ADVANCES IN THE MULTIDISCIPLINARY MANAGEMENT OF ORAL CANCER

EDITED BY: Alberto Paderno, Paolo Bossi, Sat Parmar and Cesare Piazza
PUBLISHED IN: Frontiers in Oncology

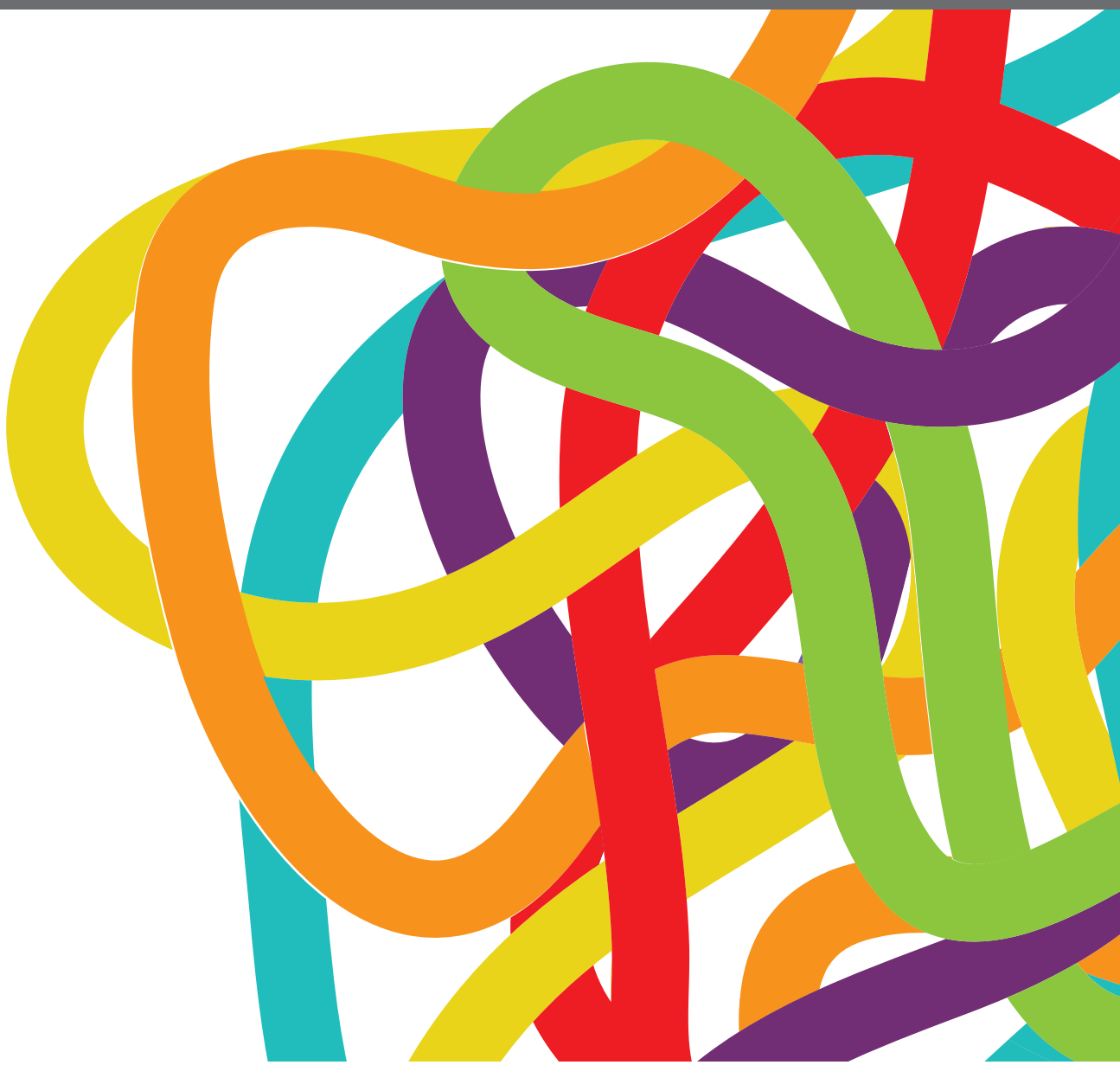

frontiers Research Topics

ISSN 1664-8714
ISBN 978-2-88974-238-7
DOI 10.3389/978-2-88974-238-7

About Frontiers

Frontiers is more than just an open-access publisher of scholarly articles: it is a pioneering approach to the world of academia, radically improving the way scholarly research is managed. The grand vision of Frontiers is a world where all people have an equal opportunity to seek, share and generate knowledge. Frontiers provides immediate and permanent online open access to all its publications, but this alone is not enough to realize our grand goals.

Frontiers Journal Series

The Frontiers Journal Series is a multi-tier and interdisciplinary set of open-access, online journals, promising a paradigm shift from the current review, selection and dissemination processes in academic publishing. All Frontiers journals are driven by researchers for researchers; therefore, they constitute a service to the scholarly community. At the same time, the Frontiers Journal Series operates on a revolutionary invention, the tiered publishing system, initially addressing specific communities of scholars, and gradually climbing up to broader public understanding, thus serving the interests of the lay society, too.

Dedication to Quality

Each Frontiers article is a landmark of the highest quality, thanks to genuinely collaborative interactions between authors and review editors, who include some of the world's best academicians. Research must be certified by peers before entering a stream of knowledge that may eventually reach the public - and shape society; therefore, Frontiers only applies the most rigorous and unbiased reviews.
Frontiers revolutionizes research publishing by freely delivering the most outstanding research, evaluated with no bias from both the academic and social point of view. By applying the most advanced information technologies, Frontiers is catapulting scholarly publishing into a new generation.

What are Frontiers Research Topics?

Frontiers Research Topics are very popular trademarks of the Frontiers Journals Series: they are collections of at least ten articles, all centered on a particular subject. With their unique mix of varied contributions from Original Research to Review Articles, Frontiers Research Topics unify the most influential researchers, the latest key findings and historical advances in a hot research area! Find out more on how to host your own Frontiers Research Topic or contribute to one as an author by contacting the Frontiers Editorial Office: frontiersin.org/about/contact

ADVANCES IN THE MULTIDISCIPLINARY MANAGEMENT OF ORAL CANCER

Topic Editors:
Alberto Paderno, University of Brescia, Italy
Paolo Bossi, University of Brescia, Italy
Sat Parmar, University Hospital, Birmingham
Cesare Piazza, University of Brescia, Italy

Citation: Paderno, A., Bossi, P., Parmar, S., Piazza, C., eds. (2022). Advances In The Multidisciplinary Management of Oral Cancer. Lausanne: Frontiers Media SA. doi: 10.3389/978-2-88974-238-7

Table of Contents

frontiers in Oncology

EDITORIAL
published: 15 December 2021
doi: 10.3389/fonc.2021.817756

Editorial: Advances in the Multidisciplinary Management of Oral Cancer

Alberto Paderno[1,2]*, *Paolo Bossi*[3] *and Cesare Piazza*[1,2]

[1] Unit of Otorhinolaryngology – Head and Neck Surgery, Azienda Socio Sanitaria Territoriale (ASST) Spedali Civili of Brescia, Brescia, Italy, [2] Department of Medical and Surgical Specialties, Radiological Sciences, and Public Health, School of Medicine, University of Brescia, Brescia, Italy, [3] Medical Oncology, Department of Medical and Surgical Specialties, Radiological Sciences, and Public Health University of Brescia, Azienda Socio Sanitaria Territoriale (ASST) Spedali Civili, Brescia, Italy

Keywords: oral cancer, multidisciplinary, management, oral cavity, squamous cell carcinoma

Editorial on the Research Topic

Advances in the Multidisciplinary Management of Oral Cancer

Oral squamous cell carcinoma (OSCC) is the 16th most common neoplasm worldwide, with almost 355,000 newly diagnosed cases and over 177,000 deaths estimated in 2018 (1). Notwithstanding, it remains an often-neglected and significantly underfunded pathology, together with all neoplasms associated with stigmatized behaviors such as alcohol and tobacco consumption (2, 3). For this reason, advancements are comparatively more difficult than in more prevalent and socially accepted diseases. Furthermore, the significant incidence of high-risk behaviors in patients affected by OSCC represents an adjunctive layer of complexity in the practical application of novel achievements. Nowadays, clinicians and researchers should strive to optimize and progressively refine each aspect of OSCC management, raising awareness on its most pressing issues and selecting interventions that are applicable in everyday clinical practice.

A significant step forward in the diagnostic, therapeutic, and rehabilitative approach of OSCC (and head and neck cancers in general) has been the broad recognition of the fundamental role of multidisciplinary teams. This concept has been confirmed by the current evaluation from Shang et al., showing that patients undergoing proper multidisciplinary management had a significantly higher survival rate. This result further reinforces the need for centralization of care in OSCC, favoring institutes with the availability of a comprehensive multidisciplinary team and all the professional figures needed for the entire diagnostic and therapeutic processes, as well as post-treatment care.

As reflected by the current Research Topic, the entire patient management pathway should be optimized to obtain measurable improvements in survival and quality of life. In particular, the main fields herein addressed are tumor diagnosis and staging, surgical approaches, non-surgical treatments, and risk stratification by conventional and molecular techniques.

Proper and timely diagnosis remains a weak point in management of OSCC. Tumors are often referred to specialists with significant delay and after reaching advanced stages. This factor has a significant impact on prognosis and is the first variable that should be optimized. Bioendoscopic filters such as Narrow Band Imaging (NBI) can improve the diagnostic potential of conventional oral examination (4, 5). However, these techniques require a significant learning curve and are burdened by subjectivity in interpretation. The study by Paderno et al. showed for the first time the possibility to apply fully convolutional neural networks to NBI endoscopic frames of oral lesions in

OPEN ACCESS

Edited and reviewed by:
Jan Baptist Vermorken, University of Antwerp, Belgium

***Correspondence:**
Alberto Paderno
albpaderno@gmail.com

Specialty section:
This article was submitted to Head and Neck Cancer, a section of the journal Frontiers in Oncology

Received: *18 November 2021*
Accepted: *29 November 2021*
Published: *15 December 2021*

Citation:
Paderno A, Bossi P and Piazza C (2021) Editorial: Advances in the Multidisciplinary sManagement of Oral Cancer. Front. Oncol. 11:817756. doi: 10.3389/fonc.2021.817756

order to automatically identify tumors and delineate their margins. This preliminary report confirms the potential of the newly developing field of "Videomics" for diagnosis and in-depth characterization of OSCC (6). In parallel, efforts should be made to refine diagnosis and stratification of oral potentially malignant diseases, thus identifying those at higher risk of malignant transformation. These two fields of research, i.e. the definition of high-risk premalignant lesions and early identification of OSCC, have a lot of common ground, being part of the continuum process of cancerization.

When considering OSCC treatment, surgery still remains the first-line option, potentially followed by adjuvant therapies. However, surgery is not a static discipline, and techniques should be refined and evolve according to new evidence and technologies. In recent years, the concept of compartmental surgery for OSCC has gained significant momentum (7–9). In this regard, Carta et al. and Grammatica et al., respectively, provided a retrospective analysis confirming the good oncologic outcomes obtainable by compartmental tongue resections and a step-by-step guide describing such a surgical technique.

At the same time, the growing acceptance of sentinel lymph node biopsy in oral oncology may lead to improvements in prophylactic management of contralateral neck metastases. As Mahieu et al. reported, the contralateral neck is generally not addressed by elective neck dissection in early stage OSCC not involving the midline, while sentinel lymph node biopsy may stage both the ipsilateral and contralateral neck. Interestingly, the authors described a higher rate of contralateral regional recurrence in patients receiving elective neck dissection than those who underwent sentinel lymph node biopsy. This result shows the effectiveness of such a procedure in detecting unexpected contralateral nodal spread, possibly opening new applications for this technique in the setting of minimally invasive contralateral neck staging.

However, optimization of surgical treatment is not limited to the simple therapeutic stage. van Baar et al., in fact, assessed a novel treatment concept for advanced mandibular osteoradionecrosis combining isodose curve visualization and alveolar nerve preservation. This pilot study showed the promise of three-dimensional planning in mandibular resection and reconstruction, taking into account previous radiotherapy fields and maximizing sensory preservation. In adjunction, non-surgical therapies have also been assessed, given the progressive improvements of radiation techniques and chemotherapy regimens. Kim et al. compared postoperative chemoradiation with radiotherapy alone using new generation techniques, showing comparable results except for tumors with extranodal extension. Different schedules of induction chemotherapy have been presented, attesting the better tolerability of weekly induction taxane – platinum – fluorouracil in comparison to a 3-week schedule (Tousif et al.). These results should, however, be put within the context of the lack of survival benefit obtained with induction chemotherapy in OCSCC. Looking to drug repurposing, a potential synergic effect has been found when low molecular weight heparin is added to cisplatin (Camacho-Alonso et al.). Still, drug discovery may conceivably offer novel tools for treatment of OSCC. In this regard, melatonin can exert anti-proliferative, anti-invasive, and anti-migrative effects on OSCC *via* the miR-25-5p/NEDD9 pathway, thus warranting further assessment of its potential (Wang et al.).

However, alternative treatments in inoperable and oligometastatic OSCC should also be explored. Lambert et al. reported a single-center experience on the use of photodynamic therapy as an alternative treatment tool in inoperable oral and oropharyngeal cancer. While limited to highly selected patients, functional and oncologic outcomes were satisfying considering the specific setting. Swallowing and airway patency were preserved in 77% and 96% of patients, respectively, and the recurrence-free rate at two years was 32%.

Furthermore, according to Szturz et al., mounting evidence suggests that patients with few and slowly progressive distant metastases of small size may benefit from various local ablation techniques. The authors summarize the potential of surgery and stereotactic radiotherapy in this specific setting. In particular, patients presenting with late development of slowly progressive oligometastatic lesions in the lungs are deemed to be potential candidates for metastasectomy or other local therapies. While literature data is still limited, this review highlights and carefully describes the often-neglected issue of oligometastatic disease in head and neck cancer, where the areas of research will increase in the future, thanks to the exploitation of combinations with immunotherapy.

Of note, significant effort has been directed towards predicting prognosis and treatment response in OSCC, resulting in improved patient stratification. This possibility has been explored through various methods, starting from conventional risk-factor selection to the evaluation of gene expression and genomic signatures.

As demonstrated, the clinical and pathologic features can be effectively integrated to optimize risk stratification through prognostic scoring systems (Zhou et al.). This is the first step towards treatment personalization, an ever-growing trend in modern oncology that aims to refine patient management by carefully assessing individual characteristics. However, accurate in-depth disease modeling requires considering a wide variety of variables that go beyond conventional clinical and histopathological characteristics. The overall microenvironment and immune-context have a leading role in determining tumor initiation, progression, and clinical features. The oral microbiota is an adjunctive player that adds complexity to the intricate web of tumor-host relations, and dysbiosis of the oral microbiome was also shown to play a critical role in the initiation and progression of OSCC. Here, Sarkar et al. precisely described the changes in the oral microbial community in Indian patients, giving a point of reference for future assessments. Considering the analysis of the tumor-immune system interplay, Fan et al. investigated the role of frequency of heterotypic neutrophil-in-tumor structure for the prognosis of patients with OSCC, highlighting its independent association with both recurrence-free and disease-specific survivals. Finally, diving into deeper and finer characteristics, gene expression profiling is showing significant promise in assessing and stratifying OSCC. In particular, mitochondrial serine hydroxymethyltransferase overexpression appears to correlate with advanced pathological

grade and recurrence (Wu Z-Z et al.). In addition, interleukin 1 receptor associated kinase 2 (IRAK2) overexpression is associated with enhanced radiosensitivity of OSCC cells, and tumors with high IRAK2 expression had better post-irradiation local control than those with low expression (Yu et al.). However, while targeted evaluations of single-gene expression may be helpful to fully clarify mechanisms and potential as therapeutic targets, complete transcriptomic analysis may give a comprehensive view of tumor biologic characteristics and risk profile. In this regard, Wu X et al. developed a 5-metabolic pathway prognostic signature for OSCC based on dysregulated metabolic cascades and provides support for the aberrant metabolism underlying tumorigenesis. The signature effectively stratified patients in groups according to survival and served as an independent prognostic factor.

Finally, the vast majority of tumors in the oral cavity are definitively squamous cell carcinoma. Nevertheless, while significantly less prevalent, salivary gland cancers also warrant consideration. Park et al. provided an overall view of minor salivary gland cancers originating from the oral cavity and compared them with OSCC. Interestingly, patients with small salivary gland malignancies showed >90% survival at 5 years, and local control was often successful even with close or positive margins. However, treatment choice should still take into account the vast heterogeneity of biological behavior in salivary gland tumors. In fact, different subtypes, even if defined by the same histology (Piwowarczyk et al.), may present diverse growth rates, patterns of spreading, and likelihood of recurrence.

In conclusion, the management of OSCC has significant room for improvement, and this should be primarily obtained by optimizing current strategies. Indeed, many factors that decrease survival are related to late diagnosis or inadequate treatment and could be addressed by prompt referral to leading oncologic centers. Once this issue has been solved, the introduction of molecular analyses and artificial intelligence tools have the potential to further improve treatment personalization and outcomes.

AUTHOR CONTRIBUTIONS

AP, PB, and CP wrote the manuscript, contributed to manuscript revision, read, and approved the submitted version.

REFERENCES

1. Bray F, Ferlay J, Soerjomataram I, Siegel RL, Torre LA, Jemal A. Global Cancer Statistics 2018: GLOBOCAN Estimates of Incidence and Mortality Worldwide for 36 Cancers in 185 Countries. *CA Cancer J Clin* (2018) 68:394–424. doi: 10.3322/caac.21492
2. Kamath SD, Kircher SM, Benson AB. Comparison of Cancer Burden and Nonprofit Organization Funding Reveals Disparities in Funding Across Cancer Types. *J Natl Compr Canc Netw* (2019) 17:849–54. doi: 10.6004/jnccn.2018.7280
3. Carter AJ, Nguyen CN. A Comparison of Cancer Burden and Research Spending Reveals Discrepancies in the Distribution of Research Funding. *BMC Public Health* (2012) 12:526. doi: 10.1186/1471-2458-12-526
4. Piazza C, Del Bon F, Paderno A, Grazioli P, Perotti P, Barbieri D, et al. The Diagnostic Value of Narrow Band Imaging in Different Oral and Oropharyngeal Subsites. *Eur Arch Otorhinolaryngol* (2016) 273:3347–53. doi: 10.1007/s00405-016-3925-5
5. Piazza C, F DB, Peretti G, Nicolai P. 'Biologic Endoscopy': Optimization of Upper Aerodigestive Tract Cancer Evaluation. *Curr Opin Otolaryngol Head Neck Surg* (2011) 19:67–76. doi: 10.1097/MOO.0b013e328344b3ed
6. Paderno A, Holsinger FC, Piazza C. Videomics: Bringing Deep Learning to Diagnostic Endoscopy. *Curr Opin Otolaryngol Head Neck Surg* (2021) 29:143–8. doi: 10.1097/MOO.0000000000000697
7. Piazza C, Grammatica A, Montalto N, Paderno A, Del Bon F, Nicolai P. Compartmental Surgery for Oral Tongue and Floor of the Mouth Cancer: Oncologic Outcomes. *Head Neck* (2019) 41:110–5. doi: 10.1002/hed.25480
8. Piazza C, Montalto N, Paderno A, Taglietti V, Nicolai P. Is It Time to Incorporate 'Depth of Infiltration' in the T Staging of Oral Tongue and Floor of Mouth Cancer? *Curr Opin Otolaryngol Head Neck Surg* (2014) 22:81–9. doi: 10.1097/MOO.0000000000000038
9. Grammatica A, Piazza C, Montalto N, Del Bon F, Frittoli B, Mazza M, et al. Compartmental surgery for oral tongue cancer: Objective and subjective functional evaluation. *Laryngoscope* (2021) 131:E176–83. doi: 10.1002/lary.28627

Conflict of Interest: The authors declare that the research was conducted in the absence of any commercial or financial relationships that could be construed as a potential conflict of interest.

frontiers in Oncology

ORIGINAL RESEARCH
published: 03 June 2020
doi: 10.3389/fonc.2020.00881

Clinical Outcome of Minor Salivary Gland Cancers in the Oral Cavity: A Comparative Analysis With Squamous Cell Carcinomas of the Oral Cavity

*Song I Park[1], Woori Park[1], Sungyong Choi[1], Yunjeong Jang[2], Hyunjin Kim[2], Seok-Hyung Kim[2], Jae Myoung Noh[3], Man Ki Chung[1], Young-Ik Son[1], Chung-Hwan Baek[1] and Han-Sin Jeong[1]**

[1] Department of Otorhinolaryngology - Head and Neck Surgery, Samsung Medical Center, Sungkyunkwan University School of Medicine, Seoul, South Korea, [2] Department of Pathology, Samsung Medical Center, Sungkyunkwan University School of Medicine, Seoul, South Korea, [3] Department of Radiation Oncology, Samsung Medical Center, Sungkyunkwan University School of Medicine, Seoul, South Korea

Purpose: Salivary gland cancer (SGC) in the oral cavity is not common and has been less studied in comparison with oral squamous cell carcinoma (SCC). This study aimed to identify the clinical characteristics and outcomes of SGC in the oral cavity compared with oral SCC.

Methods: The medical charts of the patients with SGC ($N = 68$) arising from minor salivary glands and SCC ($N = 750$) in the oral cavity between 1995 and 2017 were reviewed retrospectively. The clinical and pathological factors and treatment outcomes were compared to identify clinical differences between oral SGC and SCC in total cases and in tumor size and subsite (propensity score)-matched pairs ($N = 68$ in each group). In addition, pattern of local invasion was pathologically assessed in a subset of SGC and SCC tumors.

Results: Patients with SGC in the oral cavity showed >90% survival at 5 years. Most common pathologies of SGC were mucoepidermoid carcinoma (39.7%) and adenoid cystic carcinoma (35.3%), where high-grade tumors (including adenoid cystic carcinomas having solid components, grade 2 or 3) represented only 36.8%. Compared with oral SCC, surgery for SGC had narrow surgical safety margin. However, local control was very successful in SGC even with <5 mm or positive resection margin through surgery plus adjuvant radiation treatments or surgery alone for small low-grade tumors. Pathologic analysis revealed that the frequency of oral SGC with infiltrative tumor border was significantly lower than that of oral SCC (46.4 vs. 87.2%, $P < 0.001$).

Conclusions: SGC in the oral cavity represents relatively good prognosis and has a locally less aggressive pathology compared with oral SCC. Adjuvant radiation can be very effective to control minimal residual disease in oral SGC. Our study proposed that a different treatment strategy for oral SGC would be reasonable in comparison with oral SCC.

Keywords: minor salivary gland, neoplasms, oral cavity, surgery, radiation, outcomes

OPEN ACCESS

Edited by:
Cesare Piazza, Istituto Nazionale dei Tumori (IRCCS), Italy

Reviewed by:
Patrick James Bradley, Queen's Medical Centre, United Kingdom
Laura Deborah Locati, National Cancer Institute (IRCCS), Italy

***Correspondence:**
Han-Sin Jeong
hansin.jeong@gmail.com

Specialty section:
This article was submitted to Head and Neck Cancer, a section of the journal Frontiers in Oncology

Received: *24 February 2020*
Accepted: *05 May 2020*
Published: *03 June 2020*

Citation:
Park SI, Park W, Choi S, Jang Y, Kim H, Kim S-H, Noh JM, Chung MK, Son Y-I, Baek C-H and Jeong H-S (2020) Clinical Outcome of Minor Salivary Gland Cancers in the Oral Cavity: A Comparative Analysis With Squamous Cell Carcinomas of the Oral Cavity. Front. Oncol. 10:881. doi: 10.3389/fonc.2020.00881

INTRODUCTION

Oral cancer is the sixth most common cancer worldwide (1). While the most common malignant disease in the oral cavity is squamous cell carcinoma (SCC), other pathologic types of malignancy including salivary gland cancers (SGC) can also occur in the oral cavity (1, 2). SGC is relatively rare and comprises 1–6% of all head and neck cancers (3–7). It has heterogeneous types of pathology with diverse tumor biology (4, 5, 8). Therefore, the clinical courses, outcomes and prognosis of intraoral SCC and SGC can be different, although they share the same anatomical site. Regarding adjuvant treatment, concurrent chemoradiation is a standard treatment modality for high-risk oral SCC as a postoperative adjuvant treatment (9). In contrast, adjuvant concurrent chemoradiation is not validated yet for high-risk SGC (currently under clinical trial) (10), and postoperative radiation is still a standard of care as an adjuvant treatment for SGC (11). In terms of prognosis, 5-year survival rate for patients with SCC ranges from 40 to 63% (2), while that for SGC is 71.8–90.1% and is characterized by late recurrence (6, 12, 13).

As for resectable SCC and SGC in the oral cavity, surgery is the primary treatment option (11). According to the National Comprehensive Cancer Network (NCCN) guidelines, a surgical safety margin of 5 mm is recommended to lower recurrence in SCC (9). Because of disease rarity, it is unclear whether this cutoff value in resection is valid for oral SGC. Previously, we demonstrated that close surgical margin <5 mm in SGC of the major salivary gland was not a significant risk factor for recurrence and not a good determinant for adjuvant radiation, particularly in low-grade tumors (14). As oral SGC is a submucosal lesion, it seems difficult to define the clear boundary of tumors due to the anatomical complexity. Therefore, it is clinically important to evaluate the local microscopic invasion into the surrounding tissues in oral SGC, which determines the surgical extent and post-operative adjuvant radiation treatments.

In the first attempt to answer this clinical question in decision making of surgical extent, we tried to identify the clinical outcomes, treatment response, and pattern of local invasion of oral SGC in comparison with those of oral SCC in this study. Unlike most previous studies dealing with SGC solely, we conducted a comparative study of oral SCC and SGC with tumor size and subsite-matched pairs. Thus, this study will provide clinically relevant information in treatment decision for oral SGC and will capture the biological differences of SCC and SGC with the same anatomic site of oral cavity.

MATERIALS AND METHODS

Study Population

This retrospective study was approved by the Institutional Review Board of Samsung Medical Center. We collected and reviewed the medical records of SGC and SCC cases in the oral cavity that had been diagnosed and managed in our facility from 1995 to 2017. The diagnoses were confirmed by pathology. The SGCs in the oral cavity originated from minor salivary glands in the oral cavity, and we excluded the cases from sublingual glands. A total of 818 patients (68 SGC and 750 SCC) were included in this study, after exclusion of cases with incomplete clinical information or undetermined pathology.

Clinical and Pathological Variables

Clinical and pathological data of age, gender, site of tumor, tumor grade, tumor-node-metastasis (TNM) stage, surgical margin status, extranodal extension, type of treatment and treatment outcome were analyzed. The staging of all cases was based on the TNM classification of the American Joint Committee on Cancer (AJCC) staging manual (15). As for the cases included in this study, we reviewed the pathology again by experienced pathologists who has more than 10 years of experience in salivary gland pathology. The histological typing was made or revised according to the 2017 World Health Organization classification of salivary tumors (16). If two or more pathology types were mixed, the tumor was classified as the pathological type with the worst prognosis. The histological grade of tumor was defined as low, intermediate or high according to cytological features and architectures (16–18). Mucoepidermoid carcinomas were divided into 3 grades, based on the accepted criteria (17). Adenoid cystic carcinomas were graded according to the proportion of solid component; grade 1: predominantly tubular type with no solid component, grade 2: predominantly cribriform type with solid component less than 30%, grade 3: solid component more than 30% (17, 19). Adenocarcinoma were classified as high or low group by histological type and cytological variants (17). Acinic cell, clear cell and myoepithelial carcinoma were classified as low grade, while salivary duct carcinoma was classified as high grade (17).

Treatments and Follow-Ups

Most patients were managed with initial surgery-based treatments for resectable disease. Surgery was intended to remove all cancer tissues in the primary site and neck lymph nodes. Neck dissection was conducted simultaneously for clinically suspicious (therapeutic) or occult (elective) lymph nodes in the neck, following the accepted surgical guidelines (NCCN guidelines). Surgical defects were reconstructed with a flap or local tissue, if indicated.

During the study period, radiation techniques were mainly three-dimensional conformal radiation or intensity-modulated radiation, with a mean dose of 61.0 Gy (range 50.0–70.0) by 2.0 or 2.2 Gy (mean 2.1 Gy, range 1.8–2.5) per fraction (mean 29.6 fractions, range 24–35) over 5.5–6 weeks.

For radiotherapy (RT) plan, patients underwent computed tomography (CT) scans with a thermoplastic mask. In adjuvant RT, clinical target volume (CTV) included the primary tumor bed and pathologically involved regional lymphatics with adequate margins. Elective neck irradiation (ENI) including the remote and uninvolved lymphatic levels was determined on an individual basis, considering the estimated risk of metastasis based on location, histologic type, extent, and grade of primary tumor. RT was delivered with 4- or 6-MV photons generated from a linear accelerator.

For patients receiving definitive RT, gross tumor volume (GTV) was defined as volume of primary tumor and involved lymph nodes based on all available clinical information. The

CTV of primary tumor was delineated by adding 5 mm margins in all directions from GTV, and the margins were optionally modified in accordance with the anatomic boundaries of the tumor location and/or the adjacent organs.

Chemotherapy was administered concurrently with radiation in the adjuvant setting (oral SCC), or independently in the palliative setting. Cisplatin was the major drug for chemotherapy, in combination with other drugs depending on medical oncologist decision and clinical situation.

In terms of treatment outcome, recurrence was defined when suspicious lesions were apparent on imaging or confirmed by biopsy. The survival period was defined as the time from diagnosis to death of any cause.

A Propensity Score-Matching Analysis

A propensity score-matching method was used between oral SGC and oral SCC groups to minimize differences in baseline characteristics by using JMP macro software (SAS Institute Inc., Cary, NC, USA). T status and subsites were included in the propensity matching model. Tumor subsites in the oral cavity were roughly divided into three subsites; tongue and floor of mouth (central soft tissues), hard palate and retromolar trigone (mucoperiosteal tissue), and lip and buccal area (lateral soft tissues).

Patients were matched at a 1:1 ratio using the caliper method (caliper width = 0.25 standard deviation). Finally, 136 cases (N = 68 in the oral SGC group and N = 68 in the oral SCC group) were allocated to the comparison groups (**Supplementary Material**). Comparisons between the two groups were performed by stratified Chi-square test for categorical variables.

Pathologic Analysis

Under propensity score matching, 120 patients (out of 136) had been managed with surgical treatments alone or in combination with other treatment modalities. To evaluate the pathological pattern of the tumor border (the surgical margin between tumors and adjacent tissues), we excluded 19 tumor samples of positive cancer cells at the resection margin (where there was no adjacent normal tissues in the surgical margin) or unknown cases. Another 26 cases were excluded from pathologic analyses, because of unavailable or poor quality of surgical pathology tissues. Therefore, a total of 75 patient samples were included in the pathologic analysis (28 SGC and 47 SCC tumors). The status of resection margin (pathological local infiltration) included the presence of perineural invasion. If there were perineural invasion at the resection margin or less than 5 mm away from the resection margin, we regarded them as positive or close resection margin.

As for each tumor, multiple pathology slides (three to seven) were reviewed by two pathologists. Through pathology review, the tumor margin was classified as a pushing or infiltrative border. A pushing border was defined as cancer cells forming a single lump with a clear boundary. Meanwhile, an infiltrative border was defined as tumor cells penetrating into the surrounding matrix without linear demarcation between tumor and adjacent tissues (20–22). In equivocal cases, the joint decision was made by a consensus or discussion of two raters.

Statistical Analysis

Propensity score analysis with 1:1 matching was used as previously described to match a cohort of patients with oral SGC to patients with oral SCC. All variables were examined using Fisher's exact test or Pearson chi-square test. Survival analysis was performed using Kaplan-Meier estimate and statistical significance was determined by log-rank test. The data were analyzed using the statistical package for social science (SPSS) (IBM Corporation, Armonk, NY, USA). Differences for P-value less than 0.05 were regarded as statistically significant.

RESULTS

Comparison of Outcomes in a Pooled Cohort

The detailed characteristics of patients in the oral SGC (N = 68) and SCC (N = 750) groups are presented in **Table 1**. Female was significantly dominant in SGC compared to SCC. Hard palate/retromolar trigone and tongue/floor of the mouth were the most common origin of SGC and SCC in the oral cavity, respectively. The most common pathology type in SGC was mucoepidermoid carcinoma (39.7%), followed by adenoid cystic carcinoma and adenocarcinoma not otherwise specified (**Table 2**). Unlike SCC, low grade tumor (excluding adenoid cystic carcinomas) was the most common tumor grade in oral SGC, comprising 54.4%.

Regarding T and N status, there was a higher T tendency for oral SGC and higher N status for oral SCC, which were similar to the previous report (23). The percentage of M1 was higher in SGC group, mainly due to the adenoid cystic carcinoma pathology. Pre-operative histopathological diagnosis was made by fine needle aspiration cytology or biopsy which was correct in 54.7% of surgical cases (29 out of 53 cases). Tumor grade was correctly predicted in 30.2% of cases (16 out of 53 cases) preoperatively.

Surgery was the primary treatment option in SCC, and surgery with adjuvant radiation (52.9%) was the main treatment for SGC. Adjuvant chemoradiation was only performed in oral SCC, but not SGC, in our institute. Notably in patients with surgery, half of SCC group (49.1%) had more than 5 mm of resection margin; meanwhile a larger proportion of patients (75.4%) had close or positive resection margin in the SGC group. In clinical courses, regional recurrence and disease-related deaths were more frequent in SCC, while distant metastasis more commonly occurred in SGC. The overall survival difference between the two groups was significant (**Figure 1A**). The 5-year overall survival rate was 91.9% in SGC and 73.2% in SCC, respectively (P = 0.0015). Ten- and fifteen-year overall survival rates for oral SGC were 72.9 and 54.7%, and those for oral SCC were 61.8 and 48.6%, respectively.

Outcome Comparison in a Propensity Score-Matched Cohort

In this study, we focused on local tumor control and local extension (pathological infiltration) of oral SGC and SCC. Thus,

TABLE 1 | Comparison of total subjects diagnosed with minor salivary gland origin cancer or mucosal squamous cell carcinomas of the oral cavity (Salivary gland cancer $N = 68$, oral squamous cell carcinoma $N = 750$).

No. (%)	Salivary gland cancer ($N = 68$)	Squamous cell carcinoma ($N = 750$)	Difference (P)
Age (median, range, years)	51.0 (23.0–86.0)	56.0 (18.0–97.0)	0.074
Gender (Male: Female)	26:42 (38.2:61.8)	473:277 (63.1:36.9)	**<0.001**
Tumor subsite			**<0.001**
Hard palate/ Retromolar trigone	41 (60.3)	70 (9.3)	
Tongue/ Floor of the mouth	17 (25.0)	580 (77.3)	
Buccal/ Lip	10 (14.7)	100 (13.3)	
TNM status			
T T1	23 (33.8)	319 (42.5)	**0.028**
T2	24 (35.3)	238 (31.7)	
T3	5 (7.4)	76 (10.1)	
T4	16 (23.5)	87 (11.6)	
Tx	0 (0.0)	30 (4.0)	
N N0	55 (80.9)	461 (61.5)	**<0.001**
N1	3 (4.4)	75 (10.0)	
N2	3 (4.4)	177 (23.6)	
N3	7 (10.3)	11 (1.5)	
Nx	0	26 (3.5)	
M M1 at presentation	4 (5.9)	5 (0.7)	**0.004**
TNM stage			0.078
I	22 (32.4)	271 (36.1)	
II	16 (23.5)	133 (17.7)	
III	4 (5.9)	95 (12.7)	
IV	26 (38.2)	220 (29.3)	
Unknown	0	31 (4.1)	
Extranodal extension	6 (9.8)	128 (18.6)	0.055
Treatments			**<0.001**
Surgery alone	25 (36.8)	363 (48.4)	
Surgery + radiation	36 (52.9)	200 (26.7)	
Surgery + chemoradiation	0 (0.0)	126 (16.8)	
Chemoradiation	3 (4.4)	33 (4.4)	
Radiation alone	3 (4.4)	21 (2.8)	
Chemotherapy	0 (0.0)	5 (0.7)	
No treatments[a]	1 (1.5)	2 (0.3)	
Status of resection margin in cases of surgery	$N = 61$	$N = 689$	**<0.001**
Safety margin ≥ 5 mm	11 (18.0)	338 (49.1)	
Close margin < 5 mm	33 (54.1)	296 (43.0)	
Positive cancer cells at resection margin	13 (21.3)	27 (3.9)	
Unknown	4 (6.6)	28 (4.1)	
Treatment outcomes (No. %) and event time points (median, [interquartile range], months)			
No evidence of disease at the last follow up	42 (61.8)	424 (56.5)	0.444
Local recurrence[b]	5 (7.4) (16.0 [13.4–52.3])	122 (16.3) (8.5 [4.3–27.0])	0.054
Regional recurrence[b]	4 (5.9) (43.1 [33.5–49.9])	123 (16.4) (6.4 [3.9–9.9])	**0.022**
Distant metastasis[b]	19 (27.9) (41.1 [10.8–58.5])	44 (5.9) (6.3 [3.9–11.8])	**<0.001**
Disease progression[c]	0	38 (5.1) (2.8 [1.2–4.4])	0.066
Death of disease	9 (13.2) (46.0 [38.1–89.9])	195 (26.0) (17.3 [10.7–33.6])	**0.019**
Unknown	2 (2.9)	15 (2.0)	0.645
Follow-up (median, range, months)	49.9 (0.9–245.8)	31.3 (0.7–235.3)	

[a] No cancer treatments due to acute tumor bleeding, poor medical condition or refusal of recommended treatment.
[b] Number overlapped.
[c] Disease progression on non-surgical treatment.
Bold P-values indicate P<0.05.

TABLE 2 | Pathology diagnosis of enrolled subjects.

No. (%)	Salivary gland cancer ($N = 68$)
Pathology and tumor grade	
Mucoepidermoid carcinoma	27 (39.7)
High/ Intermediate/ Low	4/ 1/ 22 (14.8/ 3.7/ 81.5)
Adenoid cystic carcinoma[a]	24 (35.3)
Grade 3/ Grade 2/ Grade 1	3/ 16/ 5 (12.5/ 66.7/ 20.8)
Adenocarcinoma, NOS	11 (16.2)
High/ Intermediate/ Low	1/ 0/ 10 (9.1/ 0/ 90.9)
Acinic cell carcinoma (low grade)	2 (2.9)
Salivary duct carcinoma (high grade)	1 (1.5)
Clear cell carcinoma (low grade)	1 (1.5)
Myoepithelial carcinoma (low grade)	2 (2.9)

Adenocarcinoma, NOS: Adenocarcinoma, not otherwise specified.
[a] Grade 1: predominantly tubular type, no solid component), grade 2: predominantly cribriform type, solid component equal to or less than 30%, and grade 3: solid component more than 30%.

we adjusted three potential factors in comparison between oral SGC and SCC: T status, tumor subsites, and tumor grade.

First, we constructed a propensity score-matched cohort, using T status and tumor subsite. In this propensity score matching, we tried a matching between two groups with various ratios (1:1, 1:2, 1:3) and caliper widths (0.05, 0.1, 0.2, 0.25), but the matching outcomes were suboptimal (standard mean differences in matching variables > 0.1) except 1:1 matching and caliper width = 0.25. Thus, patients with SCC ($N = 68$) were matched with 68 patients diagnosed with SGC at a 1:1 ratio using the caliper method (caliper width = 0.25 standard deviation). The

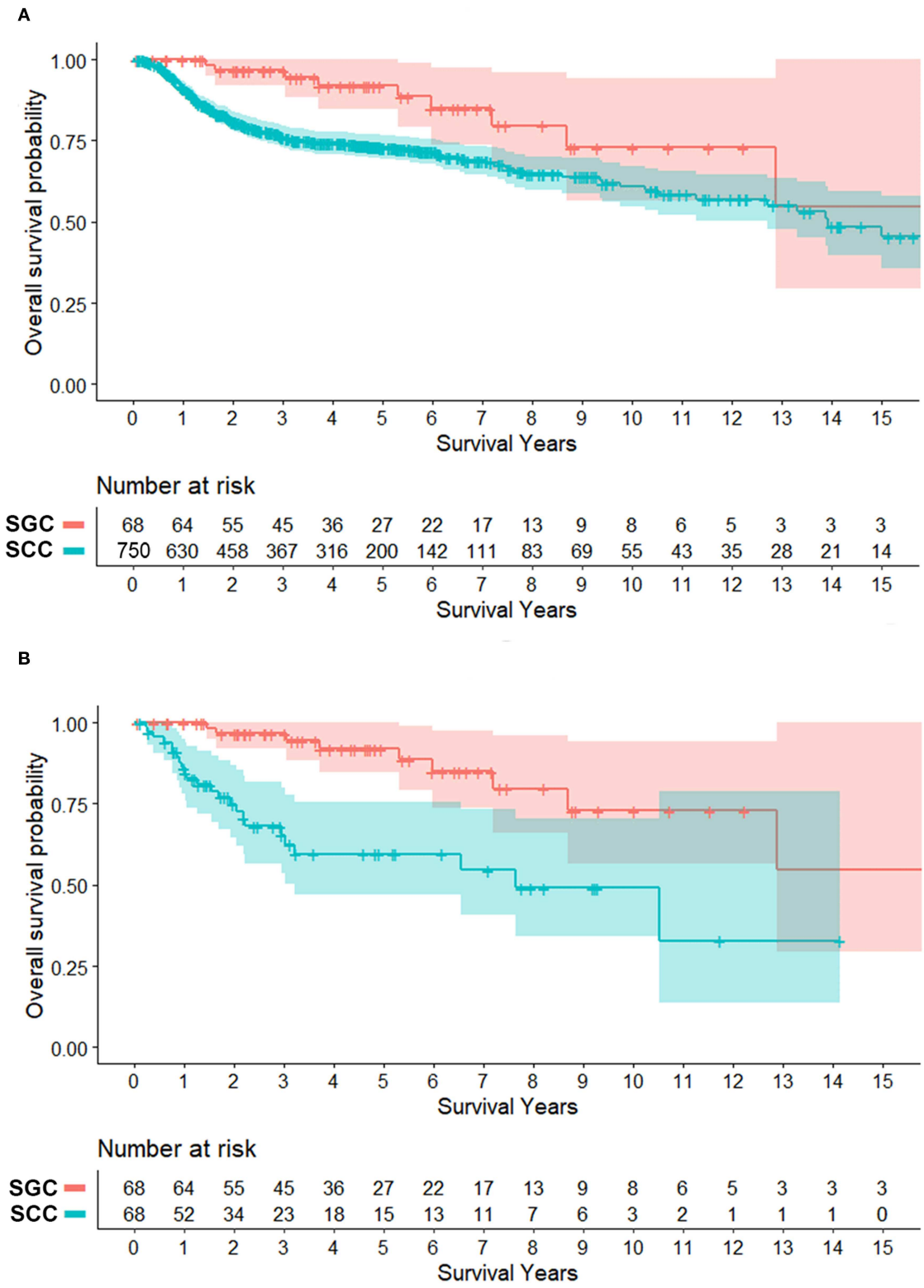

FIGURE 1 | Survival plots of patients with minor salivary gland cancer (SGC) and mucosal squamous cell carcinoma (SCC) in the oral cavity (overall survival). **(A)** Total patients. **(B)** Patients matched for tumor size (T status) and subsite (propensity score, 1:1). Shaded area = 95% confidence interval. Overall survival rates at 5, 10, and 15 years for oral SGC were 91.9, 72.9, and 54.7%, respectively. Those for oral SCC were 73.2, 61.8% and 48.6% ($N = 750$) and 59.6, 49.1, and 32.8% ($N = 68$ in matched cases).

TABLE 3 | Results of propensity score-matching (1:1) using a caliper of 0.25.

	Before propensity score matching			After a propensity score-matching		
Standardized mean difference in matching variables						
Subsite		1.543			<0.001	
T status		0.025			0.029	
Matching variables (No. %)						
	SGC (*N* = 68)	**SCC (*N* = 750)**	***P*-value**	**SGC (*N* = 68)**	**SCC (*N* = 68)**	***P*-value**
Subsite			<0.001			>0.999
Hard palate/ Retromolar trigone	41 (60.3)	70 (9.3)		41 (60.3)	41 (60.3)	
Tongue/ Floor of the mouth	17 (25.0)	580 (77.3)		17 (25.0)	17 (25.0)	
Buccal/ Lip	10 (14.7)	100 (13.3)		10 (14.7)	10 (14.7)	
T status			0.072			>0.999
T1–2	47 (69.1)	557 (74.3)		47 (69.1)	47 (69.1)	
T3–4	21 (30.9)	163 (21.7)		21 (30.9)	21 (30.9)	
Tx		30 (4.0)				

result of a propensity-score matching was satisfactory according to the T status and tumor subsite (**Table 3**).

After propensity score matching (**Table 4**), oral SGC and SCC groups had unique features regarding gender distribution (female predominance in SGC), nodal metastasis, extranodal extension and treatment types. Similarly to those of a pooled cohort, surgical safety margin more than 5 mm was more frequent in the oral SCC group (18.0% in SGC vs. 33.9% in SCC), and the rate of presence of cancer cells at the resection margin was higher in SGC than in SCC (21.3 vs. 3.4%) ($P = 0.001$).

In clinical course, local and regional recurrence rates were higher in SCC even with wider resection of SCC, but distant metastasis was detected frequently in SGC (27.9 vs. 5.9%, $P = 0.001$). The overall survival plot was also similar to that of a pooled cohort. The 5-year overall survival rates were 91.9 and 59.6% ($P < 0.001$) (**Figure 1B**). Ten- and fifteen-year overall survival rates for oral SGC were 72.9 and 54.7%, and those for oral SCC were 49.1 and 32.8%, respectively.

Response to Treatment and Pattern of Failure

Considering better oncological outcomes even with high rate of marginal surgical resection in SGC (close or positive resection margin), we evaluated the potential effectiveness of adjuvant treatments in cases with close or positive resection margin in surgical specimens (**Table 5**).

When comparing the two groups with close resection margin according to treatment type and clinical outcomes, the SGC group had more adjuvant radiation (66.7 vs. 24.3%, $P < 0.001$), and higher local control rate (100.0 vs. 70.3%, $P = 0.001$), lower regional recurrence rate (3.0 vs. 21.6%, $P = 0.03$) and higher distant metastasis rate (30.3 vs. 8.1%, $P = 0.029$). This suggested that adjuvant radiation may play an essential role in local control of oral SGC. Even in cases with positive resection margin, adjuvant radiation successfully achieved local control in oral SGC (76.9 vs. 0.0%, $P = 0.038$).

Another interesting finding was that there was just one local recurrence even with surgery alone (without any adjuvant treatment) for oral SGC with marginal resection surgery (**Table 5**). These tumors were usually small and low grade tumors. Thus, it appeared that a surgery of <5 mm safety margin would be acceptable for low-risk oral SGC tumors.

Subgroup Analysis With Tumor Grade Adjustment

In the initial subjects, the number of high-grade tumors (including grade 2 or 3 adenoid cystic carcinomas) in oral cavity SGC was not big enough ($N = 25$ of 68, 36.8%). Thus, we could not include tumor grade as a variable in a propensity score matching. Rather, we adjusted tumor grade in this subgroup comparison.

To understand the effect of tumor grade on local tumor control, we only included in a subset with high grade tumors from a previous propensity score-matched cohort (**Table 6**). In this analysis, we included adenoid cystic carcinoma cases, because they are locally aggressive (infiltrative) regardless of grade (18). Similarly, use of adjuvant radiation (not chemoradiation) (63.3 vs. 22.1%, $P < 0.001$) and safety resection margin $\geq$ 5 mm (8.3 vs. 33.9%, $P < 0.001$) were different between SGC and SCC groups. In patients with high grade SGC, systemic spread occurred in the clinical course in 33.3% (5.9% in SCC). In line with the previous findings, adjuvant radiation treatment in close or positive resection margin even in high-grade SGC appeared to be very effective in terms of local control (**Table 7**).

Pathologic Analysis of Microscopic Tumor Extension

Even with marginal surgical resection of oral cavity SGC, we found excellent local tumor control with surgery alone or surgery plus adjuvant radiation in our series, regardless of tumor grade. In addition to the effective role of adjuvant radiation, we compared microscopic tumor borders of oral SGC, with those of oral cavity SCC. Thus, we pathologically re-analyzed the surgical specimens (cases with close and clear resection margins) from a propensity-matched cohort. Remarkably, most SCC tumors had an infiltrative border (41 out of 47, 87.2%); while only 46.4% (13 out of 28) of SGC tumors had an infiltrative border ($P < 0.001$)

TABLE 4 | Clinical characteristics of tumor size (T status) and subsite (propensity score, 1:1)-matched salivary gland cancer (*N* = 68) and squamous cell carcinoma (*N* = 68) in the oral cavity.

No. (%)		Salivary gland cancer (*N* = 68)	Squamous cell carcinoma (*N* = 68)	Difference (*P*)
Age (median, range, years)		52.8 (23.0–86.0)	59.8 (34.0–82.0)	**0.003**
Gender (Male: Female)		26:42 (38.2:61.8)	47:21 (69.1:30.9)	**0.001**
Tumor subsite				>0.999
	Hard palate/ Retromolar trigone	41 (60.3)	41 (60.3)	
	Tongue/ Floor of the mouth	17 (25.0)	17 (25.0)	
	Buccal/ Lip	10 (14.7)	10 (14.7)	
TNM status				
T	T1–2	47 (69.1)	47 (69.1)	>0.999
	T3–4	21 (30.9)	21 (30.9)	
N	N0	55 (80.9)	37 (54.4)	**0.002**
	N1–3	13 (19.1)	30 (44.1)	
	Nx	0 (0.0)	1 (1.5)	
M	M1 at presentation	4 (5.9)	0 (0.0)	0.119
TNM stage				0.271
	I	22 (32.4)	21 (30.9)	
	II	16 (23.5)	8 (11.8)	
	III	4 (5.9)	7 (10.3)	
	IV	26 (38.2)	31 (45.6)	
	Unknown	0 (0.0)	1 (1.5)	
Extranodal extension		6 (9.8)	16 (27.1)	**0.018**
Treatments				**<0.001**
	Surgery alone	25 (36.8)	29 (42.6)	
	Surgery + radiation	36 (52.9)	15 (22.1)	
	Surgery + chemoradiation	0 (0.0)	15 (22.1)	
	Chemoradiation	3 (4.4)	6 (8.8)	
	Radiation alone	3 (4.4)	3 (4.4)	
	No treatment[a]	1 (1.5)	0 (0.0)	
Status of resection margin in cases of surgery		*N* = 61	*N* = 59	**0.001**
	Safety margin ≥ 5 mm	11 (18.0)	20 (33.9)	
	Close margin < 5 mm	33 (54.1)	37 (62.7)	
	Positive cancer cells at resection margin	13 (21.3)	2 (3.4)	
	Unknown	4 (6.6)	0 (0.0)	
Treatment outcomes (No. %) and event time points (median, [interquartile range], months)				
	No evidence of disease at the last follow up	42 (61.8)	34 (50.0)	0.227
	Local recurrence[b]	5 (7.4) (16.0 [13.4–52.3])	14 (20.6) (6.4 [3.5–11.6])	**0.046**
	Regional recurrence[b]	4 (5.9) (43.1 [33.5–49.9])	14 (20.6) (7.3 [3.1–11.7])	**0.021**
	Distant metastasis[b]	19 (27.9) (41.1 [10.8–58.5])	4 (5.9) (1.5 [1.1–8.8])	**0.001**
	Disease progression[c]	0	4 (5.9) (3.7 [3.2–4.7])	0.119
	Death of disease	9 (13.2) (46.0 [38.1–89.9])	24 (35.3) (17.4 [10.5–30.0])	**0.005**
	Unknown	0	2 (2.9)	0.496
Follow-ups (median, range, months)		49.9 (0.9–245.8)	24.4 (0.7–176.9)	

[a] Poor medical condition.
[b] Number overlapped.
[c] Disease progression on non-surgical treatment.
Bold P-values indicate P<0.05.

(**Figure 2**). Thus, oral SGC had a locally less aggressive pathology, compared with oral SCC.

DISCUSSION

Most malignancies arising from the oral cavity are SCC, and SGC of the oral cavity is relatively rare (23). Therefore, determination of an optimal treatment strategy for oral SGC is difficult due to lack of sufficient evidence. For this reason, current treatment for oral SGC largely depends on clinical data from SCC of the oral cavity and of the head and neck (7, 24). However, it is not yet clear whether the current surgical treatment and indications for adjuvant treatment are suitable for treatment of oral SGC, even though these two types of carcinomas have different clinical and biological characteristics (25). In this study, we tried to identify the clinical and treatment characteristics of oral SGC, compared to oral SCC. There had been several studies investigating the clinical features of SGC arising from the oral cavity or oropharynx (23–32), but no comparative analysis of oral SGC and SCC has been published.

The mean age at diagnosis in our patients with oral SGC was 51.0 years, which is similar to those of other reports (6, 23, 27, 29, 30). In terms of male/female ratio, our female preponderance was also comparable with other studies with a ratio range from 1:1.2 to 1.9 (Male: Female) (27, 29, 30, 32, 33). The most common site of origin was hard palate/retromolar trigone in our series and other papers (5, 27, 30, 31). This can be explained by densely populated minor salivary gland in the hard palate of the oral cavity (28). The majority of tumors (39.7%) in this study were mucoepidermoid carcinoma, followed by adenoid cystic carcinoma and adenocarcinoma. This was consistent with some studies (23, 27, 32), while others reported adenoid cystic carcinomas was the most common histological type (5, 6, 31). According to our results, most tumors were early T (T1–2) and N0 status at the time of diagnosis. Low frequency of nodal metastasis was also line with other studies even though the dominant T status was slightly different across studies (5, 6, 23, 26).

TABLE 5 | Response to treatments and pattern of failures in cases with close or positive resection margins (Salivary gland cancer $N = 46$, Squamous cell carcinoma $N = 39$).

No. (%)	Salivary gland cancer ($N = 46$)	Squamous cell carcinoma ($N = 39$)	Difference (P)
Close resection margin (<5 mm in surgical safety margin)	$N = 33$	$N = 37$	
No adjuvant radiation	11 (33.3)[a]	17 (45.9)[b]	**<0.001**
Adjuvant radiation	22 (66.7)	9 (24.3)[c]	
Adjuvant chemoradiation	0	11 (29.7)	
Treatment outcomes (No. %) and event time points (median, [interquartile range], months)			
Local control	33 (100.0)	26 (70.3)	**0.001**
Local recurrence	0	8 (21.6) (9.1 [2.9–16.1])	
Unknown at primary site	0	3 (8.1)	
Regional recurrence[d]	1 (3.0) (41.1)	8 (21.6) (7.4 [3.5–13.7])	**0.03**
Distant metastasis[d]	10 (30.3) (32.3 [13.4–44.7])	3 (8.1) (1.7 [1.5–15.8])	**0.029**
Positive cancer cells at resection margin	$N = 13$	$N = 2$	
No adjuvant radiation	3 (23.1)[e]	1 (50.0)[b]	0.476
Adjuvant radiation	10 (76.9)	1 (50.0)[c]	
Adjuvant chemoradiation	0	0	
Treatment outcomes (No. %) and event time points (median, [interquartile range], months)			
Local control	10 (76.9)	0	**0.038**
Local recurrence	1 (7.7) (83.7)	2 (100.0) (20.6 [12.7–18.6])	
Unknown at primary site	2 (15.4)	0	
Regional recurrence[d]	1 (7.7) (10.8)	2 (100.0) (20.6 [12.7–18.6])	**0.029**
Distant metastasis[d]	5 (38.5) (59.5 [10.8–83.7])	0	0.524
Follow-ups (median, range, months)	45.8 (0.9–152.9)	26.0 (0.7–146.8)	

[a] *Cases with low-grade salivary gland cancer and small tumor burden.*
[b] *Cases with small tumor burden without pathologic risk factors, reluctant to undergo radiation treatment, or occurrence of systemic metastasis.*
[c] *Poor patient performance status for concurrent chemo-radiation.*
[d] *Number overlapped.*
[e] *Loss of follow-up loss in 1 patient and clinical follow-up only due to systemic disease in 1 patient.*
Bold P-values indicate P<0.05.

As surgery has been the primary treatment option for resectable SGC and radiation is the main adjuvant therapy for tumors with high-risk factors (34, 35), surgery with adjuvant radiation treatments was the most frequently used modality in many studies including the present paper (24, 35, 36). Despite

TABLE 6 | Comparison of tumor size, subsite, and tumor grade-matched salivary gland cancer (high-grade, including adenoid cystic carcinoma) ($N = 30$) and squamous cell carcinoma ($N = 68$) in the oral cavity.

No. (%)	High-grade salivary gland cancer ($N = 30$)	Squamous cell carcinoma ($N = 68$)	Difference (P)
Age (mean, range, years)	58.3 (28.0–82.0)	59.8 (34.0–82.0)	0.596
Gender (Male: Female)	9:21 (30.0:70.0)	47:21 (69.1:30.9)	**<0.001**
Pathology			
Squamous cell carcinoma		68 (100.0)	**<0.001**
Mucoepidermoid carcinoma	4 (13.3)		
Adenocarcinoma, NOS	1 (3.3)		
Salivary duct carcinoma	1 (3.3)		
Adenoid cystic carcinoma	24 (80.0)		
Tumor subsite			0.555
Hard palate/ Retromolar trigone	15 (50.0)	41 (60.3)	
Tongue/ Floor of the mouth	11 (36.7)	17 (25.0)	
Buccal/ Lip	4 (13.3)	10 (14.7)	
TNM status			
T T1–2	16 (53.3)	47 (69.1)	0.171
T3–4	14 (46.7)	21 (30.9)	
N N0	21 (70.0)	37 (54.4)	0.330
N1–3	9 (30.0)	30 (44.1)	
Nx	0	1 (1.5)	
M M1 at presentation	4 (13.3)	0 (0.0)	**0.008**
TNM stage			**0.004**
I	1 (3.3)	21 (30.9)	
II	9 (30.0)	8 (11.8)	
III	2 (6.7)	7 (10.3)	
IV	18 (60.0)	31 (45.6)	
Unknown	0	1 (1.5)	
Extranodal extension	3 (12.5)	16 (27.1)	0.248
Treatments			**<0.001**
Surgery alone	5 (16.7)	29 (42.6)	
Surgery + radiation	19 (63.3)	15 (22.1)	
Surgery + chemoradiation	0	15 (22.1)	
Chemoradiation	3 (10.0)	6 (8.8)	
Radiation alone	2 (6.7)	3 (4.4)	
No treatments	1 (3.3)	0	
Status of resection margin in cases with surgery	$N = 24$	$N = 59$	**<0.001**
Safety margin ≥ 5 mm	2 (8.3)	20 (33.9)	
Close margin < 5 mm	11 (45.8)	37 (62.7)	
Positive cancer cells at resection margin	11 (45.8)	2 (3.4)	
Treatment outcomes (No. %) and event time points (median, [interquartile range], months)			
No evidence of disease at the last follow-up	10 (13.5)	34 (50.0)	0.186
Local recurrence[b]	1 (3.3) (83.6)	14 (20.6) (6.4 [3.5–11.6])	**0.033**

(Continued)

TABLE 6 | Continued

No. (%)	High-grade salivary gland cancer (*N* = 30)	Squamous cell carcinoma (*N* = 68)	Difference (*P*)
Regional recurrence[b]	2 (6.7) (43.1 [42.1–44.2])	14 (20.6) (7.3 [3.4–11.7])	0.137
Distant metastasis[b]	10 (33.3) (44.3 [27.9–59.8])	4 (5.9) (1.5 [1.1–8.8])	**0.001**
Death of disease	5 (16.7) (18.7 [10.7–43.4])	24 (35.3) (17.4 [10.5–30.0])	0.092
Unknown	2 (6.7)	2 (2.9)	0.584
Follow-ups (median, range, months)	53.3 (0.9–109.9)	24.4 (0.7–176.9)	

Adenocarcinoma, NOS: Adenocarcinoma, not otherwise specified.
[b]Number overlapped.
Bold P-values indicate P<0.05.

TABLE 7 | Response to treatments and pattern of failures in cases with close or positive resection margins in high-grade salivary gland cancer (including adenoid cystic carcinoma) (*N* = 22) and squamous cell carcinoma (*N* = 39).

No. (%)	High-grade salivary gland cancer (*N* = 22)	Squamous cell carcinoma (*N* = 39)	Difference (*P*)
Close resection margin	*N* = 11	*N* = 37	
No adjuvant radiation	1 (9.1)[a]	17 (45.9)[b]	**<0.001**
Adjuvant radiation	10 (90.9)	9 (24.3)[c]	
Adjuvant chemoradiation	0	11 (29.7)	
Treatment outcomes (No. %) and event time points (median, [interquartile range], months)			
Local control	11 (100.0)	26 (70.3)	**0.048**
Local recurrence[d]	0	8 (21.6) (9.1 [2.9–16.1])	0.170
Unknown at primary site	0	3 (8.1)	0.999
Regional recurrence[d]	1 (9.1) (41.1)	8 (21.6) (7.4 [3.5–13.7])	0.662
Distant metastasis[d]	7 (63.6) (41.1 [17.2–44.3])	3 (8.1) (1.5 [1.1–8.8])	**<0.001**
Positive cancer cells at resection margin	*N* = 11	*N* = 2	
No adjuvant radiation	3 (27.3)[a]	1 (50.0)[b]	0.999
Adjuvant radiation	8 (72.7)	1 (50.0)[c]	
Adjuvant chemoradiation	0	0	
Treatment outcomes (No. %) and event time points (median, [interquartile range], months)			
Local control	8 (72.7)	0 (0.0)	0.128
Local recurrence[d]	1 (9.1) (3.3)	2 (100.0) (4.5 [4.5–8.8])	**0.038**
Unknown at primary site	2 (18.2)	0	
Regional recurrence[d]	0	2 (100.0) (6.0 [6.0–8.0])	0.333
Distant metastasis[d]	3 (27.3)	0	
Follow-up (median, range, months)	44.5 (0.9–110.6)	25.9 (0.7–146.8)	

[a]Cases with small tumor burden or reluctant to undergo adjuvant treatment.
[b]Cases with small tumor burden without pathology risk factors, reluctant to undergo radiation treatment, or occurrence of systemic metastasis.
[c]Poor patient performance status for concurrent chemo-radiation.
[d]Number overlapped.
Bold P-values indicate P<0.05.

frozen section analysis of the resection margin during surgery, 21.3% of the patients in this study had a positive resection margin (presence of cancer cells at the resection margin) and other studies have reported the rates ranging from 3.4 to 40% (5, 6, 12, 37). After treatment, more than half of the patients remained cancer free. In our series, 7.4% of patients had local recurrence while 5.9 and 27.9% of patients experienced regional and distant metastasis, respectively (**Tables 1** and **4**). Because of the low incidence and diversity of SGC, there are some differences in reported statistics for recurrence. Garden et al. reported 12% local recurrence and 27% distant metastases. For regional recurrence, 3 of 13 patients with initially node-positive disease had regional failure, while <5% of patient with node-negative disease had regional failure (34). Strick et al. reported 14.3% local recurrence and 33.3% distant metastases (38).

Even with some discrepancies in loco-regional outcomes, most studies indicated relatively high occurrence of distant metastasis compared to loco-regional recurrence. This is in contrast to oral SCC, which has a higher rate of loco-regional recurrence than isolated distant metastasis (39, 40). This result can be partly explained by effective suppressive role of radiation in loco-regional control of oral SGC. In 224 patients with minor salivary gland cancer, Spiro et al. reported a local failure rate of 47% after initial treatment, of which more than 90% was surgery alone (41). Weber et al. reported a local failure rate of 35% in patients with submandibular gland tumors with surgery alone, while patients with postoperative radiation showed a 15% local failure rate (42).

As tumor (T) status and subsites can affect local biological and clinical outcomes in oral cancer (1, 5, 12, 34), a propensity matching analysis was performed on these two variables in SGC and SCC groups. In a propensity-matched cohort with close resection margin, radiation was mainly used for adjuvant therapy of SGC and adjuvant chemoradiation was exclusively used in SCC. Adjuvant radiation successfully achieved 76.9–100% local control and >90% regional control in oral SGC with a >5 mm or positive resection margin (**Table 5**). Since SGCs are composed of tumors with various grades, only high-grade SGC was analyzed to determine whether this excellent local control of adjuvant radiation was observed in high-grade SGC. Also, we confirmed good loco-regional control by adjuvant radiation in a subgroup of high-grade SGC in the oral cavity (**Table 7**). Our finding was consistent with other reports (42, 43); meanwhile one recent study indicated that postoperative radiotherapy was not a statistically significant variable for overall survival in minor salivary gland cancer of the head and neck (HR, 0.64; 95% CI, 0.39-1.03, $P = 0.068$) (44). However, only 37.8% of patients had postoperative radiation in this report,

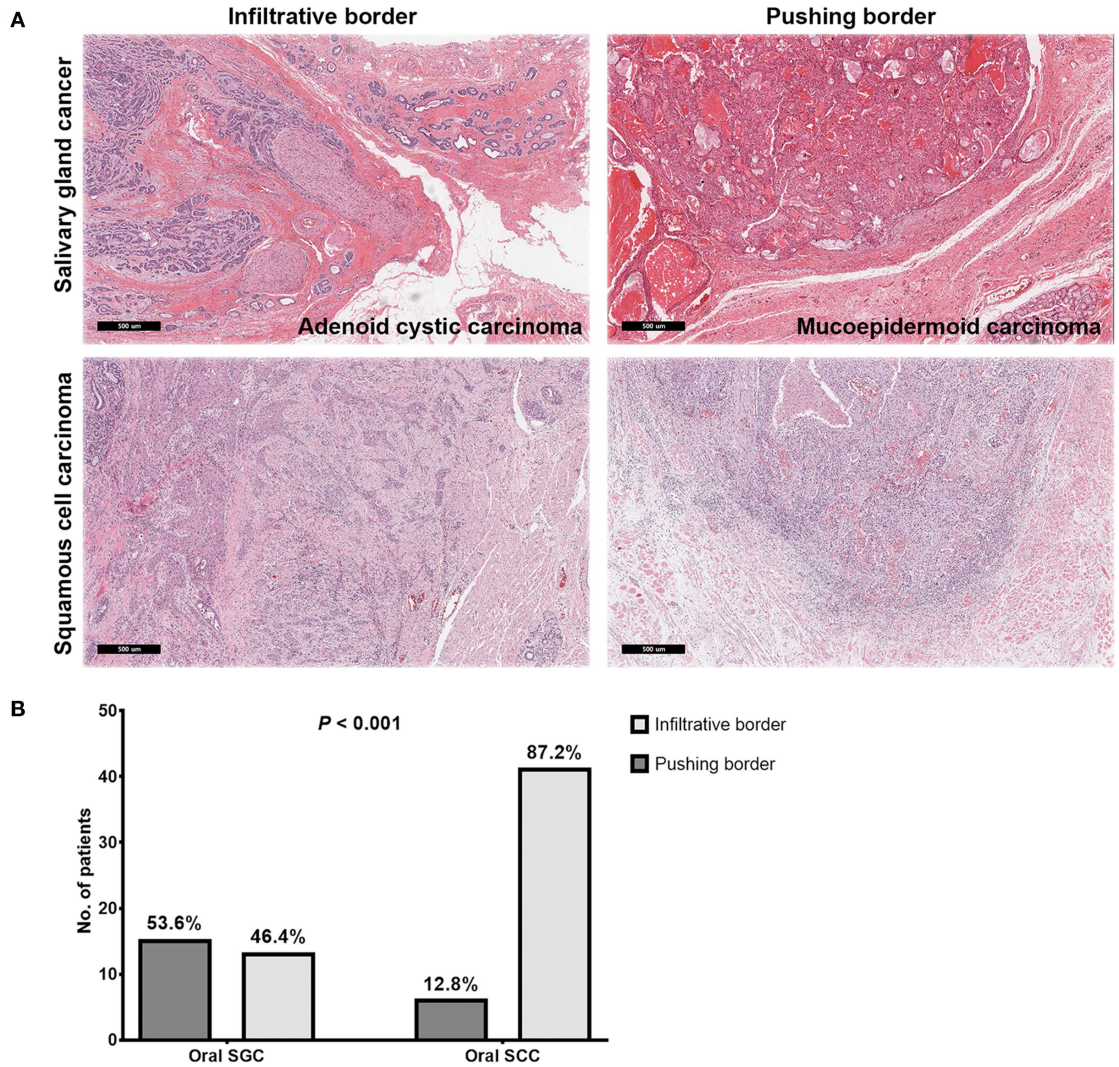

FIGURE 2 | Representative images of microscopic invasion of tumors in salivary gland cancer and squamous cell carcinoma of the oral cavity **(A)** and comparison of tumor border pattern between oral salivary gland cancer and squamous cell carcinomas **(B)**.

which suggested somewhat a different treatment strategy (wider surgery) from our series (cases with a clear, negative margin = 48.3%). This point should be further validated through future studies.

In overall survival rate for the initial cohort, the survival rate of oral SCC was lower than that of oral SGC. Strick et al. reported that patients with SGC tend to have late recurrence with a 10- year survival of only 40% (38). However, Garden et al. showed a 5-year survival rate of 81%, a 10-year survival rate of 65% even with metastases within 5 years and late local failure events after 5 years (34). This was similar to clinical courses in our series and the survival difference between the two cancer types remained similar as the initial cohort after matching. The 5-, 10-, 15-year overall survival rate in SGC were 91.9, 72.9, and 54.7% in our series, which were comparable with other studies (78–94% at 5 years, 40–84% at 10 years, 43–73% at 15 years) (34, 38, 43, 44).

Excellent local control of oral SGC even with marginal surgical resection of the primary tumor in the oral cavity might be due to less aggressive behavior at the primary site, in addition to the effective role of adjuvant radiation treatments. Next, we examined microscopic extension from the gross tumor border in SGC and SCC. In SGC, a pushing border was more prevalent, whereas an infiltrative border occupied the majority of SCC at 87.2%. These results are consistent with previous studies reporting slow growth of SGC (24). Thus, these pathology findings can be one reason explaining the good local control in oral SGC, even with a higher rate of close or positive resection margin, compared to SCC. More interestingly, high grade SGC and adenoid cystic carcinomas had infiltrative pattern of local tumor growth (71.4%, data not shown) in our series. This emphasize that multimodal treatments (surgery with radiation) can yield a better local control in a subset of oral SGC with locally invasive features (43).

In our paper, despite the rarity and heterogeneity of SGC, we suggest a comparative overview that can be applied in management of SGC arising from the oral cavity, using a propensity score-matching and stratification according to tumor grade. However, there are some limitations to our study. The number of patients was insufficient to extrapolate our results to patients with minor pathology in SGC. Also, the results were driven from a single institution; our cohort may be under-representative of the whole SGC patients. Furthermore, since it was a retrospective study, cases with limited information were excluded or omitted from the analysis. These limitations can be solved through future studies such as multi-center research.

Compared with oral SCC, the disease course of salivary gland cancer is more indolent, slow-progressing, resulting in longer patient survival. Thus, it seems possible to adjust treatments (extent and intensity of treatments) based on the tumor biology (indolent disease course and natural history, pathology and tumor grade), which is different from oral SCC.

CONCLUSION

In this study, we provided a comparative overview of clinical courses of oral SGC and SCC by a propensity-score matching analysis. To summarize, we confirmed that SGC in the oral cavity represented relatively good prognosis. A surgery with adjuvant radiation was very effective to control minimal residual disease in oral SGC, which had a locally less aggressive pathology compared with oral SCC. Our study proposed that a different treatment strategy for oral SGC based on tumor biology (pathology and tumor grade) would be reasonable in comparison with oral SCC.

DATA AVAILABILITY STATEMENT

All datasets generated for this study are included in the article/ **Supplementary Material**.

ETHICS STATEMENT

The studies involving human participants were reviewed and approved by The Institutional Review Board of Samsung Medical Center. Written informed consent for participation was not required for this study in accordance with the national legislation and the institutional requirements.

AUTHOR CONTRIBUTIONS

SP wrote the draft of the manuscript and evaluated patient record. WP and SC evaluated patient records. YJ, HK, and S-HK performed pathological investigation. JN conducted an analysis of radiation treatment. MC, Y-IS, and C-HB supervised the study and participated in quality control of data. H-SJ conceived the study concept and supervised the project and wrote and edited the manuscript. All authors read and approved the final manuscript.

FUNDING

This work was supported by a grant of the National Research Foundation of Korea (NRF) funded by the Korean government (MEST) (no. 2018R1A2B6002920). The above funders had no further role in the study design; collection, analysis, and interpretation of data; writing of the manuscript; or decision to submit this manuscript for publication.

SUPPLEMENTARY MATERIAL

The Supplementary Material for this article can be found online at: https://www.frontiersin.org/articles/10.3389/fonc.2020.00881/full#supplementary-material

Supplementary Data Sheet 1 | The raw dataset.

REFERENCES

1. Zini A, Czerninski R, Sgan-Cohen HD. Oral cancer over four decades: epidemiology, trends, histology, and survival by anatomical sites. *J Oral Pathol Med*. (2010) 39:299–305. doi: 10.1111/j.1600-0714.2009.00845.x
2. Chi AC, Day TA, Neville BW. Oral cavity and oropharyngeal squamous cell carcinoma–an update. *CA Cancer J Clin*. (2015) 65:401–21. doi: 10.3322/caac.21293
3. Chandana SR, Conley BA. Salivary gland cancers: current treatments, molecular characteristics and new therapies. *Expert Rev Anticancer Ther*. (2008) 8:645–52. doi: 10.1586/14737140.8.4.645
4. Dhanuthai K, Boonadulyarat M, Jaengjongdee T, Jiruedee K. A clinico-pathologic study of 311 intra-oral salivary gland tumors in Thais. *J Oral Pathol Med*. (2009) 38:495–500. doi: 10.1111/j.1600-0714.2009.00791.x
5. Vaidya AD, Pantvaidya GH, Metgudmath R, Kane SV, D'Cruz AK. Minor salivary gland tumors of the oral cavity: a case series with review of literature. *J Cancer Res Ther*. (2012) 8(Suppl. 1):S111–5. doi: 10.4103/0973-1482.92224
6. Copelli C, Bianchi B, Ferrari S, Ferri A, Sesenna E. Malignant tumors of intraoral minor salivary glands. *Oral Oncol*. (2008) 44:658–63. doi: 10.1016/j.oraloncology.2007.08.018
7. Nobis CP, Rohleder NH, Wolff KD, Wagenpfeil S, Scherer EQ, Kesting MR. Head and neck salivary gland carcinomas–elective neck dissection, yes or no? *J Oral Maxillofac Surg*. (2014) 72:205–10. doi: 10.1016/j.joms.2013.05.024
8. Warner KA, Adams A, Bernardi L, Nor C, Finkel KA, Zhang Z, et al. Characterization of tumorigenic cell lines from the recurrence and lymph node metastasis of a human salivary mucoepidermoid carcinoma. *Oral Oncol*. (2013) 49:1059–66. doi: 10.1016/j.oraloncology.2013.08.004
9. Gill A, Vasan N, Givi B, Joshi A. AHNS series: do you know your guidelines? evidence-based management of oral cavity cancers. *Head Neck*. (2018) 40:406–16. doi: 10.1002/hed.25024
10. Amini A, Waxweiler TV, Brower JV, Jones BL, McDermott JD, Raben D, et al. Association of adjuvant chemoradiotherapy vs radiotherapy alone with survival in patients with resected major salivary gland carcinoma: data from the national cancer data base. *JAMA Otolaryngol Head Neck Surg*. (2016) 142:1100–10. doi: 10.1001/jamaoto.2016.2168
11. Pfister DG, Spencer S, Brizel DM, Burtness B, Busse PM, Caudell JJ, et al. Head and neck cancers, version 1.2015. *J Natl Compr Canc Netw*. (2015) 13:847–55. doi: 10.6004/jnccn.2015.0102
12. Mucke T, Robitzky LK, Kesting MR, Wagenpfeil S, Holhweg-Majert B, Wolff KD, et al. Advanced malignant minor salivary glands tumors of the oral cavity. *Oral Surg Oral Med Oral Pathol Oral Radiol Endod*. (2009) 108:81–9. doi: 10.1016/j.tripleo.2009.01.013
13. Baddour HM, Jr, Fedewa SA, Chen AY. Five- and 10-year cause-specific survival rates in carcinoma of the minor salivary gland. *JAMA Otolaryngol Head Neck Surg*. (2016) 142:67–73. doi: 10.1001/jamaoto.2015.2805

14. Cho JK, Lim BW, Kim EH, Ko YH, Oh D, Noh JM, et al. Low-grade salivary gland cancers: treatment outcomes, extent of surgery and indications for postoperative adjuvant radiation therapy. *Ann Surg Oncol*. (2016) 23:4368–75. doi: 10.1245/s10434-016-5353-6
15. Amin MB, Greene FL, Edge SB, Compton CC, Gershenwald JE, Brookland RK, et al. The eighth edition AJCC cancer staging manual: continuing to build a bridge from a population-based to a more "personalized" approach to cancer staging. *CA Cancer J Clin*. (2017) 67:93–9. doi: 10.3322/caac.21388
16. Seethala RR, Stenman G. Update from the 4th edition of the world health organization classification of head and neck tumours: tumors of the salivary gland. *Head Neck Pathol*. (2017) 11:55–67. doi: 10.1007/s12105-017-0795-0
17. Seethala RR. An update on grading of salivary gland carcinomas. *Head Neck Pathol*. (2009) 3:69–77. doi: 10.1007/s12105-009-0102-9
18. Seethala RR. Salivary gland tumors: current concepts and controversies. *Surg Pathol Clin*. (2017) 10:155–76. doi: 10.1016/j.path.2016.11.004
19. Szanto PA, Luna MA, Tortoledo ME, White RA. Histologic grading of adenoid cystic carcinoma of the salivary glands. *Cancer*. (1984) 54:1062–9. doi: 10.1002/1097-0142(19840915)54:6<1062::AID-CNCR2820540622>3.0.CO;2-E
20. Carlon CA, Fabris G, Arslan-Pagnini C, Pluchinotta AM, Chinelli E, Carniato S. Prognostic correlations of operable carcinoma of the rectum. *Dis Colon Rectum*. (1985) 28:47–50. doi: 10.1007/BF02553907
21. Compton C, Fenoglio-Preiser CM, Pettigrew N, Fielding LP. American joint committee on cancer prognostic factors consensus conference: colorectal working group. *Cancer*. (2000) 88:1739–57. doi: 10.1002/(SICI)1097-0142(20000401)88:7<1739::AID-CNCR30>3.0.CO;2-T
22. Harrison JC, Dean PJ, El-Zeky F, Vander Zwaag R. From dukes through jass: pathological prognostic indicators in rectal cancer. *Hum Pathol*. (1994) 25:498–505. doi: 10.1016/0046–8177(94)90122–8
23. Kakarala K, Bhattacharyya N. Survival in oral cavity minor salivary gland carcinoma. *Otolaryngol Head Neck Surg*. (2010) 143:122–6. doi: 10.1016/j.otohns.2010.02.033
24. Guzzo M, Locati LD, Prott FJ, Gatta G, McGurk M, Licitra L. Major and minor salivary gland tumors. *Crit Rev Oncol Hematol*. (2010) 74:134–48. doi: 10.1016/j.critrevonc.2009.10.004
25. Gold DR, Annino DJ Jr. Management of the neck in salivary gland carcinoma. *Otolaryngol Clin North Am*. (2005) 38:99–105. doi: 10.1016/j.otc.2004.09.006
26. Chijiwa H, Sakamoto K, Umeno H, Nakashima T, Suzuki G, Hayafuchi N. Minor salivary gland carcinomas of oral cavity and oropharynx. *J Laryngol Otol Suppl*. (2009) 31:52–7. doi: 10.1017/S002221510900509X
27. Jansisyanont P, Blanchaert RH, Jr. Ord RA. Intraoral minor salivary gland neoplasm: a single institution experience of 80 cases. *Int J Oral Maxillofac Surg*. (2002) 31:257–61. doi: 10.1054/ijom.2002.0223
28. Parsons JT, Mendenhall WM, Stringer SP, Cassisi NJ, Million RR. Management of minor salivary gland carcinomas. *Int J Radiat Oncol Biol Phys*. (1996) 35:443–54. doi: 10.1016/S0360-3016(96)80005-8
29. Spiro RH, Thaler HT, Hicks WF, Kher UA, Huvos AH, Strong EW. The importance of clinical staging of minor salivary gland carcinoma. *Am J Surg*. (1991) 162:330–6. doi: 10.1016/0002-9610(91)90142-Z
30. Toida M, Shimokawa K, Makita H, Kato K, Kobayashi A, Kusunoki Y, et al. Intraoral minor salivary gland tumors: a clinicopathological study of 82 cases. *Int J Oral Maxillofac Surg*. (2005) 34:528–32. doi: 10.1016/j.ijom.2004.10.010
31. Wang D, Li Y, He H, Liu L, Wu L, He Z. Intraoral minor salivary gland tumors in a Chinese population: a retrospective study on 737 cases. *Oral Surg Oral Med Oral Pathol Oral Radiol Endod*. (2007) 104:94–100. doi: 10.1016/j.tripleo.2006.07.012
32. Yih WY, Kratochvil FJ, Stewart JC. Intraoral minor salivary gland neoplasms: review of 213 cases. *J Oral Maxillofac Surg*. (2005) 63:805–10. doi: 10.1016/j.joms.2005.02.021
33. Wang XD, Meng LJ, Hou TT, Zheng C, Huang SH. Frequency and distribution pattern of minor salivary gland tumors in a northeastern Chinese population: a retrospective study of 485 patients. *J Oral Maxillofac Surg*. (2015) 73:81–91. doi: 10.1016/j.joms.2014.08.019
34. Garden AS, Weber RS, Ang KK, Morrison WH, Matre J, Peters LJ. Postoperative radiation therapy for malignant tumors of minor salivary glands. outcome and patterns of failure. *Cancer*. (1994) 73:2563–9. doi: 10.1002/1097-0142(19940515)73:10<2563::AID-CNCR2820731018>3.0.CO;2-X
35. Witten J, Hybert F, Hansen HS. Treatment of malignant tumors in the parotid glands. *Cancer*. (1990) 65:2515–20. doi: 10.1002/1097-0142(19900601)65:11<2515::AID-CNCR2820651121>3.0.CO;2-B
36. Andry G, Hamoir M, Locati LD, Licitra L, Langendijk JA. Management of salivary gland tumors. *Expert Rev Anticancer Ther*. (2012) 12:1161–8. doi: 10.1586/era.12.92
37. van Weert S, Bloemena E, van der Waal I, de Bree R, Rietveld DH, Kuik JD, et al. Adenoid cystic carcinoma of the head and neck: a single-center analysis of 105 consecutive cases over a 30-year period. *Oral Oncol*. (2013) 49:824–9. doi: 10.1016/j.oraloncology.2013.05.004
38. Strick MJ, Kelly C, Soames JV, McLean NR. Malignant tumours of the minor salivary glands–a 20 year review. *Br J Plast Surg*. (2004) 57:624–31. doi: 10.1016/j.bjps.2004.04.017
39. Lim JY, Lim YC, Kim SH, Kim JW, Jeong HM, Choi EC. Predictive factors of isolated distant metastasis after primary definitive surgery without systemic treatment for head and neck squamous cell carcinoma. *Oral Oncol*. (2010) 46:504–8. doi: 10.1016/j.oraloncology.2010.02.005
40. Cho JK, Hyun SH, Choi JY, Choi N, Kim MJ, Lee SH, et al. Prognostic significance of clinical and (18) F-FDG PET/CT parameters for post-distant metastasis survival in head and neck squamous cell carcinoma patients. *J Surg Oncol*. (2016) 114:888–94. doi: 10.1002/jso.24412
41. Spiro RH, Koss LG, Hajdu SI, Strong EW. Tumors of minor salivary origin. a clinicopathologic study of 492 cases. *Cancer*. (1973) 31:117–29. doi: 10.1002/1097-0142(197301)31:1<117::AID-CNCR2820310116>3.0.CO;2--7
42. Weber RS, Byers RM, Petit B, Wolf P, Ang K, Luna M. Submandibular gland tumors. adverse histologic factors and therapeutic implications. *Arch Otolaryngol Head Neck Surg*. (1990) 116:1055–60. doi: 10.1001/archotol.1990.01870090071011
43. Tran L, Sidrys J, Sadeghi A, Ellerbroek N, Hanson D, Parker RG. Salivary gland tumors of the oral cavity. *Int J Radiat Oncol Biol Phys*. (1990) 18:413–7. doi: 10.1016/0360-3016(90)90109-W
44. Hay AJ, Migliacci J, Karassawa Zanoni D, McGill M, Patel S, Ganly I. Minor salivary gland tumors of the head and neck-memorial sloan kettering experience: incidence and outcomes by site and histological type. *Cancer*. (2019) 125:3354–66. doi: 10.1002/cncr.32208

Conflict of Interest: The authors declare that the research was conducted in the absence of any commercial or financial relationships that could be construed as a potential conflict of interest.

frontiers in Oncology

ORIGINAL RESEARCH
published: 14 July 2020
doi: 10.3389/fonc.2020.00984

Compartmental Surgery With Microvascular Free Flap Reconstruction in Patients With T1–T4 Squamous Cell Carcinoma of the Tongue: Analysis of Risk Factors, and Prognostic Value of the 8th Edition AJCC TNM Staging System

Filippo Carta[1†], Daniela Quartu[1†], Cinzia Mariani[1], Melania Tatti[1], Valeria Marrosu[1], Edoardo Gioia[1], Clara Gerosa[2], Jacopo S. A. Zanda[2], Natalia Chuchueva[3], Andrea Figus[4] and Roberto Puxeddu[1]*

[1] Unit of Otorhinolaryngology, Department of Surgery, Azienda Ospedaliero-Universitaria di Cagliari, University of Cagliari, Cagliari, Italy, [2] Unit of Pathology, Department of Surgery, Azienda Ospedaliero-Universitaria di Cagliari, University of Cagliari, Cagliari, Italy, [3] ENT Department, I. M. Sechenov First Moscow State Medical University, Moscow, Russia, [4] Unit of Plastic Surgery, Department of Surgery, Azienda Ospedaliero-Universitaria di Cagliari, University of Cagliari, Cagliari, Italy

OPEN ACCESS

Edited by:
Cesare Piazza,
Istituto Nazionale dei Tumori (IRCCS), Italy

Reviewed by:
Giuseppe Mercante,
Humanitas University, Italy
Alberto Grammatica,
University of Brescia, Italy

***Correspondence:**
Filippo Carta
filippocarta@unica.it;
pippocarta@tiscali.it

[†] These authors have contributed equally to this work

Specialty section:
This article was submitted to Head and Neck Cancer, a section of the journal Frontiers in Oncology

Received: 22 February 2020
Accepted: 19 May 2020
Published: 14 July 2020

Citation:
Carta F, Quartu D, Mariani C, Tatti M, Marrosu V, Gioia E, Gerosa C, Zanda JSA, Chuchueva N, Figus A and Puxeddu R (2020) Compartmental Surgery With Microvascular Free Flap Reconstruction in Patients With T1–T4 Squamous Cell Carcinoma of the Tongue: Analysis of Risk Factors, and Prognostic Value of the 8th Edition AJCC TNM Staging System. Front. Oncol. 10:984. doi: 10.3389/fonc.2020.00984

Compartmental surgery and primary reconstruction with microvascular free flaps represent the gold-standard in the treatment of oral tongue squamous cell carcinoma (OTSCC). However, there are still unclear clinical features that negatively affect the outcomes. This retrospective study included 80 consecutive patients with OTSCC who underwent compartmental surgery and primary reconstruction by free flap. The oncologic outcomes, the reliability of the 8th edition American Joint Committee on Cancer (AJCC) staging system and the prognostic factors were evaluated. Fifty-nine males and 21 females (mean age 57.8 years, range 27–81 years) were treated between November 2010 and March 2018 (one patient had two metachronous primaries). Seventy-one patients (88.75%, 52 males, 19 females, mean age of 57.9 years, range of 27–81 years) had no clinical history of previous head and neck radiotherapy and were considered as naive. Histology showed radical surgery on 80/81 lesions (98.8%), with excision margins >0.5 cm, while in 1 case (1.2%), a close posterior margin was found. According to the 8th AJCC classification, 37 patients (45.7%) were upstaged shifting from the clinical to the pathological stage, and 39 (48.1%) showed an upstaging while shifting from the 7th to the 8th AJCC staging system (no tumors were downstaged). Nodal involvement was confirmed in 33 patients (40.7%). Perineural and lymphovascular invasion were present in 9 (11.1%) and 11 (13.6%) cases, respectively. Twenty-two patients (27.1%) underwent adjuvant therapy. The 5-years disease-specific, overall, overall relapse-free, locoregional relapse-free and distant metastasis-free survival rates were 73.2, 66.8, 62.6, 67.4, and 86%, respectively. Patients with a lymph node ratio >0.09 experienced significantly worse outcomes. Univariate analysis showed that patients with previous radiotherapy,

stage IV disease, nodal involvement, and lymphovascular invasion had significantly worse outcomes. Multivariate analysis focused naive patients and showed that lymphovascular invasion, advanced stage of disease, and node involvement resulted reliable prognostic factors, and patients with the same tumor stage and histological risk factors who did not undergo adjuvant therapy experienced significantly worse outcomes. In our series, surgery played a major role in the treatment of local extension; adjuvant therapy resulted strictly indicated in patients with advanced-stage disease associated with risk factors.

Keywords: tongue cancer, compartmental surgery, head and neck, free flaps, American Joint Committee on Cancer

INTRODUCTION

The incidence of oral tongue squamous cell carcinoma (OTSCC) is currently estimated at 5.21/100,000 population, and ∼3.06/100,000 new cases per year are documented in Italy (1–3).

OTSCC is classically associated with the main risk factors for all squamous cell carcinomas of the upper aerodigestive tract, such as smoking, alcohol consumption, human papillomavirus (HPV), environmental factors (chemical and physical), diet, and occupation (4).

The prognosis of OTSCC in patients with advanced disease is generally poor; in addition, patients with T1-T2N0 disease experience a greater than expected rate of regional and locoregional relapse if inadequately treated (5).

In recent decades, oncologic outcomes of patients with OTSCC have improved due to the introduction of two main concepts: anatomy-based compartmental tongue surgery (CTS) and the systematic reconstruction of oral defects by microvascular free flaps. The principles of compartmental surgery advocate the removal of compartments (anatomic-functional units) containing the primary tumor, with the excision of the lesion along with the potential muscular, vascular, nervous, and lymphatic pathways that may lead to spread and recurrence (6). The diffusion of CTS has been facilitated by the increasing popularity of microvascular free flap reconstruction because three-dimensional radical resection cannot be performed without the reconstruction that allows the restoration of important functions of the tongue, such as voice articulation, swallowing and breathing. The improvement of disease local control after CTS has been significant (6), positively affecting prognosis and locoregional spread and allowing a better understanding of important prognostic factors (7). As a result, the revision of the 7th edition American Joint Committee on Cancer (AJCC) TNM staging system included depth of invasion (DOI) and extranodal extension (ENE) as fundamental predictors of disease-specific survival (DSS), providing a more reliable prognosis (8, 9).

However, despite the improvement in the understanding and management of OTSCC, there are still unclear clinical features that negatively impact the locoregional control and the incidence of distant metastasis that should be better understood.

Therefore, the authors performed a retrospective/prospective study of 80 patients consecutively treated for OTSCC with the aim of evaluating the oncologic outcomes after CTS and contemporary reconstruction with microvascular free flap. A comparison of the prognostic reliability of the two TNM staging systems (AJCC 2010 vs. AJCC 2017) and an evaluation of clinical and histological features were performed. An additional objective was to evaluate the weight of adjuvant therapy based on particular histological and clinical findings.

MATERIALS AND METHODS

The present study was approved by the Ethics Committee "Commissione del Comitato Etico Indipendente della Azienda Ospedaliero-Universitaria di Cagliari" (NP/2018/895).

All consecutive patients who underwent CTS and microvascular reconstructive surgery with curative intent between November 2010 and March 2018 for OTSCC at any stage of disease were included. Patients with previous chemotherapy (CHT) and/or radiotherapy (RT) were also included in the enrollment but the analysis focused patients without previous RT for head and neck malignancies who were considered "naive." Patients with a clinical history of previous transoral surgery alone performed elsewhere were considered as naive since, in such cases, the CTS allows a resection including the relapsed lesion and the surrounding scar tissue.

Eligible for CTS were patients affected by OTSCC more than 2 cm in greatest dimension or with more than 5 mm of DOI at computer tomography (CT) and/or magnetic resonance imaging (MRI) and extended also to pelvis and mandible. CTS was also performed in cT1 tumors when the epicentrum of the lesion was localized in the posterior and lateral aspect of the tongue or in case of any proximity of the tumor to the paramedian and/or lateral septum. Patients with contraindications for microvascular procedures, such as advanced arteriosclerosis underwent pedicled flap reconstruction and were not included in the present study.

Correlations of age and comorbidities were established according to the Age Adjusted Charlson Comorbidity Index (AACCI) (10–14).

Preoperative head and neck CT and MRI (from 2013 the MRI method has been routinely preferred since considered more accurate during the preoperative evaluation as shown in **Figure 1**), total body PET-CT (in case of relapse/persistence of disease), and color Doppler ultrasound of neck vessels and free-flap donor vessels (to evaluate anatomy and caliber of the vessels with the perforator's anatomy) were routinely performed.

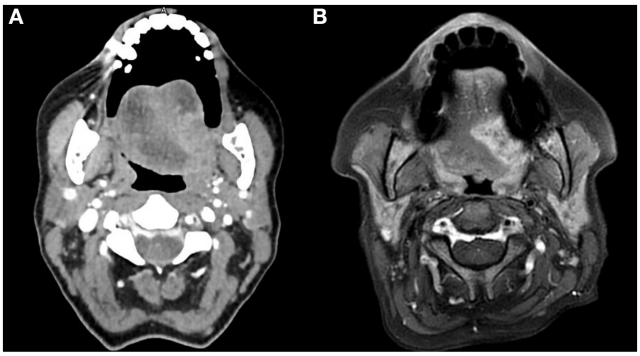

FIGURE 1 | CT **(A)** and MRI **(B)** preoperative evaluation of a patient with OTSCC. The image shows the higher definition of the boundaries of the tumor obtained with the MRI.

From 2013 the superficial spread of the tumor was assessed with the Narrow Band Imaging (Olympus Medical System Corporation Tokyo, Japan), and subsequently with the IMAGE 1S (Karl Storz, Tuttlingen, German), with 0 and 30° rigid endoscope (Andrea-Dias Contact Micro Laryngoscope, Karl Storz, Tuttlingen, Germany and Hamou Micro Contact Hysteroscope, Karl Storz, Tuttlingen, Germany) (15).

Preoperative histologic diagnosis was obtained for all patients.

All patients were clinically and pathologically staged according to the 7th and subsequently to the 8th edition of the AJCC TNM staging system and classified with clinical (preoperative) TNM and pathological (post-operative) TNM (8, 9, 16, 17).

Authors performed a precise retrospective analysis from a histopathological perspective, nevertheless the CTS was applied to all patients with tongue cancer in a prospective way from 2010. The analysis on the basis of the 2017 AJCC classification was performed by a dedicate pathologist to all surgical specimens of all patients treated since 2010.

All patients underwent compartmental radical excision of the primary tumor transorally, median mandibulotomy or with a pull-through approach, with ipsilateral or bilateral, selective or radical/modified radical neck dissection (according to the site of the tumor to the midline and the clinical neck node status).

Surgical procedures were classified according to Ansarin et al. (18): type I glossectomy (mucosectomy), type II glossectomy (partial glossectomy), type IIIa glossectomy (hemiglossectomy), type IIIb glossectomy (compartmental hemiglossectomy), type IVa glossectomy (subtotal glossectomy), type IVb glossectomy (near-total glossectomy), and type V glossectomy (total glossectomy).

Surgical resections were performed following an anatomic-based strategy: unilateral resections were extended from the lingual septum (the medial margin) to the pelvis or mucosa of the mandible (the lateral margin), the stylohyoid muscle (posterior margin), and the mylohyoid muscle, which was considered the floor of the compartment (type III glossectomy). Lesions involving both sides of the tongue were resected from pelvis to pelvis and inferiorly to the hyoid bone (type IV–V glossectomy). Patients with mandibular involvement underwent a wider resection, including the corresponding mandibular bone (marginal or segmental mandibulectomy).

All surgical defects of the oral cavity were primarily reconstructed with microvascular free flaps. The radial forearm (RF) and anterolateral thigh (ALT) free flaps were the first choice for intraoral reconstruction. Partial glossectomy was reconstructed with RF or perforator ALT flaps, total glossectomy was reconstructed with an ALT free flap or vertical rectus abdominis myocutaneous (VRAM) free flap, and the composite bony iliac crest deep circumflex iliac artery (DCIA) free flap was the procedure of choice in cases in which glossectomy was associated with segmental mandibulectomy to reconstruct composite intra-oral defects since the cutaneous and muscular component of this flap (external oblique, internal oblique and transverse muscles) provides abundant tissue for the reconstruction.

Anastomoses were performed using an operative microscope (ZEISS S7 Microscope, Carl Zeiss, USA; focal length 250 mm). Arterial anastomosis was performed with synthetic non-absorbable 8/0 or 9/0 nylon sutures. Venous anastomosis was performed with a coupler device (Microvascular Anastomotic Coupling System, Synovis Life Technologies). All patients received a single bolus of heparin sodium (1,500 IU) at least 5 min before the transfer of the flap.

Temporary tracheostomy was performed in all patients to avoid post-operative respiratory distress.

Intraoperative and post-operative fluid balance was routinely evaluated with the goal of maintaining intravascular fluid volume for optimal tissue blood flow and oxygenation (19).

All patients had nasogastric feeding tube inserted, which was kept in place until acceptable swallowing function was restored. After 30 post-operative days, percutaneous endoscopic gastrostomy (PEG) was indicated in cases with inadequate post-operative swallowing function.

Post-operative treatment consisted of the antibiotic protocol for the head and neck (ceftriaxone 2 g/day iv and metronidazole 500 mg 3 times/day iv for 7–10 days), and low molecular weight heparin (enoxaparin sodium, range of 3,000–8,000 IU/day) associated with an antiembolism stocking for the prophylaxis of deep venous (DVT) and microvascular. An Ear Nose and Throat specialist-in-training monitored the free flap every hour during the first 48 h and every 4 h up to 5 post-operative days according to the internal protocol to detect early signs of vascular impairment that could require surgical exploration/revision of the anastomosis.

Hospitalization time and complications were evaluated. According to the Clavien-Dindo System (20) and Genden et al. (21). Complications were divided into surgical donor-site and flap complications, which require surgical revision, and non-surgical donor-site and flap complications, which were treated with medical therapy. Donor-site complications consisted of hematoma, seroma, infection, wound dehiscence, venous congestion and skin loss; flap complications included partial or total flap failure, cervical hematoma, infection, wound dehiscence, and fistula. Additionally, systemic complications

were documented and included post-operative hypertension (PH), post-operative arrhythmia (PA), myocardial infarction (MI), pulmonary edema (PO), pulmonary embolism (PE), DVT, acute renal failure (ARF), respiratory distress (RD), pneumonia and sepsis.

Perineural invasion (PNI), lymphovascular invasion (LVI), DOI and ENE were evaluated in all patients. The ratio between the positive and overall number of removed nodes was calculated as the lymph node ratio (LNR), which was considered a prognostic value when higher than 0.09 (22).

Adjuvant RT was planned in cases with pT3–pT4 lesions, close margins, multiple nodal involvement, and neural, lymphatic and/or vascular invasion (23).

All patients were included in our post-operative follow-up, planned according to the American Head & Neck Society (AHNS) guidelines (24). Disease-free was defined as the absence of persistence or recurrence as demonstrated by a clinical examination performed by an experienced Head and Neck surgeon, with imaging followed by histopathology if needed. The definition of evidence of disease referred to the presence of a local, regional or locoregional relapse that was histologically proved and/or distant metastases.

Recurrence time was assessed from the date of surgery to the date of the first recurrence. The 5-years DSS, overall survival (OS), overall relapse-free survival (ORFS), local relapse-free survival (LRFS), and distant metastasis-free survival (DMFS) were calculated using the Kaplan-Meier method. Statistical analysis was performed using GraphPad Prism software (GraphPad, San Diego, CA, USA). Univariate analysis was performed to determine the statistical significance of the oncologic results observed according to different risk factors/clinical features (stage, previous treatments, neural, lymphatic and/or vascular invasion, and adjuvant treatments) in all patients and in naive patients (those without a clinical history of previous head and neck RT); multivariate analysis focused only naive patients to remove the possible bias due to the changes in lymphatic and vascular network induced by RT that could make outcomes unpredictable; statistical significance was defined as $p < 0.05$.

According to Cramer et al. (25) we evaluated five quality metrics for our series: negative surgical margins, neck dissection yielding 18 nodes, appropriateness of adjuvant RT indication, appropriateness of adjuvant CHT-RT indication, and timing of adjuvant CHT-RT.

RESULTS

Fifty-nine males and 21 females (mean age of 57.8 years, range of 27–81 years) were definitively enrolled in the present study. Seventy-one patients (88.75%, 52 males, 19 females, mean age of 57.9 years, range of 27–81 years) had no clinical history of previous hand and neck radiotherapy (naive patients), and, among them, one patient (1.25%) underwent CTS with primary free flap reconstruction for two metachronous primaries, and 2 patients were treated for recurrent OTSCC treated elsewhere with conventional transoral surgery alone. Three patients (3.7%) were treated after failure of CHT-RT, and six procedures (7.4%) were performed in patients with recurrent disease who were previously treated elsewhere with surgery and adjuvant RT.

According to the 8th AJCC staging system, 19 patients (23.5%) were staged as cT1, 48 patients (59.3%) as cT2, 1 patient (1.2%) as cT3, and 13 patients (16%) as cT4a. Fifty-two patients (64.2%) were staged as cN0, 11 patients (13.6%) as cN1 and 18 patients (22.2%) as cN2. Eighteen patients (22.2%) had malignancies classified as stage I, 28 patients (34.6%) as stage II, 9 patients (11.1%) as stage III, 25 patients (30.9%) as stage IVA, and 1 patient (1.2%) as stage IVC.

Patients underwent 81 surgical procedures: 65 type IIIb glossectomy (80.3%), 7 type IVa glossectomy (8.6%), 5 type IVb glossectomy (6.2%), and 4 type V glossectomy (4.9%). Resection of the mandible was necessary in 7 patients (8.6%): marginal mandibulotomy in 4 cases (4.9%) and segmental mandibulectomy in 3 cases (3.7%). A total of 19 patients (23.5%) underwent CTS through a transmandibular approach with a lower lip splitting incision, and 55 patients (67.9%) were treated by a combined transoral and transcervical approach without mandibular splitting.

A total of 57 patients (70.4%) underwent unilateral neck dissection, and 22 (27.1%) underwent bilateral neck dissection. Fifty-seven patients (56.4%) underwent selective neck dissections (SNDs), of which the removal of I-III levels was performed in 19 patients (18.8%), the removal of I-IV levels was performed in 35 patients (34.6%), and the removal of II–V levels was performed in 3 patients (3%). A total of 41 patients (40.6%) underwent type III modified radical neck dissections (MRNDs), 2 patients (2%) underwent type I MRND, and 1 patient (1%) underwent type II MRND. Two patients (2.5%) with a clinical history of previous neck dissection underwent CTS solely followed by microvascular reconstruction with neck dissection limited to the area of the vascular pedicle. The age distribution, procedures, reconstruction and histology are detailed in **Table 1**.

All patients underwent immediate microsurgical reconstruction. RF free flap was performed in 64 cases (79%), ALT free flap in 9 cases (11.1%), VRAM free flap in 5 cases (6.2%), and DCIA free flap in 3 cases (3.7%). All free flap procedures are reported in **Table 2**.

The recipient artery for the microvascular anastomosis was the facial artery in 55 cases (67.9%), the superior thyroid artery in 24 cases (29.6%) and the lingual artery in 2 cases (2.5%). The recipient vein for the microanastomosis was one of the branches of the thyro-lingual-facial trunk in 77 cases (95.1%), followed by termino-lateral anastomosis to the internal jugular vein in 4 cases (4.9%). Venous drainage was obtained with a single anastomosis in the majority of cases (91.4%), and in all cases, it was performed with the coupler device. When a double anastomosis was performed ($n = 7$), one of the branches of the thyro-lingual-facial trunk was used in all cases, and it was coupled with the internal jugular vein in 3 cases (3.7%), with the middle thyroid vein in 3 cases (3.7%), and with the external jugular vein in 1 case (1.2%).

In 5 cases (6.2%), admission to the Intensive Care Unit (ICU) with hemodynamic and airway monitoring was considered necessary due to the chronic impairment of one or more organ systems (26).

TABLE 1 | Patients' age distribution, site of reconstruction and histology.

Age		No. of cases/ Frequency%
All patients	Mean age 57.8 years	80
	Range 27–81 years	
	Younger: <65 years	58/72.5
	Young old: 65–74 years	16/20
	Older and oldest old: ≥75 years	6/7.5
Male	Mean age 56.7 years	59/73.8
	Range 27–79 years	
Female	Mean age 61.3 years	21/26.2
	Range 42–81 years	
Naive patients	Mean age 57.9 years	71
	Range 27–81 years	
	Younger: <65 years	52/73.3
	Young old: 65–74 years	14/19.7
	Older and oldest old: ≥75 years	5/7
Male	Mean age 57.1 years	52/73.2
	Range 27–79 years	
Female	Mean age 61.1 years	19/26.8
	Range 42–81 years	
	Oral cavity procedures	**No. of procedures/ Frequency%**
All patients	Type IIIb glossectomy	65/80.3
	+ Marginal mandibulotomy	4/4.9
	+ Segmental mandibulectomy	1/1.2
	Type IVa glossectomy	7/8.6
	+ Segmental mandibulectomy	3/2.5
	Type IVb glossectomy	5/6.2
	Type V glossectomy	4/4.9
	All procedures	81*
Naive	Type IIIb glossectomy	61/84.7
	+ Marginal mandibulotomy	4/5.6
	+ Segmental mandibulectomy	1/1.4
	Type IVa glossectomy	6/8.3
	+ Segmental mandibulectomy	3/4.2
	Type IVb glossectomy	3/4.2
	Type V glossectomy	2/2.8
	All procedures	72*
	Microvascular procedures	**No. of cases/ Frequency%**
All patients	Forearm flee flap	64/79
	ALT free flap	9/11.1
	VRAM free flap	5/6.2
	DCIA free flap	3/3.7
	All procedures	81*
Naïve	Forearm free flap	61/84.7
	ALT free flap	7/9.7
	VRAM free flap	3/4.2
	DCIA free flap	1/1.4
	All procedures	72*
	Histology features	**No. of cases/ Frequency%**
All patient	G1	28/34.6
	G2	41/50.6
	G3	12/14.8
	p16	2/2.5
	Perineural invasion	9/11.1
	Lymphovascular invasion	11/13.6
	Perineural and lymphovascular invasion	15/18.5
	Absence of perineural/lymphovascular invasion	46/56.8
Naive	G1	26/36.1
	G2	35/48.6
	G3	11/15.3
	p16	2/2.8
	Perineural invasion	20/27.8
	Lymphovascular invasion	21/29.2
	Perineural and lymphovascular invasion	11/15.3
	Absence of perineural/lymphovascular invasion	42/58.3

One patient underwent two CTS procedures for two different metachronous lesions.

TABLE 2 | Microvascular free flap procedures of our series.

Free flap procedures	No. of procedures/%	Type of glossectomy			
		IIIb	IVa	IVb	V
Forearm	64/79	59	5	–	–
ALT	9/11.1	4	–	4	1
VRAM	5/6.2	1	–	1	3
DCIA	3/3.7	1	2	–	–
Total	81	65	7	5	4

TABLE 3 | Complications observed in patients who underwent CTS.

Complications	Forearm	ALT	VRAM	DCIA	All series%
Flap failure	–	–	–	–	0 (0.0)
Near flap failure*	3	–	–	–	3 (3.7)
Cervical bleeding without flap sufferance	13	–	–	–	13 (16)
Head and neck suture dehiscence**	1	1	–	1	3 (3.7)
Salivary fistula**	1	–	1		2 (2.5)
Total	18	1	1	1	21 (25.9)

In 3 cases, the compression on the pedicle was associated with cervical hematoma; in 2 cases, bleeding originated from the pedicle; and in 1 case, the flap congestion was due to thrombosis of the venous pedicle.

***These complications were managed by a conservative approach.*

Twenty-one patients (25.9%) experienced post-operative complications that required surgical revision in 17 cases (21%). The most experienced complication was bleeding (13 cases, 16%), followed by free flap sufferance due to venous congestion, which

TABLE 4 | TNM staging system, AJCC 2010 and 2017, 7th and 8th edition.

AJCC 2010		pN0	pN1	pN2a	pN2b	pN2c	pN3b	Total
pT1	2010	17 (2)	2	0	0	0	0	19 (2)
	2017	6 (1)	0	0	0	0	0	6 (1)
pT2	2010	24 (3)	10	0	10	1	0	45 (3)
	2017	22 (3)	3	0	5	1	0	31 (3)
pT3	2010	1 (1)	0	0	1	1	0	3 (1)
	2017	14 (2)	8	1	6	0	0	29 (2)
pT4a	2010	6 (1)	2	1	1	4 (2)	0	14 (3)
	2017	6 (1)	2	1	1	3 (2)	2	15 (3)
Total	2010	48 (7)	14	1	12	6 (2)	0	81 (9)
	2017	48 (7)	13	2	12	4 (2)	2	

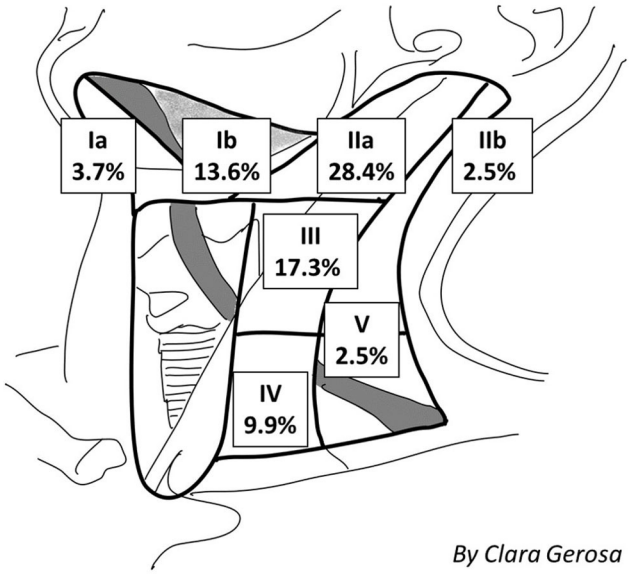

FIGURE 2 | Percentage and site of incidence of nodal metastasis.

was managed with the revision of the anastomosis (3 cases, 3.7%), wound dehiscence (3 cases, 3.7%) and fistula (2 cases, 2.5%). No total flap failure was observed in the present series (**Table 3**).

The mean time to the removal of the temporary tracheostomy was 8 days (range, 6–21 days). The mean duration of nasogastric feeding tube use was 18.1 days (range, 8–38 days), and 2 patients underwent PEG for supplemental nutrition. The mean hospitalization time was 19.3 days (range, 9–40 days).

Definitive histology showed that 80 lesions (98.8%) were completely removed with free margin, while a close posterior margin was found in 1 patient (1.2%) treated after the failure of CHT-RT for an advanced OTSCC extending to the base of tongue; the patient underwent close follow-up but experienced recurrent disease after 6 months; then, the patient underwent palliative CT and died of the disease 12 months after surgery.

Neck dissection yielded a mean number of lymph nodes of 53.1 (range of 0–139); in 77 cases (95.1%), the neck dissection yielded 18 or more lymph nodes, and in 4 cases (4.9%), <18 lymph nodes (3 of these patients were previously treated with neck dissection and underwent revision surgery for recurrent OTSCC).

Thirty-seven patients (45.7%) showed an upstage while shifting from a clinical to a pathological stage; according to the 8th AJCC staging system, 19 patients initially staged as cT1 resulted in 6 pT1 (31.6%), 8 pT2 (42.1%), and 5 pT3 (26.3%); 48 patients initially staged as cT2 resulted in 24 pT2 (50%), 22 pT3 (45.8%) and 2 pT4a (4.2%); 1 patient initially staged as cT3 and 13 patients initially staged as cT4a resulted in 1 pT3 (100%) and 13 pT4a (100%); 52 patients initially staged as cN0 resulted in 48 pN0 (92.3%) and 4 pN1 (7.7%); 11 patients initially staged as cN1 resulted in 9 pN1 (81.8%) and 2 pN2 (18.2%); and 18 patients initially staged as cN2 resulted in 16 pN2 (88.9%) and 2 pN3 (11.1%).

Thirty-nine patients (48.1%) showed upstaging while shifting from the 7th to the 8th AJCC staging system, and none of the patients were downstaged (see **Table 4**). A total of 19 patients initially staged as pT1 resulted in 6 pT1 (31.6%), 8 pT2 (42.1%) and 5 pT3 (26.3%); 45 patients initially staged as pT2 resulted in 23 pT2 (51.1%), and 22 pT3 (48.9%); 3 patients initially staged as pT3 resulted in 2 pT3 (66.7%) and 1 pT4a (33.3%); and 14 patients initially staged as pN1 resulted in 13 pN1 (92.9%) and 1 pN2a (7.1%). The histological identification of ENE was crucial; 6 patients initially staged as pN2c resulted in 4 pN2c (66.7%) and 2 pN3b ENE+ (33.3%).

Definitive nodal involvement was confirmed in 33 patients (40.7%); in 27 patients (33.3%), it was ipsilateral, while in 6 patients (7.4%), it was bilateral or contralateral. In the majority of cases, lymph node involvement was localized: at the IIa cervical level in 23 patients (28.4%), the III level in 14 cases (17.3%), the Ib level in 11 cases (13.6%), the IV level in 8 cases (9.9%), the Ia level in 3 cases (3.7%), the llb level in 2 cases (2.5%), and the V level in 2 cases (2.5%), as shown in **Figure 2**. The mean LNR was 0.017; the LNR was 0 in 48 patients (59.3%), ≤0.09 in 30 patients (37%), and >0.09 in 3 patients (3.7%).

PNI was present in 9 cases (11.1%), LVI was present in 11 cases (13.6%), and concomitant PNI and LVI were present in 15 cases (18.5%). The absence of PNI or LVI was reported in 46 cases (56.8%). Only two lesions showed positive p16.

Twenty-two patients (27.1%) underwent adjuvant therapy (**Table 5**). Eleven patients (13.6%) underwent adjuvant RT, which was indicated on the basis of the advanced T stage (pT2 in 3 cases, 27.3%; pT3 in 7 cases, 63.6%; and pT4 in 1 case, 9.1%), pN+ (observed in 7 cases, 63.6%), PNI (observed in 9 cases, 81.8%), and LVI (observed in 4 cases, 36.4%). Nine patients (11.25%) underwent adjuvant CHT-RT, which was indicated on the basis of the advanced T stage (pT2 in 3 cases, 28.6%; pT3 in 4 cases, 42.8%; and pT4 in 2 cases, 28.6%), pN+ and LVI in 7 cases, LVI alone in 1 case, and pN+ alone in one case, while PNI was observed in 3 cases (42.8%). The mean RT dose was 58 Gy (range of 54–69.3 Gy) in 30–33 fractions (mean number of fractions was 31.1). Two patients previously treated by RT for other head and neck malignancy (2.5%) underwent adjuvant CHT alone, which was indicated on the basis of the advanced T stage (pT3 in 1 case, and pT4a in 1 case). Adjuvant therapy (RT alone, CHT alone or CHT-RT) was performed 8–16 weeks after surgery (mean time

of 10 weeks) in 22 patients. In 8 patients, RT was not performed for different reasons despite being indicated: 2 patients refused RT, and 6 patients could not attend the RT sessions due to logistic/personal problems.

Mean time of follow-up was 3.3 years, median time was 1.8 years with a range of 6 months−7 years.

During the follow-up, 18 patients (22.3%) experienced recurrence of the disease (mean time of recurrence of 10.1 months): 3 patients (3.7%) showed local recurrence (mean time of recurrence of 12 months), 5 patients (6.2%) showed lymph node recurrence (mean time of recurrence of 12.4 months), 1 patient local and node recurrence (1.2%) after 8 months, 5 patients (6.2%) showed locoregional recurrence associated with distant metastases (mean time of recurrence of 7.8 months), and 4 patients (5%) experienced distant metastases alone (mean time of recurrence of 9.8 months) (**Table 5**). Of the patients who experienced relapse of the disease during the follow-up, 9 (50%) were upstaged according to the 8th Edition of the AJCC staging system (1 pT1 was restaged as pT2, 5 pT2 as pT3, 1 pT3 as pT4a, and 2 pN2c as pN3b ENE+).

The 5-years DSS, OS, ORFS, LRFS and DMFS were 73.2, 66.8, 62.6, 67.4, and 86%, respectively (**Table 6**). The survival rates and univariate and multivariate analyses based on the different clinical characteristics are reported in **Tables 6–10**.

Patients with a LNR $>$ 0.09 experienced significantly worse outcomes than patients with a LNR lower than 0.09 (**Table 7**).

Univariate analysis showed that patients with previous RT, stage IV disease, nodal involvement, and LVI had significantly worse survival rates (**Table 7**).

Multivariate analysis focused to naive patients ($n = 71$) showed that LVI, LVI-PNI (**Table 8**), advanced stage of disease (**Tables 8**, **9**), and node involvement (**Table 10**) resulted as reliable prognostic factors, and patients with the same tumor stage and histological risk factors who did not undergo adjuvant therapy experienced significantly worse outcomes.

DISCUSSION

The treatment of OTSCC remains a major therapeutic challenge, and surgery plays a fundamental role in achieving locoregional control (27–29) with the main goal of removing the primary tumor with adequate margins of healthy tissue; however, the definition of an "acceptable free margin" is essentially unclear (6, 30–32). Calabrese et al. (33) showed that DSS and OS improved in patients with advanced-stage OTSCC after CTS because of a tridimensional control of the superficial and deep extension of the tumor; as a consequence, CTS can be considered a sound oncologic option and could be applied routinely with the aid of primary microvascular free flap reconstruction, which has replaced, in the majority of cases, the use of loco-regional flaps. After wide resection, a reconstructive procedure is needed to fill the anatomical defect, reduce the risk of post-operative complications (such as salivary fistula), and recreate a functional volume, thereby improving residual tongue movements and functions (34). Obtaining healthy vascularized tissue from the donor site protects the mandible, thereby reducing eventual radio-induced complications (35). In our series, no fistula or radionecrosis occurred after RT; indeed, radionecrosis and fistula were present before CTS in two cases previously treated elsewhere with local resection without reconstruction followed by RT, which recovered after our microvascular reconstruction. The CTS approach associated with microvascular reconstruction has been adopted routinely in our department since November 2010 and allowed the resection on healthy tissue in 98.8% of patients despite the pT stage; a single close margin was observed in one patient. This surgical approach also allows the radical removal of microscopic peritumoral buds and all the lymphatics within the anatomical compartment where the tumor can develop (**Figures 3A,B**). Although this surgical strategy is technically more complex than the classic "wide resection" approach, which includes a transtumoral approach (36) without reconstruction, in our series, CTS was not burdened by a higher incidence of major complications than has been reported in the literature (33, 36): we observed one post-operative death (1.2% of all patients; an elderly patient whose AACCI score was 7 and who died of heart failure the day after the surgical procedure), and no patient experienced flap failure. The additional operating time was defined as the time required to perform the microanastomosis since the harvesting of the flap was contemporary to the resection, and the suturing of the flap was performed during the time spent waiting for frozen sections.

The literature review showed that patients with OTSCC have a 5-years DSS, OS and ORFS from 51.1 to 77.8%, 31.5 to 70.7%, and 50 to 68.1% respectively (6, 37–39); our results are comparable with the best reported in the literature (**Table 6**). The OS observed in our series could be related to the high incidence of comorbidities: only 31 patients did not have any comorbidities (38.3%), while 27 patients had 1 or 2 comorbidities (33.3%), and 23 patients had $\geq$3 comorbidities (28.4%) since the last condition was not considered an absolute contraindication to CTS. Although CTS followed by microvascular reconstruction could be considered more aggressive than excision, it produces better loco-regional control than more limited resections. Sinha et al. (36) treated their T1 and T2 patients by multiblock transoral resection with a 1 cm free margin evaluated intraoperatively with the operative microscope, achieving the following oncologic results: 5-years DSS, ORFS and OS: 88.6, 70, and 78%, respectively, in T1 patients and 74.4, 56.8, and 60.2%, respectively, in T2 patients. Five-years DSS, OS, and RFS rates of T1 and T2 lesions reported in literature in patients are 91.7–95, 75–84, 71.9–73% and 79.3–92, 59–73.3, 66.9–80%, respectively (40, 41). These results seem lower than those achieved in our study (**Table 6**) and in the experience of Calabrese et al. (33).

After CTS, 28% of patients in the study of Calabrese et al. (6) and 22.3% of our patients experienced recurrent disease; in our series, relapse of the disease was observed in 2 patients with stage II disease (2.5%), in 5 patients with stage III disease (6.2%) and 11 patients with stage IV disease (13.6%).

Recurrence, which can occur despite radical histologically-proven resection, remains a challenge to improving understanding of OTSCC biology. These neoplasms do not always show the same biological behavior, and different clinical

TABLE 5 | Series of patients who underwent adjuvant therapy and who experienced relapse of disease.

Patient	Previous therapies	Surgery	pTNM	PNI/LVI	Adjuvant therapy	Recurrence/ Time of relapse (years)	rTNM	Salvage therapy
1	–	Type IIIb glossectomy, SND, forearm free flap	pT2N0M0	LVI	CHT (Taxit + 63 Gy)	–	–	–
2	–	Type IIIb glossectomy, SND, forearm free flap	pT2N2bM0	LVI	–	Nodal relapse (contralateral lymph node)	rpTxN2cM0	SND
3	–	Type IIIb glossectomy, MRND, forearm free flap	pT3N2bM0	–	CHT (Al Sarraf + 63 Gy)	Nodal relapse (contralateral lymph node)	rypTxN3M0	SND + CHT (Taxit)
4	–	Type IIIb glossectomy, FND + SND, forearm free flap	pT4aN1M0	LVI	CHT-RT (Taxit + 63 Gy)	Nodal relapse (contralateral lymph node)	rypTxN3M0	RND
5	–	Type IIIb glossectomy, FND, forearm free flap	pT2N2bM0	LVI	CHT-RT (CDDP + 63 Gy)	–	–	–
6	Surgery + RT	Type IVb glossectomy, SND, VRAM free flap	rpT4aN0M0	–	CHT (Taxit)	Local (floor of mouth)	rycT4aN0M0	Palliative CHT
7	Surgery + RT	Type IIIb glossectomy, marginal mandibulectomy, DCIA free flap	rypT3N0M0	–	CHT (Taxit)	Local extended to pterygoid space	rycT4bN0M0	Palliative CHT
8	–	Type IVa glossectomy, FND + FND, forearm free flap	pT2N2cM0	–	CHT-RT (Taxit + 63 Gy)	–	–	–
9	–	Type IIIb glossectomy, SND, forearm free flap	pT3N2bM0	LVI	CHT-RT (Platin + 60 Gy)	–	–	–
10	CHT-RT	Type V glossectomy, SND + SND, VRAM free flap	ypT4aN0M0	PNI-LVI	–	Local (floor of mouth)	rycT4aN0M0	CHT
11	Surgery + RT	Type IIIb glossectomy, SND, forearm free flap	ypT2N0M0	–	–	Local (floor of mouth) Distant (lung)	rycT4aN0M1	Palliative CHT
12	–	Type V glossectomy, SND + SND, VRAM free flap	pT3N0M0	–	–	Nodal relapse (homolateral lymph node)	rpT0N2aM0 ENE+	SND + CHT-RT
13	–	Type IIIb glossectomy, FND, forearm free flap	pT3N2bM0	PNI-LVI	CHT-RT (Taxit + 59 Gy)	–	–	–
14	–	Type IIIb glossectomy, SND, forearm free flap	pT3N1M0	LVI	–	Local (base of tongue) Distant (lung)	rcT4aN2cM1	CHT
15	–	Type IIIb glossectomy, FND, forearm free flap	pT2N1M0	LVI	–	Local (floor of mouth) Distant (mediastinum)	rcT4aN2bM1	CHT
16	–	Type IIIb glossectomy, FND, forearm free flap	pT4aN2bM0	PNI-LVI	CHT-RT (Taxit + 63 Gy)	–	–	–
17	–	Type IVa glossectomy, FND + FND, forearm free flap	pT4aN3bM1 ENE+	PNI-LVI	–	Local (tongue) Distant (C1)	rcT4aN0M1	Palliative CHT
18	–	Type IIIb glossectomy, FND, forearm free flap	pT3N2bM0	PNI-LVI	RT (63 Gy)	Distant (lung, T11, L1)	rycT0N0M1	Palliative CHT
19	–	Type IIIb glossectomy, SND, forearm free flap	pT3N0M0	PNI	RT (63 Gy)	–	–	–
20	–	Type IIIb glossectomy, FND, forearm free flap	pT3N2bM0	PNI-LVI	CHT-RT (Taxit + 63 Gy)	Distant (lung)	rycT0N0M1	CHT
21	–	Type IIIb glossectomy, SND + SND, forearm free flap	pT2N0M0	PNI	RT (54 Gy)	Nodal relapse (contralateral lymph node)	rypTxN2cM0	SND
22	–	Type IIIb glossectomy, FND, forearm free flap	pT2N2bM0	PNI-LVI	RT (54 Gy)	–	–	–

(Continued)

TABLE 5 | Continued

Patient	Previous therapies	Surgery	pTNM	PNI/LVI	Adjuvant therapy	Recurrence/ Time of relapse (years)	rTNM	Salvage therapy
23	–	Type IIIb glossectomy, SND, forearm free flap	pT3N1M0	PNI-LVI	RT (54 Gy)	Distant (supraclavicular fat)	rcT0N0pM1	MRND
24	–	Type IIIb glossectomy, SND + SND, forearm free flap	pT4aN0M0	–	RT (60 Gy)	–	–	–
25	–	Type IVa glossectomy, FND + SND, forearm free flap	pT4aN2cM0	–	–	Local (tongue) Distant (lung)	rcT4aN0M1	Palliative CHT
26	–	Type IIIb glossectomy, FND, forearm free flap	pT3N1M0	PNI	RT (63 Gy)	–	–	–
27	–	Type IIIb glossectomy, FND, forearm free flap	pT2N2bM0	PNI-LVI	RT (63 Gy)	–	–	–
28	CHT (TPF) + CHT-RT (Erbitux)	Total glossectomy, FND + FND, ALT free flap	ypT4aN2cM0	PNI-LVI	–	Locoregional (tongue, contralateral lymph node)	rycT4aN2cM0	CHT (CDDP + Erbitux)
29	–	Total glossectomy, FND + FND, ALT free flap	pT4aN3bM0 ENE+	PNI-LVI	–	Distant (brain)	rcT0N0M1	–
30	Surgery	Type IIIb glossectomy, SND, forearm free flap	(m)pT3N0M0	PNI	RT (60 Gy)	–	–	–
31	–	Type IVb glossectomy, FND + SND, ALT free flap	pT3N1M0	–	RT (63 Gy)	–	–	–
32	–	Type IVa glossectomy, SND + SND, forearm free flap	pT3N1M0	PNI	RT (63 Gy)	–	–	–

Taxit, Taxotere; CDDP, Cisplatinum; Al Sarraf, Cisplatinum + 5-Fluorouracil.

risk factors may be associated with a higher aggressiveness of the tumor and could require different therapeutic strategies.

An association between HPV and oral cavity cancer has been described in the literature (42). In the present series, only 2 lesions were p16-positive, and the virus genome was detected in only 1 patient with OTSCC. However, in this patient, the lesion showed only the focal expression of p16 and was not considered an HPV-related disease.

Xu et al. (43) demonstrated that when ECE-1 is overexpressed in head and neck squamous cell carcinoma (HNSCC), poor tumor differentiation is associated with worse prognosis; however, in our series, patients with poorly differentiated disease did not experience significantly worse survival rates than patients with well-differentiated lesions (**Table 7**).

Recurrence after previous treatment was associated with worse local control: of the 71 naive patients, 16 (22.5%) experienced relapse of the disease, while of the 9 patients with previous RT for head and neck malignancies, 5 (55.6%) relapsed, $p = 0.034$.

Advanced T stage, nodal involvement, ENE, and poorer differentiation are well-known prognostic factors for OTSCC (44), and the latest edition of the AJCC TNM staging system has been changed on the basis of DOI and ENE (8, 9). The evaluation of the tumor's thickness was defined by Moore et al. (45) as the deepest point of tumor invasion (from the mucosal surface) in the tissue. The tumor's thickness is currently expressed by the DOI at histology, defined as the distance from the level of the basement membrane of the closest adjacent normal mucosa (22). DOI is considered a main prognostic factor associated with the risk of lymph node involvement (46–49). The significance of the DOI in the TNM staging system has been recently validated in several studies. Lydiatt et al. (8). evaluated a large population of 1,788 patients and confirmed that the DOI is a significant prognostic factor for the prediction of DSS and OS. Matos et al. (38) observed that both RFS and OS were significantly lower in patients undergoing upstaging after the application of the 8th edition of the TNM staging system ($p = 0.007$ and $p = 0.017$, respectively). Tirelli et al. (39) observed a major correlation between increased pT categories and DSS ($p = 0.01$) using the 8th edition of the TNM staging system, concluding that DOI > 10 mm is an independent prognostic factor that significantly impacts DSS ($p = 0.001$). In our series, 39 lesions (48.1%) were upstaged after restaging with the 8th edition of the TNM staging system, and in accordance to the recent literature, DSS decreases progressively according to the increasing pT category. The DSS rates based on the 7th and 8th editions were as follows: pT1 100 vs. 100%, pT2 78.4 vs. 88.7%, pT3 33.3 vs. 71%, and pT4 33.9 vs. 31.2% (**Table 6**), confirming that as found in the present

TABLE 6 | Univariate analysis of the survival rates according to pT based on the TNM staging systems (AJCC 2010 and 2017) in all patients, and in naive patients.

Patients' groups		5-years DSS%	SE	5-years OS%	SE	5-years ORFS%	SE	5-years LRFS%	SE	5-years DMFS%	SE
All patients ($n = 80$)		73.2	6.2	66.8	6.6	62.6	7.3	67.4	7.4	86	4.4
pT1	AJCC 2010	100	0	69.7	15.7	87.1	8.6	87.1	8.6	94.1	5.7
	AJCC 2017	100	0	83.3	15.2	100	0	100	0	100	0
pT2	AJCC 2010	78.4	7.4	74.5	7.6	65.3	9.7	74.2	9.5	84.2	6.6
	AJCC 2017	88.7	6.3	78.7	9	83.1	8	83.1	8	96.4	3.5
pT3	AJCC 2010	33.3	27.2	33.3	27.2	33.3	27.2	33.3	27.2	66.7	27.2
	AJCC 2017	71	12.1	68.5	11.9	48.3	13.4	58.2	14.8	74.3	10.2
pT4a	AJCC 2010	33.9	16.8	33.8	16.8	33.8	16.8	36.9	18.1	84.5	11.3
	AJCC 2017	31.2	15.7	31.2	15.7	31.2	15.7	33.8	16.8	75.5	12.3
Naive patients ($n = 71$)		80.6	11	72.2	6.7	60.1	7.3	74	9.5	84.2	6.5
pT1	AJCC 2010	100	0	77.8	15.2	85.1	9.7	85.1	9.7	93.3	6.4
	AJCC 2017	100	0	40	29.7	100	0	100	0	100	0
pT2	AJCC 2010	81.8	6.8	77.6	7.1	67.9	9.7	77.4	9.3	83.6	6.9
	AJCC 2017	92.6	5.1	88.7	6.1	86.4	7.6	86.4	7.6	96	3.9
pT3	AJCC 2010	50	35.4	50	35.4	50	35.4	50	35.4	50	35.4
	AJCC 2017	80.7	8.7	77.7	8.9	55.3	12.7	67.4	13.3	72.8	10.7
pT4	AJCC 2010	53	18.7	53	18.7	53	18.7	58.3	19.8	80.8	12.3
	AJCC 2017	48.1	17.6	48.1	17.6	48.1	17.6	52.5	18.7	73.3	13.2
Patients previously treated by RT ($n = 9$)		0	0	0	0	0	0	0	0	–	–

DSS, Disease-specific Survival; OS, Overall Survival; ORFS, Overall Relapse-free Survival; LRFS, Local Relapse-free Survival; DMFS, Distant Metastasis-free Survival.

study, the recent revision of the TNM staging system improves the correlation between T stage and prognosis and allows a better classification of OTSCC patients.

The involved margins, close margins, tumor's size and the depth of invasion of the extrinsic muscles are considered as negative prognostic factors (50, 51) and, in some cT2 tumors, it is difficult to determine before surgery whether or not the extrinsic lingual muscles are involved (51). The CTS approach allows for a resection performed along anatomic boundaries to the neoplastic spread with a complete resection even when the lesion present insidious paths of spread. Despite the three-dimensional extension of the disease, CTS, in the present series, seemed to ensure that free margins were achieved in all cases and had a positive impact on locoregional control of the disease; the neoplastic spread routes were removed *en bloc*.

The restaging of all our patients according to the 8th edition of the TNM staging system confirmed that CTS was not an overtreatment in patients previously staged as pT1 according to the 7th edition of the TNM staging system: 29 patients (35.8%) showed an upstage while shifting from a clinical T1-T2 to a T3-T4 pathological stage according to the 8th AJCC staging system and, among them, 5 were initially staged as cT1 and 24 were cT2; in these patients, a different surgical approach could have been associated with incomplete resections that were never observed in the present series. Furthermore, before 2017, the choice of the CTS approach resulted in the removal of the T-N tract potentially affected by satellite lesions or micrometastases in 27 patients (33.3%) who showed upstaging from pT1-pT2 to pT3-pT4 while shifting from the 7th to the 8th AJCC staging system; if we had performed a transoral resection in this class of tumors, we would probably have obtained worse prognoses.

Tagliabue et al. showed that on 95 patients classified as pT1-3 only 6 patients had the T-N tract involved while in 138 classified as pT4, 31 patients had a positive T-N tract (52); these findings could justify a "tailored" less aggressive resection (i.e., transoral laser resection without CTS) in case of cT1 lesions of the anterior tongue and without preoperative signs at MRI and or CT of involvement of the "anatomical barriers" for neoplastic spread. Less aggressive excisions could also be considered on the basis of age, comorbidities, previous treatments, immunological status, and patient's choice.

In the study by Tirelli et al. (39) and in our series, the new pT classification showed a better correlation with survival and oncologic outcomes. We observed that pT1–pT3 lesions according to the 8th AJCC staging system showed a significantly better prognosis than pT4 lesions; the worse prognosis of more extended lesions does not seem to be strongly related to the surgical procedure (histology confirmed free margins of resection in all advanced cases), and recurrences may be due to the insidious ways of diffusion that cannot be controlled through surgery alone.

In our series, the recent revision of the TNM staging system led to an upstaging of the pN in three patients (3.7% of the whole series). The main changes were due to the status of the pathological ENE, defined as the extension of metastatic carcinoma from the lymph node outside the nodal capsule (8). The presence of the stromal

TABLE 7 | Univariate analysis of the survival rates according to histological risk factors.

Patients' groups		5-years DSS% SE	*p*	5-years OS% SE	*p*	5-years ORFS% SE	*p*	5-years LRFS% SE	*p*	5-years DMFS% SE	*p*
Previous RT	Naive patients	80.6	**0.011**	72.2	**0.006**	60.1	**0.049**	74	**0.01**	84.2	–
		11		6.7		7.3		9.5		6.5	
	Previous RT	0		0		0		0		–	
		0		0		0		0			
Stage AJCC 2017	All patients										
	I	100	**0.0002**	42	**0.002**	100	**0.003**	100	**0.02**	100	0.07
		0		30.4		0		0		0	
	II	93.8		80.4		86.5		86.5		100	
		6.1		10.7		8.9		8.9		0	
	III	79.5		79.5		51.3		55.6		77.9	
		11.9		11.9		15.2		15.9		10	
	IV	42.9		41.2		42.9		50.7		76.1	
		11.9		11.5		11.9		13.1		9.4	
	Naive patients										
	I	100	**0.0031**	40	**0.0135**	100	**0.0383**	100	0.1494	100	0.1109
		0		29.7		0		0		0	
	II	100		94.7		91.7		91.7		100	
		0		5.1		7.8		8		0	
	III	89.9		89.9		56		61.6		75	
		6.7		6.8		15.5		16		11.2	
	IV	55.9		53.6		55.9		66.1		76.1	
		11.7		11.4		11.7		12.2		9.4	
pN	All patients										
	0	86.9	**0.0001**	72.5	**0.0001**	72.4	**0.0001**	72.4	**0.0001**	97.2	**0.0001**
		6.6		9.1		9.3		9.3		2.7	
	1	53		53		53		53		63.6	
		23.3		23.3		23.3		23.3		17.7	
	2	52.8		49.9		63.3		63.3		76.9	
		13.2		12.8		13.6		13.6		11.7	
	3	0		0		0		0		0	
		0		0		0		0		0	
	Naive patients										
	0	97.5	**<0.0001**	86	**<0.0001**	81.2	**<0.0001**	81.2	**<0.0001**	96.9	**<0.0001**
		2.5		7.2		8.4		8.4		3.1	
	2	53		53		42.4		53		63.6	
		23.3		23.3		21		23.3		17.7	
	3	61.2		57.4		61.3		74.9		75	
		13.8		13.4		13.8		13		12.5	
	4	0		0		0		0		0	
		0		0		0		0		0	
LNR	All patients										
	0	92.1	**<0.0001**	76.5	**<0.0001**	74.5	**<0.0001**	74.5	**<0.0004**	97.1	**<0.0001**
		4.4		8.6		8.8		8.8		2.8	
	≤0.09	54		52.2		49		61		70.1	
		11.6		11.3		11.5		12		10.6	
	>0.09	0		0		0		0		33.3	
		0		0		0		0		27.2	
	Naive patients										

(Continued)

TABLE 7 | Continued

Patients' groups		5-years DSS% SE	*p*	5-years OS% SE	*p*	5-years ORFS% SE	*p*	5-years LRFS% SE	*p*	5-years DMFS% SE	*p*
	0	97.4	**<0.0001**	85.9	**<0.0001**	81.1	**<0.0001**	81.1	**<0.0001**	96.9	**<0.0001**
		2.5		7.2		8.4		8.4		3	
	≤0.09	63		60.7		57.2		72		68	
		12		11.8		12.2		12		11	
	>0.09	0		0		0		0		33.3	
		0		0		0		0		27.2	
Grading	All patients										
	1	80.5	0.6	68.6	0.8	80.5	0.1	80.5	0.3	96.3	0.14
		7.9		9.4		7.9		7.9		3.6	
	2	60.1		58.5		37.8		44.1		75.2	
		13.1		12.9		14.2		16.1		8.5	
	3	83.3		55.6		69.4		76.4		90.1	
		10.8		23.8		15.5		15.5		8.7	
	Naive patients										
	1	82.3	0.8265	74.8	0.9927	82.3	0.2765	82.3	0.5431	95.8	0.1543
		8.2		8.9		8.2		8.2		4.1	
	2	78.6		76.4		52.6		61.7		73.5	
		7.9		8		14		15.4		8.9	
	3	90.9		90.9		75.8		83.3		90.9	
		8.7		8.7		15.6		15.2		8.7	
PNI	All patients										
	Absent	78.7	0.07	68	0.08	71.6	**0.006**	71.6	0.17	91.5	0.53
		6.6		7.8		7.9		7.9		4.1	
	Present	63.1		60.5		43.8		59		72.3	
		11.5		11.3		12.8		14.4		11	
	Naive patients										
	Absent	83.9	0.3313	75.8	0.2963	76.6	**0.0271**	76.6	0.6917	90.9	**0.0285**
		5.7		7		7.4		7.4		4.4	
	Present	76.4		72.6		49.3		70.3		67.2	
		10.4		10.6		15		17		12.7	
LVI	All patients										
	Absent	84.5	**0.001**	71.9	**0.004**	73.5	**0.0008**	73.5%	**0.04**	98%	**0.0001**
		6.2		8.2		8.6		8.6		2	
	Present	48.3		46.5		38.7		51.9		59.1	
		12.7		12.3		11.9		13.7		11.6	
	Naive patients										
	Absent	91	**0.0028**	81.3%	**0.008**	79.5%	**0.0019**	79.5%	0.1241	97.8%	**<0.0001**
		4.3		6.9		7.8		7.8		2.2	
	Present	53.4		50.8		41.5		59		52.2	
		14.9		14.4		13.8		16.2		12.7	
PNI-LVI	All patients										
	Absent	82.4	**0.002**	69.3	**0.002**	76.1	**0.0013**	76.1	0.06	97.5	**0.0006**
		6.8		8.6		8.8		8.8		2.5	
	Both present	42.7		39.9		32.1		57.9		53.7	
		14.8		14.1		14.4		17.2		16.2	
	Naive patients										
	Absent	85.9	**0.0081**	78.1%	**0.0036**	74.7%	**0.0033**	74.7%	0.9396	92.9%	**<0.0001**
		5.1		16.6		7.2		7.2		3.8	
	Both present	56.3		51.1		37.5		87.5		37.5	
		16.5		15.8		18.9		11.7		18.9	

DSS, Disease-specific Survival; LRFS, Local Relapse-free Survival; ORFS, Overall Relapse-free Survival; DMFS, Distant Metastasis-free Survival; OS, Overall Survival; PNI, Perineural Invasion; LVI, Lymphovascular Invasion; LNR, Lymph node ratio.

TABLE 8 | Multivariate analysis of ORFS, LRSF, and DMFS rates according to stage and histological risk factors in naive patients.

Variables		5-years ORFS%	SE	*p*	5-years LRFS%	SE	*p*	5-years DMFS%	SE	*p*
Stage I–II	**PNI-LVI**			**0.004**	**PNI-LVI**		0.1038	**PNI-LVI**		**0.0002**
	Absent	100	0		100	0		100	0	
	Present	75	21.7		75	21.7		100	0	
Stage III–IV	**PNI-LVI**				**PNI-LVI**			**PNI-LVI**		
	Absent	**69.3**	10.3		62.3	10.3		**86.2**	6.5	
	Present	37.5	18.9		87.5	11.7		37.5	18.9	
Variables		**5-years ORFS%**	**SE**	***p***	**5-years LRFS%**	**SE**	***p***	**5-years DMFS%**	**SE**	***p***
Stage I–II	**LVI**			**0.0008**	**LVI**		0.074	**LVI**		**<0.0001**
	Absent	92.9	6.9		92.9	6.9		100	0	
	Present	100	0		100	0		100	0	
Stage III–IV	**LVI**				**LVI**			**LVI**		
	Absent	**70.1**	11.7		70.1	11.7		**96**	3.9	
	Present	32.8	14		51.1	18.1		43.7	13.7	

ORFS, Overall Relapse-free Survival; LRFS, Local Relapse-free Survival; DMFS, Distant Metastasis-free Survival; PNI, Perineural Invasion; LVI, Lymphovascular Invasion.

TABLE 9 | Multivariate analysis of the survival rates of III-IV stage naive patients according to histological risk factors and adjuvant treatment.

Patients' groups		5-years DSS%	SE	*p*	5-years OS%	SE	*p*
Stage III–IV	**LVI absent**			**0.0008**	**LVI absent**		**0.0008**
	CHRT/RT				**CHRT/RT**		
	No	94.8	5.5		82.8	7.6	
	Yes	70	18.2		70	18.2	
	LVI present				**LVI present**		
	CHRT/RT				**CHRT/RT**		
	No	47.6	17.4		42.9	17.4	
	Yes	65.5	17.3		65.6	17.3	
Patients' groups		**5-years ORFS%**	**SE**	***p***	**5-years LRFS%**	**SE**	***p***	**5-years DMRFS%**	**SE**	***p***
Stage III–IV	**LVI absent**			**0.0001**	**LVI absent**		**0.0001**	**LVI absent**		**0.0001**
	CHRT/RT				**CHRT/RT**			**CHRT/RT**		
	No	86.8	8.3		86.8	8.3		97.2	2.7	
	Yes	40	20.3		40	20.3		100	0	
	LVI present				**LVI present**			**LVI present**		
	CHRT/RT				**CHRT/RT**			**CHRT/RT**		
	No	23.8	19.3		26.8	21.4		23.8	19.3	
	Yes	56.1	17.2		80	17.9		70.1	14.7	

DSS, Disease-specific Survival; OS, Overall Survival; LRFS, Local Relapse-free Survival; ORFS, Overall Relapse-free Survival; DMFS, Distant Metastasis-free Survival; LVI, Lymphovascular Invasion; CHRT/RT, Chemoradiotherapy/Radiotherapy.

inflammatory reaction has been considered in the recent TNM staging system as an independent and reliable prognostic factor (8, 9, 33). The poor prognosis of patients with pathological ENE has been evaluated in our series: ENE was confirmed in 3 cases (1 pN2a and 2 pN3b), and after a 3-years follow-up, two patients died from the disease, whereas one patient died from stroke. Univariate analysis showed that pathological ENE was the worst histological prognostic factor and was associated with significantly worse oncologic outcomes (**Table 7**).

PNI, LVI and LNR are clear signs of an increased "imbalance" between oncogenes and tumor suppressor genes that promotes the neoplastic spread showing aggressiveness of the tumor also if they are not at the margin of the resection. It is hypothesized a morph-functional sequence when defining the steps of the metastatic cascade that includes the promotion of tumor

TABLE 10 | Multivariate analysis of the survival rates in pN+ naive patients according to histological risk factors and adjuvant therapy.

Variables		5-years DSS%	SE	*p*	5-years OS%	SE	*p*
pN+	**LVI absent**			**0.0008**	**LVI absent**		**0.0002**
	CHRT/RT				**CHRT/RT**		
	No	61.7	18		61.7	18	
	Yes	100	0		100	0	
	LVI present				**LVI present**		
	CHRT/RT				**CHRT/RT**		
	No	0	0		0	0	
	Yes	60	19.7		60	19.7	

Variables		5-years ORFS%	SE	*p*	5-years LRFS%	SE	*p*	5-years DMRFS%	SE	*p*
pN+	**LVI absent**			**0.0009**	**LVI absent**		**0.0035**	**LVI absent**		**<0.0001**
	CHRT/RT				**CHRT/RT**			**CHRT/RT**		
	No	61.7	18		61.7	18		85.7	13.2	
	Yes	100	0		100	0		100	0	
	LVI present				**LVI present**			**LVI present**		
	CHRT/RT				**CHRT/RT**			**CHRT/RT**		
	No	0	0		0	0		0	0	
	Yes	50	18.8		75	21.7		66.7	16.1	

DSS, Disease-specific Survival; LRFS, Local Relapse-free Survival; ORFS, Overall Relapse-free Survival; DMRFS, Distant Metastasis-free Survival; OS, Overall Survival; LVI, Lymphovascular Invasion; CHRT/RT, Chemoradiotherapy/Radiotherapy.

neo-angiogenesis, synthesis of proteinases that helps cell intra and extravasation, synergism between altered adhesion molecules and proteinases, and loss of local immune-surveillance (53).

Many authors have associated PNI with local recurrence and lower OS (54–58) and have also observed that adjuvant therapy can have a significant positive impact on survival rates ($p = 0.022$). In our series, PNI did not significantly impact locoregional control or survival rates (**Table 7**). These data can be explained in our cases because PNI, although it is an indicator of histological aggressiveness, it was observed within the tumor but always far from the surgical margins, supporting the application of CTS, that allows wide resections, minimizing the negative impact of the presence of PNI on prognosis. Conversely, the presence of PNI in the surgical margins or the histological finding of cranial nerve invasion [defined as *perineural spread* by Brown (59)] could play a strong negative prognostic role, but it was never observed in our series. The impact of LVI on locoregional control and recurrence and survival rates has been widely demonstrated in other malignancies, such as hypopharyngeal and esophageal carcinoma, in which LVI is an independent prognostic factor (60, 61). In a recent study, Fives et al. (62) showed that the DOI ($p = 0.009$), LVI ($p = 0.006$), PNI (0.003) and nodal metastases ($p = 0.02$) had a significant negative impact on OS, and after the multivariate analysis, only LVI was associated with significantly worse OS ($p = 0.009$). In a cohort of 289 patients with OSCC, Quinlan-Davidson et al. (63) observed that LVI was associated with nodal involvement ($p = 0.01$) and DOI > 1.5 cm ($p = 0.003$) and suggested that it could be considered an independent negative prognostic factor ($p = 0.006$). Cassidy et al. (64) reported that the presence of LVI in patients without nodal involvement (N0) is associated with worse local control ($p < 0.01$), worse locoregional control ($p < 0.01$) and a lower OS ($p = 0.01$); consequently, it should be considered an indication for adjuvant therapy. In our series, univariate analysis showed that LVI is a prognostic factor associated with a significantly worse ORFS ($p = 0.0025$) and DMFS ($p = 0.0006$). Compared with the findings of Chen et al. (65) the prognostic value of LVI was more evident in our patients with stage III-IV disease (ORFS: $p = 0.002$; DMFS: $p = 0.0014$), especially when associated with PNI (**Table 8**). Multivariate analysis confirmed that patients with stages III-IV disease, node involvement and LVI experienced significantly worse outcomes especially when they refused adjuvant CHT-RT (**Tables 9**, **10**).

In the literature, the LNR has been considered an additional factor for estimating prognosis (66, 67). In our series, we considered the cut-off value of 0.09 on the basis of the meta-analysis of Talmi et al. (22) who identified 28 studies in the literature that addressed the prognostic value of the LNR and reported a range of cut-off values of the LNR associated with prognosis between 0.02 and 0.20, with an average of 0.09. In our series, patients with an LNR higher than 0.09 experienced significantly worse outcomes. In these patients the higher LNR was due to the high number of metastatic nodes since the neck dissections yielded a mean number of lymph nodes of 53.1 (range of 18–134 nodes removed). The systematic use of this parameter should be associated with high-quality neck dissection (number of lymph nodes removed per level) to avoid statistical bias due to limited neck dissections.

AHNS guidelines (24) support adjuvant therapy in high-risk OTSCC (advanced stages, multiple nodal involvement, ENE+, positive margins) and for intermediate-risk OTSCC only when one or more negative prognostic

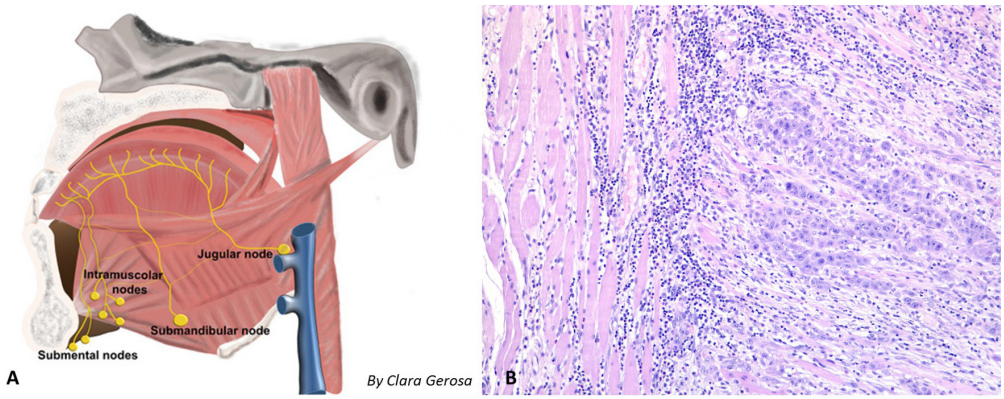

FIGURE 3 | (A) Shema of the locoregional lymphatic spread of tongue malignancy, with possible intramuscular metastasis. **(B)** 10× Histology of an intramuscular metastasis (geniohyoid muscle) observed in a patient with pT3N2a squamous cell carcinoma of the tongue; the muscle fibers dissociated by a proliferation of epithelioid cells organized in solid nests with infiltrative growth pattern. The epitelioid cells showed polimorphic and polidimensional nuclei with prominent nucleoli, atypical mitosis and wide eosinophilic cytoplasms. In the background around and inside the tumor there is an inflammatory response composed by lymphocytes and monocytes.

factors, such as LVI or multiple nodal involvement, are observed; adjuvant therapy is also indicated in specific situations, such as early-stage OSCC with positive margins, which otherwise has a negative prognosis (68). The appropriateness of this multidisciplinary management was underlined in our series: adjuvant therapy showed a significant positive role in improving the prognosis of patients with stage III and IV disease associated with LVI, while patients with early-stage disease or without LVI did not experience a significant benefit from adjuvant therapies (**Table 8**).

In the majority of the patients, the five quality metric criteria according to Cramer et al. (25) were met, although eight patients did not undergo RT despite indications due to personal choice or logistic/personal problems that could not be overcome by patients or relatives. DSS, OS, and ORFS were significantly worse in these patients who did not undergo adjuvant RT than in patients who underwent RT (**Tables 9**, **10**).

Functional outcomes after CTS showed a high recovery rate of adequate chewing and swallowing functions (97.5%). Complete removal of the extrinsic muscles from their bony insertions does not increase the functional defect any more than partial removal of the muscle involved (51). In our patients, the free flap allowed for a complete closure of the oral pelvis and an adequate volume of the reconstructed tongue, facilitating the oral phase of swallowing. In our series, all but two patients could be discharged from the hospital without a nasogastric feeding tube. Type IV and V glossectomies, although rarely performed, was burdened by higher disfunction, needing in two cases compensatory PEG.

In conclusion, our study pointed out that CTS was associated with a high rate of tumor-free margins in all stages of OTSCC. Oncologic results obtained with CTS were better than those obtained with traditional transoral or multiblock resections. Immediate free flap reconstruction was not burdened by major complications. Adequate or normal function was regained in all but two patients. Adjuvant therapy was indicated in patients with advanced disease and negative prognostic factors according to AJCC 2017 and was not burdened by complications probably due to the presence of a well-vascularized transplanted tissue.

DATA AVAILABILITY STATEMENT

All datasets generated for this study are included in the article/**Supplementary Material**.

ETHICS STATEMENT

The studies involving human participants were reviewed and approved by Comitato Etico dell'Azienda Ospedaliero-Universitaria di Cagliari. The patients/participants provided their written informed consent to participate in this study.

AUTHOR CONTRIBUTIONS

FC, DQ, and RP designed the study, analyzed the data, and wrote the manuscript. EG, CM, VM, and MT collected and analyzed the data. CG and JZ performed the experiments. NC and AF edited the manuscript. All authors contributed to the article and approved the submitted version.

SUPPLEMENTARY MATERIAL

The Supplementary Material for this article can be found online at: https://www.frontiersin.org/articles/10.3389/fonc.2020.00984/full#supplementary-material

REFERENCES

1. Ferlay J, Soerjomataram I, Dikshit R, Eser S, Mathers C, Rebelo M, et al. Cancer incidence and mortality worldwide: sources, methods and major patterns in GLOBOCAN 2012. *Int J Cancer*. (2015) 136:E359–86. doi: 10.1002/ijc.29210
2. International Agency for Research on Cancer. *Globocan 2012: Estimated Cancer Incidence, Mortality and Prevalence Worldwide in 2012*. Lyon: WHO (2012).
3. International Agency for Research on Cancer. *Fast Stats-Italy in Globocan 2012: Estimated Cancer Incidence, Mortality and Prevalence Worldwide in 2012*. Lyon: International Agency for research on Cancer-WHO (2012).
4. Ghantous Y, Elnaaj IA. Global incidence and risk factors of oral cancer. *Harefuah*. (2017) 156:645–9.
5. Ganly I, Goldstein D, Carlson DL, Patel'G, O'Sullivan B, Lee N, et al. Long-term regional control and survival in patients "ith low-isk," early stage oral tongue cancer managed by partial glossectomy and neck dissection without postoperative radiation: the importance of tumor thickness. *Cancer*. (2013) 119:1168–76. doi: 10.1002/cncr.27872
6. Calabrese L, Tagliabue M, Maffini F, Massaro MA, Santoro L. From wide excision to a compartmental approach in tongue tumors: what is going on? *Curr Opin Otolaryngol Head Neck Surg*. (2013) 21:112–7. doi: 10.1097/MOO.0b013e32835e28d2
7. O'Charoenrat P, Pillai G, Patel S, Fisher C, Archer D, Eccles S, et al. Tumour thickness predicts cervical nodal metastases and survival in early oral tongue cancer. *Oral Oncol*. (2003) 39:386–90. doi: 10.1016/S1368-8375(02)00142-2
8. Lydiatt WM, Patel'G, O'Sullivan B, Brandwein MS, Ridge JA, Migliacci JC, et al. Head and neck cancers-major changes in the American joint committee on cancer eighth edition cancer staging manual. *CA Cancer J Clin*. (2017) 67:122–37. doi: 10.3322/caac.21389
9. Amin MB, Greene FL, Edge SB, Compton CC, Gershenwald JE, Brookland RK, et al. The eighth edition AJCC cancer staging manual: continuing to build a bridge from a population-based to a "ore personaized" approach to cancer staging. *CA Cancer J Clin*. (2017) 67:93–9. doi: 10.3322/caac.21388
10. Charlson ME, Pompei P, Ales KL, MacKenzie CR. A new method of classifying prognostic comorbidity in longitudinal studies: development and validation. *J Chronic Dis*. (1987) 40:373–83. doi: 10.1016/0021-9681(87)90171-8
11. Charlson M, Szatrowski TP, Peterson J, Gold J. Validation of a combined comorbidity index. *J Clin Epidemiol*. (1994) 47:1245–51. doi: 10.1016/0895-4356(94)90129-5
12. de Groot V, Beckerman H, Lankhorst GJ, Bouter LM. How to measure comorbidity. a critical review of available methods. *J Clin Epidemiol*. (2003) 56:221–9. doi: 10.1016/S0895-4356(02)00585-1
13. Chang CM, Yin WY, Wei CK, Wu CC, Su YC, Yu CH, et al. Adjusted age-adjusted charlson comorbidity index score as a risk measure of perioperative mortality before cancer surgery. *PLoS ONE*. (2016) 11:e0148076. doi: 10.1371/journal.pone.0148076
14. Grammatica A, Piazza C, Paderno A, Taglietti V, Marengoni A, Nicolai P. Free flaps in head and neck reconstruction after oncologic surgery: expected outcomes in the elderly. *Otolaryngol Head Neck Surg*. (2015) 152:796–802. doi: 10.1177/0194599815576905
15. Carta F, Sionis S, Cocco D, Gerosa C, Ferreli C, Puxeddu R. Enhanced contact endoscopy for the assessment of the neoangiogenetic changes in precancerous and cancerous lesions of the oral cavity and oropharynx. *Eur Arch Otorhinolaryngol*. (2016) 273:1895–903. doi: 10.1007/s00405-015-3698-2
16. Sobin LH, Gospodarowicz MK, Wittekind C. *TNM Classification of Malignant Tumours*. Hoboken, NJ: John Wiley & Sons (2011). doi: 10.1002/9780471420194.tnmc26.pub2
17. Amin M, Greene FL, Edge SB, Compton CC, Gershenwald JE, Brookland RK, et al. *AJCC Cancer Staging Manual*. New York, NY: Springer (2017). doi: 10.1007/978-3-319-40618-3
18. Ansarin M, Bruschini R, Navach V, Giugliano G, Calabrese L, Chiesa F, et al. Classification of GLOSSECTOMIES: proposal for tongue cancer resections. *Head Neck*. (2019) 41:821–7. doi: 10.1002/hed.25466
19. Schrey A, Kinnunen I, Vahlberg T, Minn H, Grenman R, Taittonen M, et al. Blood pressure and free flap oxygenation in head and neck cancer patients. *Acta Otolaryngol*. (2011) 131:757–63. doi: 10.3109/00016489.2011.554438
20. Clavien PA, Barkun J, de Oliveira ML, Vauthey JN, Dindo D, Schulick RD, et al. The Clavien-Dindo classification of surgical complications: five-year experience. *Ann Surg*. (2009) 250:187–96. doi: 10.1097/SLA.0b013e3181b13ca2
21. Genden EM, Rinaldo A, Suarez C, Wei WI, Bradley PJ, Ferlito A. Complications of free flap transfers for head and neck reconstruction following cancer resection. *Oral Oncol*. (2004) 40:979–84. doi: 10.1016/j.oraloncology.2004.01.012
22. Talmi YP, Takes RP, Alon EE, Nixon IJ, Lopez F, de Bree R, et al. Prognostic value of lymph node ratio in head and neck squamous cell carcinoma. *Head Neck*. (2018) 40:1082–90. doi: 10.1002/hed.25080
23. Gooi Z, Fakhry C, Goldenberg D, Richmon J, Kiess AP. AHNS series: do you know your guidelines? Principles of radiation therapy for head and neck cancer: a review of the National Comprehensive Cancer Network guidelines. *Head Neck*. (2016) 38:987–92. doi: 10.1002/hed.24448
24. Roman BR, Goldenberg D, Givi B. AHNS s–ies–do you know your guidelines? Guideline recommended follow-up and surveillance of head and neck cancer survivors. *Head Neck*. (2016) 38:168–74. doi: 10.1002/hed.24100
25. Cramer JD, Speedy SE, Ferris RL, Rademaker AW, Patel UA, Samant S. National evaluation of multidisciplinary quality metrics for head and neck cancer. *Cancer*. (2017) 123:4372–81. doi: 10.1002/cncr.30902
26. Arshad H, Ozer HG, Thatcher A, Old M, Ozer E, Agarwal A, et al. Intensive care unit versus non-intensive care unit postoperative management of head and neck free flaps: comparative effectiveness and cost comparisons. *Head Neck*. (2014) 36:536–9. doi: 10.1002/hed.23325
27. Choi KK, Kim MJ, Yun PY, Lee JH, Moon HS, Lee TR, et al. Independent prognostic factors of 861 cases of oral squamous cell carcinoma in Korean adults. *Oral Oncol*. (2006) 42:208–17. doi: 10.1016/j.oraloncology.2005.07.005
28. Kansy K, Mueller AA, Mucke T, Koersgen F, Wolff KD, Zeilhofer HF, et al. A worldwide comparison of the management of surgical treatment of advanced oral cancer. *J Craniomaxillofac Surg*. (2018) 46:511–20. doi: 10.1016/j.jcms.2017.12.031
29. Gore SM, Crombie AK, Batstone MD, Clark JR. Concurrent chemoradiotherapy compared with surgery and adjuvant radiotherapy for oral cavity squamous cell carcinoma. *Head Neck*. (2015) 37:518–23. doi: 10.1002/hed.23626
30. Lee DY, Kang SH, Kim JH, Kim MS, Oh KH, Woo JS, et al. Survival and recurrence of resectable tongue cancer: resection margin cutoff value by T classification. *Head Neck*. (2018) 40:283–91. doi: 10.1002/hed.24944
31. Zanoni DK, Migliacci JC, Xu B, Katabi N, Montero PH, Ganly I, et al. A proposal to redefine close surgical margins in squamous cell carcinoma of the oral tongue. *JAMA Otolaryngol Head Neck Surg*. (2017) 143:555–60. doi: 10.1001/jamaoto.2016.4238
32. Kain JJ, Birkeland AC, Udayakumar N, Morlandt AB, Stevens TM, Carroll WR, et al. Surgical margins in oral cavity squamous cell carcinoma: current practices and future directions. *Laryngoscope*. (2019) 130:128–38. doi: 10.1002/lary.27943
33. Calabrese L, Bruschini R, Giugliano G, Ostuni A, Maffini F, Massaro MA, et al. Compartmental tongue surgery: long term oncologic results in the treatment of tongue cancer. *Oral Oncol*. (2011) 47:174–9. doi: 10.1016/j.oraloncology.2010.12.006
34. Almadori G, Rigante M, Bussu F, Parrilla C, Gallus R, Adesi LB, et al. Impact of microvascular free flap reconstruction in oral cavity cancer: our experience in 130 cases. *Acta Otorhinolaryngol Ital*. (2015) 35:386–93. doi: 10.14639/0392-100X-919
35. Frederick JW, Sweeny L, Carroll WR, Peters GE, Rosenthal EL. Outcomes in head and neck reconstruction by surgical site and donor site. *Laryngoscope*. (2013) 123:1612–7. doi: 10.1002/lary.23775
36. Sinha P, Hackman T, Nussenbaum B, Wu N, Lewis JS Jr, Haughey BH. Transoral laser microsurgery for oral squamous cell carcinoma: oncologic outcomes and prognostic factors. *Head Neck*. (2014) 36:340–51. doi: 10.1002/hed.23293
37. Nair D, Singhvi H, Mair M, Qayyumi B, Deshmukh A, Pantvaidya G, et al. Outcomes of surgically treated oral cancer patients at a tertiary cancer center in India. *Indian J Cancer*. (2017) 54:616–20. doi: 10.4103/ijc.IJC_445_17
38. Matos LL, Dedivitis RA, Kulcsar MAV, de Mello ES, Alves VAF, Cernea CR. External validation of the AJCC cancer staging manual, 8th edition, in

an independent cohort of oral cancer patients. *Oral Oncol*. (2017) 71:47–53. doi: 10.1016/j.oraloncology.2017.05.020
39. Tirelli G, Gatto A, Nata FB, Bussani R, Piccinato A, Marcuzzo AV, et al. Prognosis of oral cancer: a comparison of the staging systems given in the 7th and 8th editions of the American joint committee on cancer staging manual. *Br J Oral Maxillofac Surg*. (2018) 56:8–13. doi: 10.1016/j.bjoms.2017.11.009
40. Rogers SN, Brown JS, Woolgar JA, Lowe D, Magennis P, Shaw RJ, et al. Survival following primary surgery for oral cancer. *Oral Oncol*. (2009) 45:201–11. doi: 10.1016/j.oraloncology.2008.05.008
41. Ganly I, Patel S, Shah J. Early stage squamous cell cancer of the oral tongue—clinicopathologic features affecting outcome. *Cancer*. (2012) 118:101–11. doi: 10.1002/cncr.26229
42. Syrjänen S, Rautava J, Syrjänen K. HPV in head and neck cancer-30 years of history. *Recent Results Cancer Res*. (2017) 206:3–25. doi: 10.1007/978-3-319-43580-0_1
43. Xu ES, Yang MH, Huang SC, Liu CY, Yang TT, Chou TY, et al. ECE-1 overexpression in head and neck cancer is associated with poor tumor differentiation and patient outcome. *Oral Dis*. (2018) 25:44–53. doi: 10.1111/odi.12935
44. Wreesmann VB, Katabi N, Palmer FL, Montero PH, Migliacci JC, Gonen M, et al. Influence of extracapsular nodal spread extent on prognosis of oral squamous cell carcinoma. *Head Neck*. (2016) 38:E1192–9. doi: 10.1002/hed.24190
45. Moore C, Kuhns JG, Greenberg RA. Thickness as prognostic aid in upper aerodigestive tract cancer. *Arch Surg*. (1986) 121:1410–4. doi: 10.1001/archsurg.1986.01400120060009
46. Huang SH, Hwang D, Lockwood G, Goldstein'P, O'Sullivan B. Predictive value of tumor thickness for cervical lymph-node involvement in squamous cell carcinoma of the oral cavity: a meta-analysis of reported studies. *Cancer*. (2009) 115:1489–97. doi: 10.1002/cncr.24161
47. Russolo M, Giacomarra V, Papanikolla L, Tirelli G. Prognostic indicators of occult metastases in oral cancer. *Laryngoscope*. (2002) 112:1320–3. doi: 10.1097/00005537-200207000-00035
48. Spiro RH, Huvos AG, Wong GY, Spiro JD, Gnecco CA, Strong EW. Predictive value of tumor thickness in squamous carcinoma confined to the tongue and floor of the mouth. *Am J Surg*. (1986) 152:345–50. doi: 10.1016/0002-9610(86)90302-8
49. Preda L, Chiesa F, Calabrese L, Latronico A, Bruschini R, Leon ME, et al. Relationship between histologic thickness of tongue carcinoma and thickness estimated from preoperative MRI. *Eur Radiol*. (2006) 16:2242–8. doi: 10.1007/s00330-006-0263-9
50. Piazza C, Grammatica A, Montalto N, Paderno A, Del Bon F, Nicolai P. Compartmental surgery for oral tongue and floor of the mouth cancer: oncologic outcomes. *Head Neck*. (2019) 41:110–5. doi: 10.1002/hed.25480
51. Calabrese L, Giugliano G, Bruschini R, Ansarin M, Navach V, Grosso E, et al. Compartmental surgery in tongue tumours: description of a new surgical technique. *Acta Otorhinolaryngol Ital*. (2009) 29:259–64.
52. Tagliabue M, Gandini S, Maffini F, Navach V, Bruschini R, Giugliano G, et al. The role of the T-N tract in advanced stage tongue cancer. *Head Neck*. (2019) 41:2756–67. doi: 10.1002/hed.25761
53. Albera R, Cavalot A, Cortesina G, De Sanctis A, Ferrero V, Martone T, et al. *Oncogenes and Carcinogenesis of Head and Neck Carcinomas*. Torino: Edizioni Minerva Medica (2002).
54. Tai SK, Li WY, Yang MH, Chang SY, Chu PY, Tsai TL, et al. Treatment for T1–2 oral squamous cell carcinoma with or without perineural invasion: neck dissection and postoperative adjuvant therapy. *Ann Surg Oncol*. (2012) 19:1995–2002. doi: 10.1245/s10434-011-2182-5
55. Ling W, Mijiti A, Moming A. Survival pattern and prognostic factors of patients with squamous cell carcinoma of the tongue: a retrospective analysis of 210 cases. *J Oral Maxillofac Surg*. (2013) 71:775–85. doi: 10.1016/j.joms.2012.09.026
56. Chatzistefanou I, Lubek J, Markou K, Ord RA. The role of perineural invasion in treatment decisions for oral cancer patients: a review of the literature. *J Craniomaxillofac Surg*. (2017) 45:821–5. doi: 10.1016/j.jcms.2017.02.022
57. Jardim JF, Francisco AL, Gondak R, Damascena A, Kowalski LP. Prognostic impact of perineural invasion and lymphovascular invasion in advanced stage oral squamous cell carcinoma. *Int J Oral Maxillofac Surg*. (2015) 44:23–8. doi: 10.1016/j.ijom.2014.10.006
58. Nair D, Mair M, Singhvi H, Mishra A, Nair S, Agrawal J, et al. Perineural invasion: independent prognostic factor in oral cancer that warrants adjuvant treatment. *Head Neck*. (2018) 40:1780–7. doi: 10.1002/hed.25170
59. Brown IS. Pathology of perineural spread. *J Neurol Surg B Skull Base*. (2016) 77:124–30. doi: 10.1055/s-0036-1571837
60. Saito Y, Omura G, Yasuhara K, Rikitake R, Akashi K, Fukuoka O, et al. Prognostic value of lymphovascular invasion of the primary tumor in hypopharyngeal carcinoma after total laryngopharyngectomy. *Head Neck*. (2017) 39:1535–43. doi: 10.1002/hed.24705
61. Zhang H, Chen X, Wang S, Fan J, Lu L. Poorer prognosis associated with simultaneous lymphatic and vascular invasion in patients with squamous carcinoma of the thoracic oesophagus. *Eur J Cardiothorac Surg*. (2017) 52:378–84. doi: 10.1093/ejcts/ezx081
62. Fives C, Feeley'L, O'Leary G, Sheahan P. Importance of lymphovascular invasion and invasive front on survival in floor of mouth cancer. *Head Neck*. (2016) 38:E1528–34. doi: 10.1002/hed.24273
63. Quinlan-Davidson SR, Mohamed ASR, Myers JN, Gunn GB, Johnson FM, Skinner H, et al. Outcomes of oral cavity cancer patients treated with surgery followed by postoperative intensity modulated radiation therapy. *Oral Oncol*. (2017) 72:90–7. doi: 10.1016/j.oraloncology.2017.07.002
64. Cassidy RJ, Switchenko JM, Jegadeesh N, Sayan M, Ferris MJ, Eaton BR, et al. Association of lymphovascular space invasion with locoregional failure and survival in patients with node-negative oral tongue cancers. *JAMA Otolaryngol Head Neck Surg*. (2017) 143:382–8. doi: 10.1001/jamaoto.2016.3795
65. Chen TC, Wang CP, Ko JY, Yang TL, Hsu CW, Yeh KA, et al. The impact of perineural invasion and/or lymphovascular invasion on the survival of early-stage oral squamous cell carcinoma patients. *Ann Surg Oncol*. (2013) 20:2388–95. doi: 10.1245/s10434-013-2870-4
66. Iocca O, Farcomeni A, De Virgilio A, Di Maio P, Golusinski P, Malvezzi L, et al. Prognostic significance of lymph node yield and lymph node ratio in patients affected by squamous cell carcinoma of the oral cavity and oropharynx: study protocol for a prospective, multicenter, observational study. *Contemp Clin Trials Commun*. (2019) 14:100324. doi: 10.1016/j.conctc.2019.100324
67. Huang TH, Li KY, Choi WS. Lymph node ratio as prognostic variable in oral squamous cell carcinomas: systematic review and meta-analysis. *Oral Oncol*. (2019) 89:133–43. doi: 10.1016/j.oraloncology.2018.12.032
68. Fridman E, Naara S, Agarwal J, Amit M, Bachar G, Villaret AB, et al. The role of adjuvant treatment in early-stage oral cavity squamous cell carcinoma: an international collaborative study. *Cancer*. (2018) 124:2948–55. doi: 10.1002/cncr.31531

Conflict of Interest: The authors declare that the research was conducted in the absence of any commercial or financial relationships that could be construed as a potential conflict of interest.

frontiers in Oncology

ORIGINAL RESEARCH
published: 06 August 2020
doi: 10.3389/fonc.2020.01284

Randomized Controlled Study Comparing Efficacy and Toxicity of Weekly vs. 3-Weekly Induction Chemotherapy in Locally Advanced Head and Neck Squamous Cell Carcinoma

Devale Tousif[1]*, *Vinu Sarathy*[1,2]*, *Rajesh Kumar*[1] and *Radheshyam Naik*[1]

[1] HealthCare Global Enterprises Ltd (HCG), Bangalore, India, [2] HCG Cancer Hospital, Bengaluru, India

Background: Head and Neck Cancer is a major public health problem in India, majority of which are lifestyle related, male predominant requiring dedicated infrastructure and human resource. The 5-year survival is 59% for all stages combined and only 45% in patients with locally advanced inoperable head and neck cancer using current chemoradiation schedules. Chemotherapy agents administered in the induction or concurrent setting comprise of taxanes (Docetaxel, paclitaxel), platinum compounds (Cisplatin, carboplatin) and fluorouracil (TPF). For patients with advanced Head and neck squamous cell carcinoma (HNSCC), 3-weekly TPF regimen is the established standard induction chemotherapy (ICT) option based on overall survival benefit. However, TPF regimen is known to be associated with significant dose limiting toxicities which may impair tolerance and effectiveness of therapy. In this study we assessed the efficacy and toxicity of weekly vs. 3-weekly Docetaxel, Cisplatin, and Fluoro-uracil (TPF) induction chemotherapy in locally advanced Head and neck squamous cell carcinoma (LA-HNSCC).

Methods: This was an open labeled randomized two arm study with 41 patients in the 3-weekly TPF arm and 41 patients in the weekly arm. Patients were randomized using numbers from a randomization software, data recorded, and results were analyzed.

Results: The weekly group achieved far greater symptom relief than 3-weekly group (72 vs. 64%). The overall response rates were similar in both arms (ORR 75.6 and 73.1% in the weekly and 3-weekly groups, respectively). Renal toxicity was significantly lower in the weekly group as compared to 3 weekly arm post three cycles of chemotherapy (CrCl 91.49 ml/min vs. 76.67 ml/min, respectively). The weekly group had predominantly grade I and II neutropenia (19.5 and 17.1%, respectively) as compared to 3-weekly group where grade III and IV neutropenia (31 and 12%, respectively) was more prominent (p-0.003). Among non-hematological toxicities, mucositis, nausea/vomiting, and diarrhea in the weekly group were significantly lower when compared to 3-weekly group. Progression free survival was slightly higher in the weekly group (18 months) when compared to 3-weekly group (15 months) which was not statistically significant.

OPEN ACCESS

Edited by:
Alberto Paderno, University of Brescia, Italy

Reviewed by:
Maria Cossu Rocca, European Institute of Oncology (IEO), Italy
Jonathan Michael Bernstein, Imperial College London, United Kingdom

***Correspondence:**
Devale Tousif
devaletousif@gmail.com
Vinu Sarathy
sarathy.vinu.88@gmail.com

Specialty section:
This article was submitted to Head and Neck Cancer, a section of the journal Frontiers in Oncology

Received: *17 April 2020*
Accepted: *22 June 2020*
Published: *06 August 2020*

Citation:
Tousif D, Sarathy V, Kumar R and Naik R (2020) Randomized Controlled Study Comparing Efficacy and Toxicity of Weekly vs. 3-Weekly Induction Chemotherapy in Locally Advanced Head and Neck Squamous Cell Carcinoma. Front. Oncol. 10:1284. doi: 10.3389/fonc.2020.01284

Conclusion: Weekly induction with TPF had lower toxicity and similar efficacy as compared to 3-weekly regimen in locally advanced HNSCC patients. Myelosuppression, which was the most serious and common complication of 3-weekly TPF regimens was notably low using the weekly regimen. Our results suggest that weekly TPF regimen may be a safer and effective alternative to 3-weekly TPF for treatment of LA-HNSCC. To our knowledge this is the first study reporting the efficacy of weekly TPF regimen in LA-HNSCC till date.

Keywords: induction chemotherapy, weekly docetaxel, weekly cisplatin in head and neck cancer, locally advanced head and neck cancer, weekly 5-fluro uracil, weekly TPF

INTRODUCTION

Head and Neck Cancers (HNCs) comprise of malignancies of the oral/nasal cavity, lips, salivary glands, pharynx (hypo pharynx, oropharynx and nasopharynx), and larynx. Squamous cell carcinomas (SCCs) constitute ∼90% of Head and Neck Cancers with adenocarcinomas, melanomas, and sarcomas forming the rest (1). Head and Neck Cancers are emerging as a major health problem in India. Overall 57.5% of global head and neck cancers occur in Asia out of which around 30–35% occur in India (2). The 5-year relative survival rate is 81% for patients with localized disease and 59% for all stages combined (3, 4).

To improve response rates and functional outcomes, chemotherapy has been included into various schedules. Chemotherapy agents with proven activity in squamous cell carcinoma commonly used in either induction or concurrent chemotherapy regimens consist of the platinum compounds (Cisplatin, carboplatin), fluorouracil, and taxanes (Docetaxel, paclitaxel). The three-drug combination of platinum, fluorouracil plus taxane is the preferred regimen for induction chemotherapy (ICT). Randomized trials found that addition of a taxane (Docetaxel, paclitaxel) to PF regimen improved efficacy of induction chemotherapy (5, 6). The most extensive data on TPF regimen comes from the TAX 324 trial, in which 501 patients were randomly assigned to induction with Docetaxel, Cisplatin, plus fluorouracil (TPF) or PF followed by concurrent chemo radiotherapy using weekly carboplatin. Although TPF regimen had an improved overall survival than PF, TPF regimen was also associated with significant acute toxicities and myelosuppression (7, 8).

We hypothesized that weekly induction chemotherapy with TPF regimen may have similar efficacy and lower toxicity further improving tolerability and response rates. In this study we assessed the efficacy and toxicity of weekly vs. 3-weekly Docetaxel, Cisplatin, and Fluoro-uracil (TPF) induction chemotherapy in locally advanced Head and neck squamous cell carcinoma (HNSCC).

MATERIALS AND METHODS

The study was conducted in HealthCare Global Hospital, Bangalore after approval from institutional ethics committee. The study was a prospective two arm open labeled randomized controlled study which included locally advanced HNSCC (LA-HNSCC) patients recruited during 1st April 2015 to 31st March 2017. The study included a total of 82 LA-HNSCC patients. After taking informed consent the patients were randomized into two groups; Group A and Group B (41 patients in each group), to receive 3 cycles of weekly and 3-weekly TPF regimen, respectively. Randomization was done using random numbers generated by the software (www.randomizer.org) (9).

Treatment Protocol

The following treatment protocol was used for patients allotted to GROUP A or B.

Group A: Patients in this group received weekly chemotherapy for 9 weeks.

1. Docetaxel-30 mg/m^2 i/v infusion on D1
2. Cisplatin-40 mg/m^2 i/v infusion on D1
3. 5FU-750 mg/m^2 i/v infusion over 6 h on D1

Group B: Patients in this group received three-weekly chemotherapy for 3 cycles (from D1 to D5).

1. Docetaxel-75 mg/m^2 i/v infusion on D1
2. Cisplatin-75 mg/m^2 i/v infusion on D1
3. 5-FU-750 mg/m^2 i/v infusion over 24 h from D1-D5

Response Evaluation

Radiological Response assessment was done by Response Evaluation Criteria in Solid Tumors RECIST (version 1.1) based on PET scan imaging modality. Clinical response grading was done according to National Cancer Institute- Common Terminology Criteria for Adverse Events (NCI- CTCAE) version 4.0 (10).

Statistical Methods

SPSS version 23 was used for data analysis. Frequencies and percentage were reported for categorical variables. Continuous variables were expressed as mean and standard deviation for normally distributed data and median and range for skewed data. Kaplan Meier survival analysis was carried for progression free survival. Patient characteristics were evaluated by using Chi-Square test. Results are graphically represented where deemed necessary. Probability values below 0.05 were considered as statistically significant.

RESULTS

Patient's Characteristics

The patients' baseline characteristics are summarized in **Table 1**. Majority of patients were between 51 and 60 years of age in both the study groups. Both the groups had a male preponderance. It is a well-known fact that co-morbid conditions are associated with poorer tolerance and response rates, thus being a major confounding factor in the study. Most patients in both groups of our study did not have any major co-morbidity. The few patients with co-morbid conditions were well-controlled during the study period. All the three variables were well-matched in our study (**Table 1**).

TABLE 1 | Patient baseline characteristics of the two groups.

Variable	Weekly TPF (%)	3-weekly TPF (%)	*p*-value
Age (mean ± SD)			
21–30	2 (4.9)	1 (2.4)	0.263
31–40 years	4 (9.8)	10 (24.4)	
41–50 years	7 (17.1)	10 (24.4)	
51–60 years	28 (68.3)	20 (48.8)	
Gender			
Male	33 (80.5)	35 (85.4)	0.345
Female	8 (19.5)	6 (14.6)	
Comorbidities[1]			
Nil	28 (68.3)	30 (73.2)	0.872
DM (Grade 1)	8 (19.5)	5 (12.2)	
HTN (Grade 1 and 2)	4 (9.8)	5 (12.2)	
IHD (Grade 1)	1 (2.4)	1 (2.4)	
Subsite			
Oropharynx	26	25	0.601
Hypopharynx	15	15	
Oral cavity	0	1	
Performance status (ECOG)			
1	40	41	0.314
2	1	0	
HPV – p16			
Oropharynx	5	4	0.532
Hypopharynx	2	1	
Symptoms			
Dysphagia			0.587
Grade 1	0	0	
Grade 2	0	0	
Grade 3	21	19	
Grade 4	8	7	
Pain			
Grade 1	0	0	
Grade 2	0	0	
Grade 3	8	7	
Hoarseness			
Grade 1	0	0	
Grade 2	0	1	
Grade 3	4	7	
Total	41 (100)	41 (100)	

[1]*Available online at: https://www.rtog.org/LinkClick.aspx?fileticket=oClaTCMufRA%3D&tabid=290 (accessed June 15, 2020).*

Assessment of Clinical Symptoms

Severity of clinical symptoms before and after chemotherapy in the weekly and 3-weekly groups is summarized in **Table 2**. Clinical symptoms of patients were recorded as per NCI-CTCAE Version 4.0.

Pre Chemotherapy

In both groups GR III symptoms were more common. The weekly group had 80.5 and 19.5% of GR III and IV clinical symptoms, respectively, while the 3-weekly group had 2.4, 80.5 and 17.5% of GR II, III, and IV symptoms, respectively.

Post Chemotherapy

Overall better symptom relief was achieved in the weekly group as compared to 3-weekly group. The weekly group showed a 72% reduction of grade III clinical symptoms as opposed to 64% reduction in the 3-weekly group.

Radiological Responses

Post treatment radiological responses are represented in **Figure 1**. Radiological response was evaluated using RECIST criteria (1.1). Overall response rate (ORR) included complete and partial responses. The weekly group had an ORR of 75.6 and an almost similar ORR of 73.1% was seen in 3-weekly group (p-0.687). The number of patients with stable and progressive disease were also similar between the two groups.

Evaluation of Toxicities in the Weekly and 3-Weekly Group

The hematological and non-hematological toxicities in both groups are summarized in **Table 3**.

The weekly group had more grade I and II neutropenia (19.5 and 17.1%, respectively) while the 3 weekly group had predominantly grade III and IV neutropenia (31 and 12%, respectively) which was statistically significant (p-0.003). Most of the patients in the weekly group tolerated ICT well without any major hematological adverse events.

The weekly ICT group had predominantly a lower grade of mucositis which included GR II and I (34 and 29%, respectively) as compared to 3-weekly group who had more of GR III and IV mucositis (9 and 26%, respectively; p-0.003). 26% of weekly-ICT group had no episode of mucositis. Higher grades of nausea and vomiting were seen in the 3-weekly group (58 and 14% in GR III and IV, respectively) while majority of weekly group had no symptoms (39%) or lower grades of nausea/vomiting (31 and 22% in GR II and GR I, respectively) with significant p-value (0.000). High grade diarrhea was seen chiefly in the 3-weekly group (36 and 9% GR II and III, respectively) while majority of weekly group patients had minimal or no symptoms (80%), P-value (0.001). Majority of patients in both groups tolerated chemotherapy well with mainly incidences of grade I (19% in each group) neurological symptoms in both groups (p-0.028) (**Table 3**).

TABLE 2 | Grade of clinical symptoms - Pre and Post chemotherapy in Weekly and 3-Weekly groups.

Grade of clinical symptoms	At presentation				Post chemotherapy			
	Weekly		3-weekly		Weekly		3-weekly	
Grade 1	-	-	-	-	27	65.9	17	41.5
Grade 2	0	0	1	2.4	11	26.8	18	43.9
Grade 3	33	80.5	33	80.5	3	7.3	6	14.6
Grade 4	8	19.5	7	17.1	-	-	-	-
Total	41	100	41	100	41	100	41	100

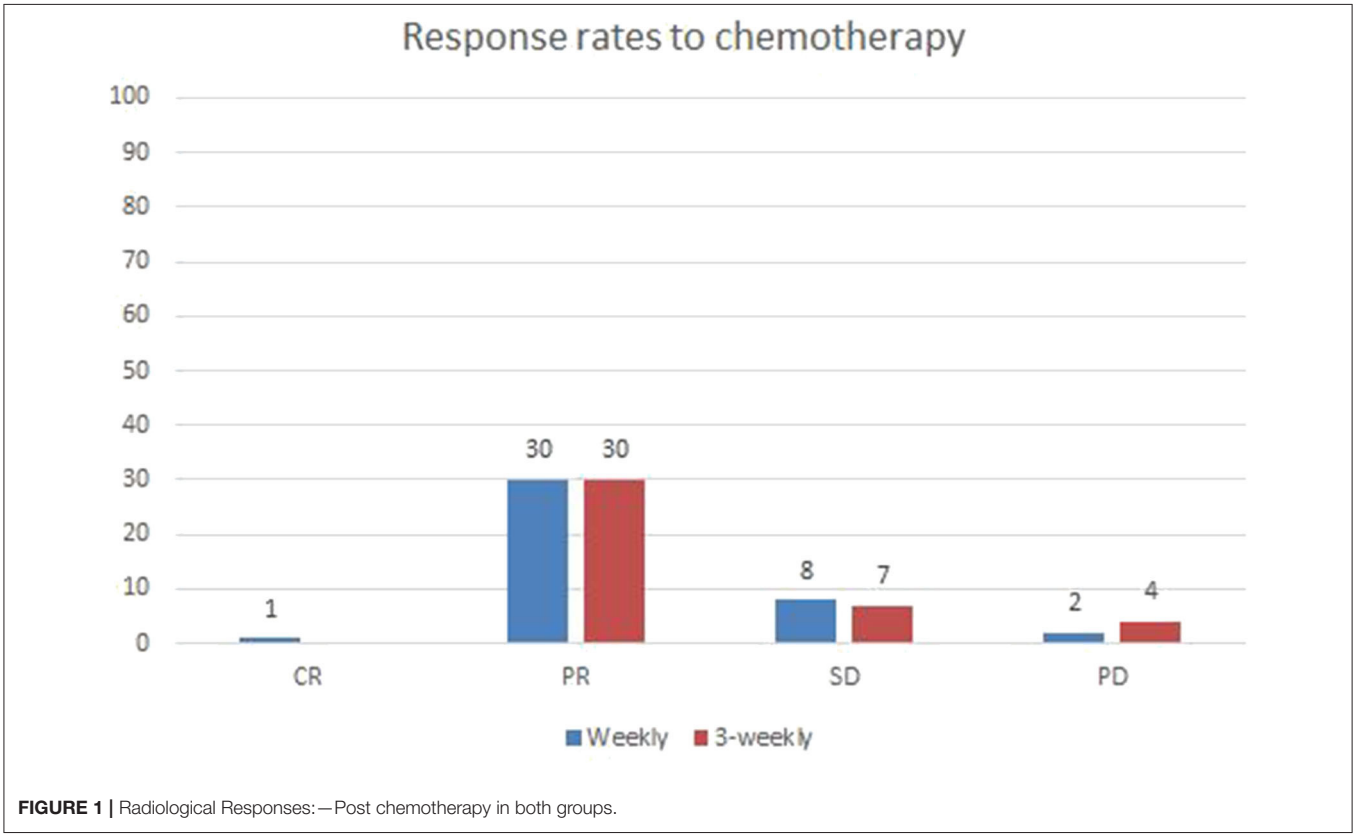

FIGURE 1 | Radiological Responses:—Post chemotherapy in both groups.

Nephropathy

Renal toxicity was analyzed using creatinine clearance (CrCl). The mean CrCl in weekly and 3-weekly groups was 91 and 76 ml/min, respectively (p-0.003). The weekly group had better renal function than 3-weekly group at the end of 3 cycles of chemotherapy. Assessment of renal function post chemotherapy is illustrated in **Figure 2.**

Survival Analysis

The progression free survival was 18 and 15 months in the weekly and 3-weekly groups, respectively which was not statistically significant ($p = 0.905$) (**Figure 3**).

DISCUSSION

Induction chemotherapy has been mentioned as a first line option especially in oropharyngeal and hypopharyngeal locally advanced SCC (11). This has been demonstrated effectively in the landmark TAX-323 and TAX-324 trials (7, 8).

Posner et al., reported longer overall and progression free survival and a non-significant reduction of toxicities in the TPF group as compared with PF (7). However, this study also reported more myelo-suppression in the TPF group (83%) as compared to PF (56%). In the TAX 323 and TAX 324 studies, the main toxicity associated with TPF regimen was leukopenia and neutropenia indicating a clear need for regimens with improved tolerability and lower toxicity (12). Hence our study was designed to establish an effective, safe and tolerable daycare regimen using TPF as ICT for locally advanced HNSCC.

The early phase I/II trials of 3-weekly TPF in advanced HNSCC where docetaxel given at 75 mg/m^2 every 3 weeks showed 95% grade 3–4 neutropenia and 19% febrile neutropenia (13). Rapidis et al. conducted a study aiming at reduction of myelosuppression and reported that using biweekly Docetaxel

TABLE 3 | Details of toxicity observed in weekly and 3-weekly groups.

Details	Neutropenia				Mucositis				Nausea/vomiting				Diarrhea				Neuropathy			
	Weekly		3-Weekly		Weekly		3-Weekly		Weekly		3-Weekly		Weekly		3-Weekly		Weekly		3-Weekly	
	N	%	*N*	%	*N*	%	*N*	%	*N*	%	*N*	%	*N*	%	*N*	%	*N*	%	*N*	%
Grade-I and II	15	36.6	13	31.7	26	63.4	12	29.3	22	53.7	11	26.8	8	19.6	21	51.2	8	19.5	15	36.6
Grade III	1	2.4	5	12.2	4	9.8	18	43.9	3	7.3	24	58.5	0	0	4	9.8	0	0	1	2.4
Grade IV	2	4.9	13	31.7	0	0	11	26.8	0	0	6	14.6	0	0	0	0	0	0	0	0
Nil	23	56.1	10	24.4	11	26.8	0	0	16	39	0	0	33	80.5	16	39	33	80.5	25	61
Total	41	100	41	100	41	100	41	100	41	100	41	100	41	100	41	100	41	100	41	100

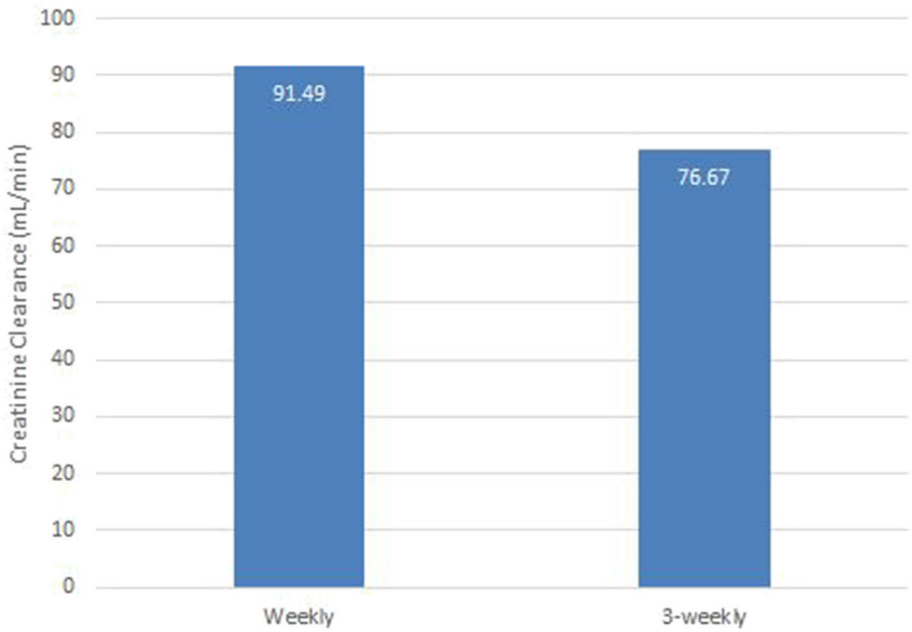

FIGURE 2 | Nephropathy; Post chemotherapy in both groups.

(40 mg/m^2) with Cisplatin and 5-FU significantly decreased grade 3–4 neutropenia to 37% (14). This response suggested that biweekly or weekly Docetaxel could be an effective alternative for the 3-weekly regimen. Kean f, HO et al. demonstrated more delays (29 vs. 41%) and omission of chemotherapy (5.6 vs. 17.4%) occurred in 3-weekly arm as compared to the weekly group. They concluded that 100 mg/m^2 of Cisplatin given every 3-weekly with radiotherapy was much less tolerated than 40 mg/m^2 administered weekly and hence fewer patients achieved the effective cumulative dose of >200 mg/m^2, possibly compromising on efficacy (15). A retrospective study by Patil et al. used induction chemotherapy with weekly paclitaxel and carboplatin in patients with LA-HNSCC and found that the above regimen was safe and effective even in elderly and those with poor performance status (16). Recently, the Japanese trial found that weekly cisplatin+RT is non-inferior to 3-weekly cisplatin+RT in LA-SCCHN pts and has a favorable toxicity profile, though this was reported in adjuvant setting (17). This formed the rationale for our study comparing standard 3-weekly with modified weekly TPF regimen using docetaxel at a dose of 30 mg/m^2, Cisplatin 40 mg/m^2 and 5-FU 750 mg/m^2, all administered weekly for 9 weeks followed by re-assessment. To our knowledge this is the first studying comparing weekly TPF induction with standard 3-weekly regimen in locally advanced head and neck squamous cell cancer.

CUMULATIVE DOSE INTENSITY AND ITS SIGNIFICANCE

The weekly group received a higher cumulative dose of taxanes and platinum by 16.7 and 37.5%, respectively at the end of 3 weeks as compared to the 3-weekly group. Whereas, the cumulative dose of 5-FU was 40% lower in the weekly group when compared to 3-weekly group. Despite higher dose intensity achieved for docetaxel and cisplatin in the weekly group, hematological and non-hematological toxicity was predominantly only grade I or II.

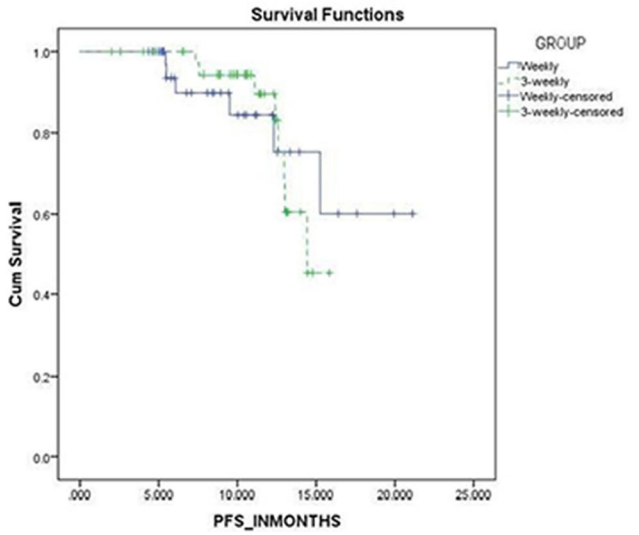

FIGURE 3 | Kaplan Meier analysis of progression free survival.

At presentation, the weekly group mainly had GR III and IV clinical symptoms in 80.5 and 19.5%, respectively while the 3-weekly group presented with GR II, III, and IV symptoms in 2.4, 80.5, and 17.5%, respectively. Post 3 cycles, the weekly group showed greater relief in symptoms with objective reduction from clinical grade III to grade I as compared to the 3-weekly group. The above effect was close to significant ($p = 0.084$). The response rate (RR) was almost similar in both groups with an ORR of 75.6% in weekly group and 73.1% in the 3-weekly group. Difference in hematological toxicities was analyzed and the weekly group had more grade I and II neutropenia (19.5 and 17.1%, respectively) as compared to 3-weekly group where grade III and IV neutropenia (31 and 12%, respectively) was more significant. The above observation was statistically significant (p-0.003). Among the non-hematological toxicities: mucositis, nausea/vomiting and diarrhea were significantly lower in the weekly group as compared to 3-weekly group.

A single arm retrospective study done at TATA Memorial Hospital, Mumbai in 2014 by Patil et al., reported an overall response rate (CR + PR) of 67% (10 patients) (16). Overall grade 3–4 toxicity was seen in 6 patients. No toxicity related mortality was observed. The median PFS and OS were 10.36 and 16.53 months, respectively. Similarly, our study reported an ORR (CR + PR) of 75.6% (31 patients) in the weekly group. Only 2 patients had grade 3–4 toxicity. Summarizing, the weekly TPF group had significantly lower incidences of both hematological and non-hematological toxicities as compared to 3-weekly group.

The progression free survival was 18 and 15 months in the weekly and 3-weekly groups, respectively which was not statistically significant ($p = 0.905$).

The proposed mechanisms are that the dose dense approach facilitates for constant exposure of taxane to cells in G2-M phase thus preventing emergence of resistance clones and enhancing anti-tumor effect. Furthermore, weekly taxane may have direct angiogenic effects disrupting microtubule dynamics in the endothelial cells. This was particularly seen at a cytostatic concentration <10 nm. Weekly taxane may theoretically also reverse the resistance acquired to 3-weekly taxanes (18). Weekly taxanes may also be beter tolerated as myelosuppression depends on peak plasma concentration >50 nm. Hence weekly paclitaxel may decrease myelosuppression, maintain dose intensity and quicker rates of plasma concentration decline could limit toxicity (19, 20). Similarly regardless of treatment regimen, it has been suggested that a cumulative dose of 200 mg/m^2 needs to be reached for therapeutic benefit in cisplatin studies (21, 22). A retrospective analysis indicated an inferior outcome with a cumulative cisplatin dose of ≤200 mg/m^2 in HPV-negative patients. In our study the weekly cisplatin arm received a much higher cumulative dose (360 mg/m^2) than the 3-weekly arm (225 mg/m^2) possibly contributing to increased efficacy. Short 5-FU infusional schedules have also been reportedly used with considerable success in advanced head and neck cancers (23, 24).

The limitation of our study is small sample size. Assessment of HPV status was done by p16 Immunohistochemistry and not by Polymerase Chain Reaction (PCR). Quality of life post ICT was not recorded which may have helped in further analysis of effectiveness. Assessment of chronic toxicity was not part of our study protocol which can help to assess quality of life in long term survivors.

CONCLUSION

Weekly TPF combination as an ICT showed significantly lower toxicity and similar efficacy as 3-weekly regimen in locally advanced HNSCC patients. Myelosuppression, which was the most serious and common complication of 3-weekly TPF regimen was notably low using the weekly regimen. Our results suggest that a weekly TPF regimen represents a safer and effective alternative to 3-weekly TPF for the treatment of LA-HNSCC. Further large-scale studies with longer follow up are needed to assess survival and long term toxicities using weekly TPF regimen in locally advanced head and neck cancers.

DATA AVAILABILITY STATEMENT

The raw data supporting the conclusions of this article will be made available by the authors, without undue reservation.

ETHICS STATEMENT

The studies involving patients with locally advanced squamous cell carcinoma of head and neck were reviewed and approved by HCG-Central Ethics Committee bearing register no. ECR/386/INST/KA/2013. The patients/participants provided their written informed consent to participate in this study.

AUTHOR CONTRIBUTIONS

All authors listed have made a substantial, direct and intellectual contribution to the work, and approved it for publication.

REFERENCES

1. MCCOMB WS. Treatment of cancer of the head and neck. *An Cir.* (1961). 26:1–20.
2. Kulkarni MR. Head and neck cancer burden in India. *Int J Head Neck Surg.* (2013) 4:29–35. doi: 10.5005/jp-journals-10001-1132
3. Pulte D, Brenner H. Changes in survival in head and neck cancers in the late 20th and early 21st Century: a period analysis. *Oncologist.* (2010) 15:994–1001. doi: 10.1634/theoncologist.2009-0289
4. Forastiere A, Koch W, Trotti A, Sidransky D. Head and neck cancer. *N Engl J Med.* (2001) 345:1890–900. doi: 10.1056/NEJMra001375
5. Hitt R, López-Pousa A, Martínez-Trufero J, Escrig V, Carles J, Rizo A, et al. Phase III study comparing cisplatin plus fluorouracil to paclitaxel, cisplatin, and fluorouracil induction chemotherapy followed by chemoradiotherapy in locally advanced head and neck cancer. *J Clin Oncol.* (2005) 23:8636–45. doi: 10.1200/JCO.2004.00.1990
6. Janoray G, Pointreau Y, Garaud P, Chapet S, Alfonsi M, Sire C, et al. Long-term results of a multicenter randomized phase iii trial of induction chemotherapy with cisplatin, 5-fluorouracil, ± Docetaxel for larynx preservation. *J Natl Cancer Inst.* (2016) 108:djv368. doi: 10.1093/jnci/djv368
7. Posner MR, Hershock DM, Blajman CR, Mickiewicz E, Winquist E, Gorbounova V, et al. Cisplatin and fluorouracil alone or with docetaxel in head and neck cancer. *N Engl J Med.* (2007) 357:1705–15. doi: 10.1056/NEJMoa070956
8. Lorch JH, Goloubeva O, Haddad RI, Cullen K, Sarlis N, Tishler R, et al. Induction chemotherapy with cisplatin and fluorouracil alone or in combination with docetaxel in locally advanced squamous-cell cancer of the head and neck: long-term results of the TAX 324 randomised phase 3 trial. *Lancet Oncol.* (2011) 12:153–9. doi: 10.1016/S1470-2045(10)70279-5
9. *Research Randomizer*. Available online at: https://www.randomizer.org/(accessed April 16, 2020).
10. *Common Terminology Criteria for Adverse Events (CTCAE) Version 4.0*. (2009). Available online at: http://www.meddramsso.com(accessed April 13, 2020).
11. *NCCN Clinical Practice Guidelines in Oncology*. Available online at: https://www.nccn.org/professionals/physician_gls/default.aspx (accessed January 21, 2020).
12. Vermorken JB, Remenar E, van Herpen C, Gorlia T, Mesia R, Degardin M, et al. Cisplatin, fluorouracil, and docetaxel in unresectable head and neck cancer. *N Engl J Med.* (2007) 357:1695–704. doi: 10.1056/NEJMoa071028
13. Haddad R, O'Neill A, Rabinowits G, Tishler R, Khuri F, Adkins D, et al. Induction chemotherapy followed by concurrent chemoradiotherapy (sequential chemoradiotherapy) versus concurrent chemoradiotherapy alone in locally advanced head and neck cancer (PARADIGM): a randomised phase 3 trial. *Lancet Oncol.* (2013) 14:257–64. doi: 10.1016/S1470-2045(13)70011-1
14. Rapidis AD, Trichas M, Stavrinidis E, Roupakia A, Ioannidou G, Kritselis G, et al. Induction chemotherapy followed by concurrent chemoradiation in advanced squamous cell carcinoma of the head and neck: final results from a phase II study with docetaxel, cisplatin and 5-fluorouracil with a four-year follow-up. *Oral Oncol.* (2006) 42:675–84. doi: 10.1016/j.oraloncology.2005.12.006
15. Ho KF, Swindell R, Brammer C V. Dose intensity comparison between weekly and 3-weekly Cisplatin delivered concurrently with radical radiotherapy for head and neck cancer: a retrospective comparison from new cross hospital, wolverhampton, UK. *Acta Oncol.* (2008) 47:1513–8. doi: 10.1080/02841860701846160
16. Patil VM, Noronha V, Joshi A, Muddu VK, Dhumal S, Arya S, et al. Weekly chemotherapy as induction chemotherapy in locally advanced head and neck cancer for patients ineligible for 3 weekly maximum tolerable dose chemotherapy. *Indian J Cancer.* (2014) 51:20–4. doi: 10.4103/0019-509X.134608
17. Kiyota N, Tahara M, Fujii H, Yamazaki T, Mitani H, Iwae S, et al. Phase II/III trial of post-operative chemoradiotherapy comparing 3-weekly cisplatin with weekly cisplatin in high-risk patients with squamous cell carcinoma of head and neck (JCOG1008). *J Clin Oncol.* (2020) 38(15Suppl.):6502. doi: 10.1200/JCO.2020.38.15_suppl.6502
18. Marchetti P, Urien S, Cappellini GA, Ronzino G, Ficorella C. Weekly administration of paclitaxel: theoretical and clinical basis. *Crit Rev Oncol Hematol.* (2002) 44(Suppl.): S3–13. doi: 10.1016/S1040-8428(02)00109-9
19. Baird RD, Tan DSP, Kaye SB. Weekly paclitaxel in the treatment of recurrent ovarian cancer. *Nat Rev Clin Oncol.* (2010) 7:575–82. doi: 10.1038/nrclinonc.2010.120
20. Gianni L, Kearns CM, Giani A, Capri G, Viganó L, Locatelli A, et al. Nonlinear pharmacokinetics and metabolism of paclitaxel and its pharmacokinetic/pharmacodynamic relationships in humans. *J Clin Oncol.* (1995) 13:180–90. doi: 10.1200/JCO.1995.13.1.180
21. Pignon JP, Maître A le, Maillard E, Bourhis J. Meta-analysis of chemotherapy in head and neck cancer (MACH-NC): an update on 93 randomised trials and 17,346 patients. *Radiother Oncol.* (2009) 92:4–14. doi: 10.1016/j.radonc.2009.04.014
22. Strojan P, Vermorken JB, Beitler JJ, Saba NF, Haigentz M, Bossi P, et al. Cumulative cisplatin dose in concurrent chemoradiotherapy for head and neck cancer: a systematic review. *Head Neck.* (2016) 38:E2151–8. doi: 10.1002/hed.24026
23. Jassem J, Gyergyay F, Kerpel-Fronius S, Nagykálnai T, Baumöhl J, Verweij J, et al. Combination of daily 4-h infusion of 5-fluorouracil and cisplatin in the treatment of advanced head and neck squamous-cell carcinoma: a South-East European Oncology Group study. *Cancer Chemother Pharmacol.* (1993) 31:489–94. doi: 10.1007/BF00685041
24. Aich RK, Deb AR, Ray A. Neo-adjuvant chemotherapy with cisplatin and short infusional 5-FU in advanced head and neck malignancies. *J Cancer Res Ther.* (2005) 1:46–50. doi: 10.4103/0973-1482.16091

Conflict of Interest: VS was employed by HealthCare Global Enterprises Ltd.

The remaining authors declare that the research was conducted in the absence of any commercial or financial relationships that could be construed as a potential conflict of interest.

frontiers in Oncology

ORIGINAL RESEARCH
published: 09 October 2020
doi: 10.3389/fonc.2020.588530

Increased Expression of SHMT2 Is Associated With Poor Prognosis and Advanced Pathological Grade in Oral Squamous Cell Carcinoma

Zhi-Zhong Wu[1], Shuo Wang[1], Qi-Chao Yang[1], Xiao-Long Wang[1], Lei-Lei Yang[1], Bing Liu[1,2] and Zhi-Jun Sun[1,2]**

[1] The State Key Laboratory Breeding Base of Basic Science of Stomatology (Hubei-MOST), Key Laboratory of Oral Biomedicine Ministry of Education, School and Hospital of Stomatology, Wuhan University, Wuhan, China, [2] Department of Oral Maxillofacial Head and Neck Oncology, School and Hospital of Stomatology, Wuhan University, Wuhan, China

This study focused on the expression of mitochondrial serine hydroxymethyltransferase (SHMT2) in oral squamous cell carcinoma (OSCC) and its correlation with clinical traits and the prognosis of OSCC patients. Immunochemical staining and Western blotting were used to quantify the expression of SHMT2 and related immune markers in OSCC. Using OSCC microarrays and The Cancer Genome Atlas (TCGA) database, we evaluated the association between SHMT2 and various clinical traits. We found that increased expression of SHMT2 was detected in OSCC and correlated with advanced pathological grade and recurrence of OSCC. By a multivariate Cox proportional hazard model, high expression of SHMT2 was shown to indicate a negative prognosis. In addition, in the OSCC microenvironment, increasing the expression of SHMT2 was associated with high expression levels of programmed cell death-ligand 1 (PD-L1), CKLF-like MARVEL transmembrane domain containing 6 (CMTM6), V-type immunoglobulin domain-containing suppressor (VISTA), B7-H4, Slug, and CD317. In the future, more effort will be required to investigate the role of SHMT2 in the OSCC microenvironment.

Keywords: SHMT2, oral squamous cell carcinoma, prognosis, TCGA, tumor microenvironment

OPEN ACCESS

Edited by:
Cesare Piazza,
University of Brescia, Italy

Reviewed by:
Angela Tramonti,
Italian National Research Council, Italy
Maria Cossu Rocca,
European Institute of Oncology (IEO), Italy

****Correspondence:***
Zhi-Jun Sun
sunzj@whu.edu.cn
Bing Liu
liubing9909@whu.edu.cn

Specialty section:
This article was submitted to Head and Neck Cancer, a section of the journal Frontiers in Oncology

Received: *29 July 2020*
Accepted: *11 September 2020*
Published: *09 October 2020*

Citation:
Wu Z-Z, Wang S, Yang Q-C, Wang X-L, Yang L-L, Liu B and Sun Z-J (2020) Increased Expression of SHMT2 Is Associated With Poor Prognosis and Advanced Pathological Grade in Oral Squamous Cell Carcinoma. Front. Oncol. 10:588530. doi: 10.3389/fonc.2020.588530

INTRODUCTION

Mainly originating from the oral cavity, oral squamous cell carcinoma (OSCC) is one of the most common malignant tumors of the head and neck (excluding non-melanoma skin cancer) (1, 2). Of note, OSCC results in negative consequences, as advanced OSCC has a poor 5-year-survival rate, impacts activities of daily living, and disfigures the appearance of patients after surgeries (1, 3). Though increasing numbers of OSCC patients have benefited from novel immunotherapies, such as immune checkpoint blockade (ICB), the OSCC microenvironment is complicated and heterogeneous and only approximately 20% of OSCC patients can undergo treatment successfully (4–6). The mechanism of the OSCC microenvironment is not yet clear, and previous studies have demonstrated that both Epstein–Barr virus (EBV) infection and human papilloma virus (HPV) infection independently act as biomarkers of prognosis in head and neck squamous cell carcinoma (HNSCC) (6, 7). However, EBV infection and HPV infection are external factors, and neither

of them can reflect the changes in intracellular molecules related to OSCC. Hence, these facts motivated us to research the biomarkers that can indicate the prognosis and the alteration of intracellular molecules related to OSCC in the OSCC microenvironment (7, 8).

Recently, it has been reported that the tumor microenvironment under hypoxia promotes immune escape and hypoxia in the OSCC microenvironment, indicating poor prognosis and reflecting the involvement of the metabolic activity in mitochondria (9). Since the Warburg effect was discovered to be associated with tumor progression, increasing numbers of scholars have investigated energy metabolism in the tumor microenvironment (10). Coincidentally, mitochondrial serine hydroxymethyltransferase (SHMT2) is a vital enzyme involved in one-carbon unit metabolism that catalyzes the metabolism of serine into glycine in OSCC (11). Intriguingly, serine, as a substrate of SHMT2, is related to the Warburg effect by the active one-carbon unit metabolism (10). Furthermore, it has been reported that SHMT2 is highly expressed in glioma, intrahepatic cholangiocarcinoma, and hepatocellular carcinoma (12), reflecting that SHMT2 is partly involved in the process of tumorigenicity (10, 12, 13). It has been suggested that SHMT2 is downstream of signal transducer and activator of transcription 3 (STAT3) and plays a key role in the conversion of prostate cancer to a more aggressive phenotype (14, 15). However, it is not clear if SHMT2 is expressed in the OSCC microenvironment and whether SHMT2 is related to the prognosis of OSCC patients. In this study, we evaluate the expression levels of SHMT2 in both OSCC and oral normal mucosa and its influence on prognosis outcome. Furthermore, we related SHMT2 expression to case information of the OSCC patients we enrolled and analyzed the correlations between SHMT2 and clinical traits (16).

Immune checkpoints including programmed cell death-ligand 1 (PD-L1), V-type immunoglobulin domain-containing suppressor (VISTA), and B7-H4 have been demonstrated to be associated with the OSCC microenvironment, and ICB has become a novel immunotherapy to overcome cancer (16–19). The epithelial–mesenchymal transition (EMT) is an oncogenicity mechanism in OSCC, and Slug is one of the classical markers involved in EMT (20, 21). For the sake of investigating the correlations between SHMT2 and the OSCC microenvironment, we analyzed the association between SHMT2 expression and related markers in the OSCC microenvironment, including immune checkpoints and EMT markers, by OSCC microarrays.

MATERIALS AND METHODS

Bioinformatics Analysis

A total of 307 OSCC cases are available from The Cancer Genome Atlas (TCGA) database[1]. Meanwhile, the normalized FPKM (fragments per kilobase million) values, as corresponding expression samples originated from RNA-sequencing and Gene Expression Quantification data, were acquired from TCGA Data Portal (22). We then utilized the expression data from 2,452 genes, including the *SHMT2* gene (Ensembl ID: ENSG00000182199), and corresponding clinical characteristics of OSCC patients to construct a weighted gene co-expression network analysis (WGCNA). We used the R package "WGCNA" (version 1.68), which possesses the function of module clustering and network analysis, to perform co-expression network analysis using R software (version 3.6.1). We first preprocessed the expression sample into a format suitable for network analysis, removed obvious outlier samples with excessive numbers of missing entries, and matched the trait samples to the expression samples (23). Second, using the methods of automatic network construction and module detection, we selected $\beta = 4$ as the soft thresholding power, where co-expression similarity was raised to calculate adjacency to meet the fitness of the scale-free topology index (roughly 0.90). Meanwhile, we chose a relatively large minimum module size of 30 and a medium sensitivity (deepSplit = 2) to perform cluster splitting. Subsequently, we visualized the results of clustering using the hierarchical clustering dendrogram constructed by the R package "WGCNA" (version 1.68) (23). Third, we correlated modules clustered with external characteristics and identified the association between them, defined as gene significance (GS). Further, for each module, we defined a quantitative measure of module membership (MM) as the correlation of the module eigengenes (MEs) and the gene expression profile, allowing us to quantify the similarity of all genes on the array to every module. By plotting a scatterplot of GS vs. MM, we conducted intramodular analysis to determine the correlation between MM and GS for the most positive traits. Finally, we conducted Gene Ontology (GO) and Kyoto Encyclopedia of Genes and Genomes (KEGG) analysis for the MEs using the R package "clusterProfiler" (version 3.12.0).

Oral Squamous Cell Carcinoma Patients and Tissue Microarrays

Typical OSCC tissues and adjacent epithelial tissues, originated from OSCC patients and fixed by paraffin, were selected to punch cylindrical cores (1.5 mm) to construct OSCC and adjacent tissue microarrays. The corresponding case information of the OSCC patients has been reported as previously described (24). The OSCC and tissue microarrays consist of 176 primary OSCC samples, 25 recurrent OSCC samples, 68 metastatic lymph node samples of OSCC, 69 dysplasia tissue samples, and 42 adjacent normal oral mucosa samples. All the OSCC patients in this study signed an informed consent before surgery.

Immunochemistry Staining and Immunochemistry Scoring Analysis, Hierarchical Clustering, and Visualization

An immunochemistry experiment was performed as previously described (25). After deparaffinization and dehydration by graded ethanol, the tissues on the microarrays were subjected to antigen retrieval with citric acid buffer (pH = 6.0) in a microwave. The tissues were incubated with 3% H_2O_2 and 10% normal goat serum at 37°C for 1 h in sequence. Next, we mixed the tissues of microarrays with the diluent antibody [SHMT2, Cell Signaling Technology (CST); CKLF-like MARVEL transmembrane domain

[1]https://portal.gdc.cancer.gov/

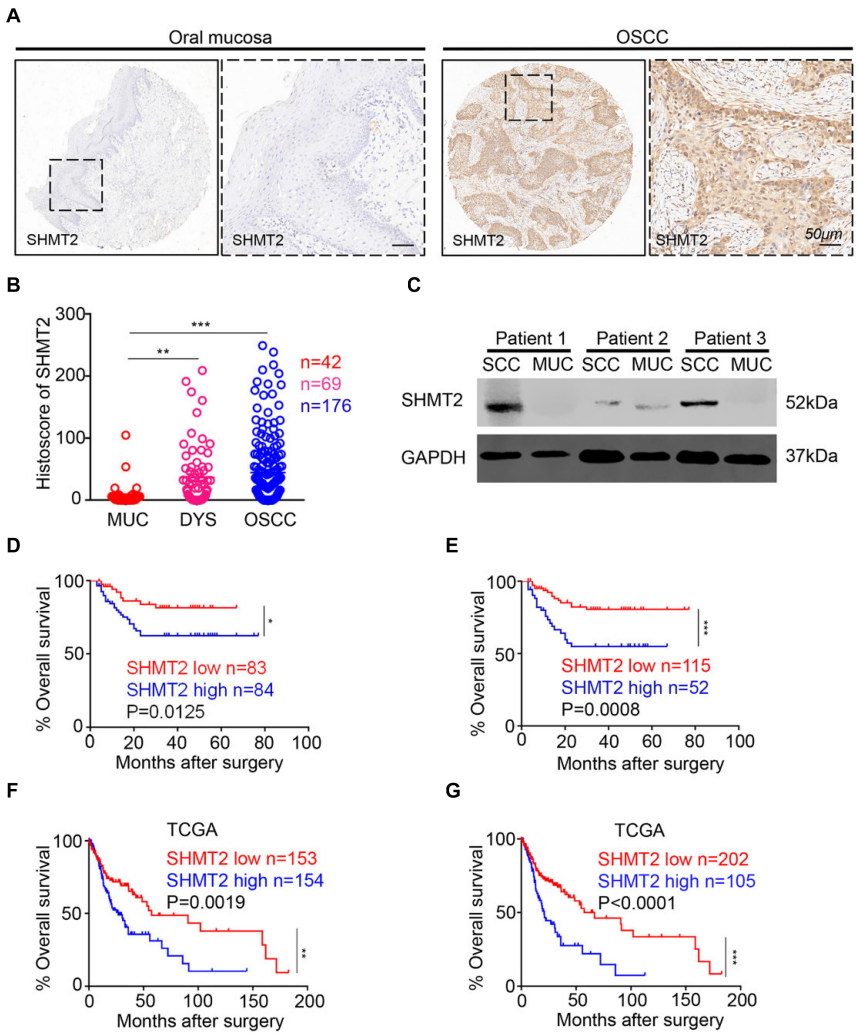

FIGURE 1 | Overexpression of serine hydroxymethyltransferase (SHMT2) in primary oral squamous cell carcinoma (OSCC). **(A)** Representative immunohistochemical staining of SHMT2 in oral mucosa (left) and primary OSCC (right). The scale bar represents 50 μm. **(B)** Histoscores of SHMT2 as SHMT2 expression levels in OSCC (n = 176), dysplasia tissue (DYS, n = 69), and normal oral mucosa (MUC, n = 42). **(C)** The expression of SHMT2 in OSCC sample and oral mucosa sample of each OSCC patient (n = 3) was shown by Western blotting, and glyceraldehyde 3-phosphate dehydrogenase (GAPDH) was defined as a loading control. **(D,E)** Kaplan–Meier survival analysis of low and high expression of SHMT2 in OSCC based on microarrays]the median value was used for **(D)**, log-rank analysis; the best cutoff value was used for **(E)**, log-rank analysis]. **(F,G)** Kaplan–Meier survival analysis of low and high expression of SHMT2 in OSCC based on The Cancer Genome Atlas (TCGA) database [the median value was used for **(F)**, log-rank analysis; the best cutoff value was used for **(G)**, log-rank analysis]. Data are represented as the mean ± SEM and analyzed by one-way ANOVA with *post hoc* Tukey test or log-rank analysis. $^{*}P < 0.05$; $^{**}P < 0.01$; $^{***}P < 0.001$.

containing 6 (CMTM6), Sigma-Aldrich; VISTA, CST; B7-H4, CST; PD-L1, CST; Slug, CST; CD317, Abcam] solution at 4°C in the refrigerator overnight. The next day, the tissues of the microarrays were mixed with the goat anti-rabbit IgG solution and avidin–biotin–peroxidase reagent solution at 37°C for 1 h in sequence. After staining with 3,3′-diaminobenzidine tetrachloride, the tissues were stained with hematoxylin again. To analyze the sample staining results, we utilized an Aperio ScanScope CS2 scanner (Vista, CA, United States) to scan the samples of microarrays and to quantify the histoscore at the area we chose from each microarray tissue using Aperio quantification software (Version 9.1) (26, 27). The detailed method for the analysis was as reported previously (25). Using Cluster 3.0, we performed hierarchical clustering analysis among SHMT2 and other correlative proteins (25). Java TreeView was applied to visualize the correlations described above (28).

Human Oral Squamous Cell Carcinoma Specimens

Three pairs of OSCC samples and normal oral mucosa samples from three OSCC patients, who received treatment or surgery at the Hospital of Stomatology of Wuhan University during October 2019∼December 2019, were prepared for protein extraction. All patients were informed of and agreed with this study before the surgery. Additionally, the Medical Ethics

TABLE 1 | Multivariate analysis for overall survival in primary OSCC patient cohort of microarrays (best cutoff value was used as a cutoff value).

Parameters	HR (95% CI)	*P*-value
Gender	0.996 (0.380∼2.609)	0.993
Age	1.640 (0.783∼3.435)	0.190
Smoking	0.999 (0.416∼2.398)	0.998
Drinking	0.587 (0.243∼1.422)	0.238
Pathological grade		
I + II vs. III	1.275 (0.514∼3.164)	0.600
Node stage		
N1 vs. N0	0.914 (0.368∼2.272)	0.846
N2 vs. N0	2.490 (0.952∼6.513)	0.063
Tumor size		
T2 vs. T1	1.202 (0.393∼3.676)	0.747
T3 vs. T1	1.675 (0.496∼5.650)	0.406
T4 vs. T1	2.101 (0.473∼9.329)	0.329
SHMT2 expression	2.474 (1.214∼5.044)	0.013*

*Cox proportional hazards regression model; HR, hazard ratio; 95% CI, 95% confidence interval; *P < 0.05. OCSS, oral squamous cell carcinoma; SHMT2, serine hydroxymethyltransferase.*

TABLE 2 | Multivariate analysis for overall survival in primary OSCC patient cohort of TCGA database (median value was used as a cutoff value).

Parameters	HR (95% CI)	*P*-value
Gender	1.044 (0.680∼1.604)	0.844
Age	1.290 (0.819∼2.034)	0.272
Race	1.148 (0.774∼1.702)	0.492
Pathological grade		
II vs. I	1.308 (0.704∼2.433)	0.396
III vs. I	1.757 (0.913∼3.381)	0.091
Node stage		
N1 vs. N0	1.050 (0.579∼1.094)	0.873
N2 vs. N0	1.733 (0.864∼3.476)	0.122
N3 vs. N0	0.000 (0.000)	0.983
Tumor size		
T2 vs. T1	2.354 (0.271∼20.407)	0.437
T3 vs. T1	4.402 (0.520∼31.441)	0.182
T4 vs. T1	3.262 (0.416∼25.564)	0.260
Stage		
Stage 2 vs. Stage 1	0.735 (0.062∼8.784)	0.808
Stage 3 vs. Stage 1	0.554 (0.051∼6.011)	0.627
Stage 4 vs. Stage 1	0.439 (0.040∼4.882)	0.503
SHMT2 expression	1.845 (1.203∼2.828)	0.005*

*Cox proportional hazards regression model; HR, hazard ratio; 95% CI, 95% confidence interval; *P < 0.05. OCSS, oral squamous cell carcinoma; SHMT2, serine hydroxymethyltransferase; TCGA, The Cancer Genome Atlas.*

Committee of the School and the Hospital of Stomatology of Wuhan University agreed with the study.

Western Blotting

We performed Western blotting according to the established protocol (29). The protein samples extracted in the experiment mentioned above were first measured by a bicinchoninic acid assay (Beyotime Biotechnology, China) to detect the protein concentrations of the samples. We used 10% polyacrylamide gel (Servicebio, Wuhan, China) to conduct electrophoresis and transferred the protein (30 mg/lane) onto a polyvinylidene fluoride (PVDF) membrane. The proteins on the PVDF membrane were blocked in 5% defatted milk (Servicebio, Wuhan, China) for 1 h at room temperature. The PVDF membrane was then placed in dilute-antibody solution [SHMT2, CST, 1:1,000; glyceraldehyde-3-phosphate dehydrogenase (GAPDH), CST, 1:1,000] at 4°C in the refrigerator overnight. In the next morning, we took the PVDF membrane out of the solution, washed it with TBST solution three times, and placed it in 5% defatted milk with goat anti-rabbit IgG (HRP-label, Proteintech, Wuhan, China) at a dilution concentration of 1:10,000 at room temperature on a shaking table for 1 h. Finally, we utilized the WesternBright Sirius Chemiluminescent Detection Kit (Advansta, San Jose, CA, United States) to detect the membrane. The experiment was performed three times.

TABLE 3 | Multivariate analysis for overall survival in primary OSCC patient cohort of TCGA database (best cutoff value was used as a cutoff value).

Parameters	HR (95% CI)	*P*-value
Gender	0.958 (0.622∼1.478)	0.848
Age	1.193 (0.751∼1.895)	0.455
Race	1.099 (0.739∼1.635)	0.642
Pathological grade		
II vs. I	1.309 (0.699∼2.450)	0.400
III vs. I	1.611 (0.831∼3.123)	0.158
Node stage		
N1 vs. N0	1.016 (0.559∼1.849)	0.958
N2 vs. N0	1.484 (0.739∼2.980)	0.267
N3 vs. N0	0.000 (0.000)	0.983
Tumor size		
T2 vs. T1	2.538 (0.289∼22.254)	0.401
T3 vs. T1	5.024 (0.636∼39.678)	0.126
T4 vs. T1	3.169 (0.404∼24.829)	0.272
Stage		
Stage 2 vs. Stage 1	0.796 (0.066∼9.604)	0.858
Stage 3 vs. Stage 1	0.515 (0.047∼5.656)	0.587
Stage 4 vs. Stage 1	0.558 (0.050∼6.212)	0.635
SHMT2 expression	2.306 (1.502∼3.542)	0.000*

*Cox proportional hazards regression model; HR, hazard ratio; 95% CI, 95% confidence interval; *P < 0.05. OSCC, oral squamous cell carcinoma; SHMT2, serine hydroxymethyltransferase; TCGA, The Cancer Genome Atlas.*

Statistical Analysis

The analyses were carried out and visualized using GraphPad Prism (version 7.0) and Statistical Product and Service Solutions (SPSS, version 20.0). We used one-way ANOVA to conduct multiple group comparisons, and we used the *t*-test to conduct two-group comparisons. We arrayed the histoscore and the FPKM value in order of size and regarded the medial value of the histoscore and FPKM value as their median value. The best cutoff value is defined as the most significant cutoff value to separate two parts from a group based on the overall survival rate. Kaplan–Meier survival and multivariate analyses were conducted as

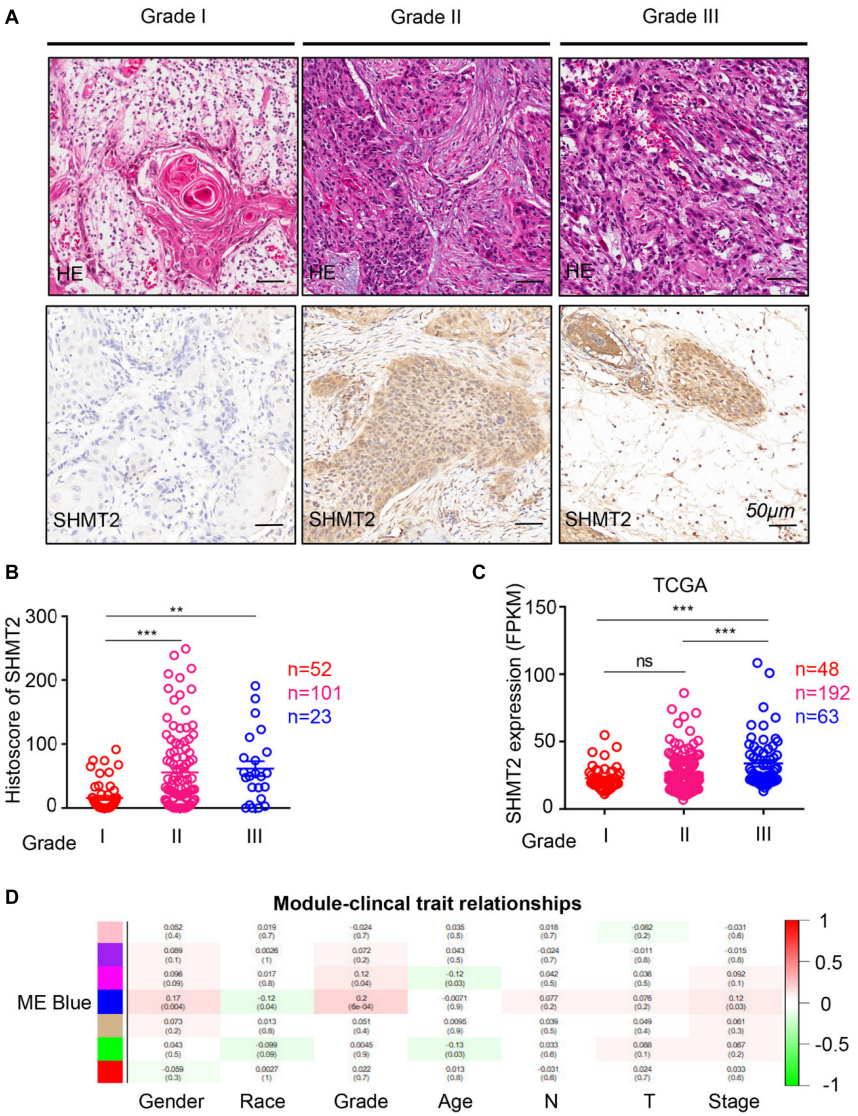

FIGURE 2 | Increased expression of serine hydroxymethyltransferase (SHMT2) of oral squamous cell carcinoma (OSCC) patients with advanced pathological grade. **(A)** Representative hematoxylin–eosin (HE, Top) and immunohistochemical staining (bottom) of SHMT2 in Grade I tissue, Grade II tissue, and Grade III tissue. The scale bar represents 50 μm. **(B)** Histoscores of SHMT2 based on microarrays among Grade I tissues (n = 52), Grade II tissues (n = 101), and Grade III tissues (n = 23). **(C)** Expression of SHMT2 in OSCC based on The Cancer Genome Atlas (TCGA) database among Grade I tissues (n = 48), Grade II tissues (n = 192), and Grade III tissues (n = 63). **(D)** Correlations between module eigengenes (the *SHMT2* gene in the blue module) and clinical traits. Each unit of the table consists of the corresponding correlation coefficient and P-value. The color scale represents the strength of the correlation. Data are represented as the mean ± SEM and analyzed by one-way ANOVA with *post hoc* Tukey's test. ns, no significance; $^{**}P < 0.01$; $^{***}P < 0.001$.

described (25). For the correlation analysis of protein expression, we conducted a two-tailed Pearson statistical analysis.

RESULTS

Overexpression of SHMT2 in Human Oral Squamous Cell Carcinoma

In this study, we utilized human OSCC tissue microarrays to investigate the expression of SHMT2 among human normal oral mucosa, dysplasia tissues, and OSCC by immunohistochemistry. As shown in **Figure 1A**, SHMT2, mostly expressed in cytoplasm, was stained in epithelial tissues and cancer cells and was rarely detected in stroma and immune cells. Meantime, lower expression of SHMT2 was detected in human normal oral mucosae compared with the expression of SHMT2 in dysplasia tissues (**Figure 1B**) and OSCC (**Figure 1B**), while there was no significant difference between dysplasia tissues and OSCC. In addition, we found that SHMT2 was indeed expressed at a high level in OSCC by comparison of the protein expression of the OSCC and normal oral mucosae of three OSCC patients (**Figure 1C**).

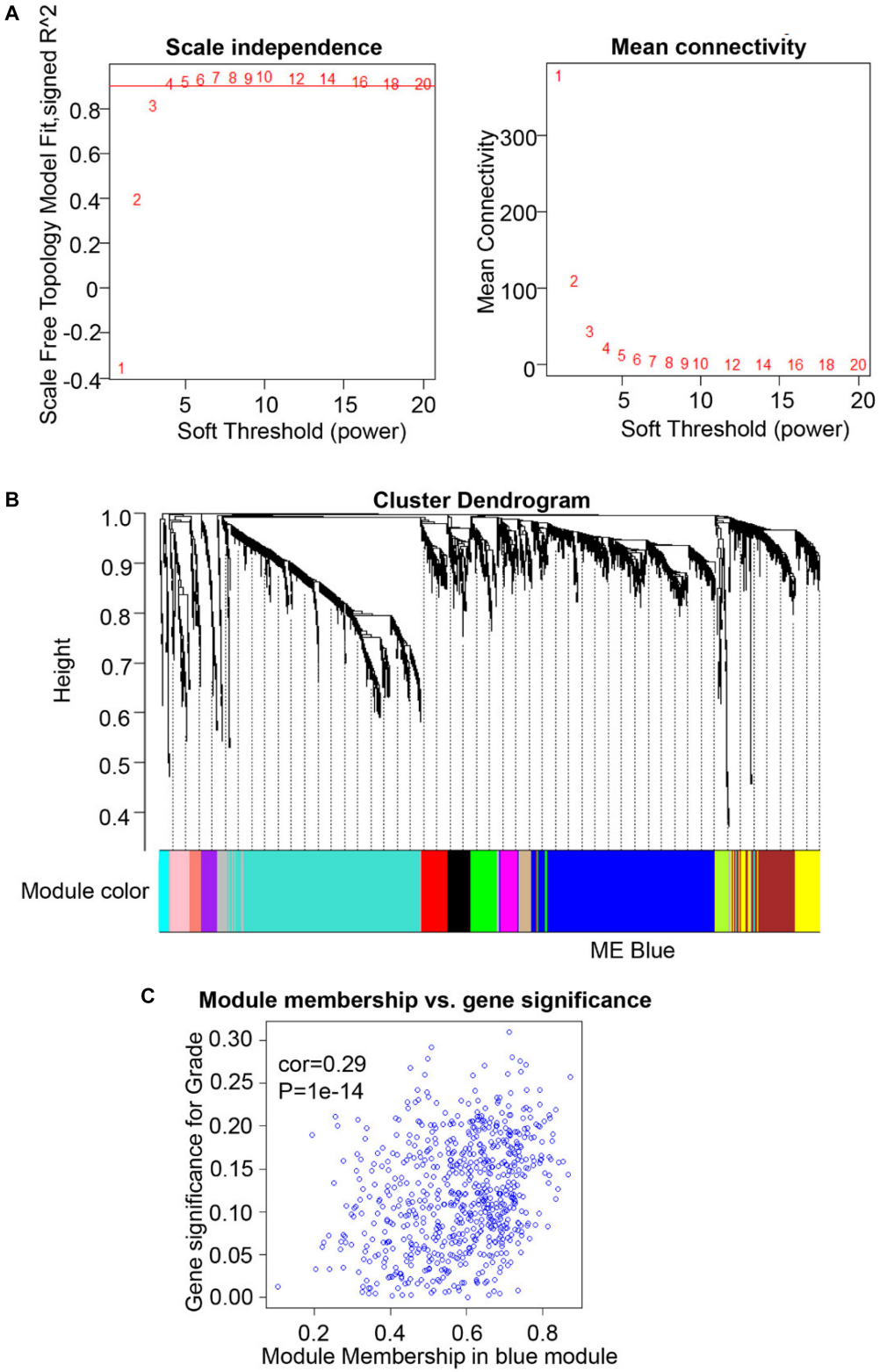

FIGURE 3 | Weighted gene co-expression network analysis (WGCNA) of serine hydroxymethyltransferase (SHMT2)-related genes. **(A)** Analysis of scale-free topology for various soft-thresholding power. We selected β = 4 as the soft thresholding power. **(B)** Dendrogram of genes was clustered based on a dissimilarity measure (1-TOM). The genes were divided into several modules. Module Blue contained the *SHMT2* gene. **(C)** Scatter plot of gene significance for grade vs. module membership in the blue module (correlation coefficient = 0.29, $P < 0.001$).

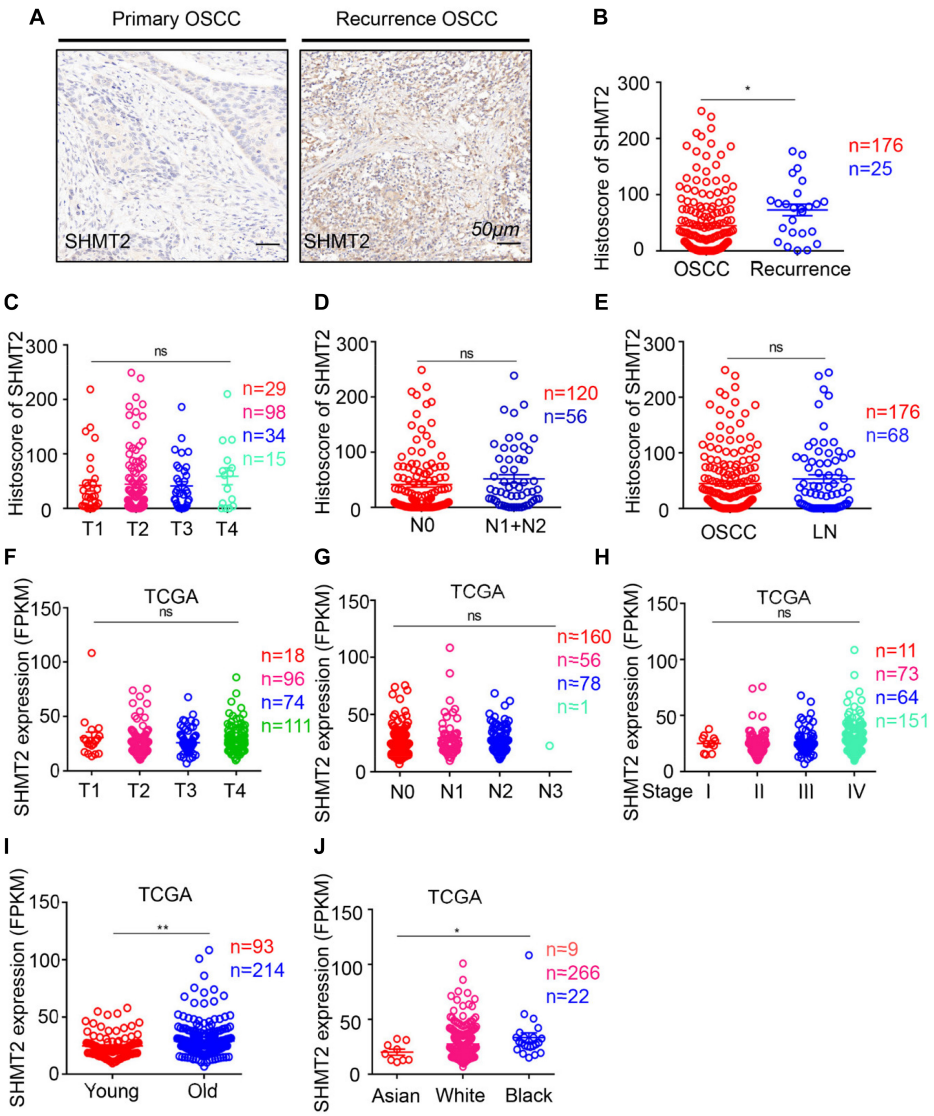

FIGURE 4 | Escalated expression of serine hydroxymethyltransferase (SHMT2) of oral squamous cell carcinoma (OSCC) patients with recurrent OSCC. **(A)** Representative immunohistochemical staining of SHMT2 in primary OSCC (left) and recurrent OSCC (right). The scale bar represents 50 μm. **(B)** Histoscores of SHMT2 based on microarrays between primary OSCC (n = 176) and recurrent OSCC (n = 25). **(C–E)** Histoscores of SHMT2 based on microarrays in different tumor sizes, lymph node stages, and lymph node metastasis. **(F–J)** Expression of SHMT2 in OSCC based on The Cancer Genome Atlas (TCGA) database in different tumor sizes, lymph node stages, clinical stages, ages, and races. Data are represented as the mean ± SEM and analyzed by unpaired t-test or one-way ANOVA with *post hoc* Tukey test. ns, no significance; *$P < 0.05$; **$P < 0.01$.

Escalated Expression of SHMT2 Indicates a Negative Prognosis of Oral Squamous Cell Carcinoma Patients

To study the influence of the expression level of SHMT2 on the prognosis of OSCC patients, we performed Kaplan–Meier survival analysis on the data from the microarrays and TCGA database. Using the median value (histoscore = 21.57) and the best cutoff value (histoscore = 49.74) of microarrays as cutoff values, respectively, the results showed that the OSCC patients with a high SHMT2 expression had a poorer survival rate in comparison with those with a low SHMT2 expression (**Figures 1D,E**). Of note, the survival analysis based on the data from TCGA database demonstrated the same results: the high SHMT2 expression of OSCC patients is associated with a poorer survival outcome compared with low SHMT2 expression of OSCC patients when the median value (FPKM = 24.64) or best cutoff value (FPKM = 28.26) was used as a cutoff value (**Figures 1F,G**).

In addition, we put the clinical information for the OSCC patient cohort of microarrays, including gender, sex, history of drinking and smoking, pathological grade, node stage, tumor size and survival outcome, and expression of SHMT2, together to construct the multivariate Cox proportional hazard model. By

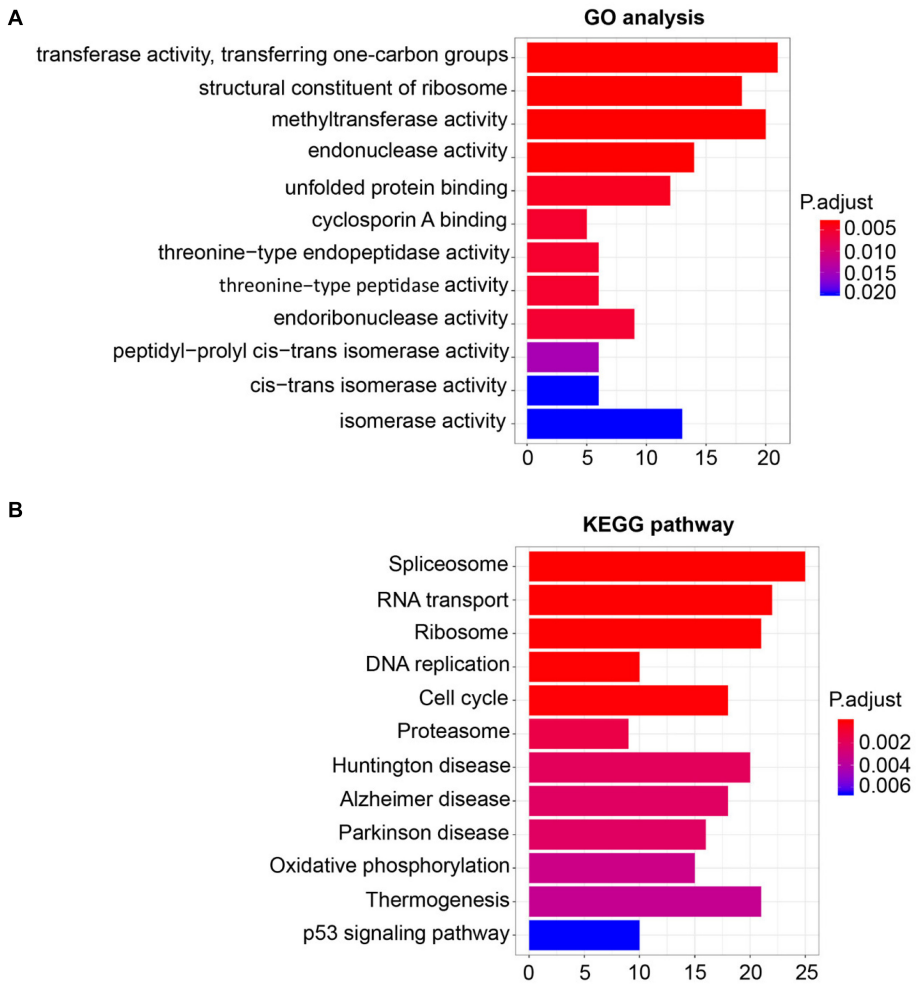

FIGURE 5 | Gene Ontology (GO) and Kyoto Encyclopedia of Genes and Genomes (KEGG) pathway enrichment analysis for module eigengenes (MEs) of the blue module. **(A)** Plot of the enrichment GO terms GO analysis for MEs of the blue module (including the *SHMT2* gene). *Y*-axis represents the GO terms. *X*-axis represents the amount of MEs of the blue module enriched in the corresponding GO terms. **(B)** Plot of the enrichment KEGG pathway KEGG analysis for MEs of the blue module. *Y*-axis represents the KEGG pathways. *X*-axis represents the amount of MEs of the blue module enriched in the corresponding KEGG pathways. *P*-values were adjusted with the false discovery rate (FDR), and the adjusted *P*-value < 0.05 was the boundary to select GO terms and KEGG pathways.

multivariate analysis and using the best cutoff value, the results showed that escalated expression of SHMT2 was related to poor prognosis in OSCC (**Table 1**). Moreover, we utilized acquired data from TCGA database to reconstruct the multivariate Cox proportional hazard model, and the results of the multivariate analysis suggest that SHMT2 is a negative prognosis marker of OSCC patients (**Tables 2**, **3**).

Expression Level of SHMT2 Is Associated With Pathological Grades and Recurrence of Oral Squamous Cell Carcinoma Among Oral Squamous Cell Carcinoma Patients

To compare the SHMT2 expression of OSCC patients with different pathological grades based on microarrays and TCGA database, we used one-way ANOVA with a *post hoc* Tukey's test and clearly observed that SHMT2 expression was related to different pathological grades (**Figures 2A–C**). According to the microarray data, the SHMT2 expression of OSCC patients with Grade I was significantly different from the expression in patients with Grade II and Grade III (**Figure 2B**), while the SHMT2 expression levels of OSCC patients with Grade I and Grade II were lower than those with Grade III according to TCGA database (**Figure 2C**). These results suggest that overexpression of SHMT2 of OSCC patients is related to advanced pathological grade. Furthermore, we utilized a transcription matrix of 2,452 genes, including the gene encoding SHMT2, acquired from TCGA database, to perform WGCNA (**Figures 3A–C**). Intriguingly, the outcome shows that Module Blue, which contains SHMT2, was strongly correlated with gender, tumor stage, and especially pathological grade (**Figure 2D**).

Moreover, to determine the correlation between the SHMT2 and other clinical characteristics, we quantified the expression of

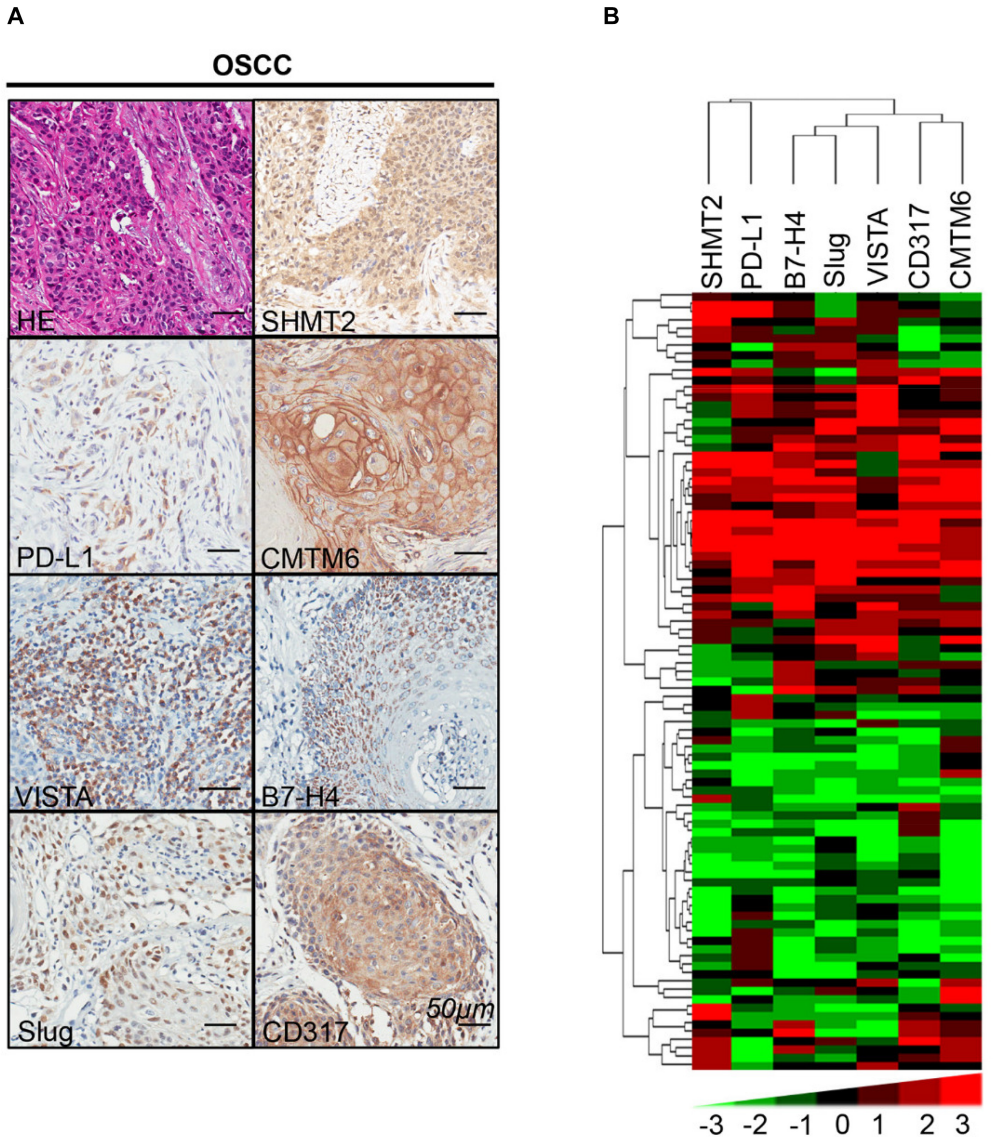

FIGURE 6 | Correlations among serine hydroxymethyltransferase (SHMT2), programmed cell death-ligand 1 (PD-L1), CKLF-like MARVEL transmembrane domain containing 6 (CMTM6), V-type immunoglobulin domain-containing suppressor (VISTA), B7-H4, Slug, and CD317 in the oral squamous cell carcinoma (OSCC) microenvironment. **(A)** Representative hematoxylin–eosin and immunohistochemical staining of SHMT2, PD-L1, CMTM6, VISTA, B7-H4, Slug, and CD317 in OSCC. The scale bar represents 50 μm. **(B)** Strongly positive correlations among SHMT2, PD-L1, CMTM6, VISTA, B7-H4, Slug, and CD317 in OSCC shown by hierarchical clustering. The color scale represents the levels of histoscores.

SHMT2 by an immunochemistry scoring system and evaluated the differences in the target protein expression associated with different clinical traits. According to the microarray data, we identified a positive significance between increasing expression of SHMT2 and recurrent OSCC (**Figures 4A,B**), and there was no distinct difference in target protein expression among different tumor sizes (**Figure 4C**), lymph node stages (**Figure 4D**), and lymph node metastasis (**Figure 4E**). Coincidentally, an analysis based on the OSCC cases from TCGA database shows the similar consequence that there was no significance of SHMT2 expression among diverse tumor sizes (**Figure 4F**), lymph node stages (**Figure 4G**), and clinical stages (**Figure 4H**) but demonstrates that both age (**Figure 4I**) and race (**Figure 4J**) are correlated with SHMT2 expression to a certain extent.

Gene Ontology and Kyoto Encyclopedia of Genes and Genomes Analysis

For the sake of deeply detecting of the function of SHMT2, we utilized all genes of Module Blue to perform GO and KEGG analyses (30). As exhibited in **Figure 5A**, the most relative functions with the module genes, including SHMT2, include transferase activity transferring one-carbon groups, methyltransferase activity, and structural constituent

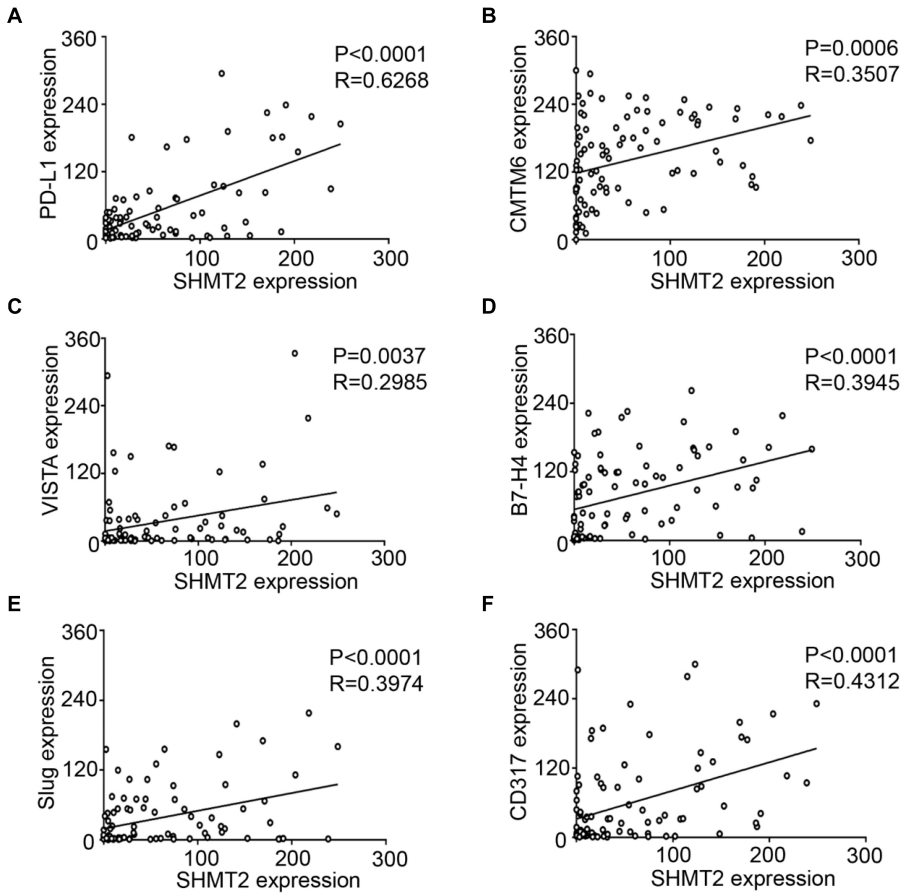

FIGURE 7 | Statistical analysis of correlations among serine hydroxymethyltransferase (SHMT2), programmed cell death-ligand 1 (PD-L1), CKLF-like MARVEL transmembrane domain containing 6 (CMTM6), V-type immunoglobulin domain-containing suppressor (VISTA), B7-H4, Slug, and CD317 in the oral squamous cell carcinoma (OSCC) microenvironment. **(A–F)** The positive correlations among SHMT2 and PD-L1, CMTM6, VISTA, B7-H4, Slug, and CD317 in the OSCC microenvironment.

of ribosome. Interestingly, by KEGG analysis, SHMT2-related genes were associated with some oncogenicity pathways, such as DNA replication, cell cycle, and especially the p53 signaling pathway (**Figure 5B**).

Positive Correlations Among SHMT2 and PD-L1, CMTM6, VISTA, B7-H4, Slug, and CD317 in Oral Squamous Cell Carcinoma

We found that SHMT2 expression was associated with related markers in the OSCC microenvironment (**Figures 6A,B**). The scatter plot shows that SHMT2 was strongly correlated with PD-L1 (**Figure 7A**), CMTM6 (**Figure 7B**), VISTA (**Figure 7C**), B7-H4 (**Figure 7D**), Slug (**Figure 7E**), and CD317 (**Figure 7F**) in OSCC patients. Of note, Slug is one of the protein markers involved in EMT, suggesting that SHMT2 may be involved in EMT or may be related to EMT in OSCC (20). Moreover, a high expression of SHMT2 is associated with increasing expression of some immune checkpoints, such as PD-L1 and VISTA, in OSCC, reflecting that SHMT2 is related to immune signaling in the OSCC microenvironment.

DISCUSSION

Being essential for a series of anabolic pathways, serine and glycine have been shown to be significant for the Warburg effect in cancer (31). Also, as an enzyme transferring serine and tetrahydrofolate into glycine and 5,10-methylenetetrahydrofolate, SHMT catalyzes the reaction that is required for *de novo* nucleotide biosynthesis and DNA methylation (31, 32). Owing to these characteristics, both SHMT isoforms including SHMT1 and SHMT2 play a key role in chemotherapeutic intervention (32). In the one hand, SHMT1, mostly located in the cytoplasm, regulates the partitioning of one-carbon units between deoxythymidine monophosphate (dTMP) and methionine (33). On the other hand, SHMT2, which exists in mitochondria, is more likely to give priority to take part in the synthesis of mitochondrial dTMP (32). In addition, SHMT2, as an enzyme involved in the metabolism of serine, is involved in tumorigenicity mediated *via* glycine (10, 34). However, the association between SHMT2 and clinical and pathological characteristics of OSCC has yet to be elucidated. In this article, we found an elevated expression of SHMT2 in OSCC

compared to normal oral mucosa and a poor overall survival rate of OSCC patients with high SHMT2 expression. Of note, SHMT2 as an independent biomarker can indicate the prognosis of an OSCC patient cohort. More specifically, an escalated expression level of SHMT2 is related to a negative prognosis consequence in OSCC. In contrast, OSCC patients with a lower SHMT2 expression possess higher overall survival rates and better prognoses, similar with the results in breast cancer. These findings suggested that SHMT2, the high expression of which can slow down the process of glycolysis and augment the ratio of lactate and pyruvate, plays a vital role in the transition of PKM2, resulting in the glycolytic metabolic shift (10, 15, 34). It is known that one of the OSCC microenvironment features is hypoxia and that normal epithelial cells cannot adjust at poor oxygen pressure, so a high expression of SHMT2 may promote tumor cell survival for a long time in the OSCC microenvironment (9). Moreover, it is exactly that SHMT2 in mitochondria, not SHMT1 in the cytoplasm, was expressed highly in rapidly proliferating cancer cells (31, 35). When SHMT2 was inhibited, the proliferation of cancer cells was subsequently inhibited (31, 35).

In addition, an increasing expression of SHMT2 in OSCC is associated with advanced pathological grade and recurrent OSCC. In TCGA database, black people and aged individuals with OSCC are correlated with high expression levels of SHMT2 compared with Asians and young individuals, respectively. This discovery matched the previous finding that the role of the STAT3/SHMT2/PKM2 loop was found to convert prostate cancer to a more aggressive phenotype (34). Thus far, high expression levels of SHMT2 have been discovered in glioma and hepatocellular carcinoma (10, 12). SHMT2 expression was correlated with pathological grade, cell proliferation, migration, and EMT in hepatocellular carcinoma (12). Hence, gradually increasing levels of SHMT2 expression indicate a poor pathological state and one of the factors explaining why high SHMT2 expression represents a poor prognosis. These findings demonstrated that SHMT2 was correlated with tumors, particularly OSCC. Moreover, it has been proved that downregulation of SHMT2 can inhibit tumor occurrence rate and growth (34).

In our study, SHMT2 was found to be not only a biomarker of prognosis in OSCC but also a bridge correlating metabolic glycolysis with related markers of OSCC. In detail, SHMT2 was correlated with PD-L1, CMTM6, VISTA, B7-H4, Slug, and CD317 in the OSCC microenvironment. On the one hand, PD-L1, VISTA, and B7-H4 were correlated with the OSCC microenvironment, and their high expression indicates a suppressive status in OSCC (16–18). Additionally, CMTM6 is an important protein involved in the regulation of PD-L1, and CD317 is associated with B7-H4 and PD-L1 (36, 37). On the other hand, Slug is one of the classical markers related to EMT (20). The existence of EMT and immune checkpoints is significant for tumor escape (20, 38–40). Taken together, the correlations among SHMT2 and the related markers described above in OSCC may indicate a suppressive or impaired immune system preventing cancer cells from being attacked by T cells. Hence, the role and correlation of SHMT2 in the OSCC microenvironment possibly promote cancer cell growth in OSCC and lead to the poor prognosis of OSCC patients. Interestingly, SHMT2-related genes are associated with DNA replication, cell cycle, and the p53 signaling pathway of OSCC patients from TCGA database.

To conclude, SHMT2, as an independent marker indicating prognosis, was highly expressed in OSCC patients, and overexpression of SHMT2 was found in advanced OSCC and recurrent OSCC. Moreover, SHMT2 is involved in some processes of tumorigenesis and is related to PD-L1, CMTM6, VISTA, B7-H4, Slug, and CD317 expression in the tumor microenvironment of OSCC. We still require more research into SHMT2 as an enzyme involved in glycolysis to determine what role SHMT2 plays in the OSCC microenvironment and the specific mechanism between SHMT2 and the immune microenvironment in OSCC.

DATA AVAILABILITY STATEMENT

The raw data supporting the conclusion of this article will be made available by the authors, without undue reservation.

ETHICS STATEMENT

The studies involving human participants were reviewed and approved by the School and Hospital of Stomatology Wuhan University Medical Ethics Committee. Written informed consent to participate in this study was provided by the participants' legal guardian/next of kin. Written informed consent was obtained from the individual(s), and minor(s)' legal guardian/next of kin, for the publication of any potentially identifiable images or data included in this article.

AUTHOR CONTRIBUTIONS

Z-ZW contributed to the conception, design, data acquisition, and analysis, and drafted and critically revised the manuscript. SW, Q-CY, X-LW, and L-LY contributed to data acquisition and critically revised the manuscript. BL and Z-JS contributed to conception, data analysis, and interpretation, and drafted and critically revised the manuscript. All authors gave final approval and agreed to be accountable for all aspects of the study.

FUNDING

This study was supported by the National Nature Science Foundation of China 81872203, 81874131, and 81672668. Z-JS was supported by Fundamental Research Funds for the Central Universities of China 2042017kf0171 (Outstanding Young Scholars) and Hubei Province Nature Science Funds for Distinguished Young Scholar 2017CFA062.

ACKNOWLEDGMENTS

We appreciate all the patients participating in this study.

REFERENCES

1. Chi AC, Day TA, Neville BW. Oral cavity and oropharyngeal squamous cell carcinoma–an update. *CA Cancer J Clin.* (2015) 65:401–21. doi: 10.3322/caac.21293
2. Perera M, Al-Hebshi NN, Perera I, Ipe D, Ulett GC, Speicher DJ, et al. Inflammatory bacteriome and oral squamous cell carcinoma. *J Dent Res.* (2018) 97:725–32. doi: 10.1177/0022034518767118
3. Torre LA, Bray F, Siegel RL, Ferlay J, Lortet-Tieulent J, Jemal A. Global cancer statistics, 2012. *CA Cancer J Clin.* (2015) 65:87–108. doi: 10.3322/caac.21262
4. Chow LQM, Haddad R, Gupta S, Mahipal A, Mehra R, Tahara M, et al. Antitumor activity of pembrolizumab in biomarker-unselected patients with recurrent and/or metastatic head and neck squamous cell carcinoma: results from the Phase Ib KEYNOTE-012 expansion cohort. *J Clin Oncol.* (2016) 34:3838–45. doi: 10.1200/jco.2016.68.1478
5. Ferris RL, Blumenschein G Jr., Fayette J, Guigay J, Colevas AD, Licitra L, et al. Nivolumab for recurrent squamous-cell carcinoma of the head and neck. *N Engl J Med.* (2016) 375:1856–67. doi: 10.1056/NEJMoa1602252
6. Neal JT, Li X, Zhu J, Giangarra V, Grzeskowiak CL, Ju J, et al. Organoid Modeling of the tumor immune microenvironment. *Cell.* (2018) 175:1972–88.e16. doi: 10.1016/j.cell.2018.11.021
7. Kang H, Kiess A, Chung CH. Emerging biomarkers in head and neck cancer in the era of genomics. *Nat Rev Clin Oncol.* (2015) 12:11–26. doi: 10.1038/nrclinonc.2014.192
8. Hill SJ, D'Andrea AD. Predictive potential of head and neck squamous cell carcinoma organoids. *Cancer Discov.* (2019) 9:828–30. doi: 10.1158/2159-8290.Cd-19-0527
9. Vito A, El-Sayes N, Mossman K. Hypoxia-driven immune escape in the tumor microenvironment. *Cells.* (2020) 9:992. doi: 10.3390/cells9040992
10. Wang B, Wang W, Zhu Z, Zhang X, Tang F, Wang D, et al. Mitochondrial serine hydroxymethyltransferase 2 is a potential diagnostic and prognostic biomarker for human glioma. *Clin Neurol Neurosurg.* (2017) 154:28–33. doi: 10.1016/j.clineuro.2017.01.005
11. Hebbring SJ, Chai Y, Ji Y, Abo RP, Jenkins GD, Fridley B, et al. Serine hydroxymethyltransferase 1 and 2: gene sequence variation and functional genomic characterization. *J Neurochem.* (2012) 120:881–90. doi: 10.1111/j.1471-4159.2012.07646.x
12. Ji L, Tang Y, Pang X, Zhang Y. Increased expression of serine hydroxymethyltransferase 2 (SHMT2) is a negative prognostic marker in patients with hepatocellular carcinoma and is associated with proliferation of HepG2 cells. *Med Sci Monit.* (2019) 25:5823–32. doi: 10.12659/MSM.915754
13. Ning S, Ma S, Saleh AQ, Guo L, Zhao Z, Chen Y. SHMT2 overexpression predicts poor prognosis in intrahepatic cholangiocarcinoma. *Gastroenterol Res Pract.* (2018) 2018:4369253. doi: 10.1155/2018/4369253
14. Yang X, Wang Z, Li X, Liu B, Liu M, Liu L, et al. SHMT2 desuccinylation by SIRT5 drives cancer cell proliferation. *Cancer Res.* (2018) 78:372–86. doi: 10.1158/0008-5472.CAN-17-1912
15. Marrocco I, Altieri F, Rubini E, Paglia G, Chichiarelli S, Giamogante F, et al. Shmt2: a Stat3 signaling new player in prostate cancer energy metabolism. *Cells.* (2019) 8:1048. doi: 10.3390/cells8091048
16. Wu L, Deng W, Huang C, Bu L-L, Yu G, Mao L, et al. Expression of VISTA correlated with immunosuppression and synergized with CD8 to predict survival in human oral squamous cell carcinoma. *Cancer Immunol Immunother.* (2017) 66:627–36. doi: 10.1007/s00262-017-1968-0
17. Yu GT, Bu LL, Huang CF, Zhang WF, Chen WJ, Gutkind JS, et al. PD-1 blockade attenuates immunosuppressive myeloid cells due to inhibition of CD47/SIRPα axis in HPV negative head and neck squamous cell carcinoma. *Oncotarget.* (2015) 6:42067–80. doi: 10.18632/oncotarget.5955
18. Wu L, Deng W, Yu G, Mao L, Bu L, Ma S, et al. B7-H4 expression indicates poor prognosis of oral squamous cell carcinoma. *Cancer Immunol Immunother.* (2016) 65:1035–45. doi: 10.1007/s00262-016-1867-9
19. Chow LQM. Head and neck cancer. *N Engl J Med.* (2020) 382:60–72. doi: 10.1056/NEJMra1715715
20. Ye X, Tam WL, Shibue T, Kaygusuz Y, Reinhardt F, Ng Eaton E, et al. Distinct EMT programs control normal mammary stem cells and tumour-initiating cells. *Nature.* (2015) 525:256–60. doi: 10.1038/nature14897
21. Puram SV, Tirosh I, Parikh AS, Patel AP, Yizhak K, Gillespie S, et al. Single-cell transcriptomic analysis of primary and metastatic tumor ecosystems in head and neck cancer. *Cell.* (2017) 171:e24. doi: 10.1016/j.cell.2017.10.044
22. Liu T, Li C, Jin L, Li C, Wang L. The prognostic value of m6A RNA methylation regulators in colon adenocarcinoma. *Med Sci Monitor.* (2019) 25:9435–45. doi: 10.12659/msm.920381
23. Zhang B, Horvath S. A general framework for weighted gene co-expression network analysis. *Stat Appl Genet Mol Biol.* (2005) 4:17. doi: 10.2202/1544-6115.1128
24. Wu CC, Li H, Xiao Y, Yang LL, Chen L, Deng WW, et al. Over-expression of IQGAP1 indicates poor prognosis in head and neck squamous cell carcinoma. *J Mol Histol.* (2018) 49:389–98. doi: 10.1007/s10735-018-9779-y
25. Yang Q-C, Wu C-C, Cao L-Y, Xiao Y, Li H, Liu B, et al. Increased expression of LAMTOR5 predicts poor prognosis and is associated with lymph node metastasis of head and neck squamous cell carcinoma. *Int J Med Sci.* (2019) 16:783–92. doi: 10.7150/ijms.33415
26. Sun ZJ, Zhang L, Hall B, Bian Y, Gutkind JS, Kulkarni AB. Chemopreventive and chemotherapeutic actions of mTOR inhibitor in genetically defined head and neck squamous cell carcinoma mouse model. *Clin Cancer Res.* (2012) 18:5304–13. doi: 10.1158/1078-0432.Ccr-12-1371
27. Kirkegaard T, Edwards J, Tovey S, McGlynn LM, Krishna SN, Mukherjee R, et al. Observer variation in immunohistochemical analysis of protein expression, time for a change? *Histopathology.* (2006) 48:787–94. doi: 10.1111/j.1365-2559.2006.02412.x
28. Saldanha AJ. Java treeview–extensible visualization of microarray data. *Bioinformatics.* (2004) 20:3246–8. doi: 10.1093/bioinformatics/bth349
29. Xiong H, Li H, Xiao Y, Yang Q, Yang L, Chen L, et al. Long noncoding RNA MYOSLID promotes invasion and metastasis by modulating the partial epithelial-mesenchymal transition program in head and neck squamous cell carcinoma. *J Exp Clin Cancer Res.* (2019) 38:278. doi: 10.1186/s13046-019-1254-4
30. Li H, Su Q, Li B, Lan L, Wang C, Li W, et al. High expression of WTAP leads to poor prognosis of gastric cancer by influencing tumour-associated T lymphocyte infiltration. *J Cell Mol Med.* (2020) 24:4452–65. doi: 10.1111/jcmm.15104
31. di Salvo ML, Contestabile R, Paiardini A, Maras B. Glycine consumption and mitochondrial serine hydroxymethyltransferase in cancer cells: the heme connection. *Med Hypotheses.* (2013) 80:633–6. doi: 10.1016/j.mehy.2013.02.008
32. Amelio I, Cutruzzolá F, Antonov A, Agostini M, Melino G. Serine and glycine metabolism in cancer. *Trends Biochem Sci.* (2014) 39:191–8. doi: 10.1016/j.tibs.2014.02.004
33. MacFarlane AJ, Perry CA, McEntee MF, Lin DM, Stover PJ. Shmt1 heterozygosity impairs folate-dependent thymidylate synthesis capacity and modifies risk of Apcmin-mediated intestinal cancer risk. *Cancer Res.* (2011) 71:2098–107. doi: 10.1158/0008-5472.Can-10-1886
34. Woo CC, Chen WC, Teo XQ, Radda GK, Lee PT. Downregulating serine hydroxymethyltransferase 2 (SHMT2) suppresses tumorigenesis in human hepatocellular carcinoma. *Oncotarget.* (2016) 7:53005–17. doi: 10.18632/oncotarget.10415
35. Jain M, Nilsson R, Sharma S, Madhusudhan N, Kitami T, Souza AL, et al. Metabolite profiling identifies a key role for glycine in rapid cancer cell proliferation. *Science.* (2012) 336:1040–4. doi: 10.1126/science.1218595
36. Yang LL, Wu L, Yu GT, Zhang WF, Liu B, Sun ZJ. CD317 signature in head and neck cancer indicates poor prognosis. *J Dent Res.* (2018) 97:787–94. doi: 10.1177/0022034518758604
37. Chen L, Yang QC, Li YC, Yang LL, Liu JF, Li H, et al. Targeting CMTM6 suppresses stem cell-like properties and enhances antitumor immunity in head and neck squamous cell carcinoma. *Cancer Immunol Res.* (2020) 8:179–91. doi: 10.1158/2326-6066.CIR-19-0394

38. Adams S, Gatti-Mays ME, Kalinsky K, Korde LA, Sharon E, Amiri-Kordestani L, et al. Current landscape of immunotherapy in breast cancer. *JAMA Oncol.* (2019) 5:1205–14. doi: 10.1001/jamaoncol.2018.7147
39. Dongre A, Weinberg RA. New insights into the mechanisms of epithelial-mesenchymal transition and implications for cancer. *Nat Rev Mol Cell Biol.* (2019) 20:69–84. doi: 10.1038/s41580-018-0080-4
40. Auslander N, Zhang G, Lee JS, Frederick DT, Miao B, Moll T, et al. Robust prediction of response to immune checkpoint blockade therapy in metastatic melanoma. *Nat Med.* (2018) 24:1545–9. doi: 10.1038/s41591-018-0157-9

Conflict of Interest: The authors declare that the research was conducted in the absence of any commercial or financial relationships that could be construed as a potential conflict of interest.

frontiers in Oncology

ORIGINAL RESEARCH
published: 15 October 2020
doi: 10.3389/fonc.2020.541878

Role of Heterotypic Neutrophil-in-Tumor Structure in the Prognosis of Patients With Buccal Mucosa Squamous Cell Carcinoma

Jie Fan[1,2†], Qigen Fang[1†], Yang Yang[3], Meng Cui[1], Ming Zhao[1], Jinxing Qi[1], Ruihua Luo[1], Wei Du[1,4], Shanting Liu[1*] and Qiang Sun[2*]*

[1] Department of Head Neck and Thyroid Surgery, Affiliated Cancer Hospital of Zhengzhou University, Henan Cancer Hospital, Zhengzhou, China, [2] Laboratory of Cell Engineering, Institute of Biotechnology, Beijing, China, [3] Department of Nephrology, The First Affiliated Hospital of Zhengzhou University, Zhengzhou, China, [4] Department of Anatomy, Zhengzhou University, Zhengzhou, China

OPEN ACCESS

Edited by:
Paolo Bossi,
University of Brescia, Italy

Reviewed by:
Tommaso Gualtieri,
Civil Hospital of Brescia, Italy
Stefania Staibano,
University of Naples Federico II, Italy

****Correspondence:***
Wei Du
ddww@zzu.edu.cn
Shanting Liu
liushanting@163.com
Qiang Sun
sunq@bmi.ac.cn

[†]These authors have contributed equally to this work

Specialty section:
This article was submitted to Head and Neck Cancer, a section of the journal Frontiers in Oncology

Received: *10 March 2020*
Accepted: *28 September 2020*
Published: *15 October 2020*

Citation:
Fan J, Fang Q, Yang Y, Cui M, Zhao M, Qi J, Luo R, Du W, Liu S and Sun Q (2020) Role of Heterotypic Neutrophil-in-Tumor Structure in the Prognosis of Patients With Buccal Mucosa Squamous Cell Carcinoma. Front. Oncol. 10:541878. doi: 10.3389/fonc.2020.541878

Objective: To analyze the role of frequency of heterotypic neutrophil-in-tumor structure (FNiT) in the prognosis of patients with buccal mucosa squamous cell carcinoma (BMSCC).

Methods: *In vitro*, we cocultured BMSCC cell line-H157 with neutrophils to form heterotypic neutrophil-in-tumor structures, which were then subject to fluorescence staining. Clinically, 145 patients were retrospectively enrolled. Associations between FNiT and clinicopathological variables including age, sex, smoking history, drinking history, betel nut chewing, tumor stage, node stage, metastasis, disease stage, lymphovascular invasion, extranodal extension, perineural invasion, and tumor grade were analyzed by chi-square test, and the main endpoints of interest were recurrence-free survival (RFS) and disease-specific survival (DSS) which were analyzed by the Kaplan-Meier method and Cox model.

Results: Fluorescent staining results of typical heterotypic neutrophil-in-tumor structure showed that well-differentiated H157 cells had a stronger ability to internalize more neutrophils than poorly-differentiated H157 cells, with the latter often internalizing only one neutrophil or nothing. The mean FNiT was 4.2‰, with a range from 2.3‰ to 7.8‰. A total of 80 patients relapsed and 84 patients died of the disease. The 5-year RFS and DSS rate was 42% and 42%, respectively. Patients with an FNiT≥4.2‰ had a significantly higher risk for locoregional recurrence and cancer-caused death than those with an FNiT<4.2‰ ($p=0.001$ and $p<0.001$, respectively). The FNiT alone was independently significant in predicting poor RFS, and the FNiT along with tumor grade was an independent predictor for DSS.

Conclusion: The FNiT as a novel predictor is significantly negatively associated with both the RFS and DSS of patients with BMSCC.

Keywords: cell-in-cell, frequency of heterotypic neutrophil-in-tumor structure, buccal mucosa squamous cell carcinoma, prognosis, recurrence-free survival, disease-specific survival

INTRODUCTION

Cell-in-cell (CIC) is an evolutionarily conserved cytobiological phenomenon (1, 2), which was first reported 150 years ago by a German scholar (3). It refers to the presence of one or more living cells within another living one and has ever since been found in varieties of tumors tissues, such as breast carcinoma (4, 5), pancreatic ductal adenocarcinoma (6), and head and neck squamous cell carcinoma (HNSCC) (7) and the like. CIC has two typical forms: one is homotypic CIC, and the other is heterotypic CIC, with the latter often occurring between tumor cells and immune cells that include neutrophils (8). Neutrophils are the most well-known marker and promoter of inflammation (9). Recent findings have indicated that inflammation, metabolic response, and immune response are the three main components of tumor microenvironment, which are of significance in cancer pathogenesis and progression by interacting with tumor cells (9–13). Several chemokines, cytokines and angiogenic factors produced by neutrophils may result in inflammatory cell recruitment and activation that crucially impact the tumor microenvironment, which could facilitate tumor cell proliferation, microvascular regeneration and tumor progression (9, 14, 15). The formation of CIC structure in tumors is a functional result of active intercellular interactions within heterogeneous tumor microenvironments, which is driven by a set of core molecular elements (16, 17) that are regulated by multiple factors, such as cholesterol and IL-8 (18–21).

Neutrophil-in-tumor (NiT) structures, previously found in HNSCC, are typical heterotypic CIC structures (hCIC), which refer to the presence of living neutrophils inside living tumor cells (7, 22, 23). The FNiT is defined as the **f**requency of heterotypic NiT structures formation and is calculated by the total number of NiT structures divided by the total number of tumor cells, reflecting the severity of tumor-infiltrating neutrophils in the tumor microenvironment based on our previous studies. Some clinical researches with limited cases had preliminarily found that NiT structures were associated with poor prognosis in patients with HNSCC (7, 23). However, the prognostic role of the FNiT in patients with BMSCC remained unclear.

MATERIALS AND METHODS

In Vitro Study

Cells and Culture Conditions

H157 cells were maintained in Dulbecco's modified Eagle's medium supplemented with 10% fetal bovine serum (PAN-Biotech). Approximately 1×10^5 H157 cells were adherently cultured in 12-well plates. Neutrophils were maintained in RPMI-1640 supplemented with 10% fetal bovine serum (PAN-Biotech). Approximately 1×10^6 neutrophils were cultured in suspension in a 10-cm dish.

Abbreviations: FNiT, Frequency of heterotypic neutrophil-in-tumor structure; BMSCC, Buccal mucosa squamous cell carcinoma; HNSCC, Head and neck squamous cell carcinoma.

Heterotypic CIC Formation Assay

Briefly, approximately 1×10^5 H157 cells were adherently cultured in 12-well plates for 8 h. Then, neutrophils and H157 cells were cocultured for 8 h. Cytospins were then made by centrifugation at 800 rpm for 4 min. Then, the cells were fixed and underwent both Phalloidin-568 and Hoechst staining to quantify hCIC structures. The presence of internalized cells wrapped by one outer cell was considered as one hCIC structure.

Fluorescence Staining

First, neutrophils were stained with CellTracker Green (Invitrogen). Second, cytospins were fixed in 4% paraformaldehyde and then proceeded to both routine Phalloidin-568 (Life) and Hoechst (Thermo) staining for 30 min before being mounted with Prolong Gold antifade reagent (Invitrogen). Confocal images were captured and processed by the Ultraview Vox confocal system (Perkin Elmer) on Nikon Ti-E microscope.

Retrospective Case Series Study

Patients and Methods

The Institutional Research Committee of Henan Cancer Hospital approved our study. All patients participating in the study signed an informed consent agreement for medical research before initial treatment, and all methods were performed in accordance with relevant guidelines and regulations.

From March 2009 to October 2018, we conducted a retrospective study on 145 patients (≥29 years old) with previously untreated history undergoing radical resection of BMSCC (RRB). Of the enrolled patients, no one had synchronous head and neck carcinoma, immunological disorders, or previous chemotherapy and/or radiation of the head and neck area. Data regarding age, sex, smoker, drinker, betel nut chewing, FNiT, tumor stage, node stage, metastasis, disease stage, lymphovascular invasion, extranodal extension, perineural invasion, tumor grade, postoperative pathological report, operation record, adjuvant treatment, and follow-up information were extracted and analyzed. All pathologic sections made from primary tumor were re-evaluated *via* immunohistochemistry. In our cancer center, preoperative ultrasound and CT or MRI were routinely performed. The disease stage was defined based on the AJCC 8th edition staging system, and the tumor grade was categorized according to the 2017 classification of the WHO. In addition, frozen sectioning of the primary tumor was routinely performed; if the pathology was malignant, a RRB was performed.

The FNiT was observed and calculated in the pathologic sections of BMSCC. The cutoff value calculated from the ROC curve, mean, tertile, or median in previous studies varied. Thus, the standard cutoff value remains unknown. In the current study, the cutoff value was defined as the mean value of the FNiT according to relevant published reports.

The chi-squared test was used to assess the association between the FNiT and the clinicopathological variables. The Kaplan-Meier method was used to calculate the RFS and DSS rates. The Cox proportional hazards method was used to

determine the independent risk factors for RFS and DSS. All statistical analyses were conducted with the help of SPSS version 20 (IBM Corporation, Armonk, NY, USA). A $P<0.05$ was considered significant.

Immunohistochemistry Staining

Prepared pathological sections were blocked with 5% (w/v) BSA for 1 h at room temperature followed by incubation with the primary antibodies against E-cadherin overnight at 4°C, HRP-conjugated secondary antibodies (1:2000) were applied for 1 h at room temperature before developed by DAB reagent.

RESULTS

In Vitro Study

In vitro, we cocultured BMSCC cell line-H157 with neutrophils to form NiT structures. Fluorescent staining results of typical heterotypic NiT structures are shown in **Figure 1**. H157-L1 and H157-L2 were two subpopulations of poorly differentiated BMSCC cell lines, while H157-H1 and H157-H2 were two subpopulations of well-differentiated BMSCC cell lines. Cells marked in red and green were H157 and neutrophils, respectively. The region marked in blue was the nuclei of H157 and neutrophils. We discovered that well-differentiated H157-H1 and H157-H2 had stronger ability to internalize more neutrophils than poorly differentiated H157-L1 and H157-L2, with the latter often internalizing only one neutrophil or nothing.

Retrospective Case Series Study

Clinically, in total, 145 patients (68 females and 77 males) were enrolled with a mean age of 56.4 (range: 29–87) years. An FNiT≥4.2‰ was detected in 78 (54%) patients, while an FNiT<4.2‰ was detected in 67 (46%) patients. A history of smoking was found in 81 (56%) patients. A history of drinking was noted in 45 (31%) patients. Betel nut chewing was prevalent in 15 (10%) patients. Tumor stage was distributed as follows: T1 in 43 (30%) patients, T2 in 22 (15%) patients, T3 in 55 (38%) patients, and T4 in 25 (17%) patients. Distant metastasis was noted in 11 (8%) patients. Lymphovascular invasion was noted in

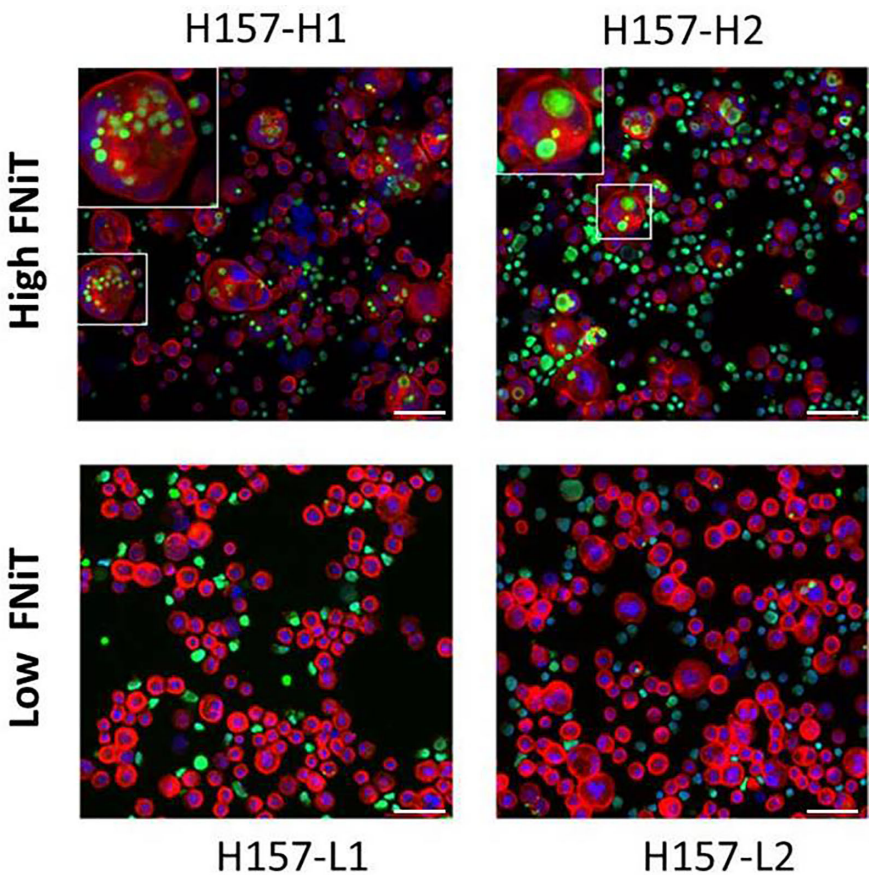

FIGURE 1 | Fluorescent staining result of typical heterotypic NiT structure formed between H157 cells and neutrophils. H157-H1 and H157-H2 are well-differentiated BMSCC cell lines with high FNiT, and H157-L1 and H157-L2 are poorly differentiated BMSCC cell lines with low FNiT. Cells marked in red and green are H157 cells and neutrophils, respectively. The regions marked in blue are the nuclei of H157 cells and neutrophils. Scale bar of all: 100 mm.

10 (7%) patients. Extranodal extension was found in 21 (14.5%) patients. Perineural invasion was noted in 8 (5.5%) patients. Tumor grade was distributed as follows: low grade in 10 (7%) patients, median grade in 26 (18%) patients, high grade in 109 (75%) patients (**Table 1**). A negative margin was achieved in 145 (100%) patients. The mean FNiT was 4.2‰, with a range from 2.3‰ to 7.8‰.

In total, all the patients underwent RRB and neck dissection whatever the clinical node stage. Pathologically negative and positive neck disease was reported in 100 (69%) and 45 (31%) patients, respectively (**Table 1**). A total of 110 patients received adjuvant radiotherapy, and adjuvant chemotherapy was performed in 29 patients.

TABLE 1 | General clinicopathological information of enrolled patients.

Variables	Number(%)
Age(years)	
<60	67(46%)
≥60	78(54%)
Sex	
Male	77(53%)
Female	68(47%)
FNiT	
Low	67(46%)
High	78(54%)
Smoker	
Y	81(56%)
N	64(44%)
Drinker	
Y	45(31%)
N	100(69%)
Betel nut chewing	
Positive	15(10%)
Negative	130(90%)
Tumor stage	
T1+T2	65(45%)
T3+T4	80(55%)
Node stage	
N0	100(69%)
N+	45(31%)
Metastasis	
Positive	11(8%)
Negative	134(92%)
Disease stage	
I+II	59(41%)
III+IV	86(59%)
Lymphovascular invasion	
Positive	10(7%)
Negative	135(93%)
Locoregional recurrence	
Y	80(55%)
N	65(45%)
Extranodal extension	
Y	21(14.5%)
N	124(85.5%)
Perineural invasion	
Y	8(5.5%)
N	137(94.5%)
Tumor Grade	
Low	10(7%)
Median	26(18%)
High	109(75%)

When re-evaluating all pathologic sections made from primary tumors *via* immunohistochemistry, we discovered the existence of typical NiT structures formation in BMSCC tissue (**Figure 2**). Representative image for E-cadherin staining in BMSCC pathologic tissue showed that tumor tissue was infiltrated with extensive neutrophils and substantial NiT structures were formed by tumor cells internalizing neutrophils (**Figure 2A**). Typical NiT structures were indicated with red asterisks, of which three boxed NiTs in **Figure 2A** were zoomed in as shown in **Figures 2B–D**. Each of them was one typical NiT structure. The inserted picture of each image was a schematic cartoon for the indicated NiT structure. We calculated the FNiT value of each pathologic section according to the formula: FNiT=**t**/**T** (**t**: the total number of NiT structures; **T**: the total number of the tumor cells).

We exhibited the images of BMSCC tissue with different levels of FNiT and FNiT distribution in enrolled patients in **Figure 3**. In **Figures 3A, B**, two representative pathologic tissues from two patients with BMSCC were shown with high FNiT (7.8‰ and 6.6‰, respectively). In **Figures 3C, D**, two representative pathologic tissues from two patients with BMSCC were shown with low FNiT (2.3‰ and 2.5‰, respectively). Histogram plot for FNiT distribution in all enrolled patients was shown in **Figure 3E**. The cutoff value of FNiT calculated by the mean value of FNiT in all the enrolled patients was 4.2‰.

When analyzing the association between the FNiT and clinicopathological variables, it was noted that the FNiT was significantly associated with tumor grade (**Table 2**).

During our follow-up with a mean time of 52.4 (range: 13–115) months, a total of 80 (55%) patients relapsed locoregionally. Salvage surgery was performed successfully in 65 patients by local resection of BMSCC or radical neck dissection. The 5-year RFS rate was 42%, with 54.2 months of median survival time of RFS. When evaluating the predictors for RFS in the univariate analysis, betel nut chewing, FNiT, tumor stage, metastasis, disease stage, and tumor grade were significantly associated with locoregional recurrence (LRR). Furthermore, the FNiT was confirmed as the only independent predictor for RFS in the Cox model (**Table 3**). In patients with an FNiT<4.2‰, the 5-year RFS rate was 56%, and in patients with an FNiT≥4.2‰, the 5-year RFS was 27%; the difference was significant (p=0.018, **Figure 4**).

A total of 84 patients died of the disease. The 5-year DSS rate was 42% with 54.0 months of median survival time of DSS. In the univariate analysis, betel nut chewing, FNiT, tumor stage, metastasis, disease stage, lymphovascular invasion and tumor grade were significantly associated with terminal death. The Cox model was further utilized to identify that the FNiT and tumor grade were two independent factors predicting DSS in patient with BMSCC (**Table 4**). In patients with an FNiT<4.2‰, the 5-year DSS rate was 58%, and in patients with an FNiT≥4.2‰, the 5-year DSS rate was 28%; the difference was significant (p=0.034, **Figure 5**). Patients with high tumor grade tended to have a shorter DSS than those with low or median tumor grade (p=0.003, **Figure 6**).

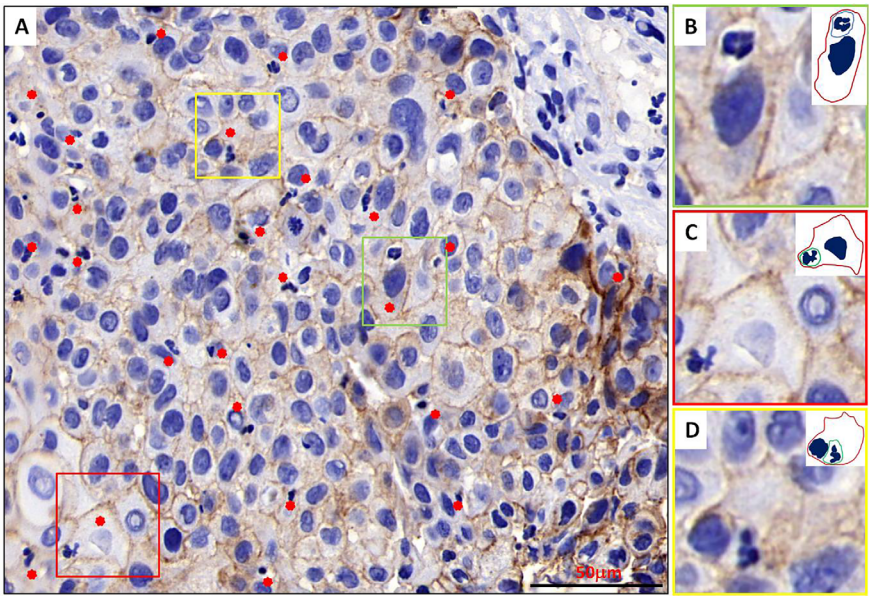

FIGURE 2 | Typical NiT structures formation in BMSCC tissue. **(A)** Representative image for E-cadherin staining in BMSCC pathologic tissue with extensive neutrophils infiltration. Typical NiT structures are indicated with red asterisks. Scale bar: 50 mm. **(B–D)** Zoomed in images for boxed NiT structures in **(A)**. Each of them is one typical NiT structure. Inserted pictures of each image are schematic cartoons for the indicated NiT structures. FNiT=t/T. (t: the total number of NiT structures. T: the total number of the tumor cells.)

DISCUSSION

Heterotypic CIC structures are generally formed by internalization of immune cells into tumor cells (24). Many tumor cells were confirmed to have the ability to internalize immune cells (25, 26), for example, HNSCC, melanoma, ductal carcinoma of the salivary gland, breast cancer, liver cancer and other tumor cells (8, 22, 27). The immune cells engulfed by tumor cells are diverse, including neutrophils (14, 15) NK cells (24, 28), T lymphocytes, and LAK cells, and neutrophils were recently mostly investigated. It has been reported that tumor progression and prognosis are associated with hCIC structure to some extent. Tetikkurt (7) and Sarode (23) described the inverse association between frequency of hCIC structure and prognosis of HNSCC, which indicates that hCIC plays an important role in predicting the progression of HNSCC.

Tumor cells internalize neutrophils to form heterotypic neutrophil-in-tumor structures, which have been discovered in HNSCC as a novel phenomenon (8, 29, 30). In our study, we cocultured BMSCC cell line-H157 with neutrophils *in vitro* to form NiT structures. We noted that H157-H1 and H157-H2 had higher ability to internalize more neutrophils than H157-L1 and H157-L2. The former cells were generally morphologically better differentiated than the latter ones. We noted that tumor grade was positively correlated with the FNiT in the association between the FNiT and clinicopathological characteristics. That is, the FNiT in well-differentiated tumor tissue is lower than that of poorly differentiated tumor tissue. This is not contradictory to the findings of the *in vitro* hCIC assays mentioned above. We supposed that the tumor tissues with high FNiT have more neutrophil infiltration than those with low FNiT, although the proportion of well-differentiated tumor cells in the low-FNiT tumor tissues surpassed that in the high-FNiT tumor tissues. We could further infer that the level of FNiT value was mainly attributed to the neutrophils infiltration within tumor tissues rather than the proportion of well-differentiated tumor cells, and the neutrophils infiltration within tumor tissues had a vital impact on the prognosis in patients with BMSCC.

To date, the role of the FNiT in the prognosis of patients with BMSCC has scarcely been investigated. A few papers have reported the existence of neutrophil-in-tumor structures in other tumors of HNSCC. Arya et al. (8) reported striking neutrophil-in-tumor cell cannibalism associated with a high grade, aggressive and metastatic duct carcinoma of the parotid gland. Magalhaes et al. (29) reviewed the role of neutrophils in the tumor microenvironment and as signaling modulators of oral squamous cell carcinoma (OSCC) and their possible role as biomarkers of OSCC prognosis and reported a pro-tumor role for NiT structure in OSCC. Tetikkurt et al. (7) presented a case related to significant neutrophilic emperipolesis in squamous cell carcinoma of the hard palate and maxilla and found that patients with high frequency of neutrophil-in-tumor structure were prone to relapse. Furthermore, neutrophil-in-tumor structures have been identified in other solid tumors such as microscopy evaluation of pleomorphic cell (giant cell) carcinomas of the lung, invasive micropapillary carcinomas of the ampulopancreaticobiliary region, gastric carcinomas, and lymphomas (31–33).

For BMSCC, alcohol consumption, tobacco use and betel quid chewing are well-known risk factors (34, 35). In the current study, we demonstrated that 31% of the patients had a history of

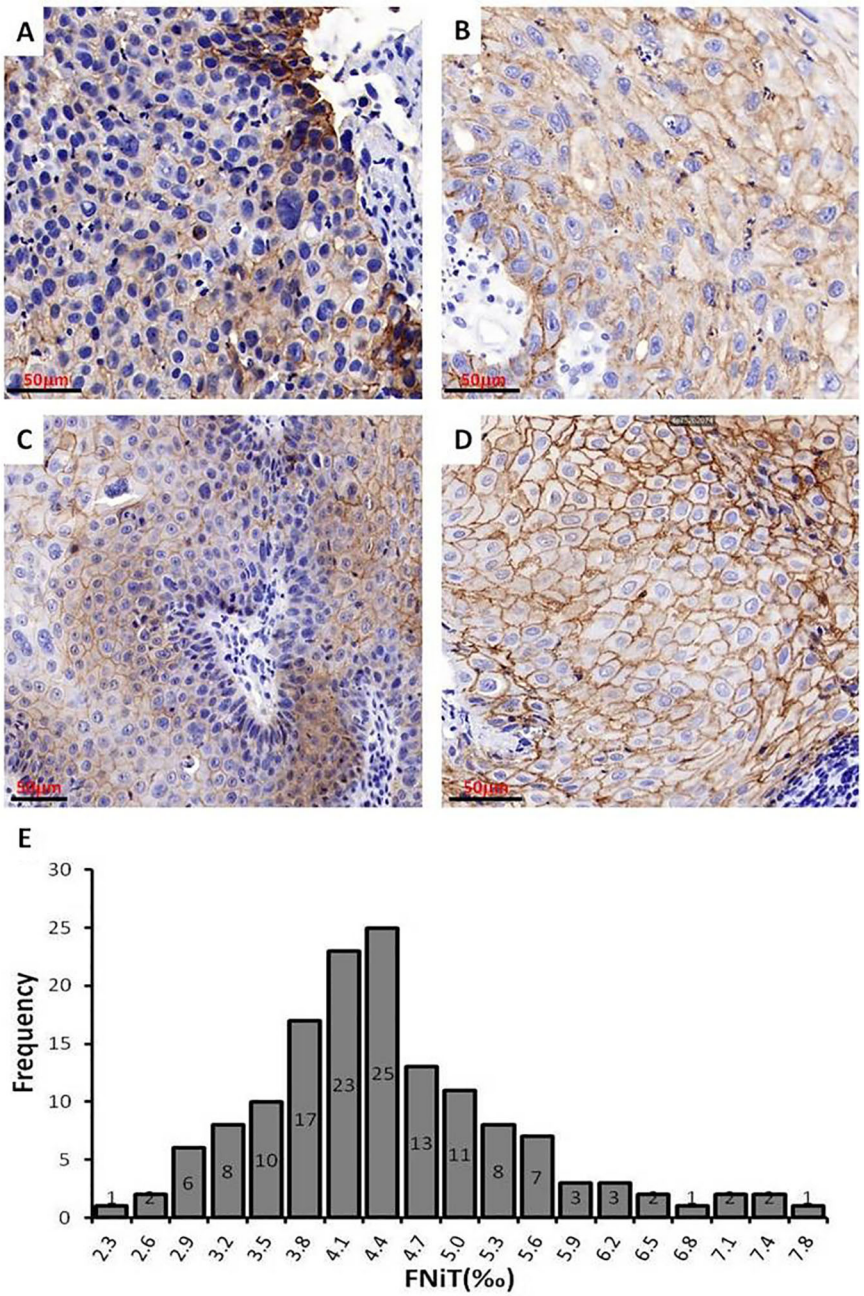

FIGURE 3 | Images of BMSCC tissue with different levels of FNiT and FNiT distribution in enrolled patients. **(A, B)** Representative images of pathologic tissues with high FNiT in two patients with BMSCC. Scale bar: 50 mm. **(C, D)** Representative images of pathologic tissues with low FNiT in two patients with BMSCC. Scale bar: 50 mm. **(E)** Histogram plot for FNiT distribution in enrolled patients. The cutoff value of the FNiT was calculated by the mean value of the FNiT in enrolled patients.

alcohol consumption, and 56% had a history of tobacco product consumption, which is consistent with previous studies. However, the proportion of betel nut chewing was 10%, which was lower than the reported result. We attributed the regional differences and human species diversity to the abnormal phenotype, as people in Hunan Province of China tended to consume more betel nuts than the ones in other region. For prognosis of BMSCC, we discovered that betel nut chewing was significantly associated with RFS and DSS ($p<0.001$ and $p=0.001$, respectively). This was in accordance with previous studies.

The LRR rate of BMSCC was generally high, as published papers have already indicated. DeConde et al. (36) found that 21 (44%) out of 48 patients with BMSCC relapsed during postoperative follow-up. In our current study, the LRR rate was 55%, which was higher than the average value previously reported. First, we speculated that it was possibly due to the high

TABLE 2 | Association between FNiT and clinicopathological characteristics.

Variables	FNiT		P-value
	Low (<4.2‰) n = 67	High (≥4.2‰) n = 78	
Age(years)			0.749
<60	30	37	
≥60	37	41	
Sex			0.298
Male	32	44	
Female	35	34	
Smoker			0.886
Y	37	44	
N	30	34	
Drinker			0.519
Y	19	26	
N	48	52	
Betel nut chewing			0.291
Positive	5	10	
Negative	62	68	
Tumor stage			0.510
T1+T2	32	33	
T3+T4	35	45	
Node stage			0.941
N0	46	54	
N+	21	24	
Metastasis			0.190
Positive	3	8	
Negative	64	70	
Disease stage			0.353
I+II	30	29	
III+IV	37	49	
Lymphovascular invasion			0.085
Positive	2	8	
Negative	65	70	
Extranodal extension			0.697
Y	9	12	
N	58	66	
Perineural invasion			0.296
Y	3	5	
N	65	72	
Tumor Grade			<0.001
Low	8	2	
Median	19	7	
High	40	69	

TABLE 3 | Univariate and multivariate analyses of predictors for recurrence-free survival in patients with BMSCC.

Variables	Univariate	Cox model	
	P-value	P-value	OR(95% CI)
Age,years(<60 vs ≥60)	0.591		
Sex(male vs female)	0.220		
Smoker (Y vs N)	0.681		
Drinker (Y vs N)	0.580		
Betel nut chewing(Y vs N)	<0.001	0.180	2.046(0.718–5.831)
FNiT(Low vs High)	0.001	0.018	1.803(1.106–2.940)
Tumor stage(T1+T2 vs T3+T4)	0.016	0.953	1.036(0.327–3.276)
Node stage(N0 vs N+)	0.342		
Metastasis(Y vs N)	<0.001	0.744	1.252 (0.325–4.821)
Disease stage(I+II vs III+IV)	0.001	0.313	1.907(0.545–6.671)
Lymphovascular invasion(Y vs N)	0.634		
Extranodal extension(Y vs N)	0.268		
Perineural invasion(Y vs N)	0.521		
Tumor Grade	0.042	0.176	1.365(0.870–2.143)
Low			
Median			
High			

proportion (75%) of high tumor grade of the enrolled patients. Secondly, regional lymph node metastasis occurred in 45 (31%) of the 145 total patients, which was relatively higher than previous results. Coppen et al. (37) reported that the prevalence of regional lymph node involvement was only 25%. Thirdly, although 110 (76%) out of 145 patients received postoperative radiotherapy, the majority of relapsed patients were continuously addicted to tobacco or alcohol.

We innovatively investigated the prognostic role of the FNiT in patients with BMSCC in the current study. We fortunately discovered that the FNiT as a novel predictor is significantly independently associated with RFS and DSS. However, the mechanism underlying the association between the FNiT and prognosis of BMSCC remains unclear. As we indicated above, the FNiT reflects the proportion of tumor-infiltrating neutrophils within the tumor microenvironment. Several chemokines, cytokines, and angiogenic factors produced by neutrophils may induce inflammatory cell recruitment and activation that have an impact on the tumor microenvironment, which could in turn facilitate tumor cell proliferation, microvascular regeneration and tumor progression (7, 9, 11, 13). In our study, patients with high FNiT tended to have both a shorter RFS and DSS than those with low FNiT, which may be better explained by the role of neutrophils in the tumor microenvironment mentioned above. Tetikkurt et al. (7) proposed that neutrophils may play a crucial role in cancer biology and may act as tumor promoters in tumor progression. Gregory et al. (38) declared that neutrophils may be vital biomarkers and targets for the administration and control of HNSCC.

In the analysis on the association between the FNiT and clinicopathological characteristics, we found that tumor stage was significantly associated with the FNiT ($p<0.001$). In the univariate analysis of the predictors for RFS in patients with BMSCC, betel nut chewing, FNiT, tumor stage, metastasis, disease stage, and tumor grade were proved to be associated with RFS; however, we unexpectedly discovered that only the FNiT was an independent predictor for RFS in Cox model. Particularly, our data indicated that tumor stage may be correlated with RFS dependent on FNiT (but not independently). In the univariate analysis of the predictors for DSS in patients with BMSCC, betel nut chewing, FNiT, tumor stage, metastasis, disease stage, lymphovascular invasion and tumor grade were related with DSS, but only the FNiT and tumor grade were independently associated with DSS. Other candidate predictors were not expected to be independently associated with RFS. Possible explanations may be that the proportions of the patients positive for betel nut chewing, metastasis, and lymphovascular invasion factors were relatively small, which may in turn cause strong error and bias in the survival analysis.

Recent advances in the role of tumor-associated neutrophils reveal that in the tumor microenvironment, neutrophils have varied functions and have been classified using different terms, including N1/N2 neutrophils, tumor-associated neutrophils

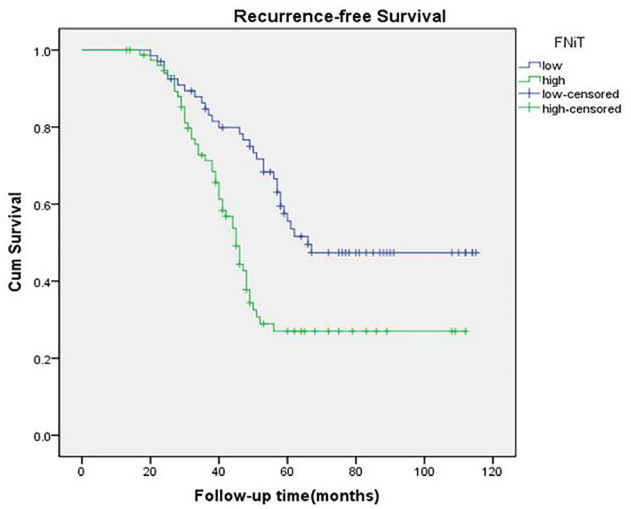

FIGURE 4 | Recurrence-free survival function in patients with different FNiT (p = 0.018).

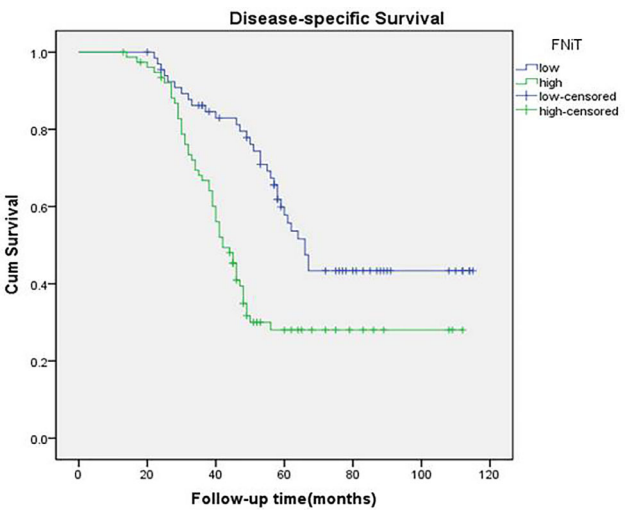

FIGURE 5 | Disease-specific survival function in patients with different FNiT (p = 0.034).

TABLE 4 | Univariate and multivariate analyses of predictors for disease-specific survival in patients with BMSCC.

Variables	Univariate	Cox model	
	P-value	P-value	OR(95% CI)
Age,years(<60 vs ≥60)	0.456		
Sex(male vs female)	0.558		
Smoker (Y vs N)	0.993		
Drinker (Y vs N)	0.701		
Betel nut chewing(Y vs N)	0.001	0.236	1.888(0.660–5.398)
FNiT(Low vs High)	<0.001	0.034	1.677(1.039–2.706)
Tumor stage(T1+T2 vs T3+T4)	0.001	0.941	0.954(0.275–3.305)
Node stage(N0 vs N+)	0.533		
Metastasis(Y vs N)	0.002	0.907	0.920 (0.228–3.709)
Disease stage(I+II vs III+IV)	<0.001	0.174	2.524(0.664–9.586)
Lymphovascular invasion(Y vs N)	0.038	0.068	2.122(0.946–4.757)
Extranodal extension(Y vs N)	0.467		
Perineural invasion(Y vs N)	0.573		
Tumor Grade	<0.001	0.003	2.371(1.337–4.203)
Low			
Median			
High			

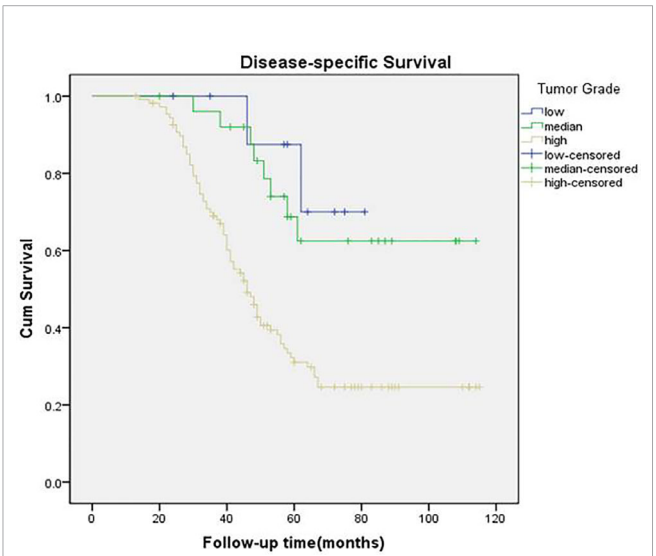

FIGURE 6 | Disease-specific survival function in patients with different levels of tumor grade (p = 0.003).

(TANs), and polymorphonuclear neutrophil myeloid–derived suppressor cells (PMN-MDSCs) (11, 39). Fridlender et al. first delineated antitumorigenic and protumorigenic neutrophils, termed N1 and N2, respectively (40). Antitumor neutrophils can directly kill tumor cells through release of reactive oxygen species (ROS) and reactive nitrogen species (RNS). In contrast, protumor neutrophils can release matrix metalloproteinase 9 (MMP9), which promotes angiogenesis and dissemination of tumor cells, and they can also suppress NK cell function. PMN-MDSCs, as well as other protumor neutrophils, can suppress CD8 T-cell function (11, 39, 40). In our work, tumor-infiltrating neutrophils that were subsequently internalized by tumor cells played a protumorigenic role as N2 type, which better explains our conclusion: the FNiT as a novel predictor is significantly negatively associated with RFS and DSS of patients with BMSCC.

Of course, we still have large amounts of work to do, and our ultimate goal is to provide novel targets and strategies for the diagnosis, treatment and prognosis management of BMSCC, and to create a new field for the fundamental research on the tumor microenvironment of BMSCC.

Limitations

The limitations of the study should be acknowledged. First, our current study has a retrospective design, so the inherent bias might

reduce the statistical power. Second, the clinicopathological factors were disproportionally distributed in the enrolled patients, which resulted in obvious error in the statistical analysis.

CONCLUSIONS

The FNiT as a novel predictor is significantly negatively associated with both the RFS and DSS of patients with BMSCC.

DATA AVAILABILITY STATEMENT

All datasets generated for this study are included in the article/supplementary material.

ETHICS STATEMENT

The studies involving human participants were reviewed and approved by: The Zhengzhou University Institutional Research and Ethics Committee. The patients/participants provided their written informed consent to participate in this study. Written informed consent was obtained from the individual(s) for the publication of any potentially identifiable images or data included in this article.

AUTHOR CONTRIBUTIONS

JF wrote the manuscript. QS, SL, WD, and QF made manuscript preparation suggestions and final manuscript revision. QS funded the research. YY and MC did routine work on approval procedures of IRC. JF and MZ collected clinical data and performed statistical analysis. JQ and RL performed fluorescence staining assay and figure preparation. All authors contributed to the article and approved the submitted version.

FUNDING

This research was supported by the National Natural Science Foundation of China (8157110152, 81872314).

REFERENCES

1. Huang H, Chen Z, Sun Q. Mammalian Cell Competitions, Cell-in-Cell Phenomena and Their Biomedical Implications. *Curr Mol Med* (2015) 15 (9):852–60. doi: 10.2174/1566524015666151026101101
2. Sun Q, Luo T, Ren Y, Florey O, Shirasawa S, Sasazuki T, et al. Competition between human cells by entosis. *Cell Res* (2014) 24(11):1299–310. doi: 10.1038/cr.2014.138
3. Overholtzer M, Brugge JS. The cell biology of cell-in-cell structures. *Nat Rev Mol Cell Biol* (2008) 9(10):796–809. doi: 10.1038/nrm2504
4. Zhang X, Niu Z, Qin H, Fan J, Wang M, Sun Q, et al. Subtype-Based Prognostic Analysis of Cell-in-Cell Structures in Early Breast Cancer. *Front Oncol* (2019) 9:895. doi: 10.3389/fonc.2019.00895
5. Ruan B, Niu Z , Jiang X , Tai Y, Huang H, Sun Q, et al. High Frequency of Cell-in-Cell Formation in Heterogeneous Human Breast Cancer Tissue in a Patient With Poor Prognosis: A Case Report and Literature Review. *Front Oncol* (2019) 9:1444. doi: 10.3389/fonc.2019.01444
6. Huang H, He M, Zhang Y, Zhang B, Wang X, Sun Q, et al. Identification and validation of heterotypic cell-in-cell structure as an adverse prognostic predictor for young patients of resectable pancreatic ductal adenocarcinoma. *Signal Transduct Tar* (2020) p:2020.07.08.20148825. doi: 10.1038/s41392-020-00346-w
7. Tetikkurt S, Taş F, Emre F, Özsoy Ş, Bilece Z. Significant Neutrophilic Emperipolesis in Squamous Cell Carcinoma. *Case Rep Oncol Med* (2018) 2018:1301562–1301562. doi: 10.1155/2018/1301562
8. Arya P, Khalbuss W, Monaco S, Pantanowitz L. Salivary duct carcinoma with striking neutrophil-tumor cell cannibalism. *CytoJournal* (2011) 8:15–5. doi: 10.4103/1742-6413.84222
9. Powell DR, Huttenlocher A. Neutrophils in the Tumor Microenvironment. *Trends Immunol* (2016) 37(1):41–52. doi: 10.1016/j.it.2015.11.008
10. Calabretta E, d'Amore F, Carlo-Stella C. Immune and Inflammatory Cells of the Tumor Microenvironment Represent Novel Therapeutic Targets in Classical Hodgkin Lymphoma. *Int J Mol Sci* (2019) 20(21):5503–21. doi: 10.3390/ijms20215503
11. Giese MA, Hind LE, Huttenlocher A. Neutrophil plasticity in the tumor microenvironment. *Blood* (2019) 133(20):2159–67. doi: 10.1182/blood-2018-11-844548
12. Hinshaw DC, Shevde LA. The Tumor Microenvironment Innately Modulates Cancer Progression. *Cancer Res* (2019) 79(18):4557–66. doi: 10.1158/0008-5472.CAN-18-3962
13. Kim J, Bae J-S. Tumor-Associated Macrophages and Neutrophils in Tumor Microenvironment. *Mediators Inflamm* (2016) 2016:6058147. doi: 10.1155/2016/6058147
14. Jeong J, Suh Y, Jung K. Context Drives Diversification of Monocytes and Neutrophils in Orchestrating the Tumor Microenvironment. *Front Immunol* (2019) 10:1817. doi: 10.3389/fimmu.2019.01817
15. SenGupta S, Subramanian BC, Parent CA. Getting TANned: How the tumor microenvironment drives neutrophil recruitment. *J Leukoc Biol* (2019) 105 (3):449–62. doi: 10.1002/JLB.3RI0718-282R
16. Wang M, Niu Z, Qin H, Ruan B, Zheng Y, Sun Q, et al. Mechanical Ring Interfaces between Adherens Junction and Contractile Actomyosin to Coordinate Entotic Cell-in-Cell Formation. *Cell Rep* (2020) 32(8):108071. doi: 10.1016/j.celrep.2020.108071
17. Sun Q, Cibas E, Huang H, Hodgson L, Overholtzer M. Induction of entosis by epithelial cadherin expression. *Cell Res* (2014) 24p:1288–98. doi: 10.1038/cr.2014.137
18. Ruan B, Zhang B, Chen A, Yuan L, Liang J, Sun Q, et al. Cholesterol inhibits entotic cell-in-cell formation and actomyosin contraction. *Biochem Biophys Res Commun* (2018) 495(1):1440–6. doi: 10.1016/j.bbrc.2017.11.197
19. Ruan B, Wang C, Chen A, Liang J, Fan J, Sun Q, et al. Expression profiling identified IL-8 as a regulator of homotypic cell-in-cell formation. *BMB Rep* (2018) 51(8):412–7. doi: 10.5483/BMBRep.2018.51.8.089
20. Wang C, Chen A, Ruan B, Niu Z, Su Y, Sun Q, et al. PCDH7 Inhibits the Formation of Homotypic Cell-in-Cell Structure. *Front Cell Dev Biol* (2020) 8p:329(329). doi: 10.3389/fcell.2020.00329
21. Liang J, Fan J, Wang M, Niu Z, Huang H, Sun Q, et al. CDKN2A inhibits formation of homotypic cell-in-cell structures. *Oncogenesis* (2018) 7(6):1–8. doi: 10.1038/s41389-018-0056-4
22. Caruso RA, Fedele F, Finocchiaro G, Arena G, Venuti A. Neutrophil-tumor cell phagocytosis (cannibalism) in human tumors: an update and literature review. *Exp Oncol* (2012) 34(3):306–11.
23. Sarode SC, Sarode GS. Neutrophil-tumor cell cannibalism in oral squamous cell carcinoma. *J Oral Pathol Med* (2014) 43(6):454–8. doi: 10.1111/jop.12157

24. Wang S, Guo Z, Xia P, Liu T, Wang X, Yao X, et al. Internalization of NK cells into tumor cells requires ezrin and leads to programmed cell-in-cell death. *Cell Res* (2009) 19(12):1350–62. doi: 10.1038/cr.2009.114
25. Singhal N, Handa U, Bansal C, Mohan H. Neutrophil phagocytosis by tumor cells–a cytological study. *Diagn Cytopathol* (2011) 39(8):553–5. doi: 10.1002/dc.21421
26. Takeuchi M, Inoue T, Otani T, Yamasaki F, Nakamura S, Kibata M. Cell-in-cell structures formed between human cancer cell lines and the cytotoxic regulatory T-cell line HOZOT. *J Mol Cell Biol* (2010) 2(3):139–51. doi: 10.1093/jmcb/mjq002
27. Lugini L, Matarrese P, Tinari A, Lozupone F, Federici C, Fais S. Cannibalism of live lymphocytes by human metastatic but not primary melanoma cells. *Cancer Res* (2006) 66(7):3629–38. doi: 10.1158/0008-5472.CAN-05-3204
28. Wang S, He MF, Chen YH, Wang MY, Wang Y, Wang XN. Rapid reuptake of granzyme B leads to emperitosis: an apoptotic cell-in-cell death of immune killer cells inside tumor cells. *Cell Death Dis* (2013) 4(10):e856–6. doi: 10.1038/cddis.2013.352
29. Magalhaes MAO, Glogauer JE, Glogauer M. Neutrophils and oral squamous cell carcinoma: lessons learned and future directions. *J Leukocyte Biol* (2014) 96(5):695–702. doi: 10.1189/jlb.4RU0614-294R
30. Sarode GS, Sarode SC, Patil S. Emperipolesis: An Unreported Novel Phenomenon in Oral Squamous Cell Carcinoma. *J Contemp Dental Pract* (2017) 18(4):345–7. doi: 10.5005/JCDP-18-4-345
31. Caruso RA, Muda AO, Bersiga A, Rigoli L, Inferrera C. Morphological evidence of neutrophil-tumor cell phagocytosis (cannibalism) in human gastric adenocarcinomas. *Ultrastruct Pathol* (2002) 26(5):315–21. doi: 10.1080/01913120290104593
32. Fishback NF, Fishback NF, Travis WD, Moran CA, McCarthy WF, Koss MN. Pleomorphic (spindle/giant cell) carcinoma of the lung. A clinicopathologic correlation of 78 cases. *Cancer* (1994) 73(12):2936–45. doi: 10.1002/1097-0142(19940615)73:12<2936::AID-CNCR2820731210>3.0.CO;2-U
33. Khayyata S, Basturk O, Adsay NV. Invasive micropapillary carcinomas of the ampullo-pancreatobiliary region and their association with tumor-infiltrating neutrophils. *Modern Pathol* (2005) 18(11):1504–11. doi: 10.1038/modpathol.3800460
34. Ghoshal S, Mallick I, Panda N, Sharma SC. Carcinoma of the buccal mucosa: analysis of clinical presentation, outcome and prognostic factors. *Oral Oncol* (2006) 42(5):533–9. doi: 10.1016/j.oraloncology.2005.10.005
35. Huang C-H, Chu ST, Ger LP, Hou YY, Sun CP. Clinicopathologic evaluation of prognostic factors for squamous cell carcinoma of the buccal mucosa. *J Chin Med Assoc JCMA* (2007) 70(4):164–70. doi: 10.1016/S1726-4901(09)70351-X
36. DeConde A, Miller ME, Palla B, Lai C, Elashoff D, St John MA. Squamous cell carcinoma of buccal mucosa: a 40-year review. *Am J Otolaryngol* (2012) 33(6):673–7. doi: 10.1016/j.amjoto.2012.04.006
37. Coppen C, de Wilde PC, Pop LA, van den Hoogen FJ, Merkx MA. Treatment results of patients with a squamous cell carcinoma of the buccal mucosa. *Oral Oncol* (2006) 42(8):795–9. doi: 10.1016/j.oraloncology.2005.11.017
38. Gregory AD, Houghton AM. Tumor-associated neutrophils: new targets for cancer therapy. *Cancer Res* (2011) 71(7):2411–6. doi: 10.1158/0008-5472.CAN-10-2583
39. Mukaida N, Sasaki SI, Baba T. Two-Faced Roles of Tumor-Associated Neutrophils in Cancer Development and Progression. *Int J Mol Sci* (2020) 21(10):3457–78. doi: 10.3390/ijms21103457
40. Fridlender ZG, Sun J, Kim S, Kapoor V, Cheng G, Albelda SM, et al. Polarization of tumor-associated neutrophil phenotype by TGF-beta: "N1" versus "N2" TAN. *Cancer Cell* (2009) 16(3):183–94. doi: 10.1016/j.ccr.2009.06.017

Conflict of Interest: The authors declare that the research was conducted in the absence of any commercial or financial relationships that could be construed as a potential conflict of interest.

frontiers in Oncology

ORIGINAL RESEARCH
published: 18 November 2020
doi: 10.3389/fonc.2020.549412

In Vitro Study of Synergic Effect of Cisplatin and Low Molecular Weight Heparin on Oral Squamous Cell Carcinoma

*Fabio Camacho-Alonso[1], T. Gómez-Albentosa[2], R. E. Oñate-Sánchez[3], M. R. Tudela-Mulero[1], M. Sánchez-Siles[2], Francisco J. Gómez-García[4] and Yolanda Guerrero-Sánchez[5]**

[1] Department of Oral Surgery, University of Murcia, Murcia, Spain, [2] Private Practitioner, Murcia, Spain, [3] Department of Dentistry for Special Patients, University of Murcia, Murcia, Spain, [4] Department of Oral Medicine, University of Murcia, Murcia, Spain, [5] Department of Human Anaothomy and Psicobiology, University of Murcia, Murcia, Spain

OPEN ACCESS

Edited by:
Alberto Paderno, University of Brescia, Italy

Reviewed by:
Kumar Prabhash, Tata Memorial Hospital, India
Francesco Bussu, University of Sassari, Italy
Marco Guerrini, Istituto di Ricerche Chimiche e Biochimiche G. Ronzoni, Italy

***Correspondence:**
Yolanda Guerrero-Sánchez
yolanda.guerreros@um.es

Specialty section:
This article was submitted to Head and Neck Cancer, a section of the journal Frontiers in Oncology

Received: *06 April 2020*
Accepted: *26 October 2020*
Published: *18 November 2020*

Citation:
Camacho-Alonso F, Gómez-Albentosa T, Oñate-Sánchez RE, Tudela-Mulero MR, Sánchez-Siles M, Gómez-García FJ and Guerrero-Sánchez Y (2020) In Vitro Study of Synergic Effect of Cisplatin and Low Molecular Weight Heparin on Oral Squamous Cell Carcinoma. Front. Oncol. 10:549412. doi: 10.3389/fonc.2020.549412

Objectives: To evaluate the possible synergic effect of cisplatin and low molecular weight heparin (LMWH) on oral squamous cell carcinoma (OSCC).

Materials and Methods: Cisplatin and enoxaparin sodium, alone or in combination, were administered at doses of 1, 2, 4, 8 and 10 μM and 0.1, 0.5, 1, 5, 10, 50, and 100 μg/ml, respectively, to the H357 human OSCC line. The effects on cell viability and apoptosis were evaluated after 24, 48, and 72 h and on cell migration after 18 and 24 h.

Results: 10 μM concentration of cisplatin produced the greatest decrease in cell viability, with significant differences at 24 (p=0.009), 48 (p=0.001) and 72 h (p = 0.003); the 100 μg/ml dose of enoxaparin produced the greatest decrease in cell viability but without significant differences (p>0.05). When different concentrations of cisplatin and enoxaparin were combined, it was found that 100 μg/ml enoxaparin sodium produced the greatest synergic effect on cell viability reduction. In analyses of apoptosis and cell migration, it was found that the combination of cisplatin at 8 or 10 μM and 100 μg/ml enoxaparin produced a higher rate of apoptosis at 24, 48, and 72 h and a greater reduction in cell migration at 18 and 24 h.

Conclusions: A combination of cisplatin and enoxaparin sodium shows a synergic effect that reduces cell viability and cell migration capacity and increases the apoptosis of human OSCC cells.

Clinical relevance: Enoxaparin may be beneficial in chemotherapy for patients with OSCC; this finding requires further clinical and laboratory investigation.

Keywords: cisplatin, low molecular weight heparin, oral squamous cell carcinoma, enoxaparin sodium, *in vitro* cell line

INTRODUCTION

Cancer is the main cause of death in both the developed and the developing worlds. It is predicted that numbers of death resulting from cancer will grow as populations and life expectancy increase, especially in the developing world where 82% of the world's population is located. In the least developed countries, lifestyle habits that constitute risk factors for developing cancer are spreading – smoking, alcohol consumption, a nutritionally poor diet (low consumption of fruit and vegetables), physical inactivity (obesity), and changing reproductive habits (fewer births, later in life) – and the numbers of cases of cancer have increased (1). Squamous cell carcinoma of the head and neck (SCCHN) is the fifth most common form of cancer and the sixth main cause of cancer mortality in the world (2), with approximately 600,000 new cases diagnosed worldwide each year (3). Oral squamous cell carcinoma (OSCC) is the most common SCCHN and represents approximately 3% of new cases of cancer diagnosed (4). Current OSCC treatment includes surgery, radiotherapy and chemotherapy. But long-term survival remains low. In fact, the survival rate of patients with OSCC beyond 5 years is about 50% (5).

Conventional chemotherapy for OSCC is based on cisplatin (cis-diammine-dichloro-platinum), the first of a family of drugs that currently include carboplatin, oxaliplatin, satraplatin, and picoplatin. Among medical cancer treatments, chemotherapy with cisplatin has the greatest impact and its introduction has changed the therapeutic management of a range of tumors over the last 40 years. These include cancers of the bladder, breast, lung, lymphomas, testicles, ovaries (6), as well as SCCHN including OSCC (7). Cisplatin's mechanism of cytotoxic action on cancer cells is based on inducing apoptosis and cell cycle arrestthrough its interaction with DNA that leads to the formation of cisplatin-DNA adducts, which activate multiple signaling pathways see (8) and (9). In comparison with other types of anticancer cell, cisplatin enters cells relatively slowly. This is regulated by various factors such as sodium and potassium ions, pH regulation, and the action of transporters (10). Before attaching to DNA in cell cytoplasm, cisplatin activates by replacing one of its two chlorine atoms with water molecules. In this way, it covalently binds to DNA, which produces what are known as DNA adducts. The resulting products can cause damage to the DNA of the carcinogenic cells, blocking their division (by blocking cells in the G2 phase of the cell cycle, the mitotic phase) and leading to cell death resulting from apoptosis (11).

In addition to the adverse effects of this drug (nausea, vomiting, dose- and time-dependent toxicities, in particular nephrotoxicity, cardiotoxicity, neurotoxicity and ototoxicity) (12), there are various routes by which cells can develop resistance to the anticarcinogenic action of cisplatin on OSCC. The molecular mechanisms responsible for cell resistance to cisplatin are complex, and may be related to limited cisplatin entrance into cells, intracellular cisplatin deactivation, increased tolerance by the cells, or even increased cisplatin exit to the cell's exterior (13). As a consequence, the formation of cisplatin-DNA adducts decreases, reducing cytotoxicity, which results in greater resistance (11). Furthermore, according to theories of cancer stem cell behavior (CSC), tumors organize themselves hierarchically in similar ways to healthy tissue, with a sub-population of CSCs that may be resistant to the chemotherapy administered, and that generate differentiated cancer cells (14). This subpopulation of CSCs was first identified in leukemia and later isolated in solid tumors including breast, brain, lung, liver, prostate, colon, and pancreatic cancers (15–19), as well as SCCHN (20–22). The CSCs express high levels of ATB-binding-cassette (ABC), transporter proteins in numerous drugs that are the cause of resistance to treatment by chemotherapy. Some ABC protein families are responsible for the cytoprotective effect of cancer cells against cisplatin (23–25). For this reason, there is a need to develop new anticarcinogenic therapies.

Low molecular weight heparins (LMWHs) were approved by the US Food and Drug Administration (FDA) in 1998 as an anticoagulant treatment and have been administered satisfactorily ever since (26). More recently, several studies have shown that LMWHs reduce death by cancer in patients with deep-vein thrombosis, and different types of cancer (27–29). Although various clinical studies have shown that LMWHs prolong survival and reduce mortality in patients with advanced solid cancer, the exact mechanism whereby LMWHs exercise their anticarcinogenic action has not yet been determined (30–33). Their anticarcinogenic action is probably produced through an antiproliferative action (due to their anti-angiogenic action) (34–36) and antimetastatic action (37–40). Regarding their antiproliferative action, LMWHs have been shown to exert an anti-angiogenic action that regulates tumoral angiogenesis *via* two paths; on the one hand, by impeding thrombin generation, which inhibits the tissue factor pathway through the release of an endothelial tissue factor (TF) pathway inhibitor (TFPI) (41), and on the other, by inhibiting the formation of Xa factor through the attachment of the antithrombin-herapin complex to this factor (42). Its antimetastatic activity would appear to be related to its capacity for attachment to selectins (mainly P- and L-selectin), integrins (mainly VLA-4), cytokines, and enzymes such as heparanases that are able to degrade the extracellular matrix and the components of the basal membrane (38–40).

Enoxaparin sodium is an LMWH obtained by an alkaline depolymerization method; it has an average molecular weight of 4.5 kDa, and its anticarcinogenic activity has been studied in cases of pancreatic adenocarcinoma cells, human breast carcinoma cells, human lung adenocarcinoma epithelial cells, glioma cells, melanoma cells (37, 43–47) and against metastasis from brain and colon cancer (48, 49). But its anticarcinogenic action on OSCC, alone or in combination with cisplatin, is unknown.

The aim of this study was to evaluate the possible synergic effect of cisplatin and enoxaparin sodium on OSCC.

MATERIALS AND METHODS

Cell Line

The study used the H357 human OSCC line (European Collection of Cell Cultures), belonging to stage 1 OSCC

(T1N0M0) located at the base of the tongue of a male patient. Cells were cultured in Iscove's Modified Dulbecco's Medium (IMDM) supplemented with 10% fetal calf serum (FCS), glutamine (2 mM), 0.5 µg/ml hydrocortisone sodium succinate, 1% penicillin, and 1% streptomycin (full medium) at 37°C, in an atmosphere of 95% oxygen and 5% CO_2.

The medium (IMDM), 3-(4,5-dimethyl-2-thiazolyl)-2,5-diphenyl-2H-tetrazolium bromide (MTT), dimethylsulfoxide (DMSO), cisplatin, and enoxaparin sodium used in the study were supplied by Sigma-Aldrich® (Sigma-Aldrich Chemistry, S.A., Madrid, Spain).

Drug Preparation

Cisplatin was dissolved in 0.5% DMSO and enoxaparin sodium in phosphate buffered saline (PBS), with 1 mg/ml of cisplatin or enoxaparin sodium being used as a stock solution. The working solutions were diluted with Iscove's modified Dulbecco's medium (IMDM). All manipulations with cisplatin and enoxaparin sodium were performed under subdued lighting. The dose range was 1, 2, 4, 8 and 10 µM of cisplatin and 0.1, 0.5, 1, 5, 10, 50, and 100 µg/ml of enoxaparin sodium.

Cell Viability Test (MTT)

The technique described by Carmichael et al. (50, 51) was used for cell viability quantification, adapted to the study's culture conditions. The cells were cultured at a density of 3,200 cells per well in 96-microwell plates, after which cisplatin or enoxaparin sodium were added at different concentrations (1, 2, 4, 8, and 10 µM of cisplatin and 0.1, 0.5, 1, 5, 10, 50, and 100 µg/ml of enoxaparin sodium), individually or in combination.

At different time points after the start of treatment (24, 48, and 72 h), the medium was eliminated and the cells were incubated with MTT (Sigma-Aldrich Chemistry, S.A.) (1 mg/ml) for 4 h, after which the non-metabolized MTT was discarded and 100 µl of DMSO were added to each well. Absorbance in each well was measured with an enzyme-linked immunosorbent assay (ELISA), using a Multiskan MCC/340P plate spectrophotometer at a reading wavelength of 570 nm and a reference wavelength of 690 nm. Each test was performed in triplicate.

Apoptosis (Histone/DNA Fragment ELISA)

The ELISA cell death detection kit was used (following the manufacturer's instructions) to detect apoptosis in cells treated with cisplatin and enoxaparin sodium. Briefly, cells were seeded in 96-well plates at a density of 3,200 cells per well for 24 h, adding the medium containing the two highest concentrations of cisplatin used in the cell viability test (8 and 10 µM) combined with the highest concentration of enoxaparin sodium used in the cell viability test (100 µg/ml). After 24, 48, or 72 h, the cytoplasm inthe control and treatment groups was transferred to the 96-well plate, peridiumed by streptavidin, and incubated with biotinylated histone antibody and peroxidase-tagged mouse anti-human DNA for 2 h at room temperature. Absorbance at 405 nm was measured with EXL-800 type Enzyme-Linked Immunosorbent apparatus. Each test was performed in triplicate.

Migration (Scratch Wound Healing)

Scratch wounds were generated in confluent monolayers of cells using a sterile 200 µl pipette tip (52). After washing away suspended cells with phosphate buffer saline (PBS), the culture medium was changed and added at different concentrations: the two highest concentrations of cisplatin used in cell viability testing (8 and 10 µM) combined with the highest concentration of enoxaparin sodium used in cell viability testing (100 µg/ml). Migration into the wound space was photographed using an inverted microscope equipped with a digital camera at the time of the initial wound and at time intervals up to 18 and 24 h after wounding. The relative distances between edges of the injured monolayer were obtained by means of pixel counts at a minimum of 10 sites per wound, using MIP-4® image software (CID, Barcelona, Spain) and applying the formula: migration distance = initial distance of free-of-cells space – distance at 18 or 24 h of free-of-cells space (53). Each test was performed in triplicate.

Statistical Analysis

Data were analyzed using the SPSS version 20.0 statistical software package (SPSS® Inc., Chicago, IL, USA). A descriptive study was made of each variable. The associations between different quantitative variables were studied using one-way analysis of variance (ANOVA) for more than two samples, verifying in each case whether variances were homogeneous. Statistical significance was accepted for $p \leq 0.05$.

RESULTS

Effects of Cisplatin, Enoxaparin Sodium, and the Combination of the Two on H357 Cell Viability

At all incubation times (24, 48 and 72 h), it was found that as the dose of cisplatin increased, OSCC cell viability decreased. The 10 µM cisplatin concentration produced the greatest reduction in cell viability, with statistically significant differences at 24 h (p=0.009), 48 h (p=0.001), and 72 h (p=0.003) (**Figure 1A**). When the effect of enoxaparin sodium on cell viability was analyzed at 24, 48, and 72 h incubation, it was found that as the dose of LMWH increased, cell viability decreased, with the greatest reduction seen with the 100 µg/ml dose of enoxaparin sodium, although without statistically significant differences at 24 h (p= 0.215), 48 h (p=0.558), or 72 h (p=0.303) incubation (**Figure 1B**).

When the different doses of cisplatin assayed (1, 2, 4, 8 and 10 µM) were combined with different concentrations of enoxaparin sodium (0.1, 0.5, 1, 5, 10, 50, and 100 µg/ml) it was found that combining any concentration of cisplatin with 100 µg/ml enoxaparin sodium produced the greatest synergic effect OSCC cell viability reduction, with statistically significant differences for combinations of 8 and 10 µM cisplatin at 24 h incubation (p<0.001 and p<0.001, respectively), and for 1, 2, 4 and 8 µM cisplatin at 48 h incubation (p<0.001, p=0.006, p=0.030, p<0.001, respectively) (**Figures 2** and **3**).

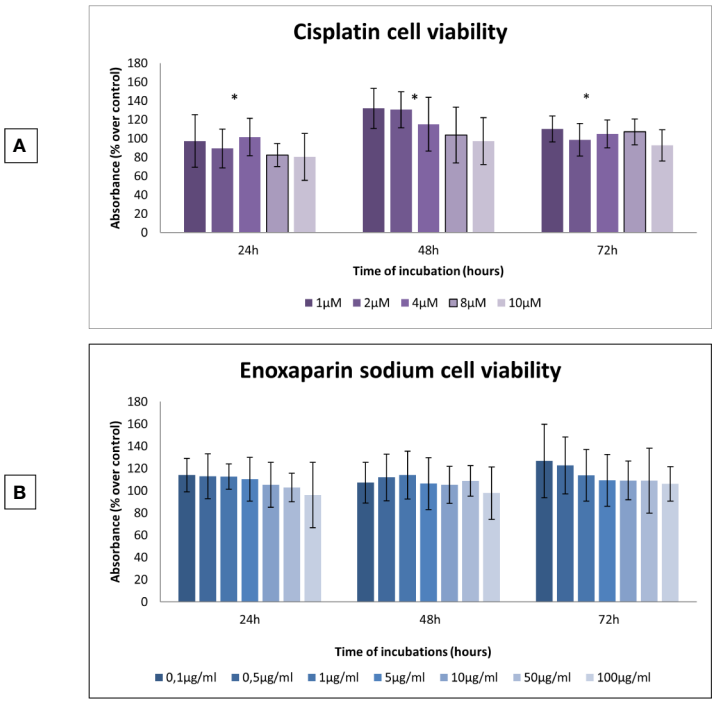

FIGURE 1 | Effects of cisplatin or enoxaparin sodium on H357 cell viability. **(A)** 24 h, $p = 0.009$; 48 h, $p = 0.001$; 72 h, $p = 0.003$. **(B)** 24 h, $p = 0.215$; 48 h, $p = 0.558$; 72 h, $p = 0.303$. * means that there is significative differences at such picture.

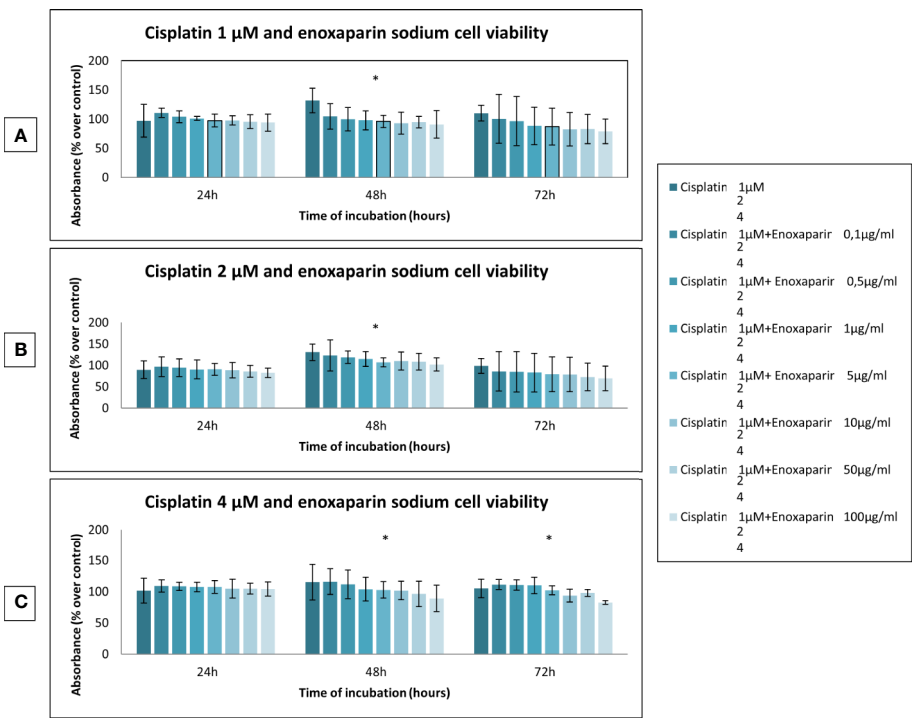

FIGURE 2 | Effects of cisplatin (1, 2, and 4 µM) and enoxaparin sodium (0.1, 0.5, 1, 5, 10, 50, and 100 µg/ml) on H357 cell viability. **(A)** 24 h, $p = 0.228$; 48 h, $p < 0.001$; 72 h, $p = 0.077$. **(B)** 24 h, $p = 0.729$; 48 h, $p = 0.006$; 72 h, $p = 0.502$. **(C)** 24 h, $p = 0.774$; 48 h, $p = 0.030$; 72 h, $p < 0.001$. * means that there is significative differences at such picture.

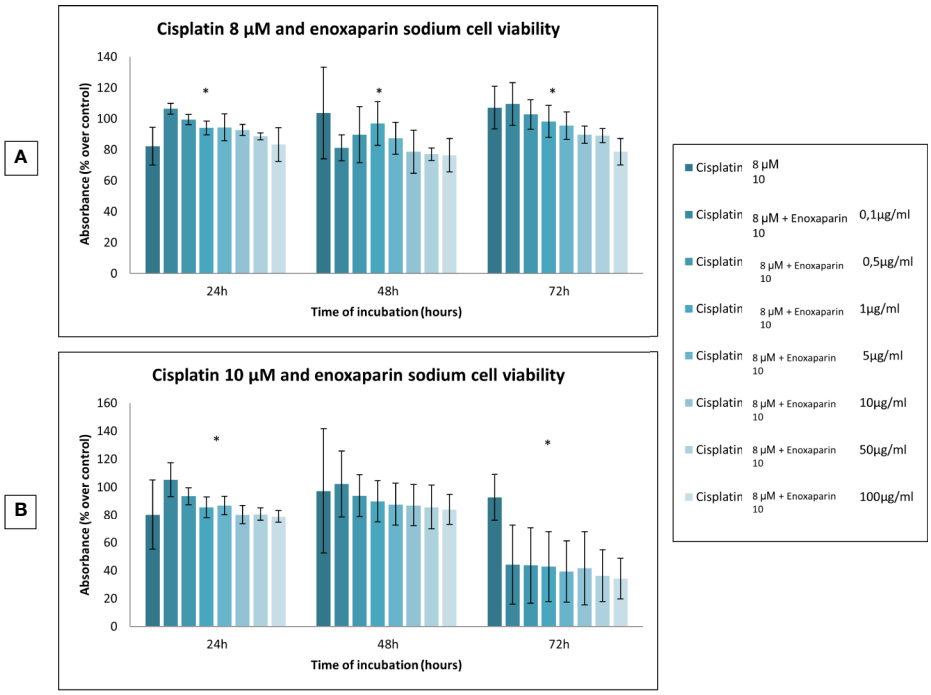

FIGURE 3 | Effects of cisplatin (8 and 10 µM) and enoxaparin sodium (0.1, 0.5, 1, 5, 10, 50, and 100 µg/ml) on H357 cell viability. **(A)** 24 h, $p < 0.001$; 48 h, $p < 0.001$; 72 h, $p < 0.001$. **(B)** 24 h, $p < 0.001$; 48 h, $p = 0.616$; 72 h, $p < 0.001$. * means that there is significative differences at such picture.

Effects of Cisplatin and Enoxaparin Sodium on H357 Cell Apoptosis

Both the cell death test and the cell migration assay, investigated the two highest concentrations of cisplatin (8 and 10 µM), and enoxaparin sodium (100 µg/ml), as these doses led to the greatest reductions in cell viability.

In the cell apoptosis test it was found that 24, 48, and 72 h incubation times all produced higher rates of apoptosis with the combination of 8 or 10 µM cisplatin and 100 µg/ml enoxaparin sodium, obtaining statistically significant differences at 48 h treatment (p=0.008 and p=0.009, respectively) (**Figure 4**).

Effects of Cisplatin and Enoxaparin Sodium on H357 Cell Migration

When 8 or 10 µM cisplatin were combined with 100 µg/ml enoxaparin sodium, a greater reduction in cell migration capacity was observed, with statistically significant differences when 8 µM cisplatin were combined with 100 µg/ml enoxaparin sodium, both at 18 h (p=0.003) and 24 h (p=0.004) (**Figures 5–7**).

DISCUSSION

Most tumors in the oral cavity, pharynx and larynx (>90%) are squamous cell carcinomas. OSCC represents 6% of all malign neoplasias and constitutes the eighth most common cancer in terms of worldwide incidence (1). Mortality associated with OSCC remains high due to the fact that most cases are detected at an advanced stage, and also to treatment failure in the form of locoregional recurrence (15–50%) or distant metastasis (54, 55). The survival rate of patients with OSCC over 5 years is over 80% providing they receive treatment while the cancer is at an early stage. However, when the disease has spread to the cervical lymph nodes, this percentage decreases to 40%, and falls to only 20% when the case presents metastasis (56).

Cisplatin is the most often used chemotherapy in OSCC treatment, often administered in combination with taxanes and/or 5-fluoruracil (57). But in addition to the adverse effects of this drug (nausea, vomiting and toxic effects on different organs) (12), there are various routes by which the cancer can develop resistance to cisplatin's anticarcinogenic action on OSCC: reduced formation of cisplatin-DNA adducts (which causes a reduction in cytotoxicity against carcinogenic cells) and generation of subpopulations of CSCs capable of ABC expression (drug transporter proteins) that may be responsible for OSCC resistance to cisplatin (23–25). In this context, development of an oral cancer-specific, anticancer drug is needed; new therapeutic strategies need to be identified and evaluated in preclinical models before entering clinical trials.

Heparin and LMWHs have shown substantial anticarcinogenic properties in addition to their traditional anticoagulant properties (34, 58, 59). It is possible that their anticarcinogenic action is due to: a) antiproliferative activity (due to their antiangiogenic activity) that

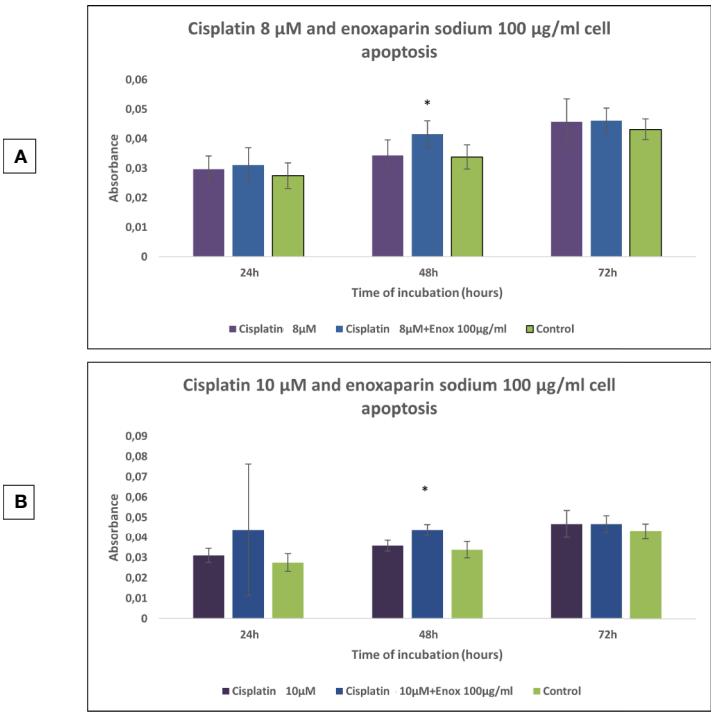

FIGURE 4 | Effects of cisplatin (8 and 10 µM) and enoxaparin sodium 100 µg/ml on H357 cell apoptosis. **(A)** 24 h, $p = 0.582$; 48 h, $p = 0.008$; 72 h, $p = 0.716$. **(B)** 24 h, $p = 0.413$; 48 h, $p = 0.009$; 72 h, $p = 0.592$. * means that there is significative differences at such picture.

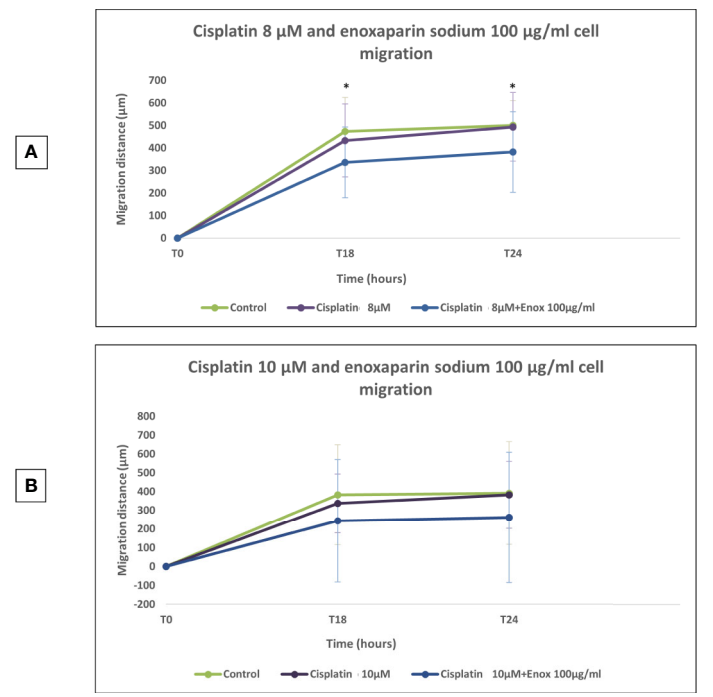

FIGURE 5 | Effects of cisplatin (8 and 10 µM) and enoxaparin sodium 100 µg/ml on H357 cell migration. **(A)** 18 h, $p = 0.003$; 24 h, $p = 0.004$. **(B)** 18 h, $p = 0.116$; 24 h, $p = 0.133$. * means that there is significative differences at such picture.

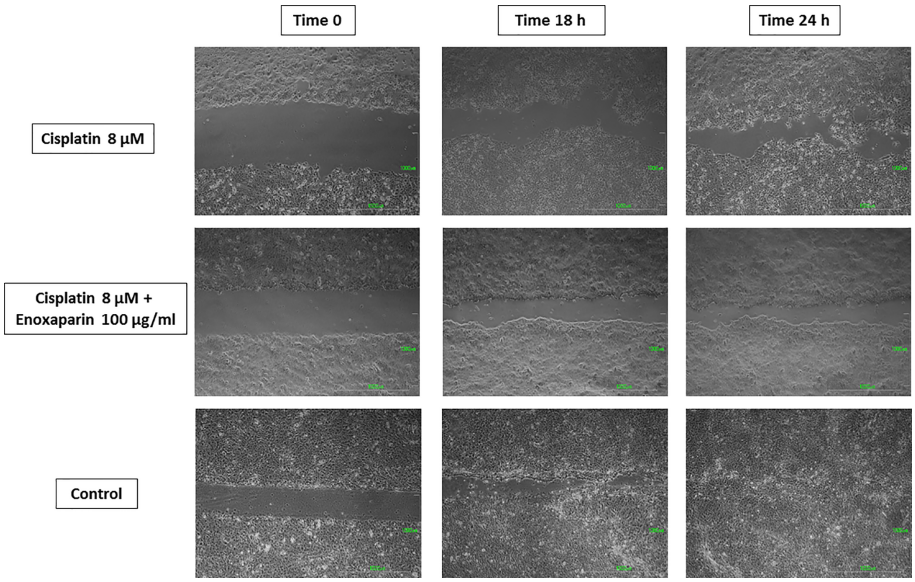

FIGURE 6 | Cell migration into the wound space photographed at the time of initial wounding and at time intervals up to 18 and 24 h after wounding. Results of cisplatin 8 µM alone and combined with 100 µg/ml enoxaparin sodium.

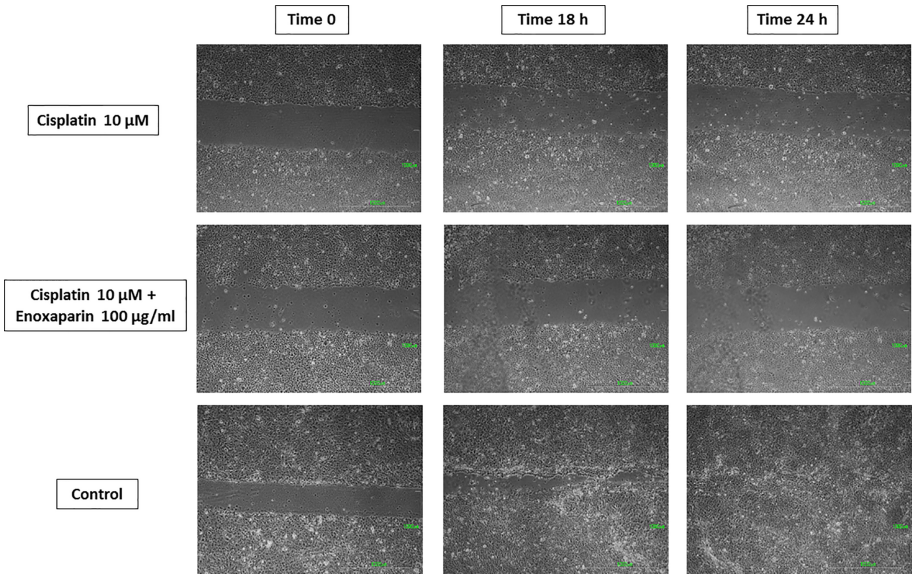

FIGURE 7 | Cell migration into the wound space photographed at the time of initial wounding and at time intervals up to 18 and 24 h after wounding. Results of 10 µM cisplatin alone or combined with 100 µg/ml enoxaparin sodium.

impedes thrombin generation and so inhibits TF expression (41) and fibrin formation (42); and b) their antimetastatic activity deriving from their capacity for attachment to selectins, integrins, cytokines and enzymes such as heparanases (38–40). However, the action of LMWH, whether alone or in combination with cisplatin, on cell viability, apoptosis and cell migration capacity on human OSCC cells remains unknown.

The present study used enoxaparin sodium, which is an LMWH whose anticarcinogenic activity has been investigated inpancreatic adenocarcinoma cells, human breast carcinoma cells, human lung adenocarcinoma epithelial cells, glioma cells, melanoma cells (37, 43–47), and against metastasis of brain and colon cancer (48, 49) but never on human OSCC cells.

TABLE 1 | Effects of cisplatin or enoxaparin sodium on H357 cell viability (ANOVA test).

Treatment/Time point	Absorbance (% over control) mean ± SD*	*p-value*
Cisplatin/24 h		0.009
1 μM	97.21 ± 27.91	
2 μM	89.45 ± 20.53	
4 μM	101.51 ± 19.82	
8 μM	82.26 ± 12.23	
10 μM	80.33 ± 24.92	
Cisplatin/48 h		0.001
1 μM	131.92 ± 21.19	
2 μM	130.52 ± 19.24	
4 μM	115.09 ± 28.51	
8 μM	103.69 ± 29.54	
10 μM	97.12 ± 44.61	
Cisplatin/72 h		0.003
1 μM	110.11 ± 13.66	
2 μM	98.65 ± 17.26	
4 μM	105.01 ± 14.81	
8 μM	107.13 ± 13.78	
10 μM	92.61 ± 16.64	
Enoxaparin sodium/24 h		0.215
0.1 μg/ml	114.08 ± 15.01	
0.5 μg/ml	112.89 ± 20.24	
1 μg/ml	112.57 ± 11.37	
5 μg/ml	110.33 ± 19.54	
10 μg/ml	105.32 ± 20.21	
50 μg/ml	102.83 ± 12.78	
100 μg/ml	96.07 ± 29.31	
Enoxaparin sodium/48 h		0.558
0.1 μg/ml	107.21 ± 18.36	
0.5 μg/ml	111.94 ± 21-06	
1 μg/ml	114.04 ± 21.57	
5 μg/ml	106.41 ± 23.36	
10 μg/ml	105.30 ± 16.59	
50 μg/ml	108.82 ± 13.61	
100 μg/ml	97.76 ± 23.72	
Enoxaparin sodium/72 h		0.303
0.1 μg/ml	126.71 ± 33.14	
0.5 μg/ml	122.77 ± 25.51	
1 μg/ml	113.84 ± 23.14	
5 μg/ml	109.31 ± 23.28	
10 μg/ml	109.25 ± 17.37	
50 μg/ml	108.98 ± 29.21	
100 μg/ml	106.18 ± 15.51	

**SD, standard deviation.*

TABLE 2 | Effects of cisplatin (8 and 10 μM) and enoxaparin sodium (0.1, 0.5, 1, 5, 10, 50, and 100 μg/ml) on H357 cell viability (ANOVA test).

Treatment/Time point	Absorbance (% over control) mean ± SD*	*p-value*
Cisplatin 8 μM/24 h		<0.001
Cisplatin 8 μM	82.26 ± 12.23	
Cisplatin 8 μM + Enoxaparin sodium 0.1 μg/ml	106.42 ± 3.59	
Cisplatin 8 μM + Enoxaparin sodium 0.5 μg/ml	99.48 ± 3.32	
Cisplatin 8 μM + Enoxaparin sodium 1 μg/ml	94.04 ± 4.54	
Cisplatin 8 μM + Enoxaparin sodium 5 μg/ml	94.37 ± 8.69	
Cisplatin 8 μM + Enoxaparin sodium 10 μg/ml	92.37 ± 3.57	
Cisplatin 8 μM + Enoxaparin sodium 50 μg/ml	88.61 ± 2.16	
Cisplatin 8 μM + Enoxaparin sodium 100 μg/ml	83.26 ± 10.92	<0.001
Cisplatin 8 μM/48 h		
Cisplatin 8 μM	103.69. ± 29.54	
Cisplatin 8 μM + Enoxaparin sodium 0.1 μg/ml	81.13 ± 8.39	
Cisplatin 8 μM + Enoxaparin sodium 0.5 μg/ml	89.60 ± 18.11	
Cisplatin 8 μM + Enoxaparin sodium 1 μg/ml	96.82 ± 14.07	
Cisplatin 8 μM + Enoxaparin sodium 5 μg/ml	87.29 ± 10.33	
Cisplatin 8 μM + Enoxaparin sodium 10 μg/ml	78.65 ± 13.95	
Cisplatin 8 μM + Enoxaparin sodium 50 μg/ml	77.07 ± 4.09	
Cisplatin 8 μM + Enoxaparin sodium 100 μg/ml	76.39 ± 10.78	
Cisplatin 8 μM/72 h		<0.001
Cisplatin 8 μM	107.13 ± 13.78	
Cisplatin 8 μM + Enoxaparin sodium 0.1 μg/ml	109.57 ± 13.82	
Cisplatin 8 μM + Enoxaparin sodium 0.5 μg/ml	102.78 ± 9.52	
Cisplatin 8 μM + Enoxaparin sodium 1 μg/ml	98.25 ± 10.45	
Cisplatin 8 μM + Enoxaparin sodium 5 μg/ml	95.54 ± 8.92	
Cisplatin 8 μM + Enoxaparin sodium 10 μg/ml	89.68 ± 5.71	
Cisplatin 8 μM + Enoxaparin sodium 50 μg/ml	89.08 ± 4.61	
Cisplatin 8 μM + Enoxaparin sodium 100 μg/ml	78.61 ± 8.62	
Cisplatin 10 μM/24 h		<0.001
Cisplatin 10 μM	80.33 ± 24.92	
Cisplatin 10 μM + Enoxaparin sodium 0.1 μg/ml	105.32 ± 11.96	
Cisplatin 10 μM + Enoxaparin sodium 0.5 μg/ml	93.59 ± 6.11	
Cisplatin 10 μM + Enoxaparin sodium 1 μg/ml	85.58 ± 7.36	
Cisplatin 10 μM + Enoxaparin sodium 5 μg/ml	86.88 ± 6.57	
Cisplatin 10 μM + Enoxaparin sodium 10 μg/ml	80.21 ± 6.81	
Cisplatin 10 μM + Enoxaparin sodium 50 μg/ml	80.58 ± 4.65	
Cisplatin 10 μM + Enoxaparin sodium 100 μg/ml	78.92 ± 4.41	
Cisplatin 10 μM/48 h		0.616
Cisplatin 10 μM	97.12 ± 44.61	
Cisplatin 10 μM + Enoxaparin sodium 0.1 μg/ml	102.21 ± 23.52	
Cisplatin 10 μM + Enoxaparin sodium 0.5 μg/ml	93.97 ± 14.99	
Cisplatin 10 μM + Enoxaparin sodium 1 μg/ml	89.82 ± 14.93	
Cisplatin 10 μM + Enoxaparin sodium 5 μg/ml	87.65 ± 15.31	
Cisplatin 10 μM + Enoxaparin sodium 10 μg/ml	86.92 ± 14.91	
Cisplatin 10 μM + Enoxaparin sodium 50 μg/ml	85.71 ± 15.85	
Cisplatin 8 μM + Enoxaparin sodium 100 μg/ml	83.91 ± 10.98	
Cisplatin 10 μM/72 h		<0.001
Cisplatin 10 μM	92.61 ± 16.64	
Cisplatin 10 μM + Enoxaparin sodium 0.1 μg/ml	44.22 ± 28.11	
Cisplatin 10 μM + Enoxaparin sodium 0.5 μg/ml	43.71 ± 26.87	
Cisplatin 10 μM + Enoxaparin sodium 1 μg/ml	42.83 ± 24.83	
Cisplatin 10 μM + Enoxaparin sodium 5 μg/ml	39.31 ± 21.81	
Cisplatin 10 μM + Enoxaparin sodium 10 μg/ml	41.64 ± 26.09	
Cisplatin 10 μM + Enoxaparin sodium 50 μg/ml	36.36 ± 18.53	
Cisplatin 10 μM + Enoxaparin sodium 100 μg/ml	34.23 ± 14.57	

**SD, standard deviation.*

The present study assayed the effect of enoxaparin sodium on cell viability at 24, 48 and 72 h incubation, observing that, as the dose of LMWH increased, cell viability decreased, with the greatest reduction found with the 100 μg/ml dose, although no statistically significant differences were found at any of the incubation times assayed. Nevertheless, in 2011, Abu Arab et al. (45) observed an antiproliferative effect on human lung adenocarcinoma epithelial cell line A549 cultured with different concentrations of enoxaparin sodium (5, 10, 20, and 30 U/ml), obtaining statistically significant differences in comparison with a control group.

On the basis of the present results, it was found that cisplatin concentrations combined with 100 μg/ml enoxaparin sodium produced the greatest synergic effect on OSCC cell viability reduction, with statistically significant differences at concentrations of 8 and 10 μM cisplatin at 24 h incubation ($p<0.001$ and $p<0.001$, respectively), and for 1, 2, 4 and 8 μM cisplatin at 48 h incubation ($p<0.001$, $p=0.006$, $p=0.030$, and $p<0.001$, respectively). The present results for the action of cisplatin in combination with enoxaparin sodium up OSCC cells

cannot be compared with any previous investigation of the possible synergic effects of these drugs for treating OSCC. Nevertheless, in 2016, Djaafar et al. (49) observed that enoxaparin sodium (200 μg/ml) reduced proto-oncogene regulator (cyclin D1) expression in mouse colon carcinoma cells MCA38. Cyclin D1 is related to the progression of G1 phase to S phase in the cell cycle. Its expression is generally increased in most tumors, but was seen to decrease through the action of enoxaparin sodium. Cell viability of colon cancer cells used in the study (MCA38) was seen to decrease after the reduction in cyclin D1 expression. This action of enoxaparin sodium combined with cisplatin's action (whereby it induces apoptosis and arrest of the cell cycle resulting from its interaction with DNA, such as the formation of cisplatin-DNA adducts, which activate multiple signaling pathways) (8) could explain the synergic effect of the cisplatin/enoxaparin sodium combination on cell viability of the H357 human OSCC line.

When the action of cisplatin combined with enoxaparin sodium on cell apoptosis was assayed it was found that at 24-, 48-, and 72-h incubation times, higher rates of apoptosis were producedwhen treatment combined 8 or 10 μM cisplatin and 100 μg/ml enoxaparin sodium, obtaining statistically significant differences after 48 h treatment (p=0.008 and p=0.009, respectively). In 2006, Balzarotti et al. (47) obtained similar results, although these researchers investigated enoxaparin sodium alone, using primary cell cultures obtained from high-grade glioma; a statistically significant increase in cell apoptosis was produced with doses of 10 and 100 U/ml enoxaparin sodium in comparison with a control group. Recently, Niu et al. (29) have studied the possible synergic effect of another LMWH (Low-molecular weight heparin calcium) (Bopuquin, TianJing Chase Sun Pharmacological Co, Ltd, TianJing, China) on cell apoptosis in cisplatin-resistant and cisplatin-sensitive lung adenocarcinoma A459/DDP cells. The authors found statistically significant differences for both cell lines when cisplatin was applied combined with 5 IU/ml LMWH, compared with treatment by cisplatin alone and a control group.

Lastly, when 8 or 10 μM cisplatin were combined with 100 μg/ml enoxaparin sodium, this produced the greatest reduction in cell migration capacity, with statistically significant differences for 8 μM cisplatin with 100 μg/ml enoxaparin sodium, at both 18 h (p=0.003) and 24 h (p=0.004) incubation. The interaction of enoxaparin sodium with heparanase at the start of the tumor metastasis process would appear to be closely related to the phenomenon of reduction in cell migration. During this step in the process, carcinogenic cells degrade the extracellular matrix and the basal membrane (including its main components—heparan sulfate proteoglycans [PGHS]) through heparanase, subsequently releasing cytokines, chemokines, and angiogenic growth factors [VEGF, bFGF]), so favoring angiogenesis, tumoral growth and metastasis. However, the reduction in heparanase expression (overexpressed in most human tumors) by the action of enoxaparin sodium will reduce this cell migration mechanism. In a study by Djaafar et al. (49), treatment of mouse colon carcinoma cells MCA38 with 200 μg/ml enoxaparin sodium, significantly reduced heparanase expression after 24 h by up to 50% (both ARN and proteins). Enoxaparin sodium's mode of action on the extracellular matrix will slow the cancer's invasion process (related to the action of heparanase) and could explain the results obtained in the present study. Mousa et al. (37) using the B16 melanoma mouse model of metastasis, found that a pre-tumor cell injection of enoxaparin sodium followed by daily doses (for 14 days) reduced lung tumor formation by 70%, with significant differences in comparison with an animal control group. The best enoxaparin sodium results were published by Seeholzer et al. (46) who studied 25 patients with advanced breast cancer, pointing to good clinical outlook for the use of this LMWH for treating cancer.

In conclusion, the combination of cisplatin and enoxaparin sodium showed a synergic effect in reducing cell viability and migration capacity and increased the apoptosis of H357 human OSCC cells. The present results suggest enoxaparin sodium could be beneficial in chemotherapy for OSCC patients. Further laboratory and clinical assays should be conducted to confirm and develop the present findings (see **Tables 1** and **2**).

DATA AVAILABILITY STATEMENT

The original contributions presented in the study are included in the article/supplementary material. Further inquiries can be directed to the corresponding author.

AUTHOR CONTRIBUTIONS

All authors have worked in an equal way in research duties for developing this work. The authors declare that there is no any conflict interest regarding this submission. All authors contributed to the article and approved the submitted version.

FUNDING

The fee will be paid with the grant of University of Murcia provided to Department of Oral Surgery. This paper is partially supported by Ministerio de Ciencia, Innovación y Universidades grant number PGC2018-097198-B-I00 and Fundación Séneca de la Región de Murcia grant number 20783/PI/18.

REFERENCES

1. Chi AC, Day TA, Neville BW. Oral cavity and oropharyngeal squamous cell carcinoma-an Update. *CA Cancer J Clin* (2015) 65:401–21. doi: 10.3322/caac.21293
2. Parkin DM, Bray F, Ferlay J, Pisani P. Global cancer statistic, 2002. *CA Cancer J Clin* (2005) 55:74–108. doi: 10.3322/canjclin.55.2.74
3. Kamangar F, Dores GM, Anderson WF. Patterns of cancer incidence, mortality, and prevalence across five continents: defining priorities to reduce cancer disparities in different geographic regions on the world. *J Clin Oncol* (2006) 24:2137–50. doi: 10.1200/JCO.2005.05.2308
4. Reid BC, Winn DM, Morse DE, Pendrys DG. Head and neck in situ carcinoma: incidence, trends, and survival. *Oral Oncol* (2000) 36:414–20. doi: 10.1016/S1368-8375(00)00028-2

5. Peterson PE. Oral cancer prevention and control-the approach of the World Health Organization. *Oral Oncol* (2009) 45:454–60. doi: 10.1016/j.oraloncology.2008.05.023
6. Price PM, Yu F, Kaldis P, Aleem E, Nowak G, Safirstein RL, et al. Dependence of cisplatin-induced cell death in vitro and in vivo on cyclin-dependent kinase 2. *J Am Soc Nephrol* (2006) 17:2434–42. doi: 10.1681/ASN.2006020162
7. Hiraishi Y, Wada T, Kakatani K, Tojyo I, Matsumoto T, Kiga N, et al. EGFR inhibitor enhances cisplatin sientivity of oral squamous cell carcinoma cell lines. *Pathol Oncol Res* (2008) 14:39–43. doi: 10.1007/s12253-008-9020-5
8. Wang G, Reed E, Li QQ. Molecular basis of cellular response to cisplatin chemotherapy in non-small cell lung cancer. *Oncol Rep* (2004) 12:955–65. doi: 10.3892/or.12.5.955
9. Bussu F, Pozzoli G, Giglia V, Rizzo D, Limongelli A, De CE, et al. Effects of the administration of epidermal growth factor receptor specific inhibitor cetuximab, alone and in combination with cisplatin, on proliferation and apoptosis of Hep-2 laryngeal cancer cells. *J Laryngol Otol* (2014) 128:902–8. doi: 10.1017/S002221511400190X
10. Kelland L. The resurgence of platinum-based cancer chemotherapy. *Nat Rev Cancer* (2007) 7:573–84. doi: 10.1038/nrc2167
11. Dasari S, Tchounwou PB. Cisplatin in cancer therapy: molecular mechanisms of action. *Eur J Pharmacol* (2014) 740:364–78. doi: 10.1016/j.ejphar.2014.07.025
12. Lee DY, Kim SK, Kim YS, Son DH, Nam JH, Kim IS, et al. Suppression of angiogenesis and tumor growth by orally active deoxycholic acid-heparin conjugate. *J Control Release* (2007) 118:310–7. doi: 10.1016/j.jconrel.2006.12.031
13. Pfankuchen DB, Stölting DP, Schlesinger M, Royer HD, Bendas G. Low molecular weight heparin tinzaparin antagonizes cisplatin resistance of ovarian cancer cells. *BiochemPharmacol* (2015) 97:147–57. doi: 10.1016/j.bcp.2015.07.013
14. Eramo A, Haas TL, De Maria R. Lung cancer stem cells: tools and targets to fight lung cancer. *Oncogene* (2010) 29:4625–35. doi: 10.1038/onc.2010.207
15. Bonnet D, Dick JE. Human acute myeloid leukemia is organized as a hierarchy that originates from a primitive hematopoietic cell. *Nat Med* (1997) 3:730–7. doi: 10.1038/nm0797-730
16. Lessard J, Sauvageau G. Bmi-1 determines the proliferative capacity of normal and leukemia stem cells. *Nature* (2003) 423:255–60. doi: 10.1038/nature01572
17. Eramo A, Lotti F, Sette G, Pilozzi E, Biffoni M, Di Vigilio A, et al. Identification and expansion of the tumorigenic lung cancer stem cell population. *Cell Death Differ* (2008) 15:504–14. doi: 10.1038/sj.cdd.4402283
18. Ricchi-Vitiani L, Lombardi DG, Pilozzi E, Biffoni M, Todaro M, Peschle C, et al. Identificacion and expansión of human colon-cancer-initiating cells. *Nature* (2007) 445:111–5. doi: 10.1038/nature05384
19. Singh SK, Hawkins C, Clarke IS, Squire JA, Bayani J, Hide T. Identification of human brain tumor initiating cells. *Nature* (2004) 432:396–401. doi: 10.1038/nature03128
20. Harper LJ, Costea DE, Gammon L, Fazil B, Biddle A, Mackenzie IC. Normal and malignant epithelial cells with stem-line properties have an extended G2 cell cycle phase that is associated with apoptotic resistance. *BMC Cancer* (2010) 10:166. doi: 10.1186/1471-2407-10-166
21. Major AG, Pitty LP, Farah CS. Cancer stem cell markers in head and neck squamous cell carcinoma. *Stem Cells Int* (2013) 2013:319489. doi: 10.1155/2013/319489
22. Tonigold M, Rossmann A, Meinold M, Bette M, Märken M, Henkenius K, et al. A cisplatin-resistant head and neck cancer cell line with cytoplasmic p53 (mut) exhibits ATP-binding cassette transporter upregulation and high glutathione levels. *J Cancer Res Clin Oncol* (2014) 140:1689–704. doi: 10.1007/s00432-014-1727-y
23. Dean M, Fojo T, Bates S. Tumour stem cells and drug resistance. *Nat Rev Cancer* (2005) 5:275–84. doi: 10.1038/nrc1590
24. Hirshmann JC, Foster AE, Wulf GG, Nuchtern JG, Jax TW, Gobel U, et al. A distinct "side population" of cells with high drug efflux capacity in human tumor cells. *Proc Natl Acad Sci USA* (2004) 101:14228–33. doi: 10.1073/pnas.0400067101
25. Yoh K, Ishii G, Yokose T, Minegishi Y, Tsuta K, Goto K, et al. Breast cancer resistance protein impacts clinical outcome in platinum-based chemotherapy for advanced non-small cell lung cancer. *Clin Cancer Res* (2004) 10:1691–7. doi: 10.1158/1078-0432.CCR-0937-3
26. Prandoni P, Lensing AW, Büller HR, Carta M, Cogo A, Vigo M, et al. Comparison of subcutaneous low-molecular-weight heparin with intravenous standard heparin in proximal deep-vein thrombosis. *Lancet* (1992) 339:441–5. doi: 10.1016/0140-6736(92)91054-C
27. Akl EA, von Doormaal FF, Barba M, Kamath G, Kim SY, Kuipers S, et al. Parenteral anticoagulation may prolong the survival of patients with limited small cell lung cancer: a Cochrane systematic review. *J Exp Clin Cancer Res* (2008) 27:4. doi: 10.1186/1756-9966-27-4
28. Bendas G, Borsig L. Cancer cell adhesion and metastasis: selectins, integrins, and the inhibitory potential of heparins. *Int J Cell Biol* (2012) 2012:676731. doi: 10.1155/2012/676731
29. Niu Q, Wang W, Li Y, Ruden DM, Wang F, Li Y, et al. Low molecular weight heparin ablates lung cancer cisplatin-resistance by inducing proteasome-mediated ABCG2 protein degradation. *PloS One* (2012) 7:e41035. doi: 10.1371/journal.pone.0041035
30. Thodiyil P, Kakkar AK. Can low-molecular-weight heparins improve outcome in patients with cancer? *Cancer Treat Rev* (2002) 28:151–5. doi: 10.1016/S0305-7372(02)00040-3
31. Chatzinikolaou G, Nikitovic D, Berdiaki A, Zafiropoulos A, Katonis P, Karamanos NK, et al. Heparin regulates colon cancer cell growth through p38 mitogen-activated protein kinase signaling. *Cell Prolif* (2010) 43:9–18. doi: 10.1111/j.1365-2184.2009.00649.x
32. van Doormaal FF, Nisio MD, Otte HM, Richel DJ, Prins MH, Buller HR. Randomized trial of the effect of the low molecular weight heparin nadroparin on survival in patients with cancer. *J Clin Oncol* (2011) 29:2071–6. doi: 10.1200/JCO.2010.31.9293
33. Klerk CP, Smorenburg SM, Otten HM, Lensing AWA, Prins MH, Piovella F, et al. The effect of low molecular weight heparin on survival in patients with advanced malignancy. *J Clin Oncol* (2005) 23:2130–5. doi: 10.1200/JCO.2005.03.134
34. Mousa SA, Petersen LJ. Anti-cancer properties of low-molecular-weight heparin: preclinical evidence. *TrombHaemost* (2009) 102:258–67. doi: 10.1160/TH08-12-0832
35. Lee DY, Lee SW, Kim SK, Lee M, Chang HW, Moon HT, et al. Antiangiogenic activity of orally absorbable heparin derivate in different types of cancer cells. *Pharm Res* (2009) 26:2667–76. doi: 10.1007/s11095-009-9989-9
36. Dogan OT, Polat ZA, Karahan O, Epozturk K, Altum A, Akkurt I, et al. Antiangiogenic activities of bemiparin sodium, enozaparin sodium, nadroparin calcium and tinzaparin sodium. *Thromb Res* (2011) 128:29–32. doi: 10.1016/j.thromres.2011.05.005
37. Mousa SA, Linhardt R, Francis JL, Amirkhosravi A. Anti-metastatic effect of a non-anticoagulant low-molecular-weight heparin versus the standard low-molecular-weight heparin, enoxaparin. *TrombHaemost* (2006) 96:816–21. doi: 10.1160/TH06-05-0289
38. Hostettller N, Naggi A, Torri G, Ishaj-Michaeli R, Casu B, Vlodaysky I, et al. P-selectin- and heparanase-dependent antimetastatic activity of non-aticoagulant heparins. *FASEB J* (2007) 21:3562–72. doi: 10.1096/fj.07-8450com
39. Naggi A, Casu B, Perez M, Torri G, Cassinelli G, Penco S, et al. Modulation of the heparanase-inhibiting activity of heparin through selective desulfation, graded N-acetylation, and glicol splitting. *J Biol Chem* (2005) 280:12103–13. doi: 10.1074/jbc.M414217200
40. Fritzsche J, Simonis D, Bendas G. Melanoma cell adhesion can be blocked by heparin in vitro: suggestion of VLA-4 as a novel target for antimetastatic approaches. *ThrombHaemost* (2008) 100:1166–75. doi: 10.1160/TH08-05-0332
41. Ahmad S, Ansari AA. Therapeutic roles of heparin anticoagulants in cancer and related disorders. *Med Chem* (2011) 7:504–17. doi: 10.2174/157340611796799104
42. Falanga A, Vignoli A, Diani E, Marchetti M. Comparative assessment of low-molecular-weight heparins in cancer from the perspective of patient outcomes and survival. *Patient Relat Outcomes Meas* (2011) 2:175–88. doi: 10.2147/PROM.S10099
43. Rousseau A, Van Dreden P, Mbemba E, Elalamy I, Larsen A, Gerotziafas GT. Cancer cells BXPC3 and MCF7 differentially reverse the inhibition of thrombin generation by apixaban, fondaparinux and enoxaparin. *Thromb Res* (2015) 136:1273–9. doi: 10.1016/j.thromres.2015.08.009
44. Gerotziafas GT, Galea V, Mbemba E, Sassi M, Roman MP, Khaterchi A, et al. Effect of low molecular weight heparins and fondaparinux upon thrombin generation triggered by human pancreatic cells BXPC3. *CurrVascPharmacol* (2014) 12:893–902. doi: 10.2174/15701611120614121012144 1

45. Abu Arab W, Kotb R, Sirois M, Rousseau E. Concentration and time dependent effects of enoxaparin on human adenocarcinomicapithelial cell line A549 proliferation in vitro. *Can J Physiol Pharmacol* (2011) 89:705–11. doi: 10.1139/y11-068
46. Seeholzer N, Thürlimann B, Köberle D, Dagmar H, Korte W. Combining chemotherapy and low-molecular-weight heparin for the treatment of advanced breast cancer: results on clinical response, transforming growth factor-beta 1 and fibrin monomer in a phase II study. *Blood Coagul Fibrinolysis* (2007) 18:415,423. doi: 10.1097/MBC.0b013e3281139c1d
47. Balzarotti M, Fontana F, Marras C, Boiardi A, Croci D, Ciusani E, et al. In vitro of low molecular weight heparin effect on cell growth and cell invasion in primary cell cultures of high-grade gliomas. *Oncol Res* (2006) 16:245–50. doi: 10.3727/000000006783981053
48. Vitale FV, Rotondo S, Sessa E, Parisi A, Giaimo V, D'Angelo A, et al. Low molecular weight heparin administration in cancer patients with hypercoagulability-realted complications and carrying brain metastases: a case series study. *J Oncol Phar Pract* (2012) 18:10–6. doi: 10.1177/1078155210390254
49. Djaafar S, Dunand-Sautier I, Gonelle-Gispert C, Lacotte S, DE Agostini A, Petro M, et al. Enoxaparin Attenuates Mouse Colon Cancer Liver Metastases by Inhibiting Heparanase and Interferon-γ-inducible Chemokines. *Anticancer Res* (2016) 36:4019–32.
50. Carmichael J, DeGraff WG, Gazdar AF, Minna JD, Mitchell JB. Evaluation of a tetrazolium-based semiautomated colorimetric assay: assessment of chemosensitivity testing. *Cancer Res* (1987) 47:936–42.
51. Carmichael J, DeGraff WG, Gazdar AF, Minna JD, Mitchell JB. Evaluation of a tetrazolium-based semiautomated colorimetric assay: assessment of radiosensitivity. *Cancer Res* (1987) 47:943–6.
52. Gerharz M, Baranowsky A, Siebolts U, Eming S, Nischt R, Krieg T, et al. Morphometric analysis of murine skin wound healing: standardization of experimental procedures and impact of an advanced multitissue array technique. *Wound Repair Regener* (2007) 15:105–12. doi: 10.1111/j.1524-475X.2006.00191.x
53. Valster A, Tran NL, Nakada M, Berens ME, Chan AY, Symons M. Cell migration and invasion assays. *Methods* (2005) 37:208–15. doi: 10.1016/j.ymeth.2005.08.001
54. Hyakusoku H, Sano D, Takahashi H, Hatano T, Isono Y, Shimada S, et al. JunB promotes cell invasion, migration and distant metastasis of head and neck squamous cell carcinoma. *J Exp Clin Cancer Res* (2006) 35:6. doi: 10.1186/s13046-016-0284-4
55. Chang JH, Wu CC, Yuan KS, Wu ATH, Wu SY. Locoregionally recurrent head and neck squamous cell carcinoma: incidence, survival, prognostic factors, and treatment outcomes. *Oncotarget* (2017) 8(33):55600–12. doi: 10.18632/oncotarget.16340
56. Kalavrezos N, Bhandari R. Current trends and future perspectives in the surgicalmanagement of oral cancer. *Oral Oncol* (2010) 46:429–32. doi: 10.1016/j.oraloncology.2010.03.007
57. Moreno-Jiménez M, Valero J, López.Picazo JM, Arbea L, Aristu J, Cambeiro M, et al. Concomitant cisplatin, paclitaxed, and hyperfractionated radiotherapy in locally advanced head and neck cancer: comparison of two different schedules. *Am J Clin Oncol* (2010) 33:137–43. doi: 10.1097/COC.0b013e31819d369d
58. Smorenburg SM, Van Nooeren CJ. The complex effects of heparins on cancer progression and metastasis in experimental studies. *Pharmacol Rev* (2001) 53:93–105.
59. Niers TM, Klerk CP, DiNisio M, Van Noorden CJ, Buller HR, Reitsma PH, et al. Mechanisms of heparin induced anti-cancer activity in experimental cancer models. *Crit Rev Oncol Hematol* (2007) 61:195–207. doi: 10.1016/j.critrevonc.2006.07.007

Conflict of Interest: The authors declare that the research was conducted in the absence of any commercial or financial relationships that could be construed as a potential conflict of interest.

frontiers in Oncology

ORIGINAL RESEARCH
published: 02 December 2020
doi: 10.3389/fonc.2020.572919

Identification of a Transcriptional Prognostic Signature From Five Metabolic Pathways in Oral Squamous Cell Carcinoma

Xiang Wu[1†], *Yuan Yao*[1†], *Zhongwu Li*[1], *Han Ge*[1,2], *Dongmiao Wang*[2] *and Yanling Wang*[1,2*]

[1] Jiangsu Key Laboratory of Oral Disease, Nanjing Medical University, Nanjing, China, [2] Department of Oral and Maxillofacial Surgery, Affiliated Hospital of Stomatology, Nanjing Medical University, Nanjing, China

Dysregulated metabolic pathways have been appreciated to be intimately associated with tumorigenesis and patient prognosis. Here, we sought to develop a novel prognostic signature based on metabolic pathways in patients with primary oral squamous cell carcinoma (OSCC). The original RNA-seq data of OSCC from The Cancer Genome Atlas (TCGA) project and Gene Expression Omnibus (GEO) database were transformed into a metabolic pathway enrichment score matrix by single-sample gene set enrichment analysis (ssGSEA). A novel prognostic signature based on metabolic pathways was constructed by LASSO and stepwise Cox regression analysis in the training cohort and validated in both testing and validation cohorts. The optimal cut-off value was obtained using the Youden index by receiver operating characteristic (ROC) curve. The overall survival curves were plotted by the Kaplan-Meier method. A time-dependent ROC curve analysis with 1, 3, 5 years as the defining point was performed to evaluate the predictive value of this prognostic signature. A 5-metabolic pathways prognostic signature (5MPS) for OSCC was constructed which stratified patients into subgroups with favorable or inferior survival. It served as an independent prognostic factor for patient survival and had a satisfactory predictive performance for OSCC. Our results developed a novel prognostic signature based on dysregulated metabolic pathways in OSCC and provided support for aberrant metabolism underlying OSCC tumorigenesis.

Keywords: oral squamous cell carcinoma, metabolic pathways, prognostic signature, single sample gene-set enrichment, LASSO

OPEN ACCESS

Edited by:
Alberto Paderno, University of Brescia, Italy

Reviewed by:
Catriona M. Douglas, NHS Greater Glasgow and Clyde, United Kingdom
Chiara Romani, University of Brescia, Italy

***Correspondence:**
Yanling Wang
wangyanling@njmu.edu.cn

[†]These authors have contributed equally to this work

Specialty section:
This article was submitted to Head and Neck Cancer, a section of the journal Frontiers in Oncology

Received: *15 June 2020*
Accepted: *02 November 2020*
Published: *02 December 2020*

Citation:
Wu X, Yao Y, Li Z, Ge H, Wang D and Wang Y (2020) Identification of a Transcriptional Prognostic Signature From Five Metabolic Pathways in Oral Squamous Cell Carcinoma. Front. Oncol. 10:572919. doi: 10.3389/fonc.2020.572919

INTRODUCTION

Oral squamous cell carcinoma (OSCC) is a common malignant tumor in the head and neck region which is closely associated with smoking and alcohol abuse (1). Currently, it is frequently treated with a combination of surgery, radiotherapy and chemotherapy in the clinic. Despite significant advances in clinical management of OSCC, its prognosis still remains poor over the past years (2). The reasons for unfavorable prognosis might be due to limited understanding of genetic, molecular

and metabolic events underlying oral tumorigenesis as well as the lack of effective prognostic predictors and therapeutic targets (3). Furthermore, these traditional prognostic indicators such as tumor size, margin status and tumor stage remain far from optimal and usually fail to meet clinical needs due to substantial survival variations in patients within the same catalogs (2, 4). Thus, it is necessary and urgently required to identify new, effective, sensitive biomarkers for early detection, diagnosis and prognosis of OSCC.

The intricate link between dysregulated metabolism and tumorigenesis has been increasingly appreciated. Metabolic reprogramming such as glycolysis has been identified as a well-established hallmark of cancer (5). Altered metabolic pathways in cancer have become a driving force for cancer cells to gain beneficial energy or evade immune surveillance, thus suggesting that these changes can be exploited for biomarkers and therapeutic targets developments (6). Indeed, dysregulation of individual or multiple metabolic pathways has been explored as diagnostic or prognostic biomarkers across several human cancers. Several metabolic signatures at the transcriptional level have been reported to predict patients' survival in hepatocellular carcinoma and ovarian cancer (7, 8). However, most of these studies usually focused on the prognostic signatures based on genes involved in a single metabolic pathway, while some other metabolic abnormalities in cancer might be neglected. Thus, an integrative signature based on multiple metabolism-related gene sets might be better to capture the full metabolic dysregulations in cancer and have superior performance in prediction. Comprehensive analyses of metabolic pathways in head and neck squamous cell carcinoma (HNSCC) have yielded predictive models and established prognostic predictors with high performance (9). However, HNSCC is a heterogeneous group of epithelial malignancies with diverse etiologic factors, tumorigenic processes and treatment modalities, as exemplified by HPV infection and its distinct roles between OSCC and oropharyngeal SCC (2, 10). To the best of our knowledge, the prognostic significance of metabolic signature in OSCC remains largely underexplored until now.

Burgeoning development of genome-wide sequencing technology and assembly of The Cancer Genome Atlas (TCGA) and Gene Expression Omnibus (GEO) databases provide rich resources for biomarker development to better early diagnosis, patient stratification, personalized treatment as well as prognostic prediction (11). Based on these datasets, several biomarkers derived from aberrant DNA methylation, mRNA/microRNA/lncRNA expression or combinations of these abnormalities such as gene signatures have been identified and validated to predict survival in patients with OSCC (12–14). For example, a three lncRNA-based signature and a 7 CpG-based signature coupled with gene expression have been successfully established for OSCC prognostic prediction (15, 16).

In the present study, we utilized publicly available RNA sequencing (RNA-seq) data of OSCC samples from TCGA project, constructed and validated a novel prognostic signature based on 5-metabolic pathway-related gene sets by bioinformatics approaches *via* integrating single-sample gene set enrichment analysis (ssGSEA), least absolute shrinkage and selection operator (LASSO) and Cox regression analyses.

MATERIALS AND METHODS

Data Acquisition and Preprocessing

TCGA represents international collaborative efforts to comprehensively delineate the biological characteristics of common human cancers and becomes the rich source to establish the link between genomic features and clinicopathological information among individual types of cancer largely based on the detailed datasets including RNA-seq, demographic information, clinical stage and patient survival (11). The original HNSCC RNA-seq data were downloaded from TCGA database and all OSCC relevant datasets were further retrieved from TCGA-HNSC dataset. A total number of 328 OSCC tumors and 32 normal counterparts were identified and enrolled. All relevant epidemiological, clinicopathological as well as follow-up data were obtained and collated in **Supplementary Table S1**. Moreover, two independent OSCC datasets (GSE41613 and GSE42743) deposited by Chen C's group in GEO database were found and utilized (14). And "Combat" in R package "sva" was used to remove batch effects. Patient informed consent and approval of the institutional review board were waived given the use of the existing, publically available datasets. Moreover, the immunohistochemical images from the Human Protein Atlas (HPA) database were used to detect the expression of the genes at the translational level (17).

Acquisition of Metabolism-Related Gene Dataset

These metabolism-related gene datasets were downloaded from the KEGG pathway database (18). There are 90 metabolic pathways including nucleotide metabolism, amino acid metabolism, sand glycan biosynthesis and metabolism. All gene sets of these metabolic pathways were listed in **Supplementary Table S2**.

Construction of Metabolism-Based Prognostic Signature for OSCC

All OSCC patients from TCGA-HNSC dataset were randomly divided into two cohorts (training cohort: testing cohort=7:3). Datasets from GSE41613 (97) and GSE42743 (74) were pooled and defined as an independent, validation cohort (14). The prognostic signature was constructed according to the following steps (**Supplementary Figure S1**). Firstly, single-sample GSEA (ssGSEA) was used to calculate and standardize the enrichment scores of individual metabolism-related gene set in each sample (19, 20). Secondly, dysregulated metabolic pathways between tumors and normal samples were screened by cut-off FDR<0.05. Thirdly, the univariate Cox regression was used to identify survival-related metabolic pathways with the *P*-value <0.05. Fourthly, the LASSO regression was performed on these survival-related metabolic pathways, and the non-zero coefficients' metabolic pathways were filtered out for further

analyses. Finally, the final metabolism-based prognostic model was constructed by stepwise multivariate Cox regression analysis. The calculation formula for risk scores of five metabolic pathways was as follows: Risk score = $\sum_{i=1}^{n} \beta i * xi$. x was the ssGSEA score for each metabolic pathways and β was the regression coefficients in the multivariable Cox regression analysis in the training set All these analyses were performed using the R software (version 3.6.3).

Statistical Analyses

A receiver operating characteristic (ROC) curve was plotted by "survival ROC" package in R and the optimal cut-off value for risk score was identified using Youden index. All patients were divided into low-risk and high-risk groups based on the cut-off value. The overall survival was counted with Kaplan-Meier method and the difference was compared with log-rank test. A time-dependent ROC curve with 1, 3, 5 years as the defining point was performed to evaluate the predictive value of risk score. The calibration curve was plotted to evaluate the difference between the predicted and actual values of the predictive model. The comparisons of clinicopathological parameters (age, gender, grade, tumor stage and margin status) between high-risk and low-risk groups were analyzed *via* Chi-square test. The evaluation of statistically significant differences of metabolic pathways risk score between subgroups was performed by one-way ANOVA analyses. Univariate and multivariate Cox regression analyses were employed to determine prognostic factors associated with survival. All these analyses were performed using the R software (version 3.6.3). All statistical tests were two sided and *P* values less than 0.05 were considered statistically significant.

RESULTS

Patient Cohorts and RNA-Seq Datasets

After data screening and filtering, 328 OSCC samples and 32 normal samples with original RNA-seq data and clinical follow-up information from TCGA were retrieved and randomly divided into training and testing cohorts. RNA-seq data and clinical information of 171 OSCC samples (defined as validation cohort) were obtained from GSE41613 and GSE42743 (14).

Identification of Dysregulated Metabolic Pathways and Construction of Metabolic Prognostic Signature in OSCC

The detailed analytic pipeline for signature development was shown in **Supplementary Figure S1**. Initially, we determined enrichment scores of 90 known metabolic pathways in the training datasets by ssGSEA and assigned individual score for every metabolic pathways in each sample. Then, we identified 75 dysregulated metabolic pathways which significantly differed between OSCC and normal samples with FDR<0.05 and 16 survival-related metabolic pathways by univariate Cox regression analysis (*P*<0.05) were found. As shown in **Figures 1A, B**, 7 survival-related metabolic pathways were selected by LASSO regression for further stepwise multiple Cox regression analyses. Finally, we developed a prognostic signature consisting of 5 metabolic pathways: hsa00561 (Glycerolipid metabolism), hsa00910 (Nitrogen metabolism), hsa00534 (Glycosaminoglycan biosynthesis-heparan sulfate/heparin), hsa01230 (Biosynthesis of amino acids) and hsa00670 (One carbon pool by folate). The coefficients of 5 metabolic pathways were shown: hsa00561: 0.22332, hsa00910: 0.18382, hsa00534: 0.20845, hsa01230: 0.33467, and hsa00670: 0.19317.

The 5-Metabolic Pathways Signature Predicts Survival of Patients With OSCC

The risk score formula was developed based on enrichment score and coefficients of these 5 metabolic pathways, which was named as 5-metabolic pathways signature (5MPS). An optimal cut-off value was selected as 0.831 with maximal sensitivity and specificity as evidenced by AUC 0.693 (**Figure 1C**). All patients in the training sets were divided into high-risk group and low-risk group according to this optimal cut-off value. The Kaplan-Meier analyses indicated that patients in high-risk subgroup had a worse prognosis than those in low-risk subgroup (*P*<0.0001, **Figures 1D, E**). Moreover, a time-dependent receiver operating characteristic (ROC) curve was performed to estimate the sensitivity and specificity of this 5MPS. Data listed in **Figure 1F** indicated that this signature to predict patient survival in 1, 3 and 5 years was satisfactory with AUC 0.666, 0.657, and 0.680 in the training cohort. In addition, the calibration curve was plotted to evaluate the performance of this signature. And the result shown in **Supplementary Figure S2** revealed that the prediction was close to a 45 degree slash, thus indicating that 5MPS prediction was well consistent with actual observation.

Validation of 5MPS Predictive Values in Multiple Independent OSCC Cohorts

Patients in testing and validation cohorts were stratified into high-risk and low-risk subgroups according to the 5MPS. As shown in **Figures 1G, H**; **Supplementary Figure S3**, the results from Kaplan-Meier analyses indicated that patients in high-risk subgroup had a lower OS ratio than those in low-risk subgroup in testing cohort (*P*=0.0191), validation cohort (*P*=0.0269) and TCGA-OSCC cohort (*P*<0.0001). As shown in **Supplementary Figure S4**, the AUC from time-dependent ROC curves were 0.702, 0.618, and 0.626 in testing cohort and 0.616, 0.628 and 0.688 in validation cohort, respectively.

Correlations Between 5MPS With Clinicopathological Characteristics in OSCC

As shown in **Figure 2A**, the heatmap showed the distributions of enrichment scores and several clinicopathological parameters including age, gender, grade, margin status, tumor stage between patients in high- and low-risk subgroups. We found that 5MPS was significantly associated with margin status (*P*<0.05) and survival status (*P*<0.0001). Moreover, as shown in **Figure 2B**, patents stratified with differentiation degree or margin status had

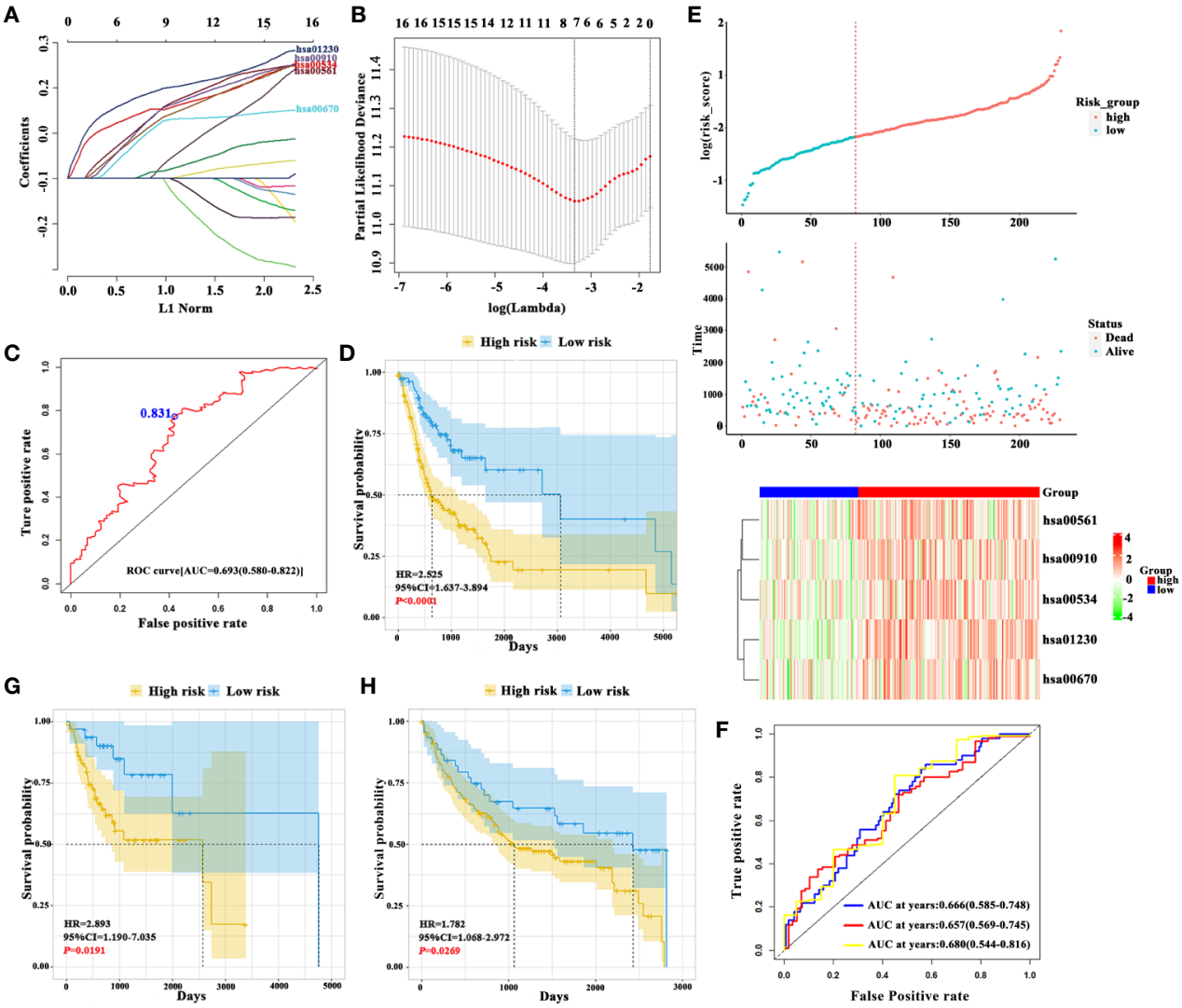

FIGURE 1 | Construction of 5-metabolic pathways signature and its prognostic value **(A)**. The coefficient profile plot of 16 survival-related metabolic pathways was produced against the log lambda sequence **(B)**. Tuning parameter (lambda) selection in the LASSO model used tenfold cross-validation *via* minimum criteria. Dotted vertical lines were drawn at the optimal values using the minimum criteria and the 1 standard error of the minimum criteria (the 1-SE criteria) **(C)**. ROC analysis of sensitivity and specificity of overall survival time by the 5-metabolic pathways signature based risk score. The blue dot represents the optimal cut-off value in training cohort using ROC analysis **(D)**. The Kaplan-Meier analyses revealed significant associations between 5MPS and OS in patients from the training cohort **(E)**. From top to bottom: The survival status of patients with OSCC in training cohort. Patient subgroups with high and low-risk score were classified by the optimal cut-off value. The heatmap show the distribution of 5 metabolic pathways enrichment score in high risk and low risk groups in training cohort **(F)**. The time-dependent ROC curve analysis with 1, 3, 5 years as the defining point was performed to evaluate the predictive value of the 5-metabolic pathways risk score in training cohort **(G, H)**. The Kaplan-Meier analyses revealed significant associations between 5MPS and OS in patients from the testing **(G)** and validation cohorts **(H)**.

significantly different risk scores, which indicated higher risk score was associated with higher pathological grade and positive margin status.

Univariate and Multivariate Cox Regression Analyses for 5MPS

To further delineate the prognostic value of 5MPS in OSCC, we performed univariate and multivariate Cox regression using the whole OSCC cohort from TCGA-HNSC dataset. Our data revealed that 5MPS was associated with overall survival in OSCC patients (HR, 2.384; 95% CI: 1.606–3.541; P <0.0001). In addition, some well-established clinicopathological parameters such as margin status and tumor stage were also identified to be prognostic. Moreover, we performed multivariate Cox regression analyses to eliminate confounding factors and highlight the prognostic value of 5MPS. As shown in **Figure 3**, 5MPS was identified as an independent predictive factor for OSCC (HR, 1.743; 95% CI: 1.154-2.635; P =0.0083). Consistently,

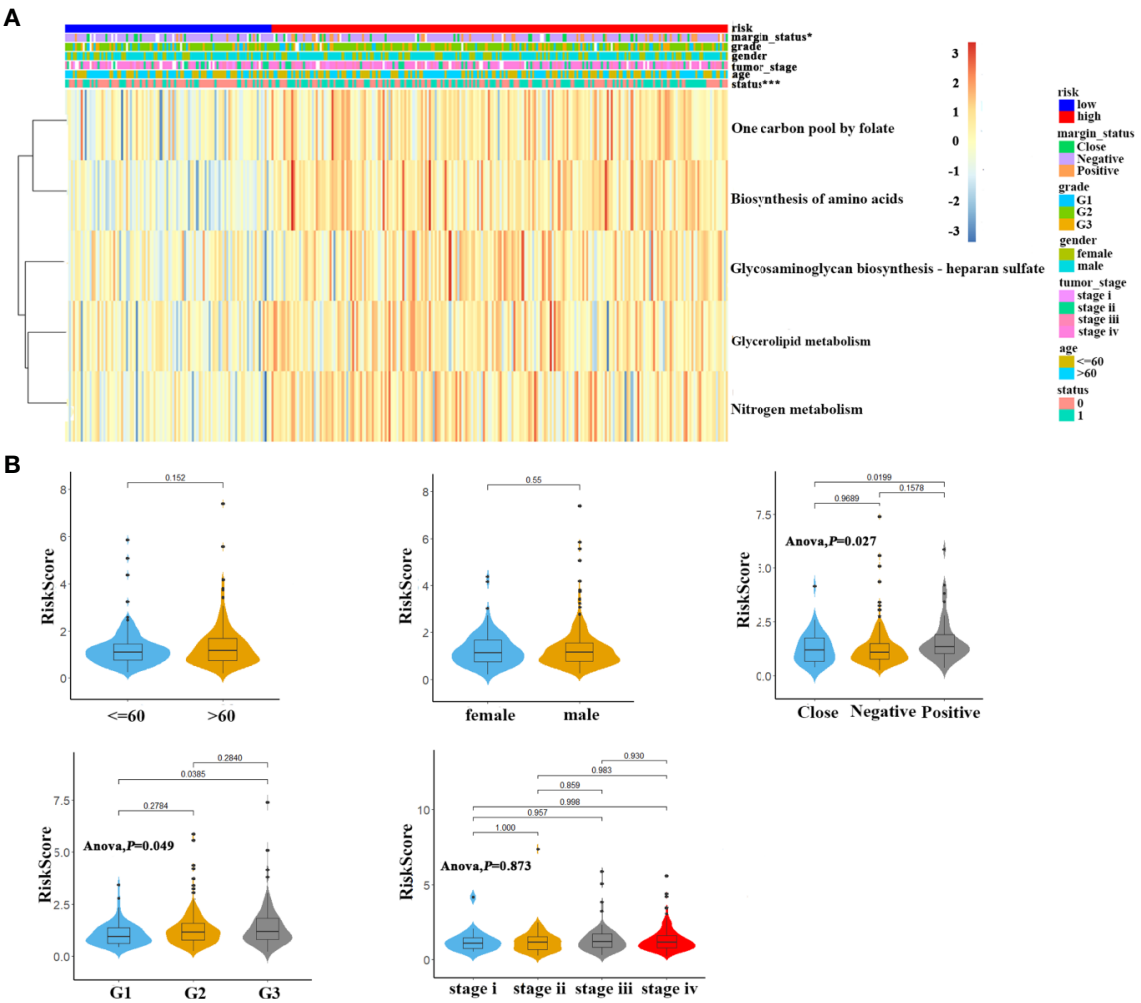

FIGURE 2 | The association of 5-metabolic pathways risk score and clinicopathological parameters **(A)**. The heatmap shows the distribution of 5 metabolic pathways enrichment score and clinicopathological parameters between high risk and low risk groups in TCGA OSCC cohort **(B)**. Distribution of 5-metabolic pathways risk score in different subgroups was compared, which stratified by age, gender, margin status, grade and tumor stage.

as shown in **Figures 4A–J**, this 5MPS robustly predicted overall survival in OSCC patients stratified by epidemiological, clinical and pathological parameters.

The Representative Genes in Five Metabolic Pathways Predict Survival in Patients With OSCC

To further characterize these 5 metabolic pathways integrated into 5MPS, we selected representative genes such as DGKG (Diacylglycerol kinase gamm), CA9 (Carbonic anhydrase 9), EXTL2 (Exostosin like glycosyltransferase 2), PGAM1 (Phosphoglycerate mutase 1), TYMS (Thymidylate Synthase) from these dysregulated metabolic pathways. The expression of these 5 genes was compared between 32 paired tumor and normal samples from TCGA OSCC cohort. As shown in **Figures 5A–E**, expression levels of these genes were significantly higher in OSCC as compared to their normal counterparts. Consistently, as shown in **Supplementary Figure S5**, we retrieved the data from the human protein atlas (HPA) platform and found that the protein abundance of these 5 genes in HNSCC samples appeared to be upregulated relative to their healthy counterparts based on both intensity and quantity of staining, although we can't definitively perform these comparisons by statistical analyses due to the lack of detailed staining data (17).

Moreover, we divided patients into low and high expression subgroups based on the median values of gene expression. Kaplan-Meier analyses indicated that these five genes were significantly associated with OS in OSCC patients (**Figures 5F–J**).

DISCUSSION

OSCC is a lethal malignancy characterized by rapid progression, cervical lymph node involvement and relatively high mortality.

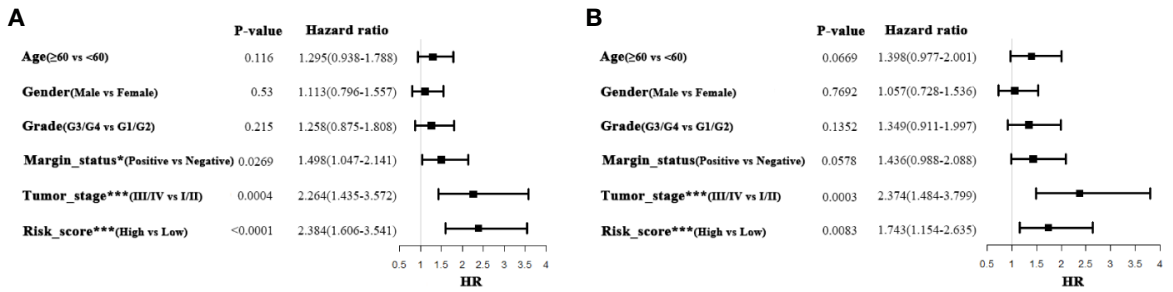

FIGURE 3 | Univariate and Multivariate Cox-regression analyses of 5-metabolic pathways signature and clinicopathological parameters in TCGA OSCC cohort (**A** Univariate analysis; **B** Multivariate analysis).

However, the traditional prognostic parameters fail to fully satisfy the clinical demands for accurate and individualized prognostic evaluation (2). Therefore, it is imperative to develop more accurate and sensitive biomarkers for OSCC diagnosis and prognostic prediction. Here, we constructed and validated a novel prognostic biomarker namely 5-metabolic pathways signature (5MPS) for OSCC *via* an integrative bioinformatics approach.

Most metabolic processes such as those involving energy and amino acid catabolism are common and pivotal to all living cells. However, compared to normal cells, some metabolic pathways such as glycolysis and fatty-acid oxidation have undergone tremendous changes in cancer cells due to their high energy requirements to support highly proliferation and metastasis. Recently, cancer metabolomics has been proposed to comprehensively characterize hallmarks of cancer-related metabolic changes (21). However, most of previous studies have largely focused on individual metabolic pathway underlying oral tumorigenesis and identified multiple biomarkers with diagnostic and prognostic significance as well as potential therapeutic targets (22, 23). Here, we exploited an integrative bioinformatics approach to comprehensively characterize the survival-related metabolic changes in OSCC. By utilizing RNA-seq datasets from TCGA and GEO, we developed a novel prognostic signature based on 5 dysregulated metabolic pathways in OSCC.

Cancer metabolomics have provided sensitive and thorough metabolic signatures as effective biomarkers for cancer diagnosis, treatment and prevention (24). Comprehensive analyses of metabolites in clinical samples such as saliva, urine and serum have identified valuable biomarkers for cancer diagnosis and prognostic prediction in multiple cancers including OSCC (25–28). Deregulated metabolic pathways including glucose metabolism, glutaminolysis and tricarboxylic acid cycle have been reported in OSCC (26). However, these abovementioned studies largely focused on a few metabolites or individual metabolites in cancer. Here, we constructed an integrative signature based several metabolic gene sets in OSCC. This analytic approach enabled simultaneous integration of dysregulated metabolic pathways that had impact on patient prognosis. As expected, our 5MPS robustly stratified patients into subgroups and served as an independent factor affecting patient survival. We believe that this 5MPS will be beneficial for predicting patient survival when it is added into current clinical regime. Of course, to reinforce its translational potentials, the predictive performance of 5MPS should be further validated.

Beyond this prognostic value of 5MPS, our 5MPS also reflected the importance of these dysregulated metabolic pathways involved in OSCC tumorigenesis. These aberrant metabolic pathways provided nutrients and biomass to meet the high energy and biosynthetic demand of cancer cells (21). For example, glycerolipid metabolism and fatty-acid oxidation have undergone tremendous changes in cancer cells to support their proliferation and metastasis (29, 30). In addition, oncogene-driven activation of cell growth was associated with increased amino acid uptake and biosynthesis (31). Folates promoted one-carbon metabolism essential for purines and thymidylate biosynthesis and enhanced DNA replication in cancer cells (32). In line with these, our results from 5 representative genes in these pathways showed that they were significantly upregulated in OSCC relative to their normal counterparts and associated with unfavorable survival. Previous studies have reported that CA9, EXTL2, PGAM1, and TYMS were dysregulated across multiple human cancers and intricately associated with tumorigenesis by functioning as key enzymes underlying metabolism (33–36). Moreover, high expression of CA9 and PGAM1 were associated with inferior prognosis in OSCC, which in part strengthened our data (33, 35). Noticeably, Yang et al. utilized gas chromatography-mass spectrometry high-throughput analysis to determine the amino acid metabolic characteristics of OSCC and found that a panel including three amino acids (glutamate, aspartic acid, and proline) was identified as potential diagnostic biomarkers of OSCC (37). These findings may add further support to the key roles of dysregulated metabolism responsible for OSCC initiation and progression, thus ultimately impacting patient prognosis.

Although, 5MPS identified here was robust and promising, there were still several limitations. Firstly, the number of OSCC samples is relatively small. This signature is still needed to be independently validated in more cohorts. However, the data from multiple databases and our training-testing-validation cohort design might compensate for this disadvantage. Secondly, 5MPS mainly depended on RNA-seq data whose procedures of detection, quantification should be standardized and normalized. Thirdly, 5MPS was based on gene sets so that might limit its clinical application to a certain degree.

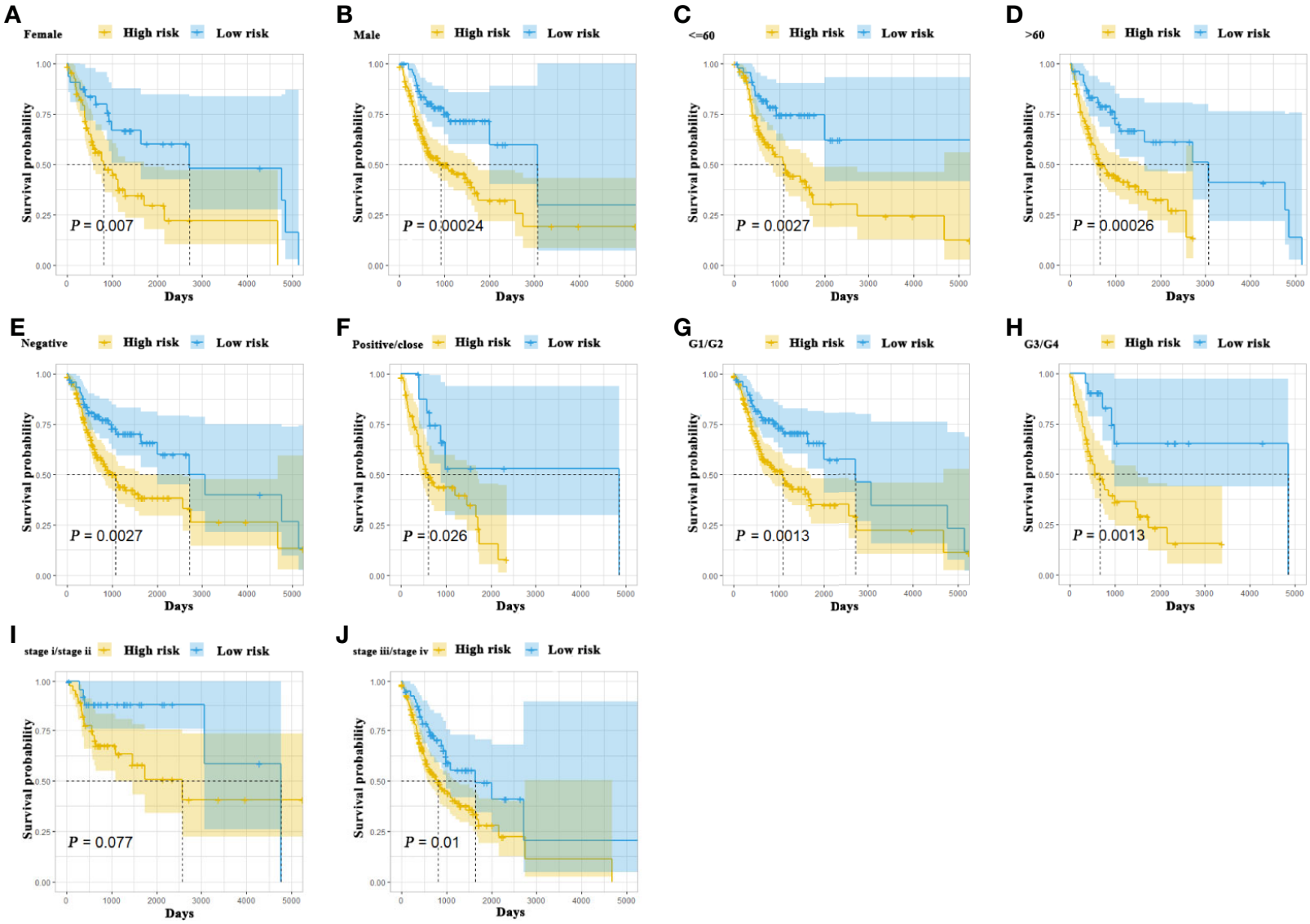

FIGURE 4 | The Kaplan-Meier analyses revealed significant associations between 5MPS and OS of OSCC patients in different clinical subgroups, grouping based on their age, gender, margin status, grade, and tumor stage **(A-J)**.

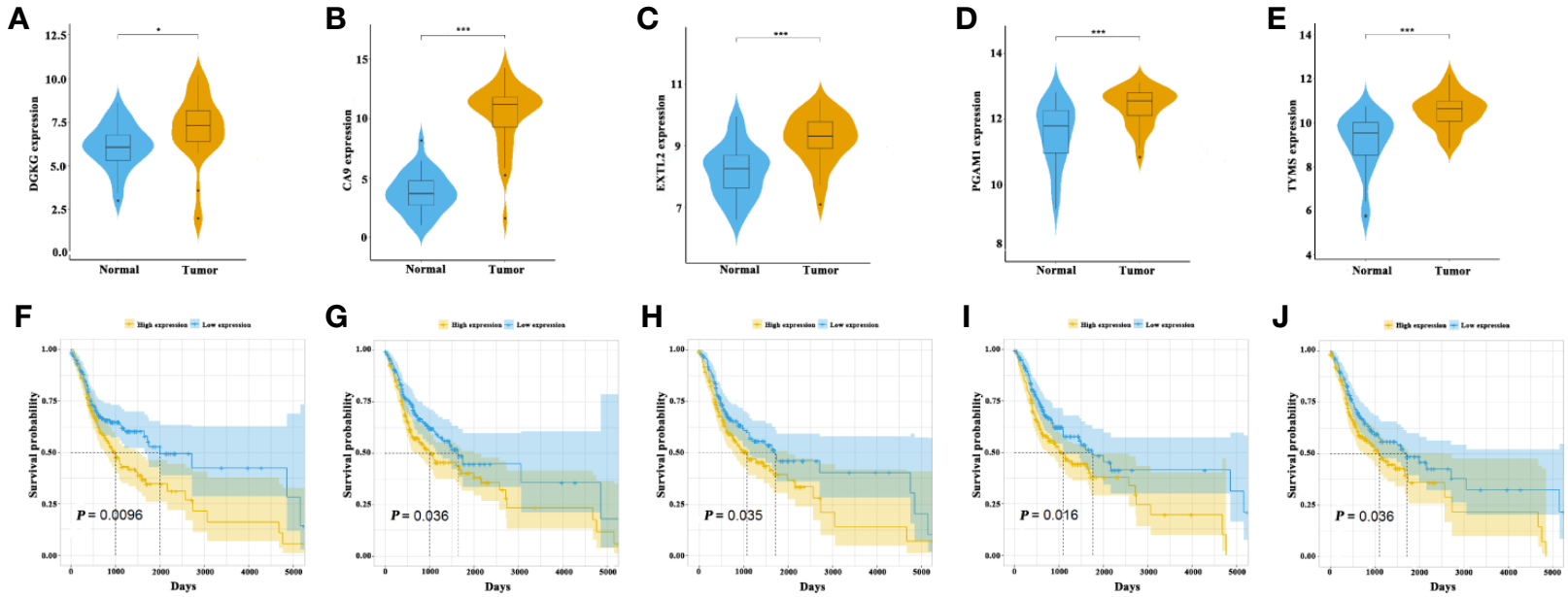

FIGURE 5 | The association of five metabolism-related genes from these five metabolic pathways with OS in OSCC patients **(A–E)**. The expression of DGKG, CA9, EXTL2, PGAM1 and TYMS were compared between tumor and normal **(F–J)**. The Kaplan-Meier analyses revealed significant associations between DGKG **(F)**, CA9 **(G)**, EXTL2 **(H)**, PGAM1 **(I)** and TYMS **(J)** and OS of OSCC patients in TCGA OSCC cohort, *P < .05,***P < .001.

CONCLUSION

In conclusion, our study identified a novel 5-metabolic pathways signature (5MPS) based on RNA-seq data which reflected dysregulated metabolic pathways and their prognostic significance in OSCC. This 5MPS served as a novel prognostic biomarker for OSCC, which was warranted to be validated further in a large amount of prospectively enrolled patients.

DATA AVAILABILITY STATEMENT

The datasets presented in this study can be found in online repositories. The names of the repository/repositories and accession number(s) can be found in the article/**Supplementary Material**.

AUTHOR CONTRIBUTIONS

XW and YY performed the data collection, analysis and manuscript writing. ZL, HG, and DW assisted out data collection and statistical analyses. YW conceived and supervised the whole project. All authors contributed to the article and approved the submitted version.

FUNDING

This work is financially supported, in whole or in part, by National Natural Science Foundation of China (81572669, 81602386, 81602378), Natural Science Foundation of Jiangsu Province (BK20161564, BK20161024), A Project Funded by the Priority Academic Program Development of Jiangsu Higher Education Institutions (2018-87), Research grant from Nanjing Medical University and Southeast University (2017DN20) and Project from Nanjing Municipal Committee of Science and Technology (201803044). The funders had no role in study design, data collection, data analysis, interpretation, or writing of the report.

SUPPLEMENTARY MATERIAL

The Supplementary Material for this article can be found online at: https://www.frontiersin.org/articles/10.3389/fonc.2020.572919/full#supplementary-material

SUPPLEMENTARY FIGURE 1 | The procedures for analyzing 5MPS in oral squamous cell carcinoma (OSCC).

SUPPLEMENTARY FIGURE 2 | The calibration curve was plotted to evaluate 5-metabolic pathways signature predictive performance for predicting OS of patients at 1, 3, 5 years in training cohort.

SUPPLEMENTARY FIGURE 3 | The Kaplan-Meier analysis revealed significant associations between 5-metabolic pathways signature and OS in patients from the TCGA OSCC cohort.

SUPPLEMENTARY FIGURE 4 | The time-dependent ROC curve analysis with 1, 3, 5 years as the defining point was performed to evaluate the predictive value of the 5-metabolic pathways risk score in testing cohort **(A)** and validation cohort **(B)**.

SUPPLEMENTARY FIGURE 5 | The immunohistochemical images from the Human Protein Atlas (HPA) database were used to compare the expression of DGKG, CA9, EXTL2, PGAM1 and TYMS at the translational level between HNSCC and normal samples. Both intensity and quantity of immunohistochemical staining in HNSCC and Normal oral mucosa were retrieved and shown in the right panel for each gene of interest.

REFERENCES

1. Siegel RL, MillerA Jemal KD. Cancer statistics, 2019. *CA Cancer J Clin* (2019) 69(1):7–34. doi: 10.3322/caac.21551
2. Chi AC, Day TA, Neville BW. Oral cavity and oropharyngeal squamous cell carcinoma–an update. *CA Cancer J Clin* (2015) 65(5):401–21. doi: 10.3322/caac.21293
3. Hasegawa T, Tanakura M, Takeda D, Sakakibara A, Akashi M, Minamikawa T, et al. Risk factors associated with distant metastasis in patients with oral squamous cell carcinoma. *Otolaryngol Head Neck Surg* (2015) 152(6):1053–60. doi: 10.1177/0194599815580980
4. Dissanayaka WL, Pitiyage G, Kumarasiri PV, Liyanage RL, Dias KD, Tilakaratne WM. Clinical and histopathologic parameters in survival of oral squamous cell carcinoma. *Oral Surg Oral Med Oral Pathol Oral Radiol* (2012) 113(4):518–25. doi: 10.1016/j.oooo.2011.11.001
5. DeBerardinis RJ, Chandel NS. Fundamentals of cancer metabolism. *Sci Adv* (2016) 2(5):e1600200. doi: 10.1126/sciadv.1600200
6. Chiaradonna F, Moresco RM, Airoldi C, Gaglio D, Palorini R, Nicotra F, et al. From cancer metabolism to new biomarkers and drug targets. *Biotechnol Adv* (2012) 30(1):30–51. doi: 10.1016/j.biotechadv.2011.07.006
7. Liu GM, Xie WX, Zhang CY, Xu JW. Identification of a four-gene metabolic signature predicting overall survival for hepatocellular carcinoma. *J Cell Physiol* (2020) 235(2):1624–36. doi: 10.1002/jcp.29081
8. Wang L, Li X. Identification of an energy metabolismrelated gene signature in ovarian cancer prognosis. *Oncol Rep* (2020) 43(6):1755–70. doi: 10.3892/or.2020.7548
9. Xing L, Guo M, Zhang X, Zhang X, Liu F. A transcriptional metabolic gene-set based prognostic signature is associated with clinical and mutational features in head and neck squamous cell carcinoma. *J Cancer Res Clin Oncol* (2020) 146(3):621–30. doi: 10.1007/s00432-020-03155-4
10. D'Souza G, Westra WH, Wang SJ, van Zante A, Wentz A, Kluz N, et al. Differences in the Prevalence of Human Papillomavirus (HPV) in Head and Neck Squamous Cell Cancers by Sex, Race, Anatomic Tumor Site, and HPV Detection Method. *JAMA Oncol* (2017) 3(2):169–77. doi: 10.1001/jamaoncol.2016.3067
11. Liu J, Lichtenberg T, Hoadley KA, Poisson LM, Lazar AJ, Cherniack AD, et al. An Integrated TCGA Pan-Cancer Clinical Data Resource to Drive High-Quality Survival Outcome Analytics. *Cell* (2018) 173(2):400–416 e11. doi: 10.1016/j.cell.2018.02.052
12. El-Sakka H, Kujan O, Farah CS. Assessing miRNAs profile expression as a risk stratification biomarker in oral potentially malignant disorders: A systematic review. *Oral Oncol* (2018) 77:57–82. doi: 10.1016/j.oraloncology.2017.11.021
13. Guo Y, Ma Y, Hu X, Song R, Zhu L, Zhong M. Long non-coding RNA CEBPA-AS1 correlates with poor prognosis and promotes tumorigenesis via CEBPA/Bcl2 in oral squamous cell carcinoma. *Cancer Biol Ther* (2018) 19(3):205–13. doi: 10.1080/15384047.2017.1416276
14. Lohavanichbutr P, Mendez E, Holsinger FC, Rue TC, Zhang Y, Houck J, et al. A 13-gene signature prognostic of HPV-negative OSCC: discovery and external validation. *Clin Cancer Res* (2013) 19(5):1197–203. doi: 10.1158/1078-0432.CCR-12-2647
15. Zhao C, Zou H, Wang J, Shen J, Liu H. A Three Long Noncoding RNA-Based Signature for Oral Squamous Cell Carcinoma Prognosis Prediction. *DNA Cell Biol* (2018) 37(11):888–95. doi: 10.1089/dna.2018.4317
16. Shen S, Wang G, Shi Q, Zhang R, Zhao Y, Wei Y, et al. Seven-CpG-based prognostic signature coupled with gene expression predicts survival of oral

squamous cell carcinoma. *Clin Epigenet* (2017) 9:88. doi: 10.1186/s13148-017-0392-9
17. Uhlen M, Zhang C, Lee S, Sjostedt E, Fagerberg L, Bidkhori G, et al. A pathology atlas of the human cancer transcriptome. *Science* (2017) 357(6352). doi: 10.1126/science.aan2507
18. Kanehisa M. The KEGG database. *Novartis Found Symp* (2002) 247:91–101; discussion 101-3, 119-28, 244-52.
19. Foroutan M, Bhuva DD, Lyu R, Horan K, Cursons J, Davis MJ. Single sample scoring of molecular phenotypes. *BMC Bioinformatics* (2018) 19(1):404. doi: 10.1186/s12859-018-2435-4
20. Barbie DA, Tamayo P, Boehm JS, Kim SY, Moody SE, Dunn IF, et al. Systematic RNA interference reveals that oncogenic KRAS-driven cancers require TBK1. *Nature* (2009) 462(7269):108–12. doi: 10.1038/nature08460
21. Pavlova NN, Thompson CB. The Emerging Hallmarks of Cancer Metabolism. *Cell Metab* (2016) 23(1):27–47. doi: 10.1016/j.cmet.2015.12.006
22. Grimm M, Cetindis M, Lehmann M, Biegner T, Munz A, Teriete P, et al. Association of cancer metabolism-related proteins with oral carcinogenesis - indications for chemoprevention and metabolic sensitizing of oral squamous cell carcinoma? *J Transl Med* (2014) 12:208. doi: 10.1186/1479-5876-12-208
23. Hu Q, Peng J, Chen X, Li H, Song M, Cheng B, et al. Obesity and genes related to lipid metabolism predict poor survival in oral squamous cell carcinoma. *Oral Oncol* (2019) 89:14–22. doi: 10.1016/j.oraloncology.2018.12.006
24. Zhang F, Zhang Y, Zhao W, Deng K, Wang Z, Yang C, et al. Metabolomics for biomarker discovery in the diagnosis, prognosis, survival and recurrence of colorectal cancer: a systematic review. *Oncotarget* (2017) 8(21):35460–72. doi: 10.18632/oncotarget.16727
25. Shintani S, Hamakawa H, Ueyama Y, Hatori M, Toyoshima T. Identification of a truncated cystatin SA-I as a saliva biomarker for oral squamous cell carcinoma using the SELDI ProteinChip platform. *Int J Oral Maxillofac Surg* (2010) 39(1):68–74. doi: 10.1016/j.ijom.2009.10.001
26. Vitorio JG, Duarte-Andrade FF, Dos Santos Fontes Pereira T, Fonseca FP, Amorim LSD, Martins-Chaves RR, et al. Metabolic landscape of oral squamous cell carcinoma. *Metabolomics* (2020) 16(10):105. doi: 10.1007/s11306-020-01727-6
27. Lin X, Xu R, Mao S, Zhang Y, Dai Y, Guo Q, et al. Metabolic biomarker signature for predicting the effect of neoadjuvant chemotherapy of breast cancer. *Ann Transl Med* (2019) 7(22):670. doi: 10.21037/atm.2019.10.34
28. Bouatra S, Aziat F, Mandal R, Guo AC, Wilson MR, Knox C, et al. The human urine metabolome. *PloS One* (2013) 8(9):e73076. doi: 10.1371/journal.pone.0073076
29. Prentki MS, Madiraju R. Glycerolipid metabolism and signaling in health and disease. *Endocr Rev* (2008) 29(6):647–76. doi: 10.1210/er.2008-0007
30. Ma Y, Temkin SM, Hawkridge AM, Guo C, Wang W, Wang XY, et al. Fatty acid oxidation: An emerging facet of metabolic transformation in cancer. *Cancer Lett* (2018) 435:92–100. doi: 10.1016/j.canlet.2018.08.006
31. Schworer S, Vardhana SA, Thompson CB. Cancer Metabolism Drives a Stromal Regenerative Response. *Cell Metab* (2019) 29(3):576–91. doi: 10.1016/j.cmet.2019.01.015
32. Zheng Y, Lin TY, Lee G, Paddock MN, Momb J, Cheng Z, et al. Mitochondrial One-Carbon Pathway Supports Cytosolic Folate Integrity in Cancer Cells. *Cell* (2018) 175(6):1546–1560 e17. doi: 10.1016/j.cell.2018.09.041
33. Guan C, Ouyang D, Qiao Y, Li K, Zheng G, Lao X, et al. CA9 transcriptional expression determines prognosis and tumour grade in tongue squamous cell carcinoma patients. *J Cell Mol Med* (2020) 24(10):5832–41. doi: 10.1111/jcmm.15252
34. Sembajwe LF, Katta K, Gronning M, Kusche-Gullberg M. The exostosin family of glycosyltransferases: mRNA expression profiles and heparan sulphate structure in human breast carcinoma cell lines. *Biosci Rep* (2018) 38(4). doi: 10.1042/BSR20180770
35. Zhang D, Wu H, Zhang X, Ding X, Huang M, Geng M, et al. Phosphoglycerate Mutase 1 Predicts the Poor Prognosis of Oral Squamous Cell Carcinoma and is Associated with Cell Migration. *J Cancer* (2017) 8(11):1943–51. doi: 10.7150/jca.19278
36. Zhao M, Tan B, Dai X, Shao Y, He Q, Yang B, et al. DHFR/TYMS are positive regulators of glioma cell growth and modulate chemo-sensitivity to temozolomide. *Eur J Pharmacol* (2019) 863:172665. doi: 10.1016/j.ejphar.2019.172665
37. Yang XH, Jing Y, Wang S, Ding F, Zhang XX, Chen S, et al. Integrated Non-targeted and Targeted Metabolomics Uncovers Amino Acid Markers of Oral Squamous Cell Carcinoma. *Front Oncol* (2020) 10:426. doi: 10.3389/fonc.2020.00426

Conflict of Interest: The authors declare that the research was conducted in the absence of any commercial or financial relationships that could be construed as a potential conflict of interest.

frontiers in Oncology

ORIGINAL RESEARCH
published: 02 December 2020
doi: 10.3389/fonc.2020.543591

Melatonin Inhibits the Progression of Oral Squamous Cell Carcinoma *via* Inducing miR-25-5p Expression by Directly Targeting NEDD9

Yanling Wang[1†], *Bo Tao*[2†], *Jiaying Li*[3†], *Xiaoqun Mao*[4], *Wei He*[5*] and *Qinbiao Chen*[6*]

[1] Department of Stomatology, Henan Province Hospital of Traditional Chinese Medicine, Zhengzhou, China, [2] Department of Orthopedics, Tianjin Medical University General Hospital, Tianjin, China, [3] Huiqiao Medical Center, Southern Medical University Nanfang Hospital, Guangzhou, China, [4] Nursing Department, Sun Yat-Sen Memorial Hospital of Sun Yat-Sen University, Guangzhou, China, [5] Department of Oral and Maxillofacial Surgery, The First Affiliated Hospital of Zhengzhou University, Zhengzhou, China, [6] Neurosurgery Department, Sun Yat-Sen Memorial Hospital of Sun Yat-Sen University, Guangzhou, China

OPEN ACCESS

Edited by:
Cesare Piazza,
University of Brescia, Italy

Reviewed by:
Augusto Schneider,
Federal University of Pelotas, Brazil
Shaoshan Hu,
Second Affiliated Hospital of Harbin Medical University, China
Yuan Li,
Shandong University, China

***Correspondence:**
Wei He
lbandye@foxmail.com
Qinbiao Chen
CQBSHEN@163.com

[†]These authors have contributed equally to this work

Specialty section:
This article was submitted to Head and Neck Cancer, a section of the journal Frontiers in Oncology

Received: 17 March 2020
Accepted: 29 October 2020
Published: 02 December 2020

Citation:
Wang Y, Tao B, Li J, Mao X, He W and Chen Q (2020) Melatonin Inhibits the Progression of Oral Squamous Cell Carcinoma via Inducing miR-25-5p Expression by Directly Targeting NEDD9. Front. Oncol. 10:543591. doi: 10.3389/fonc.2020.543591

Melatonin exerts anti-cancer roles in various types of cancers. However, to the best of our knowledge, its role in oral squamous cell carcinoma (OSCC) is unknown. The present study aimed to investigate the role of melatonin and its underlying mechanism in OSCC. MTT, colony formation, wound healing, and transwell invasion assays proved that melatonin played anti-tumor effects in OSCC cells by inhibiting cell viability, proliferation, migration, and invasion in a concentration-dependent manner. The RT-qPCR analysis showed that miR-25-5p was significantly upregulated after melatonin treatment. Further, miR-25-5p might be involved in melatonin-induced inhibitory effects on the biological behavior of OSCC. The expression of miR-25-5p was decreased in tumor tissues and OSCC cells detected by RT-qPCR. MTT assay, colony formation assay, and TUNEL staining indicated miR-25-5p overexpression inhibited OSCC cell viability, proliferation, and induced OSCC cell apoptosis. Furthermore, wound healing, transwell invasion assay, and animal experiments suggested that miR-25-5p might exert suppressive effects on the migration, invasion, and tumor formation of OSCC cells, while miR-25-5p knockdown exhibited the opposite effects in OSCC cells. Bioinformatics analysis, western blot analysis, and luciferase reporter assay suggested that neural precursor cell expressed developmentally downregulated protein 9 (NEDD9) was proved to be a putative target for miR-25-5p. The role of NEDD9 in inhibiting OSCC cell proliferation, invasion, and migration was verified with NEDD9 siRNA transfection. Thus, melatonin exerted anti-proliferative, anti-invasive, and anti-migrative effects on OSCC *via* miR-25-5p/NEDD9 pathway. Melatonin could be applied as a potential novel drug on treating OSCC.

Keywords: melatonin, oral squamous cell carcinoma, miR-25-5p, anti-tumor, NEDD9

INTRODUCTION

Oral cancer, as a global health problem, brings a huge challenge to the health care system. Oral squamous cell carcinoma (OSCC) occupies more than 90% of oral cancer (1). OSCC ranks as the 6th cancer type among the most common cancer types all over the world with a low 5-year overall survival rate and high incidence rate (2). It is estimated that there are 0.3 million new cases each year (3). Although considerable diagnostic and therapeutic progress has been made in recent years, the prognosis of the patients with OSCC remains particularly unfavorable because of its invasive characteristics and high malignancy (4). It is demonstrated that traditional treatments are not effective (5, 6). Thus, it is extremely urgent for us to widen the understanding of the mechanism underlying OSCC progression and identify novel and effective therapeutic methods.

Melatonin (N-acetyl-5-methoxytryptamine), a natural indoleamine, is mainly synthesized by the mammalian pineal gland and other tissues, such as lymphocytes, Harderian gland, liver, and gastrointestinal tract (7, 8). Interestingly, melatonin can regulate the circadian rhythms in living organisms, showing a wide distribution from bacteria to humans (9, 10). It has been shown that melatonin plays a vital role in the different physiological events, including the regulation of light/darkness responses, inhibition of tumor progression, improvement of immune system actions, and controlling of homeostasis in the different tissues (11–14). Besides, several pieces of evidence have revealed that melatonin could also serve as an antioxidant and oncostatic attributes (15, 16). According to the reports, melatonin exerts anti-cancer roles in various types of cancers, including breast cancer, lung cancer, colorectal cancer, gastric cancer, and cervical cancer (17–21). However, the underlying mechanism of the anti-cancer effects of melatonin on cancers needs further investigation.

Neural precursor cell expressed developmentally downregulated protein 9 (NEDD9) is a member of the Crk-associated substrate family. NEDD9 is located at 6p24.2 and also known as HEF1 and CasL. NEDD9 acts as a scaffold to regulate SRC and focal adhesion kinase pathways to modulate tumor cell adhesion, invasion, migration, proliferation, apoptosis, and survival (22–26). NEDD9 could activate multi-pathways, like PI3K/AKT, ERK, E-cadherin, Aurora-A (AURKA), and HDAC6. NEDD9 could also be activated by many stimuli, like TGF-β. At the end of mitosis, NEDD9 is degraded by proteasome. Although NEDD9 overexpression or inhibition does not induce tumorigenesis, its expression is upregulated in many cancers (27). NEDD9 could also regulate cancer metastasis. The upregulation of NEDD9 promotes multi cancer metastasis, like epithelial ovarian cancer, epithelial ovarian cancer, lung cancers, hepatocellular carcinoma, and cervical cancer (22, 28–34). NEDD9 could serve as a biomarker of tumor aggression and a prognostic gene of solid cancers. Further, NEDD9 could serve as one of the biomarkers for therapeutic resistance (27). Thus, NEDD9 might also regulate OSCC development.

MicroRNAs are a type of short (approximately 20~25 nucleotide), single-stranded non-coding RNAs, which are generally expressed in a diversity of tissues and cell types and mediate post-transcriptional gene silencing *via* binding to mRNA 3'UTR (35–37). Accumulating studies on the biological behaviors of miRNAs in the development, prognosis, proliferation, apoptosis, and differentiation have attracted the people's attention (38). MicroRNAs (miRNAs) have been reported to exhibit a fundamental role in regulating a variety of physiological and pathological processes, including cancers (39). Recently, miRNAs, including miR-25-5p, have been shown to participate in the progression and metastasis of many cancers, including colorectal cancers (CRCs), non-small cell lung cancer (NSCL), and cutaneous squamous cell carcinoma (CSCC) (15, 40, 41). However, the expression, clinical significance, and functions of miR-25-5p in OSCC remain unclear. In the present study, we aimed to characterize the effects of melatonin on the development of OSCC and identify the underlying mechanisms.

MATERIALS AND METHODS

Clinical Specimens

During the surgical procedure, the OSCC tissues (n=35) and adjacent tissues (n=35) were collected from patients with OSCC who had undergone surgical operation in Henan Province Hospital of TCM from January 2017 to October 2017 for research purpose. The patients with OSCC were diagnosed by histopathological analysis of tumor tissues from the surgical resection specimen. The specimen was examined and divided into OSCC tissues and adjacent tissues by faculties of the Pathology Department. Among the patients, a total of 35 patients, including 22 males and 13 females, were enrolled in this study. The age range was from 30 to 60 years old, with an average age of 41.5 ± 10.18 years. The clinical and pathologic characteristics of patients were obtained from the Medical Records Room. Patient information is shown in **Table 1**. All human tissues were snap frozen in liquid nitrogen and stored in a liquid nitrogen container (Thermo, USA) prior to further experiments. All the patients signed the informed consent before the study. The present study was approved by the Ethics Committee of Henan Province Hospital of TCM.

Cell Culture

Human OSCC cells (SCC9) and the normal human oral keratinocytes (HOK) cells were purchased from the Biological Resources Center of ATCC, USA. The SCC9 cells were cultured in F12-Dulbecco's modified Eagle's medium (DMEM) culture medium supplemented with 10% fetal bovine serum (FBS) (Thermo, USA). The HOK cells were grown in DMEM culture medium with 10% FBS. All the cells were cultured in a 37°C, 5% CO_2 humidified incubator (Thermo, USA). All cell lines were passaged for fewer than 6 months.

MiRNA Transfection

The miR-25-5p mimic, miR-25-5p inhibitor or negative control (NC) mimic, and NC inhibitor used in this study were designed and synthesized by GenePharma, China. Human OSCC cells

TABLE 1 | The clinical characteristics of OSCC patients.

Characteristics	n	%
Age		
<41	19	54.29
≥41	16	45.71
Sex		
male	22	62.86
female	13	37.14
Tumor location		
Tongue	13	37.14
Gingival	8	22.86
Mouth floor	4	11.43
Lip	3	8.57
Cheek	4	11.43
Soft palate	3	8.57
Pathological differentiation grade		
Well	21	60.00
Moderate	11	31.43
Poor	3	8.57
Clinical stage		
I+II	19	55.47
III+IV	16	44.53

Clinical stage I: T1N0M0; Stage II: T2N0M0; Stage III: T3N0M0, T(1-3)N1M0; Stage IV: T4aN(0,1)M0, T(1-4a)N2M0, TN3M0, T4bNM0.

were transfected with miR-25-5p mimic or miR-25-5p inhibitor using the transfection reagent Lipofectamine2000 (Invitrogen, USA) according to the manufacturer's instructions. The transfection concentration for either miR-25-5p mimic or NC mimic was 50 nM. The transfection concentration for either miR-25-5p inhibitor or NC inhibitor was 100 nM. Then, the cells were cultured for 48 h. RT-qPCR analysis was performed to confirm the transfection efficiency of miR-25-5p.

Melatonin Treatment

Different concentrations (0 mM, 0.01 mM, 0.1 mM, and 1 mM) of melatonin (trans-3,5-dimethoxy-4-hydroxystilbene) (Selleckchem, USA) were added to the culture medium for 48 h to detect the effects of melatonin on the human OSCC cells.

Real Time qPCR Analysis

RNA was extracted from tissues and cells using Trizol reagents (Invitrogen, USA) according to the manufacturer's instructions. The concentrations and purification of RNAs were assessed by NanoDrop2000 spectrophotometer (Thermo, USA). For detecting the expression of miRNAs, a tissue/cell miRNA extraction kit (HaiGene, China) was used. The cDNAs were synthesized immediately from the RNAs to avoid RNA degradation using Reverse Transcription Kit (ABI, USA). The expression analysis of target genes was performed on Applied Biosystems StepOne Plus real-time PCR system (ABI, USA) by using TaqMan Universal PCR Master Mix (ABI, USA). The conditions were as follows: 95°C for 5 min, followed by 35~40 cycles of amplification (95°C for 30s, 60°C for 30s, and 72°C for 30s), and 72°C for 10 min. At last, the expression level of miRNA primers (forward and reverse) and U6 served as an endogenous control. GAPDH mRNA was used as an internal control to assess the relative expression of NEDD9 mRNA. The $2^{-\Delta\Delta Ct}$ method was utilized to detect the expression of target genes. In our study, the primers were designed and synthesized by GeenPharma, China. The primer sequences were shown in **Table 2**.

Methyl Thiazolyl Tetrazolium (MTT) Analysis

MTT assay was performed to investigate the cell viability of human OSCC cells. The cells were plated into 96-well plates. Then, 20 μL MTT solution (Biosharp, China) was added to each well. After incubation for 4 h, the MTT solution was discarded and 150 μL dimethyl sulfoxide (DMSO) was added. After incubation for additional 10 min, the absorbance at a wavelength of 490 nm were measured using a microplate reader (TECAN, Switzerland) to determine cell viability.

Colony Formation Assay

Colony formation assay was performed to determine the proliferation ability of cells. First, 3500 cells were seeded into six-well plates (Corning, USA) and cultured for 14 days. The culture medium was replaced by free medium every three days. After three times washes with PBS, the cells were fixed with 4% paraformaldehyde (Solarbio, China) for 25 min at room temperature and stained with 0.2% crystal violet solution (Biosharp, China) for 20 min. The colonies (≥50 cells/colony) were observed and imaged under a light microscope (Nikon, Japan).

TABLE 2 | The sequence of primers used for real-time qPCR analysis.

Genes	Primers sequences (5' to 3')
miR-21	Forward: GCTTATCAGACTGATGTTG
	Reverse: GAACATGTCTGCGTATCTC
miR-133a	Forward: TTTGGTCCCCTTCAACC
	Reverse: GAACATGTCTGCGTATCTC
miR-148a-3p	Forward: GTTCTGAGACACTCCGA
	Reverse: GAACATGTCTGCGTATCTC
miR-25-5p	Forward: CGGAGACTTGGGCAATT
	Reverse: GAACATGTCTGCGTATCTC
miR-155	Forward: TGCTAATCGTGATAGGGG
	Reverse: GAACATGTCTGCGTATCTC
U6	Forward: CTGACATCAGTGTCACAGACCC
	Reverse: CGCATCCTGTAGCAACTGTGTG
NEDD9	Forward: CCCATCCAGATACCAAAAGGACG
	Reverse: CACTGGAACTGAAAACACAGGGC
KLK9	Forward: TCAACCTCAGCCAGACCTGTGT
	Reverse: TCTCCAGGATGCTGATGTTGGC
WNT3A	Forward: ATGAACCGCCACAACAACGAGG
	Reverse: GTCCTTGAGGAAGTCACCGATG
FGF18	Forward: ACGATGTGAGCCGTAAGCAGCT
	Reverse: ACCGAAGGTGTCTGTCTCCACT
SRSF4	Forward: CAGATTAGTTGAAGACAAGCCAGG
	Reverse: CACTTCGGCTTCTGCTCTTACG
FIBP	Forward: CAAGGTGGTAGAGGAAATGCGG
	Reverse: CCTGTCTCAAAGCGGTTGTTAGC
SOX12	Forward: GACATGCACAACGCCGAGATCT
	Reverse: GTAATCCGCCATGTGCTTGAGC
TGFBI	Forward: GGACATGCTCACTATCAACGGG
	Reverse: CTGTGGACACATCAGACTCTGC
GAPDH	Forward: GTCTCCTCTGACTTCAACAGCG
	Reverse: ACCACCCTGTTGCTGTAGCCAA

Apoptosis Assay

Forty-eight hours after transfection, the cells were used for apoptosis assay. Transferase dUTP nick end labeling (TUNEL) assay was conducted using TUNEL staining kit (Ribo, China) according to the instructions. The TUNEL-positive cells were examined under a microscope (Nikon, Japan). The pictures from 10 random fields were observed and taken to assess the apoptosis of cells.

Wound Healing Assay

Cell migration ability was examined by wound healing assay, and 5×10^5 cells/well were plated into six-well plates (Corning, USA). When the density of cells reached about 90%, a wound was created at the bottom of plates using a sterile pipette tip. The cells were washed three times with PBS to clear cell debris and then cultured in the culture medium for 48 h. Finally, the images were captured under an inverted microscope (Nikon, Japan) at 0 h, 24 h, and 48 h.

Transwell Invasion Assay

Cell invasion ability was tested by transwell invasion assay. For the transwell invasion assay, human OSCC cells were plated in the transwell chambers with 8 μm pore size polycarbonic membrane (Corning, USA) to separate the top chamber and the lower chamber. In brief, 1×10^5 cells were seeded in serum-free DMEM in the upper chamber, which was coated with 20 μL extracellular matrix gel (Sigma, USA). The culture medium with 10% FBS was added into the lower chamber. After incubation for about 24 h, the cells on the top surface of the membrane were wiped off. The cells were then stained with crystal violet (Biosharp, China) at room temperature for 30 min. Finally, the cells were observed under a light and inverted microscope (Nikon, Japan).

Animal Experiments

The animal experiments were performed with the approval of the Ethics Committee of Henan Province Hospital of TCM. Animal experiments were carried out according to the National Institutes of Health Guidelines to the Care and Use of Laboratory Animals. Forty Balb/c nude mice (4~6 weeks of age, male, Charles River, China) housed and maintained in a specific pathogen-free room, and were allowed free access to water and food. The mice were divided randomly into 4 groups (n=10 per group). To initiate OSCC xenografts, 5×10^6 human OSCC cells transfected with miR-25-5p were injected subcutaneously into to the flanks of the nude mice. After 4 weeks, the animals were euthanized in a CO_2 chamber and tumors were collected. Tumor nodules were collected and calculated by the following formula: V = (Width2 × Length)/2. The weights of tumors were weighed and analyzed.

Bioinformatics Analysis

The candidate target genes of miR-25-5p were predicted using the TargetScanHuman 7.2 (http://www.targetscan.org/vert_72/) and miRWalk (http://mirwalk.umm.uni-heidelberg.de/). In Targetscan and miRWalk databases, the species was set as human. The miRNA was set as miR-25-5p. In Targetscan database, the predicted target genes of miR-25-5p was shown by searching the presence of conserved 8mer, 7mer, and 6mer sites that match the seed region of miR-25-5p. In miRWalk database, the interaction score of miR-25-5p and NEDD9 mRNA was 0.92. The binding sites of miR-25-5p and target genes' mRNA 3'UTR were predicted and showed with TargetScan. NEDD9 could be predicted by both databases and might be a putative target for miR-25-5p.

Western Blot Analysis

Human OSCC cells were lysed by using RIPA lysis buffer containing proteinase inhibitors (Beyotime, China). The concentration of proteins was detected according to the instruction of the BCA Protein Quantitation kit (Beyotime, China). Then, the total proteins (60 μg) were subjected to 10% sodium dodecyl sulfate (SDS)-polyacrylamide gel electrophoresis (PAGE) and transferred onto a PVDF membrane (Millipore, USA). Then, 5% skim milk was applied to block the membranes at room temperature for 120 min. Subsequently, immunoblotting was performed with specific antibodies against NEDD9 (1:1000, ab18056, Abcam, Cambridge, UK) and β-actin (1:2000, β-actin, Abcam, Cambridge, UK). β-actin was used as an internal control. The membranes were incubated with primary antibodies at 4°C temperature overnight. Next day, the secondary antibodies (Abcam, Cambridge, UK) were added and incubated at room temperature for 2 h. Ultimately, the signals were detected by an enhanced chemiluminescence (ECL) detection system (PerkinElmer, USA) and quantified with ImageJ software.

Luciferase Reporter Assay

The 3'-UTR sequence of NEDD9 containing the predicted binding site for miR-25-5p was obtained and cloned into psiCHECK-2 vector (Promega, USA) to obtain the wild-type (WT) reporter plasmid NEDD9-WT. To generate the NEDD9 mutant (MUT) reporter plasmid, NEDD9-MUT, the seed region was mutated to eliminate all complementary nucleotides to miR-25-5p. Human OSCC were transfected with the reporter plasmid together with miR-25-5p mimic/miR-25-5p inhibitor and NEDD9-WT/NEDD9-MUT. After 48 h of transfection, a dual-luciferase reporter assay system (Promega, USA) was applied to monitor the relative luciferase activity.

Statistical Analysis

All quantitative results were from at least three independent experiments and presented as the mean ± SD. Differences among various groups were evaluated by one-way analysis of variance (ANOVA) followed by Turkey's post-hoc analysis. Diffeerences between two groups were analyzed with Student's t-tests. All the statistical analysis was carried out using GraphPad Prism. A p-value of less than 0.05 was considered statistically significant.

RESULTS

Anti-Tumor Effects of Melatonin on Human Oral Squamous Cell Carcinoma Cells

To test whether melatonin could exert the inhibitory effects in the biological functions of OSCC (SCC9) cells, various concentrations of melatonin were used. First, SCC9 cells were treated with 0.01, 0.1, and 1 mM of melatonin for 48 h. MTT assay indicated that, compared to control, melatonin decreased the cell viability of SCC9 cells in a concentration-dependent manner, and the maximum effect was 1 mM group (**Figure 1A**). The concentration-dependent effects of melatonin on the proliferation ability of SCC9 cells were also observed as confirmed by colony formation assay (**Figure 1B**). The number of colonies was significantly reduced by melatonin at concentrations of 0.01, 0.1, and 1 mM in SCC9 cells (**Figure 1B**). Wound healing assay showed that the number of migrating cells was reduced after melatonin treatment at 0.01, 0.1, and 1 mM, especially at 1 mM. These results suggested that melatonin showed a significant inhibitory effect on cell migration ability (**Figure 1C**). Dose-dependent inhibitory roles of melatonin in the invasion ability of SCC9 cells were displayed by the Transwell invasion assay (**Figure 1D**). These results suggested that melatonin played anti-tumor effects in SCC9 cells by inhibiting the cell viability, proliferation, migration, and invasion at a millimolar concentration.

Melatonin Upregulates the Expression of miR-25-5p

To understand the underlying mechanism of melatonin inhibiting the biological behaviors of OSCC cells, the RT-qPCR analysis was performed to identify the dysregulated expression of miRNAs in different concentrations of melatonin treated SCC9 cells. The results of RT-qPCR analysis revealed no significant

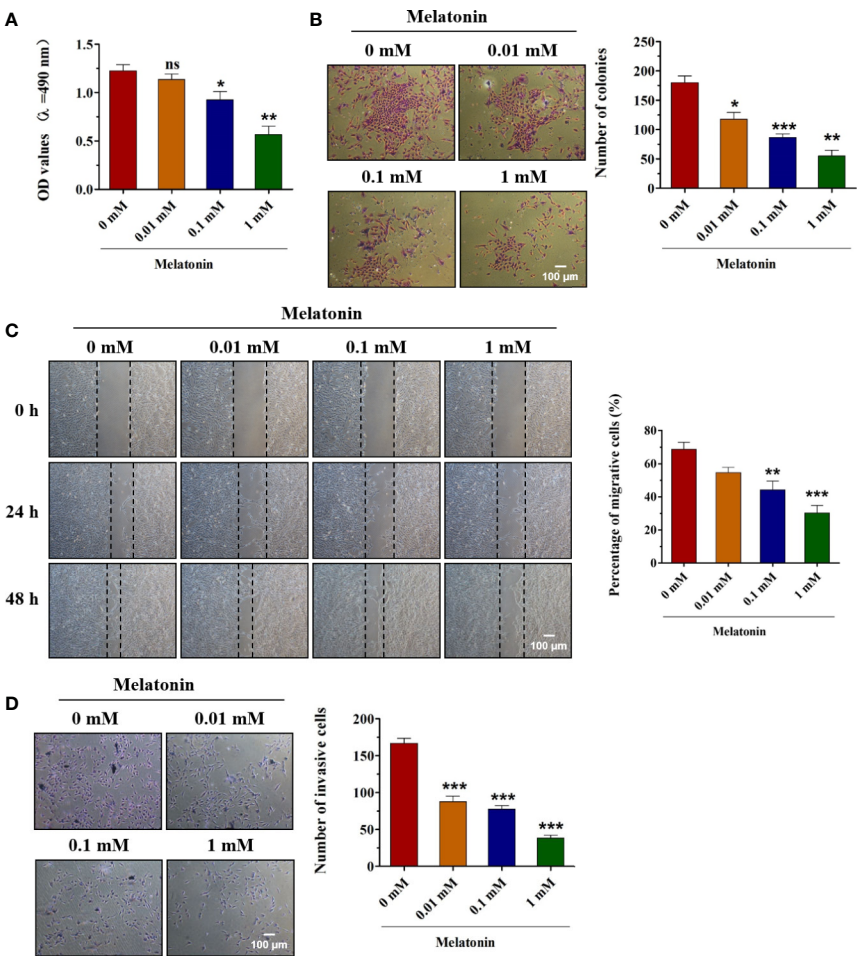

FIGURE 1 | Effects of melatonin on the biological functions of OSCC cells. **(A)** SCC9 cells were treated with melatonin at 0.01, 0.1, and 1 mM for 48 h, and MTT assay was performed to detect the cell viability. **(B)** SCC9 cells were exposed to different concentrations of melatonin for 48 h and subjected to colony formation assay to examine the proliferation ability. **(C)** Effects of melatonin on the migration of SCC9 cells after exposure to melatonin (0.01, 0.1, and 1 mM) for wound healing assay. **(D)** The invasion ability of SCC9 cells after melatonin treatment by Transwell invasion assay. (n=4, One way ANOVA followed by the Tukey's test, * indicated the differences compared with 0 mM Melatonin group, *p < 0.05, **p < 0.01, ***p < 0.001, ns, no statistical differences, Scale bar, 100 μm).

changes in miR-21 or miR-133a expression after melatonin administration (**Figures 2A, B**). As shown in **Figures 2D, E**, melatonin elevated the expression of miR-148a-3p and miR-25-5p, but it inhibited the expression of miR-155 (**Figures 2C–E**). Among these miRNAs, miR-25-5p was the most significantly upregulated miRNA after melatonin treatment (**Figure 2C**). We hypothesized that miR-25-5p might be involved in the development of OSCC and the inhibitory effects of melatonin on OSCC cells. To further confirm this observation, the OSCC tissues and adjacent tissues were collected to detect the expression level of miR-25-5p. RT-qPCR assay based on 35 paired tumor tissues and matched tumor-adjacent tissues showed that miR-25-5p was significantly decreased in the OSCC tissues compared with the adjacent tissues (**Figure 2F**). In addition, as indicated in **Figure 2G**, the expression of miR-25-5p was markedly decreased in SCC9 cells compared with that in the normal human oral keratinocytes (HOK) cells (**Figure 2G**). These results suggested that miR-25-5p might be involved in melatonin-induced inhibitory effects on the biological functions of OSCC cells.

Overexpression of miR-25-5p Inhibits Cell Viability, Proliferation, and Induces OSCC Cell Apoptosis

As miR-25-5p was downregulated in OSCC, we hypothesized that miR-25-5p might serve as a tumor-suppressive miRNA in OSCC. To confirm this hypothesis, we transfected miR-25-5p mimics/mimics NC in OSCC cells. The expression levels of miR-25-5p in SCC9 cells were examined with RT-qPCR analysis 48 h after transfection. The results of RT-qPCR displayed that the miR-25-5p expression was significantly upregulated in SCC9 cells transfected with miR-25-5p mimic compared with that in the NC mimic group (**Figure 3A**). MTT assays showed that the cell viability of miR-25-5p mimic group was much lower than that in the NC mimic group (**Figure 3B**). The colony formation assay revealed that miR-25-5p mimic transfection significantly inhibited the proliferation ability compared with that in NC mimic-transfected cells (**Figure 3C**). TUNEL staining revealed that miR-25-5p overexpression led to an increase in apoptotic cell number in SCC9 cells (**Figure 3D**). These results supported the hypothesis that miR-25-5p inhibited the cell viability, proliferation, and induced the apoptosis of OSCC cells.

Upregulation of miR-25-5p Suppresses the Migration, Invasion, and Tumor Formation of OSCC Cells

To unravel the function of miR-25-5p in OSCC cells, the oncogenic phenotypes, including migration, invasion, and tumor formation were detected. Wound healing assay showed that the SCC9 cells transfected with miR-25-5p mimic showed lower migratory capacity than the cells transfected with NC mimic, indicating that the increase of miR-25-5p led to a decrease in migratory ability of SCC9 cells (**Figure 4A**). The Transwell invasion analysis revealed that miR-25-5p overexpression was able to reduce the invasion of SCC9 cells (**Figure 4B**). To further determine the potential roles of miR-25-5p in OSCC tumor formation, animal experiments were performed. The SCC9 cells treated with miR-25-5p mimic or NC mimic were injected subcutaneously into the flanks of the nude mice. After 4 weeks, the tumors were collected and the tumor nodules were collected and calculated. As presented in **Figures 4C, D**, the tumor weights and tumor volumes in miR-

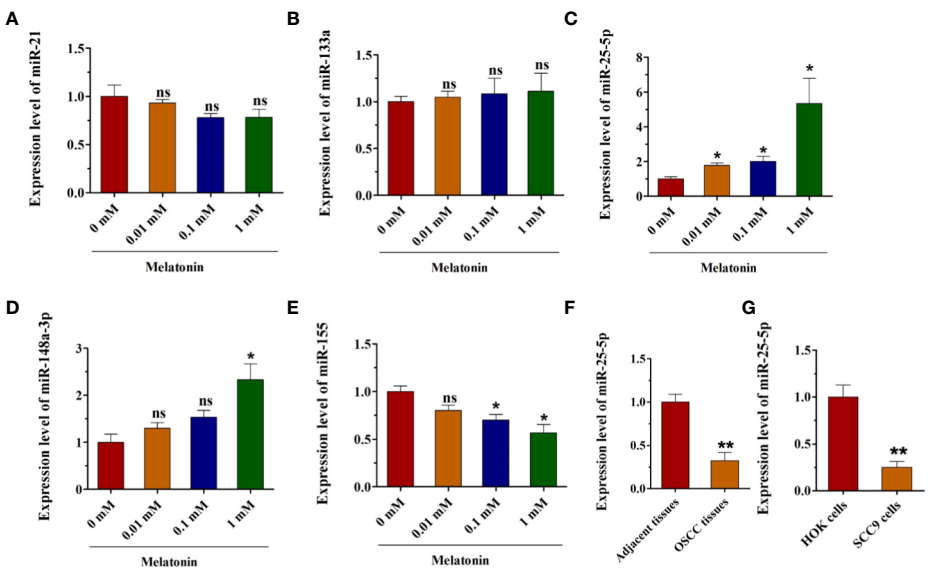

FIGURE 2 | Melatonin increases the expression of miR-25-5p in OSCC cells. **(A–E)** RT-qPCR analysis of miR-21, miR-133a, miR-25-5p, miR-148a-3p, miR-155 expression was performed in SCC9 cells after treating with melatonin at 0.01, 0.1, and 1 mM for 48 h (n=4, One way ANOVA followed by the Tukey's test, * indicated the differences compared with 0 mM Melatonin group). **(F)** Relative miR-25-5p levels in OSCC tissues (n=35, Student's t-test). **(G)** RT-qPCR analysis was utilized to examine the expression of miR-25-5p in SCC9 and HOK cells (n=4, Student's t-test) (*p < 0.05, **p < 0.01, ns, no statistical differences).

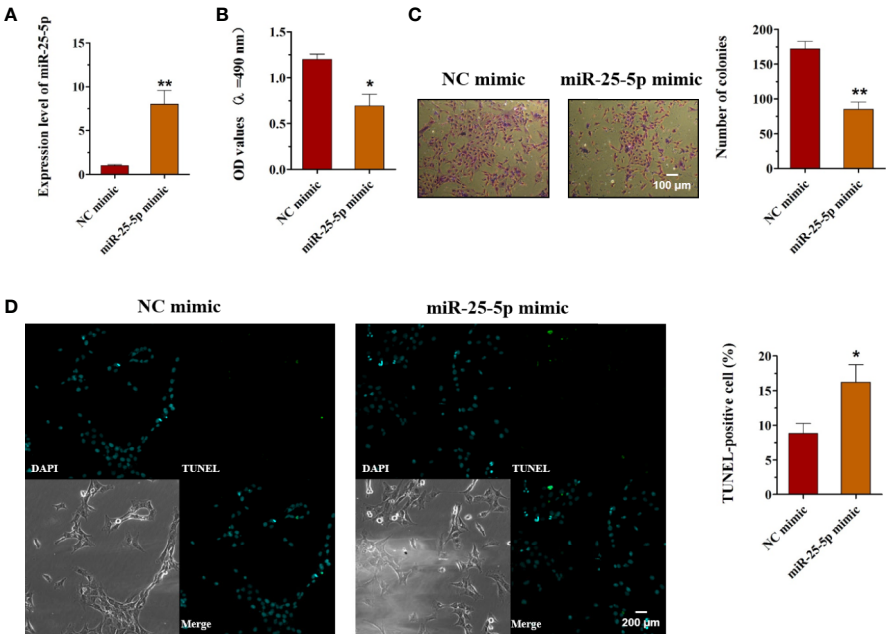

FIGURE 3 | Overexpression of miR-25-5p inhibits the cell viability, proliferation but promotes the apoptosis of OSCC cells. **(A)** RT-qPCR analysis of miR-25-5p in SCC9 cells transfected with miR-25-5p mimic or NC mimic. **(B)** MTT assay of cell viability in SCC9 cells treated with miR-25-5p mimic or NC mimic. **(C)** Colony formation of SCC9 cells exposed to miR-25-5p mimic or NC mimic (Scale bar, 100 μm). **(D)** The apoptosis of SCC9 cells detected by TUNEL staining. Nuclei were stained by DAPI (blue) stain and apoptotic cells were stained by TUNEL (green) (Scale bar, 200 μm). (n=4, Student's t-test, *p < 0.05, **p < 0.01).

25-5p mimic group were much lower than that in NC mimic group (**Figures 4C, D**). These data suggested that miR-25-5p might exert suppressive effects on the migration, invasion, and tumor formation of OSCC cells.

Knockdown of miR-25-5 Promotes the Viability, Proliferation, and Inhibits the Apoptosis of OSCC Cells

To explore the role of miR-25-5p in OSCC, SCC9 cells were transfected with miR-25-5p inhibitor or NC inhibitor, and the cell viability, proliferation, and apoptosis were evaluated using MTT assay, colony formation assay, and TUNEL staining, respectively. First, the SCC9 cells were transfected with miR-25-5p inhibitor or NC inhibitor, and the expression of miR-25-5p was analyzed by RT-qPCR analysis (**Figure 5A**). As shown in **Figure 5A**, miR-25-5p inhibitor significantly inhibited miR-25-5p expression in SCC9 cells compared with NC inhibitor group (**Figure 5A**). Then, the transfected cells were selected for subsequent experiments. As shown in **Figure 5B**, knockdown of miR-25-5p markedly elevated the cell viability of SCC9 cells in comparison with the NC inhibitor group (**Figure 5B**). Furthermore, the number of colonies of SCC9 cells transfected with miR-25-5p inhibitor were significantly increased compared with SCC9 cells transfected with NC inhibitor (**Figure 5C**). Subsequently, TUNEL staining was utilized to determine the apoptosis of SCC9 cells. The results of TUNEL staining demonstrated that downregulation of miR-25-5p markedly suppressed the apoptosis of SCC9 cells compared with the NC inhibitor group (**Figure 5D**). The above results indicated that knockdown of miR-25-5p elevated the viability and proliferation but inhibited the apoptosis of OSCC cells.

Knockdown of miR-25-5p Accelerates the Migration, Invasion, and Tumor Formation of OSCC Cells

To explore the functions of miR-25-5p in OSCC, we employed the miR-25-5p inhibitor and NC inhibitor in cultured SCC9 cells. The results of the wound healing and transwell invasion assays indicated that transfection of the miR-25-5p inhibitor obviously promoted both migration (**Figure 6A**) and invasion (**Figure 6B**) of SCC9 cells. Meanwhile, the knockdown of miR-25-5p increased the tumor weights and tumor volumes of Balb/c nude mice (**Figures 6C, D**). To conclude, the knockdown of miR-25-5p accelerated the migration, invasion, and tumor formation of OSCC cells.

Inhibition of miR-25-5p Reverses the Inhibitory Effects of Melatonin in OSCC Cells

Then, we further investigated whether melatonin could exert the anti-proliferative, anti-invasive, and anti-migratory effects on OSCC cells by regulating the expression of miR-25-5p. According to the results of **Figure 1C**, the expression of miR-25-5p was the highest when the cells were treated with 1 mM melatonin. Therefore, the cells were treated with 1 mM melatonin and miR-25-5p inhibitor. MTT assay indicated that

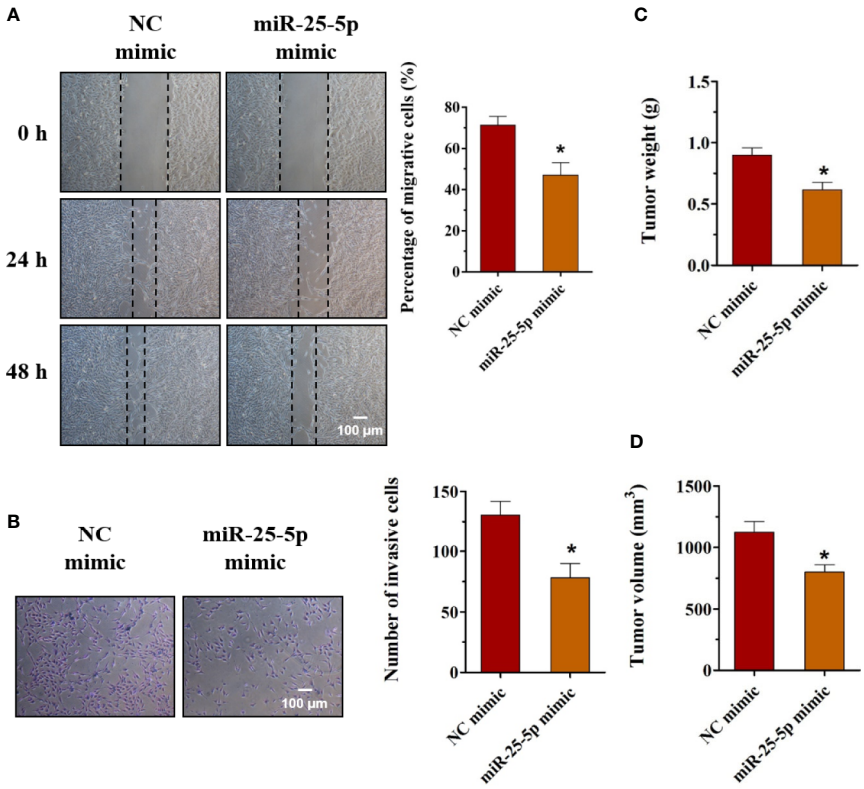

FIGURE 4 | Upregulation of miR-25-5p suppresses the migration, invasion, and tumor formation of OSCC cells. **(A)** Wound healing assay was used to determine the migration of SCC9 cells transfected with miR-25-5p mimic or NC mimic (n=4). **(B)** SCC9 cells were transfected with miR-25-5p mimic or NC mimic and allowed to migrate through an 8 μm pore size polycarbonic membrane in Transwell chambers. The invasive cells were stained and counted (n=4, Scale bar, 100 μm). **(C, D)** Animal experiments of tumor formation of OSCC cells were conducted using SCC9 cells. Tumor weights and volumes were measured (n=10, Student's t-test, *p < 0.05).

compared with the control group, the cell viability of OSCC cells were inhibited by 1 mM melatonin, while the inhibitory effects were abolished in the presence of miR-25-5p inhibitor (**Figure 7A**). As shown in **Figure 7B**, the number of colonies were markedly reduced by 1 mM melatonin, but it was increased in the OSCC cells treated with both 1 mM melatonin and miR-25-5p inhibitor (**Figure 7B**). Furthermore, the migratory ability of OSCC cells were obviously inhibited after 1 mM melatonin treatment. However, the inhibitory effects of melatonin on OSCC cell migration was offset by miR-25-5p inhibitor (**Figure 7C**). Transwell invasion analysis revealed that the inhibition of miR-25-5p could reverse the anti-invasive effects of melatonin in OSCC cells (**Figure 7D**). Above results indicated that melatonin exerted the anti-proliferative, anti-invasive, and anti-migratory effects on OSCC cells by regulating miR-25-5p.

miR-25-5p Regulates OSCC Cell Proliferation, Invasion, and Migration *via* Targeting NEDD9

To determinate the mechanism underlying the effects of miR-25-5p in OSCC cells, the candidate target genes of miR-25-5p were predicted using the TargetScanHuman7.2 (http://www.targetscan.org/vert_72/) and miRWalk (http://mirwalk.umm.uni-heidelberg.de/). Among these target genes of miR-25-5p, KLK9, WNT3A, FGF18, SRSF4, FIBP, SOX12, TGFBI, and NEDD9 have been reported to participate in the development human cancers (42–49). Thus, we selected these genes for further investigation. The binding sequences between miR-25-5p and these target genes were shown in **Figure 8A**. The results of RT-qPCR indicated that among KLK9, WNT3A, FGF18, SRSF4, FIBP, SOX12, TGFBI, and NEDD9, the expression of NEDD9 was much higher in OSCC tissues than adjacent tissues. NEDD9 was the most obviously upregulated gene between OSCC tissues and adjacent tissues that isolated from OSCC patients (**Figure 8B**). Thus, we selected NEDD9 for further analysis. To further investigate the role of NEDD9, OSCC cells were transfected with miR-25-5p inhibitor, miR-25-5p inhibitor+siRNA-NEDD9 respectively. As shown in **Figure 8C**, compared with NC group, the proliferation ability of OSCC cells was elevated by miR-25-5p inhibitor, but it was inhibited in the presence of siRNA-NEDD9 (**Figure 8C**). The transwell assay showed that knockdown of miR-25-5p promoted the invasion ability of OSCC cells, which was reversed by siRNA-NEDD9 (**Figure 8D**). Furthermore, wound healing assay indicated that the

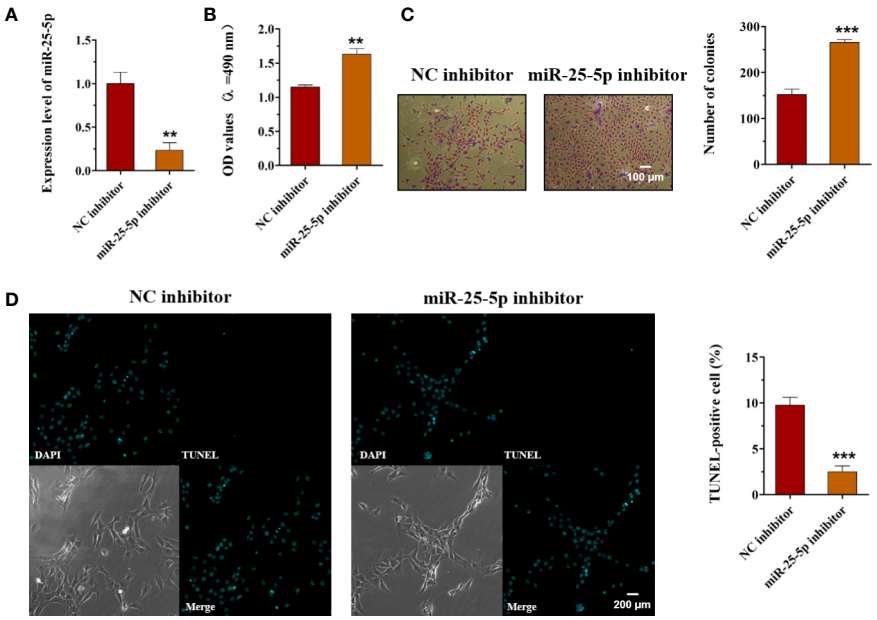

FIGURE 5 | Knockdown of miR-25-5p promotes cell viability, proliferation, and inhibits the apoptosis of OSCC cells. **(A)** SCC9 cells transfected with miR-25-5p or NC inhibitor were used to analyze the expression of miR-25-5p with RT-qPCR. **(B)** MTT assay of cell viability in SCC9 cells in the presence of miR-25-5p or NC inhibitor. **(C)** Effect of miR-25-5p inhibitor on the proliferation ability of SCC9 cells (Scale bar, 100 μm). **(D)** The apoptosis of SCC9 cells detected by TUNEL staining. Nuclei were stained by DAPI (blue) stain and apoptotic cells were stained by TUNEL (green) (Scale bar, 200 μm). (n=4, Student's t-test, $^{**}p < 0.01$ $^{***}p < 0.001$).

migratory ability of OSCC cells in the miR-25-5p inhibitor group was higher than that in the NC group, while the elevated migratory ability was inhibited by NEDD9 siRNA (**Figure 8E**). To further confirm the relationship between miR-25-5p and NEDD9, dual-luciferase reporter assay was conducted. Luciferase reporter assay revealed that miR-25-5p mimic significantly decreased the luciferase activity in SCC9 cells transfected with NEDD9-WT, but not the NEDD9-MUT compared with NC group (**Figure 8F**). RT-qPCR analysis was conducted to determine the expression levels of NEDD9 in SCC9 cells after miR-25-5p modulation (**Figure 8G**). The results indicated that miR-25-5p mimic inhibited the mRNA expression of NEDD9, while miR-25-5p inhibitor elevated the mRNA expression of NEDD9 (**Figure 8G**). Western blot analysis demonstrated that miR-25-5p mimics reduced the protein level of NEDD9 and miR-25-5p inhibitor elevated the protein level of NEDD9 (**Figure 8H**). The results provided that NEDD9 was a direct target of miR-25-5p that regulated OSCC cell behaviors.

DISCUSSION

OSCC is one of the most malignant neoplasms worldwide and ranks first with 90% in oral cancers. There are about 0.3 billion new patients every year. Unhealthy living habits like smoking, alcohol uptake, and papillomavirus infection are the main risk factors of OSCC. With the progress of medical science in the recent decades, the 5-year survival rate of OSCC patients improves to approximate 50%. However, over 60% patients are at stage III or IV when diagnosed, which leaves a poor survival rate for these patients. It is necessary to clarify the mechanism of origination and development of OSCC, so as to find treatment targets and novel therapeutics (1–3).

Melatonin is an endogenous hormone secreted from pineal and could regulate circadian rhythms and mitochondrial homeostasis (12, 50, 51). Melatonin and its metabolites are proved to have an antioxidative role against oxidative stress (51). More interestingly, this hormone exerts anti-tumor effect on kinds of solid tumors *via* its receptor that exists in tumor tissues (13). It is thought that the anti-tumor effect of melatonin is based in its anti-oxidation and anti-inflammatory roles (52, 53). Melatonin inhibits triple negative breast cancer cell proliferation, migration *via* increasing miR-152-3p (54, 55). Melatonin inhibits breast tumor cell survival, migration, and invasion and upregulates miR-148a-3p (56). Melatonin represses 5-FU resistant colorectal cancer cell growth *via* miR-215-p/thymidylate synthase (TYMS) pathway (57). Melatonin inhibits gastric cancer cell growth *via* miR-16-5p/Smad3 pathway (58). Glioma cell proliferation and invasion are inhibited by melatonin *via* repressing miR-155 (59). In a random clinic trial, after neoadjuvant chemotherapy, melatonin was applied to treat OSCC patients. The residual tumor percentage and miR-210 were reduced. However, the decrease of miR-210 had no statistical significance (60). Thus, there could be other miRNAs downstream melatonin. After literature research, we chose miR-21, miR-133a, miR-148a-3p, miR-25-5p, and miR-155, which have been reported to regulate tumor progression in other cancers and

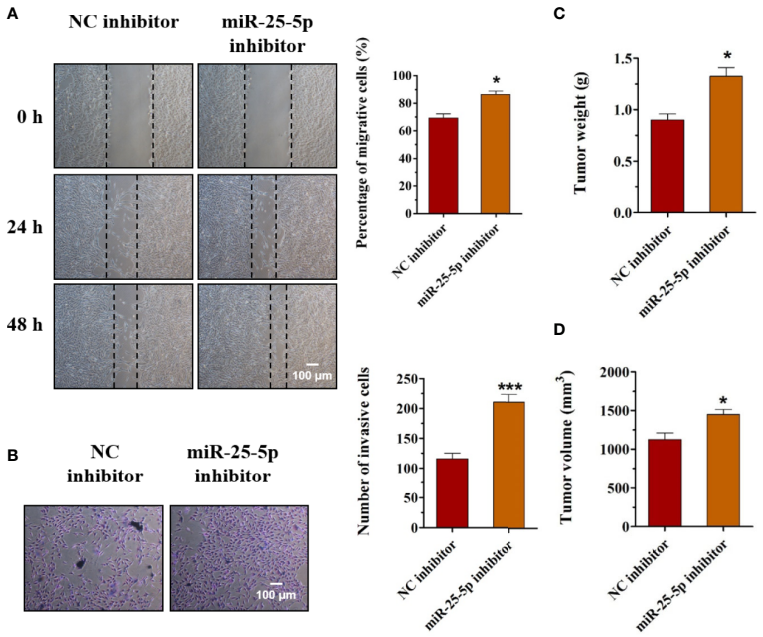

FIGURE 6 | Knockdown of miR-25-5p accelerates the migration, invasion, and tumor formation of OSCC cells. **(A, B)** The effects of miR-25-5p inhibitor on the migration and invasion of SCC9 cells were detected by wound healing assay and transwell invasion assay, respectively (n=4). **(C, D)** The SCC9 cells transfected with miR-25-5p inhibitor or NC inhibitor were injected subcutaneously into the flanks of the nude mice. After 4 weeks, the tumor nodules were collected and the tumor formation was examined (n=10). (Student's t-test, *p < 0.05 and ***p < 0.001, Scale bar, 100 μm).

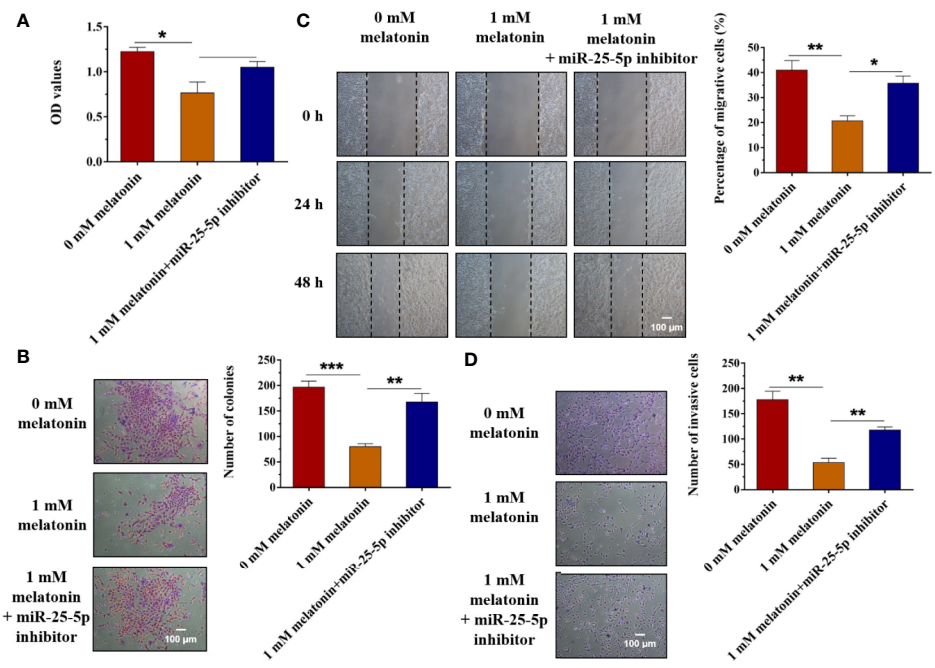

FIGURE 7 | Inhibition of miR-25-5p reverses the inhibitory effects of melatonin in OSCC cells. **(A)** SCC9 cells were treated with melatonin at 1 mM and miR-25-5p inhibitor, and MTT assay was performed to detect the cell viability. **(B)** SCC9 cells were exposed to 1 mM melatonin and miR-25-5p inhibitor and then were subjected to colony formation assay to examine SCC9 cell proliferation ability. **(C)** Effects of melatonin on the migration of SCC9 cells in the presence of miR-25-5p by wound healing assay. **(D)** The invasion ability of SCC9 cells after melatonin treatment and miR-25-5p transfection by Transwell invasion assay. (n=4, One way ANOVA followed by the Tukey's test, * indicated the differences compared with 0 mM Melatonin group,*p < 0.05, **p < 0.01, ***p < 0.001, Scale bar, 100 μm).

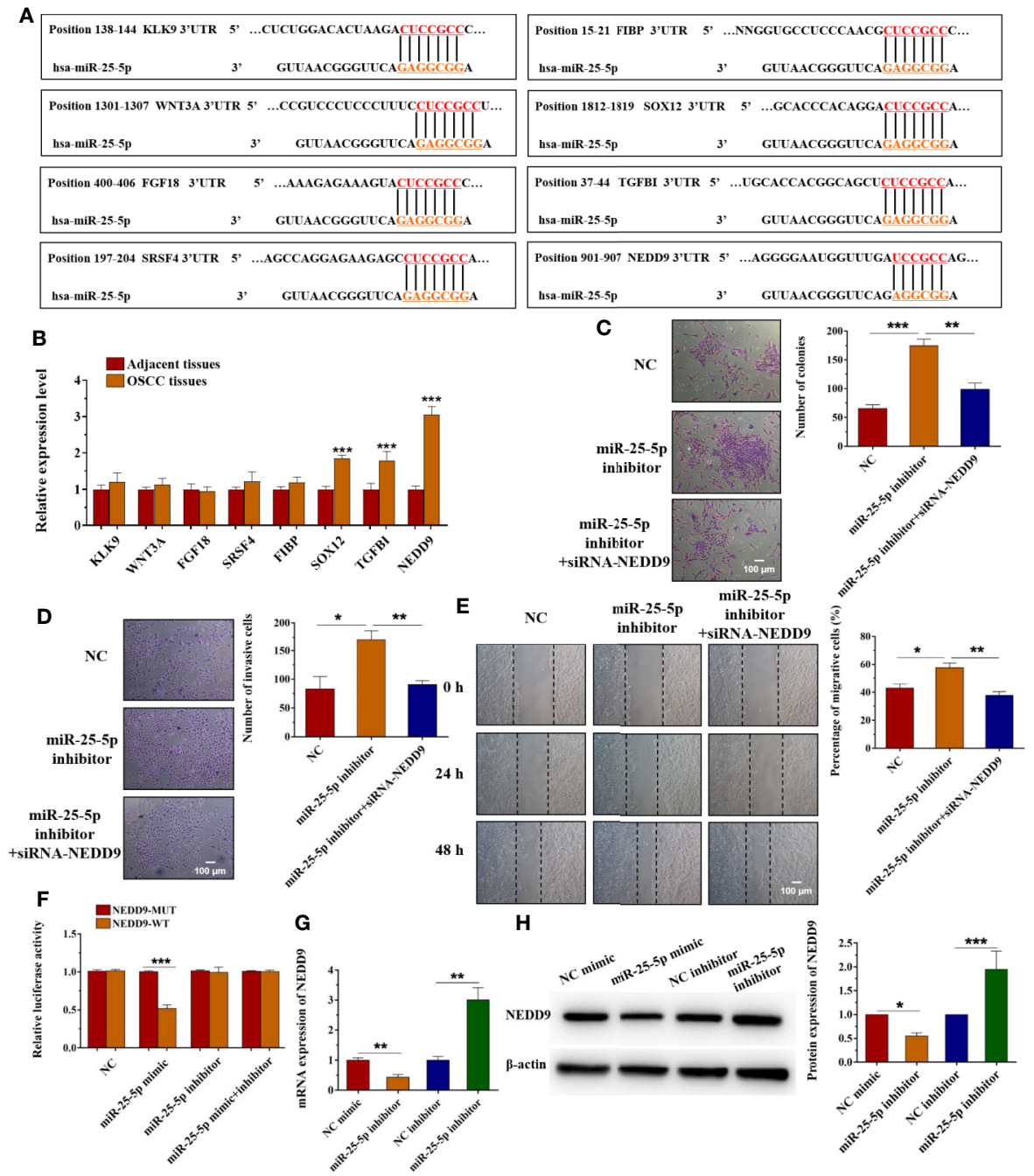

FIGURE 8 | miR-25-5p regulates OSCC cell proliferation, invasion, and migration *via* targeting NEDD9. **(A)** Schematic representation of the predicted miR-25-5p binding region in the 3′-UTR of target genes. **(B)** The expression of KLK9, WNT3A, FGF18, SRSF4, FIBP, SOX12, TGFBI, and NEDD9 in OSCC tissues and adjacent tissues. **(C)** Colony formation assay was used to examine the proliferation ability. **(D)** Transwell invasion assay was performed to detect the invasion ability. **(E)** Wound healing assay was applied to assess the migration ability. **(F)** Luciferase activity was analyzed to confirm the relationship between miR-25-5p and NEDD9. **(G, H)** RT-qPCR **(G)** and western blotting **(H)** were performed to examine the NEDD9 level in SCC9 cells transfected with miR-25-5p mimic or NC mimic. (n=4, B: Student's t-test; C-H: One way ANOVA followed by the Tukey's test, * indicated the differences compared with NC mimics/inhibitor group, *p < 0.05, **p < 0.01, ***p < 0.001, Scale bar, 100 μm).

have not been studied in OSCC. Among these miRNAs, miR-25-5p was downregulated in OSCC tissues and cells, and melatonin treatment upregulated miR-25-5p expression in OSCC cell. Further, we confirmed miR-25-5p was the downstream miRNA of melatonin in OSCC. Melatonin could inhibit multi tumor, like breast cancer, glioma, colorectal cancer, and gastric cancer. However, the involved pathways downstream melatonin in multi tumors are different.

MiRNAs, a cluster of noncoding RNAs, could regulate cell biological behaviors in tumors *via* targeting the 3'UTR of target genes (61). The role of miRNAs has been studied in multi tumors like breast and colon cancers (62, 63). In OSCC, the role of miRNAs has also been studied. Many miRNAs in the body fluids of OSCC patients are common, which indicated they could be set as biomarkers to predict diagnosis, prognosis, and therapeutic efficiency (64). MiRNAs are crucial therapeutic targets to handle oral cancer related pain (65). Thus, it might also be the targets to treat OSCC. According to the previous reports, miR-21, miR-133a, miR-148a-3p, miR-25-5p, and miR-155 participated in the development of various cancers. However, there were no studies that investigate the role of miR-21, miR-133a, miR-148a-3p, miR-25-5p, and miR-155 in OSCC cells and the relationship between melatonin and the expression of these miRNAs. Therefore, in our study, we performed RT-qPCR analysis to identify the dysregulated expression of miRNAs by using SCC9 cells, which were pretreated with melatonin at different concentrations. The results of RT-qPCR analysis revealed that no significant changes in miR-21 or miR-133a expression were observed under melatonin administration. As shown in the results, melatonin elevated the expression of miR-148a-3p and miR-25-5p, but it inhibited the expression of miR-155. Among these miRNAs, miR-25-5p was the most significantly upregulated miRNA after melatonin treatment. Therefore, we chose miR-25-5p for further analysis. MiR-25-5p has been reported to inhibit the proliferation of colorectal cancer cells (15, 66). In our study, melatonin upregulated the expression of miR-25-5p *in vitro*. Melatonin has been reported to upregulate lncRNA H19 *via* enhancing its transcription efficiency. H19 could target miR-675 to upregulate miR-675 expression (67). Thus, in this study, melatonin might upregulate miR-25-5p expression by promoting the expression of lncRNAs or transcription factors that binding to the promoter of miR-25-5p. This hypothesis needed further confirmation. The overexpression of miR-25-5p inhibited OSCC cell viability, proliferation, and induced cell apoptosis. The migration, invasion, and tumor formation were also inhibited by miR-25-5p. Our data confirmed the potential inhibitory role of miR-25-5p on OSCC. Besides, in our study, the results indicated that melatonin exerted anti-proliferative, anti-invasive, and anti-migratory effects on OSCC and promoted the expression of miR-25-5p. Further, inhibition of miR-25-5p could reverse the inhibitory effects of melatonin in OSCC cells. Therefore, we concluded that melatonin exerted anti-proliferative, anti-invasive, and anti-migratory effects on OSCC cells by regulating the expression of miR-25-5p.

As is widely known, miRNAs exert their posttranscriptional regulation role *via* inhibiting target genes expression. The potential target genes were predicted by two databases. There are lots of target genes of miR-25-5p according to the results of quick search on TargetScan databases. Among these target genes, KLK9, WNT3A, FGF18, FIBP, SOX12, TGFBI, and NEDD9 have been reported to participate in the development of human cancers (42–49). The results of RT-qPCR indicated that among KLK9, WNT3A, FGF18, SRSF4, FIBP, SOX12, TGFBI, and NEDD9, the expression of NEDD9 was much higher in OSCC tissues than adjacent tissues. NEDD9 displayed the most obviously upregulated gene between OSCC tissues and adjacent tissues that isolated from OSCC patients. Therefore, we speculated that NEDD9 might play a vital role in the development of OSCC. According to the results, NEDD9 might be the potential target gene of miR-25-5p, and we selected NEDD 9 for further analysis. Dual-luciferase reporter assay confirmed the interaction of miR-25-5p and NEDD9 mRNA. The mRNA expression of NEDD9 could be regulated by miR-25-5p. In OSCC cells, NEDD9 induced MMP9 secretion is an important process to form invadopodia (68). Abnormal expression of NEDD9 has been proved in colorectal cancer, lung cancer, and melanoma (69–71). The inhibition of NEDD9 could induce cancer cell apoptosis in colorectal cancer (15). NEDD9 could regulate many cellular behaviors like proliferation, invasion, mitosis, and migration (72). Overexpressed NEDD9 could enhance the metastasis of hepatocellular carcinoma, while inhibition of NEDD9 could suppress the metastasis (73).

In conclusion, our results proved miR-25-5p/NEDD9 was the downstream pathway of melatonin in OSCC. This study clarified a new mechanism and provided novel therapeutic targets in OSCC. Melatonin could be a potential treatment drug to handle OSCC.

DATA AVAILABILITY STATEMENT

All datasets generated for this study are included in the article/supplementary material.

ETHICS STATEMENT

All the patients have signed the written informed consent before the study. And the present study was approved by the Research Ethics Committee of Henan Province Hospital of TCM. The animal experiments were performed with the approval of the Ethics Committee of Henan Province Hospital of TCM. Animal experiments were carried out according to the National Institutes of Health guidelines to the Care and Use of Laboratory Animals.

AUTHOR CONTRIBUTIONS

Authors WH and QC designed the study and wrote the protocol. Authors YW, BT, and JL conducted the experiments. Author BT managed the literature searches and analyses. Authors JL and XM undertook the statistical analysis, and author YW wrote the first draft of the manuscript. All authors contributed to the article and approved the submitted version.

FUNDING

Funding for this study was provided by Henan Provincial Science and Technology Department Project (172102310613, 142300410086).

REFERENCES

1. Momen-Heravi F, Bala S. Extracellular vesicles in oral squamous carcinoma carry oncogenic miRNA profile and reprogram monocytes via NF-κB pathway. *Oncotarget* (2018) 9:34838–54. doi: 10.18632/oncotarget.26208
2. Chen R, Zhang Y, Zhang X. MiR-1254 Functions as a Tumor Suppressor in Oral Squamous Cell Carcinoma by Targeting CD36. *Technol Cancer Res Treat* (2019) 18:1–9. doi: 10.1177/1533033819859447
3. Xu Y, Liu Y, Xiao W, Yue J, Xue L, Guan Q, et al. MicroRNA-299-3p/FOXP4 Axis Regulates the Proliferation and Migration of Oral Squamous Cell Carcinoma. *Technol Cancer Res Treat* (2019) 18:1–6. doi: 10.1177/1533033819874803
4. Shi B, Ma C, Liu G, Guo Y. MiR-106a directly targets LIMK1 to inhibit proliferation and EMT of oral carcinoma cells. *Cell Mol Biol Lett* (2019) 24:1. doi: 10.1186/s11658-018-0127-8
5. Shi J, Bao X, Liu Z, Zhang Z, Chen W, Xu Q. Serum miR-626 and miR-5100 are Promising Prognosis Predictors for Oral Squamous Cell Carcinoma. *Theranostics* (2019) 9:920–31. doi: 10.7150/thno.30339
6. Kurihara-Shimomura M, Sasahira T, Shimomura H, Nakashima C, Kirita T. The Oncogenic Activity of miR-29b-1-5p Induces the Epithelial-Mesenchymal Transition in Oral Squamous Cell Carcinoma. *J Clin Med* (2019) 8:1–12. doi: 10.3390/jcm8020273
7. Wu H, Liu J, Yin Y, Zhang D, Xia P, Zhu G. Therapeutic Opportunities in Colorectal Cancer: Focus on Melatonin Antioncogenic Action. *BioMed Res Int* (2019) 2019:1–6. doi: 10.1155/2019/9740568
8. Madigan AP, Egidi E, Bedon F, Franks AE, Plummer KM. Bacterial and Fungal Communities Are Differentially Modified by Melatonin in Agricultural Soils Under Abiotic Stress. *Front Microbiol* (2019) 10:2616. doi: 10.3389/fmicb.2019.02616
9. Lu KH, Lin RC, Yang JS, Yang WE, Reiter RJ, Yang SF. Molecular and Cellular Mechanisms of Melatonin in Osteosarcoma. *Cells* (2019) 8:1–14. doi: 10.3390/cells8121618
10. Chang MC, Pan YH, Wu HL, Lu YJ, Liao WC, Yeh CY, et al. Stimulation of MMP-9 of oral epithelial cells by areca nut extract is related to TGF-β/Smad2-dependent and -independent pathways and prevented by betel leaf extract, hydroxychavicol and melatonin. *Aging* (2019) 11:11624–39. doi: 10.18632/aging.102565
11. Fathizadeh H, Mirzaei H, Asemi Z. Melatonin: an anti-tumor agent for osteosarcoma. *Cancer Cell Int* (2019) 19:319. doi: 10.1186/s12935-019-1044-2
12. García-Macia M, Santos-Ledo A, Caballero B, Rubio-González A, de Luxán-Delgado B, Potes Y, et al. Selective autophagy, lipophagy and mitophagy, in the Harderian gland along the oestrous cycle: a potential retrieval effect of melatonin. *Sci Rep* (2019) 9:18597. doi: 10.1038/s41598-019-54743-5
13. Iravani S, Eslami P, Dooghaie Moghadam A, Moazzami B, Mehrvar A, Hashemi MR, et al. The Role of Melatonin in Colorectal Cancer. *J Gastrointestinal Cancer* (2019) 51(3):748–53. doi: 10.1007/s12029-019-00336-4
14. Zhang J, Lu X, Liu M, Fan H, Zheng H, Zhang S, et al. Melatonin inhibits inflammasome-associated activation of endothelium and macrophages attenuating pulmonary arterial hypertension. *Cardiovasc Res* (2019) 116 (13):2156–69. doi: 10.1093/cvr/cvz312
15. Jung JH, Shin EA, Kim JH, Sim DY, Lee H, Park JE, et al. NEDD9 Inhibition by miR-25-5p Activation Is Critically Involved in Co-Treatment of Melatonin- and Pterostilbene-Induced Apoptosis in Colorectal Cancer Cells. *Cancers* (2019) 11:1–17. doi: 10.3390/cancers11111684
16. Kleszczyński K, Kim TK, Bilska B, Sarna M, Mokrzynski K, Stegemann A, et al. Melatonin exerts oncostatic capacity and decreases melanogenesis in human MNT-1 melanoma cells. *J Pineal Res* (2019) 67:e12610. doi: 10.1111/jpi.12610
17. Jablonska K, Nowinska K, Piotrowska A, Partynska A, Katnik E, Pawelczyk K, et al. Prognostic Impact of Melatonin Receptors MT1 and MT2 in Non-Small Cell Lung Cancer (NSCLC). *Cancers* (2019) 11:1–24. doi: 10.3390/cancers11071001
18. Anderson G. Breast cancer: Occluded role of mitochondria N-acetylserotonin/melatonin ratio in co-ordinating pathophysiology. *Biochem Pharmacol* (2019) 168:259–68. doi: 10.1016/j.bcp.2019.07.014
19. Mirza-Aghazadeh-Attari M, Mohammadzadeh A, Mostavafi S, Mihanfar A, Ghazizadeh S, Sadighparvar S, et al. Melatonin: An important anticancer agent in colorectal cancer. *J Cell Physiol* (2020) 235:804–17. doi: 10.1002/jcp.29049
20. Liu H, Zhu Y, Zhu H, Cai R, Wang KF, Song J, et al. Role of transforming growth factor β1 in the inhibition of gastric cancer cell proliferation by melatonin in vitro and in vivo. *Oncol Rep* (2019) 42:753–62. doi: 10.3892/or.2019.7190
21. Shafabakhsh R, Reiter RJ, Mirzaei H, Teymoordash SN, Asemi Z. Melatonin: A new inhibitor agent for cervical cancer treatment. *J Cell Physiol* (2019) 234:21670–82. doi: 10.1002/jcp.28865
22. Natarajan M, Stewart JE, Golemis EA, Pugacheva EN, Alexandropoulos K, Cox BD, et al. HEF1 is a necessary and specific downstream effector of FAK that promotes the migration of glioblastoma cells. *Oncogene* (2006) 25:1721–32. doi: 10.1038/sj.onc.1209199
23. O'Neill GM, Golemis EA. Proteolysis of the docking protein HEF1 and implications for focal adhesion dynamics. *Mol Cell Biol* (2001) 21:5094–108. doi: 10.1128/MCB.21.15.5094-5108.2001
24. van Seventer GA, Salmen HJ, Law SF, O'Neill GM, Mullen MM, Franz AM, et al. Focal adhesion kinase regulates beta1 integrin-dependent T cell migration through an HEF1 effector pathway. *Eur J Immunol* (2001) 31:1417–27. doi: 10.1002/1521-4141(200105)31:5<1417::AID-IMMU1417>3.0.CO;2-C
25. Tikhmyanova N, Golemis EA. NEDD9 and BCAR1 negatively regulate E-cadherin membrane localization, and promote E-cadherin degradation. *PloS One* (2011) 6:e22102. doi: 10.1371/journal.pone.0022102
26. Jemal A, Bray F, Center MM, Ferlay J, Ward E, Forman D. Global cancer statistics. *CA Cancer J Clin* (2011) 61:69–90. doi: 10.3322/caac.20107
27. Shagisultanova E, Gaponova AV, Gabbasov R, Nicolas E, Golemis EA. Preclinical and clinical studies of the NEDD9 scaffold protein in cancer and other diseases. *Gene* (2015) 567:1–11. doi: 10.1016/j.gene.2015.04.086
28. Sima N, Cheng X, Ye F, Ma D, Xie X, Lü W. The overexpression of scaffolding protein NEDD9 promotes migration and invasion in cervical cancer via tyrosine phosphorylated FAK and SRC. *PloS One* (2013) 8:e74594. doi: 10.1371/journal.pone.0074594
29. Kong C, Wang C, Wang L, Ma M, Niu C, Sun X, et al. NEDD9 is a positive regulator of epithelial-mesenchymal transition and promotes invasion in aggressive breast cancer. *PloS One* (2011) 6:e22666. doi: 10.1371/journal.pone.0022666
30. Budhu A, Forgues M, Ye QH, Jia HL, He P, Zanetti KA, et al. Prediction of venous metastases, recurrence, and prognosis in hepatocellular carcinoma based on a unique immune response signature of the liver microenvironment. *Cancer Cell* (2006) 10:99–111. doi: 10.1016/j.ccr.2006.06.016
31. Chang JX, Gao F, Zhao GQ, Zhang GJ. Expression and clinical significance of NEDD9 in lung tissues. *Med Oncol* (2012) 29:2654–60. doi: 10.1007/s12032-012-0213-0
32. Wang H, Mu X, Zhou S, Zhang J, Dai J, Tang L, et al. NEDD9 overexpression is associated with the progression of and an unfavorable prognosis in epithelial ovarian cancer. *Hum Pathol* (2014) 45:401–8. doi: 10.1016/j.humpath.2013.10.005
33. Izumchenko E, Singh MK, Plotnikova OV, Tikhmyanova N, Little JL, Serebriiskii IG, et al. NEDD9 promotes oncogenic signaling in mammary tumor development. *Cancer Res* (2009) 69:7198–206. doi: 10.1158/0008-5472.CAN-09-0795
34. Wei H, Li J, Xie M, Lei R, Hu B. Comprehensive analysis of metastasis-related genes reveals a gene signature predicting the survival of colon cancer patients. *PeerJ* (2018) 6:e5433. doi: 10.7717/peerj.5433
35. Zhao Z, Gao D, Ma T, Zhang L. MicroRNA-141 suppresses growth and metastatic potential of head and neck squamous cell carcinoma. *Aging* (2019) 11:921–32. doi: 10.18632/aging.101791
36. Cheng J, Cheng A, Clifford BL, Wu X, Hedin U, Maegdefessel L, et al. MicroRNA-144 Silencing Protects Against Atherosclerosis in Male, but Not Female Mice. *Arteriosclerosis Thrombosis Vasc Biol* (2020) 40:412–25. doi: 10.1161/ATVBAHA.119.313633
37. Xu H, Sun Y, You B, Huang CP, Ye D, Chang C. Androgen receptor reverses the oncometabolite R-2-hydroxyglutarate-induced prostate cancer cell invasion via suppressing the circRNA-51217/miRNA-646/TGFβ1/p-Smad2/3 signaling. *Cancer Lett* (2020) 472:151–64. doi: 10.1016/j.canlet.2019.12.014
38. Zheng J, Xu T, Chen F, Zhang Y. MiRNA-195-5p Functions as a Tumor Suppressor and a Predictive of Poor Prognosis in Non-small Cell Lung Cancer by Directly Targeting CIAPIN1. *Pathol Oncol Res POR* (2019) 25:1181–90. doi: 10.1007/s12253-018-0552-z
39. Salomão KB, Pezuk JA, de Souza GR, Chagas P, Pereira TC, Valera ET, et al. MicroRNA dysregulation interplay with childhood abdominal tumors. *Cancer Metastasis Rev* (2019) 38(4):783–811. doi: 10.1007/s10555-019-09829-x
40. Zhan JW, Jiao DM, Wang Y, Song J, Wu JH, Wu LJ, et al. Integrated microRNA and gene expression profiling reveals the crucial miRNAs in

curcumin anti-lung cancer cell invasion. *Thoracic Cancer* (2017) 8:461–70. doi: 10.1111/1759-7714.12467
41. Singh A, Willems E, Singh A, Ong IM, Verma AK. Ultraviolet radiation-induced differential microRNA expression in the skin of hairless SKH1 mice, a widely used mouse model for dermatology research. *Oncotarget* (2016) 7:84924–37. doi: 10.18632/oncotarget.12913
42. Geng X, Liu Y, Diersch S, Kotzsch M, Grill S, Weichert W, et al. Clinical relevance of kallikrein-related peptidase 9, 10, 11, and 15 mRNA expression in advanced high-grade serous ovarian cancer. *PloS One* (2017) 12:e0186847. doi: 10.1371/journal.pone.0186847
43. Shen G, Gao Q, Liu F, Zhang Y, Dai M, Zhao T, et al. The Wnt3a/β-catenin/TCF7L2 signaling axis reduces the sensitivity of HER2-positive epithelial ovarian cancer to trastuzumab. *Biochem Biophys Res Commun* (2020) 526:685–91. doi: 10.1016/j.bbrc.2020.03.154
44. Re Cecconi AD, Forti M, Chiappa M, Zhu Z, Zingman LV, Cervo L, et al. Musclin, A Myokine Induced by Aerobic Exercise, Retards Muscle Atrophy During Cancer Cachexia in Mice. *Cancers (Basel)* (2019) 11:1–27. doi: 10.3390/cancers11101541
45. Park S, Brugiolo M, Akerman M, Das S, Urbanski L, Geier A, et al. Differential Functions of Splicing Factors in Mammary Transformation and Breast Cancer Metastasis. *Cell Rep* (2019) 29:2672–88.e7. doi: 10.1016/j.celrep.2019.10.110
46. Huang YF, Niu WB, Hu R, Wang LJ, Huang ZY, Ni SH, et al. FIBP knockdown attenuates growth and enhances chemotherapy in colorectal cancer via regulating GSK3β-related pathways. *Oncogenesis* (2018) 7:77. doi: 10.1038/s41389-018-0088-9
47. Umeh-Garcia M, Simion C, Ho PY, Batra N, Berg AL, Carraway KL, et al. A Novel Bioengineered miR-127 Prodrug Suppresses the Growth and Metastatic Potential of Triple-Negative Breast Cancer Cells. *Cancer Res* (2020) 80:418–29. doi: 10.1158/0008-5472.CAN-19-0656
48. Steitz AM, Steffes A, Finkernagel F, Unger A, Sommerfeld L, Jansen JM, et al. Tumor-associated macrophages promote ovarian cancer cell migration by secreting transforming growth factor beta induced (TGFBI) and tenascin C. *Cell Death Dis* (2020) 11:249. doi: 10.1038/s41419-020-2438-8
49. Wang Y, Dan L, Li Q, Li L, Zhong L, Shao B, et al. ZMYND10, an epigenetically regulated tumor suppressor, exerts tumor-suppressive functions via miR145-5p/NEDD9 axis in breast cancer. *Clin Epigenet* (2019) 11:184. doi: 10.1186/s13148-019-0785-z
50. Reiter RJ. The pineal and its hormones in the control of reproduction in mammals. *Endocrine Rev* (1980) 1:109–31. doi: 10.1210/edrv-1-2-109
51. Coto-Montes A, Boga JA, Rosales-Corral S, Fuentes-Broto L, Tan DX, Reiter RJ. Role of melatonin in the regulation of autophagy and mitophagy: a review. *Mol Cell Endocrinol* (2012) 361:12–23. doi: 10.1016/j.mce.2012.04.009
52. Karbownik M, Lewinski A, Reiter RJ. Anticarcinogenic actions of melatonin which involve antioxidative processes: comparison with other antioxidants. *Int J Biochem Cell Biol* (2001) 33:735–53. doi: 10.1016/S1357-2725(01)00059-0
53. Klaunig JE, Xu Y, Isenberg JS, Bachowski S, Kolaja KL, Jiang J, et al. The role of oxidative stress in chemical carcinogenesis. *Environ Health Perspect* (1998) 106 Suppl 1(Suppl 1):289–95. doi: 10.1289/ehp.98106s1289
54. Marques JHM, Mota AL, Oliveira JG, Lacerda JZ, Stefani JP, Ferreira LC, et al. Melatonin restrains angiogenic factors in triple-negative breast cancer by targeting miR-152-3p: In vivo and in vitro studies. *Life Sci* (2018) 208:131–8. doi: 10.1016/j.lfs.2018.07.012
55. Ferreira LC, Orso F, Dettori D, Lacerda JZ, Borin TF, Taverna D, et al. The role of melatonin on miRNAs modulation in triple-negative breast cancer cells. *PloS One* (2020) 15:e0228062. doi: 10.1371/journal.pone.0228062
56. Lacerda JZ, Ferreira LC, Lopes BC, Aristizábal-Pachón AF, Bajgelman MC, Borin TF, et al. Therapeutic Potential of Melatonin in the Regulation of MiR-148a-3p and Angiogenic Factors in Breast Cancer. *Microrna* (2019) 8:237–47. doi: 10.2174/2211536608666190219095426
57. Sakatani A, Sonohara F, Goel A. Melatonin-mediated downregulation of thymidylate synthase as a novel mechanism for overcoming 5-fluorouracil associated chemoresistance in colorectal cancer cells. *Carcinogenesis* (2019) 40:422–31. doi: 10.1093/carcin/bgy186
58. Zhu C, Huang Q, Zhu H. Melatonin Inhibits the Proliferation of Gastric Cancer Cells Through Regulating the miR-16-5p-Smad3 Pathway. *DNA Cell Biol* (2018) 37:244–52. doi: 10.1089/dna.2017.4040
59. Gu J, Lu Z, Ji C, Chen Y, Liu Y, Lei Z, et al. Melatonin inhibits proliferation and invasion via repression of miRNA-155 in glioma cells. *BioMed Pharmacother* (2017) 93:969–75. doi: 10.1016/j.biopha.2017.07.010
60. Kartini D, Taher A, Panigoro SS, Setiabudy R, Jusman SW, Haryana SM, et al. Effect of melatonin supplementation in combination with neoadjuvant chemotherapy to miR-210 and CD44 expression and clinical response improvement in locally advanced oral squamous cell carcinoma: a randomized controlled trial. *J Egypt Natl Canc Inst* (2020) 32:12. doi: 10.1186/s43046-020-0021-0
61. Li B, Wang Z, Yu M, Wang X, Wang X, Chen C, et al. miR-22-3p enhances the intrinsic regenerative abilities of primary sensory neurons via the CBL/p-EGFR/p-STAT3/GAP43/p-GAP43 axis. *J Cell Physiol* (2020) 235:4605–17. doi: 10.1002/jcp.29338
62. Seung EL. MicroRNA and gene expression analysis of melatonin-exposed human breast cancer cell lines indicating involvement of the anticancer effect. *J Pineal Res* (2011) 3:345–52. doi: 10.1111/j.1600-079X.2011.00896.x.
63. Li Q, Zou C, Zou C, Han Z, Xiao H, Wei H, et al. MicroRNA-25 functions as a potential tumor suppressor in colon cancer by targeting Smad7. *Cancer Lett* (2013) 335:168–74. doi: 10.1016/j.canlet.2013.02.029
64. Mazumder S, Datta S, Ray JG, Chaudhuri K, Chatterjee R. Liquid biopsy: miRNA as a potential biomarker in oral cancer. *Cancer Epidemiol* (2019) 58:137–45. doi: 10.1016/j.canep.2018.12.008
65. Pereira CM, Sehnem D, da Fonseca EO, Barboza HFG, de Carvalho ACP, DaSilva AFM, et al. miRNAs: Important Targets for Oral Cancer Pain Research. *BioMed Res Int* (2017) 2017:4043516. doi: 10.1155/2017/4043516
66. Zhang S, Zhang Y, Cheng Q, Ma Z, Gong G, Deng Z, et al. Silencing protein kinase C ζ by microRNA-25-5p activates AMPK signaling and inhibits colorectal cancer cell proliferation. *Oncotarget* (2017) 8:65329–38. doi: 10.18632/oncotarget.18649
67. Yang S, Tang W, He Y, Wen L, Sun B, Li S, et al. and microRNA-675/let-7a mediates the protective effect of melatonin against early brain injury after subarachnoid hemorrhage via targeting TP53 and neural growth factor. *Cell Death Dis* (2018) 9:99. doi: 10.1038/s41419-017-0155-8
68. Grauzam S, Brock AM, Holmes CO, Tiedeken JA, Boniface SG, Pierson BN, et al. NEDD9 stimulated MMP9 secretion is required for invadopodia formation in oral squamous cell carcinoma. *Oncotarget* (2018) 9:25503–16. doi: 10.18632/oncotarget.25347
69. Dai J, Van Wie PG, Fai LY, Kim D, Wang L, Poyil P, et al. Downregulation of NEDD9 by apigenin suppresses migration, invasion, and metastasis of colorectal cancer cells. *Toxicol Appl Pharmacol* (2016) 311:106–12. doi: 10.1016/j.taap.2016.09.016
70. Kim M, Gans JD, Nogueira C, Wang A, Paik JH, Feng B, et al. Comparative oncogenomics identifies NEDD9 as a melanoma metastasis gene. *Cell* (2006) 125:1269–81. doi: 10.1016/j.cell.2006.06.008
71. Chang JX, Gao F, Zhao GQ, Zhang GJ. Effects of lentivirus-mediated RNAi knockdown of NEDD9 on human lung adenocarcinoma cells in vitro and in vivo. *Oncol Rep* (2014) 32:1543–9. doi: 10.3892/or.2014.3347
72. Singh M, Cowell L, Seo S, O'Neill G, Golemis E. Molecular basis for HEF1/NEDD9/Cas-L action as a multifunctional co-ordinator of invasion, apoptosis and cell cycle. *Cell Biochem Biophysics* (2007) 48:54–72. doi: 10.1007/s12013-007-0036-3
73. Zheng Y, Nie P, Xu S. Long noncoding RNA linc00467 plays an oncogenic role in hepatocellular carcinoma by regulating the miR-18a-5p/NEDD9 axis. *J Cell Biochem* (2020) 121(5-6):3135–44. doi: 10.1002/jcb.29581

Conflict of Interest: The authors declare that the research was conducted in the absence of any commercial or financial relationships that could be construed as a potential conflict of interest.

frontiers in Oncology

REVIEW
published: 22 December 2020
doi: 10.3389/fonc.2020.617793

Oligometastatic Disease Management: Finding the Sweet Spot

Petr Szturz[1], *Daan Nevens*[2,3] *and Jan B. Vermorken*[3,4]*

[1] Medical Oncology, Department of Oncology, Lausanne University Hospital (CHUV), Lausanne, Switzerland, [2] Department of Radiation Oncology, IridiumNetwork, Wilrijk (Antwerp), Belgium, [3] Faculty of Medicine and Health Sciences, University of Antwerp, Antwerp, Belgium, [4] Department of Medical Oncology, Antwerp University Hospital, Edegem, Belgium

Hematogenous dissemination represents a common manifestation of squamous cell carcinoma of the head and neck, and the recommended therapeutic options usually consist of systemically administered drugs with palliative intent. However, mounting evidence suggests that patients with few and slowly progressive distant lesions of small size may benefit from various local ablation techniques, which have already been established as standard-of-care modalities for example in colorectal and renal cell carcinomas and in sarcomas. In principle, serving as radical approaches to eradicate cancer, these interventions can be curative. Their impact on local control and overall survival has been shown in numerous retrospective and prospective studies. The term oligometastatic refers to the number of distant lesions which should generally not surpass five in total, ideally in one organ. Currently, surgical resection remains the method of choice supported by the majority of published data. More recently, stereotactic (ablative) body radiotherapy (SABR/SBRT) has emerged as a viable alternative. In cases technically amenable to such local interventions, several other clinical variables need to be taken into account also, including patient-related factors (general health status, patient preferences, socioeconomic background) and disease-related factors (primary tumor site, growth kinetics, synchronous or metachronous metastases). In head and neck cancer, patients presenting with late development of slowly progressive oligometastatic lesions in the lungs secondary to human papillomavirus (HPV)-positive oropharyngeal cancer are the ideal candidates for metastasectomy or other local therapies. However, literature data are still limited to say whether there are other subgroups benefiting from this approach. One of the plausible explanations is that radiological follow-up after primary curative therapy is usually not recommended because its impact on survival has not been unequivocal, which is also due to the rarity of oligometastatic manifestations in this disease. At the same time, aggressive treatment of synchronous metastases early in the disease course should be weighed against the risk of futile interventions in a disease with already multimetastatic microscopic dissemination. Therefore, attentive treatment sequencing, meticulous appraisal of cancer extension, refinement of post-treatment surveillance, and understanding of tumor biology and kinetics are crucial in the management of oligometastases.

Keywords: head and neck cancer, oligometastatic, metastasectomy, surgery, stereotactic ablative body radiotherapy, immunotherapy, surveillance, cure

OPEN ACCESS

Edited by:
Alberto Paderno, University of Brescia, Italy

Reviewed by:
Sandro J. Stoeckli, Kantonsspital St. Gallen, Switzerland
Maria Cossu Rocca, European Institute of Oncology (IEO), Italy

***Correspondence:**
Jan B. Vermorken
JanB.Vermorken@uza.be

Specialty section:
This article was submitted to Head and Neck Cancer, a section of the journal Frontiers in Oncology

Received: *15 October 2020*
Accepted: *16 November 2020*
Published: *22 December 2020*

Citation:
Szturz P, Nevens D and Vermorken JB (2020) Oligometastatic Disease Management: Finding the Sweet Spot. Front. Oncol. 10:617793. doi: 10.3389/fonc.2020.617793

INTRODUCTION

Recent therapeutic achievements in head and neck cancer managed to reduce the risk of death from recurrences and metastatic dissemination or at least contributed to delaying disease progression and quality of life deterioration. Apart from new systemic modalities leveraging the immune cells to combat cancer, increasing attention has been drawn towards local ablative approaches, which either as complementary or stand-alone therapies demonstrated encouraging activity against distant lesions. In particular, cases with few slowly growing metastases seem to constitute the ideal candidates (1). These patients present with different forms of oligometastatic disease. Besides a de-novo diagnosis, it may develop in the context of a controlled primary tumor (oligorecurrence) or otherwise controlled polymetastatic disease (oligoprogression). Herein, we will discuss the current state of the art in management of oligometastatic head and neck cancer in order to assist physicians in finding the optimal spot in the disease course where such treatment brings the maximum benefit to patients. However, before doing that, we will briefly review some important facts about metastatic outgrowth defining the patients at risk, addressing different diagnostic methods, and introducing available treatment options.

DISTANT METASTASES: WHO, HOW, AND WHAT

Who is at risk of developing distant lesions? Compared with other malignancies, the proportion of head and neck cancer patients presenting with hematogenous dissemination is generally smaller and varies from 3%–17% at presentation (before any therapy). This may increase during the course of the disease to 10%–40% and can be even found higher at autopsy studies (40%–50%). The clinical presentations are variable according to the primary tumor site, disease stage, local and regional control, duration of follow-up, histological type, and delivered treatment. High-risk features include hypopharyngeal origin, advanced locoregional disease characterized by large tumors and extensive lymphadenopathies, poor histological differentiation, and the presence of extracapsular spread (2). Moreover, advanced age, black race, and radiological evidence of low jugular, posterior triangle, paratracheal, and contralateral lymph nodes were associated with increased risk of metastases (3, 4). The aforementioned features hold true for the most frequent histological type, i.e. squamous cell carcinoma, which will also be the principal subject of this article unless otherwise specified. Furthermore, some tumors both within this group, such as basaloid squamous cell carcinoma, and beyond, such as nasopharyngeal, adenoid cystic, and neuroendocrine carcinomas, are known for even a higher propensity to develop distant lesions (5). Typically involved sites are the lungs (70%–85% of patients with metastases), albeit a distinction from a primary pulmonary tumor can be challenging, then the bones (15%–39%) and liver (10%–30%), while skin (10%–15%) and brain (about 5%) affections remain less frequent (2). They usually occur within 2–3 years of diagnosis with the notable exception of a small proportion (probably more than 10%) of human papillomavirus (HPV)-positive oropharyngeal cancer cases, which continue to metastasize for a longer period of time, even beyond 6 years (6, 7). Interestingly, in a recent meta-analysis of seven studies, time to distant progression was 0.2–106 months and 0.2–33 months in HPV-positive and HPV-negative oropharyngeal cancer patients, respectively (8).

How to detect them? This is the pivotal question because imaging modalities differ in their diagnostic accuracy, which is partially responsible for the higher incidence of macrometastases found at autopsies than radiological surveys (5). In addition, our knowledge of micrometastases sometimes identified in tissue specimens remains elusive, including their clinical significance. Currently, fluorine-18-fluorodeoxyglucose (FDG) positron emission tomography with or without simultaneous computed tomography (PET/CT) scanning represents the optimal modality for detection of head and neck cancer distant spread at initial staging (9, 10). In a prospective trial of 233 patients, the addition of FDG-PET to a conventional work-up (physical examination, head and neck CT or magnetic resonance [MR], and thoracic CT) changed the M-stage in 8.6% of the study cohort (11). On the other hand, its role in follow-up of head and neck cancer survivors has been proved only for an early evaluation of regional control after definitive chemoradiotherapy but still needs to be defined for metastatic disease (12–14). One of the new, promising techniques that could find its place especially in surveillance protocols is liquid biopsy. It is based on early detection of circulating tumor deoxyribonucleic acid (DNA) mostly in the blood but also in saliva and other body fluids (15). Finally, special attention should be paid to patients with polymetastatic disease on systemic therapy, in whom close response monitoring by CT or PET/CT scans is usually performed every 6 to 12 weeks for a timely detection of disease progression, which in some highly selected cases may be treated with local ablation.

What are the treatment options? Although the traditional approach of oncology care in patients with metastatic tumors relies on systemic treatment with palliative intent, mounting evidence has demonstrated the utility of local ablation in certain clinical situations. Surgical resection of metastases, especially in the lungs, has been known to medical professionals since the 19th century. In 1882, Weinlechner removed sarcoma metastases localized near the primary tumor infiltrating the thoracic wall. However, the first pulmonary metastasectomy as a planned and separate procedure was carried out by Divis in Prague in 1926 (16). When in 1995 Hellman and Weichselbaum thus coined the term "oligometastatic state", surgery had already been widely accepted as a curative approach to a rather small proportion of patients, typically with lung metastases from soft tissue sarcomas, osteosarcomas, and renal cell cancers and with hepatic metastases from colorectal cancer (17). More recently, the armamentarium of local approaches has been complemented by radiotherapy and thermal ablation treatments, such as radiofrequency ablation or cryotherapy, which spare patients

from a more invasive procedure at the cost of unknown treatment margins. At present, patients with oligometastatic disease of various origins are routinely offered such a potentially curative treatment, sometimes using a sequential combination of different modalities, planned in a stepwise fashion and even repeatedly in the case of accessible recurrences (18, 19).

APPROACH TO OLIGOMETASTATIC DISEASE

Over the past year, growing efforts have been undertaken to define oligometastatic disease and its different states in order to standardize reporting thereof (20, 21). As a result, the following two conditions must be met: the maximum number of five metastases should not be surpassed, and all of them must be safely treatable, whereas a controlled primary is optional (21). According to the timing of its appearance, several distinct clinical presentations, discussed further in the text, are recognized (20–22). Since a standard approach has not been determined in these situations, all patients who could potentially be considered for a local approach should be discussed in multidisciplinary tumor boards. In this regard, we propose a multistep evaluation procedure respecting not only the technical feasibility of a given procedure but also its clinical relevance (**Figure 1**). While the former aspect is beyond the scope of this paper, we will address important pre-treatment factors here, some of which are specific for head and neck cancer, and then outline the main treatment modalities, among which the surgical approach is grounded in the strongest body of scientific evidence, followed by stereotactic radiotherapy reserved for inoperable cases. In the last section, we will deliberate over the intriguing role of combining systemic treatment with local therapies. The key message is that primary intent of these therapeutic endeavors is curative, although they may also be beneficial in consolidating response to systemic palliative treatment or postponing initiation or change thereof. Finally, the advantages of active approach should be weighed against watchful waiting, particularly in heavily pre-treated patients with repeatedly recurring and slowly progressing oligometastases.

Clinical Pre-Treatment Considerations

The following three patient-related factors should be acknowledged before performing a planned intervention, feasible from a technical point of view.

General health status. The majority of head and neck cancer cases occur in the elderly, and global epidemiological projections predict increasing proportions of older people, people with cancer, and also older people with head and neck cancer, which further stimulates the strengthening position of geriatric evaluation in oncology practices. Prior to a tumor-directed treatment, all cancer patients of 70 years of age or older should undergo a frailty screening test and, according to the result, be subjected to a comprehensive geriatric assessment comprising a thorough evaluation of functional status, comorbidities, cognition, nutritional status, social support, psychological state, and polypharmacy (23). These variables are relevant, albeit to lesser extent, to the younger counterparts as well, who have usually an overall higher life expectancy and functional reserve capacity, so that the medical assessment is often limited to the appraisal of performance status and comorbidities (24). Of note, frailty, characterized by at least three of the following five criteria: weakness (grip strength), slowness, low physical activity, exhaustion, and weight loss, or pre-frailty (comprising only one or two of these criteria) can develop even in younger patients, particularly in the presence of chronic diseases, socioeconomic deprivation, and specific lifestyle behaviors (smoking, obesity) (25). Estimating overall health status of an individual and detecting unknown deficits help select an appropriate local therapy and decide on its timing and possible combinations with systemic treatment.

Patient preference. Shared-decision making with a well-informed patient should be encouraged whenever possible and has particular importance in borderline cases, such as when watchful waiting is proposed. Sometimes, patients can decide whether they opt for an invasive procedure or radiotherapy or thermal ablation if assumed equipotent in a given situation.

Socioeconomic background. It has been well recognized that socioeconomic and other disparities negatively impact on cancer incidence and survival due to associated inequalities in harmful lifestyle behaviors (smoking, alcohol intake, dietary patterns, physical inactivity), screening, and treatment (26). In head and neck cancer, lower income, high school education or less, and older age correlate with decreased overall and disease-free survival, at least in the USA (27). All these factors are particularly relevant in resource-limited countries. Moreover, the COVID-19 pandemic has disrupted oncologic care in many areas and amplified the pre-existing gap in its delivery (28).

In order to optimize the planned therapeutic intervention, the following three disease-related factors should be taken into account in patients deemed suitable according to the above-mentioned characteristics.

Primary tumor site. Among squamous cell carcinomas of the head and neck, HPV-positive oropharyngeal cancer represents a separate entity with distinct biological and epidemiological behavior (29). Not only is overall survival after distant failure longer in these patients, but about one third of oligometastatic cases in the lungs can be cured with either surgery or radiotherapy (7, 30). Noteworthy, compared with their HPV-negative; counterparts, patients with HPV-positive oropharyngeal cancer present more often with dissemination to more than two organs (about one third of cases) that can also involve unusual localizations such as the skeletal muscles, pericardial lymph nodes, kidney, or pancreatic tail (6–8). Therefore, careful evaluation and sometimes even multiple biopsies are warranted in these cases. Another notable exception sharing with HPV-positive oropharyngeal cancer the prominent trend of developing distant metastases is nasopharyngeal carcinoma (31). Although less evidence is available on using local ablation alone to treat metastatic lesions in nasopharyngeal carcinoma, improved outcomes have been noted if palliative systemic therapy for disseminated disease is complemented with radiotherapy of the primary lesion (32, 33).

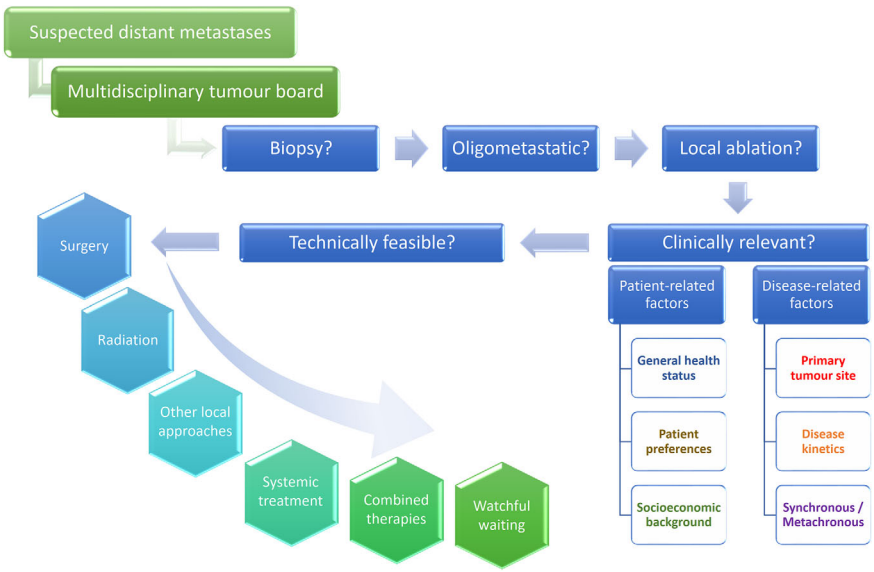

FIGURE 1 | Multistep process of decision making in oligometastatic head and neck cancer patients. Patients with suspected hematogenous spread should be discussed at tumor board meetings in order to decide whether a biopsy confirmation is needed and whether local ablation can be proposed in case of an oligometastatic manifestation. Such treatment should not only be technically feasible but also clinically sound. Metastasectomy remains the treatment of choice and could be replaced by stereotactic body radiation or other local therapies in patients not suitable for a surgical intervention. Incorporating chemo- or immunotherapy or both, systemic treatment can be combined with local ablation according to the clinical setting. Watchful waiting is reserved for highly selected cases, usually as a temporary solution in heavily pre-treated patients with known disease kinetics.

Disease kinetics. Pace of the disease is one of the critical decision-making factors in patients presenting with distant spread (34). When applying local ablation to eradicate a disseminated cancer, the major concern is that the few visible macroscopic lesions represent merely the inception of an explosive manifestation. Logically, a follow-up imaging in 2–3 months gives us the desired answer but that's actually what we try to avoid doing in the majority of cases, if not deemed suitable candidates for a wait-and-watch strategy, due to the following three reasons. First, lesions that can be treated now may progress in a couple of months in size rendering them unsuitable for the initially planned procedure. Second, new distant lesions may develop, and third, the patient's condition may alter, either because of disease progression or underlying comorbidities, to an extent which can contraindicate further antitumor efforts. In some cases, distant metastases, particularly in the lung parenchyma, can be traced back on preceding imaging methods carried out even for other, non-oncologic reasons. In other cases, we may encounter oligoprogression which means that one or a few nodules progress during systemic palliative therapy while at the same time multiple other lesions remain under control. Subsequently, retrospective review of tumor size and other characteristics will help estimate the disease kinetics. However, in the majority of patients, the decisive factor is whether the metastases were detected at the time of initial diagnosis or whether they appeared in the course of the disease. These aspects are detailed in the following paragraph.

Synchronous or metachronous metastases. In the former scenario, partially owing to the insufficient information on tumor kinetics, patients usually receive systemic treatment in the first place, and if the disease is well-controlled, a local therapy is delivered at some point later. In the latter setting, corresponding to oligorecurrence or oligoprogression, a series of imaging studies is sometimes available allowing a more accurate appraisal of the disease pace and facilitating decisions about a single-modality local therapy. According to an arbitrary definition, metachronous metastases occur after 3 months from the initial diagnosis, which typically means that at least one radiological survey had been carried out. In this respect, it should be noted that in the majority of head and neck cancer patients treated with curative intent, no radiological surveillance is recommended as it had not consistently demonstrated survival benefit, although this does not perhaps hold true for some patient subgroups, such as with HPV-positive oropharyngeal cancer, in whom periodic imaging might be warranted (14).

Surgical Treatment

Supported by the largest body of evidence, metastasectomy has been traditionally considered the gold standard in this setting. In 2015, a meta-analysis of 11 retrospective studies enrolling a total of 387 head and neck cancer patients calculated a 5-year overall survival rate at 29% after resection of metachronous pulmonary metastases (mostly single nodules). Various poor prognostic factors were reported in the included individual studies comprising the site of the primary tumor in the oral cavity, initial lymph node involvement, shorter interval from primary diagnosis to pulmonary dissemination, particularly if it occurred within 1 year, incomplete metastasectomy, and multiple

pulmonary nodules (35). Literature on extrapulmonary surgery is less advanced but 5-year survival after resection of hepatic oligometastases may be in the same range (36). Additionally, the importance of new techniques should be brought to the forefront. In a retrospective cohort of different primary tumors, minimally invasive approaches, such as video-assisted thoracic surgery (VATS) and radiofrequency ablation (RFA), were associated with lower morbidity and similar local control and overall survival compared with an open resection (37). Besides that, surgical candidates are usually young patients in a good general condition, and this should also be kept in mind not only when making decisions in routine clinical practice but also when interpreting the results of available retrospective studies. Finally, the obtained full pathological specimen provides definitive diagnosis as well as additional material for immunohistochemical and molecular analyses if so needed. In this respect, differentiating a pulmonary metastasis from squamous cell lung carcinoma has been challenging and requires clinical and radiological inputs and in the case of oropharyngeal carcinoma also detection of high-risk HPV infection and not only p16 expression which can also be found in squamous cell carcinomas originating in the lungs, esophagus, and skin (38, 39).

Radiotherapy

In patients who are unwilling or unable to undergo an invasive procedure or deemed to be at high risk of postoperative complications due to underlying comorbidities, stereotactic (ablative) body radiotherapy (SABR/SBRT) has emerged as a viable alternative to a standard surgical intervention. Derived from intracranial stereotactic radiosurgery, the methodology was introduced to clinical practice by Lax and Blomgren at the Karolinska Hospital in Sweden in September 1991 (40, 41). Based on delivering precisely targeted high doses of radiation in one or several fractions, the concept of SABR has been rapidly adopted by many institutions to treat mainly small lung cancers either primary or secondary, liver metastases, and later on also bone, lymph node, and other less frequent locations (42, 43). The increasing popularity has been mirrored by a steadily rising implementation in treatment protocols which is expected to continue in the coming years (44). Multiple single-arm studies as well as several randomized trials showed that SABR can improve disease-free and overall survival in the oligometastatic setting while maintaining good tolerance (45–51). However, covering different primary tumor types and organ sites, the available data remain heterogeneous (44). Furthermore, no randomized trial comparing a standard surgical approach with SABR has been conducted so far.

Until now, the largest *retrospective study* in head and neck cancer evaluated 82 cases of different histological types presenting either with synchronous or metachronous oligometastases (less than three in total) or multiple metastases in the lungs. Among 43 patients with oligometastatic squamous cell carcinomas, 1- and 2-year local control was 96% and 90%, respectively, and 1- and 2-year overall survival was 74% and 66%, respectively (52). Focusing solely on oligometastatic disease, another retrospective study reported 1- and 2-year overall survival of 78% and 43%, respectively, in 27 squamous head and neck carcinoma patients with up to five synchronous and metachronous metastases mostly affecting the lungs but also other organs encompassing the bones, liver, lymph nodes, and soft tissues. Local control of treated lung nodules was 74% and 52% at 1- and 2-years, respectively (53). Contrary to the former study, in which histopathological confirmation of the lung lesions was obtained in almost 90% of cases, in the latter one, biopsy was not mandatory prior to radiotherapy.

Regarding *prospective trials* on the efficacy and safety of SABR in oligometastatic disease, only a few are randomized phase II trials while most of them are single arm studies with just a small number of head and neck cancer patients (54, 55). In the largest one, Sutera et al. recruited 147 patients with up to five metachronous, biopsy-proven metastases visualized on FDG-PET/CT in at most three organs comprising the lungs (52%), lymph nodes (17%), bones (15%), and other sites. There was a large variety of primary tumors with more than half of them represented by lung cancer (22%), colorectal cancer (21%), and head and neck cancer (11%). Owing to an excess of early deaths, median overall survival of 17.6 months in 16 patients with head and neck cancer, out of which 11 had squamous cell carcinoma, was inferior to that observed in other primary tumor subgroups. However, the 42% 5-year overall survival yielded in this cohort compares favorably to outcomes yielded in surgical studies but can be biased by the small patient number (43). As of yet, the only randomized trial exploring the addition of SABR to a standard systemic palliative treatment according to primary cancer was the SABR-COMET phase II study with a 2:1 randomization in favor of the experimental arm. Oligometastatic state was defined by a maximum of five metachronous lesions with not more than three of them per organ. Biopsy was optional, and participants were not considered candidates for surgery. The three most frequently included primary tumors were breast cancer (18%), colorectal cancer (18%), and lung cancer (18%), which were not balanced between the two study arms. The number of head and neck cancer patients was not specified except for a short comment in the supplementary materials on a case of oropharyngeal cancer treated for a lung metastasis of 3 cm in diameter complicated by a large pulmonary abscess a year later. In the whole cohort of 99 patients, SABR enhanced 5-year overall survival from 18% to 42% which is very much in line with the previous study that reported this parameter at 43% for the entire study population. The benefit observed in SABR-COMET came at the cost of increased grade 2 or worse treatment-related toxicity (29% versus 9%) including grade 5 adverse events (5% versus 0%), albeit with no impact on quality of life as measured using the FACT-G scores (48, 49). These results are encouraging and imply that even poor performance and frail patients may be considered for SABR. Nevertheless, such assumption needs to be validated in further trials involving a larger proportion of oligometastatic head and neck cancer patients.

Systemic Treatment

In the case of recurrent head and neck cancer not amenable to resection or irradiation, palliative systemic therapy can

be initiated. Hematogenous metastases per se represent a sufficient criterion for this treatment, and the available registration trials did not allow consideration of local ablative methods for their management. At present, patients are usually treated with various combinations of traditional cytotoxic drugs (5-fluorouracil, platinum, taxanes) and targeted agents (cetuximab) including also immune checkpoint inhibitors (pembrolizumab, nivolumab) according to clinical factors (biological age, disease burden, pace of the disease) and programmed cell death ligand-1 (PD-L1) expression and depending also on previous treatment lines. Interested readers are referred to two of our recent publications (1, 34). Here, we would like to point out that if treated with immunotherapy in first line, patients achieve median overall survival slightly exceeding 1 year but about one third of them can still be alive at 3 years (56). Longer follow-up data are not available yet. It is also not clear whether such treatment can indeed lead to cure, and if so, then in what proportion of patients. Concerning second-line immunotherapy, only less than 10% of patients survive 3 years (57). Importantly, no studies have shown that postponing the initiation of systemic therapy has any impact on outcome, which holds true especially for indolent and slowly progressive cases, creating thus a window of opportunity for example for local ablation strategies (34, 58).

Combination Approaches

From the above mentioned it follows that combination of local and systemic approaches might be feasible and beneficial in terms of survival parameters. Even though rigorous evidence for that is lacking, a retrospective analysis of the National Cancer Data Base provided an indirect support by identifying patients with metastatic squamous cell carcinoma of the head and neck cancer who received systemic drugs with or without locoregional therapy. With a median follow-up of 52 months, 3,269 cases were included. In propensity score-matched cohorts, 2-year overall survival was significantly enhanced in the combined treatment arm (34% versus 21%, $p<0.001$). Notably, the improvement pertained merely to those who underwent high-intensity locoregional therapy (oncologic resection or at least 60 Gy of radiotherapy) and was more pronounced if such intervention was delivered early in the disease course, i.e. within the first 6 months of diagnosis than later (adjusted hazard radio: 0.26 versus 0.62) (59). These outcomes suggest the importance of not only treating the locoregional disease adequately but at the same time also synchronous metastases, opening thus avenues for possible integration of their ablation in the management of otherwise locally or locoregionally advanced disease. In this respect, induction chemotherapy may be followed by definitive chemoradiation or resection of the primary tumor with subsequent local ablation of the distant lesion or lesions if they remain well-controlled throughout the treatment (60). On the other hand, different concepts pertain to metachronous presentation. Here, local ablation can be used in parallel to immuno- and/or chemotherapy either to delay a change of systemic treatment line in oligoprogressive disease or as oligo-consolidation in responding patients to eradicate a few persisting nodules (22, 61).

Another area of research relates to the radiation-induced bystander effect, also known as the abscopal effect, which is characterized by regression of nonirradiated distant lesions (62). This phenomenon is very rare but has recently been brought back to the spotlight due to a possible synergism with immune checkpoint inhibitors (63). It is therefore of interest to explore the beneficial effect of immunotherapy combined with SABR in oligometastatic disease. A phase II trial of ipilimumab, a cytotoxic T-lymphocyte antigen 4 (CTLA-4) inhibitor, and sequential or concurrent SABR to metastatic lesions of the lungs or liver demonstrated disease control in nonirradiated tumor volume of 26% in 95 patients evaluable for response with the highest rate of 42% observed after sequential SABR to one lung lesion. This trial did not focus on oligometastatic disease but possibly enrolled some of these patients. There were only four cases of squamous head and neck carcinoma, and all of them progressed (64). The absence of radiological signs of an abscopal effect in head and neck cancer was very recently corroborated in a randomized phase II trial investigating the addition of SABR to the anti-PD-1 agent nivolumab (65). However, another report described two polymetastatic head and neck cancer patients in whom the addition of SABR to PD-1/PD-L1 inhibitors induced an abscopal effect with an overall tumor regression (66). Therefore, further confirmation is clearly needed before accepting the abscopal effect might have clinical relevance.

CLINICAL PRACTICE CONTROVERSY

Despite the advantages of local ablation across different tumor types, the applicability in head and neck cancer remains to be established. Its role in the management of synchronous metastases still cannot be generalized, and radiological post-treatment follow-up in the primary disease setting in search for metachronous metastases has not been uniformly recommended in clinical practice because of its controversial impact on patient survival and the resulting low cost-effectiveness (14). However, oligometastatic disease amenable to local treatment tends to be asymptomatic due to its typical localization in the lungs, a paucity of nodules by definition, and their limited size and appears preferably late after the initial diagnosis. Such manifestation of cancer outgrowth can thus be detected only on imaging modalities, performed either as part of radiological surveillance, notwithstanding its unclear pertinence, or perhaps less frequently for other reasons.

As a result, the key issue is to define patient populations who should be exposed to a regular radiological assessment in order to be potentially able to undergo an aggressive local treatment with curative intent, acknowledging at the same time all the individuals who take these preventive measures in vain either because they will never become metastatic or will develop a distant recurrence not eligible for local treatment because of various patient- and disease-related factors. Moreover, even if a patient finally receives local ablation, it does not automatically mean cure, and in this difficult patient population, the majority of which had undergone bi- or trimodality treatment, severe late adverse events may sometimes have even more debilitating and life-threatening consequences

than disease recurrence. We also need to understand that local therapy of hematogenous dissemination is rarely applied in head and neck cancer patients. Among 934 oropharyngeal cancer cases initially managed with radiotherapy with or without chemotherapy, 15% were later diagnosed with distant metastases, 4% had oligometastases (not more than five lesions confined to one organ), and disease-free survival of 1.9 to 7.7 years was seen in 10 patients (1% of the initial cohort), all of which had pulmonary oligometastases treated in 90% with local therapies. Of note, nine of these 10 cases were HPV-positive (30).

CONCLUSIONS

Local ablation of oligometastases gives a second chance of long-term survival to patients failing primary curative treatment, especially with colorectal and renal cell carcinomas and sarcomas. In head and neck cancer, the evidence for such benefit is less clear, and this treatment is rarely delivered in clinical practice. We still need to figure out who will derive most benefit, when the right moment is to intervene, and how to optimize our diagnostic modalities for a timely identification of potential candidates. Despite this level of uncertainty and a lack of randomized trials, we advocate using this approach in selected patients after a discussion at a multidisciplinary tumor board. At the same time, we would like to stress the importance of conducting dedicated studies for squamous head and neck carcinoma patients, particularly with HPV-positive oropharyngeal cancer. A direct comparison between surgery and SABR in fit patients seems to be indispensable for further improvement as is resolving the question of implementing local ablation early in the disease course, possibly with the help of innovative approaches to disease kinetics measurements in order to exclude an early phase of an explosive distant spread.

AUTHOR CONTRIBUTIONS

All authors contributed to the article and approved the submitted version.

REFERENCES

1. Szturz P, Vermorken JB. Management of recurrent and metastatic oral cavity cancer: Raising the bar a step higher. *Oral Oncol* (2020) 101:104492. doi: 10.1016/j.oraloncology.2019.104492
2. Takes RP, Rinaldo A, Silver CE, Haigentz M Jr, Woolgar JA, Triantafyllou A, et al. Distant metastases from head and neck squamous cell carcinoma. Part I. Basic aspects. *Oral Oncol* (2012) 48:775–9. doi: 10.1016/j.oraloncology.2012.03.013
3. Kuperman DI, Auethavekiat V, Adkins DR, Nussenbaum B, Collins S, Boonchalermvichian C, et al. Squamous cell cancer of the head and neck with distant metastasis at presentation. *Head Neck* (2011) 33:714–8. doi: 10.1002/hed.21529
4. Ljumanovic R, Langendijk JA, Hoekstra OS, Leemans CR, Castelijns JA. Distant metastases in head and neck carcinoma: identification of prognostic groups with MR imaging. *Eur J Radiol* (2006) 60:58–66. doi: 10.1016/j.ejrad.2006.05.019
5. Ferlito A, Shaha AR, Silver CE, Rinaldo A, Mondin V. Incidence and sites of distant metastases from head and neck cancer. *ORL J Otorhinolaryngol Relat Spec* (2001) 63:202–7. doi: 10.1159/000055740
6. Huang SH, Perez-Ordonez B, Weinreb I, Hope A, Massey C, Waldron JN, et al. Natural course of distant metastases following radiotherapy or chemoradiotherapy in HPV-related oropharyngeal cancer. *Oral Oncol* (2013) 49:79–85. doi: 10.1016/j.oraloncology.2012.07.015
7. Trosman SJ, Koyfman SA, Ward MC, Al-Khudari S, Nwizu T, Greskovich JF, et al. Effect of human papillomavirus on patterns of distant metastatic failure in oropharyngeal squamous cell carcinoma treated with chemoradiotherapy. *JAMA Otolaryngol Head Neck Surg* (2015) 141:457–62. doi: 10.1001/jamaoto.2015.136
8. Tiedemann D, Jakobsen KK, von Buchwald C, Grønhøj C. Systematic review on location and timing of distant progression in human papillomavirus-positive and human papillomavirus-negative oropharyngeal squamous cell carcinomas. *Head Neck* (2019) 41:793–8. doi: 10.1002/hed.25458
9. Xu GZ, Guan DJ, He ZY. (18)FDG-PET/CT for detecting distant metastases and second primary cancers in patients with head and neck cancer. A meta-analysis. *Oral Oncol* (2011) 47:560–5. doi: 10.1016/j.oraloncology.2011.04.021
10. de Bree R, Haigentz MJr, Silver CE, Paccagnella D, Hamoir M, Hartl DM, et al. Distant metastases from head and neck squamous cell carcinoma. Part II. *Diagnosis Oral Oncol* (2012) 48:780–6. doi: 10.1016/j.oraloncology.2012.03.014
11. Lonneux M, Hamoir M, Reychler H, Maingon P, Duvillard C, Calais G, et al. Positron emission tomography with [18F]fluorodeoxyglucose improves staging and patient management in patients with head and neck squamous cell carcinoma: a multicenter prospective study. *J Clin Oncol* (2010) 28:1190–5. doi: 10.1200/JCO.2009.24.6298
12. Mehanna H, Wong WL, McConkey CC, Rahman JK, Robinson M, Hartley AG, et al. PET-CT Surveillance versus Neck Dissection in Advanced Head and Neck Cancer. *N Engl J Med* (2016) 374:1444–54. doi: 10.1056/NEJMoa1514493
13. Van Den Wyngaert T, Helsen N, Carp L, De Bree R, Martens MJ, Van Laer C, et al. ECLYPS: Multicenter trial of FDG-PET/CT to detect residual nodal disease in locally advanced head-and-neck squamous cell carcinoma (LAHNSCC) after chemoradiotherapy (CRT). *J Clin Oncol* (2016) 34 (suppl):Abstr 6021. doi: 10.1200/JCO.2016.34.15_suppl.6021
14. Szturz P, Van Laer C, Simon C, Van Gestel D, Bourhis J, Vermorken JB. Follow-Up of Head and Neck Cancer Survivors: Tipping the Balance of Intensity. *Front Oncol* (2020) 10:688. doi: 10.3389/fonc.2020.00688
15. Spector ME, Farlow JL, Haring CT, Brenner JC, Birkeland AC. The potential for liquid biopsies in head and neck cancer. *Discovery Med* (2018) 25:251–7.
16. van Dongen JA, van Slooten EA. The surgical treatment of pulmonary metastases. *Cancer Treat Rev* (1978) 5:29–48. doi: 10.1016/s0305-7372(78)80004-8
17. Hellman S, Weichselbaum RR. Oligometastases. *J Clin Oncol* (1995) 13:8–10. doi: 10.1200/JCO.1995.13.1.8
18. Nielsen K, van der Sluis WB, Scheffer HJ, Meijerink MR, Comans EFI, Slotman BJ, et al. Stereotactic Ablative Radiotherapy to Treat Colorectal Liver Metastases: Ready for Prime-Time? *J Liver* (2013) 2:139. doi: 10.4172/2167-0889.1000139
19. Galata C, Wimmer E, Kasper B, Wenz F, Reißfelder C, Jakob J. Multidisciplinary Tumor Board Recommendations for Oligometastatic Malignancies: A Prospective Single-Center Analysis. *Oncol Res Treat* (2019) 42:87–94. doi: 10.1159/000495474
20. Guckenberger M, Lievens Y, Bouma AB, Collette L, Dekker A, deSouza NM, et al. Characterisation and classification of oligometastatic disease: a European Society for Radiotherapy and Oncology and European Organisation for Research and Treatment of Cancer consensus recommendation. *Lancet Oncol* (2020) 21:e18–28. doi: 10.1016/S1470-2045(19)30718-1
21. Lievens Y, Guckenberger M, Gomez D, Hoyer M, Iyengar P, Kindts I, et al. Defining oligometastatic disease from a radiation oncology perspective: An ESTRO-ASTRO consensus document. *Radiother Oncol* (2020) 148:157–66. doi: 10.1016/j.radonc.2020.04.003

22. Sun XS, Michel C, Babin E, De Raucourt D, Péchery A, Gherga E, et al. Approach to oligometastatic disease in head and neck cancer, on behalf of the GORTEC. *Future Oncol* (2018) 14:877–89. doi: 10.2217/fon-2017-0468
23. Szturz P, Bossi P, Vermorken JB. Systemic treatment in elderly head and neck cancer patients: recommendations for clinical practice. *Curr Opin Otolaryngol Head Neck Surg* (2019) 27:142–50. doi: 10.1097/MOO.0000000000000526
24. Szturz P, Vermorken JB. The role of chemoradiotherapy in elderly patients with locoregionally advanced head and neck cancer. *Belg J Med Oncol* (2018) 12:110–7.
25. Hanlon P, Nicholl BI, Jani BD, Lee D, McQueenie R, Mair FS. Frailty and pre-frailty in middle-aged and older adults and its association with multimorbidity and mortality: a prospective analysis of 493 737 UK Biobank participants. *Lancet Public Health* (2018) 3:e323–32. doi: 10.1016/S2468-2667(18)30091-4
26. Singh GK, Jemal A. Socioeconomic and Racial/Ethnic Disparities in Cancer Mortality, Incidence, and Survival in the United States, 1950-2014: Over Six Decades of Changing Patterns and Widening Inequalities. *J Environ Public Health* (2017) 2017:2819372. doi: 10.1155/2017/2819372
27. Choi SH, Terrell JE, Fowler KE, McLean SA, Ghanem T, Wolf GT, et al. Socioeconomic and Other Demographic Disparities Predicting Survival among Head and Neck Cancer Patients. *PLoS One* (2016) 11:e0149886. doi: 10.1371/journal.pone.0149886
28. Beaudoin PL, Anchouche S, Gaffar R, Guadagno E, Ayad T, Poenaru D. Barriers in Access to Care for Patients With Head and Neck Cancer in Resource-Limited Settings: A Systematic Review. *JAMA Otolaryngol Head Neck Surg* (2020) 146:291–7. doi: 10.1001/jamaoto.2019.4311
29. Nevens D, Nuyts S. HPV-positive head and neck tumours, a distinct clinical entity. *B-ENT* (2015) 11:81–7.
30. Huang S, Waldron J, Xu W, Tong L, Ringash JG, Bayley AJ, et al. Potential Cure in HPV-Related Oropharyngeal Cancer With Oligometastases. *Int J Radiat Oncol Biol Phys* (2014) 90(suppl):S180–1. doi: 10.1016/j.ijrobp.2014.05.700
31. Zhang MX, Li J, Shen GP, Zou X, Xu JJ, Jiang R, et al. Intensity-modulated radiotherapy prolongs the survival of patients with nasopharyngeal carcinoma compared with conventional two-dimensional radiotherapy: A 10-year experience with a large cohort and long follow-up. *Eur J Cancer* (2015) 51:2587–95. doi: 10.1016/j.ejca.2015.08.006
32. Vengaloor Thomas T, Packianathan S, Bhanat E, Albert A, Abraham A, Gordy X, et al. Oligometastatic head and neck cancer: Comprehensive review. *Head Neck* (2020) 42:2194–201. doi: 10.1002/hed.26144
33. Huang T, Su N, Zhang X, Ma S, Zhong G, Tian X, et al. Systemic chemotherapy and sequential locoregional radiotherapy in initially metastatic nasopharyngeal carcinoma: Retrospective analysis with 821 cases. *Head Neck* (2020) 42:1970–80. doi: 10.1002/hed.26130
34. Szturz P, Vermorken JB. Translating KEYNOTE-048 into practice recommendations for head and neck cancer. *Ann Transl Med* (2020) 8:975. doi: 10.21037/atm.2020.03.164
35. Young ER, Diakos E, Khalid-Raja M, Mehanna H. Resection of subsequent pulmonary metastases from treated head and neck squamous cell carcinoma: systematic review and meta-analysis. *Clin Otolaryngol* (2015) 40:208–18. doi: 10.1111/coa.12348
36. Florescu C, Thariat J. Local ablative treatments of oligometastases from head and neck carcinomas. *Crit Rev Oncol Hematol* (2014) 91:47–63. doi: 10.1016/j.critrevonc.2014.01.004
37. von Meyenfeldt EM, Wouters MW, Fat NL, Prevoo W, Burgers SA, van Sandick JW, et al. Local treatment of pulmonary metastases: from open resection to minimally invasive approach? Less morbidity, comparable local control. *Surg Endosc* (2012) 26:2312–21. doi: 10.1007/s00464-012-2181-z
38. van Boerdonk RA, Daniels JM, Bloemena E, Krijgsman O, Steenbergen RD, Brakenhoff RH, et al. High-risk human papillomavirus-positive lung cancer: molecular evidence for a pattern of pulmonary metastasis. *J Thorac Oncol* (2013) 8:711–8. doi: 10.1097/JTO.0b013e3182897c14
39. Doxtader EE, Katzenstein AL. The relationship between p16 expression and high-risk human papillomavirus infection in squamous cell carcinomas from sites other than uterine cervix: a study of 137 cases. *Hum Pathol* (2012) 43:327–32. doi: 10.1016/j.humpath.2011.05.010
40. Lax I, Blomgren H, Näslund I, Svanström R. Stereotactic radiotherapy of malignancies in the abdomen. Methodological aspects. *Acta Oncol* (1994) 33:677–83. doi: 10.3109/02841869409121782
41. Blomgren H, Lax I, Näslund I, Svanström R. Stereotactic high dose fraction radiation therapy of extracranial tumors using an accelerator. Clinical experience of the first thirty-one patients. *Acta Oncol* (1995) 34:861–70. doi: 10.3109/02841869509127197
42. Wulf J, Hädinger U, Oppitz U, Thiele W, Ness-Dourdoumas R, Flentje M. Stereotactic radiotherapy of targets in the lung and liver. *Strahlenther Onkol* (2001) 177:645–55. doi: 10.1007/pl00002379
43. Sutera P, Clump DA, Kalash R, D'Ambrosio D, Mihai A, Wang H, et al. Initial Results of a Multicenter Phase 2 Trial of Stereotactic Ablative Radiation Therapy for Oligometastatic Cancer. *Int J Radiat Oncol Biol Phys* (2019) 103:116–22. doi: 10.1016/j.ijrobp.2018.08.027
44. Nevens D, Kindts I, Defourny N, Boesmans L, Van Damme N, Engels H, et al. The financial impact of SBRT for oligometastatic disease: A population-level analysis in Belgium. *Radiother Oncol* (2020) 145:215–22. doi: 10.1016/j.radonc.2020.01.024
45. Iyengar P, Wardak Z, Gerber DE, Tumati V, Ahn C, Hughes RS, et al. Consolidative Radiotherapy for Limited Metastatic Non-Small-Cell Lung Cancer: A Phase 2 Randomized Clinical Trial. *JAMA Oncol* (2018) 4:e173501. doi: 10.1001/jamaoncol.2017.3501
46. Ost P, Reynders D, Decaestecker K, Fonteyne V, Lumen N, De Bruycker A, et al. Surveillance or Metastasis-Directed Therapy for Oligometastatic Prostate Cancer Recurrence: A Prospective, Randomized, Multicenter Phase II Trial. *J Clin Oncol* (2018) 36:446–53. doi: 10.1200/JCO.2017.75.4853
47. Gomez DR, Tang C, Zhang J, Blumenschein GR Jr, Hernandez M, Lee JJ, et al. Local Consolidative Therapy Vs. Maintenance Therapy or Observation for Patients With Oligometastatic Non-Small-Cell Lung Cancer: Long-Term Results of a Multi-Institutional, Phase II, Randomized Study. *J Clin Oncol* (2019) 37:1558–65. doi: 10.1200/JCO.19.00201
48. Palma DA, Olson R, Harrow S, Gaede S, Louie AV, Haasbeek C, et al. Stereotactic ablative radiotherapy versus standard of care palliative treatment in patients with oligometastatic cancers (SABR-COMET): a randomised, phase 2, open-label trial. *Lancet* (2019) 393:2051–8. doi: 10.1016/S0140-6736(18)32487-5
49. Palma DA, Olson R, Harrow S, Gaede S, Louie AV, Haasbeek C, et al. Stereotactic Ablative Radiotherapy for the Comprehensive Treatment of Oligometastatic Cancers: Long-Term Results of the SABR-COMET Phase II Randomized Trial. *J Clin Oncol* (2020) 38:2830–8. doi: 10.1200/JCO.20.00818
50. Petrelli F, Comito T, Barni S, Pancera G, Scorsetti M, Ghidini A, et al. Stereotactic body radiotherapy for colorectal cancer liver metastases: A systematic review. *Radiother Oncol* (2018) 129:427–34. doi: 10.1016/j.radonc.2018.06.035
51. Al-Shafa F, Arifin AJ, Rodrigues GB, Palma DA, Louie AV. A Review of Ongoing Trials of Stereotactic Ablative Radiotherapy for Oligometastatic Cancers: Where Will the Evidence Lead? *Front Oncol* (2019) 9:543. doi: 10.3389/fonc.2019.00543
52. Pasalic D, Betancourt-Cuellar SL, Taku N, Ludmir EB, Lu Y, Allen PK, et al. Outcomes and toxicities following stereotactic ablative radiotherapy for pulmonary metastases in patients with primary head and neck cancer. *Head Neck* (2020) 42:1939–53. doi: 10.1002/hed.26117
53. Bates JE, De Leo AN, Morris CG, Amdur RJ, Dagan R. Oligometastatic squamous cell carcinoma of the head and neck treated with stereotactic body ablative radiotherapy: Single-institution outcomes. *Head Neck* (2019) 41:2309–14. doi: 10.1002/hed.25695
54. Kao J, Chen CT, Tong CC, Packer SH, Schwartz M, Chen SH, et al. Concurrent sunitinib and stereotactic body radiotherapy for patients with oligometastases: final report of a prospective clinical trial. *Target Oncol* (2014) 9:145–53. doi: 10.1007/s11523-013-0280-y
55. Wong AC, Watson SP, Pitroda SP, Son CH, Das LC, Stack ME, et al. Clinical and molecular markers of long-term survival after oligometastasis-directed stereotactic body radiotherapy (SBRT). *Cancer* (2016) 122:2242–50. doi: 10.1002/cncr.30058
56. Burtness B, Harrington KJ, Greil R, Soulières D, Tahara M, de Castro G Jr, et al. Pembrolizumab alone or with chemotherapy versus cetuximab with chemotherapy for recurrent or metastatic squamous cell carcinoma of the head and neck (KEYNOTE-048): a randomised, open-label, phase 3 study. *Lancet* (2019) 394:1915–28. doi: 10.1016/S0140-6736(19)32591-7
57. Ferris RL, Blumenschein G Jr, Fayette J, Guigay J, Colevas AD, Licitra L, et al. Nivolumab vs investigator's choice in recurrent or metastatic squamous cell

carcinoma of the head and neck: 2-year long-term survival update of CheckMate 141 with analyses by tumor PD-L1 expression. *Oral Oncol* (2018) 81:45–51. doi: 10.1016/j.oraloncology.2018.04.008
58. Sacco AG, Cohen EE. Current Treatment Options for Recurrent or Metastatic Head and Neck Squamous Cell Carcinoma. *J Clin Oncol* (2015) 33:3305–13. doi: 10.1200/JCO.2015.62.0963
59. Zumsteg ZS, Luu M, Yoshida EJ, Kim S, Tighiouart M, David JM, et al. Combined high-intensity local treatment and systemic therapy in metastatic head and neck squamous cell carcinoma: An analysis of the National Cancer Data Base. *Cancer* (2017) 123:4583–93. doi: 10.1002/cncr.30933
60. Tang E, Lahmi L, Meillan N, Pietta G, Albert S, Maingon P. Treatment Strategy for Distant Synchronous Metastatic Head and Neck Squamous Cell Carcinoma. *Curr Oncol Rep* (2019) 21:102. doi: 10.1007/s11912-019-0856-5
61. Bonomo P, Greto D, Desideri I, Loi M, Di Cataldo V, Orlandi E, et al. Clinical outcome of stereotactic body radiotherapy for lung-only oligometastatic head and neck squamous cell carcinoma: Is the deferral of systemic therapy a potential goal? *Oral Oncol* (2019) 93:1–7. doi: 10.1016/j.oraloncology.2019.04.006
62. Popp I, Grosu AL, Niedermann G, Duda DG. Immune modulation by hypofractionated stereotactic radiation therapy: Therapeutic implications. *Radiother Oncol* (2016) 120:185–94. doi: 10.1016/j.radonc.2016.07.013
63. Lauber K, Dunn L. Immunotherapy Mythbusters in Head and Neck Cancer: The Abscopal Effect and Pseudoprogression. *Am Soc Clin Oncol Educ Book* (2019) 39:352–63. doi: 10.1200/EDBK_238339
64. Welsh JW, Tang C, de Groot P, Naing A, Hess KR, Heymach JV, et al. Phase II Trial of Ipilimumab with Stereotactic Radiation Therapy for Metastatic Disease: Outcomes, Toxicities, and Low-Dose Radiation-Related Abscopal Responses. *Cancer Immunol Res* (2019) 7:1903–9. doi: 10.1158/2326-6066.CIR-18-0793
65. McBride S, Sherman E, Tsai CJ, Baxi S, Aghalar J, Eng J, et al. Randomized Phase II Trial of Nivolumab With Stereotactic Body Radiotherapy Versus Nivolumab Alone in Metastatic Head and Neck Squamous Cell Carcinoma. *J Clin Oncol* (2020), JCO2000290. doi: 10.1200/JCO.20.00290
66. Choi JS, Sansoni ER, Lovin BD, Lindquist NR, Phan J, Mayo LL, et al. Abscopal Effect Following Immunotherapy and Combined Stereotactic Body Radiation Therapy in Recurrent Metastatic Head and Neck Squamous Cell Carcinoma: A Report of Two Cases and Literature Review. *Ann Otol Rhinol Laryngol* (2020) 129:517–22. doi: 10.1177/0003489419896602

Conflict of Interest: PS has had in the last 3 years or has advisory relationships with Merck-Serono, Servier, and BMS and received honoraria from Merck-Serono.

JV has had in the last 3 years or has consulting/advisory relationships with: Immunomedics, Innate Pharma, Merck-Serono, Merck Sharp & Dome Corp, PCI Biotech, Synthon Biopharmaceuticals, Debiopharm, Cue Biopharma, and WntResearch and received lecture fees from Merck-Serono, MSD, and BMS.

The remaining author declares that the research was conducted in the absence of any commercial or financial relationships that could be construed as a potential conflict of interest.

frontiers in Oncology

ORIGINAL RESEARCH
published: 08 January 2021
doi: 10.3389/fonc.2020.600707

Salivary Gland Pleomorphic Adenomas Presenting With Extremely Varied Clinical Courses. A Single Institution Case-Control Study†

Krzysztof Piwowarczyk[1]*, *Ewelina Bartkowiak*[1], *Paweł Kosikowski*[2], *Jadzia Tin-Tsen Chou*[1] and *Małgorzata Wierzbicka*[1]

[1] Department of Otolaryngology and Laryngological Oncology, Poznan University of Medical Sciences, Poznan, Poland,
[2] Department of Clinical Pathology, Poznan University of Medical Sciences, Poznan, Poland

OPEN ACCESS

Edited by:
Alberto Paderno, University of Brescia, Italy

Reviewed by:
Shilpi Sharma, Narayana Superspeciality Hospital, India
Iain James Nixon, National Health Service Scotland, United Kingdom

***Correspondence:**
Krzysztof Piwowarczyk
krzysztofpiwowarczyk2@gmail.com

†This paper is dedicated to the memory of Tomasz Kopec, MD, PhD

Specialty section:
This article was submitted to Head and Neck Cancer, a section of the journal Frontiers in Oncology

Received: 30 August 2020
Accepted: 23 November 2020
Published: 08 January 2021

Citation:
Piwowarczyk K, Bartkowiak E, Kosikowski P, Chou JT-T and Wierzbicka M (2021) Salivary Gland Pleomorphic Adenomas Presenting With Extremely Varied Clinical Courses. A Single Institution Case-Control Study. Front. Oncol. 10:600707. doi: 10.3389/fonc.2020.600707

Objective: Pleomorphic adenomas (PAs) with divergent clinical behavior, differing from the vast majority of PAs, were distinguished. "Fast" PAs are characterized by an unexpectedly short medical history and relatively rapid growth. The reference group consisted of "slow" PAs with very stable biology and long-term progression. We divide the PA group as a whole into three subsets: "fast," "normal," and "slow" tumors. Our goal is a multifactorial analysis of the "fast" and "slow" PA subgroups.

Methods: Consecutive surgeries in a tertiary referral center, the Department of Otolaryngology and Laryngological Surgery, Poznan University of Medical Sciences, Poland, were carried out between 2002 and 2011. Out of 1,154 parotid tumors, 636 (55.1%) were PAs. The data were collected prospectively in collaboration with the Polish National Registry of Benign Salivary Gland Tumors. The main outcome measure was the recurrence rate in "fast" and "slow" PA subgroups. All surgical qualifications and surgeries were performed by two experienced surgeons.

Results: Slow PAs, compared to fast PAs, presented in older patients (53.25 ± 15.29 versus 47.92 ± 13.44 years). Multifactor logistic regression analysis with recurrence (yes/no) as the outcome variable, fast/slow as the predictor variable and age, gender, margin, FN status as covariates showed that fast PAs were significantly predicting recurrence vs. slow PAs ($p = 0.035$). Fast PAs were increasing the risk of PAs 10-fold vs. slow PAs, exp $\beta = 10.20$, CI_{95} [1.66; 197.87]. The variables impacting relapse were recent accelerated growth of the tumor OR = 3.35 (SE = 0.56), $p = 0.030$, positive margins OR = 7.18 (SE = 0.57), $p < 0.001$, incomplete or bare capsule OR = 9.91 (SE = 0.53), $p = 0.001$ and location III OR = 3.12 (SE = 0.53), $p = 0.033$. In the multivariate model only positive margin was selected as the best predictor of relapse, OR = 5.01 (SE = 0.60), $p = 0.007$.

Conclusions: The simple clinical aspect of slow or fast PA progression is of great practical importance and can constitute a surrogate of the final histopathological information that is derived from the surgical specimen. The slow or fast nature of the

PA to some extent indicates prognostic features such as recurrence risk. This finding requires correlation with histological and molecular features in further stages of research.

Keywords: mixed tumor, parotid gland tumor, recurrence, surgery, progression, facial nerve

INTRODUCTION

Pleomorphic adenomas (PA) are the most common parotid tumors and their trend of incidence is increasing (1, 2). These tumors are slow-growing and can remain asymptomatic and unrecognized, or unobtrusive enough that the patient decides not to undergo treatment. Though they may reach significant size over a period of years, some of them present misleadingly short histories constituting rather rapid development (3, 4).

It is important to accurately establish the histology of all benign salivary tumors in order to predict their clinical behavior, and this is particularly true in the case of PA due to its histological variants, different tumor entities, and the possibility of treatment failure (5, 6). The post-operative incidence of PA recurrence is significant and varies largely because of differences in surgical technique (1, 7, 8), as well as other factors including multi-nodularity and pseudopodia, tumor diameter, the age of the patient, and cellular and molecular changes (9–12). The risk of malignant transformation to carcinoma ex pleomorphic adenoma (Ca ex PA) occurs in only 1.8–6.2% of cases (13, 14), with a prevalence rate of 5.6 cases per 100,000 malignant tumors and an incidence rate of 0.17 tumors per million persons (15).

The histological diagnosis of the majority of PAs is straightforward. The tumor is usually well-circumscribed, encapsulated with a bosselated outer surface, and often presents with tongue-like protrusions or sometimes satellite nodules. Morphological patterns vary, with typically the following three components present: (1) epithelial and (2) myoepithelial cells, with (3) areas of mesenchymal differentiation. There are varying proportions of tubules, duct-like structures, and mesenchymal tissues (16) and different histological patterns of myoepithelial cells, which may appear as plasmacytoid, spindle, epithelioid, clear, or stellate (16, 17). Metaplastic changes and the foci of squamous cells are an integral feature of PAs, however extensive squamous metaplasia is uncommon and can easily be misinterpreted as squamous cell carcinoma (18).

Morphologic and genetic studies on PAs are scarce and there are still gaps in the knowledge concerning variations in clinical behavior and adverse outcomes (19). Furthermore, no pathological features of the tumor are available prior to surgery. We know only the tumor's dimensions and the duration and speed of its growth. Our experience with 1,154 benign salivary gland tumors over a 10-year period has prompted us to distinguish a small group of PA tumors with clinical behavior that differs from the vast majority of PA. Progression, recurrence, and malignant transformation are well-known PA behavior, but the unusually fast growth of this benign tumor has always surprised clinicians. The impact of this phenomenon on the treatment failure rate is unknown. Our goal is a multifactorial analysis of fast versus slow PA tumors, with the main end result being recurrence and the main outcome measure being the correlation of this failure with the clinical nature of the tumor (slow/fast), tumor size, tumor volume, and additional factors such as age, gender, margins, and facial nerve (FN) status.

MATERIALS AND METHODS

In total, 1,154 benign parotid tumors were consecutively operated on in a tertiary referral center, the Department of Otolaryngology and Laryngological Surgery, Poznan University of Medical Sciences, Poland, between 2002 and 2011. Of these, 636 (55.1%) were PA. The data were initially collected prospectively from a local database and, from 2015 onwards, from the Polish National Registry of Benign Salivary Gland Tumors. There were 224 (35.2%) men, 412 (64.8%) women, with ages ranging from 13 to 86 years, mean 47.93 ± 14.93 years and median 48 years. All patients were operated on by two experienced surgeons (MW, TK).

This study was conducted in accordance with a protocol approved by the Bioethics Committee of Poznan University of Medical Sciences (Resolution No. 781/16), and written consent was obtained from each patient.

Clinically "Fast" and "Slow" Tumors

The PA group was divided into three subsets: "fast," "normal/stable," and "slow" tumors, based on several clinical and radiological features. Three different criteria were used to categorize tumors. Objective criteria were history-based growth time and growth rate, determined by tumor increment in percent by volume, as per the patient's description. The subjective criteria were the radiological features assessed by the doctor in one of the imaging modalities, predominantly ultrasonography. "Slow" tumors had over 10 years' history and exhibited slow growth (<5% of tumor size over the last 10 years). "Stable" tumors constitute the vast majority of PA and are characterized by anamnesis >=3 years, stable size of the tumor or its slow growth (<5% of tumor size over the last 6 months); a well-visualized tumor capsule in the radiological investigation, and tumor homogeneity. The "fast" tumors are characterized by an unexpectedly short medical history and relatively rapid growth. The criteria were as follows: anamnesis <3 years; >5% growth of the tumor size within six months; and multi-polycyclic outline, heterogenic echostucture and loss of capsule echogenicity in radiological investigation. To accurately and unequivocally categorize a tumor as "fast," all the criteria had to be obtained.

Variables Collected for PAs

The variables age, sex, place of residence, time between first symptoms and surgery, tumor location, margins, FN status after surgery, and recurrence were collected.

Tumor location was presented according to the European Salivary Gland Society's (ESGS) classification of salivary gland surgeries (2, 20). The ESGS operative report includes the level removed, designated by the Roman numerals I to V in ascending order, and non-glandular structures removed, each identified through the use of specified acronyms.

Surgical approach. The classification of salivary gland surgeries was presented according to the ESGS (2, 20) and distinguishes two types of surgery: extracapsular dissection and parotidectomy. The ESGS operative report includes the glandular parenchyma level removed, designated by Roman numerals I to V. Extracapsular dissection, partial superficial parotidectomy, superficial parotidectomy, and total parotidectomy were noted.

Margins. In benign salivary gland tumors, there is no concept of positive or negative margins as there would be in malignant cancers. Positive margins were categorized by the following adverse findings: capsular rupture and intra-operative tumor spillage, the presence of incomplete or bare capsule or absence of encapsulation in the pathology specimen, and satellite nodules as distinct tumor nodules.

FN status. Function of the facial nerve using the House-Brackmann scale was recorded at 1 week, 1 month, and 12 months.

Follow up. Routine follow-up is based on ultrasonography performed once a year. In cases with a higher risk of recurrence, ultrasound is performed twice a year, and an additional MRI once a year if needed.

Furthermore, tumor features such as growth rate, capsule visualization in pre-operative imaging, and tumor homogeneity were taken into consideration. The main predictive value was categorization into "fast," "normal," and "slow" PA.

The outcome measure was the correlation of recurrence with tumor size, volume, and of recurrence with PA nature ("fast," "normal," and "slow"). The main outcome measure was the determination of whether tumor size, tumor nature (slow/fast), or the other variables influenced recurrence more. Subsequent multivariant analysis included additional factors such as age, gender, margins, and FN status.

Statistical Analysis

Analysis was conducted using R software version 3.5.1. Nominal variables are presented as n (% of group), and continuous variables as mean ± SD or median (Q1;Q3). Normality of distribution was validated using the Shapiro-Wilk test as well as a visual assessment of histograms, skewness, and kurtosis values. Comparison of fast and slow PA groups was conducted with a chi-square test or chi-square test with Yate's correction for nominal variables and with t-test or Mann-Whitney U test for continuous variables, as appropriate. The mean/median difference (MD) with 95% confidence interval was calculated for continuous variables. To verify the impact of fast/slow PAs on recurrence, a multifactorial logistic regression model was calculated, with age, sex, margins, and FN status as covariates. Model assessment was conducted with the Hosmer–Lemeshow goodness of fit (GOF) test. Additionally, relapse-free survival (RFS) was calculated using Kaplan-Meier survival analysis, including 95% confidence interval. RFS stratified by independent variables (i.e., sex, location, margin, etc.) was compared with log-rank chi-square test. Cox regression model with Breslow method was used to identify parameters impacting relapse. First, univariate models were prepared for each of the independent variables, and based on those models, variables with $p < 0.2$ in Wald test were included to the final multivariate model. For location variables, due to their inter-dependence, location with the lowest p-value in univariate models was included in the final model. For the margins variable (positive/negative) and the reasons for positive variable: due to inter-dependence of both variables, the final model included the variable (positive/negative) that had a lower p-value in the univariate model. The final multivariate model was created using a stepwise approach. All tests were based on $\alpha = 0.05$.

RESULTS

Of the 636 PAs over a 10-year period, there were 84 (13.2%) fast, 73 (11.5%) slow, and 479 (75.3%) normal/stable PAs. The recurrence rate was 8.2% (52/636). All recurrences were ipsilateral. There was no difference in the frequency distribution of individual groups over the years.

There was also a statistically significant relationship between fast/slow PAs and tumor volume ($p = 0.033$). Smaller tumors (≤ 4 cm^3) were more frequent with slow PAs (72.6%) vs. fast PAs (52.4%). (**Table 1**).

Next, we analyzed the categories of fast/slow tumors and the correlations with patient epidemiological data and tumor features: tumor location in individual regions of the salivary gland, margins, and condition of the facial nerve after surgery.

The time elapsed between the first symptoms and surgery was significantly different between fast (11.85 ± 6.47 months) and slow (52.03 ± 13.76 months) PA, MD = -40.18 CI_{95} [-43.50; -36.86]; ($p < 0.001$). There was no significant relationship between slow vs. fast PA and sex or place of residence. Slow PAs presented in older patients (53.25 ± 15.29 years vs. 47.92 ± 13.44 for fast PAs), MD = -5.33 CI_{95} [-9.90; -0.76]; ($p = 0.021$).

Relapse-free survival (RFS) for the whole group was 96.3% CI_{95} [94.6%; 98.1%]. RFS was significantly different in regard to the pace of recent rapid tumor growth (log-rank $p = 0.020$), positive/negative margins (log-rank $p < 0.001$), the reason for positive margin (log-rank $p < 0.001$), location of the tumor in area III (log-rank $p = 0.020$), and location in area V (log-rank $p = 0.020$). Log-rank test did not confirm statistically significant differences in RFS for the remaining variables (sex, FN status, location of the tumor in area I, II, IV, I–II, III–IV, parotidectomy type). **Figure 1** demonstrates that the recurrence risk increased during the first 4.2 years after surgery and stabilized after this time.

Localization of the tumor in area I, as designated by the ESGS classification, was significantly more frequent in slow PAs (63.0% vs. 45.2%, p = 0,012) while localization in areas II, III, and IV were more frequent in fast PAs (78.6%% vs. 52.1%, $p < 0.001$ for location II, 28.6% vs. 4.1%, $p < 0.001$ for location III, 14.3% vs.

TABLE 1 | Comparison of criteria determining fast and slow PA categorization.

Characteristic	Normal PA	Fast PA	Slow PA	Recurrence (Yes)	MD (95% CI)	p
N	479	84	73	52		
Greatest dimension [cm], mean ± SD	2.42 ± 1.07	2.60 ± 1.06	2.23 ± 0.90	2.15 ± 1.37	0.37 (0.06; 0.67)	0.021
Ratio of the greatest dimension to time*	0.22 ± 0.16	0.34 ± 0.42	0.05 ± 0.02	0.34 ± 0.29	0.29 (0.20; 0.38)	<0.001
Ratio of volume to time*	0.22 (0.08;0.55)	0.40 (0.12;0.84)	0.03 (0.01;0.09)	0.19 (0.12;0.73)	0.37 (0.15; 0.48)	<0.001
Capsule presence, n (%)	293 (61.2)	0 (0.0)	73 (100.0)	7 (13.5)		<0.001
Heterogeneous tumor, n (%)	89 (18.6)	71 (84.5)	0 (0.0)	38 (73.1)		<0.001
Polycyclic outline, n (%)	152 (31.7)	49 (58.3)	9 (12.3)	49 (94.2)		<0.001
Capsule presence + heterogeneous tumor, n (%)	0 (0.0)	0 (0.0)	0 (0.0)	3 (5.8)		>0.999
Capsule presence + polycyclic outline, n (%)	69 (14.4)	0 (0.0)	9 (12.3)	7 (13.5)		0.003
Heterogeneous tumor + polycyclic outline, n (%)	58 (12.1)	45 (53.6)	0 (0.0)	37 (71.2)		<0.001
Capsule presence + heterogeneous tumor + polycyclic outline, n (%)	0 (0.0)	0 (0.0)	0 (0.0)	3 (5.8)		>0.999

*MD, mean/median difference between fast/slow groups with 95% confidence interval; p, comparison of fast/slow groups (chi-square test for nominal variables or t-test/Mann-Whitney U test for continuous variables); *, time between first symptoms and surgery, in months.*

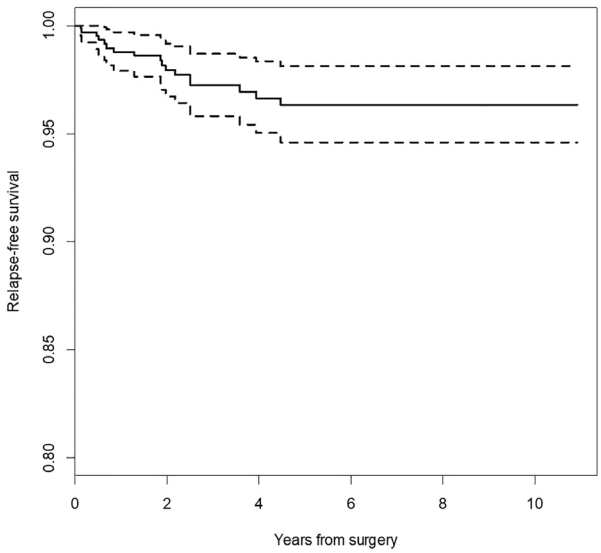

FIGURE 1 | Kaplan-Meier survival curve for relapse-free survival (RFS). Dotted lines indicate 95% confidence interval for survival curve.

0%, p = 0.002 for location IV). There was no significant relationship between location V and fast/slow PAs. Locations I and II combined, as well as locations I–IV combined were not significantly different when comparing fast vs slow PAs. However, locations III and IV combined were more frequent in fast PAs (33.3% vs. 4.1%, p < 0.001).

FN dysfunction of the marginal-mandibular branch occurred in 35 (7.3%) normal PAs, 18 (21.4%) fast Pas, and 3 (4.1%) slow PAs. Patients of 17 (3.5%) normal PAs, 9 (9.7%) fast Pas, and 2 (2.7%) slow PAs recovered facial function at 1 month; 12 (2.5%) normal PAs, 7 (8.3%) fast Pas, and 1 (1.4%) slow PA recovered facial function at 6 months, and 100% had recovered at 12 months. There were no cases of definitive involvement of FN.

The main outcome measure was the correlation of treatment failure, that is, recurrence with examined variables, with special regard to the fast/slow PA nature. Thus, the key question was, Which of the clinical parameters, age of onset, tumor volume, tumor growth rate, surgical approach, better correlated with a higher risk of recurrence? Based on univariate Cox regression models presented in **Table 2**, variables that were significantly impacting relapse were recent rapid tumor growth, OR = 3.35 (SE = 0.56), p = 0.030, positive margins vs. negative, OR = 7.18 (SE = 0.57), p < 0.001, incomplete or bare capsule vs. other reasons of positive margin, OR = 9.91 (SE = 0.53), p = 0.001 and location III vs. other, OR = 3.12 (SE = 0.53), p = 0.033. In the multivariate model only positive margin was selected as the best predictor of relapse, OR = 5.01 (SE = 0.60), p = 0.007.

As the two surgeons (MW, TK) performed all surgical qualifications as well as all surgeries, it can be assumed that such

TABLE 2 | Cox regression model for relapse.

Characteristic	Univariate models			Multivariate model		
	OR	SE	p	OR	SE	p
Age, years	1.002	0.02	0.886			
Sex, male	2.04	0.49	0.142			
Tumor volume [cm^3]	0.99	0.02	0.844			
Recent rapid tumor growth	3.35	0.56	0.030			
Margins, positive	7.18	0.57	<0.001	5.01	0.60	0.007
Incomplete or bare capsule	9.91	0.53	0.001			
FN status, intact	1.50	1.03	0.694			
Tumor location by ESGS						
I	0.82	0.49	0.684			
II	1.46	0.51	0.457			
III	3.12	0.53	0.033			
IV	2.14	0.75	0.313			
V	7.26	1.03	0.055			
I-II	0.63	0.75	0.542			
III-IV	2.31	0.53	0.116			
I-IV	0.01	0.01	0.997			
Parotidectomy type, ECD = baseline						
Partial superficial	0.87	0.56	0.800			
Superficial	0.44	0.80	0.304			
Total	1.66	0.80	0.528			
ND	0.01	0.01	0.998			

OR, odds ratio; SE, standard error; ND, no data available.

a standardization of surgical technique, considered for a given type of surgery, had a limited impact on the incidence of recurrence.

The analysis of fast and slow PA with special regard to recurrence is presented in **Table 3**. The relationship between fast/slow PAs and margins, condition of the FN after surgery, recurrence rate was significant. Positive margins were more frequent in fast PAs (47.9% vs. 17.4% of slow PAs, $p < 0.001$), and intact FN was also more frequent in fast PAs (21.4% vs. 4.1% of slow PAs, $p = 0.001$). PAs recurred in 17.9% of fast PAs vs. 1.4% of slow PAs ($p = 0.002$).

Then two entities were compared in **Table 4**: recurrent tumors (r-PA) and those successfully treated. Patients with recurrence demonstrated significantly faster tumor growth in the last few years (44% in patients with recurrence vs. 20% in patients without recurrence, $p < 0.001$). There was no significant difference in age and tumor volume between recurrence groups.

Thus, second, a multivariate analysis was performed. Using recurrence (yes/no) as the outcome variable, fast/slow categories as the predictor variable, and age, gender, margin, FN status as the covariates, multifactor logistic regression analysis showed that fast PAs significantly predicted recurrence vs. slow PAs ($p = 0.035$). Fast PAs were increasing the risk of recurrence 10-fold vs. slow PAs, exp $\beta = 10.20$, CI_{95} [1.66; 197.87]. Model assessment using Hosmer–Lemeshow GOF test ($p = 0.743$) confirmed good fit of the model to the data. Interpretation of logistic regression data for fast/slow categories indicates that in patients with fast PA, the risk of recurrence increases by 10.2-fold compared to patients with slow PA.

TABLE 3 | Analysis of fast and slow pleomorphic adenoma (PA).

Characteristic	Normal PA	Fast PA	Slow PA	Recurrence(Yes)	MD (95% CI)	p
N	479	84	73	52		
Time between first symptoms and surgery, in months (mean ± SD)	13.67 ± 6.21	11.85 ± 6.47	52.03 ± 13.76	11.32 ± 13.16	-40.18 (-43.50;-36.86)	<0.001
Sex, n (%)						
Female	311 (64.9)	52 (61.9)	49 (67.1)	29 (55.8)		0.496
Male	168 (35.1)	32 (38.1)	24 (32.9)	23 (44.2)		
Age, in years (mean ± SD)	47.13 ± 14.99	47.92 ± 13.44	53.25 ± 15.29	48.04 ± 14.14	-5.33 (-9.90;-0.76)	0.021
Place of residence, n (%)						
Rural area	104 (21.7)	14 (16.7)	14 (19.2)	5 (9.6)		0.682
City	375 (78.3)	70 (83.3)	59 (80.8)	47 (90.4)		
Imaging examinations. n (%)						
CT	115 (24.0)	40 (47.6)	29 (39.7)	10 (62.5)		0.268
MRI	44 (9.2)	26 (31.0)	20 (27.4)	37 (231.3)		
US	320 (66.8)	18 (21.4)	24 (32.9)	5 (31.3)		
Tumor location by ESGS, n (%)						
I	290 (60.5)	38 (45.2)	46 (63.0)	31 (59.6)		0.012
II	290 (60.5)	66 (78.6)	38 (52.1)	35 (67.3)		<0.001
III	82 (17.1)	24 (28.6)	3 (4.1)	16 (30.8)		<0.001
IV	30 (6.3)	12 (14.3)	0 (0.0)	7 (13.5)		0.002
V	20 (4.2)	4 (4.8)	1 (1.4)	3 (5.8)		0.434
I-II	435 (90.8)	79 (94.0)	67 (91.8)	49 (94.2)		0.579
III-IV	98 (20.5)	28 (33.3)	3 (4.1)	17 (32.7)		<0.001
I-IV	452 (94.4)	82 (97.6)	67 (91.8)	51 (98.1)		0.097
Parotidectomy type, n (%)						
Partial superficial	163 (34.0)	17 (20.2)	15 (20.5)	14 (26.9)		<0.001
Superficial	100 (20.9)	33 (39.3)	31 (42.5)	11 (21.2)		
Total	31 (6.5)	22 (26.2)	1 (1.4)	12 (23.1)		
ECD	185 (38.6)	10 (11.9)	21 (28.8)	14 (26.9)		
Other	0 (0.0)	2 (2.4)	5 (6.8)	1 (1.9)		
Tumor volume [cm^3], n (%)						
≤ 4	286 (59.7)	44 (52.4)	53 (72.6)	39 (75.0)		0.033
4-15	148 (30.9)	31 (36.9)	16 (21.9)	9 (17.3)		
≥15	45 (9.4)	9 (10.7)	4 (5.5)	4 (7.7)		
Margins, n (%)						
Positive:	130 (31.7)	35 (47.9)	12 (17.4)	34 (70.8)		<0.001
Negative	280 (68.3)	38 (52.1)	57 (82.6)	14 (29.2)		
FN status, n (%)						
Other	35 (7.3)	18 (21.4)	3 (4.1)	25 (48.1)		0.001
Intact	444 (92.7)	66 (78.6)	70 (95.9)	27 (51.9)		
Recurrence, n (%)						
Yes	36 (7.5)	15 (17.9)	1 (1.4)	52 (100.0)		0.002
No	443 (92.5)	69 (82.1)	72 (98.6)	–		

MD, mean difference between fast/slow groups with 95% confidence interval; p, comparison of fast/slow groups (chi-square test for nominal variables and t-test for continuous variables), ECD, extracapsular dissection.

TABLE 4 | Comparison of features in r-PA versus PA.

Characteristic	Recurrence (Yes)	Recurrence (No)	MD (95% CI)	p	RFS, %	95% CI	Log-rank p
Total group, N	52	584			96.3	94.6–98.1	
Age, years, mean ± SD	48.04 ± 14.14	47.92 ± 15.01	0.12 (-4.36; 4.13)	0.958			
Sex, n (%)							
Female	29 (55.8)	383 (65.6)		0.205	97.5	95.8–99.2	0.100
Male	23 (44.2)	201 (34.4)			94.3	90.7–98.1	
Tumor volume [cm^3], median (Q1;Q3)	2.00 (1.24;4.13)	2.34 (1.20;6.43)	-0.34 (-0.37; 0.90)	0.497			
Recent accelerated tumor growth, n (%)							
Yes	17 (43.6)	108 (19.9)		<0.001	92.6	87.1–98.6	0.020
No	22 (56.4)	438 (80.1)			98.0	96.6–99.5	
Margins, n (%)							
Negative	14 (29.2)	361 (71.6)		<0.001	98.5	97.0–100	<0.001
Positive	34 (70.8)	143 (28.4)			89.8	84.5–95.4	
capsular rupture*	0 (0.0)	36 (25.2)		<0.001	n/a	n/a	<0.001
tumor spillage*	1 (0.7)	38 (26.6)			n/a	n/a	
incomplete or bare capsule*	16 (11.2)	14 (9.8)			64.1	47.1–87.4	
absence of encapsulation in the pathology specimen*	7 (4.9)	37 (25.9)			93.1	84.3–100	
satellite nodules*	10 (7.0)	18 (12.6)			89.2	79.4–100	
FN status, n (%)							
Other	25 (48.1)	31 (5.3)		<0.001	96.2	94.3–98.1	0.700
Intact	27 (51.9)	553 (94.7)			98.0	94.3–100	
Tumor location by ESGS, n (%)							
I	31 (59.6)	273 (46.7)		0.102	96.7	94.3–99.2	0.700
Other	21 (40.4)	311 (53.3)			96.0	93.4–98.6	
II	35 (67.3)	336 (57.5)		0.221	95.6	93.1–98.3	0.500
Other	17 (32.7)	248 (42.5)			97.2	94.9–99.5	
III	16 (30.8)	74 (12.7)		0.001	91.4	84.4–99.0	0.020
Other	36 (69.2)	510 (87.3)			97.0	95.2–98.7	
IV	7 (13.5)	38 (6.5)		0.111	92.6	83.2–100	0.300
Other	45 (86.5)	546 (93.5)			96.6	94.8–98.3	
V	3 (5.8)	5 (0.9)		0.017	80.0	51.6–100	0.020
Other	49 (94.2)	579 (99.1)			96.5	94.8–98.2	
I-II	49 (94.2)	534 (91.4)		0.663	96.4	94.6–98.3	0.500
Other	3 (5.8)	50 (8.6)			95.0	88.3–100	
III-IV	17 (32.7)	96 (16.4)		0.006	93.5	88.0–99.3	0.100
Other	35 (67.3)	488 (83.6)			96.8	95.0–98.7	
I-IV	51 (98.1)	552 (94.5)		0.434	96.1	94.3–98.0	n/a
Other	1 (1.9)	32 (5.5)			n/a	n/a	
Parotidectomy type, n (%)							
Partial superficial	14 (26.9)	181 (31.0)		0.009	96.2	93.3–99.3	0.600
Superficial	11 (21.2)	153 (26.2)			98.1	95.6–100	
Total	12 (23.1)	42 (7.2)			92.6	83.2–100	
ECD	14 (26.9)	202 (34.6)			96.0	93.0–99.0	
ND	1 (1.9)	6 (1.0)			n/a	n/a	

*MD, mean/median difference between groups with and without recurrence with 95% confidence interval; RFS, Kaplan Meier relapse-free survival; p, comparison of groups (chi-square test for nominal variables, t-test for age and Mann-Whitney U test for tumor volume); ND, no data available; *% frequency calculated to positive margins.*

DISCUSSION

PA progression rate, differences in tumor growth rate, and impact on recurrence still remain unclear. In this study, the authors aimed to show that one of the clinical parameters—tumor growth rate—significantly correlates with a higher risk of recurrence. Despite the progress in this field, the exact causes of PA recurrence remain elusive. It has been hypothesized that the various reasons for PA recurrence can be grouped into pathology-related (capsule thickness or lack of capsule (21, 22), pseudopodia, satellite nodules (23, 24), and multi-centricity) and surgery-related factors such as rupture of the tumor, spillage of tumor contents, insufficient margins of resection due to nerve branches, and inadequate excision related to the type of surgery (25). Conceptually, re-growth of the tumor as a result of inadequate initial resection could be defined as PA persistence rather than PA recurrence. Owing to the time frame between the initial surgery and recurrence, it is generally implied that the re-operation is performed by a different surgeon who tends to blame the first inadequate procedure (25). In our setting, we can abandon the hypothesis that tumor re-growth results from inadequate surgery, as the 1,154 benign salivary gland tumors observed over a 10-year period were operated on by only two experienced surgeons.

The initial medical interview allowed us to derive data concerning the speed of tumor progression, and it is on this basis that the patient was advised on the pressing necessity to undergo surgery. Thus, the surgeon was able to make short- or long-term considerations and plan the procedure precisely according to these indications. Clinical observation has led us to distinguish a small group of PAs demonstrating clinical behavior that differs from the vast majority of PAs.

Fast PAs are characterized by an unexpectedly short medical history and relatively rapid growth. Additionally, they exhibit imaging features that, while similar to other PAs, are extremely exaggerated, that is, presenting jagged fragments instead a smooth tumor capsule, with only polycyclic pseudopodia and satellites. In a diametrically different group, we distinguished from typical PAs a group of tumors demonstrating even calmer biology, with very slow, long-term progression. Thus, we divided the whole PA group into three subsets of "fast," "normal," and "slow" tumors. The criteria for such division were based on several clinical and radiological features that differed in this seemingly homogenous benign PA group (25–29).

So far, two clinical features—patient age and tumor size—have been associated with a higher risk of recurrence, and this finding is coherent with most conclusions in the literature. Larger PAs have a tendency to exhibit incomplete capsules and are additionally associated with more numerous satellite nodules (9, 24).

Based on fast/normal/slow PA categorization, we proved that this clinical aspect is of great practical importance. Not only does it allow for preliminary selection of patients for immediate surgery, they are under greater vigilance during surgery and are more frequently monitored for relapse. Surgical access can be potentially modified, such as forgoing extracapsular access in rapid tumors in favor of parotidectomy. One may also consider a lower threshold for postoperative RT in the event of tumor spillage. We conduct follow-up visits once a year for all PAs, while select tumors demonstrating adverse findings are followed up every six months for a period of 10 years. It is of note that tumor development over a shorter period is also very probable (1, 27, 30).

Our publication delineating the clinical aspect of the course and speed of PA development is innovative and unique. It measurably defines the clinical distinctiveness of PAs. Every experienced surgeon is aware of this problem and probably intuitively schedules earlier surgeries and closely monitors rapid tumors. Nevertheless, we have proven that this feature is statistically more significant than other features for the development of recurrence, and on this basis we recommend careful and longer monitoring of these patients.

The main limitations of our study include inconsistent imaging examinations in our patients. Magnetic resonance imaging (MRI), ultrasonography (US), and computed tomography (CT) are the most commonly ordered studies for PA because these protocols describe the precise location and size of the tumor (31). However, some of the patients received US or MRI while some received CT. Another limitation of this study is patient-reported symptom duration, where we can broadly assume that symptom duration was underestimated by a few months.

CONCLUSION

The simple clinical aspect of slow or fast PA development is of great practical importance and can constitute a surrogate of the final histopathological result derived from the surgical specimen. The slow or fast nature of the PA to some extent indicates prognostic features such as recurrence risk. This finding requires correlation with histological and molecular features in further stages of research.

DATA AVAILABILITY STATEMENT

The original contributions presented in the study are included in the article/supplementary materials. Further inquiries can be directed to the corresponding author.

ETHICS STATEMENT

The studies involving human participants were reviewed and approved by Bioethics Committee of Poznan University of Medical Sciences (Resolution No. 781/16). The patients/participants provided their written informed consent to participate in this study.

AUTHOR CONTRIBUTIONS

Conceptualization, KP, MW. Data curation, KP, PK. Formal analysis, PK, JC. Investigation, KP, EB, JC. Methodology, KP, EB, MW. Project administration, MW. Resources, KP, PK, MW. Software, EB, JC. Supervision, MW. Validation, KP, EB, MW. Visualization, KP, JC. Writing—original draft, KP, JC, MW. Writing—review and editing, KP, JC, MW. All authors contributed to the article and approved the submitted version.

REFERENCES

1. Andreasen S, Therkildsen MH, Bjørndal K, Homøe P. Pleomorphic adenoma of the parotid gland 1985-2010: A Danish nationwide study of incidence, recurrence rate, and malignant transformation. *Head Neck* (2016) 38(Suppl 1):E1364–9. doi: 10.1002/hed.24228
2. Wierzbicka M, Piwowarczyk K, Nogala H, Błaszczyńska M, Kosiedrowski M, Mazurek C. Do we need a new classification of parotid gland surgery? *Otolaryngol Pol* (2016) 70:9–14. doi: 10.5604/00306657.1202390
3. Shome S, Shah N, Mahmud SA, Pal M. A miscellany of cribriform pattern, squamous metaplasia and clear cells in pleomorphic adenoma of upper lip: A diagnostic paradox. *J Oral Maxillofac Pathol* (2020) 24:46. doi: 10.4103/jomfp.JOMFP_354_19
4. Sharma S, Mehendiratta M, Chaudhary N, Gupta V, Kohli M, Arora A. Squamous Metaplasia in Pleomorphic Adenoma: A Diagnostic and Prognostic Enigma. *J Pathol Transl Med* (2018) 52:411–5. doi: 10.4132/jptm.2018.07.15
5. Hellquist H, Paiva-Correia A, Vander Poorten V, Quer M, Hernandez-Prera JC, Andreasen S, et al. Analysis of the Clinical Relevance of Histological

Classification of Benign Epithelial Salivary Gland Tumours. *Adv Ther* (2019) 36:1950–74. doi: 10.1007/s12325-019-01007-3
6. Nonitha S, Yogesh TL, Nandaprasad S, Maheshwari BU, Mahalakshmi IP, Veerabasavaiah BT. Histomorphological comparison of pleomorphic adenoma in major and minor salivary glands of oral cavity: A comparative study. *J Oral Maxillofac Pathol* (2019) 23:356. doi: 10.4103/jomfp.JOMFP_91_19
7. Valstar MH, Andreasen S, Bhairosing PA, McGurk M. Natural history of recurrent pleomorphic adenoma: implications on management. *Head Neck* (2020) 42(8):2058-2066. doi: 10.1002/hed.26137
8. Riad MA, Abdel-Rahman H, Ezzat WF, Adly A, Dessouky O, Shehata M. Variables related to recurrence of pleomorphic adenomas: outcome of parotid surgery in 182 cases. *Laryngoscope* (2011) 121:1467–72. doi: 10.1002/lary.21830
9. Zbären P, Stauffer E. Pleomorphic adenoma of the parotid gland: histopathologic analysis of the capsular characteristics of 218 tumors. *Head Neck* (2007) 29:751–7. doi: 10.1002/hed.20569
10. Soares AB, Demasi APD, Altemani A, de Araújo VC. Increased mucin 1 expression in recurrence and malignant transformation of salivary gland pleomorphic adenoma. *Histopathology* (2011) 58:377–82. doi: 10.1111/j.1365-2559.2011.03758.x
11. Salzman R, Stárek I, Kučerová L, Skálová A, Hoza J. Neither expression of VEGF-C/D nor lymph vessel density supports lymphatic invasion as the mechanism responsible for local spread of recurrent salivary pleomorphic adenoma. *Virchows Arch* (2014) 464:29–34. doi: 10.1007/s00428-013-1502-5
12. de Souza AA, Altemani A, Passador-Santos F, Turssi CP, de Araujo NS, de Araújo VC, et al. Dysregulation of the Rb pathway in recurrent pleomorphic adenoma of the salivary glands. *Virchows Arch* (2015) 467:295–301. doi: 10.1007/s00428-015-1804-x
13. Antony J, Gopalan V, Smith RA, Lam AKY. Carcinoma ex pleomorphic adenoma: a comprehensive review of clinical, pathological and molecular data. *Head Neck Pathol* (2012) 6:1–9. doi: 10.1007/s12105-011-0281-z
14. Valstar MH, de Ridder M, van den Broek EC, Stuiver MM, van Dijk BAC, van Velthuysen MLF, et al. Salivary gland pleomorphic adenoma in the Netherlands: A nationwide observational study of primary tumor incidence, malignant transformation, recurrence, and risk factors for recurrence. *Oral Oncol* (2017) 66:93–9. doi: 10.1016/j.oraloncology.2017.01.004
15. Mariano FV, Noronha ALF, Gondak RO, de A.M. Altemani AM, de Almeida OP, Kowalski LP. Carcinoma ex pleomorphic adenoma in a Brazilian population: clinico-pathological analysis of 38 cases. *Int J Oral Maxillofac Surg* (2013) 42:685–92. doi: 10.1016/j.ijom.2013.02.012
16. Dardick I, van Nostrand AW, Jeans MT, Rippstein P, Edwards V. Pleomorphic adenoma, I: Ultrastructural organization of "epithelial" regions. *Hum Pathol* (1983) 14:780–97. doi: 10.1016/s0046-8177(83)80301-3
17. Palmer RM, Lucas RB, Langdon JD. Ultrastructural analysis of salivary gland pleomorphic adenoma, with particular reference to myoepithelial cells. *Histopathology* (1985) 9:1061–76. doi: 10.1111/j.1365-2559.1985.tb02785.x
18. Lim S, Cho I, Park J-H, Lim S-C. Pleomorphic Adenoma with Exuberant Squamous Metaplasia and Keratin Cysts Mimicking Squamous Cell Carcinoma in Minor Salivary Gland. *Open J Pathol* (2013) 2013:113–5. doi: 10.4236/ojpathology.2013.33020
19. Thielker J, Weise A, Othman MAK, Carreria IM, Melo JB, von Eggeling F, et al. Molecular cytogenetic pilot study on pleomorphic adenomas of salivary glands. *Oncol Lett* (2020) 19:1125–30. doi: 10.3892/ol.2019.11198
20. Quer M, Guntinas-Lichius O, Marchal F, Poorten VV, Chevalier D, León X, et al. Classification of parotidectomies: A proposal of the European Salivary Gland Society. *Eur Arch Otorhinolaryngol* (2016) 273(10):3307–12. doi: 10.1007/s00405-016-3916-6
21. Bankamp DG, Bierhoff E. Proliferative activity in recurrent and nonrecurrent pleomorphic adenoma of the salivary glands. *Laryngorhinootologie* (1999) 78:77–80. doi: 10.1055/s-2007-996835
22. Stennert E, Guntinas-Lichius O, Klussmann JP, Arnold G. Histopathology of pleomorphic adenoma in the parotid gland: a prospective unselected series of 100 cases. *Laryngoscope* (2001) 111:2195–200. doi: 10.1097/00005537-200112000-00024
23. Orita Y, Hamaya K, Miki K, Sugaya A, Hirai M, Nakai K, et al. Satellite tumors surrounding primary pleomorphic adenomas of the parotid gland. *Eur Arch Otorhinolaryngol* (2010) 267:801–6. doi: 10.1007/s00405-009-1149-7
24. Li C, Xu Y, Zhang C, Sun C, Chen Y, Zhao H, et al. Modified partial superficial parotidectomy versus conventional superficial parotidectomy improves treatment of pleomorphic adenoma of the parotid gland. *Am J Surg* (2014) 208(1)112-118. doi: 10.1016/j.amjsurg.2013.08.036
25. Dulguerov P, Todic J, Pusztaszeri M, Alotaibi NH. Why Do Parotid Pleomorphic Adenomas Recur? A Systematic Review of Pathological and Surgical Variables. *Front Surg* (2017) 4:26 1-5. doi: 10.3389/fsurg.2017.00026
26. Kanatas A, Ho MWS, Mücke T. Current thinking about the management of recurrent pleomorphic adenoma of the parotid: a structured review. *Br J Oral Maxillofac Surg* (2018) 56:243–8. doi: 10.1016/j.bjoms.2018.01.021
27. Abu-Ghanem Y, Mizrachi A, Popovtzer A, Abu-Ghanem N, Feinmesser R. Recurrent pleomorphic adenoma of the parotid gland: Institutional experience and review of the literature. *J Surg Oncol* (2016) 114:714–8. doi: 10.1002/jso.24392
28. Rowley H, Murphy M, Smyth D, O'Dwyer TP. Recurrent pleomorphic adenoma: uninodular versus multinodular disease. *Ir J Med Sci* (2000) 169:201–3. doi: 10.1007/BF03167696
29. Witt RL, Eisele DW, Morton RP, Nicolai P, Poorten VV, Zbären P. Etiology and management of recurrent parotid pleomorphic adenoma. *Laryngoscope* (2015) 125:888–93. doi: 10.1002/lary.24964
30. Wittekindt C, Streubel K, Arnold G, Stennert E, Guntinas-Lichius O. Recurrent pleomorphic adenoma of the parotid gland: analysis of 108 consecutive patients. *Head Neck* (2007) 29:822–8. doi: 10.1002/hed.20613
31. Kato H, Kawaguchi M, Ando T, Mizuta K, Aoki M, Matsuo M. Pleomorphic adenoma of salivary glands: common and uncommon CT and MR imaging features. *Jpn J Radiol* (2018) 36:463–71. doi: 10.1007/s11604-018-0747-y

Conflict of Interest: The authors declare that the research was conducted in the absence of any commercial or financial relationships that could be construed as a potential conflict of interest.

frontiers in Oncology

ORIGINAL RESEARCH
published: 22 February 2021
doi: 10.3389/fonc.2021.630123

A Novel Treatment Concept for Advanced Stage Mandibular Osteoradionecrosis Combining Isodose Curve Visualization and Nerve Preservation: A Prospective Pilot Study

Gustaaf J. C. van Baar[1], Lars Leeuwrik[1], Johannes N. Lodders[1], Niels P. T. J. Liberton[2], K. Hakki Karagozoglu[1], Tymour Forouzanfar[1] and Frank K. J. Leusink[1]*

[1] Amsterdam UMC and Academic Centre for Dentistry Amsterdam (ACTA), Vrije Universiteit Amsterdam, Department of Oral and Maxillofacial Surgery/Pathology, Amsterdam, Netherlands, [2] Amsterdam UMC, Vrije Universiteit Amsterdam, Medical Technology, 3D Innovation Lab, Amsterdam, Netherlands

OPEN ACCESS

Edited by:
Cesare Piazza, University of Brescia, Italy

Reviewed by:
Achille Tarsitano, University of Bologna, Italy
Constantinus Politis, University Hospitals Leuven, Belgium

***Correspondence:**
Gustaaf J. C. van Baar
g.vanbaar@amsterdamumc.nl

Specialty section:
This article was submitted to Head and Neck Cancer, a section of the journal Frontiers in Oncology

Received: *16 November 2020*
Accepted: *05 January 2021*
Published: *22 February 2021*

Citation:
van Baar GJC, Leeuwrik L, Lodders JN, Liberton NPTJ, Karagozoglu KH, Forouzanfar T and Leusink FKJ (2021) A Novel Treatment Concept for Advanced Stage Mandibular Osteoradionecrosis Combining Isodose Curve Visualization and Nerve Preservation: A Prospective Pilot Study. Front. Oncol. 11:630123. doi: 10.3389/fonc.2021.630123

Background: Osteoradionecrosis (ORN) of the mandible is a severe complication of radiation therapy in head and neck cancer patients. Treatment of advanced stage mandibular osteoradionecrosis may consist of segmental resection and osseous reconstruction, often sacrificing the inferior alveolar nerve (IAN). New computer-assisted surgery (CAS) techniques can be used for guided IAN preservation and 3D radiotherapy isodose curve visualization for patient specific mandibular resection margins. This study introduces a novel treatment concept combining these CAS techniques for treatment of advanced stage ORN.

Methods: Our advanced stage ORN treatment concept includes consecutively: 1) determination of the mandibular resection margins using a 3D 50 Gy isodose curve visualization, 2) segmental mandibular resection with preservation of the IAN with a two-step cutting guide, and 3) 3D planned mandibular reconstruction using a hand-bent patient specific reconstruction plate. Postoperative accuracy of the mandibular reconstruction was evaluated using a guideline. Objective and subjective IAN sensory function was tested for a period of 12 months postoperatively.

Results: Five patients with advanced stage ORN were treated with our ORN treatment concept using the fibula free flap. A total of seven IANs were salvaged in two men and three women. No complications occurred and all reconstructions healed properly. Neither non-union nor recurrence of ORN was observed. Sensory function of all IANs recovered after resection up to 100 percent, including the patients with a pathologic fracture due to ORN. The accuracy evaluation showed angle deviations limited to 3.78 degrees. Two deviations of 6.42° and 7.47° were found. After an average of 11,6 months all patients received dental implants to complete oral rehabilitation.

Conclusions: Our novel ORN treatment concept shows promising results for implementation of 3D radiotherapy isodose curve visualization and IAN preservation. Sensory function of all IANs recovered after segmental mandibular resection.

Keywords: osteoradionecrosis, mandibular reconstruction, inferior alveolar nerve, treatment, computer-assisted surgery

INTRODUCTION

Osteoradionecrosis (ORN) of the jaws is a common side effect of radiation therapy (RT) (1–4). ORN is defined as the process where irradiated bone becomes necrotic and exposed for a time period of at least 3 months, and fails to heal (5–8). It affects the mandible, in particular the body, more often than the maxilla or any other bone of the head and neck area (9) and has an incidence in the mandible between 2% and 22% (10, 11). Although ORN is often diagnosed within 2 years after RT, there is a lifelong risk for this severe complication (12).

Risk factors associated with ORN are well documented (8, 13–15), with the most prominent being the radiation dose. A radiation dose more than 60 Gy is reported as high risk and 50–60 Gy as intermediate risk (4, 8, 15–17). In the management of ORN prevention is crucial since the process is irreversible and progression is difficult to control. Once ORN is diagnosed conservative measurements are indicated (18–20). For advanced stages of ORN these conservative measurements alone are not sufficient.

There are different ORN classification systems described in the literature, however the Notani classification (21) seems to be the most reliable for determining progression of ORN in the mandible (**Table 1**) (22). In advanced stage ORN (Notani stage III), segmental mandibular resection may be indicated (13, 18, 19). However, determining resection margins may be difficult as the extent, severity, and location of ORN do not always correlate with radiographical imaging (23).

Computer-assisted surgery (CAS) is well known in mandibular resection and reconstruction since its introduction by Hirsch in 2009 (24, 25) introducing high accuracy results and shortened operation time (26–30). In addition, CAS can facilitate incorporation of intensity modulated radiation therapy (IMRT) data in the virtual planning of segmental mandibular resection and reconstruction. As radiation dose seems to correlate with the risk for ORN (15), Kraeima et al. (2018) incorporated RT isodose curves in the virtual planning of the resection using a three-dimensional image of the administered RT dose of 50 Gy (31). With this patient-specific technique, the mandibular resection can be planned highly accurate out of the irradiated bone, leading to a minimally invasive mandibular resection.

Although the inferior alveolar nerve (IAN) is not directly affected in ORN cases, the nerve is often sacrificed during mandibular resection. Injury of the IAN may have a significant negative impact on quality of life as it may cause chronic pain (32). Additionally, maintaining sensorimotoric function of the lower lip and chin may be beneficial for oral function such as speech and mastication (33). Free handed preservation of the IAN is time consuming (34, 35) and includes a considerable risk of iatrogenic nerve injury (36). The use of CAS techniques for preserving the IAN during segmental mandibular resection has been evaluated by previous studies (37–40), showing promising results to prevent sensory disturbance of the lip and chin region. After segmental resection of necrotic bone, mandibular continuity can be restored with a vascularized bone flap covering the defect with non-irradiated soft-tissue (41). Currently, the fibula free flap (FFF) is the most commonly used reconstruction approach (42–44).

In this prospective pilot study we combined RT isodose curve visualization with 3D guided IAN preservation in order to improve quality of life. Research to date has not yet combined these two CAS techniques. The accuracy of the mandibular reconstructions were evaluated postoperatively (45). In all cases the postoperative IAN sensory function was objectified and compared with the preoperative function. A visual analog scale-based questionnaire was used to evaluate subjective sensibility.

TABLE 1 | The Notani classification for mandibular osteoradionecrosis.

Stage I	Osteoradionecrosis confined to the alveolar bone
Stage II	Osteoradionecrosis limited to the alveolar bone or the mandible, or both above the mandibular alveolar canal
Stage III	Osteoradionecrosis that extended to the mandible under the level of the mandibular alveolar canal and osteoradionecrosis with a skin fistula or a pathological fracture, or both

MATERIALS AND METHODS

Patients

This study was conducted in the Department of Oral and Maxillofacial Surgery/Oral Pathology, Amsterdam UMC, VU University Medical Center Amsterdam (the Netherlands) and was approved by the Medical Ethics Review Committee of VU University Medical Center (FWA 00017598). Between November 2017 and March 2019 all ORN stage III patients (minimum age of 18 years) who received IMRT in the past with an indication for segmental mandibular resection were included. Patients with diagnosed malignancies were excluded.

Preoperative Imaging

A preoperative multi-detector row computed tomography (MDCT) scan (kVp 120, mAs 300, slice thickness 0.625 mm) was made of the skull using a GE Discovery CT750 HD 64-slice MDCT scanner (GE Healthcare, Little Chalfont, Buckinghamshire, UK). The lower leg

was scanned with CT angiography (CTA) for visualization of the fibula including vessel anatomy. Both Digital

Imaging and Communications in Medicine (DICOM) files were uploaded in Mimics Medical 21.0 software (Materialise, Leuven, Belgium) and converted into 3D models using the thresholding tool; voxels with an HU above a selected threshold value are included in the ROI and transformed into 3D surface models in the Standard Tessellation Language (STL) file format (46).

Isodose Curve Visualization

In the RT software (Eclipse™, external beam planning V15.6, Varian medical systems, Palo Alto, CA, USA) the 50 Gy isodose borders from the IMRT data were determined, converted into a 3D model, and superimposed on the 3D model of the mandible. Subsequently the mandibular resection margins were determined on the mandible, taking into account the above mentioned isodose curve visualization and the optimal direction of the osteotomy planes for FFF reconstruction. Remnant mandibular bone outside the resection was checked for the signs of ORN on CT (mono- or bicortical destruction, central necrosis, and sequestration) (23). **Figure 1** shows an example of a 3D model with the bone that had been exposed to a high risk dose of 50 Gy or more.

IAN Localization

The mandibular canal was traced using the tool "trace thin structure" in Mimics Medical 21.0 in a coronal view from the mandibular foramen to the mental foramen in steps of 2 mm. Once the canal was marked, the tracing was checked in sagittal view of the CT scan. The same procedure was used for the other side. The traced canals were exported in STL format. The mandible was also segmented and exported in STL format (**Figure 2**).

Guide Design and Manufacturing

ProPlan CMF 2.1. software (Materialise, Leuven, Belgium) was used to design the osteotomy planes on the mandible and to determine the optimal position and configuration of the fibula segments to reconstruct the mandibular defect (25) (**Figure 3**). This virtual model was 3D printed and figured as a template to pre-bent a KLS Martin 2.7 mm reconstruction plate into a patient specific reconstruction plate (PSRP) (**Figure 4**). Subsequently a CT scan of the PSRP was made, converted to STL format, and used further along in the virtual planning to determine the locations of the fixation screws.

All cutting guides were designed using 3-Matic Medical software 14.0 (Materialise, Leuven, Belgium). To preserve the IAN a two-step mandibular guide was created with a free margin of 2 mm cranially to allow two-step deroofing of the superior and lateral cortex of the mandibular canal. When using CT data for manual mandibular canal tracing a safety zone of 1.7 mm should be taken into account (47). A template design with cutting guides is shown in **Figure 5**. The STL files of the cutting

FIGURE 2 | Frontal view of a 3D model of the mandible including inferior alveolar nerve tracing (in purple) on the left and the right.

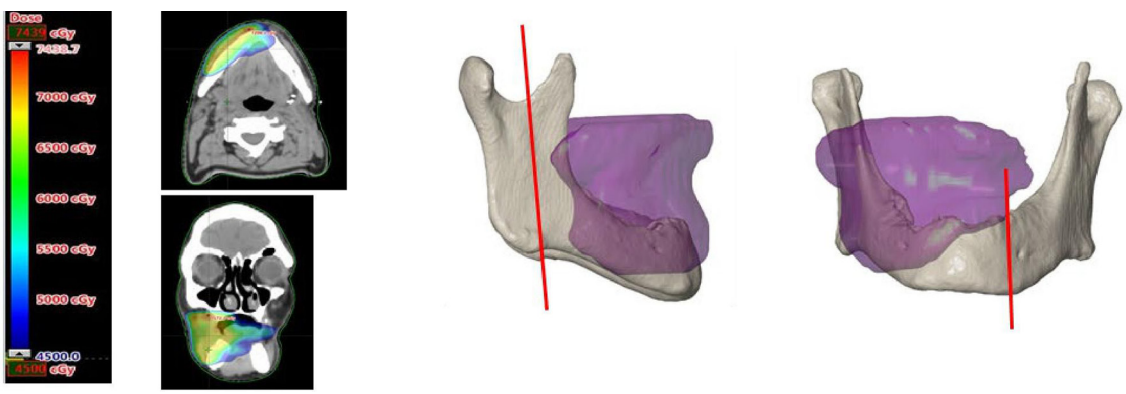

FIGURE 1 | On the left an axial and coronal CT image with superimposed the field of view exposed to 50 Gy or more. On the right a 3D image of the superimposed 50 Gy field on the 3D model of the mandible. The vertical red lines on the mandible mark the planned resection margins.

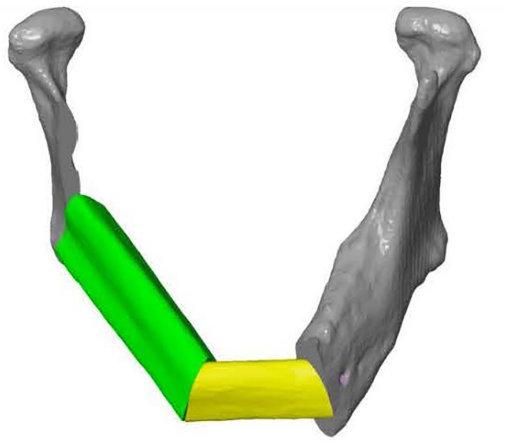

FIGURE 3 | Frontal view of a 3D model of the virtual planned reconstruction in Proplan CMF.

FIGURE 4 | KLS Martin 2.7 mm reconstruction plate bent on a 3D model of the reconstructed mandible, creating a patient specific reconstruction plate.

guides were 3D printed in PA12 material in compliance to ISO 13485 and sterilized.

Surgical Procedure

Once surgical access and mandibular exposure was obtained, the cutting guide was positioned and fixed to the mandible with four titanium screws (4× KLS Martin 1.5. × 7 mm screws). The resection started with a horizontal osteotomy 2 mm above the mandibular canal (**Figure 6A**) and completed with two vertical osteotomies on both sides. The superior part of the mandible was subsequently removed (**Figure 6B**). After removing the upper part of the IAN cutting guide with a reciprocal saw (**Figure 6C**), the superior and buccal cortex of the mandibular canal are exposed (**Figure 6D**) and can be removed with a hard steel burr (**Figure 6E**). The IAN can be exposed along its entire path with this technique. Once secured, mandibular resection is proceeded as planned (**Figure 6F**). The full surgical process is shown in **Figure 6**.

Outcome Evaluation

Accuracy of the mandibular reconstruction was evaluated according to the evaluation method for computer-assisted surgery in mandibular reconstruction described by Van Baar et al (45, 46)..

A review of Poort et al. (2009) recommends the use of Semmes Weinstein monofilaments as a reliable and reproducible test for measuring sensation in the mental nerve area, in combination with a patient's subjective function by using the visual analogue scale (VAS). We used five Semmes-Weinstein monofilaments (Baseline® tactile™ monofilament evaluator case) to objectify sensory function of the IAN (in order 300, 40.0, 2.0, 0.4, and 0.07 gram) (48). The monofilaments were placed perpendicular to the front of the chin and lower lip and pressed until the filament begins to deform. At this point, a known reproducible pressure is applied. The monofilaments are placed on a grid of 24 locations on the front of the chin and lower lip (i.e. innervation of one IAN was divided into a 12-point grid). Each approach at each individual measuring point of the grid contains two moments of attention in

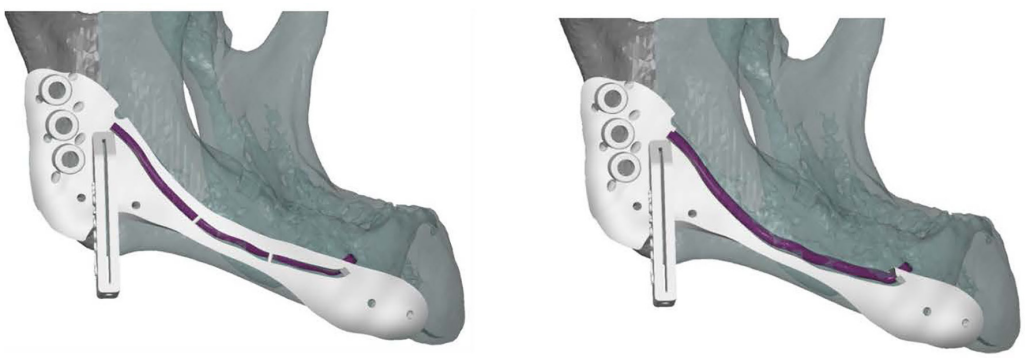

FIGURE 5 | Lateral view of a cutting guide, allowing two-step exteriorization of the inferior alveolar nerve. The purple line indicates the inferior alveolar nerve. The guide shows three drilling holes on the left for plate fixation surrounded by small holes for water cooling during drilling. The guide also includes a saw box to create the osteotomy plane. The two small holes surrounding the saw box and the two small holes on the right side of the guide are used for fixation.

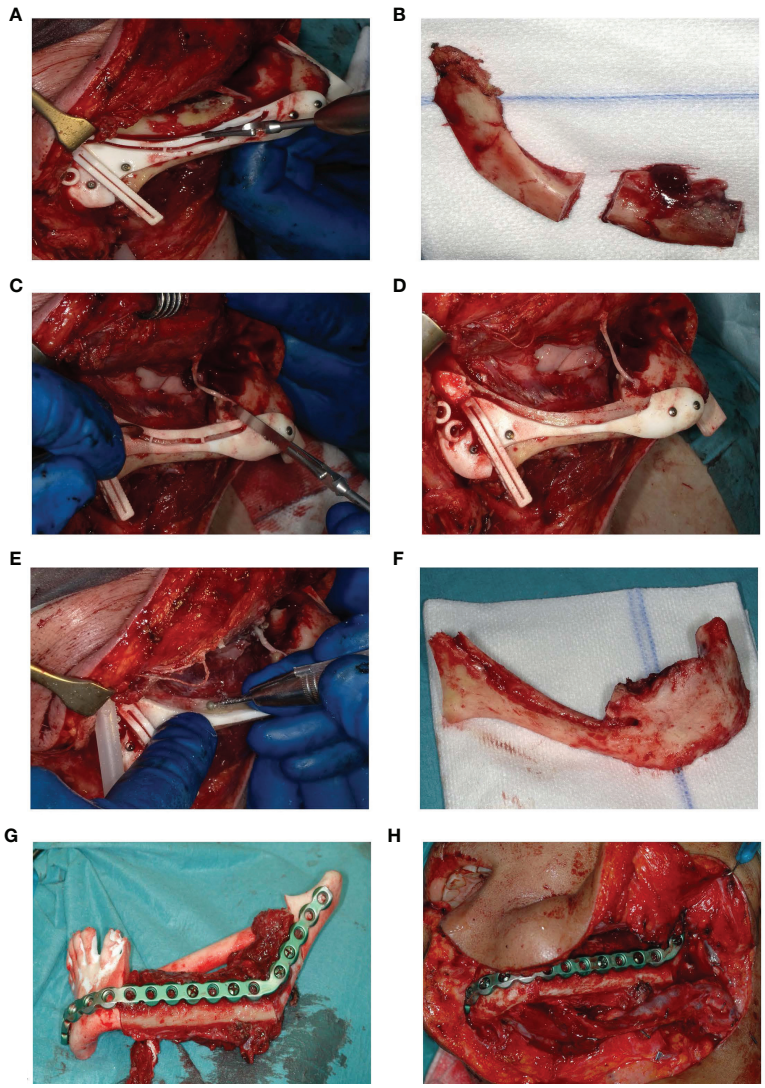

FIGURE 6 | **(A)** Deroofing of the upper part of the mandible. **(B)** Removed upper part of the mandible after two vertical osteotomies on both sides. **(C)** Removal of the upper part of the guide. **(D)** Accessible buccal bone and 2 mm roof of the IAN. **(E)** Buccal corticotomy to expose the IAN. **(F)** Resected part of the mandible without the right IAN. **(G)** Fitting of the fibula segments fixated to the patient specific reconstruction plate into a 3D printed mandible including the planned resection. **(H)** Reconstruction *in situ*.

which either a test stimulus or a fake stimulus is applied. The fake stimulus is performed by approaching the lower lip/chin with an averted monofilament. The order of test/fake stimulus in the two moments of attention is randomized. A stimulus (test or fake) is preceded by the words spoken: "test 1" and "test 2." After each offer, the patient indicates whether the test stimulus was administered during attention moment 1 or 2. If the patient does not know exactly, they have to guess ("two alternative forced choice" test procedure). The sensitivity test score is positive if the test stimulus is correctly detected in seven consecutive offers. With seven offers, the chance that a correct result will be achieved by means of guessing is less than 0.01 (<0.5). At the first error in the series of seven, the test can be terminated immediately with a negative result (49). The total amount of positive reactions were added up for all five monofilaments on each of the 12 locations (i.e. no function of the IAN resulted in a 12 × 0 score of 0 and full function resulted in a 12 × 5 score of 60). Eventually, the score was converted into a score between 0 and 5 for statistical analysis.

For subjective IAN sensory function two Visual Analog Scales (VAS) were used (**Supplementary Figure 1**), asking the following questions: "How would you describe the sensation of your lower lip and chin. Place a vertical mark on the line below to indicate the sensation on your lower lip and chin today" and "Place a vertical mark on the line below to indicate the level of sensation on your lower lip and chin you find acceptable in daily life." Both vertical marks were transformed to a score on a scale from 1 "no feeling" to 10 "normal feeling."

Subjective and objective function of the IAN were determined one day preoperatively (T0) and 2–4 weeks (T1), 2–3 months (T2), 6–7 months (T3), and 1 year or more (T4) postoperatively.

Statistical Analysis

SPSS Software package (version 26.0 Inc., Chicago, IL, USA) was used for statistical analysis. A paired samples T-test was executed for both subjective and objective IAN function between T0 measurements and T1-T4 measurements. Statistical significance was reached with a two-tailed p value of <0.05. As T0 measurements were expected to be different for cases with a pathologic fracture and those without, these cases were analyzed separately.

RESULTS

Patients

Between November 2017 and March 2019 five patients were included with a mean age of 53.4 years (49,50,51,52,53,54,55,56,57). A total of seven IAN were preserved (two patients required bilateral IAN preservation). All patient characteristics are shown in **Table 2**. No patients developed peri-operative complications, in particular there were no clinical or radiological signs of recurrent ORN or non-union for at least 1 year after surgery.

Accuracy

Table 3 shows all angle deviations (AD) in degrees per angle. The mandibular defect classification of Brown et al. was used (50). **Figure 7** shows the panoramic radiographs preoperatively, postoperatively, and after implant placement, with the 3D plan and accuracy measurements added in between.

Nerve Evaluation

The objective IAN function results are shown in **Figures 8A, B**. As can be seen in **Figure 8B**, there were two patients with a pathologic fracture (IAN 1 and IAN 4). Patients without a pathologic fracture had an average preoperative score of 4.8. At T1 these patients had an average score of 1.9, which was significantly lower than T0 (p = 0.00) (**Table 4**). However, the objective IAN function improved at T2 up to an average score of 4.3 at T4 for patients without a pathologic fracture (p = 0.07) (**Table 5**).

As shown in **Figure 8C, D**, the subjective IAN function (VAS-scores) showed similar results as the objective IAN function (**Figures 8C, D**). The light touch test results for the three control IANs were consistent throughout every evaluation moment.

TABLE 3 | Angle deviations in degrees (°) between the preoperative virtual plan and the postoperative result.

Nr.	Brown class	Axial		Coronal		Sagittal	
		L	R	L	R	L	R
1	I	2.40	6.42	0.54	0.06	0.28	0.10
2	III	0.17	2.27	0.77	2.99	1.93	1.10
3	I	0.94	0.12	0.73	0.49	2.17	0.11
4	II	2.45	2.84	1.03	0.32	3.78	1.49
5	III	0.23	1.30	0.10	2.39	7.47	2.78

DISCUSSION

ORN of the jaw is still a common side effect of RT, even after the introduction of intensity-modulated radiotherapy (1–3). ORN can be treated with conservative measures, but in more severe cases (Notani stage III) a segmental resection followed by a vascularized reconstruction flap should be considered (13, 18, 19). Due to new CAS techniques, preservation of the IAN during mandibular resection is more feasible than ever. Previous studies have evaluated these new CAS techniques for preservation of the IAN during mandibular resection (37–40). These studies have published promising results for postoperative sensory disturbance, but none of them used reliable and reproducible clinical neurosensory tests which are advised for sensory

TABLE 2 | An overview of the included patients and their characteristics.

Nr.	Age	Sex	Primary diagnosis	TNM	Treatment	Secondary diagnosis	Included IAN
1	49	F	Tonsil R SCC	T2N1	Chemoradiotherapy: 70 Gy	ORN + pathologic fracture	R
2	57	M	Floor of mouth R+L SCC	T3N1	Surgery, Radiotherapy: 70 Gy	ORN	L + R
3	54	F	Tonsil L SCC	T1N2a	Radiotherapy: 70 Gy	ORN + pathologic fracture	L
4	56	M	Buccal mucosa R SCC	T1N0	Surgery Radiotherapy: 66 Gy	ORN	R
			Buccal mucosa L SCC	T2N0	Surgery		
5	51	F	Floor of mouth L SCC	T2N2	Surgery, Chemoradiotherapy: 55 Gy	ORN	L + R

F, female; M, male; R, right; L, left; SCC, squamous cell carcinoma; ORN, Osteoradionecrosis.

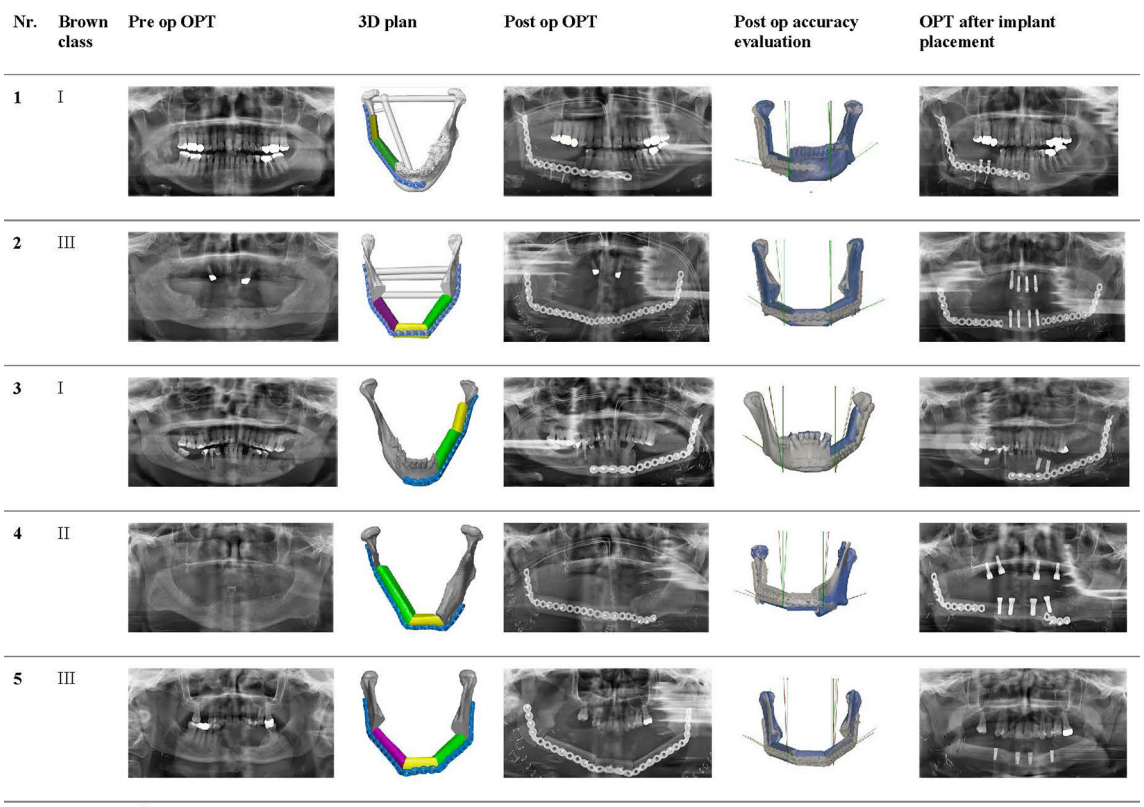

FIGURE 7 | Panoramic radiographs of all included cases preoperatively, postoperatively, and after implant placement, with the 3D plan and accuracy measurements added in between.

evaluation of trigeminal nerve branches (48, 51). In addition, the study groups consisted of patients with different preoperative diagnoses.

This study included only patients diagnosed with ORN. The sensory disturbance of the IAN was evaluated using the light touch test with Semmes-Weinstein monofilaments. We also used a VAS-score questionnaire to measure subjective feeling. Poort et al. recommended to use a follow-up regimen of 1 week, 1 month, 3 months, and 1 year (48). However, in this study we did not follow this exact regimen for patient load reasons.

Our results show that IAN preservation using CAS is possible. None of the patients experienced reoccurring ORN within at least 1 year, which suggests enough infected bone was resected. This study suggests that the use of RT isodose curves set to 50Gy can therefore be safely implemented in determining osteotomy planes. Our results show that there was some sensory disturbance of the IAN after surgery, but the mental nerve area regains its sensitivity each following evaluation moment to almost its preoperative sensitivity after 1 year. The cases with a pathological fracture, which already had an IAN sensitivity disturbance, regained even more sensitivity than before the surgery.

The statistical analysis of the average IAN sensitivity (light touch test and VAS) of the "pathological fracture" cases (n = 2) did not show a significant difference, this may be a result of the low case number. The "no pathological fracture" cases did show statistical significant results during analysis. We did not take the double inclusion of patients (two "bilateral patients") into account, which may be a weakness of the executed analysis. The three unaffected IANs, used as controls, did not show different sensitivity levels for each evaluation moment, meaning the light touch test with Semmes-Weinstein monofilaments was consistent.

The sensitivity survival and recovery indicates that the nerve tracking technique was sufficient: mandibular canal tracing in steps of 2 mm in coronal view on the CT of the skull. For the design of the IAN preservation guide we considered the discrepancy of the virtual traced IAN location and the actual location by designing a two-step deroofing process. Once the upper part of the guide was removed, the IAN was still covered with bone and could be carefully exteriorized. By approaching the IAN from the buccal side (buccal corticotomy), it could be lifted easily from the mandibular canal.

In our treatment concept, a virtual model was 3D printed and figured as a template to pre-bent a reconstruction plate into a patient specific reconstruction plate (PSRP) (**Figure 4**). Subsequently a CT scan of the pre-bent PSRP was made, converted to STL format, and used further along in the virtual

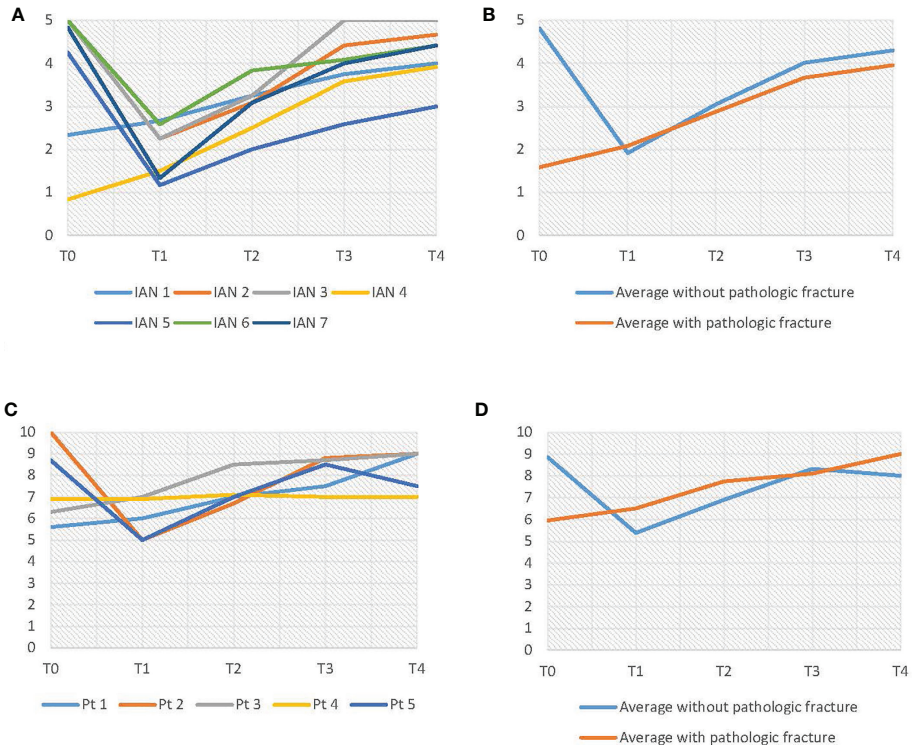

FIGURE 8 | **(A)** Results of the light touch test. **(B)** Average results of the light touch test, differentiated on pathologic fracture. **(C)** VAS-score results. **(D)** Average VAS-score results, differentiated on pathologic fracture.

TABLE 4 | Paired samples T-test between T0 and T1 for objective IAN function in patients without a pathologic fracture (n = 5). α = 0,05.

	Mean (SD)	Mean difference (SD)	t-value	p-value
T0	4,8167 (0,32489)	2,9 (0,40995)	15,818	0,000
T1	1,9167 (0,62639)			

TABLE 5 | Paired samples t-test T0–T4. Light touch test. Without pathologic fracture (n = 5). α = 0,05.

	Mean (SD)	Mean difference (SD)	t-value	p-value
T0	4,8167 (0,32489)	0,51667 (0,46173)	2,502	0,067
T4	4,3 (0,76513)			

planning. This has the same advantages as a 3D printed titanium patient specific reconstruction plate, but saves on the high costs of the selective laser sintering manufacturing technique (52). Another advantage of this treatment concept is that no third party is involved in the planning phase, which speeds up the workflow for hospitals with its own 3D lab. Our systematic review of accuracy in mandibular reconstruction using CAS showed that 14 out of the 42 included studies used a standard reconstruction plate which was pre-bent on a 3D printed model of the virtually planned reconstruction and 12 studies used a 3D printed PSRP. Even though the studies were difficult to compare, there were no striking differences in accuracy or postoperative complications between the studies using a pre-bent reconstruction plate or a 3D printed PSRP (53).

The measured accuracy of the reconstructions did not show any extreme deviations. Since the accuracy is on such a high level, we believe it is possible to perform computer guided mandibular reconstructions with direct dental implant placement in ORN cases. Especially since in ORN cases the neomandible is constructed with well vascularized donor bone and postoperative RT is not indicated. All patients received dental implants after an average time of 11.6 months (min. 8/ max. 19 months). The use of immediately placed dental implants will improve dental rehabilitation time significantly. Any data on acceptable outcome ranges regarding immediately placed dental implants during mandibular reconstruction has yet to be published.

A shortcoming of this study was the low case number, caused by small numbers of ORN cases. Future multi-center prospective studies need to be carried out in order to validate the results of our novel treatment concept.

CONCLUSION

Our novel ORN treatment concept shows promising results for implementation of 3D radiotherapy isodose curve visualization

and IAN preservation. Sensory function of all IAN recovered after segmental mandibular resection.

DATA AVAILABILITY STATEMENT

The original contributions presented in the study are included in the article/**Supplementary Material**. Further inquiries can be directed to the corresponding author.

ETHICS STATEMENT

The studies involving human participants were reviewed and approved by the Medical Ethics Review Committee of VU University Medical Center (FWA 00017598). The ethics committee waived the requirement of written informed consent for participation.

AUTHOR CONTRIBUTIONS

Conceived and designed the analysis: GV, JL, LL, TF, and FL. Collected the data: GV, LL, NL, KK, JL, TF, and FL. Contributed data or analysis tools: GV, LL, JL, and KK. Performed the analysis: GV, LL, and JL. Wrote the paper: GV, LL, JL, and FL. All authors contributed to the article and approved the submitted version.

SUPPLEMENTARY MATERIAL

The Supplementary Material for this article can be found online at: https://www.frontiersin.org/articles/10.3389/fonc.2021.630123/full#supplementary-material

Supplementary Figure 1 | Two Visual Analogue Scales (VAS) were asked to the patient to evaluate subjective sensory function of the inferior alveolar nerve.

REFERENCES

1. Lohia S, Rajapurkar M, Nguyen SA, Sharma AK, Gillespie MB, Day TA. A comparison of outcomes using intensity-modulated radiation therapy and 3-dimensional conformal radiation therapy in treatment of oropharyngeal cancer. *JAMA Otolaryngol Head Neck Surg* (2014) 140:331. doi: 10.1001/jamaoto.2013.6777
2. Setton J, Caria N, Romanyshyn J, Koutcher L, Wolden SL, Zelefsky MJ, et al. Intensity-modulated radiotherapy in the treatment of oropharyngeal cancer: an update of the Memorial Sloan-Kettering Cancer Center experience. *Int J Radiat Oncol Biol Phys* (2012) 82:291. doi: 10.1016/j.ijrobp.2010.10.041
3. Vergeer MR, Doornaert PA, Rietveld DH, Leemans CR, Slotman BJ, Langendijk JA. Intensity-modulated radiotherapy reduces radiation-induced morbidity and improves health-related quality of life: results of a nonrandomized prospective study using a standardized follow-up program. *Int J Radiat Oncol Biol Phys* (2009) 74:1. doi: 10.1016/j.ijrobp.2008.07.059
4. Reuther T, Schuster T, Mende U, Kubler A. Osteoradionecrosis of the jaws as a side effect of radiotherapy of head and neck tumour patients–a report of a thirty year retrospective review. *Int J Oral Maxillofac Surg* (2003) 32:289. doi: 10.1054/ijom.2002.0332
5. Harris M. The conservative management of osteoradionecrosis of the mandible with ultrasound therapy. *Br J Oral Maxillofac Surg* (1992) 30:313. doi: 10.1016/0266-4356(92)90181-H
6. Lambade PN, Lambade D, Goel M. Osteoradionecrosis of the mandible: a review. *Oral Maxillofac Surg* (2013) 17:243. doi: 10.1007/s10006-012-0363-4
7. Marx RE. Osteoradionecrosis: a new concept of its pathophysiology. *J Oral Maxillofac Surg* (1983) 41:283. doi: 10.1016/0278-2391(83)90294-X
8. Lyons A, Ghazali N. Osteoradionecrosis of the jaws: current understanding of its pathophysiology and treatment. *Br J Oral Maxillofac Surg* (2008) 46:653. doi: 10.1016/j.bjoms.2008.04.006
9. Schwartz HC, Kagan AR. Osteoradionecrosis of the mandible: scientific basis for clinical staging. *Am J Clin Oncol* (2002) 25:168. doi: 10.1097/00000421-200204000-00013
10. Store G, Boysen M. Mandibular osteoradionecrosis: clinical behaviour and diagnostic aspects. *Clin Otolaryngol Allied Sci* (2000) 25:378. doi: 10.1046/j.1365-2273.2000.00367.x
11. De Felice F, Musio D, Tombolini V. Osteoradionecrosis and intensity modulated radiation therapy: An overview. *Crit Rev Oncol Hematol* (2016) 107:39. doi: 10.1016/j.critrevonc.2016.08.017
12. Mendenhall WM, Suarez C, Genden EM, de Bree R, Strojan P, Langendijk JA, et al. Parameters Associated With Mandibular Osteoradionecrosis. *Am J Clin Oncol* (2018) 41:1276. doi: 10.1097/COC.0000000000000424
13. Rice N, Polyzois I, Ekanayake K, Omer O, Stassen LF. The management of osteoradionecrosis of the jaws–a review. *Surgeon* (2015) 13:101. doi: 10.1016/j.surge.2014.07.003
14. Kluth EV, Jain PR, Stuchell RN, Frich JCJr. A study of factors contributing to the development of osteoradionecrosis of the jaws. *J Prosthet Dent* (1988) 59:194. doi: 10.1016/0022-3913(88)90015-7
15. Owosho AA, Tsai CJ, Lee RS, Freymiller H, Kadempour A, Varthis S, et al. The prevalence and risk factors associated with osteoradionecrosis of the jaw in oral and oropharyngeal cancer patients treated with intensity-modulated radiation therapy (IMRT): The Memorial Sloan Kettering Cancer Center experience. *Oral Oncol* (2017) 64:44. doi: 10.1016/j.oraloncology.2016.11.015
16. Nabil S, Samman N. Incidence and prevention of osteoradionecrosis after dental extraction in irradiated patients: a systematic review. *Int J Oral Maxillofac Surg* (2011) 40:229. doi: 10.1016/j.ijom.2010.10.005
17. Caparrotti F, Huang SH, Lu L, Bratman SV, Ringash J, Bayley A, et al. Osteoradionecrosis of the mandible in patients with oropharyngeal carcinoma treated with intensity-modulated radiotherapy. *Cancer* (2017) 123:3691. doi: 10.1002/cncr.30803
18. Jacobson AS, Buchbinder D, Hu K, Urken ML. Paradigm shifts in the management of osteoradionecrosis of the mandible. *Oral Oncol* (2010) 46:795. doi: 10.1016/j.oraloncology.2010.08.007
19. Nadella KR, Kodali RM, Guttikonda LK, Jonnalagadda A. Osteoradionecrosis of the Jaws: Clinico-Therapeutic Management: A Literature Review and Update. *J Maxillofac Oral Surg* (2015) 14:891. doi: 10.1007/s12663-015-0762-9
20. Wong JK, Wood RE, McLean M. Conservative management of osteoradionecrosis. *Oral Surg Oral Med Oral Pathol Oral Radiol Endod* (1997) 84:16. doi: 10.1016/S1079-2104(97)90287-0
21. Notani K, Yamazaki Y, Kitada H, Sakakibara N, Fukuda H, Omori K, et al. Management of mandibular osteoradionecrosis corresponding to the severity of osteoradionecrosis and the method of radiotherapy. *Head Neck* (2003) 25:181. doi: 10.1002/hed.10171
22. Shaw R, Tesfaye B, Bickerstaff M, Silcocks P, Butterworth C. Refining the definition of mandibular osteoradionecrosis in clinical trials: The cancer research UK HOPON trial (Hyperbaric Oxygen for the Prevention of Osteoradionecrosis). *Oral Oncol* (2017) 64:73. doi: 10.1016/j.oraloncology.2016.12.002
23. Store G, Larheim TA. Mandibular osteoradionecrosis: a comparison of computed tomography with panoramic radiography. *Dentomaxillofac Radiol* (1999) 28:295. doi: 10.1038/sj.dmfr.4600461
24. Rodby KA, Turin S, Jacobs RJ, Cruz JF, Hassid VJ, Kolokythas A, et al. Advances in oncologic head and neck reconstruction: systematic review and future considerations of virtual surgical planning and computer aided design/computer aided modeling. *J Plast Reconstr Aesthet Surg* (2014) 67:1171. doi: 10.1016/j.bjps.2014.04.038
25. Hirsch DL, Garfein ES, Christensen AM, Weimer KA, Saddeh PB, Levine JP. Use of computer-aided design and computer-aided manufacturing to produce orthognathically ideal surgical outcomes: a paradigm shift in head and neck

reconstruction. *J Oral Maxillofac Surg* (2009) 67:2115. doi: 10.1016/j.joms.2009.02.007
26. Nilsson J, Hindocha N, Thor A. Time matters - Differences between computer-assisted surgery and conventional planning in cranio-maxillofacial surgery: A systematic review and meta-analysis. *J Craniomaxillofac Surg* (2020) 48:132. doi: 10.1016/j.jcms.2019.11.024
27. Roser SM, Ramachandra S, Blair H, Grist W, Carlson GW, Christensen AM, et al. The accuracy of virtual surgical planning in free fibula mandibular reconstruction: comparison of planned and final results. *J Oral Maxillofac Surg* (2010) 68:2824. doi: 10.1016/j.joms.2010.06.177
28. Antony AK, Chen WF, Kolokythas A, Weimer KA, Cohen MN. Use of virtual surgery and stereolithography-guided osteotomy for mandibular reconstruction with the free fibula. *Plast Reconstr Surg* (2011) 128:1080. doi: 10.1097/PRS.0b013e31822b6723
29. Hanasono MM, Skoracki RJ. Computer-assisted design and rapid prototype modeling in microvascular mandible reconstruction. *Laryngoscope* (2013) 123:597. doi: 10.1002/lary.23717
30. Avraham T, Franco P, Brecht LE, Ceradini DJ, Saadeh PB, Hirsch DL, et al. Functional outcomes of virtually planned free fibula flap reconstruction of the mandible. *Plast Reconstr Surg* (2014) 134:628e. doi: 10.1097/PRS.0000000000000513
31. Kraeima J, Steenbakkers R, Spijkervet FKL, Roodenburg JLN, Witjes MJH. Secondary surgical management of osteoradionecrosis using three-dimensional isodose curve visualization: a report of three cases. *Int J Oral Maxillofac Surg* (2018) 47:214. doi: 10.1016/j.ijom.2017.08.002
32. Smith JG, Elias LA, Yilmaz Z, Barker S, Shah K, Shah S, et al. The psychosocial and affective burden of posttraumatic neuropathy following injuries to the trigeminal nerve. *J Orofac Pain* (2013) 27:293. doi: 10.11607/jop.1056
33. Marchena JM, Padwa BL, Kaban LB. Sensory abnormalities associated with mandibular fractures: incidence and natural history. *J Oral Maxillofac Surg* (1998) 56:822. doi: 10.1016/S0278-2391(98)90003-9
34. Kuriakose MA, Lee JJ, DeLacure MD. Inferior alveolar nerve-preserving mandibulectomy for nonmalignant lesions. *Laryngoscope* (2003) 113:1269. doi: 10.1097/00005537-200307000-00029
35. Wu TC, Chen Z, Tian FC, Tian QZ, You CT. Ameloblastoma of the mandible treated by resection, preservation of the inferior alveolar nerve, and bone grafting. *J Oral Maxillofac Surg* (1984) 42:93. doi: 10.1016/0278-2391(84)90318-5
36. Nocini PF, De Santis D, Fracasso E, Zanette G. Clinical and electrophysiological assessment of inferior alveolar nerve function after lateral nerve transposition. *Clin Oral Implants Res* (1999) 10:120. doi: 10.1034/j.1600-0501.1999.100206.x
37. Chen MJ, Yang C, Huang D, He DM, Wang YW, Zhang WH. Modified technique for preservation of inferior alveolar nerve during mandibulectomy. *Head Neck* (2017) 39:2562. doi: 10.1002/hed.24924
38. Zhou Z, Zhao H, Zhang S, Zheng J, Yang C. Evaluation of accuracy and sensory outcomes of mandibular reconstruction using computer-assisted surgical simulation. *J Craniomaxillofac Surg* (2019) 47:6. doi: 10.1016/j.jcms.2018.10.002
39. Ricotta F, Battaglia S, Sandi A, Pizzigallo A, Marchetti C, Tarsitano A. Use of a CAD-CAM inferior alveolar nerve salvage template during mandibular resection for benign lesionsUtilizzo di una guida CAD-CAM per la preservazione del nervo alveolare inferiore durante le resezioni mandibolari nelle lesioni benigne. *Acta Otorhinolaryngol Italica* (2019) 39:117. doi: 10.14639/0392-100X-2408
40. Huang D, Chen M, He D, Yang C, Yuan J, Bai G, et al. Preservation of the inferior alveolar neurovascular bundle in the osteotomy of benign lesions of the mandible using a digital template. *Br J Oral Maxillofacial Surg* (2015) 53:637. doi: 10.1016/j.bjoms.2015.04.013
41. Ang E, Black C, Irish J, Brown DH, Gullane P, O'Sullivan B, et al. Reconstructive options in the treatment of osteoradionecrosis of the craniomaxillofacial skeleton. *Br J Plast Surg* (2003) 56:92. doi: 10.1016/S0007-1226(03)00085-7
42. Bak M, Jacobson AS, Buchbinder D, Urken ML. Contemporary reconstruction of the mandible. *Oral Oncol* (2010) 46:71. doi: 10.1016/j.oraloncology.2009.11.006
43. Pohlenz P, Blessmann M, Blake F, Li L, Schmelzle R, Heiland M. Outcome and complications of 540 microvascular free flaps: the Hamburg experience. *Clin Oral Investig* (2007) 11:89. doi: 10.1007/s00784-006-0073-0
44. Hayden RE, Mullin DP, Patel AK. Reconstruction of the segmental mandibular defect: current state of the art. *Curr Opin Otolaryngol Head Neck Surg* (2012) 20:231. doi: 10.1097/MOO.0b013e328355d0f3
45. van Baar GJC, Liberton N, Forouzanfar T, Winters HAH, Leusink FKJ. Accuracy of computer-assisted surgery in mandibular reconstruction: A postoperative evaluation guideline. *Oral Oncol* (2019) 88:1. doi: 10.1016/j.oraloncology.2018.11.013
46. van Baar GJC, Liberton N, Winters HAH, Leeuwrik L, Forouzanfar T, Leusink FKJ. A Postoperative Evaluation Guideline for Computer-Assisted Reconstruction of the Mandible. *J Vis Exp* (2020) 28(155). doi: 10.3791/60363
47. Gerlach NL, Meijer GJ, Maal TJ, Mulder J, Rangel FA, Borstlap WA, et al. Reproducibility of 3 different tracing methods based on cone beam computed tomography in determining the anatomical position of the mandibular canal. *J Oral Maxillofac Surg* (2010) 68:811. doi: 10.1016/j.joms.2009.09.059
48. Poort LJ, van Neck JW, van der Wal KG. Sensory testing of inferior alveolar nerve injuries: a review of methods used in prospective studies. *J Oral Maxillofac Surg* (2009) 67:292. doi: 10.1016/j.joms.2008.06.076
49. Vriens JP, van der Glas HW, Koole R. [Repair and revision 9. Peripheral trigeminal nerve injury]. *Ned Tijdschr Tandheelkd* (2002) 106(3):95–9.
50. Brown JS, Barry C, Ho M, Shaw R. A new classification for mandibular defects after oncological resection. *Lancet Oncol* (2016) 17:e23. doi: 10.1016/S1470-2045(15)00310-1
51. Devine M, Hirani M, Durham J, Nixdorf DR, Renton T. Identifying criteria for diagnosis of post-traumatic pain and altered sensation of the maxillary and mandibular branches of the trigeminal nerve: a systematic review. *Oral Surg Oral Med Oral Pathol Oral Radiol* (2018) 125:526. doi: 10.1016/j.oooo.2017.12.020
52. Zweifel DF, Simon C, Hoarau R, Pasche P, Broome M. Are virtual planning and guided surgery for head and neck reconstruction economically viable? *J Oral Maxillofac Surg* (2015) 73:170. doi: 10.1016/j.joms.2014.07.038
53. van Baar GJC, Forouzanfar T, Liberton N, Winters HAH, Leusink FKJ. Accuracy of computer-assisted surgery in mandibular reconstruction: A systematic review. *Oral Oncol* (2018) 84:52. doi: 10.1016/j.oraloncology.2018.07.004

Conflict of Interest: The authors declare that the research was conducted in the absence of any commercial or financial relationships that could be construed as a potential conflict of interest.

frontiers in Oncology

ORIGINAL RESEARCH
published: 23 February 2021
doi: 10.3389/fonc.2021.614448

Dysbiosis of Oral Microbiota During Oral Squamous Cell Carcinoma Development

*Purandar Sarkar[1], Samaresh Malik[1], Sayantan Laha[2], Shantanab Das[2], Soumya Bunk[3], Jay Gopal Ray[4], Raghunath Chatterjee[2] and Abhik Saha[1,3]**

[1] School of Biotechnology, Presidency University, Kolkata, India, [2] Human Genetics Unit, Indian Statistical Institute, Kolkata, India, [3] Department of Life Sciences, Presidency University, Kolkata, India, [4] Department of Oral Pathology, Dr. R Ahmed Dental College and Hospital, Kolkata, India

Infection with specific pathogens and alterations in tissue commensal microbial composition are intricately associated with the development of many human cancers. Likewise, dysbiosis of oral microbiome was also shown to play critical role in the initiation as well as progression of oral cancer. However, there are no reports portraying changes in oral microbial community in the patients of Indian subcontinent, which has the highest incidence of oral cancer per year, globally. To establish the association of bacterial dysbiosis and oral squamous cell carcinoma (OSCC) among the Indian population, malignant lesions and anatomically matched adjacent normal tissues were obtained from fifty well-differentiated OSCC patients and analyzed using 16S rRNA V3-V4 amplicon based sequencing on the MiSeq platform. Interestingly, in contrast to the previous studies, a significantly lower bacterial diversity was observed in the malignant samples as compared to the normal counterpart. Overall our study identified *Prevotella, Corynebacterium*, *Pseudomonas*, *Deinococcus* and *Noviherbaspirillum* as significantly enriched genera, whereas genera including *Actinomyces*, *Sutterella*, *Stenotrophomonas*, *Anoxybacillus*, and *Serratia* were notably decreased in the OSCC lesions. Moreover, we demonstrated HPV-16 but not HPV-18 was significantly associated with the OSCC development. In future, with additional validation, this panel could directly be applied into clinical diagnostic and prognostic workflows for OSCC in Indian scenario.

Keywords: oral squamous cell carcinoma, 16S rRNA sequence analysis, oral microbiology ecology, dysbiosis, human papillomavirus-16

OPEN ACCESS

Edited by:
Alberto Paderno, University of Brescia, Italy

Reviewed by:
Nora Staniene, Lithuanian University of Health Sciences, Lithuania
Bhabatosh Das, Translational Health Science and Technology Institute (THSTI), India

***Correspondence:**
Abhik Saha
abhik.dbs@presiuniv.ac.in

Specialty section:
This article was submitted to Head and Neck Cancer, a section of the journal Frontiers in Oncology

Received: *06 October 2020*
Accepted: *05 January 2021*
Published: *23 February 2021*

Citation:
Sarkar P, Malik S, Laha S, Das S, Bunk S, Ray JG, Chatterjee R and Saha A (2021) Dysbiosis of Oral Microbiota During Oral Squamous Cell Carcinoma Development. Front. Oncol. 11:614448. doi: 10.3389/fonc.2021.614448

INTRODUCTION

Oral squamous cell carcinoma (OSCC), a subset of head and neck squamous cell carcinoma (HNSCC), is the most common oral malignancy, representing approximately 90% of all cancers in the oral cavity (1, 2). It is the sixth most common cancer worldwide and every year around 400,000 new cases are diagnosed (3, 4). The number of newly diagnosed cases is predicted to increase by 62% in 2035 (5). The prevalence of oral cancer is highest in India and it represents most prevailing cancer in male population and fifth most common cancer among women (6, 7). Despite easy accessibility of the oral cavity during physical examination as well as several technological advancements in

surgical procedures in addition to adjuvant radiotherapy and chemotherapy, due to the lack of early diagnosis based on appropriate molecular markers, OSCC patients are often diagnosed at more advanced stages, leading to poor survival outcomes. The overall 5-year survival rate of OSCC patients is roughly 50% across the globe (8–10). Thus, early detection, identification of biomarkers and understanding the role of various etiological agents can significantly improve the current situation of OSCC treatment. In developing countries like India, excessive tobacco usage including smoking, chewing betel quid and areca nut along with alcohol consumption are the major risk factors for OSCC development (7, 11). However, oral cancer often arises in patients without a history of tobacco usage or alcohol consumption, indicating contribution from other potential risk factors including genetic/epigenetic alterations or microbial infection (2, 6, 12). A number of oncogenic viruses including high risk human papillomavirus (HPV) genotypes and Epstein-Barr virus (EBV) have been identified as infectious etiological agents for OSCC (13–15). However, association of these oncoviruses with OSCC development is not strong, contributing approximately 20% of all oral cancers (13, 14). Thus, identification of other microbial factors influencing OSCC development is warranted.

Human body harbors a plethora of microbial species referred to as 'commensal microbiota' including bacteria, yeast, fungi, protozoa, archaea and viruses and develops a symbiotic ecosystem without eliciting a decimating immune response. However, alterations of the microbiome architecture (dysbiosis) often lead to a variety of human diseases including cancer (16, 17). The advent of next-generation sequencing technologies for example the 16S rRNA gene amplicon based sequencing has allowed an affordable and culture-free approach of identification of overall bacterial composition in cancerous lesions and its effect on the progression of the disease (18). As one of the prime territories of microbiome in human body, the oral cavity contains distinct niches with dynamic microbial communities (19). Oral microbial ecology is a critical factor in controlling both human physiology and pathophysiology. The oral microbiome and their produced metabolites translocate through gastrointestinal tract or due to periodontal pocket ulceration can affect various distant tissues and are associated with the development of a number of diseases like cardiovascular disorder, diabetes, rheumatoid arthritis and premature birth (20–23). The dysbiosis of oral microbiome is associated with a number of clinical symptoms that ranges from dental caries, periodontal disease to oral cancer (24–28). Importantly, chronic periodontitis has also been suggested as potential risk factor for the onset of oral pre-cancerous and cancerous lesions (27). There is, however, no consensus among reports regarding microbiome signature associated with the development of OSCC. For example, Schmidt et al. demonstrated depletion of Firmicutes and Actinobacteria in a study of 15 oral cancer patients (29), while Mager *et al.* using DNA hybridization technique reported elevation of *Capnocytophaga gingivalis*, *Provatella melaningtoenica*, and *Streptococcus mitis* in the saliva of OSCC patients (30). Recently, Zhao *et al.* demonstrated that a cluster of periodontitis associated taxa such as *Fusobacterium, Dialister, Peptostreptococcus, Filifactor, Peptococcus, Catonella*, and *Parvimonas* was enriched in OSCC lesions (31). AI-hebshi et al. reported that several inflammatory bacterial species including *Pseudomonas aeruginosa* and *Fusobacterium nucleatum* are elevated in OSCC patients' samples (32). Another report by Lee *et al.* demonstrated that salivary microbiome particularly five genera including *Bacillus*, *Enterococcus*, *Parvimonas*, *Peptostreptococcus*, and *Slackia* significantly varied between samples from the epithelial precursor and OSCC lesions (33), indicating a potential prognostic marker for OSCC development. Börnigen et al. identified a number of differentially abundant genera in oral cancer samples specifically *Dialister* as enriched and *Scardovia* as depleted (34). Overall, given the diversity of identified microbiome composition as well as limited number of samples, more in depth investigations with larger-scale epidemiologically designed cohorts are warranted to assess the role of microbiome dysbiosis in OSCC development.

Despite the highest oral cancer incidence in India, till date no efforts have been made in understanding the oral microbial imbalance during OSCC development among Indian patients. Here, in an aim to explore OSCC-associated bacterial composition fifty OSCC lesions and their anatomically matched normal tissue regions was profiled using 16S rRNA gene amplicon based sequencing by targeting the hypervariable V3-V4 region. Our analyses revealed while top five genera such as *Prevotella, Corynebacterium, Pseudomonas, Deinococcus* and *Noviherbaspirillum* were significantly enriched, while genera including *Actinomyces, Sutterella, Stenotrophomonas, Anoxybacillus, and Serratia* were notably depleted in the OSCC lesions as compared to matched control adjacent tissue samples. In sum, our results provided evidence of alterations of oral bacterial community during OSCC development and indicated the possibility of utilizing the identified microbiome signature as prognostic marker of oral malignancies in patients of Indian subcontinent.

MATERIALS AND METHODS

Ethics Statement

The study was approved by the Institutional Ethics Committee for Human Research, Indian Statistical Institute, Kolkata, India. Written informed consent was obtained from all participants and all methods in this study were performed in accordance with the relevant guidelines and regulations.

Sample Information

After the clinical diagnosis of oral squamous cell carcinoma (OSCC) the patients from Dr. R Ahmed Dental College and Hospital, were enlisted for the study. 50 patients were included in the study after confirmation of well-differentiated squamous cell carcinoma from histopathological reports. All participants were not on any local or systemic antibiotics prior to sample collection. Tissue samples were collected by incisional and 3 mm punch biopsy sample collection method from both the regions of cancerous lesions (N=50) and the adjoining clinically uninvolved normal area (matched control, N=50) for each of the 50 patients recruited in this study. A portion of the tissue

samples were collected in RNA Later (Invitrogen, Thermo Fisher Scientific Inc., Waltham, MA, USA) and stored at -80°C for future use. Another portion was fixed in the formalin and used for histopathological evaluations.

DNA Extraction

DNA was isolated from the cancerous lesion and adjacent unaffected normal tissue regions using DNeasy Blood and Tissue Kit (Qiagen, Hilden, Germany) according to manufacturer's protocol. The quality and quantity of isolated DNA was determined by the A260/280 ratio using Synergy H1 Multimode Microplate Reader (BioTek Instruments, Inc., VT, USA). DNA samples were frozen at -20°C for further analysis. Approximately 50 ng of genomic DNA from each sample was used for 16S rRNA V3-V4 amplicon sequencing.

16S Ribosomal RNA Sequencing and OTU Assignment

16S ribosomal RNA (rRNA) amplicon sequencing for metagenomics studies was performed on a MiSeq platform (Illumina, San Diego, CA, USA) using 2×250 bp chemistry. Clonal libraries for 16S rRNA V3-V4 hypervariable region were prepared using NEBNext Ultra DNA Library preparation kit (New England Biolabs, Ipswich, MA, USA) with the forward primer (5′-CTTTCCCTACACGACGCT CTTCCGATCTACGGRA GGCAGCAG-3′) and the reverse primer (5′-GGAGTTCAGA CGTGTGCT CTTCCGATCTTACCAGGGTATCTAATCCT-3′). The amplicons were subjected to a number of enzymatic reactions for end-repairing, dA-tailing followed by adapter ligation and cleaning up using Solid Phase Reversible Immobilization (SPRI) technology (Beckman Coulter, Indianapolis, IN, USA). The adapter ligated fragments were indexed by limited PCR cycle to generate final libraries for paired-end sequencing. The concentration of the purified amplicons was measured using Qubit fluorometer (Thermo Fisher Scientific Inc., Waltham, MA, USA) and the quality was checked using Agilent 2100 Bioanalyzer (Agilent Technologies, Santa Clara, CA, USA). The multiplex amplified libraries were pooled in equimolar concentrations with unique indices, mixed with 15% PhiX control and sequenced using MiSeq reagent kit v2 (Illumina, San Diego, CA, USA) according to manufacturer's instruction.

The raw FASTQ sequencing files were further processed after checking base quality, base composition and GC content using FASTQC toolkit. The targeted amplicons were filtered out from other superfluous sequences by detecting the specific conserved region. Forward and reverse reads were stitched together with a minimum overlap of 30 bp and maximum overlap of 250 bp. De-replication was performed using USEARCH (35) (v11) for the identification of unique sequences and chimera sequences were filtered out using the UCHIME (36) algorithm in USEARCH package. Sequences that had a similarity of 97% were grouped together under a single operational taxonomic unit (OTU) against the GreenGenes database (release 2013-08: gg_13_8_otus) using UPARSE (37) method. The taxonomy classification and relative abundance assignments were performed using 'Quantitative Insights Into Microbial Ecology' (QIIME v. 1.9.0) (38) pipeline and singletons were discarded from the dataset to minimize the effect of low abundance sequences. To confirm the annotation, the resulting OTU representative sequences were then searched against the Ribosomal Database Project naïve Bayesian classifier (RDP 10 database, version 6) (39, 40) database, using the online program SEQMATCH (40). The taxonomy classifications at the phyla, order, family, genera and species level were performed using the GreenGenes and RDP databases.

Diversity and Bacterial Enrichment Analyses

MicrobiomeAnalyst (41) was used for statistical analysis. The α-diversity indexes including observed OTU numbers, Chao index, Simpson index, and Shannon index and the β-diversity – Bray-Curtis dissimilarity measurements were calculated. Evolutionary relation of the genera unique to the OSCC samples and the normal counterparts were analyzed and a cladogram was generated using Galaxy (42). The variation in genera as well as the unique bacterial composition in the normal and OSCC samples was identified using Random Forest (43) classification analysis within MicrobiomeAnalyst (41).

To estimate β-diversity, un-weighted and weighted UniFrac distances by Bray-Curtis method were calculated from the OTU abundance and utilized in Principal Component Analysis (PCoA) to analyze the unique clustering genera for the normal and OSCC affected tissue samples. PERMANOVA (44) algorithm on un-weighted and weighted UniFrac distance matrices was applied to generate PCoA plots. The differential abundances of OTUs and specific OTU enrichment between OSCC samples and matched controls were determined using LEfSe based on Kruskal–Wallis H test. Pairwise OTU enrichment analysis was performed to specifically identify the OTU abundance in each sample pair by comparing their true abundance values in the OSCC sample and its normal counterpart.

Functional Prediction of Distinct Bacterial Communities

Functional compositions of the bacterial communities among two different groups were predicted using Phylogenetic Investigation of Communities by Reconstruction of Unobserved States (PICRUSt) (45) according to the Kyoto Encyclopedia of Genes and Genomes (KEGG) database (46).

Real-Time PCR Primer Designing and Data Output

Primer-BLAST tool (https://www.ncbi.nlm.nih.gov/tools/primer-blast/) in National Center for Biotechnology Information (NCBI) database was used to design primers for real-time quantitative PCR (qPCR) analyses. Primers for conserved sequence of bacterial 16S rRNA gene, human Glyceraldehyde 3-phosphate dehydrogenase (GAPDH) gene and human oncogenic viruses

HPV16, HPV18 and EBV are listed in **Table S2**. qPCR primers were obtained from Integrated DNA Technologies, Inc. (Coralville, IA, USA). The optimum primer melting temperature (Tm) was chosen at 60°C and the maximum GC content was kept at 55%. qPCR analysis was performed using iTaq Universal SYBR Green Supermix (BIO-RAD, Hercules, CA, USA) in CFX Connect Real-Time PCR detection System (BIO-RAD, Hercules, CA, USA) with the following thermal profile – one cycle: 95°C for 10 min; 40 cycles: 95°C for 10 s followed by 60°C for 10 s; and finally the dissociation curve at – 95°C for 1 min, 55°C 10 s, and 95°C for 10 s. Unless and otherwise stated, each sample was performed in duplicate and calculation was made using a −ΔCT method to quantify relative abundance compared with human genomic GAPDH control. The $-\Delta C_t$ values of each OSCC samples and their match controls were plotted using GraphPad Prism 8.0.1.

RESULTS

Subject Characteristics and Oral Microbiota Profiling by 16S rRNA V3-V4 Amplicon Sequencing

To investigate changes in the oral microbiome associated with OSCC development, we prospectively collected cancerous lesions and anatomically matched adjacent normal tissue samples from four OSCC patients. Prior to proceeding into 16S rRNA amplicon based metagenomics studies, a preliminary verification was conducted for confirmatory presence of bacterial species in the isolated genomic DNA from the clinical samples. A real time quantitative PCR (qPCR) assay was performed using primer against the 16S rDNA conserved region. Excellent PCR amplification curves and $-\Delta C_t$ values calculated against the housekeeping human GAPDH gene demonstrated the presence of bacterial species in both OSCC samples and their normal counterparts (**Figure S1**). To expand and substantiate our initial observations, we further collected another 46 pair of OSCC lesions and adjacent healthy tissue samples. The bacterial DNA was isolated from all 50 pair specimens (**Table S1**), followed by PCR amplification targeting the 16S rRNA V3–V4 hypervariable region. The 16S amplicons were purified, and a second round of index PCR was performed. The multiplex amplified libraries were pooled at equimolar concentrations and sequenced on an Illumina MiSeq platform. A total of 477,411 raw sequences were generated and after quality trimming and chimera checking, 322,656 high quality sequences were recovered for downstream analysis, with an average of 3,226 reads, ranging from 1,703 to 11,411 reads per sample.

Genera Abundance and Diversity of Oral Microecology Were Depleted During OSCC Development

FASTQ files generated in 16S rRNA gene sequencing of all 50 samples containing high quality sequences were further analyzed using MicrobiomeAnalyst, a web-based online tool for comprehensive statistical analysis of microbiome data (41). Rarefaction plot generated from the mapped reads indicated a clear difference of the OTU (Operational Taxonomic Unit) richness at the genus level between OSCC and normal samples (**Figure 1A**). Most of the samples, though not entirely, reached a saturated plateau phase, indicating further sequencing would possibly generate additional genera in those samples (**Figure 1A**). The average data of rarefaction plot demonstrated elevated genus richness in anatomically matched controls (samples 1–50) as compared to the paired contralateral OSCC lesions (samples 51–100), signifying a potential loss of certain genera during OSCC progression (**Figure 1A).** The OTU richness was further analyzed by calculating alpha diversity of oral microbiota, indicating the differences and similarities of the identified genera between the two sample groups (**Figures 1B–E**). The Observed genus (p = 0.000463) and Chao1 index (p = 0.00101) indicated that the OTU richness was significantly depleted in the OSCC samples as compared to the matched controls. The diversity estimator Shannon index (p = 0.00849) indicated that relative diversity of bacterial genera was significantly decreased in cancerous lesions in contrast to the normal tissue sections (**Figures 1B–D respectively**). A similar trend of depletion in relative diversity of bacterial genera in OSCC samples as compared to the normal counterparts was also observed by employing Simpson index, although the data was not statistically significant (p = 0.070680) (**Figure 1E**).

Anatomically Matched OSCC and Normal Samples Comprised of Distinct Microbiome Composition

The beta diversity indicates the difference in the composition of bacterial community among different sample groups (47). To estimate β-diversity, weighted UniFrac distances as well as Bray-Curtis dissimilarity metric were calculated from the OTU abundance and utilized in Principal Component Analysis (PCoA) (47). Permutational Multivariate Analysis of Variance (PERMANOVA) (44) algorithm on Bray-Curtis dissimilarity and weighted UniFrac distance matrices was applied to generate PCoA plots (**Figures 2A, B**, respectively). The bacterial communities in the cancerous lesions and the anatomically matched controls clustered discretely, suggesting the overall structures of the bacterial communities in the groups were significantly different ($p < 0.002$ and $p < 0.009$, respectively in two analyses) (**Figures 2A, B**).

A 'Random Forest' algorithm (43) was applied to further confirm the difference in bacterial community among the OSCC samples and anatomically matched healthy controls (**Figure 2C**). The decision trees extracted from the random forest classification identified distinct bacterial composition in diseased samples when compared with the normal counterparts. In the error plots identified from random forest analyses, while the red-line indicated the overall genera present in both OSCC and normal samples, green-line indicated the distinct genera present in the normal samples and the blue-line indicated the specific genera present in the OSCC lesions (**Figure 2C).** Moreover, in the total of 50 OSCC samples, 32 samples revealed unique and 18 samples demonstrated overlapping genera; whereas in case of contralateral

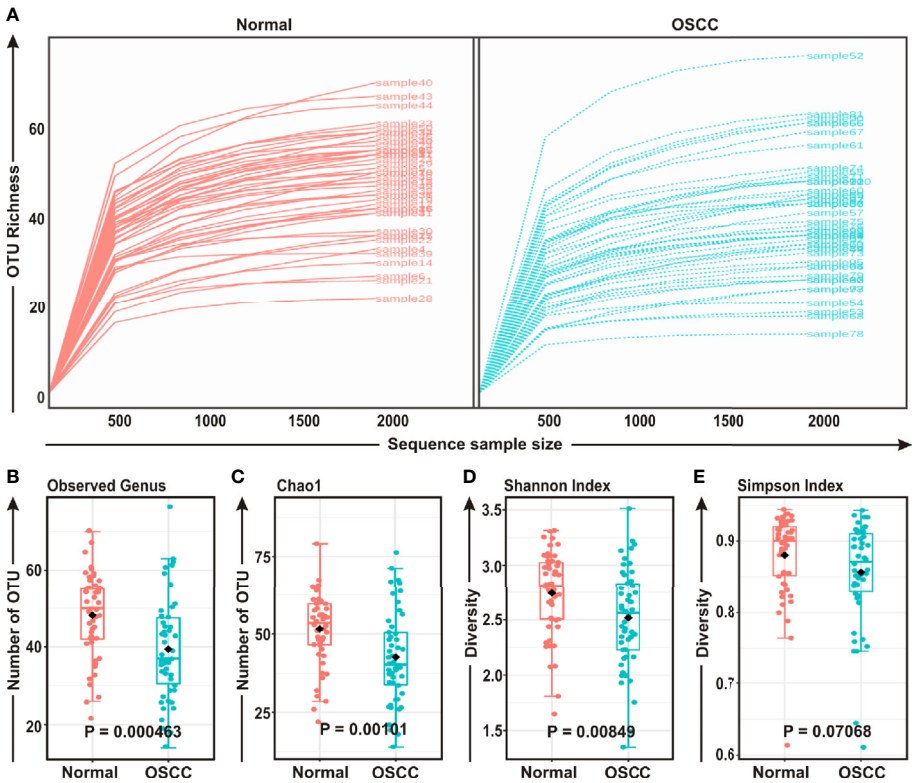

FIGURE 1 | Comparison of oral microbiome compositions in the oral squamous cell carcinoma (OSCC) lesions and contralateral normal healthy groups. **(A)** Rarefaction analysis of bacterial 16S rRNA gene sequences of normal (red) and OSCC lesions (blue). Each line represents one sample. **(B–E)** Box-Whisker plots of **(B)** Observed operational taxonomic units (OTUs), **(C)** Chao 1 and **(D)** Shannon Index, **(E)** Simpson Index respectively.

paired 50 normal tissue samples, 38 samples exhibited unique and 12 samples showed overlapping genera (**Figure 2C**).

Phylogenetic Analysis Revealed Variations Among Common and Distinct Taxa in OSCC Lesions and Anatomically Matched Healthy Controls

The bacterial communities in the OSCC lesions and the anatomically matched healthy controls were first analyzed at phylum level (**Figures 3A, B**). The top five most abundant phyla including *Firmicutes, Proteobacteria, Fusobacteria, Bacteroidetes*, and *Actinobacteria* collectively comprised of 97.3% and 93% of all sequences in matched controls and OSCC lesions, respectively (**Figure 3B**). *Firmicutes* was the most abundant phylum in all samples, accounting for 36.1% of sequences in matched controls and 30.5% in OSCC lesions. In contrast, the abundances of the other detected phyla, including *Epsilonbacteraeota*, *Spirochaetes*, *Patescibacteria*, *Tenericutes*, *Synergistetes*, and *Deinococcus*, were less than 4.0%, ranges from 0.3% to 3.96%. While abundance of phyla including *Firmicutes, Proteobacteria* and *Actinobacteria* were reduced, *Fusobacteria, Bacteroidetes*, *Epsilonbacteraeota*, and *Spirochaetes* were elevated in OSCC lesions compared to normal healthy controls (**Figures 3A, B**). At the genus level, *Streptococcus*, *Leptotrichia*, *Fusobacterium*, *Serratia*, *Neisseria*, *Haemophilus*, *Gemella*, *Campylobacter*, *Veillonella*, *Capnocytophaga*, *Prevotella*, *Porphyromonas*, *Rothia*, *Bifidobacterium*, and *Bacteroides* were the fifteen most abundant genera, comprising of 13.63%, 8.77%, 6.42%, 6.14%, 4.97%, 4.28%, 2.96%, 2.67%, 2.47%, 2.24%, 2.12%, 1.87%, 1.87%, 1.85%, and 1.84% sequence coverage, respectively (**Figures S2A-C**). Of all genera detected, 137 taxa were found common in all samples, while 26 and 29 taxa were distinctly present OSCC lesions and anatomically matched controls, respectively (**Figure S2D**). The shared genera among OSCC lesions and normal samples collectively represented more than 97.0% of all detected sequences in oral microbiota (**Figure S2**).

In order to further determine the differential presence and abundance of oral microbial community a phylogenetic tree was generated up to class level by MicrobiomeAnalyst (**Figure 3C**). The result demonstrated that Rudrobacteria class under phylum Actinobacteria was exclusively present in normal samples, whereas Deinococcus phylum was exclusively present in OSCC lesions (**Figure 3C**). A number of bacterial genera under the classes of Gammaproteobacteria, Clostridia, Negativicutes, Bacilli, Actinobacteria, Bacteroidea and Fusobacteria demonstrated an elevated abundance in both groups without significant deference in distribution between OSCC lesions and anatomically matched normal samples (**Figure 3C**).

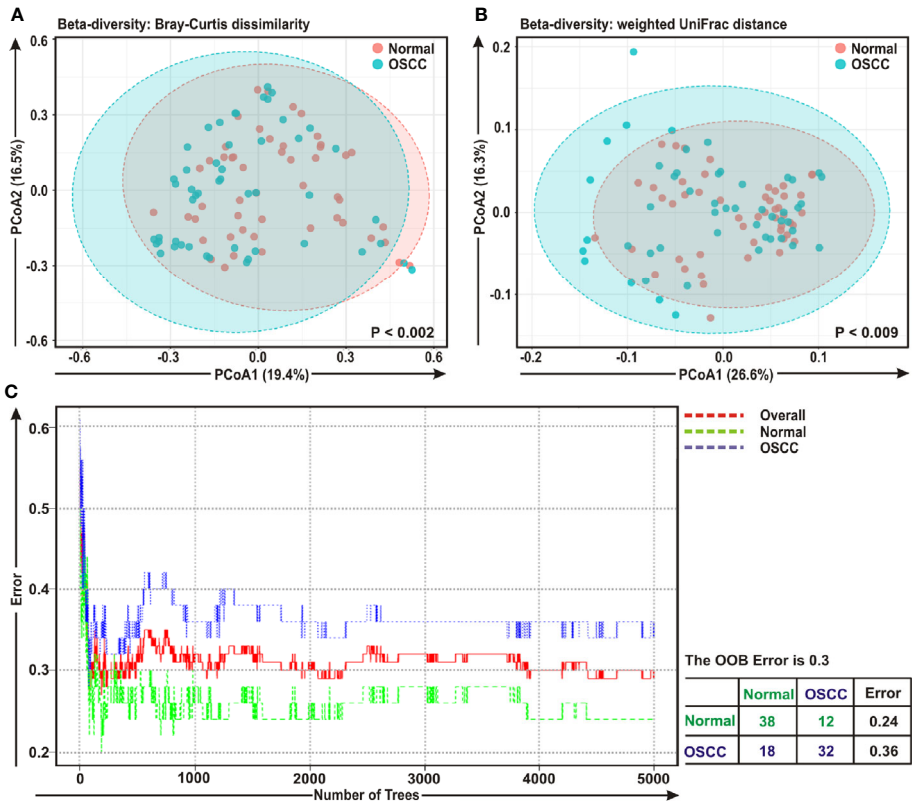

FIGURE 2 | Beta diversity analyses among cancerous and normal samples. Principal Component Analysis (PCoA) plots based on **(A)** Bray-Curtis dissimilarity and **(B)** weighted UniFrac distance matrices with respect to the bacterial abundance and composition among oral squamous cell carcinoma (OSCC) lesions and adjacent normal tissue samples. **(A)** Axis 1 (PCoA1): 19.4% of variation explained. Axis 2 (PCoA2): 16.5% of variation explained. **(B)** Axis 1 (PCoA1): 26.6% of variation explained. Axis 2 (PCoA2): 16.3% of variation explained. **(C)** The error plots identified from random forest classification analyses. Red-line indicates the overall genera present in both OSCC and normal samples, green-line indicates the distinct genera present in the normal samples and the blue-line indicates the specific genera present in the OSCC lesions.

Enrichment Analysis Identified Unique Genera for OSCC and Adjacent Normal Tissue Samples

Cladistic analysis allows for a precise definition of biological classification in which organisms are categorized in 'clades' (or groups) based on the most recent common ancestor and are best depicted by cladogram models indicating the relation between the different levels of clades in multiple sample groups. Identification of differential microbial ecology at phylum level would thus further facilitate to correlate their potential effect on OSCC progression. A cladogram was generated using Galaxy (42), a web-based platform for bioinformatic analysis, to visualize significantly enriched bacteria taxa identified in OSCC lesions and anatomically matched adjacent control tissue samples (**Figure 4A**). The result demonstrated that while *Bacteroidetes* phylum was phylogenetically predominant, a number of phyla including *Firmicutes* and *Actinobacteria* were depleted in the cancerous lesions as compared to the healthy controls (**Figure 4A**).

Linear Discrimination Analysis (LDA) Effect Size (LEfSe) algorithm allows identifying high dimensional biomarkers among multiple study groups (48). To identify the distinguishing taxa within OSCC lesions and matched controls, we applied LEfSe method (**Figures 4B, C**). At the phylum level, *Bacteroidetes* and *Deinococcus* were significantly enriched in OSCC lesions, while *Proteobacteria*, *Firmicutes* and *Actinobacteria* were considerably diminished (**Figure 4B**). At the genus level, 22 taxa including *Serratia*, *Anoxybacilus*, *Stenotrophomonas*, *Sutterella*, *Actinomyces*, *Bacillus*, *Lysobacter*, *Paenibacillus*, *Ammoniphilus*, *Bifidobacterium*, *Megamonas*, *Collinsella*, *Brevibacillus*, *Megasphaera*, *Blautia*, *Methylobacterium*, *Prevotella_9*, *Roseburia*, *Phenylobacterium*, *Pseudopropionibacterium*, *Parabacteroides*, and *Anaerobacillus* were significantly declined in the OSCC lesions as compared to the healthy controls (**Figure 4C**). In contrast, only five taxa including *Prevotella_7*, *Corynebacterium1*, *Pseudomonus*, *Deinococcus*, and *Noviherbaspirillum* were significantly enriched in the OSCC lesions as compared to the anatomically matched control samples (**Figure 4C**). Box-Whisker dot plots along with the pair-wise genus enrichment analysis were also performed to clearly visualize the differential enrichment pattern of top five bacterial genera identified by the LEfSe analyses between OSCC lesions and contralateral anatomically matched healthy controls (**Figure S3**).

In addition, a 'Random Forest' algorithm was employed to further assess the diversity in bacterial community at the species level among the OSCC samples and anatomically matched

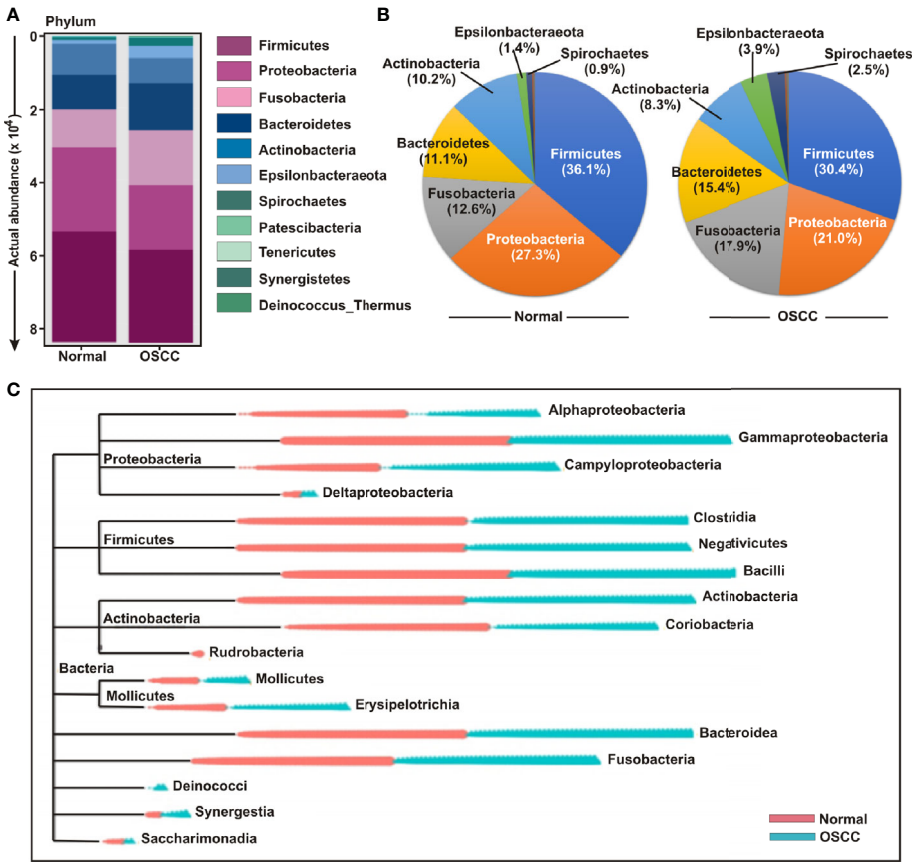

FIGURE 3 | Composition of bacterial communities across samples at the phylum and genus levels. **(A)** Actual and **(B)** relative abundance of bacterial communities at phylum level of OSCC lesions and anatomically matched controls. **(C)** Phylogenetic tree with operational taxonomic unit (OTU) abundances between OSCC and normal samples.

healthy controls (**Figure S4A**). The decision trees extracted from the random forest classification identified distinct bacterial species in OSCC lesions when compared with the normal samples (**Figure S4A**). The results demonstrated that in the total of 50 OSCC samples, 34 samples exhibited unique and 16 samples showed overlapping species, while in normal counterparts, 30 samples exhibited unique and 20 samples showed overlapping species (**Figure S4A**). LEfSe analyses further revealed *Capnocytophaga*, unidentified *Micrococcaceae* and uncultured *Cornebacterium* 1 species were considerably enriched in OSCC lesions, 29 different species, however, mostly unidentified and uncultured species, were significantly declined as compared to the paired contralateral anatomically matched controls (**Figure S4B**). Recent studies suggested that 16S rRNA based sequencing technologies targeting one or more hypervariable regions allow reliable identification of bacterial genera, but can potentially misguide identification of bacterial species (49, 50). In agreement to this, our study also demonstrated that the sequencing depth was not sufficient to accurately identify the oral microbial composition at the species level responsible for OSCC development. Therefore, to nullify the false positives at the species level, we have limited our analyses up to genus level for further investigation and subsequent conclusion.

Functional Prediction of Oral Microbiome Associated With OSCC Development

To envisage oral microbial functions connected to the development of OSCC, we employed the Phylogenetic Investigation of Communities by Reconstruction of Unobserved States (PICRUSt) (45) and accordingly Kyoto Encyclopedia of Genes and Genomes (KEGG) pathways (46) were generated specific for OSCC lesions and anatomically matched healthy controls (**Figure 5).** The LEfSe outputs demonstrated that function related to nucleotide synthesis and maintaining the fundamental functions of a cell such as pyrimidine and purine metabolism, DNA repair and recombination proteins, DNA replication, transcription machinery, amino and nucleotide sugar metabolism, protein translation related function such as ribosome, amino acid related enzymes, aminoacyl tRNA biosynthesis, peptidases, as well as peptidoglycan biosynthesis were associated with the progression of OSCC (**Figure 5A**). In contrast, parameters related to flagellar assembly, butanoate metabolism, secretion system, bacterial motility proteins, two-

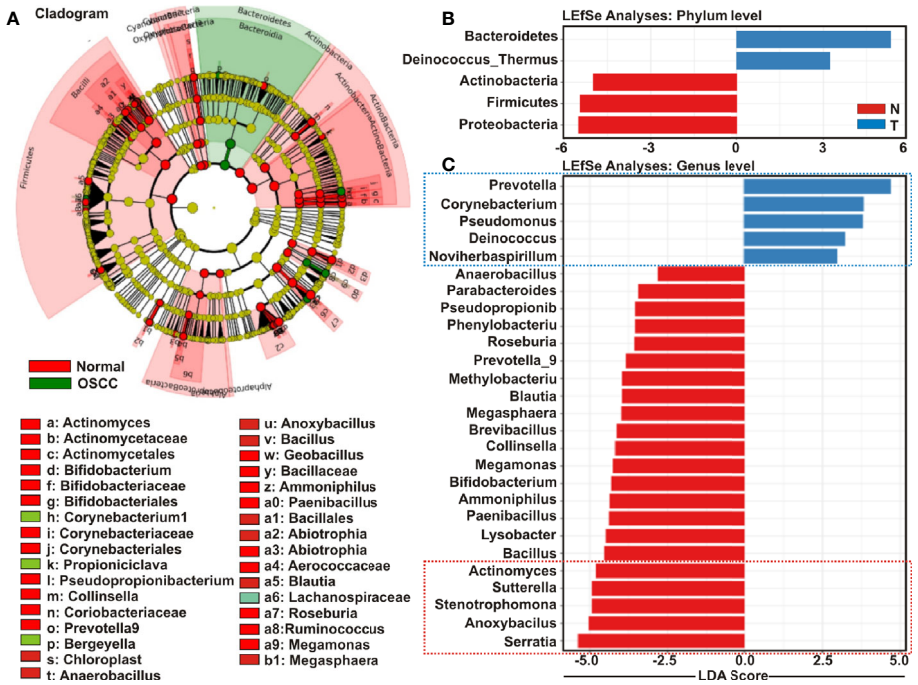

FIGURE 4 | Cladogram and enrichment analysis among among oral squamous cell carcinoma (OSCC) lesions and clinically normal tissue samples. **(A)** Cladogram for phylogenetic relation of Normal and OSCC genus. Cladogram was constructed using the Linear Discrimination Analysis (LDA) Effect Size (LEfSe) method to indicate the phylogenetic distribution of bacteria that were significantly enriched in the tumor and normal groups. LDA scores showed significant bacterial differences within groups OSCC and clinically normal counterparts at the **(B)** phylum level and **(C)** genus level.

component system and ABC transporters, were inversely associated with OSCC development (**Figure 5A).** PCoA analyses also demonstrated that the predicted functions of bacterial compositions in two groups – OSCC lesions and the anatomically matched controls were significantly clustered ($p < 0.05$) (**Figure 5B**).

Quantitative PCR Profile of Oncogenic Viruses Revealed Significant Association of HPV16 With OSCC Development

Studies suggest that a number of human oncogenic viruses including human papilloma viruses (HPVs) and Epstein-Barr virus (EBV) are associated with OSCC development (13–15). To assess the potential involvement of viral etiology in our samples we designed real time PCR primers against EBV encoded EBNA3A oncogene (GeneID: 3783762) along with two high risk HPV isotypes HPV-16 encoded E2 oncogene (GeneID: 1489080) and HPV-18 encoded E6 oncogene (GeneID: 1489088) and subsequently employed in quantitative PCR (qPCR) analyses (**Figures 6A–C).** The housekeeping gene human GAPDH gene was utilized as control assuming the genomic segment bearing GAPDH gene remained unaffected in both normal and OSCC affected tissue sections. A higher negative $-\Delta C_t$ (average GAPDH C_t value – average target primer C_t value) indicated elevated presence of the virus in the sample as detected by specific primer set targeting specific viral gene. Our results clearly demonstrated that only HPV-16 ($p = 0.004$) was significantly associated with OSCC lesions as compared to the control tissue sections (**Figure 6A**). In contrast, no significant association for both HPV-18 ($p = 0.221$) and EBV ($p = 0.326$) between the two sample groups was observed (**Figures 6B, C**, respectively). However, $-\Delta C_t$ values for both HPV-18 and EBV were higher than that of HPV-16, indicating a higher prevalence in oral tissue samples (compare **Figures 5B, C** with **5A**). Altogether these oncogenic viruses might regulate the onset as well as progression of oral cavity oncogenesis and thereby demands their detection along with bacterial dysbiosis.

Next, the co-occurrence and co-exclusion patterns of these oncogenic viruses with the 27 most abundant bacterial genera identified in LEfSe analyses in each group of OSCC lesions and contralateral matched controls were further investigated (**Figure 6D**). Overall, there was no negative correlation found in our analyses. In matched normal controls, *Prevotella_9* was found to be positively correlated with a number of bacterial genera. For example, *Prevotella_9* and *Blautia* were the most positively correlated ($\rho = 0.926$), followed by *Megamonas* ($\rho = 0.872$), *Collinsella* ($\rho = 0.852$), *Serratia* ($\rho = 0.679$), *Bifidobacterium* ($\rho = 0.673$), and *Parabacteroides* ($\rho = 0.626$). HPV-18 demonstrated moderate positive correlation with most of these genera – including *Prevotella_9* ($\rho = 0.683$), *Blautia* ($\rho = 0.660$), *Megamonas* ($\rho = 0.509$), *Collinsella* ($\rho = 0.527$), and *Parabacteroides*

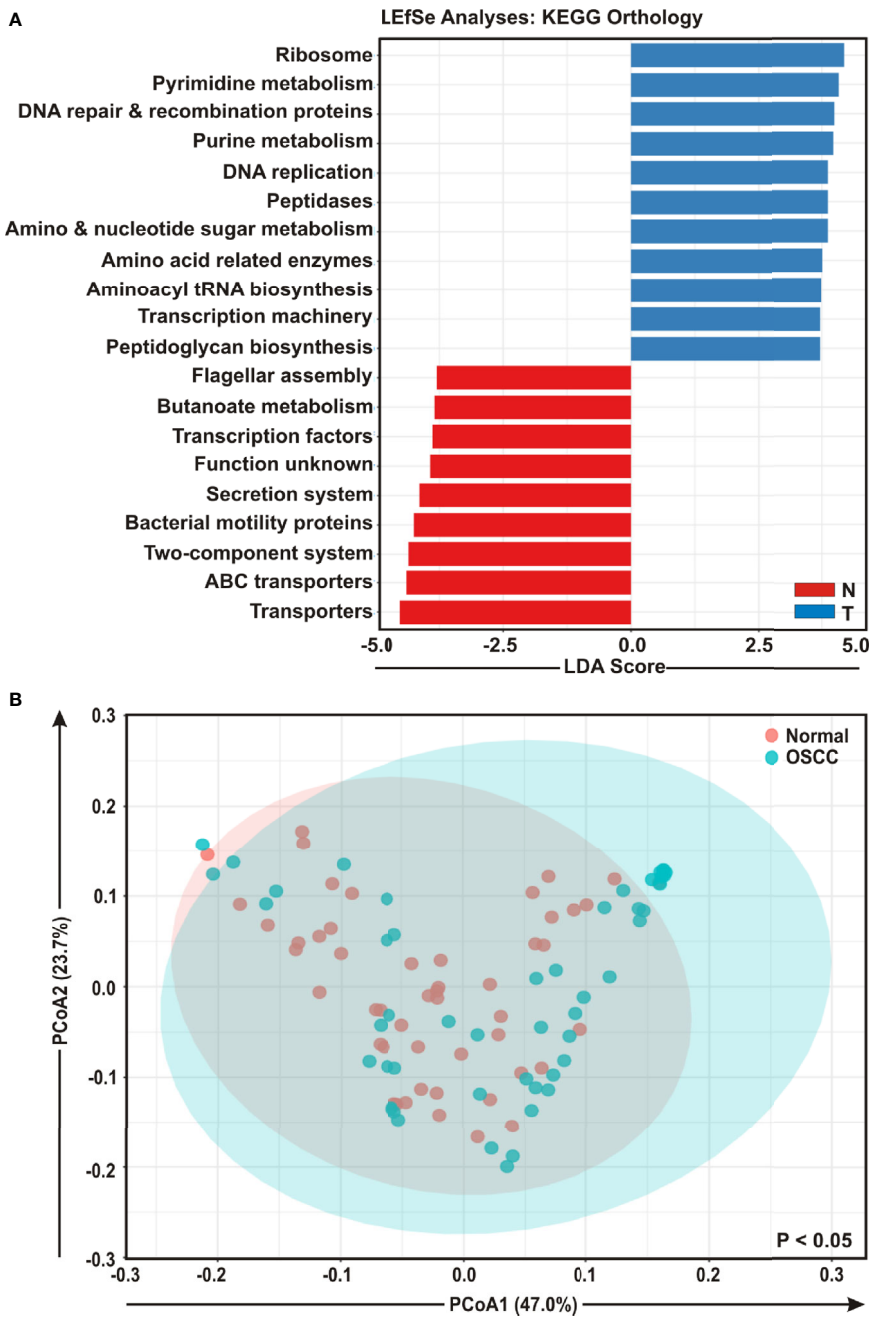

FIGURE 5 | Functional analyses of identified microbial compositions in cancerous lesions and clinically normal samples. **(A)** Linear Discrimination Analysis (LDA) scores predicting gene function enriched among two different groups of oral squamous cell carcinoma (OSCC) lesions and normal samples using Phylogenetic Investigation of Communities by Reconstruction of Unobserved States (PICRUSt) according to the Kyoto Encyclopedia of Genes and Genomes (KEGG) database. **(B)** Principal Component Analysis (PCoA) of bacterial functions associated OSCC lesions and contralateral matched controls. Axis 1 (PCoA1): 47.0% of variation explained. Axis 2 (PCoA2): 23.7% of variation explained.

(ρ = 0.514) (**Figure 6D**, **Table S3**). In contrast, HPV-16 demonstrated no positive correlation with any bacterial genera identified in cancerous lesions (**Figure 6D**). Although *Corynebacterium1* was significantly associated with OSCC lesions, it demonstrated positive correlation with several bacterial taxa abundantly enriched in normal samples (**Figure 6D**). Among these, the most positively correlated genera were *Corynebacterium1* and *Prevotella_9* (ρ = 0.785) followed by *Megamonas* (ρ = 0.657), *Blautia* (ρ = 0.643), and *Collinsella* (ρ = 0.601) (**Figure 6D**, **Table S3**).

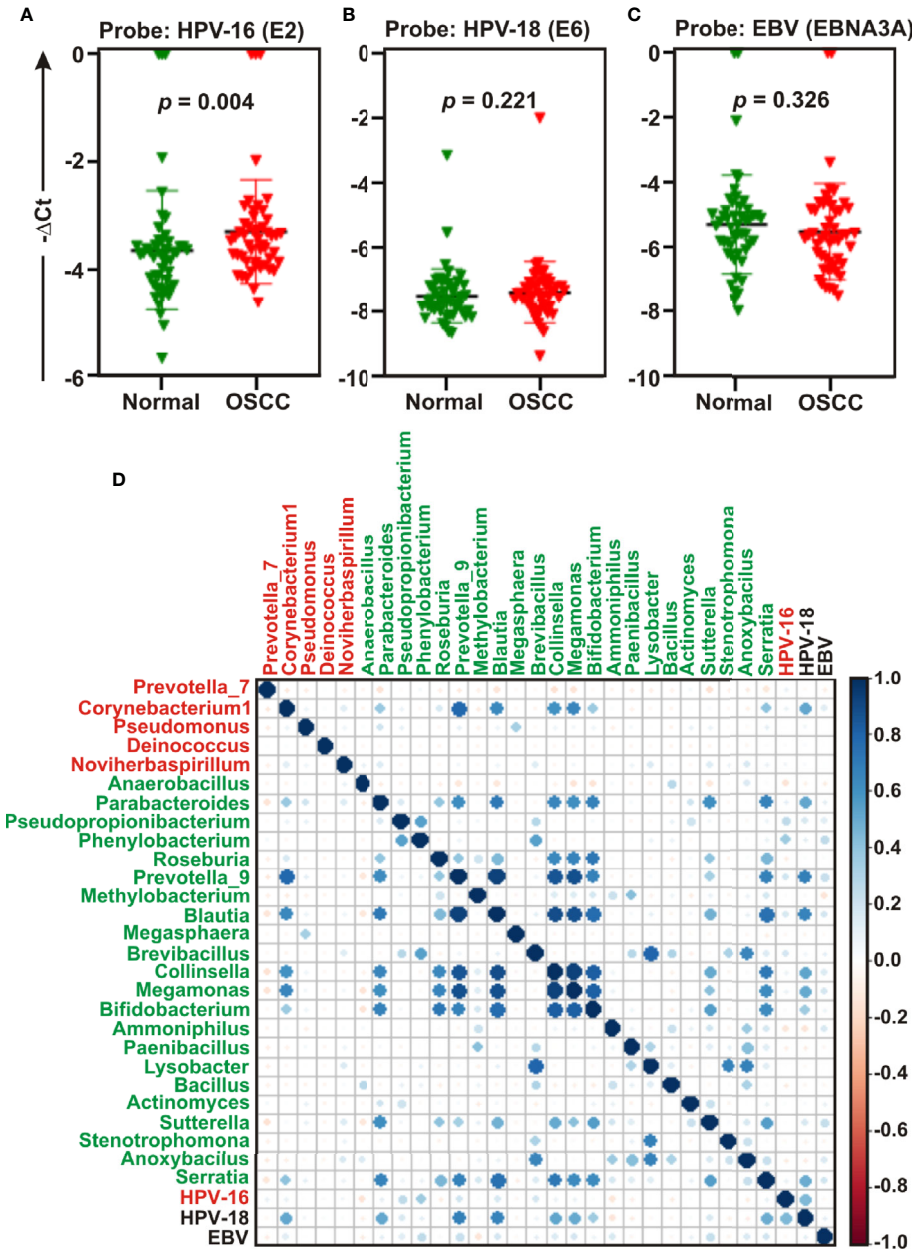

FIGURE 6 | Quantitative PCR (qPCR) and co-occurrence analysis of human oncogenic viruses with identified bacterial genera in normal and oral squamous cell carcinoma (OSCC) samples. Comparative qPCR data of **(A, B)** high risk human papilloma viruses (HPVs) - **(A)** HPV-16 **(B)** HPV-18 and **(C)** Epstein-Barr virus (EBV). PCR calculation was performed by –ΔCT method to quantify relative abundance of each tumor virus using human genomic GAPDH as control. The -ΔC_t values of each sample were plotted using GraphPad Prism 8.0.1. **(D)** Pearson correlations among human oncogenic viruses and the top 27 most abundant bacterial genera identified by Linear Discrimination Analysis (LDA) Effect Size (LEfSe) analyses were calculated and analyzed. Correlation values range from –1.00 (red) to 1.00 (blue).

DISCUSSION

In spite of the highest oral cancer incidence, accounting to 30% of all cancers in India (6, 7), so far there are no reports describing changes of oral microbiome in OSCC among Indian patients. The purpose of the current investigation was to profile the dysbiosis of oral microbiota between OSCC lesions and contralateral anatomically matched control tissue samples prospectively collected from fifty patients of eastern region of India. In agreement with Guerrero-Preston et al. study (51), we also observed a significant loss in richness and diversity of oral bacterial communities in OSCC lesions compared to matched controls. However, several reports revealed enhanced diversity of bacterial communities in OSCC samples (31, 52, 53). Nevertheless, dysbiosis of oral microbiome appears to be strongly associated with OSCC development. Overall, the

results demonstrated that *Prevotella, Corynebacterium*, *Pseudomonas*, *Deinococcus*, and *Noviherbaspirillum* genera were significantly enriched, while genera including *Actinomyces*, *Sutterella*, *Stenotrophomonas*, *Anoxybacillus*, and *Serratia* were depleted in the OSCC lesions as compared to the matched healthy controls.

Previously, several models of microbial infection and potential oral microbiome signature link to the pathology of a number of oral diseases including cancer have been established. For example, certain oral bacterial pathogens, including *Porphyromonas gingivalis* and *Fusobacterium nucleatum* have been reported to disrupt the equilibrium of oral microbiome and along with deregulated immune response eventually initiate periodontal diseases (periodontitis) (54–56). These well studied periodontal organisms subsequently prompted researchers to further investigate the precise role of dysbiotic oral micrbiota in developing oral cancer (57, 58). In general, our results agreed with the previously published data of enriched and depleted microbes associated with the OSCC development. Overall, five of the most abundant phyla including *Proteobacteria*, *Firmicutes*, *Actinobacteria*, *Bacteroidetes*, and *Fusobacteria* identified in our study were consistent with those found in previous studies. However, the less abundant phyla including *Tenericutes*, *Deinococcus*, and *Patescibacteria* detected were significantly varied among multiple studies. In addition, in line with the previous studies (29, 52, 53) *Firmicutes* was also found as the most abundant phylum in overall oral microbiome in our study. Of the significantly elevated genera in cancerous lesions, *Prevotella* and *Pseudomonus* were previously shown to be highly abundant in both periodontitis and OSCC samples when compared to healthy controls (32, 53, 59). Importantly, periodontitis has been suggested as a self-governing risk factor for OSCC development (27). Interestingly, in contrast to our finding, *Corynebacterium* was previously found to be decreased in oral cavity cancer (OCC) and oropharyngeal cancers (OPC) (60). Our results indicated presence of a unique genus *Deinococcus* although relatively less abundantly only in cancerous lesions and could not be detected in control tissue sections. Since in our study design, paired OSCC lesion and control tissue samples were obtained from single patient, it nullified the possibilities of inter-individual variation. Thus even small differences of bacterial communities among two these groups would represent significance in OSCC development. Species of the *Deinococcus* genus are recognized for their extreme resistance to ionizing radiation and oxidative stress and other damaging conditions (61). Although a number of earlier studies indicated the presence of *Deinococcus* genus (62, 63), the precise role of the members of this genus in OSCC is yet to be defined.

In our study, although *Fusobacteria* was identified as one of the most abundant phyla in overall oral bacteriome, its abundance showed no significant difference between OSCC lesions and normal tissue samples. This is in contrast to a number of recent reports which demonstrated significant abundance of several members of *Fusobacteriem* in OSCC lesions when compared to normal samples (31, 32). Mager et al. detected *F. periodonticum* in the saliva sample from OSCC patients using specific bacteria probes, but its abundance showed no significantly difference between OSCC-positive and OSCC-free patients (30). Yang et al. determined significant elevation of *F. periodonticum* species in OSCC lesions, whereas no significant difference was observed in case of *F. nucleatum* between tumor and normal samples (52). In contrast, Al-Hebshi *et al.* indicated that *F. nucleatum* was the most significantly enriched species in OSCC lesions as compared to the control normal tissues (32). The diverse presence of different members of *Fusobacterium* species identified in OSCC samples in multiple studies possibly arose due to varied sample types as well as subjects recruited of different ethnicity across the world. In addition, *Fusobacterium nucleatum* was also identified as one of the highly enriched bacterial species in colorectal cancer (64). Moreover, Komiya et al. showed that patients with colorectal cancer (CRC) have identical strains of *Fusobacterium nucleatum* in their CRC tissue section and oral cavity (65). Given the importance of *Fusobacterium* in various human cancers, further in depth investigation is required to verify *Fusobacterium* association with OSCC in Indian scenario with larger patients sample size.

Nucleotide metabolism is an important pathway that provides purine and pyrimidine molecules for DNA replication, RNA biogenesis, as well as cell bioenergetics. Increased nucleotide metabolism supports uncontrolled proliferation of cancer cells and thus represents a hallmark of cancer (66). Apart from nucleotide metabolisms, several critical pathways like DNA repair, recombination, protein synthesis and transcription machineries are frequently altered in tumor cells (67–69). Moreover, inhibitors that specifically blocks DNA replication and induce DNA damages have been widely used as chemotherapeutic agents against numerous cancers (70). In agreement to this, our PICRUSt analyses showed that function related to nucleotide metabolisms including both purine and pyrimidine synthesis as well as basic cell functions like DNA repair and replication and functions related to mRNA translation including ribosome, amino acid related enzymes, aminoacyl tRNA biosynthesis and peptidases were significantly linked to OSCC development. Although Yost et al. using metatranscriptomic analyses suggested importance of these pathways for OSCC development (71), so far there are no robust studies that directly linked microbes with these pathways in a tumor microenvironment. Moreover, in contrast to our study, Yang et al. demonstrated that parameters related to protein and amino acids metabolisms were inversely associated with OSCC progression from stage 1 to stage 4 patients (52). Previously a number of reports demonstrated that pathways related to bacterial chemotaxis and flagellar assembly were remarkably enriched in the OSCC group (32, 59). However, in contrast, our study showed that pathways related to flagellar assembly and bacterial motility proteins were inversely associated with the OSCC development.

A growing body of evidence suggested a potential association of several human tumor viruses with oral cancers (13–15, 72). For example, while low risk HPV subtypes including HPV-6 and HPV-11 are associated with a variety of oral benign papillomatous lesions such as oral squamous papilloma, oral verruca vulgaris, oral condyloma accuminatum and focal epithelial hyperplasia, high risk HPV subtypes including HPV-16 and HPV-18 are associated with malignant lesions (72–75). The transformation

of normal oral mucosa in OSCC is potentially linked to precancerous lesions, such as OLP (76, 77). Although the precise role of viral mediated malignant transformation of precancerous lesions is not clear, HPV infection is significantly associated with OLP (72, 78). Overall, previous studies suggested that HPV-16 is the most frequently detected HPV subtype in oral cancers (79) and accordingly in 2012 the International Agency of Research of Cancer (IARC) acknowledged the significant association of HPV-16 high risk group with oral cancer development (14). In agreement to this, our results also demonstrated that HPV-16 but not HPV-18 was significantly associated with OSCC lesions as compared to anatomically matched control tissue sections.

In sum, using a carefully controlled patients' cohort, herein we identified specific microbial signature associated with OSSCC development. However, the current study has several limitations including constraints associated with the 16S rRNA gene amplification based sequencing technologies (49, 50). Recent studies suggested although more than 99% of sequencing reads could be correctly classified at the genus level, a significant proportion at the species level might be misclassified during identification of bacterial populations by targeting various variable regions of the 16S rRNA gene. In agreement to this, our study also showed that the sequencing depth was not adequate to precisely classify the oral microbiota at the species level and thus, in order to nullify false positives, we restricted our analyses up to genus level. Another limitation of this study was relatively smaller sample size. In future, to validate the results a larger sample size with distinct cancer stages among population in different regions and different socioeconomic background would be highly preferable. We additionally lacked information on the involvement of other organisms particularly fungus and the association of different viruses with OSCC development. Strategies such as whole genome sequencing and metabolomics would allow in identification of changes of overall oral microbiota and their metabolities during OSCC development. Moreover, whole genome shotgun sequencing (metagenomics) would further validate the functional inferences from 16S rRNA amplicon sequences obtained using PICRUSt. Since the current study was conducted using tissue biopsy samples, it would be interesting to investigate whether the results could be extended in a non-invasive method by utilizing saliva samples. Altogether, longitudinal research activities are greatly demanded to explore the functional implications of the oral microbiota in terms of diagnosis and risk assessment of OSCC development, as well as potential expansion of current therapeutic strategies to restore the health of the oral ecosystem.

DATA AVAILABILITY STATEMENT

The 16S rRNA amplicon sequencing data from this study have been deposited in the NCBI BioProject under accession number PRJNA666746.

ETHICS STATEMENT

The studies involving human participants were reviewed and approved by the Institutional Ethics Committee for Human Research, Indian Statistical Institute, Kolkata, India. The patients/participants provided their written informed consent to participate in this study.

AUTHOR CONTRIBUTIONS

PS and AS wrote the main manuscript text. PS, SM, SL, RC, and AS performed the bioinformatic analysis. PS and SB performed the experiments. JR recruited the patients and conducted the histopathological studies. SD and RC collected the samples and performed sampling. AS conceived, designed, and successfully sought funding for the study. All authors contributed to the article and approved the submitted version.

FUNDING

This study was supported by grants from DBT/Wellcome Trust India Alliance Intermediate Fellowship research grant [IA/I/14/2/501537] and Science & Technology and Biotechnology, Govt. of West Bengal [1798 (Sanc.)/ST/P/S&T/9G-5/2019] to A.S. The funders had no role in study design, data collection and analysis, decision to publish, or preparation of the manuscript.

ACKNOWLEDGMENTS

The authors would like to thank all patients for making this study possible. The authors thank all members of both AS and RC laboratories for valuable suggestions and discussions of the experiment. AS is Wellcome Trust/DBT India Alliance Intermediate Fellow. PS and SL are recipients of CSIR-NET Research Fellowships and SM is a recipient of UGC-NET Research Fellowships.

SUPPLEMENTARY MATERIAL

The Supplementary Material for this article can be found online at: https://www.frontiersin.org/articles/10.3389/fonc.2021.614448/full#supplementary-material

Supplementary Figure 1 | Preliminary quantitative PCR (qPCR) analyses of four OSCC and anatomically matched normal samples. PCR calculation was performed by −ΔCT method to quantify relative abundance of overall bacteria using primers against the conserved region of 16S rRNA gene and human genomic GAPDH gene segment as control. The -ΔC_t values of each sample were plotted using GraphPad Prism 8.0.1.

Supplementary Figure 2 | Differentially abundant genera in OSCC lesions and anatomically matched normal samples. Relative abundance (%) of the taxa at the genus level in **(A)** all samples, **(B)** anatomically matched control tissues and **(C)** OSCC lesions. **(D)** Venn diagram depicts distinct and overlapped genera among OSCC and normal samples.

Supplementary Figure 3 | Top five taxa at genus level identified in the LEfSe analysis among OSCC lesions and healthy matched controls. Box Whisker Plot (top) and Pair-wise (bottom) genus enrichment analysis of top five bacterial genera

identified in LEFSe analysis as described in **Figure 4**among **(A)** normal samples and **(B)** OSCC lesions.

Supplementary Figure 4 | Bacterial composition at the species level between paired OSCC lesions and contralateral normal tissue samples. **(A)** The error plots identified from random forest classification analyses. Red-line indicates the overall species present in both OSCC and normal samples, green-line indicates the distinct species present in the normal samples and the blue-line indicates the specific species present in the OSCC lesions. **(B)** Linear discriminant analysis effect size (LEfSe) analysis demonstrating differential bacterial composition at the species level between the OSCC lesions and anatomically matched healthy controls.

Supplementary Table 1 | Clinical characteristics of patients' samples.

Supplementary Table 2 | Real time PCR primers.

Supplementary Table 3 | Pearson correlations among HPV-16, HPV-18, EBV and the top 27 most abundant bacterial genera identified by LEfSe analyses.

REFERENCES

1. Vigneswaran N, Williams MD. Epidemiologic trends in head and neck cancer and aids in diagnosis. *Oral Maxillofac Surg Clin North Am* (2014) 26(2):123–41. doi: 10.1016/j.coms.2014.01.001
2. Rischin D, Ferris RL, Le QT. Overview of Advances in Head and Neck Cancer. *J Clin Oncol* (2015) 33(29):3225–6. doi: 10.1200/JCO.2015.63.6761
3. Parkin DM, Bray F, Ferlay J, Pisani P. Global cancer statistics, 2002. *CA Cancer J Clin* (2005) 55(2):74–108. doi: 10.3322/canjclin.55.2.74
4. Warnakulasuriya S. Causes of oral cancer–an appraisal of controversies. *Br Dent J* (2009) 207(10):471–5. doi: 10.1038/sj.bdj.2009.1009
5. Nunez-Gonzalez S, Delgado-Ron JA, Gault C, Simancas-Racines D. Trends and Spatial Patterns of Oral Cancer Mortality in Ecuador, 2001-2016. *Int J Dent* (2018) 2018:6086595. doi: 10.1155/2018/6086595
6. Basu B, Chakraborty J, Chandra A, Katarkar A, Baldevbhai JRK, Dhar Chowdhury D, et al. Genome-wide DNA methylation profile identified a unique set of differentially methylated immune genes in oral squamous cell carcinoma patients in India. *Clin Epigenet* (2017) 9:13. doi: 10.1186/s13148-017-0314-x314
7. Byakodi R, Byakodi S, Hiremath S, Byakodi J, Adaki S, Marathe K, et al. Oral cancer in India: an epidemiologic and clinical review. *J Community Health* (2012) 37(2):316–9. doi: 10.1007/s10900-011-9447-6
8. Tajmirriahi N, Razavi SM, Shirani S, Homayooni S, Gasemzadeh G. Evaluation of metastasis and 5-year survival in oral squamous cell carcinoma patients in Isfahan (2001-2015). *Dent Res J (Isfahan)* (2019) 16 (2):117–21. doi: 10.4103/1735-3327.250974
9. Geum DH, Roh YC, Yoon SY, Kim HG, Lee JH, Song JM, et al. The impact factors on 5-year survival rate in patients operated with oral cancer. *J Korean Assoc Oral Maxillofac Surg* (2013) 39(5):207–16. doi: 10.5125/jkaoms.2013.39.5.207
10. Rogers SN, Brown JS, Woolgar JA, Lowe D, Magennis P, Shaw RJ, et al. Survival following primary surgery for oral cancer. *Oral Oncol* (2009) 45 (3):201–11. doi: 10.1016/j.oraloncology.2008.05.008
11. Parra C, Jodar-Sanchez F, Jimenez-Hernandez MD, Vigil E, Palomino-Garcia A, Moniche-Alvarez F, et al. Development, Implementation, and Evaluation of a Telemedicine Service for the Treatment of Acute Stroke Patients: TeleStroke. *Interact J Med Res* (2012) 1(2):e15. doi: 10.2196/ijmr.2163
12. Bagan J, Sarrion G, Jimenez Y. Oral cancer: clinical features. *Oral Oncol* (2010) 46(6):414–7. doi: 10.1016/j.oraloncology.2010.03.009
13. Gupta K, Metgud R. Evidences suggesting involvement of viruses in oral squamous cell carcinoma. *Patholog Res Int* (2014) 2013:642496. doi: 10.1155/2013/642496
14. Kim SM. Human papilloma virus in oral cancer. *J Korean Assoc Oral Maxillofac Surg* (2016) 42(6):327–36. doi: 10.5125/jkaoms.2016.42.6.327
15. She Y, Nong X, Zhang M, Wang M. Epstein-Barr virus infection and oral squamous cell carcinoma risk: A meta-analysis. *PloS One* (2017) 12(10): e0186860. doi: 10.1371/journal.pone.0186860PONE-D-17-18573
16. Cho I, Blaser MJ. The human microbiome: at the interface of health and disease. *Nat Rev Genet* (2012) 13(4):260–70. doi: 10.1038/nrg3182
17. Elinav E, Garrett WS, Trinchieri G, Wargo J. The cancer microbiome. *Nat Rev Cancer* (2019) 19(7):371–6. doi: 10.1038/s41568-019-0155-310.1038/s41568-019-0155-3
18. Malla MA, Dubey A, Kumar A, Yadav S, Hashem A, Abd Allah EF. Exploring the Human Microbiome: The Potential Future Role of Next-Generation Sequencing in Disease Diagnosis and Treatment. *Front Immunol* (2019) 9:2868:2868. doi: 10.3389/fimmu.2018.02868
19. Deo PN, Deshmukh R. Oral microbiome: Unveiling the fundamentals. *J Oral Maxillofac Pathol* (2019) 23(1):122–8. doi: 10.4103/jomfp.JOMFP_304_18JOMFP-23-122
20. Beck JD, Offenbacher S. Systemic effects of periodontitis: epidemiology of periodontal disease and cardiovascular disease. *J Periodontol* (2005) 76(11 Suppl):2089–100. doi: 10.1902/jop.2005.76.11-S.2089
21. Bingham CO, Moni M. Periodontal disease and rheumatoid arthritis: the evidence accumulates for complex pathobiologic interactions. *Curr Opin Rheumatol* (2013) 25(3):345–53. doi: 10.1097/BOR.0b013e32835fb8ec
22. Daniel R, Gokulanathan S, Shanmugasundaram N, Lakshmigandhan M, Kavin T. Diabetes and periodontal disease. *J Pharm Bioallied Sci* (2012) 4 (Suppl 2):S280–2. doi: 10.4103/0975-7406.100251JPBS-4-280
23. Walia M, Saini N. Relationship between periodontal diseases and preterm birth: Recent epidemiological and biological data. *Int J Appl Basic Med Res* (2015) 5(1):2–6. doi: 10.4103/2229-516X.149217IJABMR-5-2
24. Curtis MA, Zenobia C, Darveau RP. The relationship of the oral microbiotia to periodontal health and disease. *Cell Host Microbe* (2011) 10(4):302–6. doi: 10.1016/j.chom.2011.09.008
25. Preza D, Olsen I, Aas JA, Willumsen T, Grinde B, Paster BJ. Bacterial profiles of root caries in elderly patients. *J Clin Microbiol* (2008) 46(6):2015–21. doi: 10.1128/JCM.02411-07
26. Chhour KL, Nadkarni MA, Byun R, Martin FE, Jacques NA, Hunter N. Molecular analysis of microbial diversity in advanced caries. *J Clin Microbiol* (2005) 43(2):843–9. doi: 10.1128/JCM.43.2.843-849.2005
27. Tezal M, Sullivan MA, Hyland A, Marshall JR, Stoler D, Reid ME, et al. Chronic periodontitis and the incidence of head and neck squamous cell carcinoma. *Cancer Epidemiol Biomarkers Prev* (2009) 18(9):2406–12. doi: 10.1158/1055-9965.EPI-09-0334
28. Karpinski TM. Role of Oral Microbiota in Cancer Development. *Microorganisms* (2019) 7(1):20. doi: 10.3390/microorganisms7010020
29. Schmidt BL, Kuczynski J, Bhattacharya A, Huey B, Corby PM, Queiroz EL, et al. Changes in abundance of oral microbiota associated with oral cancer. *PloS One* (2014) 9(6):e98741. doi: 10.1371/journal.pone.0098741PONE-D-13-34607
30. Mager DL, Haffajee AD, Devlin PM, Norris CM, Posner MR, Goodson JM. The salivary microbiota as a diagnostic indicator of oral cancer: a descriptive, non-randomized study of cancer-free and oral squamous cell carcinoma subjects. *J Transl Med* (2005) 3:27. doi: 10.1186/1479-5876-3-27
31. Zhao H, Chu M, Huang Z, Yang X, Ran S, Hu B, et al. Variations in oral microbiota associated with oral cancer. *Sci Rep* (2017) 7(1):11773. doi: 10.1038/s41598-017-11779-910.1038/s41598-017-11779-9
32. Al-Hebshi NN, Nasher AT, Maryoud MY, Homeida HE, Chen T, Idris AM, et al. Inflammatory bacteriome featuring Fusobacterium nucleatum and Pseudomonas aeruginosa identified in association with oral squamous cell carcinoma. *Sci Rep* (2017) 7(1):1834. doi: 10.1038/s41598-017-02079-310.1038/s41598-017-02079-3
33. Lee WH, Chen HM, Yang SF, Liang C, Peng CY, Lin FM, et al. Bacterial alterations in salivary microbiota and their association in oral cancer. *Sci Rep* (2017) 7(1):16540. doi: 10.1038/s41598-017-16418-x10.1038/s41598-017-16418-x
34. Bornigen D, Ren B, Pickard R, Li J, Ozer E, Hartmann EM, et al. Alterations in oral bacterial communities are associated with risk factors for oral and oropharyngeal cancer. *Sci Rep* (2017) 7(1):17686. doi: 10.1038/s41598-017-17795-z10.1038/s41598-017-17795-z
35. Edgar RC. Search and clustering orders of magnitude faster than BLAST. *Bioinformatics* (2010) 26(19):2460–1. doi: 10.1093/bioinformatics/btq461

36. Edgar RC, Haas BJ, Clemente JC, Quince C, Knight R. UCHIME improves sensitivity and speed of chimera detection. *Bioinformatics* (2011) 27 (16):2194–200. doi: 10.1093/bioinformatics/btr381
37. Edgar RC. UPARSE: highly accurate OTU sequences from microbial amplicon reads. *Nat Methods* (2013) 10(10):996–8. doi: 10.1038/nmeth.2604
38. Caporaso JG, Kuczynski J, Stombaugh J, Bittinger K, Bushman FD, Costello EK, et al. QIIME allows analysis of high-throughput community sequencing data. *Nat Methods* (2010) 7(5):335–6. doi: 10.1038/nmeth.f.303
39. Wang Q, Garrity GM, Tiedje JM, Cole JR. Naive Bayesian classifier for rapid assignment of rRNA sequences into the new bacterial taxonomy. *Appl Environ Microbiol* (2007) 73(16):5261–7. doi: 10.1128/AEM.00062-07
40. Cole JR, Wang Q, Fish JA, Chai B, McGarrell DM, Sun Y, et al. Ribosomal Database Project: data and tools for high throughput rRNA analysis. *Nucleic Acids Res* (2014) 42(Database issue):D633–42. doi: 10.1093/nar/gkt1244
41. Dhariwal A, Chong J, Habib S, King IL, Agellon LB, Xia J. MicrobiomeAnalyst: a web-based tool for comprehensive statistical, visual and meta-analysis of microbiome data. *Nucleic Acids Res* (2017) 45(W1): W180–W8. doi: 10.1093/nar/gkx295
42. Afgan E, Baker D, Batut B, van den Beek M, Bouvier D, Cech M, et al. The Galaxy platform for accessible, reproducible and collaborative biomedical analyses: 2018 update. *Nucleic Acids Res* (2018) 46(W1):W537–W44. doi: 10.1093/nar/gky379
43. Basu S, Kumbier K, Brown JB, Yu B. Iterative random forests to discover predictive and stable high-order interactions. *Proc Natl Acad Sci U.S.A.* (2018) 115(8):1943–8. doi: 10.1073/pnas.1711236115
44. Kelly BJ, Gross R, Bittinger K, Sherrill-Mix S, Lewis JD, Collman RG, et al. Power and sample-size estimation for microbiome studies using pairwise distances and PERMANOVA. *Bioinformatics* (2015) 31(15):2461–8. doi: 10.1093/bioinformatics/btv183
45. Langille MG, Zaneveld J, Caporaso JG, McDonald D, Knights D, Reyes JA, et al. Predictive functional profiling of microbial communities using 16S rRNA marker gene sequences. *Nat Biotechnol* (2013) 31(9):814–21. doi: 10.1038/nbt.2676
46. Kanehisa M, Goto S. KEGG: kyoto encyclopedia of genes and genomes. *Nucleic Acids Res* (2000) 28(1):27–30. doi: 10.1093/nar/28.1.27
47. Goodrich JK, Di Rienzi SC, Poole AC, Koren O, Walters WA, Caporaso JG, et al. Conducting a microbiome study. *Cell* (2014) 158(2):250–62. doi: 10.1016/j.cell.2014.06.037
48. Segata N, Izard J, Waldron L, Gevers D, Miropolsky L, Garrett WS, et al. Metagenomic biomarker discovery and explanation. *Genome Biol* (2011) 12 (6):R60. doi: 10.1186/gb-2011-12-6-r60
49. Johnson JS, Spakowicz DJ, Hong BY, Petersen LM, Demkowicz P, Chen L, et al. Evaluation of 16S rRNA gene sequencing for species and strain-level microbiome analysis. *Nat Commun* (2019) 10(1):5029. doi: 10.1038/s41467-019-13036-110.1038/s41467-019-13036-1
50. Winand R, Bogaerts B, Hoffman S, Lefevre L, Delvoye M, Braekel JV, et al. Targeting the 16s Rrna Gene for Bacterial Identification in Complex Mixed Samples: Comparative Evaluation of Second (Illumina) and Third (Oxford Nanopore Technologies) Generation Sequencing Technologies. *Int J Mol Sci* (2019) 21(1):298. doi: 10.3390/ijms21010298
51. Guerrero-Preston R, Godoy-Vitorino F, Jedlicka A, Rodriguez-Hilario A, Gonzalez H, Bondy J, et al. 16S rRNA amplicon sequencing identifies microbiota associated with oral cancer, human papilloma virus infection and surgical treatment. *Oncotarget* (2016) 7(32):51320–34. doi: 10.18632/oncotarget.9710
52. Yang CY, Yeh YM, Yu HY, Chin CY, Hsu CW, Liu H, et al. Oral Microbiota Community Dynamics Associated With Oral Squamous Cell Carcinoma Staging. *Front Microbiol* (2018) 9:862:862. doi: 10.3389/fmicb.2018.00862
53. Su SC, Chang LC, Huang HD, Peng CY, Chuang CY, Chen YT, et al. Oral microbial dysbiosis and its performance in predicting oral cancer. *Carcinogenesis* (2020) 4:bgaa062. doi: 10.1093/carcin/bgaa062
54. Nagy KN, Sonkodi I, Szoke I, Nagy E, Newman HN. The microflora associated with human oral carcinomas. *Oral Oncol* (1998) 34(4):304–8. doi: 10.1016/S1368-8375(98)80012-2
55. Bolz J, Dosa E, Schubert J, Eckert AW. Bacterial colonization of microbial biofilms in oral squamous cell carcinoma. *Clin Oral Investig* (2014) 18(2):409–14. doi: 10.1007/s00784-013-1007-2
56. de Andrade KQ, Almeida-da-Silva CLC, Coutinho-Silva R. Immunological Pathways Triggered by Porphyromonas gingivalis and Fusobacterium nucleatum: Therapeutic Possibilities? *Mediators Inflammation* (2019) 2019:7241312. doi: 10.1155/2019/7241312
57. Whitmore SE, Lamont RJ. Oral bacteria and cancer. *PloS Pathog* (2014) 10(3): e1003933. doi: 10.1371/journal.ppat.1003933PPATHOGENS-D-13-03323
58. Hajishengallis G, Lamont RJ. Beyond the red complex and into more complexity: the polymicrobial synergy and dysbiosis (PSD) model of periodontal disease etiology. *Mol Oral Microbiol* (2012) 27(6):409–19. doi: 10.1111/j.2041-1014.2012.00663.x
59. Zhang L, Liu Y, Zheng HJ, Zhang CP. The Oral Microbiota May Have Influence on Oral Cancer. *Front Cell Infect Microbiol* (2019) 9:476:476. doi: 10.3389/fcimb.2019.00476
60. Lim Y, Fukuma N, Totsika M, Kenny L, Morrison M, Punyadeera C. The Performance of an Oral Microbiome Biomarker Panel in Predicting Oral Cavity and Oropharyngeal Cancers. *Front Cell Infect Microbiol* (2018) 8:267:267. doi: 10.3389/fcimb.2018.00267
61. Pavlopoulou A, Savva GD, Louka M, Bagos PG, Vorgias CE, Michalopoulos I, et al. Unraveling the mechanisms of extreme radioresistance in prokaryotes: Lessons from nature. *Mutat Res Rev Mutat Res* (2016) 767:92–107. doi: 10.1016/j.mrrev.2015.10.001
62. Zhang Z, Yang J, Feng Q, Chen B, Li M, Liang C, et al. Compositional and Functional Analysis of the Microbiome in Tissue and Saliva of Oral Squamous Cell Carcinoma. *Front Microbiol* (2019) 10:1439:1439. doi: 10.3389/fmicb.2019.01439
63. Chang C, Geng F, Shi X, Li Y, Zhang X, Zhao X, et al. The prevalence rate of periodontal pathogens and its association with oral squamous cell carcinoma. *Appl Microbiol Biotechnol* (2018) 103(3):1393–404. doi: 10.1007/s00253-018-9475-610.1007/s00253-018-9475-6
64. Yu T, Guo F, Yu Y, Sun T, Ma D, Han J, et al. Fusobacterium nucleatum Promotes Chemoresistance to Colorectal Cancer by Modulating Autophagy. *Cell* (2017) 170(3):548–63 e16. doi: 10.1016/j.cell.2017.07.008
65. Komiya Y, Shimomura Y, Higurashi T, Sugi Y, Arimoto J, Umezawa S, et al. Patients with colorectal cancer have identical strains of Fusobacterium nucleatum in their colorectal cancer and oral cavity. *Gut* (2018) 68 (7):1335–7. doi: 10.1136/gutjnl-2018-316661
66. Siddiqui A, Ceppi P. A non-proliferative role of pyrimidine metabolism in cancer. *Mol Metab* (2020) 35:100962. doi: 10.1016/j.molmet.2020.02.005
67. Dietlein F, Thelen L, Reinhardt HC. Cancer-specific defects in DNA repair pathways as targets for personalized therapeutic approaches. *Trends Genet* (2014) 30(8):326–39. doi: 10.1016/j.tig.2014.06.003
68. Bradner JE, Hnisz D, Young RA. Transcriptional Addiction in Cancer. *Cell* (2017) 168(4):629–43. doi: 10.1016/j.cell.2016.12.013
69. Lee LJ, Papadopoli D, Jewer M, Del Rincon S, Topisirovic I, Lawrence MG, et al. Cancer Plasticity: The Role of mRNA Translation. *Trends Cancer* (2020) 7(2):134–45. doi: 10.1016/j.trecan.2020.09.005
70. Berdis AJ. Inhibiting DNA Polymerases as a Therapeutic Intervention against Cancer. *Front Mol Biosci* (2017) 4:78:78. doi: 10.3389/fmolb.2017.00078
71. Yost S, Stashenko P, Choi Y, Kukuruzinska M, Genco CA, Salama A, et al. Increased virulence of the oral microbiome in oral squamous cell carcinoma revealed by metatranscriptome analyses. *Int J Oral Sci* (2018) 10(4):32. doi: 10.1038/s41368-018-0037-710.1038/s41368-018-0037-7
72. Miller CS, Johnstone BM. Human papillomavirus as a risk factor for oral squamous cell carcinoma: a meta-analysis, 1982-1997. *Oral Surg Oral Med Oral Pathol Oral Radiol Endod* (2001) 91(6):622–35. doi: 10.1067/moe.2001.115392
73. Prabhu SR, Wilson DF. Human papillomavirus and oral disease - emerging evidence: a review. *Aust Dent J* (2013) 58(1):2–10; quiz 125. doi: 10.1111/adj.12020
74. Gupta S. Role of human papillomavirus in oral squamous cell carcinoma and oral potentially malignant disorders: A review of the literature. *Indian J Dent* (2015) 6(2):91–8. doi: 10.4103/0975-962X.155877IJDENT-6-91
75. Feller L, Khammissa RA, Wood NH, Lemmer J. Epithelial maturation and molecular biology of oral HPV. *Infect Agent Cancer* (2009) 4:16. doi: 10.1186/1750-9378-4-16
76. Scheifele C, Reichart PA. [Oral leukoplakia in manifest squamous epithelial carcinoma. A clinical prospective study of 101 patients]. *Mund Kiefer Gesichtschir* (1998) 2(6):326–30. doi: 10.1007/s100060050081

77. Sudbo J, Reith A. Which putatively pre-malignant oral lesions become oral cancers? Clinical relevance of early targeting of high-risk individuals. *J Oral Pathol Med* (2003) 32(2):63–70. doi: 10.1034/j.1600-0714.2003.00054.x
78. van der Waal I. Potentially malignant disorders of the oral and oropharyngeal mucosa; present concepts of management. *Oral Oncol* (2010) 46(6):423–5. doi: 10.1016/j.oraloncology.2010.02.016
79. Licitra L, Perrone F, Bossi P, Suardi S, Mariani L, Artusi R, et al. High-risk human papillomavirus affects prognosis in patients with surgically treated oropharyngeal squamous cell carcinoma. *J Clin Oncol* (2006) 24(36):5630–6. doi: 10.1200/JCO.2005.04.6136

Conflict of Interest: The authors declare that the research was conducted in the absence of any commercial or financial relationships that could be construed as a potential conflict of interest.

frontiers in Oncology

ORIGINAL RESEARCH
published: 04 March 2021
doi: 10.3389/fonc.2021.626394

Photodynamic Therapy as an Alternative Therapeutic Tool in Functionally Inoperable Oral and Oropharyngeal Carcinoma: A Single Tertiary Center Retrospective Cohort Analysis

Arnaud Lambert[1,2], *Lotte Nees*[1], *Sandra Nuyts*[3,4], *Paul Clement*[5], *Jeroen Meulemans*[1], *Pierre Delaere*[1] *and Vincent Vander Poorten*[1,2]*

[1] Department of Otorhinolaryngology, Head and Neck Surgery, University Hospitals Leuven, Leuven, Belgium, [2] Department of Oncology—Section Head and Neck Oncology, KU Leuven, Leuven, Belgium, [3] Department of Oncology—Section Experimental Radiotherapy, KU Leuven, Leuven, Belgium, [4] Radiation Oncology, University Hospitals Leuven, Leuven, Belgium, [5] Department of Oncology—Section Experimental Oncology, KU Leuven, Leuven, Belgium

OPEN ACCESS

Edited by:
Cesare Piazza,
University of Brescia, Italy

Reviewed by:
Catriona M. Douglas,
NHS Greater Glasgow and Clyde, United Kingdom
Thomas Gander,
University Hospital Zürich, Switzerland

***Correspondence:**
Vincent Vander Poorten
vincent.vanderpoorten@uzleuven.be

Specialty section:
This article was submitted to Head and Neck Cancer, a section of the journal Frontiers in Oncology

Received: *05 November 2020*
Accepted: *08 February 2021*
Published: *04 March 2021*

Citation:
Lambert A, Nees L, Nuyts S, Clement P, Meulemans J, Delaere P and Vander Poorten V (2021) Photodynamic Therapy as an Alternative Therapeutic Tool in Functionally Inoperable Oral and Oropharyngeal Carcinoma: A Single Tertiary Center Retrospective Cohort Analysis. Front. Oncol. 11:626394. doi: 10.3389/fonc.2021.626394

Background: Head and neck cancer is typically treated with surgery, radiotherapy, chemoradiation, or a combination of these treatments. This study aims to retrospectively analyse oncological outcomes, adverse events and toxicity of treatment with temoporfin-mediated photodynamic therapy at a single tertiary referral center. More specifically, in a selected group of patients with otherwise (functionally) inoperable oral or oropharyngeal head and neck squamous cell carcinoma.

Methods: Twenty-six consecutive patients who received photodynamic therapy for oral or oropharyngeal squamous cell carcinoma from January 2002 until July 2019 at the University Hospitals Leuven were included. These were (1) patients with an accessible recurrent or new primary tumor in an extensively treated area of the head and neck, not suitable for standard treatment, or (2) patients that were judged medically unfit to undergo standard treatment modalities.

Results: Complete tumor response immediately after PDT was obtained in 76.9% of cases. During follow-up, a proportion of CR patients did recur, to reach recurrence-free rates at six months, one year and two years of 60.6%, 48.5% and 32.3%. Local control at the PDT treated area was 42.3% with a median recurrence free interval time of 9 months. Recurrence-free interval was statistically more favorable for oropharyngeal squamous cell carcinoma (with or without oral cavity extension) in comparison to oral cavity squamous cell carcinoma alone ($p < 0.001$). During a median follow-up period of 27 months, we report new tumor activity in 80.8% of patients. Median overall and disease-specific survival time was 31 and 34 months, respectively. Most reported adverse events were pain after treatment and facial edema. At the end of follow-up, swallowing and upper airway functionality were preserved in 76.9 and 95.7% of patients, respectively.

Conclusion: Photodynamic therapy is a valuable treatment option in highly selected patients with oral and/or oropharyngeal (functionally) inoperable head and neck squamous cell carcinoma. Treatment with this alternative modality can induce durable local control in an important fraction of treated patients, with an acceptable toxicity profile.

Keywords: photodynamic therapy, oral, oropharyngeal, outcome, head and neck squamous cell carcinoma

INTRODUCTION

Head and neck cancer is a major health problem with substantial morbidity and mortality. Worldwide, this is the sixth most common cancer (1) and the eight most common cause of cancer-related death (2). In Belgian men, it is the fourth most common cancer, with an incidence of 36.2 per 100,000 people in 2016. The median age of patients with oral cavity and pharyngeal cancer at diagnosis in Belgian patients is 63.7 years in men and 65.8 years in women. For newly diagnosed cases in Belgium from 2012 until 2016, the 5-year relative survival rate is 51.2 and 59.4% for men and women, respectively (3). Despite the progress in standard treatment, tumor recurrence and second primary tumors occur in many patients after extensive combined treatment, which poses the need for novel therapies.

In this study, we investigate the oncological outcome and adverse events (AE) of photodynamic therapy (PDT), as a mildly invasive treatment alternative for head and neck cancer. It combines a photosensitizing agent, oxygen and a light source of a specific activating wavelength to establish a cytotoxic effect (4). The intravenously injected photosensitizing agent concentrates preferably in tumor tissue as compared to adjacent healthy tissue because it is taken up by cells with an elevated metabolic rate that have, in addition, less potency to get rid of the drug by exocytosis compared to healthy cells. Approximately 4–5 days (96–120 h) following injection, the ratio of photosensitizer concentration in tumor as opposed to healthy tissue is maximal. Illumination is performed by a laser that is set to a specific wavelength in relation to the absorption characteristics of the administrated photosensitizer. The activation of the photosensitizer by the emitted photons during illumination, creates an excited state that can either emit fluorescence to lose excess energy or form a triplet state of the photosensitizer. Combined with oxygen, this activated state interacts with organic molecules producing free radicals that are cytotoxic and vasculotoxic, provoking apoptosis, and a local inflammatory response which can cause a systemic antitumor immunological reaction (5, 6). Consequently, it causes tumor necrosis and ischemia. The tissue neighboring the illuminated area is, in part, spared because of the significantly lower concentration of photosensitizer stored in healthy cells. As a result, its architecture and collagen framework is protected and this facilitates recovery (7). In the past, PDT was not used very widely because of the lack of an appropriate photosensitizer. Since the development of second-generation photosensitizers that have more depth of penetration and less side effects, there is an increasing interest in PDT (8). We use one of the most potent available second generation photosensitizers, meta-tetra(hydroxyphenyl)chlorin (mTHPC), which has a maximal absorption peak at 652 nm, necessitating a diode laser with exactly this wavelength (9).

Ablative surgery and radiation therapy with or without chemotherapy are the most commonly used therapeutic options in head and neck oncology. PDT offers an alternative treatment modality, in well-selected patients possibly providing local tissue preservation resulting in less post-treatment morbidity and a better functional outcome while maintaining adequate local tumor control. In contrast, ablative surgery in these instances can result in significant loss of function regarding speech and swallowing as well as a poor cosmetic outcome (5, 10). Radiotherapy, especially re-irradiation, while sparing the local anatomy, is at risk of rendering the tissue afunctional due to radiation induced fibrosis or necrosis (11). PDT, however, also has complications, such as pain, burns and edema of the tongue (5, 7).

In PDT, the photosensitizer can be activated by superficial illumination to a depth of 2–10 mm due to the physical properties of the used wavelength of light in combination with the tissue properties; as such it is effective only for superficial tumors. For tumors with a depth of more than 10 mm, interstitial PDT (iPDT), i.e., bypassing the issue of depth of tumor invasion by implanting the tumor with light sources (laser fibers) (5) can be an alternative. A systematic review by De Visscher et al. illustrated that PDT for head and neck squamous cell carcinomas (HNSCC) in the palliative setting enhanced the quality of life in patients with limited remaining treatment options. In a curative setting, they concluded that there were not enough data to support its use (12).

We conducted this retrospective cohort study in our tertiary care center to evaluate treatment with Temoporfin-mediated PDT for oral cavity and oropharyngeal cancer. This treatment option is offered to a small selected subgroup of patients with a history of head and neck cancer already treated with conventional therapeutic strategies, especially when a significant functional impairment is expected when treated with either salvage surgery or (re-)irradiation. Provided the tumor is locally accessible for illumination, our multidisciplinary tumor board typically advises the use of PDT as a means to offer a less invasive and less toxic alternative as opposed to major ablative surgery or (re-)irradiation, respectively. In this study, patient characteristics, outcome and reported adverse effects were investigated and subsequently compared to data in the literature.

MATERIALS AND METHODS

Patients

In this retrospective cohort study, all consecutive patients with oral cavity and or oropharyngeal cancer treated with mTHPC photodynamic therapy at the University Hospitals Leuven from January 2002 until July 2019 were included. All PDT treatments were performed by one senior head and neck surgeon (Vander Poorten V.). Treatment with mTHPC was offered if the tumor board concluded no other conventional treatment option to be suitable other than palliative chemotherapy or immunotherapy. Patients were selected for this treatment in case of (1) local recurrence or a new primary, without evidence distant metastasis, following extensive previous treatments including surgery, radiation or chemoradiation, where salvage surgery or re-irradiation is not an option, (2) surgically unacceptable functional impairment [functional inoperability (13)] or (3) patient refusal or being medically unfit to undergo conventional treatments. The accessibility of the tumor for superficial illumination was a prerequisite for PDT treatment selection. In tumors more difficult to access with perpendicular superficial illumination, interstitial PDT was used. The study population consists of 26 patients (10 women, 16 men) with a median mean age of 59 years old. Data of all included patients were extracted from their electronic medical file. The patient characteristics including substance abuse risk factors are listed in **Table 1**.

TABLE 1 | Patient characteristics: Age, gender, and risk factors for $n = 26$ patients, with oral cavity and/or oropharyngeal cancer treated with photodynamic therapy.

Patient characteristics ($n = 26$)		
Age at diagnosis of PDT tumor	Mean (SD)	61.09 (8,436)
Gender	***n* (%)**	
Male		16 (61.5)
Female		10 (38.5)
Risk factors	***n* (%)**	
Alcohol alone		3 (11.5)
Smoking alone		1 (3.8)
Alcohol + smoking		21 (80.8)
No abuse		1 (3.8)
Primary tumor before PDT	***n* (%)**	
Unknown primary		2 (7.7)
Oral cavity		6 (23.1)
Oropharynx		9 (34.6)
Hypopharynx		1 (3.8)
Larynx		4 (15.4)
Oral cavity and oropharynx		2 (7.7)
Hypopharynx and larynx		2 (7.7)
Second primary tumor before PDT	***n* (%)**	
Oral cavity		3 (11.5)
Oropharynx		3 (11.5)
PDT tumor origin	***n* (%)**	
New primary		12 (46.2)
First rec of first primary		7 (26.9)
Second rec of first prim		4 (15.4)
PDT tumor = first primary		1 (3.8)
First rec of second primary		2 (7.7)
Sum of treatments before PDT	***n* (%)**	
No treatment before PDT		1 (3.8)
Ablative surgery		2 (7.7)
Primary RT alone		6 (23.1)
Primary RCT alone		2 (7.7)
Ablative surgery + RT		14 (53.8)
Primary RCT + salvage surgery		1 (3.8)

Rec, recurrence; RT, radiotherapy; RCT, radiochemotherapy.

Methods

Upon selection, the tumor location was specified and the tumor area and invasion depth were measured using high resolution CT scan, MRI scan or clinically if there was no evidence for the presence of a tumor on imaging or the measurements were not specified. A senior pathologist evaluated the histology. Previous treatments details for the index head and neck tumor (radiation, surgery, or chemotherapy) and smoking and alcohol consumption were extracted from the patient's medical file. The TNM classification (UICC 7th edition) was used to describe the locoregional anatomical extent of the tumor. Seventy-two to one-hundred and twenty hours (mean: 97.8 h, SD: 9.4) following intraveneous mTHPC administration, laser illumination was performed under general anesthesia using a Ceralas® 652 nm diode laser with microlens fiber (Biolitec, Jena, Germany). Taking into account a healthy tissue margin around the tumor of 5–10 mm, the remaining surrounding tissue was protected with black shielding wax (**Figure 1**). Patients were treated with superficial or/and interstitial PDT. During follow-up the treatment specific adverse events, swallowing and upper airway function, and the patients' alcohol use and smoking habits were recorded. Treatment modalities following the (first) PDT session were listed as well. All patients were repeatedly examined in the head and neck area to look for any tumor recurrence or other primary tumor, following a fixed follow-up protocol: 1 visit every 2 months the first 2 years, then every 3 months the 3rd year, every 4 months the 4th year, every 6 months the 5th year, and finally yearly until 10 years of follow-up. Baseline imaging using MRI (magnetic resonance imaging) was routinely obtained within a 2–6 months period for treatment response evaluation (14).

The primary outcomes of this study were:

1 tumor response to PDT, according to the RECIST1.1 (15) criteria: complete response (CR), partial response (PR) (≥30% reduction), stable disease (SD) (30% reduction – 20% increase) and progressive disease (PD) (≥20% increase). "Complete response" means complete resolution without clinical and radiological (MR/CT) evidence of tumor activity after PDT;
2 overall survival (time between the mTHPC injection and death or censoring/last follow-up), disease-free survival (time between mTHPC injection and first tumor recurrence/second primary tumor or last follow-up without disease) and disease-specific survival (time between mTHPC injection and death, patients that died from another cause being censored).

FIGURE 1 | Left panel: Superficial Illumination of a tumor located on the soft palate (T2N0M0). Black shielding wax protects the surrounding tissue during illumination, including a margin of 1 cm. This patient had already received radiotherapy at this site. Right panel: tumor site necrosis of the tumor in the same patient 4 weeks after PDT.

Secondary outcome was the occurrence of adverse events. Recorded adverse events were: pain, skin burns (due to inadvertent light exposure of the skin during the hypersensitive period following Temoporfin injection; graded and followed-up by our burns center), edema (as occurring in the entire head and neck region: facial, oral cavity, pharyngeal, and laryngeal edema). "Injection site reaction" was defined as every deviation from an uncomplicated injection at the site of mTHPC injection, including erythema during or after the administration, burns, pain, itch, hematoma, and swelling. Necrosis of the illuminated area is an expected consequence of PDT. This can be an adverse event if it is too extensive. Our policy is that every side effect is systematically noted in the electronic patient file. If there were no adverse events documented in the medical file, this means none had occurred. If any AE was documented more than 1 year after PDT, this was not assumed to be caused by PDT.

Statistical Analysis

Statistical analysis was performed using IBM SPSS Statistics (version 27). Overall and disease-specific survival were assessed using the Kaplan-Meier method, as well as the recurrence-free interval. Univariate log-rank analysis was used to compare survival data between subgroups. An unpaired T-test was used to compare the means of two subgroups. Chi-square analysis was used to detect significant correlations between independent variables. Statistical significance was defined at the $p < 0.05$ level.

Ethical Considerations

This study was carried out according to the prevailing ethical standards after obtaining approval by the Ethical Committee of the University Hospitals Leuven (approval number: MP010447).

RESULTS

Patient Characteristics

Twenty-six patients received PDT in the University Hospitals Leuven. Two out of three patients were male ($n = 16$, 61.5%). The mean age at PDT was 61 years, with a minimum age of 47 and a maximum age of 79 years old. The vast majority of our patient population ($n = 21$, 80.8%) had a history of combined smoking and alcohol abuse. Three patients consumed alcohol alone. Of the remaining two patients, one was only a smoker and the other had no history in alcohol or smoking consumption whatsoever (**Table 1**). More than half ($n = 14$, 53.8%) of the patient population had undergone a combination of ablative surgery and radiotherapy before receiving PDT, six patients (23.1%) had a history of primary radiotherapy treatment, two patients (7.7%) received concurrent chemo- and radiotherapy before PDT and two patients (7.7%) had ablative surgery alone before PDT. One patient had a history of concurrent chemoradiation as well as ablative surgery before receiving PDT. Evidently, most of the patient population already had an extensive head and neck cancer history. In one patient PDT was selected as a suitable primary treatment modality: this patient had a large erythroplakia lesion with some invasive SCC spots located on the soft palate with extensions to the right retromolar trigone. This patient was very frail with a history of alcohol abuse, Korsakoff disease, and chronic kidney failure, making her unsuitable for ablative surgery or a full course of radiotherapy. The oncological and treatment history in terms of primary head and neck tumors before the oral cavity/oropharyngeal tumor treated with PDT is listed in **Table 2**, as well as an overview of recurrences before PDT treatment in **Table 3**. The mean time between the first primary tumor and the tumor treated with PDT varied from 7 to 348 months, with a median time of 66.5 months or 5.5 years.

TABLE 2 | Tumor characteristics of primary head and neck SCC before diagnosis and treatment of the PDT tumor in 26 patients.

Primary head and neck tumors before PDT tumor			
	First primary (*n* = 26)	**Second primary (*n* = 6)**	**Third primary (*n* = 1)**
Location	***n* (%)**	***n* (%)**	***n* (%)**
Oral cavity (OC)	6 (23.1)	3 (11.5)	1 (3.8)
Oropharynx	9 (34.6)	3 (11.5)	
OC + oropharynx	2 (7.7)		
Hypopharynx	1 (3.8)		
Larynx	4 (15.4)		
Hypopharynx and larynx	2 (7.7)		
Unknown primary	2 (7.7)		
TNM classification	***n* (%)**	***n* (%)**	***n* (%)**
clinical T class			
cTx	2 (7.7)	1 (3.8)	
cT1	3 (11.5)		
cT2	4 (15.4)		
cT3	4 (15.4)		
cT4	3 (11.5)		
Clinical N class			
cN0	13 (50.0)	5 (19.2)	1 (3.8)
cN1	1 (3.8)		
cN2a	1 (3.8)		
cN2b	1 (3.8)		
Pathological T class			
pT1	4 (15.4)	4 (15.4)	
pT2	1 (3.8)		1 (3.8)
pT3	2 (7.7)		
pT4a	3 (11.5)		
Pathological N class			
pN0	1 (3.8)		
pN1	1 (3.8)		
pN2a	1 (3.8)		
pN2b	5 (19.2)		
pN3b	1 (3.8)		
Not available	0	1 (3.8%)	0
Treatment	***n* (%)**	***n* (%)**	***n* (%)**
RT + MRND	2 (7.7)		
Ablative surgery alone	3 (11.5)	5 (19.2)	1 (3.8%)
AS + ND	1 (3.8)		
AS + ND + adj. RT	7 (26.9)		
Primary RT	8 (30.8)		
Primary RCT	2 (7.7)		
RT + brachytherapy	2 (7.7)	1 (3.8)	
PDT	1 (3.8)		

OC, Oral Cavity; RT, Radiotherapy; MRND, modified radical neck dissection; AS, Ablative surgery; ND, selective neck dissection; adj. RT, adjuvant radiotherapy; RCT, radiochemotherapy; PDT, photodynamic therapy.

TABLE 3 | Tumor characteristics of head and neck SCC recurrences before diagnosis and treatment of PDT tumor in 26 patients.

Recurrences before PDT tumor		
	First recurrence (*n* = 9)	**Second recurrence (*n* = 1)**
Origin of recurrence	***n* (%)**	***n* (%)**
First primary	8 (30.8)	1 (3.8)
Second primary	1 (3.8)	
No recurrence	17 (65.4)	25 (96.2)
Location	***n* (%)**	***n* (%)**
Oral cavity (OC)	6 (23.1)	1 (3.8)
Oropharynx	1 (3.8)	1 (3.8)
OC + oropharynx	1 (3.8)	
Larynx	1 (3.8)	
No recurrence	17 (65.4)	24 (92.3)
TNM classification	***n* (%)**	***n* (%)**
Clinical T class		
cT4a	1 (3.8)	
Clinical N class		
cN0	4	1 (3.8)
Pathological T class		
pT1	2 (7.7)	1 (3.8)
pT2	1 (3.8)	
pT3	1 (3.8)	
pT4a	1 (3.8)	
Pathological N class		
pN0	2 (7.7)	
not available	3 (11.5)	0
Treatment	***n* (%)**	***n* (%)**
Ablative surgery alone	3 (11.5)	1 (3.8)
AS + ND	4 (15.4)	
AS + adj. RT	1 (3.8)	
Primary RT	1 (3.8)	

OC, Oral Cavity; AS, Ablative surgery; ND, selective neck dissection; adj. RT, adjuvant radiotherapy; RT, radiotherapy.

Tumor Characteristics

The most common anatomical site where PDT treatment was performed, was the oropharynx ($n = 14$, 53.8%), followed by the oral cavity ($n = 8$, 30.8%) and a combination of both locations ($n = 4$, 15.4%). Compared to the site of the first primary head and neck tumor in each patient, half of the tumors ($n = 13$, 50%) treated with PDT were located at a different site than their primary head and neck tumor; resulting in twelve patients (46.2%) with a new primary tumor and one patient where the tumor was in fact the first primary. The other half of tumors treated with PDT presented either as a first recurrence of the first primary ($n = 7$, 26.9%), a second recurrence of the first primary ($n = 4$, 15.4%) or a first recurrence of a second primary ($n = 2$, 7.7%). Of oropharyngeal anatomical subsites, the tumors treated with PDT were most frequently located on the soft palate ($n = 10$, 38.5%). Other subsites were more or less equally distributed

between the lateral tonsillar wall or glossotonsillar sulcus ($n = 2$, 7.7%), the base of the tongue or vallecula ($n = 3$, 11.5) and the posterior pharyngeal wall ($n = 3$, 11.5%). The retromolar trigone or inner cheek area was mostly affected in the oral cavity ($n = 8$, 30.8%), usually in continuity with an adjacent subsite of the oral cavity (hard palate, lateral tongue) or oropharynx (soft palate). Only two cases presented as an isolated retromolar trigone tumor. Tumor characteristics and PDT treatment specifics per case are illustrated in **Tables 4**, **5** respectively.

Treatment Characteristics

mTHPC was administered to the patients at a dose of 0.15 mg/kg. This resulted in a mean dose of 9.28 mg (median: 9.15 mg, range 5.55–12.90 mg) during a mean intravenous infusion time of 7.7 minutes (median: 8 min, range 5–10 min). The laser illumination had a mean total energy of 0.66 Watt per spot (median: 0.67 Watt, range 0.1–1.45 Watt). The superficially illuminated area consisted of one or more spots, with a mean spot size of 3 cm and a maximum spot size of 4 cm. If larger areas needed to be illuminated, several overlapping spots were used, with a mean of 3 spots (median: 3, range 1–4 spots). As a standard for superficial PDT every spot was illuminated for 200 s. Superficial PDT with surface illumination alone was performed in 76.9% ($n = 20$) of the patients, interstitial PDT in 7.7% ($n = 2$) and a combination of both surface and interstitial PDT in 15.4% ($n = 4$) of the patients. Of the 26 patients, two patients received interstitial PDT and four patients received a combination of interstitial PDT and superficial illumination. For interstitial PDT, minimum 4 and maximum 14 bare fibers were placed in the tumor tissue (mean: 9 fibers). The mean length of stay in the hospital was 17 days (median: 12.5 days, range 7–40 days). This includes pre-operative evaluation at the first date of admission, as well as any concomitant treatments performed before illumination (e.g., planned tracheotomy, neck dissection). After PDT illumination, the median length of stay in the hospital was 7 days (range 3–34 days). Follow-up ranged from 2 to 129 months, with a median time of 29.5 months. Out of our group of 26 patients 76.9% ($n = 20$) died during follow-up and six patients were alive at the end of follow-up. Median follow-up in these 6 patients is 22.5 months with a minimum of 3 months and a maximum of 62 months (median 22.5 months).

Tumor Response

Complete response was obtained in 76.9% ($n = 20$) of the treated tumors at a mean follow-up time of 36.55 months (min: 2, max 129, and median 30.5 months). A partial tumor response was seen in 11.5% ($n = 3$) with a median follow-up time of 15 months. An equal amount of patients (11.5%, $n = 3$) presented with progressive disease within a median follow-up time of 6 months. Out of the 20 patients treated with surface illumination alone, 17 tumors showed complete response, one partial response and two tumors exhibited progressive disease. Four patients were treated with a combination of surface illumination and interstitial PDT, resulting in two complete and two partial responses. Finally, two patients were treated with interstitial PDT alone, showing complete response in one and progressive disease in the other. In **Table 6**, we provide an overview of the tumor response per PDT modality in relation to anatomical site subgroup (oral cavity alone vs. oropharynx ± oral cavity extension). Chi-square analysis shows a significant correlation favoring complete tumor response in the oropharynx subgroup ($p = 0.03$). No significant difference was found between superficial PDT, interstitial or combined PDT.

Recurrence

Recurrence at the same site as the illumination area or at another site in the head and neck region (new primary tumor) occurred in the majority of the patients (80.8%, $n = 21$). In our case series 42.3% ($n = 11$) of tumors did not recur at the illuminated area. The median follow-up period of these patients was 27 months (range: 2–90; mean: 29.55 months). Consequently 57.7% ($n = 15$) did recur locally at a median follow-up time of 5 months (mean: 8.6 months). Overall recurrence, locally as well as at other sites in the head and neck area, occurred after a median time of 8 months, with a minimum of 22 days and a maximum of 90 months. The median follow-up time in the overall non-recurring patient group was 31 months (range: 2–52 months). About one third of our patients ($n = 9$, 34.6%) developed a separate primary tumor outside of the head and neck region in their follow-up period after PDT. Notably, the sites of these new primary tumors are also notoriously associated with alcohol abuse and smoking: esophageal cancer ($n = 4$), lung cancer ($n = 3$), breast cancer ($n = 1$), and bladder cancer ($n = 1$). Other separate primary tumors were prostate cancer and sarcoma. Six patients out of the 21 with a recurrence, developed this recurrence at a different or adjacent site in relation to the PDT treated area. This could be in the same subsite, but not in the illuminated tissue area, otherwise the recurrence was labeled as a local recurrence. Hence, the other 15 recurrences were identified as local recurrences, specifically at the level of the oropharynx ($n = 8/15$, 53.3%), the oral cavity ($n = 5/15$, 30%) or a combination of both ($n = 2/15$, 13.3%). In 90.5% ($n = 19/21$) of the patients who had head and neck tumor recurrence, local or otherwise, this was proven with a biopsy. In only two patients ($n = 2/21$, 9.5%), recurrence was based on clinical and radiological findings. Both these patients presented with a local recurrence in the previously illuminated site. **Figure 2** shows a Kaplan–Meier plot of the recurrence-free interval after PDT. Two patients received more than one treatment with PDT. More specifically, one patient underwent a second (surface illumination) and third (interstitial) treatment with PDT because of incomplete response (oral cavity) and recurrence (oropharynx), respectively, with 5 and 7 months in between treatments, respectively. The second patient received a second treatment with surface illumination because of recurrence in the oropharynx, at another location as the first tumor treated with PDT 27 months earlier. After 6 months there was a new recurrence at the same site.

Median recurrence-free interval (RFI) is 9 months. Recurrence-free rates at 6 months, 1, and 2 years are 60.6, 48.5, and 32.3%. Five patients remained recurrence-free during the follow-up period. There was no statistically significant difference in RFI between tumors originating from a recurrence of an earlier primary in comparison to PDT tumors being a new primary ($p = 0.209$). A significantly worse RFI ($p < 0.001$) was

TABLE 4 | Tumor specific characteristics of 26 patients receiving photodynamic therapy for cancer of the oral cavity or oropharynx with oral cavity extension.

PDT tumor characteristics						
n°	**Location**	**L/R**	**Subsite**	**Rec. or new tumor**	**TNM**	**Tumor grade**
1	OC + OP	Left	Tonsillar fossa + trigonum retromolare	New primary	T2N0M0	NOS
2	OC + OP	Midline	Soft palate + hard palate	New primary	T2N0M0	Well-to medium diff
3	OP	Right	Base of tongue, vallecula	First rec. of first primary	T2N1M0	Poorly differentiated
4	OP	Midline	Base of tongue, vallecula	New primary	T1N1M0	Poorly differentiated
5	OP	Left	Tonsillar fossa, lateral wall	First rec. of first primary	TisN0M0	Carcinoma *in situ*
6	OP	Midline	Soft palate	First rec. of first primary	T1N0M0	NOS
7	OC	Midline	Hard palate	Second rec. of first primary	TisN0M0	Carcinoma *in situ*
8	OP	midline	Soft palate	First rec. of first primary	T2N0M0	NOS
9	OC + OP	right	Soft palate + trigonum retromolare	First primary	T1N0M0	NOS
10	OC	left	Tongue	First rec of second primary	T2N0M0	Poorly differentiated
11	OC	right	Trigonum retromolare, lateral tongue	New primary	T1N0M0	Well-to medium diff
12	OP	midline	Posterior oropharynx	New primary	T2N0M0	Well-differentiated
13	OP	right	Soft palate	First rec of second primary	T3N0M0	NOS
14	OC	right	Hard palate, trigonum retromolare	Second rec. of first primary	T1N0M0	Medium differentiation
15	OC	left	Hard palate, trigonum retromolare	Second rec. of first primary	T1N0M0	NOS
16	OC	right	Trigonum retromolare	New primary	T1N0M0	Well-to medium diff
17	OP	right	Soft palate	New primary	T2N1M0	NOS
18	OC + OP	Left	Soft palate + trigonum retromolare	New primary	T3N0M0	Well-to medium diff
19	OP	Right	Soft palate	New primary	T1N0M0	NOS
20	OP	Right	Posterior oropharynx wall	New primary	T1N0M0	NOS
21	OP	Right	Soft palate	New primary	TisN0M0	Carcinoma *in situ*
22	OP	Right	Base of tongue + floor of mouth	First rec. of first primary	T3N0M0	Well-differentiated
23	OC	Right	Floor of mouth	Second rec. of first primary	T3N0M0	Verrucous carcinoma
24	OP	Left	Soft palate, lateral wall	New primary	T2N0M0	Medium differentiation
25	OC	Left	Trigonum retromolare	First rec. of first primary	T1N0M0	Medium differentiation
26	OP	Right	Posterior oropharynx	First rec. of first primary	T2N0M0	Medium differentiation

OC, oral cavity; OP, oropharynx; rec., recurrence; NOS, not otherwise specified; diff, differentiation.

observed in patients presenting with an oral cavity (OC) tumor alone, as opposed to those with an oropharyngeal tumor with or without oral cavity extension (OP ± OC). Median RFI was 3 months in the OC alone group and 22 months in the OP ± OC group (**Figure 4**).

Survival

A lot of heterogeneity existed in whether or not the primary head and neck cancer was actually related with the tumor treated for PDT. Therefore, even though most patients were already under follow-up and care for a previous primary head and neck cancer, starting point for the survival plots was taken as the date of PDT illumination. Median overall survival (OS) of all treated patients was 31 months (mean: 36.6 months, range 2–129 months). Of 26 patients, three are alive to date and still in follow-up at 14, 46 and 47 months. Overall survival at 6 months, 1, and 2 years was 88.1, 80.1, and 59.2%, respectively. The 5-year overall survival was 24.2% (**Figure 1**). The majority of the patients died because of the tumor ($n = 16$, 61.5%), 26.9% ($n = 7$) died due to another cause (e.g., subdural hematoma, heart failure, other tumors, or unknown causes). The median disease-specific survival (DSS) was 34 months (mean: 51 months). Disease-specific survival at 6 months, 1, and 2 years was 91.7, 83.3, and 61.6%, respectively. The 5 year DSS was 36.6%. In comparing the PDT tumors regarded as a new primary in comparison to those being recurrences from earlier head and neck tumors, no statistically significant difference in survival was found (OS $p = 0.209$; DSS $p = 0.907$, and RFS $p = 0.665$). Similarly, there were no significant differences between the OC alone group and the OP ± OC when comparing OS ($p = 0.399$) and DSS plots ($p = 0.210$). **Figures 2**, **3** show the Kaplan–Meier plots on OS and DSS after PDT. Other factors such as age, gender,

TABLE 5 | Photodynamic treatment type and associated interventions for 26 patients receiving therapy for cancer of the oral cavity or oropharynx with oral cavity extension.

	PDT treatment characteristics			
n°	**PDT type**	**Concomittant R/**	**Airway R/**	**Swallowing R/**
1	Surface illumination	None	None	None
2	Surface illumination	None	None	Planned NGT
3	Surface illumination	Selective ND	None	None
4	Surface illumination	lymph node excision	Planned tracheotomy	Planned NGT
5	Surface illumination	None	None	None
6	Surface illumination	None	None	None
7	Surface illumination	None	None	None
8	Surface illumination	None	None	None
9	Surface illumination	None	NONE	None
10	Surface illumination	None	Urgent tracheotomy	Unplanned NGT
11	Surface illumination	None	Pre-existing tracheostoma	None
12	Surface illumination	None	Planned tracheotomy	Planned PEG
13	Surface illumination	None	Pre-existing tracheostoma	None
14	Surface + interstitial ill.	None	None	None
15	Surface illumination	None	None	NGT on readmission
16	Interstitial PDT	None	None	None
17	Surface + interstitial ill.	MRND	Planned tracheotomy	Planned PEG
18	Surface illumination	None	Planned tracheotomy	Planned NGT
19	Surface illumination	None	None	None
20	Surface + interstitial ill.	None	Pre-existing tracheostoma	None
21	Surface illumination	None	Planned tracheotomy	Pre-existing PEJ
22	Interstitial PDT	None	Planned tracheotomy	Planned NGT
23	Surface illumination	None	Normal airway	None
24	Surface illumination	None	Normal airway	None
25	Surface + interstitial ill.	None	Normal airway	Planned NGT
26	Surface illumination	None	Planned tracheotomy	NGT on readmission

NGT, nasogastric tube; PEG, percutaneous endoscopic gastrostomy; ill., illumination; MRND,modified radical neck dissection.

TABLE 6 | Overview of tumor response according to RECIST criteria per subgroup and per PDT modality.

		Tumor response					
Subgroup		OC alone ($n = 8$)			OP & OP + OC extension ($n = 18$)		
PDT type		SI ($n = 5$)	iPDT ($n = 1$)	SI + iPDT ($n = 2$)	SI ($n = 16$)	iPDT ($n = 1$)	SI + iPDT ($n = 2$)
Tumor Response	PD	1	0	0	1	1	0
	SD	0	0	0	0	0	0
	PR	1	0	2	0	0	0
	CR	3	1	0	14	0	2

OC, oral cavity; OP, oropharynx; rec., recurrence; SI, surface illumination; iPDT, interstitial PDT; PD, progressive disease; SD, stable disease; PR, partial response; CR, complete response.

TNM classification, and substance abuse were examined but had no statistical significant impact on any survival plot. No significant difference was found in regards to PDT treatment type (superficial PDT vs. interstitial ± superficial PDT). Notably, complete tumor response as opposed to incomplete response (defined as partial response, stable disease, or progressive disease) showed no significant difference in terms of overall or disease specific survival.

Adverse Events and Toxicity of Treatment

During hospitalization and follow-up, all adverse events (AE) were documented in the patient files. To get a clear view on PDT toxicity, we collected information on the frequency and duration of pain, swallowing impairment and the need for tube feeding, airway management (tracheostomy), treated area (tumor site) necrosis and duration of tissue healing, as well as any other local or systemic adverse event potentially linked to PDT.

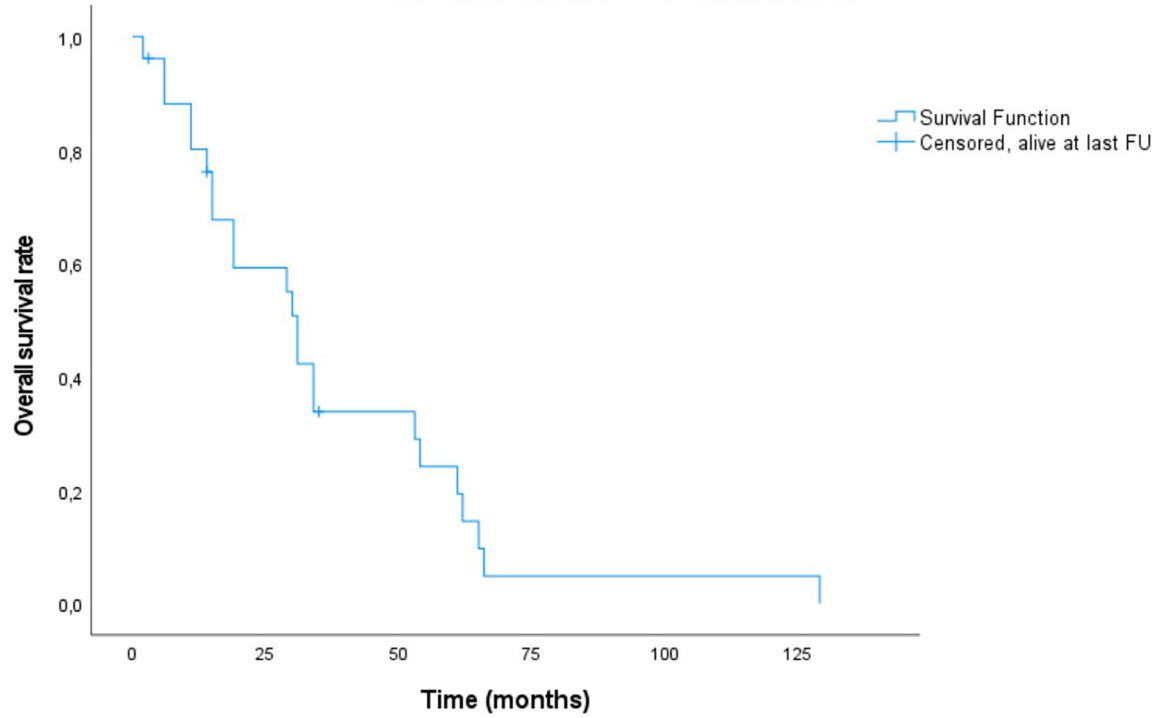

FIGURE 2 | Kaplan–Meier plot showing overall survival of PDT patients, starting from illumination date to endpoint defined as either overall death or alive at last follow-up (FU).

All patients required a variable level of pain medication during and after treatment. Our department monitors pain daily with a visual analog pain scale (VAS 0–10) since 2010, so we only have scored data on pain during hospitalization in PDT patients treated after 2010 ($n = 13$, 50%). Median pain level at the day of treatment was a VAS score of 8 ($n = 10$, range: 0–10), at 1 day post-illumination the median pain level was VAS score of 5 ($n = 13$, range 0–7) and after 7 days we noted a median VAS score of 3 ($n = 13$, range 0–6). Lastly, to assess the need for pain medication after discharge we reviewed the documented pain medication intake 1 month post PDT. We divided the need for pain medication in the following categories: no need for pain medication, conventional oral medication only (paracetamol, NSAID), conventional oral pain medication in conjunction with oral opioid medication and lastly the necessity for transcutaneous continuous opioid pain medication. In five patient case files there was no mention of pain medication and this was regarded as missing data. At 1 month, a minority of patients was pain free without any medication ($n = 7$, 26.9%), over half of our patients ($n = 14$, 53.8%) had controlled pain levels using appropriate pain medication. Of these, five (35.7%) needed conventional pain medication only, three (21.4%) needed an additional oral opioid and six (42.9%) were dependent on continuous transcutaneous opioid medication for pain relief. After discharge we documented four readmissions (15.4%) within 1 month after discharge, three because of pain and dysphagia, one patient was admitted due to an aspiration pneumonia. One patient only reported inadequate pain relief and was discharged 2 days later. Another patient with mainly dysphagia received a reintroduction of nasogastric tube for feeding and was discharged with the nasogastric tube 6 days later. The last patient who was readmitted presented with pain and secondary dysphagia, after adjusting the pain medication discharge was possible at day 11.

Swallowing capacity of these patients is undeniably affected by PDT treatment in the short-term post-treatment period. Partially on its own due to tissue necrosis and loss of function to some degree, but also due to the associated pain. Over half of the patient population did not require any tube feeding ($n = 15$, 57.5%) in the hospital. Planned tube feeding was foreseen for the remaining eight patients. The majority of planned tube feeding was anticipated for the oropharyngeal tumors ($n = 4$ NGT, $n = 2$ PEG, $n = 1$ pre-existing PEJ) as opposed to the oral cavity tumors ($n = 1$ NGT). Five patients received a nasogastric tube at the time of hospitalization, two patients a planned percutaneous gastrostomy (PEG) tube, and one patient had a pre-existing percutaneous jejunostomy (PEJ) tube. The remaining three patients that required unplanned nasogastric tube feeding for dysphagia in the short term period were: two patients during readmission and one patient due to an unforeseen emergency tracheotomy and admittance to the ICU. Four out of the five patients with planned nasogastric tube feeding had their feeding tubes successfully removed by a median time of 13.5 days

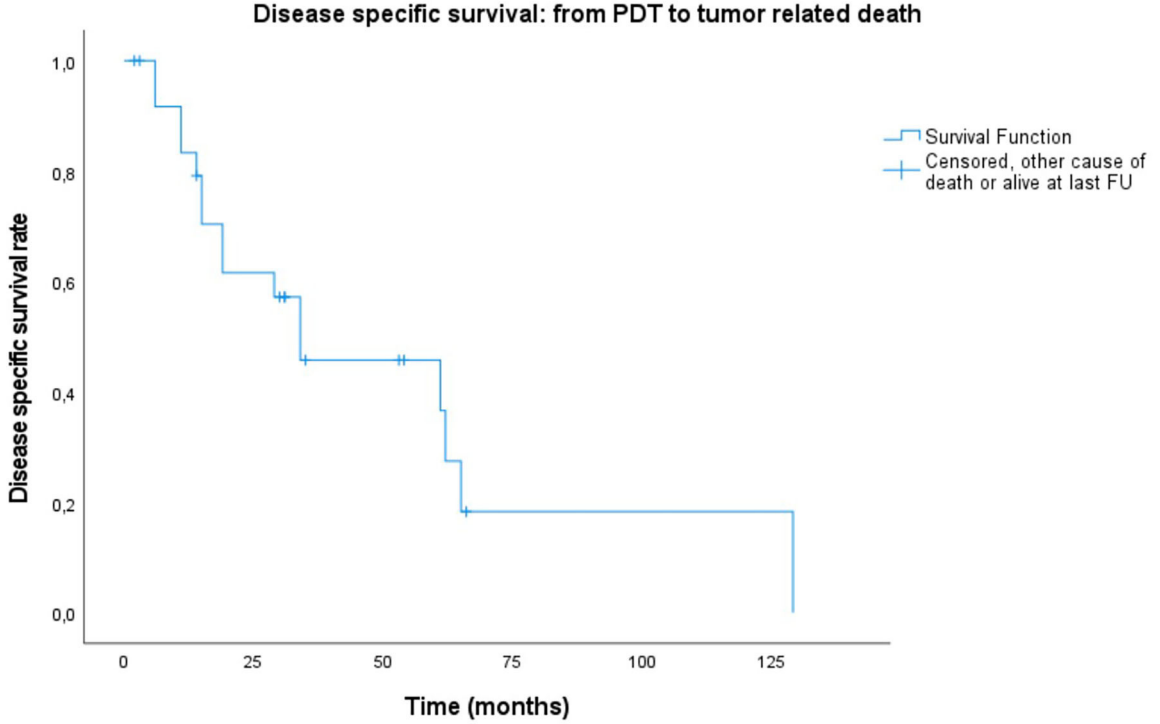

FIGURE 3 | Kaplan–Meier plot showing disease-specific survival from PDT illumination date to endpoint defined as either tumor related death, other cause of death or alive at last follow-up (FU).

(range: 5–8 days, mean 12.5). Unfortunately two patients out of those four needed their nasogastric tube reintroduced within the short term follow-up period of 1 month. One patient out of the total five could not be accounted for, regarding timing of tube removal, due to transfer to another center for revalidation purposes. Standardized swallowing scores were not routinely used to assess swallowing capabilities outside of prospective controlled studies, as this is a retrospective case study we have no standardized evaluation data to report. However, clinically at the end of a median follow-up time of 29.5 months, the majority of patients (n = 18, 69.2%) had full oral intake. In those remaining eight who did eventually receive a PEG/PEJ tube (either planned or otherwise), two patients had their PEG tube successfully removed, two patients were co-dependent on tube feeding and oral feeding, three patients had hardly any oral feeding capability and mainly relied on tube feeding. Finally, one patient was entirely dependent on tube feeding due to aspiration risk. Thus, a clinically functional and preserved swallowing function could be observed for 76.9% (n = 20/26) of cases. Partially preserved swallowing function was present in 7.7% (n = 2/26) and dysfunctional swallowing with persistent dysphagia was present in 11.5% (n = 3/26) of patients. Only one patient (3.8%) showed complete loss of swallowing function due to treatment and was completely dependent on PEG tube.

The overall majority of patients was treated with PDT without a planned tracheotomy (n = 15, 57.7%). Three patients already had a permanent tracheostoma due to a laryngectomy in the past (n = 3, 11.5%). Most tracheostomies (n = 7, 26.9%) were planned and performed in the same hospitalization as the PDT treatment, before mTHPC injection and illumination. All planned tracheostomies were performed for patients that had PDT in the oropharynx. Namely, two out of three base of tongue carcinomas and three out of eight soft palate tumors. All (n = 3) posterior oropharynx tumors had airway management: two received a planned tracheostomy and one had a pre-existing tracheostomy. In only one case an urgent unplanned bedside tracheotomy under local anesthesia was necessary, 2 days after PDT illumination, due to laryngeal edema following prolonged illumination during difficult fiberoptic intubation. Notably this patient in particular had a history of a hemi-laryngectomy with reconstruction and closure of previous tracheostoma. Median duration until decannulation for the planned tracheostomy patients was 24.5 days (n = 6, range: 11–127 days, mean 50 days). Thus, tracheotomy dependency is low with 85.7% decannulation rate (n = 6/7) after PDT treatment. One patient was never decannulated due to progressive disease.

The most expected local adverse event of tumor site necrosis (**Figure 1**) occurred in 88.5% (n = 23) of cases. In one of three cases without necrosis, progressive disease was present. In the other two cases complete tumor response was observed. We observed that local healing was complete at a median local healing time of 107 days (3–4 months; mean 143, n = 21, range: 30–604 days). In 5 patients failure of observing full healing was due to tumor recurrence in 4 and to a tumor-unrelated

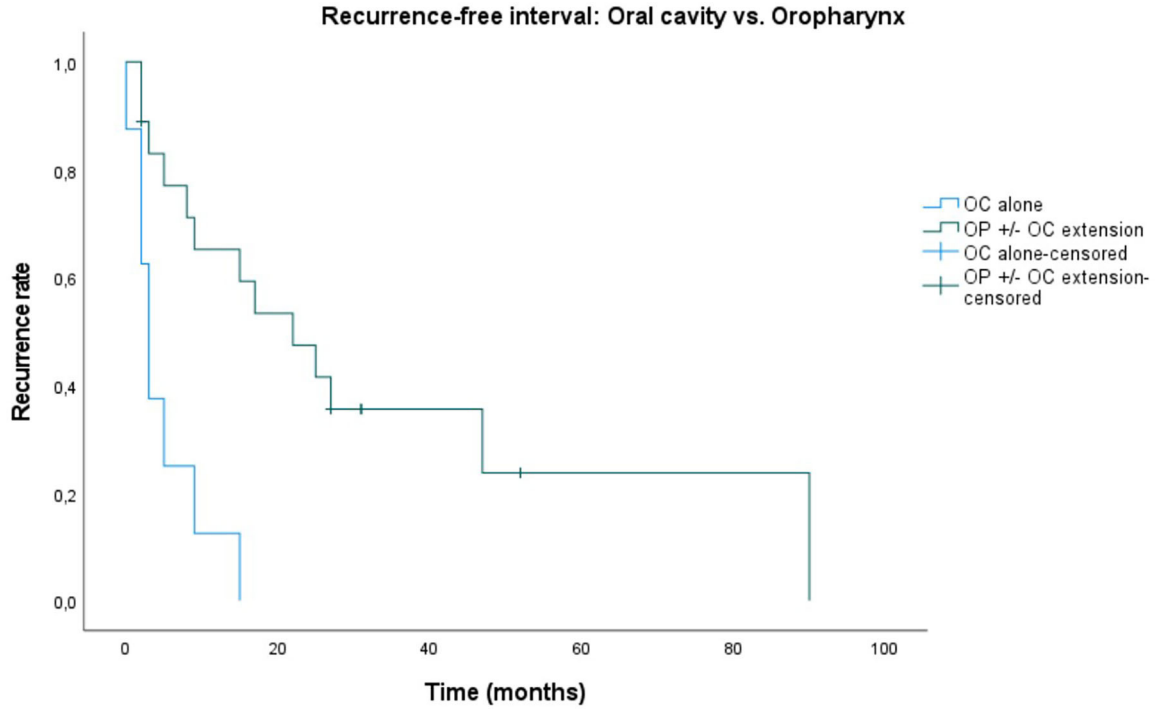

FIGURE 4 | Kaplan–Meier plot showing statistically significant difference in recurrence-free interval ($p < 0.001$) for oropharyngeal squamous cell carcinoma (with or without oral cavity extension) treated with photodynamic therapy, compared to oral cavity tumors alone. Starting point in time is PDT illumination date until local recurrence. OC, oral cavity; OP ± OC extension, oropharyngeal squamous cell carcinoma with or without oral cavity extension.

death (acute CVA) in the early follow-up period. Out of the four patients with recurrence, according to the RECIST tumor response criteria (15), two presented stable disease and the other two progressive disease at a median follow-up time of 57 days ($n = 4$, range 22–85 days, mean 55 days). Other local adverse effects in order of prevalence were: facial edema ($n = 13$, 50%), nasal regurgitation ($n = 9$, 34.6%), injection site reaction ($n = 7$, 26.9%), spontaneous burns of various degrees ($n = 7$, 26.9%), trismus ($n = 7$, 26.9%), phlebitis ($n = 5$, 19.2%), necrotizing stomatitis ($n = 5.19.2\%$), oronasal fistula ($n = 1$, 3.8%) (**Figure 5**) and velopharyngeal insufficiency ($n = 1$, 3.8%). Systemic incidental indirect adverse events during hospital stay illustrate the frailty of this patient population and the impact of PDT treatment in this instance: delirium, takotsubo cardiomyopathy, cardiac arrhythmia, urinary retention, aspiration pneumonia, acute cerebrovascular accident (CVA).

DISCUSSION

We studied 26 patients with oral and/or oropharyngeal cancer treated with photodynamic therapy (PDT). Complete tumor response occurred in 20 out of 26 patients (76.9%). Partial response was noted in three cases (11.5%) and progressive disease was observed in the remaining three cases (11.5%). Tan et al. (4) in a multicenter study of 39 patients, report a complete response in 49% of cases. In our study, local control was obtained in 42.3% ($n = 11$) of the patients. In case of recurrence ($n = 21$), almost two thirds ($n = 5$, 71.4%) of the tumors appeared at the same or adjacent site as the illuminated tumor. A possible explanation is field cancerization, which involves the expansion and migration of clonally related preneoplastic cells (16), first described by Slaughter et al. (17) who found histologically altered tissue surrounding squamous cell carcinoma.

In our case series mTHPC (Foscan) was used as the photosensitizing agent, as it is the most potent second generation photosensitizing agent currently available and approved in Europe since 2001 for the palliative use in squamous cell carcinoma of the head and neck (18). Newer alternative photosensitizers, with a more favorable photophysical and pharmacokinetic profile, are in development due to need of prolonged protection from sunlight and other sources of bright light after PDT treatment with mTHPC (19). However, further studies with larger patient populations and longer follow-up are needed to confirm the clinical efficacy of these newer agents. Targeted delivery methods of photosensitizers with various nanoparticles as a carrier system, are also being explored, hopefully further expanding the application of PDT for thick and bulky HNSCC without the need for interstitial PDT (20). In the present study, no significant difference in survival and functional outcome was observed between superficial PDT in comparison to interstitial or combined PDT.

Twenty-one of these patients (80.8%) had a history of combined smoking and alcohol abuse. A synergistic effect is proven of smoking and alcohol on the risk of oral cancer (21,

22). Four patients (15.4%) continued to combine smoking and alcohol consumption after receiving PDT. The higher number of isolated alcohol consumption ($n = 9$, 34.6%) post-PDT is most likely due to the fact that part of the combination abusers gave up smoking but were not able to stop alcohol consumption entirely. It is no surprise that all but one of these patients had an extensive oncological history in head and neck squamous cell carcinoma (HNSCC) at various sites (**Table 2**). All were histologically typed as squamous cell carcinoma (SCC) to a variable degree of differentiation, with one verrucous carcinoma. This is in line with the overall percentage of SCC, which accounts for more than 90% of all head and neck cancers (21). Only two patients had a definite negative p16 status, one in each subgroup. The p16 status of the tumors in this study was not systematically assessed, since the cohort spans a broad time-line, dating back to January 2002, before routine p16 staining and HPV *in situ* hybridization was introduced in our center.

The conventional treatment modalities of HNSCC in the curative setting are primary radio(chemo)therapy, ablative surgery alone, or a combination of both treatments (6). In this retrospective study, 15 patients (57.7%) were treated with a combination of radio(chemo)therapy and ablative surgery prior to illumination. Only one patient received PDT as a first treatment modality, and had not received any prior tumor management. Ablative surgery with broad margins is usually preferred due to higher survival rates. On the other hand, surgery has the disadvantage of being mutilating at times, and depending on the localization, size, and distribution of the tumor, the patient can be functionally inoperable or even oncologically unresectable. When performing PDT however, tumor margins need to be taken in account as well. In the multicenter study by D'cruz et al. (8) a minimal margin of 5 mm was used. Likewise, we also implemented a minimal margin of 5–10 mm healthy tissue margin whenever anatomically possible.

Common morbidity after head and neck oncological surgery for HNSCC is observed in swallowing (dysphagia), loss of speech and/or articulation, unfavorable cosmesis, etc. Nonetheless, radiotherapy also has some common non-negligible complications such as: xerostomia, dysgeusia, dysphagia, and osteoradionecrosis (6).

About one third of our patients ($n = 9$, 34.6%) developed a separate primary tumor outside of the head and neck region in their follow-up period after PDT. Notably, the sites of these new primary tumors are also notoriously associated with alcohol abuse and smoking: esophageal cancer, lung cancer, breast cancer, and bladder cancer. Other separate primary tumors were prostate cancer and sarcoma (23–25).

Median overall survival in the systematic review of by De Visscher et al. (12) was 8–16 months. In our patient population, median overall survival (OS) was 31 months (2–129 months). We created Kaplan–Meier plots for OS, and DSS (**Figures 2**, **3**, respectively) and reported the median outcome 6 months, 1, 2, and 5 years after PDT. We looked at different variables including gender, age, TNM classification, substance abuse, and number of recurrences for which treatment with PDT. No statistically significant factor with an impact on OS or DSS was identified. This is most likely at least in part due to the small sample size and the rarity of this treatment modality as well as its indication, which defines a selection of patients with superficial tumors without lymph node involvement or distant metastasis. Nevertheless, the long median survival is remarkable. Particularly in oropharyngeal SCC with or without oral cavity extension, we observed a durable local control. These patients were found to have a significantly better recurrence-free interval ($p < 0.001$) compared to oral cavity SCC alone (**Figure 4**). This difference in outcome could be due to a fraction of oropharyngeal SCC being HPV-induced, unfortunately the lack of consistent HPV/p16 data prevents us from substantiating this possibility. On the other hand, it is not unlikely that most of these oropharyngeal cancers were not HPV related: most ($n = 10$, 71.4%) were soft palate tumors and all patients had a strong tobacco and alcohol past. The rate of soft palate tumors in oropharyngeal cases is comparable to the literature, showing a 75% occurrence in the oropharyngeal tumors analyzed in the systematic review by De Visscher et al. (12). We presume that a more favorable exposure for PDT illumination may also have played a role. Finally, more than half ($n = 11$, 61%) of the oropharyngeal tumors were new primary lesions, whereas tumors in the oral cavity subgroup were more often recurrences ($n = 6$, 75%). The higher rate of new primary lesions in the oropharynx subgroup might contribute to help explain the significant difference in recurrent free interval. Although a significant correlation was not observed in our case series, De Visscher et al. (12) showed a 83% complete tumor response rate for first primary tumors as opposed to 67% in non-primary tumors ($p = 0.001$). There is a paucity of data available in regards to HPV status in PDT studies. Many noteworthy reviews (5, 21), case series (4, 19), and systematic reviews (6, 12) make no comment on it. Interestingly, a recent *in vitro* research study on HPV related sensitivity toward radiation and PDT showed an unexpected but significant difference in sensitivity patterns: Kessel et al. (26) found that a cell line derived from a donor with a HPV infection was more responsive to radiation, but significantly less responsive to PDT than a cell line derived from an HPV-free patient. The authors of this study cannot postulate a simple explanation for this finding, as they observed no impaired photosensitizer uptake or decreased reactive oxygen species formation in the HPV positive cell line. The primary goal of this study was to examine the responsiveness of HPV-negative cells to PDT through paraptosis. Their research shows morphologic evidence for paraptosis after PDT to HPV negative cells, and a significantly less responsive effect from radiotherapy in comparison with PDT due to an impaired apoptosis pathway (26).

Further *in vitro* studies, as well as clinical data, is necessary in order to better understand the effect on PDT in relation to the HPV status of the tumor.

Besides the oncological outcome, we also studied adverse events and toxicity of PDT. When evaluating PDT as a potential treatment modality, a thorough assessment of treatment toxicity on target organ functionality is paramount. Preserved swallowing function, defined as complete oral feeding with no supplementation, was observed at the end of follow-up for 76.9% of cases in our study. Upper airway functionality remained uncompromised in 95.7% of patients that did not

FIGURE 5 | Photodynamic therapy patient with oronasal fistula, 3 months after PDT illumination of the hard palate.

have a pre-existing permanent tracheostoma at the end of follow-up. Thus, tracheotomy dependency is low with a 85.7% decannulation rate after PDT treatment with planned tracheotomy. Only one patient was never decannulated due to progressive disease. The decision to perform prophylactic tracheotomy was based on a case per case evaluation of tumor stage, tumor site, and anticipated difficult airway. In general, when planning PDT for a large tumor surface area located in the oropharyngeal region (base of tongue, soft palate, and posterior pharyngeal wall), a preventive tracheotomy was performed, especially in case of risk factors for a difficult airway, such as trismus, a history of radiation or extensive surgery to the head and neck.

In first instance, out of all adverse events, pain and dysphagia are to be expected. Secondly, facial edema, injection site reactions, burns, nasal regurgitation, trismus, and phlebitis are not uncommon. Tumor necrosis can explain pain after treatment and facial edema. Extensive necrosis can cause exposed bone and oronasal fistula (**Figure 5**) and even cerebrospinal fluid leakage in case of PDT on the skull base. In our study, complete local healing was observed at a median time of 107 days or 3–4 months healing time. Four patients recurred before complete local healing could occur at a median follow-up time of 57 days. In other words, when no progressive healing or rather suspicious tissue is observed after ∼2 months, tumor progression or early recurrence needs to be considered and a low threshold for biopsy is warranted. Phlebitis and injection site reactions are caused by intravenous administration of mTHPC. Burns occur due to the phototoxic effects of mTHPC. Trismus, dysphagia and nasal regurgitation are possible complications because of tissue scarring and the development of fistula after PDT. Delirium, arrhythmia, and cardiomyopathy might be explained by intrinsic factors of the patient population, namely a frail elderly population with a history of smoking and alcohol abuse and stress caused by hospitalization. The adverse events due to photodynamic therapy are mostly mild, but in one case laryngeal edema caused an upper airway obstruction. Adverse events reported in the literature are largely similar to those in our patient population: injection site reactions (11%), edema (11%) (8), trismus (8%), necrotizing stomatitis (5%), vomiting (5%), and dysphagia(13%) (4). Local pain, pruritus (5), burns, orocutaneous fistula, skin necrosis, and acute airway obstruction (7) have also been described. Burns can be avoided if the patient stays inside, away from bright light (6). In the post-PDT illumination period, our patients are instructed on the safety measures regarding light and sun exposure. A commercially available LUX-meter is provided for each patient, which is used during the hospital admission and at home after discharge, to monitor light exposure. The PDT patients are instructed to progressively increase the light exposure by no more than 100 Lux each day. In addition, every patient receives a brochure with a timeline on progressive light exposure and the necessary information on preventive measurements such as

clothing and the avoidance of certain light-emitting appliances (computer, smart phone screens, etc.). In case of burns secondary to the PDT treatment a careful evaluation and follow-up by a specialized burn unit is essential, as second degree burns due to accidental light exposure is not uncommon. During the hospital admission local and systemic effects are monitored, pain is controlled with paracetamol, NSAID and/or opioid pain medication. Usually a prolonged course of 1.5 g metronidazole was administered in three divided daily doses for several weeks to prevent local bacterial colonization of the necrotic tumor site. Evidently, regular debridement of the necrotic tissue is indicated to further reduce the risk of surinfection and promote mucosal healing. Corticosteroid administration is ideally reserved for cases of manifest edema and possible airway risk, as it may inhibit the potential systemic antitumor immunological reaction.

Limitations of this study are the relatively small number of patients treated with PDT over a long period of time, the lack of quality of life measurements, the retrospective study design, and the fact that this study does not compare PDT to standard treatment. Quality of life increase in PDT patients with HNSCC has been demonstrated in the past (4, 8, 12), however, comparative studies to conventional treatment options are currently still lacking. New prospective trials should aim to conduct systematic quality of life assessments before, during, and after PDT therapy to better illustrate the added value of this treatment modality. Due to the long time interval of inclusion, and the inherent long history of HNSCC in many of these patients, the 7th TNM classification system was mostly implemented at the time of diagnosis. Similarly, p16 staining and HPV *in situ* hybridization was not yet routine practice. The strong prevalence of substance abuse in this population as well as the development of multiple different sites of HNSCC, suggests these tumors to be clinically p16 negative. Still, the lack of p16 staining and unknown HPV status is a limitation in this study concerning the tumor biology. There is an overall paucity on data and research on the effects of PDT in HPV positive HNSCC, further *in vitro* research and clinical studies are necessary in order to determine a possible difference in tumor response. Strong points of this analysis are the consistency of treatment protocol and single treating physician, which has remained unchanged over the entire treatment period. Few studies comparing outcomes of PDT to surgical treatment have been published, with mainly positive results (10, 27). However, survival rates should not be compared to those of primary surgical cases, as these tumors treated with PDT are highly selected patients with most often recurrences of previously failed management. More importantly, toxicity and preserved organ function need to be taken into account when comparing PDT to other treatments. To date, there is not much data to support PDT as a primary treatment modality for invasive SCC. Still, a recent systematic review of Vohra et al. (28) showed that PDT is effective in the overall management of oral premalignant lesions.

To further prove the value of PDT in clinical practice, future prospective and controlled randomized studies with a specific treatment protocol and systematic quality of life measurements before, during, and after PDT should be carried out, comparing these outcomes to conventional therapy (6).

CONCLUSION

The oncological outcome in this retrospective study is comparable to what has been previously reported in the literature. A complete response was obtained in 76% of the patients, with local control in 42.3%. Median overall survival was 24 months. The main cause of death was head and neck cancer (65%). Multiple but transient adverse events were reported in our study, mostly PDT specific.

In summary, PDT is a valuable treatment option in selected patients with oral and/or oropharyngeal HNSCC that induces durable local control in an important fraction of treated patients. The technique has an acceptable toxicity profile.

DATA AVAILABILITY STATEMENT

The datasets generated for this article are not readily available because the raw data supporting the conclusions of this article will be made available by the authors upon reasonable request. Requests to access the datasets should be directed to VV, vincent.vanderpoorten@uzleuven.be.

ETHICS STATEMENT

The studies involving human participants were reviewed and approved by Research Ethics Committee UZ/KU Leuven. Written informed consent for participation was not required for this study in accordance with the national legislation and the institutional requirements.

AUTHOR CONTRIBUTIONS

AL: data quality control, data analysis (statistics), drafting manuscript, and review of manuscript. LN: data collection, data analysis (statistics), and drafting manuscript. SN, PC, JM, and PD: drafting manuscript and review of manuscript. VV: study concept, data quality control, data analysis (statistics), drafting manuscript, and review of manuscript. All authors contributed to the article and approved the submitted version.

FUNDING

The open access publication costs were funded through the Vandeputte Walter Head and Neck cancer Fund of the Catholic University Leuven, Belgium.

REFERENCES

1. Bulsara VM, Worthington HV, Glenny AM, Clarkson JE, Conway DI, Macluskey M. Interventions for the treatment of oral and oropharyngeal cancers: surgical treatment. *Cochrane Database Syst Rev.* (2018) 12:CD006205. doi: 10.1002/14651858.CD006205.pub4
2. Kyrgias G, Hajiioannou J, Tolia M, Kouloulias V, Lachanas V, Skoulakis C, et al. Intraoperative radiation therapy (IORT) in head and neck cancer: a systematic review. *Med (United States).* (2016) 95:e5035. doi: 10.1097/MD.0000000000005035
3. Belgian Cancer Registry (2016). Available online at: https://kankerregister.org/default.aspx?url=p_132.htm#top
4. Tan IB, Dolivet G, Ceruse P, Vander Poorten V, Roest G, Rauschning W. Temoporfin-mediated photodynamic therapy in patients with advanced, incurable head and neck cancer: a multicenter study. *Head Neck.* (2010) 32:1597–604. doi: 10.1002/hed.21368
5. Civantos FJ, Karakullukcu B, Biel M, Silver CE, Rinaldo A, Saba NF, et al. A review of photodynamic therapy for neoplasms of the head and neck. *Adv Ther.* (2018) 35:324–40. doi: 10.1007/s12325-018-0659-3
6. Gondivkar SM, Gadbail AR, Choudhary MG, Vedpathak PR, Likhitkar MS. Photodynamic treatment outcomes of potentially-malignant lesions and malignancies of the head and neck region: a systematic review. *J Investig Clin Dent.* (2018) 9:1–9. doi: 10.1111/jicd.12270
7. Durbec M, Cosmidis A, Fuchsmann C, Ramade A, Céruse P. Efficacy and safety of photodynamic therapy with temoporfin in curative treatment of recurrent carcinoma of the oral cavity and oropharynx. *Eur Arch Otorhinolaryngol.* (2013) 270:1433–9. doi: 10.1007/s00405-012-2083-7
8. D'Cruz AK, Robinson MH, Biel MA. mTHPC-mediated photodynamic therapy in patients with advanced, incurable head and neck cancer: a multicenter study of 128 patients. *Head Neck.* (2004) 26:232–40. doi: 10.1002/hed.10372
9. Copper MP, Tan IB, Oppelaar H, Ruevekamp MC, Stewart FA. Meta-tetra(hydroxyphenyl)chlorin photodynamic therapy in early-stage squamous cell carcinoma of the head and neck. *Arch Otolaryngol Head Neck Surg.* (2003) 129:709–11. doi: 10.1001/archotol.129.7.709
10. De Visscher SAHJ, Melchers LJ, Dijkstra PU, Karakullukcu B, Tan IB, Hopper C, et al. MTHPC-mediated photodynamic therapy of early stage oral squamous cell carcinoma: a comparison to surgical treatment. *Ann Surg Oncol.* (2013) 20:3076–82. doi: 10.1245/s10434-013-3006-6
11. Fayter D, Corbett M, Heirs M, Fox D, Eastwood A. A systematic review of photodynamic therapy in the treatment of precancerous skin conditions, Barrett's oesophagus and cancers of the biliary tract, brain, head and neck, lung, oesophagus and skin. *Health Technol Assess (Rockv).* (2010) 14:3–129. doi: 10.3310/hta14370
12. De Visscher SAHJ, Dijkstra PU, Tan IB, Roodenburg JLN, Witjes MJH. MTHPC mediated photodynamic therapy (PDT) of squamous cell carcinoma in the head and neck: a systematic review. *Oral Oncol.* (2013) 49:192–210. doi: 10.1016/j.oraloncology.2012.09.011
13. Kreeft AM. *Functional Inoperability of Oral and Oropharyngeal Cancer*. PhD Thesis, Universiteit van Amsterdam (2013).
14. Digonnet A, Hamoir M, Andry G, Haigentz M Jr, Takes RP, Silver CE, et. al. Post-therapeutic surveillance strategies in head and neck squamous cell carcinoma. *Eur Arch Otorhinolaryngol.* (2013) 270:1569–80. doi: 10.1007/s00405-012-2172-7
15. Eisenhauer EA, Therasse P, Bogaerts J, Schwartz LH, Sargent D, Ford R, et al. New response evaluation criteria in solid tumours: revised RECIST guideline (version 1.1). *Eur J Cancer.* (2009) 45:228–47. doi: 10.1016/j.ejca.2008.10.026
16. Califano J, Van Der Riet P, Westra W, Nawroz H, Clayman G, Piantadosi S, et al. Genetic progression model for head and neck cancer: Implications for field cancerization. *Cancer Res.* (1996) 56:2488–92. doi: 10.5281/zenodo.192487
17. Sathiasekar A, Mathew D, Jaish Lal M, Arul Prakash A, Goma Kumar K. Oral field cancerization and its clinical implications in the management in potentially malignant disorders. *J Pharm Bioallied Sci.* (2017) 9:S23–5. doi: 10.4103/jpbs.JPBS_109_17
18. Biel MA. Photodynamic therapy treatment of early oral and laryngeal cancers. *Photochem Photobiol.* (2007) 83:1063–8. doi: 10.1111/j.1751-1097.2007.00153.x
19. Rigual N, Shafirstein G, Cooper MT, Baumann H, Bellnier DA, Sunar U, et al. Photodynamic therapy with 3-(1'-hexyloxyethyl) pyropheophorbide a for cancer of the oral cavity. *Clin Cancer Res.* (2013) 19:6605–13. doi: 10.1158/1078-0432.CCR-13-1735
20. Meulemans J, Delaere P, Vander Poorten V. Photodynamic therapy in head and neck cancer: indications, outcomes, and future prospects. *Curr Opin Otolaryngol Head Neck Surg.* (2019) 27:136–41. doi: 10.1097/MOO.0000000000000521
21. Rivera C. Essentials of oral cancer. *Int J Clin Exp Pathol.* (2015) 8:11884–94.
22. Dal Maso L, Torelli N, Biancotto E, Di Maso M, Gini A, Franchin G, et al. Combined effect of tobacco smoking and alcohol drinking in the risk of head and neck cancers: a re-analysis of case-control studies using bi-dimensional spline models. *Eur J Epidemiol.* (2016) 31:385–93 doi: 10.1007/s10654-015-0028-3
23. Freedman ND, Abnet CC, Caporaso NE, Fraumeni JF, Murphy G, Hartge P, et al. Impact of changing US cigarette smoking patterns on incident cancer: risks of 20 smoking-related cancers among the women and men of the NIH-AARP cohort. *Int J Epidemiol.* (2016) 45:846–56. doi: 10.1093/ije/dyv175
24. Jayasekara H, MacInnis RJ, Room R, English DR. Long-term alcohol consumption and breast, upper aero-digestive tract and colorectal cancer risk: a systematic review and meta-analysis. *Alcohol Alcohol.* (2016) 51:315–0. doi: 10.1093/alcalc/agv110
25. De Menezes RF, Bergmann A, Thuler LCS. Alcohol consumption and risk of cancer: a systematic literature review. *Asian Pacific J Cancer Prev.* (2013) 14:4965–72 doi: 10.7314/APJCP.2013.14.9.4965
26. Kessel D, Cho WJ, Rakowski J, Kim HE, Kim HC. Effects of HPV Status on responsiveness to ionizing radiation vs photodynamic therapy in head and neck cancer cell lines. *Photochem Photobiol.* (2020) 96:652–7. doi: 10.1111/php.13150
27. Karakullukcu B, Stoker SD, Wildeman APE, Copper MP, Wildeman MA, Tan IB. A matched cohort comparison of mTHPC-mediated photodynamic therapy and trans-oral surgery of early stage oral cavity squamous cell cancer. *Eur Arch Otorhinolaryngol.* (2013) 270:1093–7. doi: 10.1007/s00405-012-2104-6
28. Vohra F, Al-Kheraif AA, Qadri T, Hassan MIA, Ahmed A, Warnakulasuriya S, et al. Efficacy of photodynamic therapy in the management of oral premalignant lesions. A systematic review. *Photodiagnosis Photodyn Ther.* (2015) 12:150–9. doi: 10.1016/j.pdpdt.2014.10.001

Conflict of Interest: The authors declare that the research was conducted in the absence of any commercial or financial relationships that could be construed as a potential conflict of interest.

frontiers in Oncology

SYSTEMATIC REVIEW
published: 08 March 2021
doi: 10.3389/fonc.2021.630906

Impact of Multidisciplinary Team Management on the Survival Rate of Head and Neck Cancer Patients: A Cohort Study Meta-analysis

Changyi Shang[1], Linfei Feng[1], Ying Gu[2], Houlin Hong[3], Lilin Hong[4] and Jun Hou[1]**

[1] Department of Oral and Maxillofacial Surgery, The First Affiliated Hospital of Anhui Medical University, Hefei, China, [2] Department of General Dentistry, School of Dental Medicine, Stony Brook University, Stony Brook, NY, United States, [3] Program in Public Health, Stony Brook Medicine, Stony Brook University, Stony Brook, NY, United States, [4] Department of General Dentistry, The Fourth Affiliated Hospital of Anhui Medical University, Hefei, China

Background: Head and neck cancer (HNC) is one of the more common malignant tumors that threaten human health worldwide. Multidisciplinary team management (MDTM) in HNC treatment has been introduced in the past several decades to improve patient survival rates. This study reviewed the impact of MDTM on survival rates in patients with HNC compared to conventional treatment methods.

Methods: Only cohort studies were identified for this meta-analysis that included an exposure group that utilized MDTM and a control group. Heterogeneity and sensitivity also were assessed. Survival rate data for HNC patients were analyzed using RevMan 5.2 software.

Results: Five cohort studies (n = 39,070) that examined survival rates among HNC patients were included. Hazard ratios (HR) were calculated using the random effect model. The results revealed that exposure groups treated using MDTM exhibited a higher survival rate [HR = 0.84, 95% CI (0.76–0.92), P = 0.0004] with moderate heterogeneity (I^2 = 68%, p = 0.01). For two studies that examined the effect of MDTM on the survival rate for patients specifically with stage IV HNC, MDTM did not produce any statistically significant improvement in survival rates [HR = 0.81, 95% CI (0.59–1.10), p = 0.18].

Conclusions: The application of MDTM based on conventional surgery, radiotherapy, and chemotherapy improved the overall survival rate of patients with HNC. Future research should examine the efficacy of MDTM in patients with cancer at different stages.

Keywords: multidisciplinary team management, MDTM, head and neck cancer, HNC, survival rate, meta-analysis

OPEN ACCESS

Edited by:
Paolo Bossi,
University of Brescia, Italy

Reviewed by:
Olgun Elicin,
Bern University Hospital, Switzerland
Fausto Petrelli,
ASST di Bergamo Ovest, Italy

***Correspondence:**
Lilin Hong
hongll899@sohu.com
Jun Hou
2223409716@qq.com

Specialty section:
This article was submitted to Head and Neck Cancer, a section of the journal Frontiers in Oncology

Received: *18 November 2020*
Accepted: *16 February 2021*
Published: *08 March 2021*

Citation:
Shang C, Feng L, Gu Y, Hong H, Hong L and Hou J (2021) Impact of Multidisciplinary Team Management on the Survival Rate of Head and Neck Cancer Patients: A Cohort Study Meta-analysis. Front. Oncol. 11:630906. doi: 10.3389/fonc.2021.630906

INTRODUCTION

Head and neck cancer (HNC) consists of a group of malignant neoplasias involving different anatomical regions, including the oral cavity, pharynx, larynx, paranasal sinuses, nasal cavity, and salivary glands (1). HNC is the sixth most common type of cancer among humans, and every year, over 650,000 HNCs are diagnosed worldwide, contributing to more than 330,000 deaths annually (2, 3). High rates have been reported on the Indian subcontinent and other parts of Asia, with male incidence rates exceeding 10 per 100,000 annually (4, 5). HNC presents with the characteristics of

invasion and malignancy, and 90% of HNCs are squamous cell carcinoma (HNSCC) (6). Among the cases of HNSCC, oral squamous cell carcinoma (OSCC) comprises the majority of HNCs and accounts for approximately 90% of all oral malignancies (7). Although HNC usually is curable if diagnosed early, the lack of patient awareness of early warning signs makes early diagnosis challenging. About two-thirds of HNC patients already have advanced to stages III and IV at the time of diagnosis, leading to increased postoperative recurrence and metastasis (8, 9). The resulting poor prognosis leads to a 5-year survival rate of ∼50% for HNC patients (10, 11).

To promote better cancer treatment outcomes, medical institutions have established multidisciplinary team management (MDTM). MDTM refers to the method of clinical diagnosis and treatment drawn from two or more related disciplines with the participation of representatives from each relevant medical specialty. The core activity of MDTM utilized to improve patient prognosis is to hold MDT meetings, at which all new cases of HNC are discussed, and each patient receives a personalized diagnosis and treatment plan (12). Also, patients undergoing surgery, radiotherapy, or chemotherapy for HNC are suggested to have weekly discussions for the duration of their treatment (13). MDTM integrates the professional knowledge associated with various disciplines and breaks down professional boundaries of these disciplines, resulting in improved diagnosis and treatment. The MDTM teams usually include a trained head and neck surgeon. In addition to medical oncology and radiation oncology, MDTM teams can include radiologists, speech therapy, nutritional experts, pathology, dental services, nurses, and social work (14). However, there is no international consensus concerning the necessary professional team members from participating disciplines to be included on MDTM teams established for HNC (15, 16).

The time consumption and financial burden of regular MDT meetings are high, and some researchers believe that the cost for MDTM exceeds its benefits (17, 18). For patients with HNC, one of the greatest benefits of MDTM is improved survival rates. Recently, researchers have explored the impact of the application of MDTM to conventional surgery, radiotherapy, and chemotherapy on patient survival rates, but the results are controversial (19–22). The therapeutic effect of MDTM in improving HNC outcomes has not been studied thoroughly. In this paper, it was hypothesized that MDTM improved the survival rate of patients with HNC.

METHODS

This meta-analysis study was prepared according to the Preferred Reporting Items for Systematic Reviews and Meta-Analyses (PRISMA) guidelines (23) and the Meta-analysis of Observational Studies in Epidemiology (MOOSE) guideline (24). It was conducted using the methodology recommended by the Cochrane Collaboration (25).

Abbreviations: MDTM, Multidisciplinary team management; HNC, Head and neck cancer; OSCC, oral squamous cell carcinoma.

Selection Criteria

Studies were included in data analyses if they met the following criteria. (1) The studies were cohort studies and published as original studies. (2) They assessed head and neck cancers with MDTM as an exposure and had conventional surgery, radiotherapy, or chemotherapy treatment measures as a control for comparison. (3) The studies analyzed survival rate as an outcome measure. (4) The studies used appropriate statistical analyses, such as hazard ratios and effect sizes or translatable data between the exposure and control groups.

Search Strategy

PubMed, Cochrane, EMBASE, and Web of Science English databases were systematically searched for publications on MDTM of HNC patients. Searches were limited to articles published in English until January 2020. The main search terms included "head and neck squamous cell carcinoma," "oral cancer," "mouth tumor," "nasopharyngeal tumor," "sino-nasal tumor," "pharyngeal tumor," "laryngeal tumor," "multidisciplinary team," and "survival." Titles, abstracts, and keywords were carefully examined to retrieve all relevant articles. In addition, the reference lists from the retrieved articles also were examined, and Medical Subject Headings (MeSH) were used to identify relevant studies.

Data Extraction

Two reviewers (CS and LF) independently screened articles retrieved from databases using the inclusion criteria mentioned above. The full text of the articles was carefully reviewed, and data were extracted from each selected study. In cases of disagreement and inconsistencies, a third researcher (JH) was consulted for adjudication. For each study, the publication year, country, research type, sample size, exposure factors, and outcome measures were extracted.

Quality Assessment

Currently, the Newcastle-Ottawa scale (NOS) is the most commonly used bias risk assessment tool for cohort studies (26). The NOS is divided into two parts, which are appropriate to evaluate cohort and case-control studies. Each part has three columns, including study population selection, comparability, and exposure or outcome evaluation, and eight items in total. The NOS bias risk was evaluated using a semi-quantitative star system, with a full score of nine stars. Two evaluators (CS and LF) evaluated the methodological quality for each cohort study included in this meta-analysis. Discrepancies were resolved when a consensus was reached with the third researcher (JH).

Statistical Analysis

The effects of MDTM were presented using hazard ratios (HR) and 95% confidence intervals (CI). The study heterogeneity was evaluated using Chi-square tests or Q tests for I^2 values. The I^2 value of heterogeneity was categorized as no, small, moderate, and large heterogeneity with values of 0, 25, 50, and 75%, respectively. When the heterogeneity was small ($P_Q \geq 0.1$ or $I^2 \leq 50\%$), the combined HR and 95% CI were calculated using the Mantel-Haensel fixed-effect model.

The Dersimonian-Laird random-effect model was used if the heterogeneity between studies was large ($P_Q < 0.1$ or $I^2 > 50\%$). The impact of individual studies on combined HR values was estimated using reassessment and missing mapping in each study. Subgroup analysis was performed to explore the source of heterogeneity. All analyses were performed using Review Manager (RevMan) version 5.2 (The Cochrane Collaboration, The Nordic Cochrane Centre, Copenhagen, Denmark) and Stata version 12.0 (StataCorp LP, College Station, TX, USA). *P*-values <0.05 were considered statistically significant.

RESULTS

Search Results

Two hundred thirty-three articles were retrieved from the initial search (**Figure 1**), and 25 were removed due to duplication. A further 178 articles were excluded after the titles and abstracts were reviewed. Fourteen articles were excluded due to inappropriate research methods. Of the 16 remaining articles, four were excluded because of duplication, and seven failed to meet the inclusion criteria.

Characteristics of the Eligible Studies

Five studies involving 39,070 patients were included in this meta-analysis (see **Table 1**). All five studies used HR as the outcome measure (13, 19, 20, 27, 28). The proportion of males ranged from 72 to 93.21%, and the average age ranged from 51 to 61.4 years. All five studies were adjusted for confounding effects (e.g., sex, age, race, disease stage, tumor location, hospital level, and others) to evaluate the association between MDTM and the survival of patients with HNC using survival models.

Methodological Quality of the Included Studies

As shown in **Table 2**, the baseline consistency between the exposed group and the control group in each study was satisfactory and comparable. The median of the NOS quality evaluation for the five cohort studies was an average value of 6.00 ± 0.71 (range 5–7).

Primary Outcome

The Effect of MDTM on the Survival Rate of Patients With HNC

The five studies included in this analysis demonstrated moderate heterogeneity ($I^2 = 68\%$, $p = 0.01$). Therefore, a random-effect model was used to estimate the MDTM treatment effect. The model suggested that MDTM resulted in a significantly higher survival rate in HNC patients compared to conventional methods [Overall HR: 0.84, 95% CI (0.76–0.92), $Z = 3.52$, $P = 0.0004$]. Thus, MDTM produced a 16% improvement in survival rate (**Figure 2**).

Meta-Analysis of the Effect of MDTM on the Survival Rate of Patients With Stage IV HNC

Of the five articles included in the analysis, two studies described the effects of MDTM management on the survival rate of patients with stage IV HNC (19, 20). The cancer stages were determined by the Union for International Cancer Control (UICC) cancer staging system in Friedland's study (19); while the American Joint Committee on Cancer (AJCC) cancer staging system was used in Tsai's study (20). Greater heterogeneity was observed between these two studies ($I^2 = 80\%$. $P = 0.03$). Although MDTM showed a trend toward an improved survival rate among patients with stage IV HNC, it did not reach statistical significance [combined HR = 0.81, 95% CI (0.59–1.10), $Z = 1.35$, $P = 0.18$, **Figure 3**].

Sensitivity Analysis

Two models were used to assess sensitivity, including removing the highest gravity study (20) and removing the lowest gravity study (13) (**Figure 4**). The results of the two models were similar (HR with the removal of the highest gravity = 0.82; HR with the removal of the lowest gravity = 0.85). However, the heterogeneity reached zero when the highest gravity study was removed ($I^2 = 0\%$), indicating that the removed study was a major source of the heterogeneity (**Table 3**).

Subgroup Analyses

Subgroup analyses were performed according to the nationality of the study subjects to determine possible sources of heterogeneity. Three of the five studies (20, 27, 28) were from Asia, while the other two (13, 19) were conducted in Australia and the United States. The heterogeneity for studies from Asia was high ($I^2 = 81\%$, $p = 0.005$), while the heterogeneity for the other two countries was low ($I^2 = 0\%$, $p = 0.47$). HRs for studies from Asia and non-Asian countries were 0.86 and 0.76, respectively, (both *p*-values <0.01), and were not significantly different between Asia and non-Asian countries ($p = 0.27$).

DISCUSSION

Since HNC consists of a collection of complex and heterogeneous malignant tumors, it requires a range of treatment strategies. MDTM combines evidence-based treatment models, local experience, and well-developed management skills. To promote efficient and effective evidence-based management of HNC cases, most medical centers have established a process for MDTM that includes the participation of representatives from each relevant medical specialty. Treatment plans are made based on accurate tumor staging and other factors, including physical rehabilitation, mental health, and economic conditions that are tailored for different individuals in the MDTM meetings. A recent study evaluated multidisciplinary team meetings in a national tertiary referral center in Morocco and found that out of 105 patients (50.72%) who were scheduled for a MDTM meeting, 79 (38%) received and completed the MDTM meeting before treatment (29). According to the classification statistics for the different treatment methods for patients who were scheduled for a MDTM meeting, the proportion of patients who completed the MDTM meeting was 68% for surgery, 35% for medical treatment, and 19% for radiotherapy. Of the patients discussed at the MDTM meetings, 4–45% received changes in the post-meeting diagnostic reports, and they were more likely to receive more accurate and complete preoperative staging and new neo-adjuvant or adjuvant treatment (18).

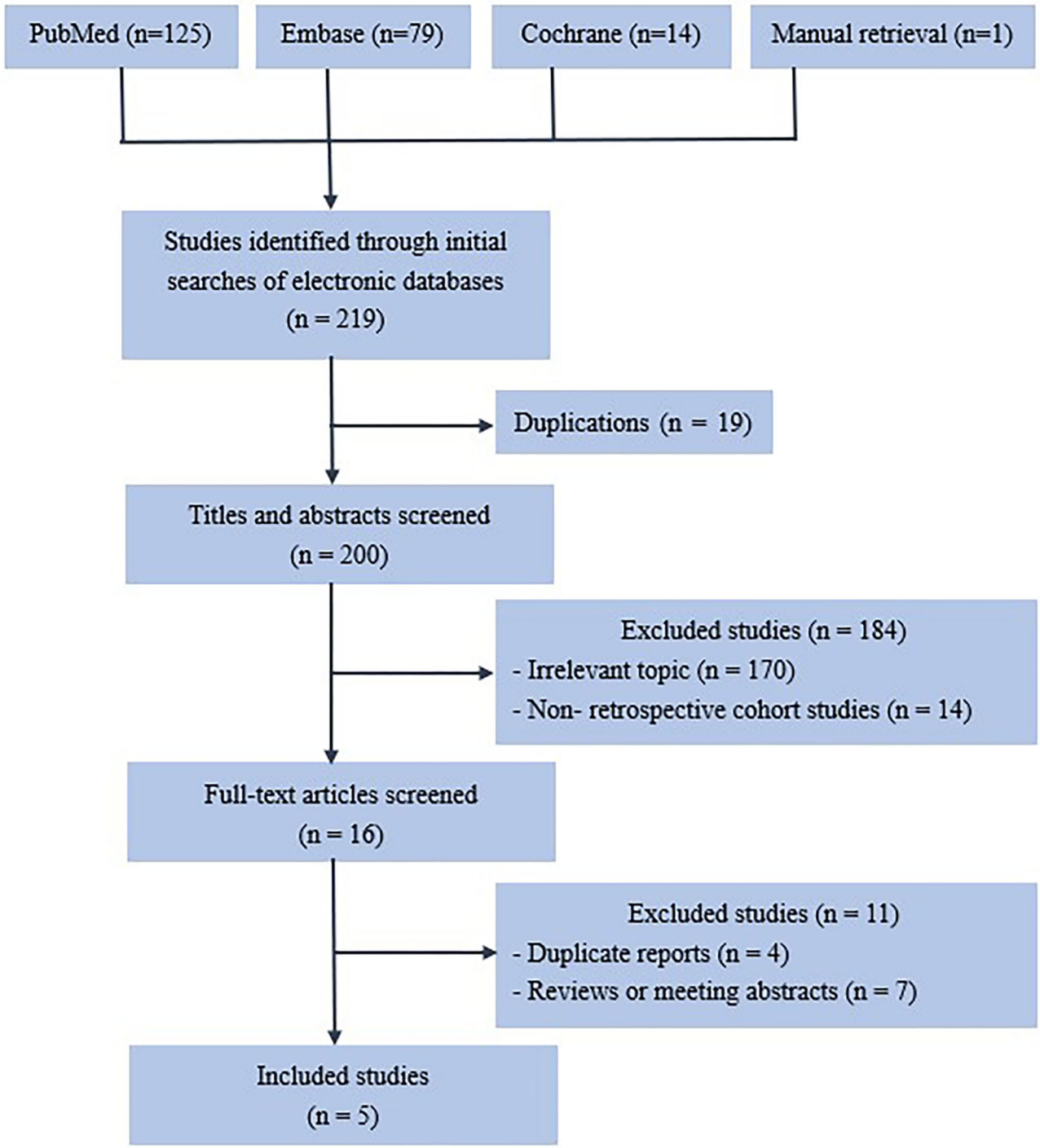

FIGURE 1 | Flow chart showing the selection of papers.

We reviewed two retrospective studies that evaluated the role of MDTM in HNC. Nguyen et al. reviewed 225 patients with locally advanced HNC to identify how treatment outcomes were affected by MDTM recommendations. The authors concluded that MDTM approaches provided optimal treatment outcomes for locally advanced HNC (30). Birchall et al. found that patients assessed using MDTM experienced improved 2-year survival outcomes compared with patients who were not assessed using MDTM ($p = 0.03$) (31). The MDTM approach for treating patients with HNC has improved the organization of standard

TABLE 1 | Main characteristics of studies included in the meta-analysis.

Study	Year	Country	Study type	Study time	Number	Study scope	Cancer stage	HR	95%CI	*P*	NOS score
P. L. Friedland et al.	2011	Australia	Retrospective cohort study	1996–2008	726	H&N	I–IV	0.79	0.64–0.97	0.024	6
Y. H. Wang et al.	2012	Taiwan,China	Retrospective cohort study	2004–2008	19,513	Oral	-	0.84	0.78–0.90	0.001	7
W. C. Tsai et al.	2015	Taiwan,China	Nationwide cohort study	2004–2010	16,991	Oral	-	0.94	0.89–1.00	0.032	6
C. T. Liao et al.	2016	Taiwan,China	Retrospective cohort study	1996–2011	1,616	Oral	III–IV	0.75	0.63–0.89	0.001	5
J. C. Liu et al.	2019	America	Retrospective cohort study	2006–2015	224	H&N	I–IV	0.67	0.46–0.98	0.041	6

TABLE 2 | NOS of studies included in the meta-analysis.

Study	Study population selection				Comparability between groups	Result measurement			NOS score
	Exposure group representativeness	Control group selection method	Methods for determining exposure factors	Whether there are outcome indicators to be observed at the beginning of the study		Sufficiency of result evaluation	Length of follow-up time	Adequacy of follow-up	
P. L. Friedland et al.	1	1	1	1	1	0	1	0	6
Y. H. Wang et al.	1	1	1	1	1	0	1	1	7
W. C. Tsai et al.	1	1	1	1	1	0	1	0	6
C. T. Liao et al.	1	1	0	1	1	0	1	0	5
J. C. Liu et al.	1	1	1	1	1	0	1	0	6

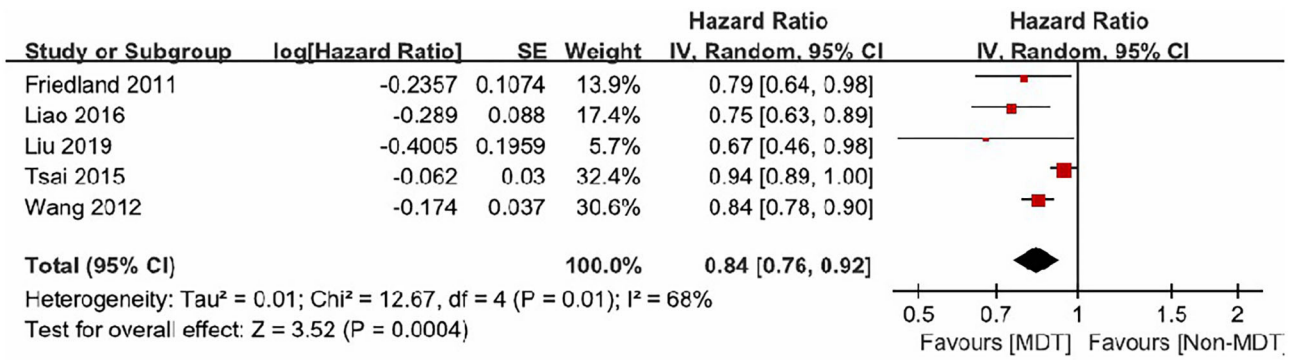

FIGURE 2 | Forest plot of MDTM patients' survival rate.

clinical guidelines, but this development has yet to translate into a demonstrable impact on survival (21). Croke et al. reported that articles showing that MDTM improved the prognosis of tumor patients have great heterogeneity after statistical analysis, so the relationship between MDTM and the prognosis of tumor patients is not clear (22). We found evidence that supported the concept that MDTM significantly influenced clinical decision-making and treatment recommendations. However, scant evidence suggested that MDTM improved patient outcomes. Because the relationship between MDTM and the survival rate of patients with HNC is still uncertain, we conducted this meta-analysis.

Based on the literature search, we did not find meta-analysis research on this specific topic. Therefore, this was the first meta-analysis to evaluate the influence of MDTM on the survival rate of HNC patients. We found that the survival rate of patients with HNC was positively correlated with the use of MDTM. Compared to conventional treatments, MDTM improved the survival rate of patients with HNC, with a combined-effect HR of 0.84. Through sensitivity analysis, we observed that the change in the estimated value of the combined effect quantity was not apparent when the highest gravity was removed and subsequently the lowest gravity. These observations indicated

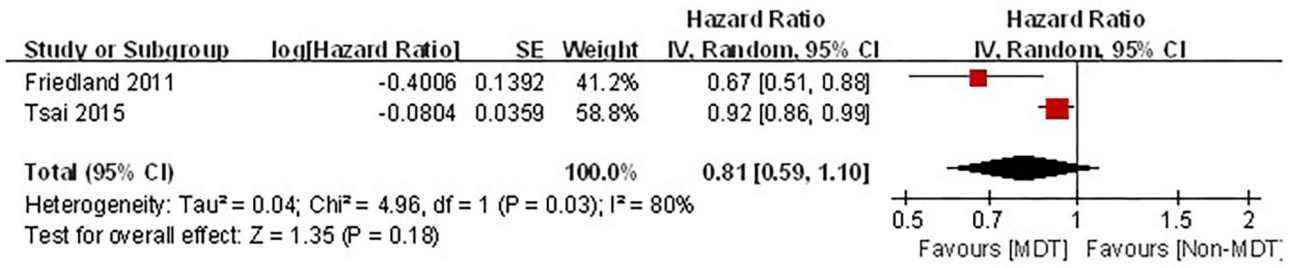

FIGURE 3 | Forest plot of MDTM survival rate of stage IV cancer patients.

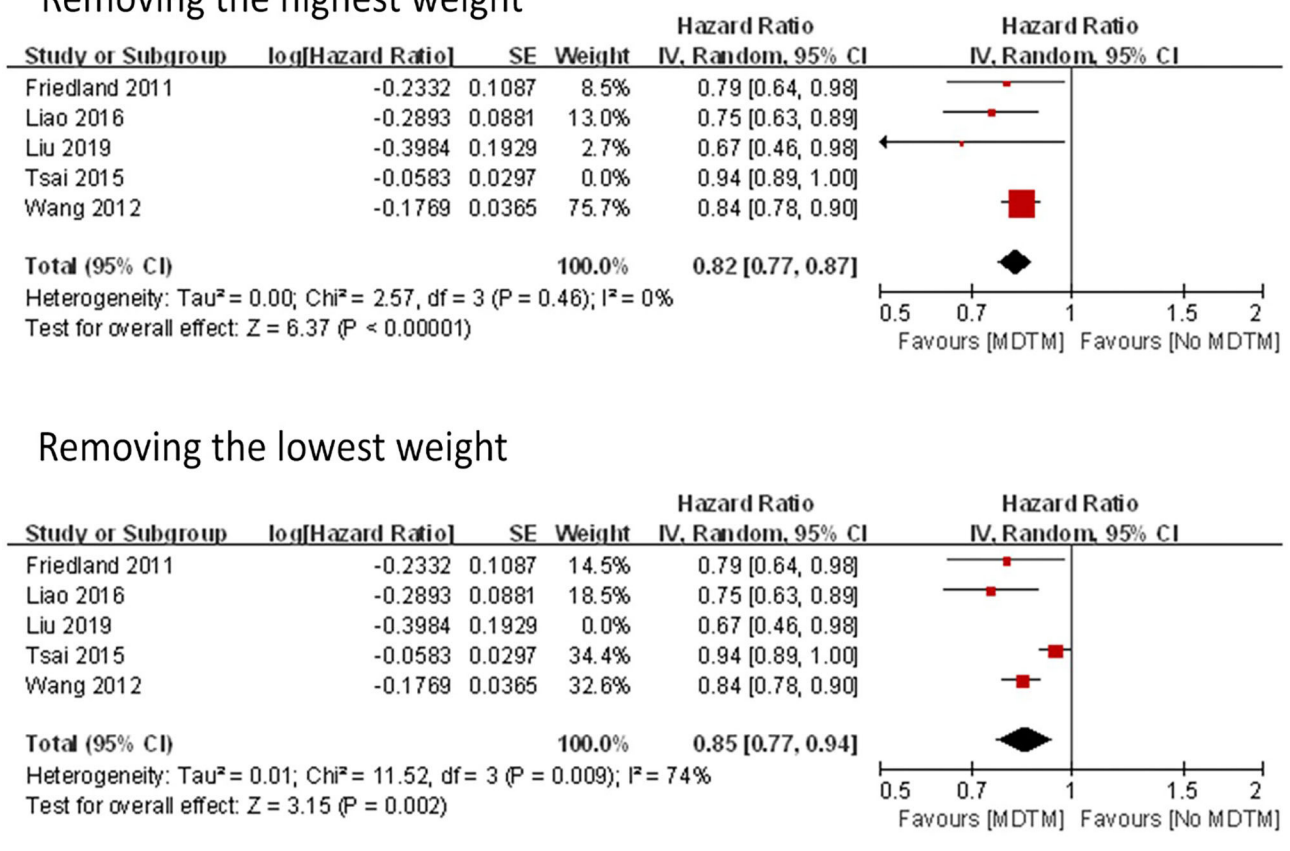

FIGURE 4 | Forest plot of MDTM survival rate removing the highest and lowest weight.

that the results of this meta-analysis were stable. However, after removing the highest proportion item, the heterogeneity disappeared, indicating that the eliminated study was a dominant source of heterogeneity. This study included five cohort studies. Therefore, this study might have been affected by a range of biases. Specifically, the overall management quality of the MDTM in the exposure group and the baseline consistency in the control group were affected, resulting in bias. Using subgroup analysis, we determined that the differences observed in the study scope where the research was conducted might have been the source of heterogeneity. There were no subgroup analyses of the HNCs for different stages in this study because most reports did not provide relevant data or lacked complete data to conduct such analyses. Other influencing factors, including gender, occupation, and use of tobacco and alcohol, also contributed to bias. Therefore, additional high-quality cohort studies are needed for large-scale meta-analysis to reduce bias and confirm the reliability of the above conclusions.

The advantages of MDTM are as follows. (1) MDTM is targeted to develop the best treatment, minimize misdiagnoses,

TABLE 3 | Sensitivity Analysis.

Analysis item	*P*	I^2	Effect model	HR	95%CI
Remove the highest proportion of literature	0.44	0%	Fixed-effect model	0.82	0.77–0.87
Remove the lowest proportion of literature	0.01	72%	Random-effect model	0.85	0.77–0.94

TABLE 4 | HNC Stage (UICC Version 6th).

Stage I	Tumor size and invasion: 2 cm or less in diameter, no invasion in adjacent tissues; Lymph node involvement: no; Distant organ involvement: no.
Stage II	Tumor size and invasion: larger than 2 cm in diameter but <4 cm in diameter, or has invaded an adjacent tissues; Lymph node involvement: no; Distant organ involvement: no.
Stage III	Tumor size and invasion: larger than 4 cm in diameter, or Lymph node involvement: no; Distant organ involvement: no.
Stage IVA	Tumor size and invasion: any size and invasion; Lymph node involvement: yes, 3–6 cm; Distant organ involvement: no.
Stage IVB	Tumor size and invasion: the space in front of the cervical spine tumor invasion,called the mediastinum between carotid artery or both lungs structures, such as the trachea and esophagus;or Lymph node involvement: yes, larger than 6 cm; Distant organ involvement: no.
Stage IVC	No matter the size of the primary tumor and lymph node involvement, distant organ involvement (distant metastasis)

and reduce the ineffective treatment of patients. (2) A reasonable treatment plan can be formulated by many experts using MDTM, which avoids inefficient and less effective treatment plans resulting from multiple referrals, repeated examinations, and treatment plan changes that often occur with the traditional treatment protocols. Clear, straightforward, and effective treatment plans can help produce emotional stability in patients that might improve their compliance with the treatment, which is conducive to a more positive outcome of the disease. (3) MDTM can avoid the need for patients to change departments numerous times. This continuity improves treatment and can shorten the time patients must wait for treatment, which also can help improve the prognosis. (4) MDTM enables multiple professional medical experts to consult on and discuss specific cases, which promotes communication and understanding between different departments. Such cooperation ensures the formulation and implementation of optimal treatment plans and facilitates the development of clinical and basic scientific research. This cooperation is critical to allow younger medical students to learn from each other and gain valuable information by participating in the MDTM meetings. (5) Finally, MDTM promotes the improvement of the hospital's overall treatment levels and the survival rates of tumor patients (32).

Among the five studies included in this meta-analysis, Tsai et al. reported that MDTM had a strong beneficial effect on the survival rate of stage IV patients but limited effects on stage I-III patients (20). Friedland et al. did not observe any significant differences in the 5-year survival rates between the MDTM group and the non-MDTM group for stage I–III patients, but the 5-year survival rate for stage IV patients in the MDTM group was significantly higher than the non-MDTM group (19). Although these two studies suggested that MDTM could improve the survival rate of patients with stage IV HNC, the results of this meta-analysis indicated that the impact of MDTM on the survival rate of patients with stage IV HNC was not clear.

There are only two published reports on stage IV HNC at present, which are not enough to prove the effectiveness of MDTM. The limited influence of MDTM on the survival rate of patients with stage IV HNC could be due to several reasons. (1) Patients with stage IV HNC are in the late stages of cancer, and their condition is more severe. The treatments in late-stage cancer are primarily palliative treatments, and the effects of treatment measures on patient survival rates are limited. (2) The survival rate of patients with stage IV HNC is affected by the physical resilience of patients and the degree of cancer metastasis. (3) The distribution of HNC stages is unique, with a distribution skewed toward stage IVA/B in regionally advanced stages (**Table 4**). The UICC stages IVA and IVB can be treated with the possibility of cure, whereas stage IVC is a metastatic disease that has spread to distant regions of the body. For stage IVC patients, oncologists only treat the metastatic disease and do not treat the primary lesions. It should be noted that among the five studies included in the current analysis, cancer stages were determined by AJCC cancer staging system in three studies and UICC cancer staging system (Sixth Edition) was used in one study. In all five studies, the authors categorized cancer stages from I to IV,

however no further subcategorization within stage IV cancers were given.

Several limitations of this study should be acknowledged. First, though the overall sample size is large, the number of studies examined is small. Second, the confounding factors controlled in each study were different, which might result in estimation bias. Third, there might be differences in MDTM levels, which could be the source of heterogeneity observed in the research results. Because only five studies were included in this meta-analysis, a funnel plot could not be used to analyze the publication bias. Fifth, MDTs are a relatively recent (past decade) introduction to the management of HNC patients. Therefore, the improvement in survival might reflect the increase in HPV oropharyngeal cancer and the improved treatment of those patients rather than the MDTM itself. Thus, conclusions should be drawn with caution. The impact of MDTM on the survival rate of patients with stage IV HNC is not clear, and more research is needed.

CONCLUSION

MDTM plays a prominent role in cancer treatment. We systematically evaluated the impact of MDTM on the survival rate of HNC patients. MDTM demonstrated a higher survival rate for HNC patients overall. This paper provided evidence for the successful application of MDTM in the treatment of HNC patients. Thus, MDTM is recommended in the treatment of HNC.

At present, there are few reports on the differences in survival rates for patients with different stages of HNC when MDTM was used. Although two studies claimed that the positive impact of MDTM on the survival rate of patients with stage IV HNC was greater than that of patients with stage I-III, the results of this meta-analysis did not demonstrate a statistical difference. Therefore, future research should focus on the difference of the effects of MDTM on the survival rate of HNC patients in different stages of the disease. This information would allow doctors and patients to judge the necessity of using MDTM, reduce unnecessary time and money invested by patients, and conserve valuable medical resources.

DATA AVAILABILITY STATEMENT

The original contributions presented in the study are included in the article/supplementary material, further inquiries can be directed to the corresponding author/s.

AUTHOR CONTRIBUTIONS

CS, LF, and JH conceived and designed the research. CS ran the model. LH contributed to materials. CS and LF searched and retrieved articles from database both also wrote the manuscript. LH, HH, and YG edited the paper. All authors contributed to the article and approved the submitted version.

ACKNOWLEDGMENTS

The authors would like to express their gratitude to EditSprings (https://www.editsprings.com/) for the expert linguistic services provided.

REFERENCES

1. Licitra L, Keilholz U, Tahara M, Lin JC, Chomette P, Ceruse P, et al. Evaluation of the benefit and use of multidisciplinary teams in the treatment of head and neck cancer. *Oral Oncol.* (2016) 59:73–9. doi: 10.1016/j.oraloncology.2016.06.002
2. Sritippho T, Chotjumlong P, Iamaroon A. Roles of human papillomaviruses and p16 in oral cancer. *Asian Pac J Cancer Prev.* (2015) 16:6193–200. doi: 10.7314/APJCP.2015.16.15.6193
3. Bray F, Ferlay J, Soerjomataram I, Siegel RL, Torre LA, Jemal A. Global cancer statistics 2018: GLOBOCAN estimates of incidence and mortality worldwide for 36 cancers in 185 countries. *CA Cancer J Clin.* (2018) 68:394–424. doi: 10.3322/caac.21492
4. Moore SR, Johnson NW, Pierce AM, Wilson DF. The epidemiology of mouth cancer: a review of global incidence. *Oral Dis.* (2000) 6:65–74. doi: 10.1111/j.1601-0825.2000.tb00104.x
5. Patel SS, Shah KA, Shah MJ, Kothari KC, Rawal RM. Cancer stem cells and stemness markers in oral squamous cell carcinomas. *Asian Pac J Cancer Prev.* (2014) 15:8549–56. doi: 10.7314/APJCP.2014.15.20.8549
6. Vigneswaran N, Williams MD. Epidemiologic trends in head and neck cancer and aids in diagnosis. *Oral Maxillofac Surg Clin North Am.* (2014) 26:123–41. doi: 10.1016/j.coms.2014.01.001
7. Sarode GS, Sarode SC, Maniyar N, Anand R, Patil S. Oral cancer databases: a comprehensive review. *J Oral Pathol Med.* (2018) 47:547–56. doi: 10.1111/jop.12667
8. Haddad RI, Shin DM. Recent advances in head and neck cancer. *N Engl J Med.* (2008) 359:1143–54. doi: 10.1056/NEJMra0707975
9. Rogers SN, Brown JS, Woolgar JA, Lowe D, Magennis P, Shaw RJ, et al. Survival following primary surgery for oral cancer. *Oral Oncol.* (2009) 45:201–11. doi: 10.1016/j.oraloncology.2008.05.008
10. Taghavi N, Yazdi I. Prognostic factors of survival rate in oral squamous cell carcinoma: clinical, histologic, genetic and molecular concepts. *Arch Iran Med.* (2015) 18:314–9.
11. Kumar M, Nanavati R, Modi TG, Dobariya C. Oral cancer: etiology and risk factors: a review. *J Cancer Res Ther.* (2016) 12:458–63. doi: 10.4103/0973-1482.186696
12. Taylor C, Atkins L, Richardson A, Tarrant R, Ramirez AJ. Measuring the quality of MDT working: an observational approach. *BMC Cancer.* (2012) 12:202. doi: 10.1186/1471-2407-12-202
13. Liu JC, Kaplon A, Blackman E, Miyamoto C, Savior D, Ragin C. The impact of the multidisciplinary tumor board on head and neck cancer outcomes. *Laryngoscope.* (2020) 130:946–50. doi: 10.1002/lary.28066
14. Borras JM, Albreht T, Audisio R, Briers E, Casali P, Esperou H, et al. Policy statement on multidisciplinary cancer care. *Eur J Cancer.* (2014) 50:475–80. doi: 10.1016/j.ejca.2013.11.012
15. Wang YH, Kung PT, Tsai WC, Tai CJ, Liu SA, Tsai MH. Effects of multidisciplinary care on the survival of patients with oral cavity cancer in Taiwan. *Oral Oncol.* (2012) 48:803–10. doi: 10.1016/j.oraloncology.2012.03.023
16. Hughes C, Homer J, Bradley P, Nutting C, Ness A, Persson M, et al. An evaluation of current services available for people diagnosed with head and neck cancer in the UK (2009–2010). *Clin Oncol.* (2012) 24:e187–92. doi: 10.1016/j.clon.2012.07.005

17. Taylor C, Munro AJ, Glynne-Jones R, Griffith C, Trevatt P, Richards M, et al. Multidisciplinary team working in cancer: what is the evidence? *BMJ.* (2010) 340:c951. doi: 10.1136/bmj.c951
18. Pillay B, Wootten AC, Crowe H, Corcoran N, Tran B, Bowden P, et al. The impact of multidisciplinary team meetings on patient assessment, management and outcomes in oncology settings: a systematic review of the literature. *Cancer Treat Rev.* (2016) 42:56–72. doi: 10.1016/j.ctrv.2015.11.007
19. Friedland PL, Bozic B, Dewar J, Kuan R, Meyer C, Phillips M. Impact of multidisciplinary team management in head and neck cancer patients. *Br J Cancer.* (2011) 104:1246–8. doi: 10.1038/bjc.2011.92
20. Tsai WC, Kung PT, Wang ST, Huang KH, Liu SA. Beneficial impact of multidisciplinary team management on the survival in different stages of oral cavity cancer patients: results of a nationwide cohort study in Taiwan. *Oral Oncol.* (2015) 51:105–11. doi: 10.1016/j.oraloncology.2014.11.006
21. Coca-Pelaz A, Takes RP, Hutcheson K, Saba NF, Haigentz M Jr, Bradford CR, et al. Head and neck cancer: a review of the impact of treatment delay on outcome. *Adv Ther.* (2018) 35:153–60. doi: 10.1007/s12325-018-0663-7
22. Croke JM, El-Sayed S. Multidisciplinary management of cancer patients: chasing a shadow or real value? An overview of the literature. *Curr Oncol.* (2012) 19:e232–8. doi: 10.3747/co.19.944
23. Shamseer L, Moher D, Clarke M, Ghersi D, Liberati A, Petticrew M, et al. Preferred reporting items for systematic review and meta-analysis protocols (PRISMA-P) 2015: elaboration and explanation. *BMJ.* (2015) 350:g7647. doi: 10.1136/bmj.g7647
24. Stroup DF, Berlin JA, Morton SC, Olkin I, Williamson GD, Rennie D, et al. Meta-analysis of observational studies in epidemiology: a proposal for reporting. Meta-analysis Of Observational Studies in Epidemiology (MOOSE) group. *JAMA.* (2000) 283:2008–12. doi: 10.1001/jama.283.15.2008
25. Meyer S. Evidence-based healthcare and the cochrane collaboration: an unfinished journey as yet! *J Evid Based Med.* (2013) 6:302–4. doi: 10.1111/jebm.12071
26. Stang A. Critical evaluation of the Newcastle-Ottawa scale for the assessment of the quality of nonrandomized studies in meta-analyses. *Eur J Epidemiol.* (2010) 25:603–5. doi: 10.1007/s10654-010-9491-z
27. Liao CT, Kang CJ, Lee LY, Hsueh C, Lin CY, Fan KH, et al. Association between multidisciplinary team care approach and survival rates in patients with oral cavity squamous cell carcinoma. *Head Neck.* (2016) 38(Suppl. 1):E1544–53. doi: 10.1002/hed.24276
28. Wang SM, Kung PT, Wang YH, Huang KH, Tsai WC. Effects of multidisciplinary team care on utilization of emergency care for patients with lung cancer. *Am J Manag Care.* (2014) 20:e353–64.
29. Chaouki W, Mimouni M, Boutayeb S, Hachi H, Errihani H, Benjaafar N. [Evaluation of multidisciplinary team meeting; the example of gynecological mammary cancers in a tertiary referral center in Morocco]. *Bull Cancer.* (2017) 104:644–51. doi: 10.1016/j.bulcan.2017.04.004
30. Nguyen NP, Vos P, Lee H, Borok TL, Karlsson U, Martinez T, et al. Impact of tumor board recommendations on treatment outcome for locally advanced head and neck cancer. *Oncology.* (2008) 75:186–91. doi: 10.1159/000163058
31. Birchall M, Bailey D, King P. South west cancer intelligence service head and neck tumour panel. effect of process standards on survival of patients with head and neck cancer in the south and west of England. *Br J Cancer.* (2004) 91:1477–81. doi: 10.1038/sj.bjc.6602118
32. Westin T, Stalfors J. Tumour boards/multidisciplinary head and neck cancer meetings: are they of value to patients, treating staff or a political additional drain on healthcare resources? *Curr Opin Otolaryngol Head Neck Surg.* (2008) 16:103–7. doi: 10.1097/MOO.0b013e3282f6a4c4

Conflict of Interest: The authors declare that the research was conducted in the absence of any commercial or financial relationships that could be construed as a potential conflict of interest.

frontiers in Oncology

MINI REVIEW
published: 08 March 2021
doi: 10.3389/fonc.2021.616629

Biomarkers for Immunotherapy of Oral Squamous Cell Carcinoma: Current Status and Challenges

Alhadi Almangush[1,2,3,4,5]*, *Ilmo Leivo*[4,6] *and Antti A. Mäkitie*[2,7,8]*

[1] Department of Pathology, University of Helsinki, Helsinki, Finland, [2] Research Program in Systems Oncology, Faculty of Medicine, University of Helsinki, Helsinki, Finland, [3] Department of Oral and Maxillofacial Diseases, University of Helsinki, Helsinki, Finland, [4] Institute of Biomedicine, Pathology, University of Turku, Turku, Finland, [5] Faculty of Dentistry, University of Misurata, Misurata, Libya, [6] Department of Pathology, Turku University Central Hospital, Turku, Finland, [7] Department of Otorhinolaryngology—Head and Neck Surgery, University of Helsinki and Helsinki University Hospital, Helsinki, Finland, [8] Division of Ear, Nose and Throat Diseases, Department of Clinical Sciences, Intervention and Technology, Karolinska Institutet and Karolinska University Hospital, Stockholm, Sweden

OPEN ACCESS

Edited by:
Cesare Piazza, University of Brescia, Italy

Reviewed by:
Renata Ferrarotto, University of Texas MD Anderson Cancer Center, United States
Christophe Le Tourneau, Maria Sklodowska-Curie National Research Institute of Oncology, Poland

***Correspondence:**
Alhadi Almangush
Alhadi.almangush@helsinki.fi
Antti A. Mäkitie
antti.makitie@helsinki.fi

Specialty section:
This article was submitted to Head and Neck Cancer, a section of the journal Frontiers in Oncology

Received: *12 October 2020*
Accepted: *29 January 2021*
Published: *08 March 2021*

Citation:
Almangush A, Leivo I and Mäkitie AA (2021) Biomarkers for Immunotherapy of Oral Squamous Cell Carcinoma: Current Status and Challenges. Front. Oncol. 11:616629. doi: 10.3389/fonc.2021.616629

Oral squamous cell carcinoma (OSCC) forms a major health problem in many countries. For several decades the management of OSCC consisted of surgery with or without radiotherapy or chemoradiotherapy. Aiming to increase survival rate, recent research has underlined the significance of harnessing the immune response in treatment of many cancers. The promising finding of checkpoint inhibitors as a weapon for targeting metastatic melanoma was a key event in the development of immunotherapy. Furthermore, clinical trials have recently proven inhibitor of PD-1 for treatment of recurrent/metastatic head and neck cancer. However, some challenges (including patient selection) are presented in the era of immunotherapy. In this mini-review we discuss the emergence of immunotherapy for OSCC and the recently introduced biomarkers of this therapeutic strategy. Immune biomarkers and their prognostic perspectives for selecting patients who may benefit from immunotherapy are addressed. In addition, possible use of such biomarkers to assess the response to this new treatment modality of OSCC will also be discussed.

Keywords: oral squamous cell carcinoma, immunotherapy, biomarkers, immune response, survival

INTRODUCTION

Survival rate of oral squamous cell carcinoma (OSCC) is about 50% of affected cases. Advances in traditional treatments (surgery, radiotherapy, chemotherapy) of OSCC have failed to increase survival and, at the same time, they have been associated with significant side effects. Prediction of survival in oral cancer depends on classical parameters such as tumor grade and depth of invasion, although many biomarkers have been introduced as potential prognosticators of OSCC (1, 2).

Recent research has introduced immunotherapy as an effective treatment option for OSCC. The hypothesis of immunotherapy was based on a theory that was introduced for more than a century ago postulating an ability of the immune system to repress cancer cells and aid in patient recovery (3). The significance of cancer immunotherapy was recognized more universally when the Nobel Prize in

Physiology or Medicine was awarded for the development of such therapies in 2018 (4). For OSCC, immunotherapy was firstly approved for recurrent/metastatic cases (similar to other cancers of head and neck region) (5). Of note, neoadjuvant immunotherapy administered preoperatively has been recently introduced for untreated OSCC (6).

With the success of immunotherapy in the treatment of OSCC, it has become important to find parameters to select patients who might benefit from this treatment strategy as well as to find a predictive marker/s for following treatment response. In this mini-review we will discuss different methods that have been introduced to assess the immune response and immune biomarkers in OSCC.

ASSESSMENT OF IMMUNE RESPONSE AS A PART OF GRADING SYSTEMS OF OSCC

Immune cells are among the main cellular components of cancer stroma tissue (7). The interaction of immune cells with tumor cells has been widely studied as one of the factors that influence tumor progression (8, 9). It has been reported in many cancers that active antitumor immune response is a feature of good prognosis (9, 10). Many proposals have suggested to assess the immune response as a part of histopathologic grading of OSCC. For example, an early study by Anneroth et al. (11) suggested to incorporate the assessment of the inflammatory cell infiltrate as a part of their malignancy grading system (11). They scored lymphoplasmacytic infiltrates into four categories as marked, moderate, slight or none (11). That system was modified later by Bryne et al. (12) who assessed malignancy grade (including the lymphoplasmacytic infiltrate) at the invasive front of OSCC (12). Brandwein-Gensler et al. (13) assessed the immune response as a part of a histologic risk score including three parameters: worst pattern of invasion, perineural invasion and lymphocytic host response (13). Most recently (2020), Bjerkli et al. proposed a histo-score based on the assessment of the lymphocytic infiltrate and tumor differentiation, and showed that the score gave a good prediction of survival in oral tongue cancer (14). Our group (15) proposed stromal classification, based on the assessment of tumor-infiltrating lymphocytes and tumor-stroma ratio, with a promising prognostic value in early oral tongue cancer.

From the above historically accumulated evidence, it seems that incorporation of the immune response as a part of the grading system of OSCC is a useful and important step which has not yet been implemented in pathology practice. A clinically relevant grading system with a robust association with tumor behavior and outcome, which considers the immune response is expected to become very useful for future immunotherapy of OSCC.

HISTOLOGIC SEMIQUANTITATIVE ASSESSMENT OF TUMOR-INFILTRATING LYMPHOCYTES

Morphological evaluation of tumor-infiltrating lymphocytes (TILs), using routine hematoxylin eosin (HE)-stained tumor sections, has been reported in many cancers including OSCC (16). A standardized method for the assessment of TILs has been introduced by the International TILs Working Group (9). Accumulating evidence has shown the significance of this method in various cancers (17–19). In OSCC, our group (15) has recently reported that the assessment of stromal TILs [as proposed by TILs Working Group (9)] can be used as a significant prognostic tool for the prediction of overall survival, disease-specific survival and disease-free survival in a large multicenter cohort of early oral tongue cancer. This assessment method has also been used successfully for other subsites of head and neck cancers (16). After further validation in large cohorts, this simple method for the assessment of TILs can be used to monitor response to immunotherapy. In addition to validation, it is important to overcome some limitations such as lack of consensus on the morphologic evaluation of TILs in OSCC and difficulty in assessing TILs using the preoperative diagnostic biopsies (20).

PROGRESS OF RESEARCH ON IMMUNE BIOMARKERS OF OSCC

In order to predict cancer response to immunotherapy, recent research (21) has tried to identify the immune profile of tumors classified into cold tumor (also known as immune desert) or hot tumor (also known as inflamed tumor). Using immunohistochemistry, several researchers have studied immune checkpoint molecules and the expression of specific TILs to identify the immune profile of OSCC. The mechanisms of such immune molecules were described in other articles (22, 23). Because so many studies have been published on immune biomarkers, we will focus here on the accumulated evidence from systematic reviews and meta-analyses. For example, Sievilainen et al. (24) in their recent systematic review covering the period from 1985 to 2017, on the prognostic value of immune checkpoints of OSCC have noted that seven immune checkpoints (PD-L1, FKBP51, B7-H4, B7-H6, ALHD1, IDO1, and B7-H3) had been reported to have an association with worse survival. In a meta-analysis of the prognostic value of TILs in OSCC, Huang et al. (25) found that high infiltration of CD8+ TILs, CD45RO+ TILs and CD57+ TILs associated with good survival; while high infiltration of CD163+ and CD68+ macrophages had an association with poor prognosis. In another meta-analysis, Hadler-Olsen et al. (26) found that CD163+ M2 and CD57+ had a promising relationship with outcome in patients with OSCC. Findings from these systematic reviews and meta-analyses should be considered as a cornerstone for future research in identifying the clinically most relevant immune biomarkers. It is necessary to acknowledge that the above-mentioned findings were reported from studies including samples mainly from patients treated with surgery and other traditional strategies, such as radiotherapy and/or chemotherapy.

For head and neck cancer including OSCC, treatment with anti-programmed cell death-1 (anti-PD-1) and anti-programmed cell death ligand-1 (anti-PD-L1) antibodies are crucial in the currently approved immunotherapy (27, 28). To

identify which cases are more likely to benefit from such treatment, many researchers have studied the two relevant biomarkers (i.e. PD-1 and PD-L1) using samples from patients treated with immunotherapy. As an example, expression of PD-L1 showed a significant association with response to durvalumab (an anti-PD-L1 antibody) in recent studies of head and neck cancer (5, 29).These studies found that a cutoff of 25% of cancer cells staining with PD-L1 is suitable to determine the patient´s response to durvalumab immunotherapy (5, 29). In another study on the anticancer activity of pembrolizumab-based immunotherapy, however, Chow et al. (30) suggested to consider scoring of PD-L1 in both cancer cells and immune cells with a cutoff point of 1%. Similarly, Emancipator et al. (31) reported that a "combined positive score", which evaluates the ratio of the number of PD-L1-expressing cells (including cancer cells and immune cells) to the number of all viable cancer cells multiplied by 100, is a powerful tool in assessing the response to pembrolizumab.

In a phase 3 trial including 361 patients with recurrent HNSCC who received nivolumab, the patient survival was improved with this kind of immunotherapy (32). However, expression of PD-L1 was not that significant in the assessment of response to the treatment (32). This might highlight the difficulty in comparing the findings across the studies that have used PD-L1 as a predictive marker if the immunotherapeutic agents were different. In addition, it is important to take into consideration that the above-mentioned findings on PD-1 and/or PD-L1 were reported from studies that included different subsites of head and neck cancer with well-known variation in their clinical behavior. Therefore, further trials should consider specific studies on OSCC to confirm the usefulness of PD-1 and PD-L1 in predicting the response to immunotherapy. In addition, whether to evaluate the expression of PD-L1 in both cancer cells and immune cells or only in immune cells needs to be determined based on the future studies. Furthermore, methods other than immunohistochemistry to assess immune biomarkers, such as immune-related signature, should be tested in OSCC cases treated with immunotherapy as this method has showed a good predictive value to immunotherapy in other tumors (33, 34).

IMMUNOSCORE FOR OSCC

Recent research efforts have introduced an immune-based assay known as immunoscore based on the assessment of a combination of immune biomarkers to identify the outcome of cancer (35). The most promising results with immunoscore have been reported in colorectal cancer where a scoring system for the quantification of CD3 and CD8 were standardized and showed a promising predictive power superior to TNM staging system (36) and showed successful results in phase 3 clinical trials (37). For oral carcinoma, identification of immune feature-based prognostic score has been recently introduced by Zhou et al. (38) who reported a promising prognostic value for an immunoscore based on the evaluation of CD3 in central areas and at invasive margins of OSCC; CD8, CD45RO, and FOXP3 in the central part of OSCC; FOXP3 and CD45RO at invasive margins of OSCC. However, the proposed immunoscore for OSCC will require further validation.

DIGITAL PATHOLOGY AND IMMUNE BIOMARKERS

Automated assessment of immune biomarkers has been widely studied in different cancers with successful performance (39–41). In OSCC, such assessment is still at an early stage as only few studies have reported on this concept. However, those few reports have shown promising findings. Shaban et al. (2019) reported a digital score for objective quantification of TILs that can successfully predict disease-free survival in OSCC and showed a better prognostic value than the manual assessment of TILs (42). Of note, this method of assessing TILs using whole-slide images of hematoxylin and eosin (HE)-stained sections was also successfully used in other cancers (43). In another recent study, Huang et al. (44) reported a promising value for digital image analysis of CD8 in a large cohort of tongue cancers. This approach of evaluating immune markers using digital analysis can be a simple tool to assess the immune response of OSCC and therefore validation studies are required.

OTHER FACTORS TO ASSESS RESPONSE TO IMMUNOTHERAPY

In addition to immune response and immune biomarkers, other existing factors including tumor mutational burden and mutational signatures might be associated with response to immunotherapy (45). Tumor mutational burden, referring to number of somatic mutations per coding area of a tumor genome, has shown a prognostic value in many cancers (46). Of note, recent research has showed that tumor mutational burden has a significant value in prediction of response to the immunotherapy (45). In a cohort including cases of head and neck cancer, Cristescu et al. (47) found that tumor mutational burden and T cell-inflamed gene expression profile can together predict the clinical responses to immunotherapy with pembrolizumab, and a longer survival was reported with higher levels of these two factors. Although pembrolizumab has been recommended for cases with high tumor mutational burden (≥ 10 mutations/megabase), some researchers have caveated against such universal threshold, and highlighted the fact that patients with cancer are often receiving cytotoxic chemotherapies that might cause higher level of tumor mutational burden (48). Thus, it is still necessary to determine the optimal cutoff point for tumor mutational burden in each tumor type to identify the group that might benefit from immunotherapy. In addition, it is necessary to take into consideration that the tumor immune microenvironment is characterized by a complexity that warrants assessment of the

clinical response from different aspects, and the measurement of tumor mutational burden being one of them.

CONCLUSIONS AND PERSPECTIVES

In the rapidly evolving field of immunotherapy, identification of biomarkers to predict the immune response can make such a therapy one of the clinically effective treatments of OSCC. There are many parameters/biomarkers and methods that have been introduced during the last three decades for the assessment of immune response. Ongoing research efforts include use of immune response in grading of OSCC, and identification of an immunoscore for OSCC. A successful clinically relevant assessment of the immune response can be considered as a cornerstone in identifying patients who will benefit from immunotherapy and also for following up the treatment response. Evidence from recent collaborative studies and/or meta-analyses highlighting the importance of evaluation of TILs and other immune biomarkers as a robust tool reveal the status of the immune response and have a strong correlation with survival outcome. There is an urgent need for validation studies to confirm the findings on these biomarkers, thus, to aid in identification of an ideal biomarker/s to select OSCC cases that can benefit from immunotherapy and to assess the patient´s response. Digital assessment of immune biomarkers in OSCC are still at an early stage and require further research. Similarly, findings on the predictive value of tumor mutational burden and mutational signatures still require further research before they can be added in the personalized prediction of OSCC treatment response.

AUTHOR CONTRIBUTIONS

All authors listed have made a substantial, direct, and intellectual contribution to the work and approved it for publication.

REFERENCES

1. Almangush A, Heikkinen I, Makitie AA, Coletta RD, Laara E, Leivo I, et al. Prognostic biomarkers for oral tongue squamous cell carcinoma: a systematic review and meta-analysis. *Br J Cancer* (2017) 117:856–66. doi: 10.1038/bjc.2017.244
2. Rivera C, Oliveira AK, Costa RAP, De Rossi T, Paes Leme AF. Prognostic biomarkers in oral squamous cell carcinoma: A systematic review. *Oral Oncol* (2017) 72:38–47. doi: 10.1016/j.oraloncology.2017.07.003
3. Adams JL, Smothers J, Srinivasan R, Hoos A. Big opportunities for small molecules in immuno-oncology. *Nat Rev Drug Discovery* (2015) 14:603–22. doi: 10.1038/nrd4596
4. Huang PW, Chang JW. Immune checkpoint inhibitors win the 2018 Nobel Prize. *BioMed J* (2019) 42:299–306. doi: 10.1016/j.bj.2019.09.002
5. Zandberg DP, Algazi AP, Jimeno A, Good JS, Fayette J, Bouganim N, et al. Durvalumab for recurrent or metastatic head and neck squamous cell carcinoma: Results from a single-arm, phase II study in patients with >/=25% tumour cell PD-L1 expression who have progressed on platinum-based chemotherapy. *Eur J Cancer* (2019) 107:142–52. doi: 10.1016/j.ejca.2018.11.015
6. Schoenfeld JD, Hanna GJ, Jo VY, Rawal B, Chen YH, Catalano PS, et al. Neoadjuvant Nivolumab or Nivolumab Plus Ipilimumab in Untreated Oral Cavity Squamous Cell Carcinoma: A Phase 2 Open-Label Randomized Clinical Trial. *JAMA Oncol* (2020) 6:1563–70. doi: 10.1001/jamaoncol.2020.2955
7. Maman S, Witz IP. A history of exploring cancer in context. *Nat Rev Cancer* (2018) 18:359–76. doi: 10.1038/s41568-018-0006-7
8. Giraldo NA, Sanchez-Salas R, Peske JD, Vano Y, Becht E, Petitprez F, et al. The clinical role of the TME in solid cancer. *Br J Cancer* (2019) 120:45–53. doi: 10.1038/s41416-018-0327-z
9. Salgado R, Denkert C, Demaria S, Sirtaine N, Klauschen F, Pruneri G, et al. The evaluation of tumor-infiltrating lymphocytes (TILs) in breast cancer: recommendations by an International TILs Working Group 2014. *Ann Oncol* (2015) 26:259–71. doi: 10.1093/annonc/mdu450
10. Fridman WH, Zitvogel L, Sautes-Fridman C, Kroemer G. The immune contexture in cancer prognosis and treatment. *Nat Rev Clin Oncol* (2017) 14:717–34. doi: 10.1038/nrclinonc.2017.101
11. Anneroth G, Batsakis J, Luna M. Review of the literature and a recommended system of malignancy grading in oral squamous cell carcinomas. *Scand J Dent Res* (1987) 95:229–49. doi: 10.1111/j.1600-0722.1987.tb01836.x
12. Bryne M, Koppang HS, Lilleng R, Kjaerheim A. Malignancy grading of the deep invasive margins of oral squamous cell carcinomas has high prognostic value. *J Pathol* (1992) 166:375–81. doi: 10.1002/path.1711660409
13. Brandwein-Gensler M, Teixeira MS, Lewis CM, Lee B, Rolnitzky L, Hille JJ, et al. Oral squamous cell carcinoma: histologic risk assessment, but not margin status, is strongly predictive of local disease-free and overall survival. *Am J Surg Pathol* (2005) 29:167–78. doi: 10.1097/01.pas.0000149687.90710.21
14. Bjerkli IH, Hadler-Olsen E, Nginamau ES, Laurvik H, Soland TM, Costea DE, et al. A combined histo-score based on tumor differentiation and lymphocytic infiltrate is a robust prognostic marker for mobile tongue cancer. *Virchows Arch* (2020) 477(6):865–72. doi: 10.1007/s00428-020-02875-9
15. Almangush A, Bello IO, Heikkinen I, Hagstrom J, Haglund C, Kowalski LP, et al. Stromal categorization in early oral tongue cancer. *Virchows Arch* (2020). doi: 10.1007/s00428-020-02930-5
16. Almangush A, Leivo I, Makitie AA. Overall assessment of tumor-infiltrating lymphocytes in head and neck squamous cell carcinoma: time to take notice. *Acta Otolaryngol* (2020) 140:246–8. doi: 10.1080/00016489.2020.1720284
17. Hwang C, Lee SJ, Lee JH, Kim KH, Suh DS, Kwon BS, et al. Stromal tumor-infiltrating lymphocytes evaluated on H&E-stained slides are an independent prognostic factor in epithelial ovarian cancer and ovarian serous carcinoma. *Oncol Lett* (2019) 17:4557–65. doi: 10.3892/ol.2019.10095
18. Liu JY, Yang GF, Chen FF, Peng CW. Evaluating the prognostic significance of tumor-infiltrating lymphocytes in solid tumor: practice of a standardized method from the International Immuno-Oncology Biomarkers Working Group. *Cancer Manag Res* (2019) 11:6815–27. doi: 10.2147/CMAR.S201538
19. Fuchs TL, Sioson L, Sheen A, Jafari-Nejad K, Renaud CJ, Andrici J, et al. Assessment of Tumor-infiltrating Lymphocytes Using International TILs Working Group (ITWG) System Is a Strong Predictor of Overall Survival in Colorectal Carcinoma: A Study of 1034 Patients. *Am J Surg Pathol* (2020) 44:536–44. doi: 10.1097/PAS.0000000000001409
20. Bello IO, Wennerstrand PM, Suleymanova I, Siponen M, Qannam A, Nieminen P, et al. Biopsy quality is essential for preoperative prognostication in oral tongue cancer. *APMIS* (2020) 129(3):118–27. doi: 10.1111/apm.13104
21. Chen DS, Mellman I. Elements of cancer immunity and the cancer-immune set point. *Nature* (2017) 541:321–30. doi: 10.1038/nature21349
22. Wei SC, Duffy CR, Allison JP. Fundamental Mechanisms of Immune Checkpoint Blockade Therapy. *Cancer Discovery* (2018) 8:1069–86. doi: 10.1158/2159-8290.CD-18-0367

23. Giraldo NA, Peske JD, Sautes-Fridman C, Fridman WH. Integrating histopathology, immune biomarkers, and molecular subgroups in solid cancer: the next step in precision oncology. *Virchows Arch* (2019) 474:463–74. doi: 10.1007/s00428-018-02517-1
24. Sievilainen M, Almahmoudi R, Al-Samadi A, Salo T, Pirinen M, Almangush A. The prognostic value of immune checkpoints in oral squamous cell carcinoma. *Oral Dis* (2019) 25:1435–45. doi: 10.1111/odi.12991
25. Huang Z, Xie N, Liu H, Wan Y, Zhu Y, Zhang M, et al. The prognostic role of tumour-infiltrating lymphocytes in oral squamous cell carcinoma: A meta-analysis. *J Oral Pathol Med* (2019) 48:788–98. doi: 10.1111/jop.12927
26. Hadler-Olsen E, Wirsing AM. Tissue-infiltrating immune cells as prognostic markers in oral squamous cell carcinoma: a systematic review and meta-analysis. *Br J Cancer* (2019) 120:714–27. doi: 10.1038/s41416-019-0409-6
27. Cramer JD, Burtness B, Ferris RL. Immunotherapy for head and neck cancer: Recent advances and future directions. *Oral Oncol* (2019) 99:104460. doi: 10.1016/j.oraloncology.2019.104460
28. Moskovitz JM, Ferris RL. Tumor Immunology and Immunotherapy for Head and Neck Squamous Cell Carcinoma. *J Dent Res* (2018) 97:622–6. doi: 10.1177/0022034518759464
29. Rebelatto MC, Midha A, Mistry A, Sabalos C, Schechter N, Li X, et al. Development of a programmed cell death ligand-1 immunohistochemical assay validated for analysis of non-small cell lung cancer and head and neck squamous cell carcinoma. *Diagn Pathol* (2016) 11:95. doi: 10.1186/s13000-016-0545-8
30. Chow LQM, Haddad R, Gupta S, Mahipal A, Mehra R, Tahara M, et al. Antitumor Activity of Pembrolizumab in Biomarker-Unselected Patients With Recurrent and/or Metastatic Head and Neck Squamous Cell Carcinoma: Results From the Phase Ib KEYNOTE-012 Expansion Cohort. *J Clin Oncol* (2016) 34:3838–45. doi: 10.1200/JCO.2016.68.1478
31. Emancipator K, Huang L, Aurora-Garg D, Bal T, Cohen EEW, Harrington K, et al. Comparing programmed death ligand 1 scores for predicting pembrolizumab efficacy in head and neck cancer. *Mod Pathol* (2020) 34 (3):532–41. doi: 10.1038/s41379-020-00710-9
32. Ferris RL, Blumenschein G Jr, Fayette J, Guigay J, Colevas AD, Licitra L, et al. Nivolumab for Recurrent Squamous-Cell Carcinoma of the Head and Neck. *N Engl J Med* (2016) 375:1856–67. doi: 10.1056/NEJMoa1602252
33. Wang Y, Chen L, Yu M, Fang Y, Qian K, Wang G, et al. Immune-related signature predicts the prognosis and immunotherapy benefit in bladder cancer. *Cancer Med* (2020) 9:7729–41. doi: 10.1002/cam4.3400
34. Xiao Y, Cui G, Ren X, Hao J, Zhang Y, Yang X, et al. A Novel Four-Gene Signature Associated With Immune Checkpoint for Predicting Prognosis in Lower-Grade Glioma. *Front Oncol* (2020) 10:605737. doi: 10.3389/fonc.2020.605737
35. Bruni D, Angell HK, Galon J. The immune contexture and Immunoscore in cancer prognosis and therapeutic efficacy. *Nat Rev Cancer* (2020) 20(11):662–80. doi: 10.1038/s41568-020-0285-7
36. Galon J, Bruni D. Approaches to treat immune hot, altered and cold tumours with combination immunotherapies. *Nat Rev Drug Discovery* (2019) 18:197–218. doi: 10.1038/s41573-018-0007-y
37. Pages F, Taieb J, Laurent-Puig P, Galon J. The consensus Immunoscore in phase 3 clinical trials; potential impact on patient management decisions. *Oncoimmunology* (2020) 9:1812221. doi: 10.1080/2162402X.2020.1812221
38. Zhou C, Diao P, Wu Y, Wei Z, Jiang L, Zhang W, et al. Development and validation of a seven-immune-feature-based prognostic score for oral squamous cell carcinoma after curative resection. *Int J Cancer* (2020) 146:1152–63. doi: 10.1002/ijc.32571
39. Zilenaite D, Rasmusson A, Augulis R, Besusparis J, Laurinaviciene A, Plancoulaine B, et al. Independent Prognostic Value of Intratumoral Heterogeneity and Immune Response Features by Automated Digital Immunohistochemistry Analysis in Early Hormone Receptor-Positive Breast Carcinoma. *Front Oncol* (2020) 10:950. doi: 10.3389/fonc.2020.00950
40. Humphries MP, Craig SG, Kacprzyk R, Fisher NC, Bingham V, McQuaid S, et al. The adaptive immune and immune checkpoint landscape of neoadjuvant treated esophageal adenocarcinoma using digital pathology quantitation. *BMC Cancer* (2020) 20:500. doi: 10.1186/s12885-020-06987-y
41. Parra ER, Behrens C, Rodriguez-Canales J, Lin H, Mino B, Blando J, et al. Image Analysis-based Assessment of PD-L1 and Tumor-Associated Immune Cells Density Supports Distinct Intratumoral Microenvironment Groups in Non-small Cell Lung Carcinoma Patients. *Clin Cancer Res* (2016) 22:6278–89. doi: 10.1158/1078-0432.CCR-15-2443
42. Shaban M, Khurram SA, Fraz MM, Alsubaie N, Masood I, Mushtaq S, et al. A Novel Digital Score for Abundance of Tumour Infiltrating Lymphocytes Predicts Disease Free Survival in Oral Squamous Cell Carcinoma. *Sci Rep* (2019) 9:13341. doi: 10.1038/s41598-019-49710-z
43. Linder N, Taylor JC, Colling R, Pell R, Alvelyn E, Joseph J, et al. Deep learning for detecting tumour-infiltrating lymphocytes in testicular germ cell tumours. *J Clin Pathol* (2019) 72:157–64. doi: 10.1136/jclinpath-2018-205328
44. Huang Y, Lin C, Kao HK, Hung SY, Ko HJ, Huang YC, et al. Digital Image Analysis of CD8+ and CD3+ Tumor-Infiltrating Lymphocytes in Tongue Squamous Cell Carcinoma. *Cancer Manag Res* (2020) 12:8275–85. doi: 10.2147/CMAR.S255816
45. Oliva M, Spreafico A, Taberna M, Alemany L, Coburn B, Mesia R, et al. Immune biomarkers of response to immune-checkpoint inhibitors in head and neck squamous cell carcinoma. *Ann Oncol* (2019) 30:57–67. doi: 10.1093/annonc/mdy507
46. Sha D, Jin Z, Budczies J, Kluck K, Stenzinger A, Sinicrope FA. Tumor Mutational Burden as a Predictive Biomarker in Solid Tumors. *Cancer Discovery* (2020) 10:1808–25. doi: 10.1158/2159-8290.CD-20-0522
47. Cristescu R, Mogg R, Ayers M, Albright A, Murphy E, Yearley J, et al. Pan-tumor genomic biomarkers for PD-1 checkpoint blockade-based immunotherapy. *Science* (2018) 362(6411):362. doi: 10.1126/science.aar3593
48. Strickler JH, Hanks BA, Khasraw M. Tumor Mutational Burden as a Predictor of Immunotherapy Response: Is More Always Better? *Clin Cancer Res* (2020). doi: 10.1158/1078-0432.CCR-20-3054

Conflict of Interest: The authors declare that the research was conducted in the absence of any commercial or financial relationships that could be construed as a potential conflict of interest.

frontiers in Oncology

ORIGINAL RESEARCH
published: 11 March 2021
doi: 10.3389/fonc.2021.614877

Mouthwash Containing Vitamin E, Triamcinolon, and Hyaluronic Acid Compared to Triamcinolone Mouthwash Alone in Patients With Radiotherapy-Induced Oral Mucositis: Randomized Clinical Trial

Farzaneh Agha-Hosseini[1,2,3], *Mona Pourpasha*[2], *Massoud Amanlou*[4] *and Mahdieh-Sadat Moosavi*[1,2*]

[1] Dental Research Center, Dentistry Research Institute, Tehran University of Medical Sciences, Tehran, Iran, [2] Department of Oral Medicine, Faculty of Dentistry, Tehran University of Medical Sciences, Tehran, Iran, [3] The Academy of Medical Sciences Tehran, Tehran, Iran, [4] Department of Medicinal Chemistry, Faculty of Pharmacy, Tehran University of Medical Sciences, Tehran, Iran

OPEN ACCESS

Edited by:
Cesare Piazza,
University of Brescia, Italy

Reviewed by:
Nicola Alessandro Iacovelli,
Istituto Nazionale dei Tumori (IRCCS), Italy
Markus Brunner,
Medical University of Vienna, Austria

***Correspondence:**
Mahdieh-Sadat Moosavi
ms-moosavi@sina.tums.ac.ir

Specialty section:
This article was submitted to Head and Neck Cancer, a section of the journal Frontiers in Oncology

Received: 07 October 2020
Accepted: 12 January 2021
Published: 11 March 2021

Citation:
Agha-Hosseini F, Pourpasha M, Amanlou M and Moosavi MS (2021) Mouthwash Containing Vitamin E, Triamcinolon, and Hyaluronic Acid Compared to Triamcinolone Mouthwash Alone in Patients With Radiotherapy-Induced Oral Mucositis: Randomized Clinical Trial. Front. Oncol. 11:614877. doi: 10.3389/fonc.2021.614877

One of the most common side effects of radiotherapy in head and neck cancers is mucositis. Despite all the studies conducted on new therapies proposed for oral mucositis caused by radiation therapy, a single standard treatment strategy has not been developed yet. In the present study, for the first time, the effectiveness of the treatment with a combined mouthwash containing vitamin E (as an antioxidant), triamcinolone (as an anti-inflammatory agent) and hyaluronic acid (HA) (as a local reducer used for reducing the effects of ROS on the mucosa, with ameliorative effects (improving the healing process) compared to triamcinolone mouthwash alone was investigated in patients with radiotherapy-induced oral mucositis. This study was a randomized triple-blind clinical trial performed on 60 patients underwent radiotherapy on an outpatient basis. The combined mouthwash containing vitamin E, triamcinolone, and hyaluronic acid compared to triamcinolone mouthwash alone was prescribed for 4 weeks. The severity of oral mucositis was assessed based on the WHO classification and the intensity of pain was assessed using the numerical pain intensity scale. According to the analysis performed in the first, second, third and fourth weeks, the reduction of oral mucositis grade in the intervention group was significantly higher than in the comparison group. In the first, second, third, and fourth weeks, the reduction in pain intensity in the intervention group was significantly higher than in the comparison group ($P < 0.001$). The combined mouthwash containing vitamin E, hyaluronic acid and triamcinolone acetonide can be used as an effective treatment for oral mucositis caused by radiation therapy, which is

probably the result of antioxidant, anti-inflammatory and improved healing process mechanisms due to the biological nature of the components of this mouthwash.

Trial registration: This study was registered in the WHO Primary registry (IRCT) with the code IRCT20190428043407N. Registered on 20 July 2019, https://www.irct.ir/trial/39231.

Keywords: head and neck cancer, hyaluronic acid, mucositis, radiotherapy, vitamin E

INTRODUCTION

One of the most common side effects of radiotherapy in head and neck cancers is mucositis (1). Studies have shown that 73–100% of patients treated with intensity-modulated radiation therapy (IMRT) experienced grade 3 and 4 mucositis (2). Finding a cure for mucositis is important in several ways. Oral mucositis is often painful and manifests as erythema or sores in the oral mucosa and can also affect the mucous membranes of the throat, larynx, and esophagus (3). Therefore, it can be said that mucositis significantly affects nutrition, oral care, and quality of life. In severe cases, mucositis can lead to the need of reducing the dose of chemotherapy and undesirable breaks in radiation therapy, which would consequently have a negative effect on treatment prognosis (4).

Several mechanisms have been identified in the etiology of oral mucositis. One of them is the Nuclear Factor NF-κB signal transduction pathway. In oral mucositis, NF-κB is involved in the initial inflammatory damage to connective tissue by increasing the expression of pro-inflammatory cytokines, including TNF-a, MMPs, COX-2, TGF-B, and IL-1B (5). Another mechanism is the production of free radicals during radiation and the generation of oxidative stress (6).

Despite all the studies conducted on new therapies for oral mucositis caused by radiation therapy, a single standard treatment strategy has not yet been developed, and studies carried out on the prevention and/or treatment of oral mucositis compared with the control group have been accompanied by contradictory results and have not been fully confirmed (7). Each of these studies has introduced some materials or biomaterials in this field to block the pathway involved in the development of mucositis.

Due to the production of free radicals during radiation, several efforts have been made to use vitamin E ointment as an antioxidant and free radical scavenger (8). The main ingredient in vitamin E, alpha-tocopherol is an antioxidant that can react with free radicals and remove them from the body and better control inflammation caused by oral mucositis. Previous studies conducted on vitamin E as a radioprotective agent have reported good results (9).

Hyaluronic acid (HA) is a natural polysaccharide with a linear chain, which is known as an important element of the extracellular matrix of many tissues in the human body (10). Hyaluronic acid, while creating a protective physical barrier (coating), repairs tissues and promotes cell proliferation by regulating inflammatory responses, and besides stimulating the proliferation of basal layer keratinocytes, gives rise to re-epithelialization, improves the healing process and plays a role in reducing the size of the erosive/injured areas of the oral mucosa (11).

Due to the pathogenesis of mucositis, corticosteroid compounds such as triamcinolone acetonide are among the common treatments for this lesion. Triamcinolone is effective in reducing pain and the course of oral mucositis caused by radiation therapy. By reducing the expression of the NFKB/P65 gene and protein, these compounds reduce the levels of anti-inflammatory cytokines such as TNF-a and IL-6, and by the same mechanism, they can reduce ulcers and inflammation in oral mucositis (12).

In the present study, for the first time, the effectiveness of treatment with a combined mouthwash containing vitamin E (as an antioxidant), triamcinolone (as an anti-inflammatory agent) and hyaluronic acid (HA) (as a local reducer used for reducing the effects of ROS on the mucosa, with ameliorative effects (improving the healing process) compared to triamcinolone mouthwash alone was investigated in patients with radiotherapy-induced oral mucositis.

MATERIALS AND METHODS

This study was a randomized triple-blind clinical trial registered in the WHO Primary registry with the code (IRCT20190428043407N1) and approved by the ethics committee with the code (IR.TUMS.DENTISTRY.REC. 1398.043). This study was conducted in parallel design to compare the effectiveness of a combined mouthwash containing vitamin E, hyaluronic acid and triamcinolone with triamcinolone mouthwash alone for the treatment of oral mucositis (grades 3 and 4) caused by radiotherapy. The patients entered the study by signing an informed consent form. Their ratio in the two study groups was one to one.

The study population included patients with any type of head and neck malignancy undergoing radiotherapy (IMRT) on an outpatient basis who referred to the university's cancer institute. The patients were treated by radiotherapy up to a total dose of 60–66 Gy during 30–33 treatment sessions. Most of the patients included in this study were in the range of 10th–25th sessions of radiation therapy. The average number of previous sessions of the treatment before the start of the study was 18.57 for the intervention group and 18.58 for the control group. This study aimed to investigate the therapeutic effect of mouthwash on grades 3 and 4 of oral mucositis, so the dose delivered to the oral cavity as an OAR (Organ at Risk) was not evaluated as an independent parameter.

After the start of radiotherapy, the patients' oral mucosa was examined every week for the incidence of oral mucositis by a specialist in oral and maxillofacial diseases.

The inclusion criteria included:

- The definitive diagnosis of head and neck cancer according to a histopathological examination and undergoing radiotherapy
- Aged at least 18 years old (no maximum age limit)
- Observing oral hygiene in a way that does not preclude the diagnosis of the degree of severity of mucositis.
- Having the ability to use mouthwash
- Patients with grades 3 and 4 of oral mucositis according to the WHO criteria, were selected for the study
- Having no history of allergy to the drugs studied (questioning patients before entering the study)
- Not having undergone other selected treatments for oral mucositis

The exclusion criteria included pregnant women, patients' use of vitamin E and other complementary antioxidants in the last 3 weeks, suffering from other active lesions in their mouth like pests, history of alcohol or drug use, history of any previous radiation therapy and current chemotherapy (for better matching the case and control groups in terms of the type of treatment and the presence or the absence of chemotherapy affects the tissue response to treatment), and bone marrow transplantation. Additionally, systemic diseases affecting the healing process of mucosal wounds (such as diabetes and hypertension) or with oral complications (such as kidney disease and autoimmune disorders) were excluded.

The Karnofsky performance status scale below 60 is known as an index used to evaluate dysfunction, as that the smaller the number, the lower the patient's survival rate. Moreover, some patients with an index below 60 require hospitalization.

The drug was prepared in the Medicinal Chemistry Laboratory of Tehran University of Medical Sciences by a Pharmacist according to the above-mentioned method. Thereafter, the drugs were prepared in similar bottles and then coded by a person who was not involved in the study.

The random allocation method was based on the simple randomization method using Microsoft Excel software and the randomization was performed by a person who was independent of the study.

To provide the same conditions for all the patients, candidiasis was monitored to be treated if necessary. Oral hygiene was also recommended for all the patients.

In this study, researchers, patients, and statistical analyzers did not know whom patients were in the intervention group and whom were in the control group. Enrolments of the subjects are shown in the CONSORT diagram.

Intervention Group

The combined mouthwash was prepared with 0.1% triamcinolone (13), 0.2% vitamin E (14), and 0.2% hyaluronic acid (15). Triamcinolone acetonide powder along with vitamin E and hyaluronic acid (with the mentioned percentages) were dissolved in propylene glycol solvent and were then brought to the required volume with double-distilled water and packed in identical glass containers unrecognizable from the glass containers of the comparison group with the dropper.

Comparison Group

0.1% triamcinolone mouthwash alone:

0.1% Triamcinolone (13) was dissolved in propylene glycol solvent, was brought to the required volume with double-distilled water, and then packed in identical glass containers that were unrecognizable from the glass containers of the intervention group with the dropper by a person who was not involved in the study, so that the drugs used for the intervention and comparison groups were similar in terms of volume and shape.

In both intervention and comparison groups, mouthwash was used for 4 weeks (16, 17), three times a day (morning, noon and night) at a rate of 2 ccs each time (without the need for dilution) and for at least one minute, without swallowing any mouthwash. It was recommended eating and drinking be avoided for 15 minutes after using the mouthwash.

During the use of mouthwash, any symptoms that indicated an allergy, such as swelling of the lips, tongue, and eyelids, hives and itching in the body gave us the permission to interrupt the intervention.

The following actions were performed during the follow-up study of patients to ensure the correct use of the drug: asking the patient's companion about regular use of mouthwash, learning how to use mouthwash properly, patients' weekly follow-up schedule, checking the amount of medicine left over in the glass bottle in the last week, and making phone calls.

Our patients' cooperation in using the patient's diaries seemed unlikely due to their illness. Therefore, as mentioned earlier, some other ways such as telephone call to the patient during the treatment period and the amount of leftover medicine were used.

Outcome Measurements

The Severity of Oral Mucositis

The severity of oral mucositis was determined based on the WHO classification (13). After beginning the intervention, this variable was evaluated in the first, second, third and fourth weeks. The grade of mucositis was determined by the same oncologist. The scale was then re-examined by the same oral medicine specialist who has been trained in this field.

Pain Intensity

Pain intensity was assessed using the numerical pain intensity scale [a segmented numeric version of the visual analog scale (VAS)]. In this regard, a score of 10 is allocated to indescribable and severe pain and a score of 0 is for the painless state. Thus, the patient's oral condition, including the grade of oral mucositis and pain intensity, and baseline were recorded in the first, second, third, and fourth weeks as well as weak zero, respectively.

Statistical Analysis

The outcome variable of oral mucositis grade, which is a qualitative ranked variable, was reported as the number and

percentage in each group, and the Mann-Whitney test was used to compare the two groups.

The outcome variable of the numerical pain intensity scale is a qualitative variable whose distribution was examined and considered abnormal and median and interquartile range (IQR) were therefore used to describe this variable. The Mann-Whitney test was used to compare the two groups. The level of statistical significance was set at $p < 0.05$.

RESULTS

The patients in the intervention group included 29 individuals and the patients in the comparison group included 30 individuals. Demographics, Tumor, and Radiotherapy characteristics of the patients are given in **Table 1**.

Oral mucositis grade, represented as a percentage at 0, 1, 2, 3, and 4 weeks in the comparison group is shown in **Figure 1** and oral mucositis grade in the intervention group is given in **Figure 2**.

According to the analysis performed in the first, second, third, and fourth weeks, the reduction of oral mucositis grade in the intervention group was significantly higher than that of the comparison group ($P < 0.001$).

TABLE 1 | Demographics, Tumor, and Radiotherapy characteristics.

	Intervention group	Comparison group
Age (Mean ± SD)	55.03 ± 9.84	55.57 ± 11.53
Sex (M/F)	17/12	17/13
Type of tumor:		
Nasopharynx	9	5
Buccal SCC	5	9
Lingual SCC	10	12
Other H&N tumors	5	4

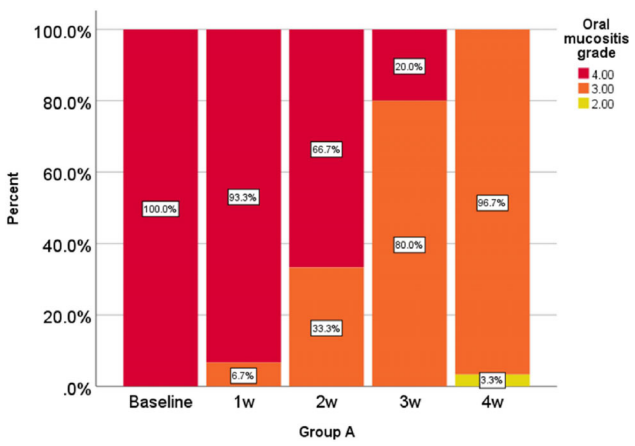

FIGURE 1 | Percentage of oral mucositis grades in the comparison group in weeks 0-1-2-3 and 4.

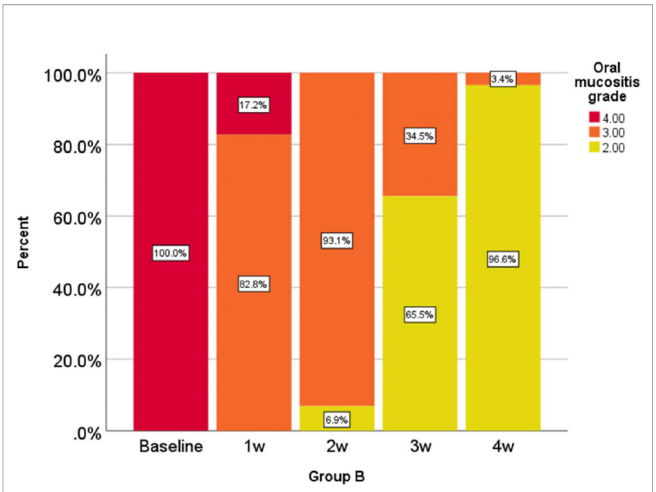

FIGURE 2 | Percentage of oral mucositis grades in the intervention group in weeks 0-1-2-3 and 4.

The pain intensity expressed as the median and interquartile range (IQR) is shown in **Figure 3**. In the first, second, third, and fourth weeks, the reduction in pain intensity in the intervention group was significantly higher than in the comparison group ($P < 0.001$). A photograph of a patient in the intervention group is shown in the first and fourth sessions (Photos 1 and 2).

DISCUSSION

The results of the present study showed that the combined mouthwash of vitamin E, hyaluronic acid and triamcinolone acetonide could be significantly ($P < 0.001$) effective on reducing the oral mucositis grade and pain intensity during the first, second, third and fourth weeks of follow-up. One of the side effects of radiation therapy and chemotherapy for head and neck cancers is the occurrence of oral mucositis, which at severe stages, besides increasing medical costs and creating negative psychological and social consequences, causes many limitations such as the prolonged hospitalization time, using liquid diets or total parenteral nutrition (TPN), the increased drug use, and the use of antibacterial, antifungal, and antiviral drugs, which can ultimately lead to the cessation of treatment processes (18). Unfortunately, research conducted from 1980 to 2019 has failed to identify an effective global intervention for the prevention and treatment of oral mucositis. Therefore, oral mucositis treatment remains a medical challenge and requires a standard evidence-based treatment approach (18).

The main bases in the management of radiotherapy-induced oral mucositis are nutritional support, pain alleviation, prophylaxis, and treatment of secondary infections. The previously suggested treatments are locally applied agents (such as Glycyrrhetinic acid/povidone/sodium hyaluronate gel, l-Glutamine, manganese superoxide dismutase, local anesthetics, corticosteroids mouthwashes, and vitamins), systemically applied agents (cyclooxygenase-2 inhibitors, N-acetyl cysteine,

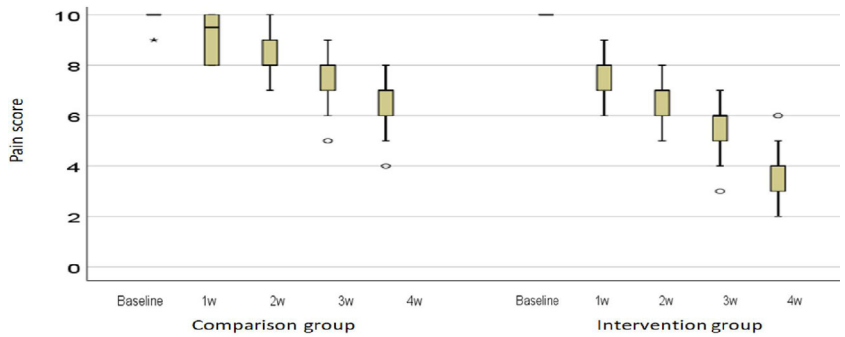

FIGURE 3 | Description of the intensity of pain in the middle and the distance between the quarters. O: outlier; *: extreme outlier.

transforming growth factor-β3, and systemic corticosteroids), and oral microbial load reduction agents such as antimicrobial and antifungal agents (14).

It is important to recognize and target the pathophysiological processes leading to oral mucositis in order to develop effective preventive and/or therapeutic strategies in this regard. Radiation-induced mucosal damage is actually the result of complex biological and cellular events that occur mainly under the mucosa and eventually lead to epithelial damage (6). Due to the initiating role of reactive oxygen species (ROS) produced during radiation therapy in epithelial cell damage, vitamin E as an antioxidant, and by stabilizing the cell membrane (protecting the cell membrane) against radiation, limit the tissue damage caused by ROS and reduces the severity of oral mucositis during the treatment of head and neck cancers (HNC). Accordingly, that in some studies, it was considered as the main mechanism used to prevent tissue damage (9). In various studies, the desired therapeutic effect of topical vitamin E in oral mucositis has been reported (9, 19). In a meta-analysis in 2017, the significant effect of vitamin E on reducing the severity of oral mucositis in all three groups of patients underwent radiation therapy and/or without chemotherapy and chemotherapy alone was confirmed. This study also showed that the topical form of vitamin E was more effective than its systemic form (8). According to the above-mentioned explanations, in our study, vitamin E was used as one of the components of the combined mouthwash to treat the patients with oral mucositis caused by radiation therapy. However, for the treatment of mucositis, despite its complex pathophysiology, which has been mentioned earlier, the use of a drug with antioxidant properties is not sufficient, and the reason for the temporary effectiveness of single-drug treatments on mucositis is probably due to the failure to observe this point.

Due to the high turnover of the epithelial mucosa, it is exposed to direct damage in chemotherapy and radiotherapy (20). To help repair this mucosal rupture, biological drugs with the ability to stimulate fibroblasts and keratinocytes can be used in topical treatments. In 2001, the U.S. Food and Drug Administration (FDA) approved a gel containing hyaluronic acid as a substance useful in the treatment of oral mucositis and relieving pain (15). Although the exact mechanism associated with the effectiveness of hyaluronic acid in improving the healing process of oral mucositis is not well known, some studies have shown the role of hyaluronic acid compounds only as a physical barrier (coating) between the oral environment and oral mucosa, which reduces pain and possibly improves the healing process (21). Hyaluronic acid (HA) may give rise to re-epithelialization, improve the healing process, and play a role in reducing the size of the erosive/injured areas of the oral mucosa by regulating inflammatory responses and stimulating the proliferation of basal layer keratinocytes (22).

Triamcinolone was chosen as the standard treatment for mucositis, which can be used both as a treatment for the control group and as a base material to be added to vitamin E and hyaluronic acid. Triamcinolone is a kind of fluoride-containing synthetic corticosteroid and an anti-inflammatory compound with medium to high power, which can inhibit all stages of the inflammatory response, from redness and erythema to cell proliferation and wound healing (12). Studies investigating the effects of corticosteroids on mucositis have shown that triamcinolone, as an antioxidant molecule and/or cell protector in the treatment of oral mucositis, can reduce the degree of oral mucositis and the intensity of the pain (12, 20). Furthermore, in previous studies conducted on the treatment of oral mucositis, the compounds of vitamin E, hyaluronic acid and triamcinolone acetonide alone have shown relatively good effects. In the present study, for the first time, the effect of a combined mouthwash containing vitamin E (as an antioxidant), triamcinolone (as an anti-inflammatory agent), and hyaluronic acid (HA) (as a local reducer used for reducing the effects of ROS on the mucosa, with ameliorative effects (improving the healing process) compared to triamcinolone mouthwash alone (comparison group) was investigated in terms of the degree of oral mucositis (according to the WHO criteria) and the severity of pain (according to the VAS criteria). The new composition used substances that have benefits for the treatment of mucositis without the fear of complications of primary tumor growth or increased mortality. For example, studies on the administration of growth factors and cytokines and their side effects are still ongoing (23).

Due to the high molecular weight of vitamin E in combination with the two above-mentioned substances, it was not possible to

use the orabase form, which has a longer shelf life in the mouth, and this limitation led to the use of its mouthwash form in this study.

In this study, the WHO classification was used to select patients, which is a combination of objective criteria such as mucosal changes including redness and ulcers and functional criteria such as inability to eat. Studies have shown that this criterion is significantly correlated with the clinical signs and symptoms of mucositis (24).

Due to the lack of a common treatment protocol for the treatment of mucositis, some studies have conducted clinical trials without placing treatment in the control group (25). One of the advantages of the present study was the use of a combination therapy base (triamcinolone) as a control group treatment, which made it possible to compare the effect or non-effect of added substances to the base compared to the base material alone and prevented unreal magnification of the results.

Moreover, previous studies have not reported any significant side effects regarding the use of separate compounds of vitamin E, hyaluronic acid and triamcinolone acetonide in the treatment of oral mucositis, and in the present study, no side effects such as swelling of the lips, tongue, and eyelids, hives or itching in the body were observed in patients either.

According to the results of our study, the use of a combined mouthwash containing vitamin E, hyaluronic acid and triamcinolone acetonide can be an effective treatment in patients with radiotherapy-induced oral mucositis. One of the limitations in the current study was the lack of quality of life's evaluation. It is suggested to add quality of life's evaluation through questionnaires into outcome measurements.

In this study, the combined mouthwash of vitamin E, hyaluronic acid and triamcinolone acetonide was found to be effective in the treatment of oral mucositis caused by radiation therapy and positive results were reported in this regard as well, probably due to the antioxidant, anti-inflammatory and improved healing process mechanisms, which are the results of the biological nature of the components of this mouthwash.

DATA AVAILABILITY STATEMENT

The raw data supporting the conclusions of this article will be made available by the authors, without undue reservation.

ETHICS STATEMENT

The studies involving human participants were reviewed and approved by Tehran University of Medical Sciences. The patients/participants provided their written informed consent to participate in this study.

AUTHOR CONTRIBUTIONS

FA-H contributed to conception and design, drafted the manuscript, and gave final approval. MP contributed to acquisition and interpretation, drafted the manuscript, and gave final approval. MA contributed to conception and design, drafted the manuscript, and gave final approval. M-SM contributed to conception and design, contributed to analysis and interpretation, drafted the manuscript, and gave final approval. All authors contributed to the article and approved the submitted version.

SUPPLEMENTARY MATERIAL

The Supplementary Material for this article can be found online at: https://www.frontiersin.org/articles/10.3389/fonc.2021.614877/full#supplementary-material

Supplementay Datasheet 1 | CONSORT diagram.

Supplementary Figure 1 | A photograph of a patient (Code 20) in the intervention group in the first sessions. Ulcerative and erosive lesions are seen in the left buccal mucosa, the lips, and the tongue (with Mucositis Grade 4).

Supplementary Figure 2 | A photograph of a patient (Code 20) in the intervention group in the fourth sessions (with Mucositis Grade 2).

REFERENCES

1. Razmara F, Khayamzadeh M. An Investigation into the Prevalence and Treatment of Oral Mucositis After Cancer Treatment. *Int J Cancer Management* (2019) 12(11):e88405. doi: 10.5812/ijcm.88405
2. Zhang H, D'Souza W. A treatment planning method for better management of radiation-induced oral mucositis in locally advanced head and neck cancer. *J Med Phys* (2018) 43:6. doi: 10.4103/jmp.JMP_78_17
3. Elting LS, Shih YC. The economic burden of supportive care of cancer patients. *Support Care Cancer* (2004) 12(4):219–26. doi: 10.1007/s00520-003-0513-1
4. Sroussi HY, Epstein JB, Bensadoun RJ, Saunders DP, Lalla RV, Migliorati CA, et al. Common oral complications of head and neck cancer radiation therapy: mucositis, infections, saliva change, fibrosis, sensory dysfunctions, dental caries, periodontal disease, and osteoradionecrosis. *Cancer Med* (2017) 6(12):2918–31. doi: 10.1002/cam4.1221
5. Ribeiro SB, de Araujo AA, Araujo Junior RF, Brito GAC, Leitao RC, Barbosa MM, et al. Protective effect of dexamethasone on 5-FU-induced oral mucositis in hamsters. *PloS One* (2017) 12(10):e0186511. doi: 10.1371/journal.pone.0186511
6. Sonis ST. Mucositis: The impact, biology and therapeutic opportunities of oral mucositis. *Oral Oncol* (2009) 45(12):1015–20. doi: 10.1016/j.oraloncology.2009.08.006
7. Villa A, Sonis ST. Mucositis: pathobiology and management. *Curr Opin Oncol* (2015) 27(3):159–64. doi: 10.1097/CCO.0000000000000180
8. Chaitanya NC, Muthukrishnan A, Babu DBG, Kumari CS, Lakshmi MA, Palat G, et al. Role of Vitamin E and Vitamin A in Oral Mucositis Induced by Cancer Chemo/Radiotherapy- A Meta-analysis. *J Clin Diagn Res* (2017) 11(5):Ze06–ze9. doi: 10.7860/JCDR/2017/26845.9905
9. El-Housseiny AA, Saleh SM, El-Masry AA, Allam AA. The effectiveness of vitamin "E" in the treatment of oral mucositis in children receiving chemotherapy. *J Clin Pediatr Dent* (2007) 31(3):167–70. doi: 10.17796/jcpd.31.3.r8371x45m42l10j7
10. Lopez M, Manzulli N, D'Angelo A, Lauritano D, Papalia R, Candotto V. The use of hyaluronic acid as an adjuvant in the management of peri-implantitis. *J Biol Regul Homeost Agents* (2017) 31(4 Suppl 2):123–7.
11. Vokurka S, Skardova J, Hruskova R, Kabatova-Maxova K, Svoboda T, Bystricka E, et al. The effect of polyvinylpyrrolidone-sodium hyaluronate gel (Gelclair) on oral microbial colonization and pain control compared with other rinsing solutions in patients with oral mucositis after allogeneic stem

cells transplantation. *Med Sci Monit* (2011) 17(10):Cr572–6. doi: 10.12659/MSM.881983
12. Gumus S, Yariktas M, Naziroglu M, Uguz AC, Aynali G, Baspinar S. Effect of a corticosteroid (triamcinolone) and chlorhexidine on chemotherapy-induced oxidative stress in the buccal mucosa of rats. *Ear Nose Throat J* (2016) 95(12): E36–e43. doi: 10.1177/014556131609501211
13. Worthington HV, Clarkson JE, Eden OB. Interventions for preventing oral mucositis for patients with cancer receiving treatment. *Cochrane Database Syst Rev* (2007) 4):Cd000978. doi: 10.1002/14651858.CD000978.pub3
14. Maria OM, Eliopoulos N, Muanza T. Radiation-Induced Oral Mucositis. *Front Oncol* (2017) 7:89. doi: 10.3389/fonc.2017.00089
15. Cirillo N, Vicidomini A, McCullough M, Gambardella A, Hassona Y, Prime SS, et al. A hyaluronic acid-based compound inhibits fibroblast senescence induced by oxidative stress in vitro and prevents oral mucositis in vivo. *J Cell Physiol* (2015) 230(7):1421–9. doi: 10.1002/jcp.24908
16. Khanjani Pour-Fard-Pachekenari A, Rahmani A, Ghahramanian A, Jafarabadi MA, Onyeka TC, Davoodi A. The effect of an oral care protocol and honey mouthwash on mucositis in acute myeloid leukemia patients undergoing chemotherapy: a single-blind clinical trial. *Clin Oral Invest* (2019) 23(4):1811–21. doi: 10.1007/s00784-018-2621-9
17. Dastan F, Ameri A, Dodge S, Shishvan HH, Pirsalehi A, Abbasinazari M. Efficacy and safety of propolis mouthwash in management of radiotherapy induced oral mucositis; A randomized, double blind clinical trial. *Rep Pract Oncol Radiother* (2020) 25(6):969–73. doi: 10.1016/j.rpor.2020.09.012
18. Ghalayani P, Emami H, Pakravan F, Nasr Isfahani M. Comparison of triamcinolone acetonide mucoadhesive film with licorice mucoadhesive film on radiotherapy-induced oral mucositis: A randomized double-blinded clinical trial. *Asia Pac J Clin Oncol* (2017) 13(2):e48–56. doi: 10.1111/ajco.12295
19. de Freitas Cuba L, Braga Filho A, Cherubini K, Salum FG, Figueiredo MA. Topical application of Aloe vera and vitamin E on induced ulcers on the tongue of rats subjected to radiation: clinical and histological evaluation. *Support Care Cancer* (2016) 24(6):2557–64. doi: 10.1007/s00520-015-3048-3
20. Pakravan F, Ghalayani P, Emami H, Isfahani MN, Noorshargh P. A novel formulation for radiotherapy-induced oral mucositis: Triamcinolone acetonide mucoadhesive film. *J Res Med Sci* (2019) 24:63. doi: 10.4103/jrms.JRMS_456_18
21. Kapoor P, Sachdeva S, Sachdeva S. Topical hyaluronic Acid in the management of oral ulcers. *Indian J Dermatol* (2011) 56(3):300–2. doi: 10.4103/0019-5154.82485
22. Colella G, Cannavale R, Vicidomini A, Rinaldi G, Compilato D, Campisi G. Efficacy of a spray compound containing a pool of collagen precursor synthetic aminoacids (l-proline, l-leucine, l-lysine and glycine) combined with sodium hyaluronate to manage chemo/radiotherapy-induced oral mucositis: preliminary data of an open trial. *Int J Immunopathol Pharmacol* (2010) 23(1):143–51. doi: 10.1177/039463201002300113
23. Logan RM, Al-Azri AR, Bossi P, Stringer AM, Joy JK, Soga Y, et al. Systematic review of growth factors and cytokines for the management of oral mucositis in cancer patients and clinical practice guidelines. *Support Care Cancer* (2020) 28:2485–98. doi: 10.1007/s00520-019-05170-9
24. Lee YH, Hong J, Kim I, Choi Y, Park HK. Prospective evaluation of clinical symptoms of chemotherapy-induced oral mucositis in adult patients with acute leukemia: A preliminary study. *Clin Exp Dent Res* (2020) 6(1):90–9. doi: 10.1002/cre2.253
25. Sayed R, El Wakeel L, Saad AS, Kelany M, El-Hamamsy M. Pentoxifylline and vitamin E reduce the severity of radiotherapy-induced oral mucositis and dysphagia in head and neck cancer patients: a randomized, controlled study. *Med Oncol* (2019) 37(1):8. doi: 10.1007/s12032-019-1334-5

Conflict of Interest: The authors declare that the research was conducted in the absence of any commercial or financial relationships that could be construed as a potential conflict of interest.

frontiers in Oncology

ORIGINAL RESEARCH
published: 12 March 2021
doi: 10.3389/fonc.2021.628320

Is the Depth of Invasion a Marker for Elective Neck Dissection in Early Oral Squamous Cell Carcinoma?

*Yassine Aaboubout[1,2], Quincy M. van der Toom[2], Maria A. J. de Ridder[3], Maria J. De Herdt[2], Berdine van der Steen[2], Cornelia G. F. van Lanschot[2], Elisa M. Barroso[1,4,5], Maria R. Nunes Soares[1,5], Ivo ten Hove[4], Hetty Mast[4], Roeland W. H. Smits[2], Aniel Sewnaik[2], Dominiek A. Monserez[2], Stijn Keereweer[2], Peter J. Caspers[5], Robert J. Baatenburg de Jong[2], Tom C. Bakker Schut[5], Gerwin J. Puppels[5], José A. Hardillo[2] and Senada Koljenović[1]**

[1] Department of Pathology, Erasmus MC, University Medical Center Rotterdam, Rotterdam, Netherlands, [2] Department of Otorhinolaryngology and Head and Neck Surgery, Erasmus MC, University Medical Center Rotterdam, Rotterdam, Netherlands, [3] Department of Medical informatics, Erasmus MC, University Medical Center Rotterdam, Rotterdam, Netherlands, [4] Department of Oral and Maxillofacial Surgery, Erasmus MC, University Medical Center Rotterdam, Rotterdam, Netherlands, [5] Department of Dermatology, Erasmus MC, University Medical Center Rotterdam, Rotterdam, Netherlands

Objective: The depth of invasion (DOI) is considered an independent risk factor for occult lymph node metastasis in oral cavity squamous cell carcinoma (OCSCC). It is used to decide whether an elective neck dissection (END) is indicated in the case of a clinically negative neck for early stage carcinoma (pT1/pT2). However, there is no consensus on the cut-off value of the DOI for performing an END. The aim of this study was to determine a cut-off value for clinical decision making on END, by assessing the association of the DOI and the risk of occult lymph node metastasis in early OCSCC.

Methods: A retrospective cohort study was conducted at the Erasmus MC, University Medical Centre Rotterdam, The Netherlands. Patients surgically treated for pT1/pT2 OCSCC between 2006 and 2012 were included. For all cases, the DOI was measured according to the 8th edition of the American Joint Committee on Cancer guideline. Patient characteristics, tumor characteristics (pTN, differentiation grade, perineural invasion, and lymphovascular invasion), treatment modality (END or watchful waiting), and 5-year follow-up (local recurrence, regional recurrence, and distant metastasis) were obtained from patient files.

Results: A total of 222 patients were included, 117 pT1 and 105 pT2. Occult lymph node metastasis was found in 39 of the 166 patients who received END. Univariate logistic regression analysis showed DOI to be a significant predictor for occult lymph node metastasis (odds ratio (OR) = 1.3 per mm DOI; 95% CI: 1.1–1.5, $p = 0.001$). At a DOI of 4.3 mm the risk of occult lymph node metastasis was >20% (all subsites combined).

Conclusion: The DOI is a significant predictor for occult lymph node metastasis in early stage oral carcinoma. A NPV of 81% was found at a DOI cut-off value of 4 mm. Therefore, an END should be performed if the DOI is >4 mm.

Keywords: oral cancer, squamous cell carcinoma of head and neck, depth of invasion, occult metastasis, elective neck dissection

OPEN ACCESS

Edited by:
Paolo Bossi,
University of Brescia, Italy

Reviewed by:
Jonathan Michael Bernstein,
Imperial College London, United Kingdom
Thomas Gander,
University Hospital Zürich, Switzerland

***Correspondence:**
Senada Koljenović
s.koljenovic@erasmusmc.nl

Specialty section:
This article was submitted to Head and Neck Cancer, a section of the journal Frontiers in Oncology

Received: *11 November 2020*
Accepted: *01 February 2021*
Published: *12 March 2021*

Citation:
Aaboubout Y, van der Toom QM, de Ridder MAJ, De Herdt MJ, van der Steen B, van Lanschot CGF, Barroso EM, Nunes Soares MR, ten Hove I, Mast H, Smits RWH, Sewnaik A, Monserez DA, Keereweer S, Caspers PJ, Baatenburg de Jong RJ, Bakker Schut TC, Puppels GJ, Hardillo JA and Koljenović S (2021) Is the Depth of Invasion a Marker for Elective Neck Dissection in Early Oral Squamous Cell Carcinoma? Front. Oncol. 11:628320. doi: 10.3389/fonc.2021.628320

INTRODUCTION

Oral cavity cancer has a worldwide incidence of 350,000, with a male:female ratio of 2.1:1 (1). The 5-year survival rate is approximately 50% in Europe (2). Histologically, more than 90% of all oral cavity cancers are squamous cell carcinoma (OCSCC) (3). The most common risk factors for developing OCSCC are tobacco and alcohol consumption (4). In Southern Asia (India, Sri Lanka, China, and Thailand), the incidence of OCSCC is even higher due to the chewing of tobacco with or without betel quid (2). The estimated annual mortality in patients with OCSCC is 145,000 worldwide (5).

Factors that are known to contribute to a patients prognosis are tumor size, regional lymph node involvement and distance metastasis (TNM classification), tumor differentiation grade, perineural invasion (PNI), and lymphovascular invasion (LVI) (6). The treatment of choice is surgery with tumor resection and neck dissection in case of clinical lymph node involvement. An elective neck dissection in OCSCC patients is recommended if the risk of occult lymph node metastasis is >20% (7).

An END increases the disease-specific survival (DSS) and overall survival (OS) compared to watchful waiting (WW), supported by a therapeutic lymph node dissection when needed (8, 9). A neck dissection can be associated with several adverse effects such as edema, pain, and disability of the shoulder. The severity of these effects is often related to the extent of dissection; neck and shoulder discomfort is still reported even if the vital structures are well preserved (10, 11). Therefore, the current international consensus is that an END should only be performed if the risk of occult lymph node metastasis is >20%.

The DOI and sentinel lymph node biopsy are currently the best predictors for occult lymph node metastasis (12). Sentinel node biopsy has high accuracy for identifying occult lymph node metastasis (13–15). However, this accuracy is very dependent on experience and technical expertise, which makes the sentinel node biopsy procedure difficult for wide implementation (12).

The DOI is used as a marker for elective neck dissection (END) in a number of centers, including ours. However, there is no unanimous cut-off value, varying from 2 mm - 10 mm between the centers (16, 17). The lack of common definition and guidelines on how to measure DOI has led to this large variation. This shortcoming has been recently addressed by the 8th edition of the cancer staging manual from the American Joint Committee on Cancer (AJCC) (18).

The aim of this study was to estimate a cut-off value of DOI for clinical decision making on END, by assessing the association of DOI and the risk of occult lymph node metastasis in early OCSCC.

Abbreviations: DOI, depth of invasion; OCSCC, oral cavity squamous cell carcinoma; END, elective neck dissection; WW, watchful waiting; OR, odds ratio; MC, Medical Center; AJCC, American Joint Committee on Cancer; NCCN, National Comprehensive Cancer Network; H&E, hematoxylin and eosin; PNI, perineural invasion; LVI, lymphovascular invasion; OS, overall survival; DSS, disease-specific survival; RRFS, regional recurrence-free survival; TT, tumor thickness; TNM, Tumor, lymph nodes, metastasis (according to the TNM Classification of Malignant Tumors).

METHOD

Study Design and Patients

A single-center retrospective cohort study was conducted at the Erasmus University Medical Center (Erasmus MC), Rotterdam, the Netherlands after Institutional Review Board approval (MEC-2016-751). Surgically treated patients with primary OCSCC (pT1 or pT2, based on the 8th edition of the AJCC) and clinically negative lymph nodes (cN0) were identified from January 2006 until December 2012 (18). Clinical lymph node status was determined by palpation of the neck, and/or by imaging (ultrasound with fine-needle aspiration biopsy, CT, and/or MRI).

Exclusion criteria were a history of head and neck cancer, presence of synchronous oral cavity tumor, unreliable assessment of the DOI, and loss to follow-up.

All patient and tumor characteristics, except the DOI, were recorded from the patient files, including age, gender, tumor localization, cTNM, pTN, differentiation grade, perineural invasion (PNI), and lymphovascular invasion (LVI). Lymphovascular invasion was regarded as positive when appreciated in the tumor and/or in the cases of a positive lymph node (pN+).

Neck lymph node treatment (*i.e.*, END or WW), follow-up (*e.g.*, local recurrence, regional recurrence, and cause of death) were also recorded. Patients were divided into two groups based on the neck treatment: the END group and the WW group. All patients were followed for at least 5 years. Patients from the END group received clinical examination and ultrasonography when indicated. Patients in the WW group always underwent ultrasonography in the first 2 years of follow-up in addition to clinical examination. The frequency of the follow-up in the first 2 years was every 2–3 months, in the 3rd year 4–6 months, and in the 4th and 5th years 6–12 months. If regional recurrence occurred, the side (ipsilateral or contralateral) was recorded.

Measurement of the Depth of Invasion

The DOI was measured for all surgical specimens based on the hematoxylin and eosin slide. The DOI was defined and measured as a plumb-line from the basal membrane of the closest normal adjacent mucosa to the deepest point of invasion, in line with the recommendation from the 8th edition of the AJCC (18).

All hematoxylin and eosin slides were collected from the Department of Pathology of the Erasmus University Medical Center and scanned by the NanoZoomer 2.0-HT slide scanner (Hamamatsu Photonics, Hamamatsu, Japan). Slides were reviewed by a head and neck pathologist (SK) using the NanoZoomer digital pathology (NDP) viewer 2.5.19 (Hamamatsu Photonics, Hamamatsu, Japan).

The patients were divided based on DOI into a group with DOI ≤4 mm and a group with DOI >4 mm, based on the DOI cut-off value >4 mm used at our institute.

Statistical Analysis

Statistical analysis was performed using the IBM SPSS Statistics version 25 software. Patients' characteristics between the two groups (DOI ≤ 4 mm DOI > 4 mm) were compared using

student T-test for continuous variables and Chi-square test for categorical variables. Univariate logistic regression was performed to assess the correlation between predictor variables and occult lymph node status. A Receiver Operator Curve (ROC) was utilized to determine the optimal cut-off value for predicting occult lymph node metastasis using DOI, for all sub-sites combined. Follow-up was calculated from the date of surgery. Regional recurrence-free survival (*i.e.*, time until an isolated regional recurrence occurs; RRFS) and disease-specific survival (*i.e.*, time until death due to disease; DSS) were assessed by Kaplan–Meier analysis and log-rank test for the DOI ≤4 mm and >4 mm and for the WW and END in the DOI group ≤4 mm. The overall survival (*i.e.*, time until the death of patients; OS) was assessed by Kaplan–Meier analysis and log-rank test for the DOI ≤4 mm and >4 mm. Two-tailed statistical tests were performed. A p-value of less than 0.05 was considered statistically significant.

TABLE 1 | Patient and tumor characteristics.

	Number (n = 222)	%
Gender		
Male	138	62.2
Female	84	37.8
Age (years)		
Median (range)	64.5 (16.1–93.1)	
pT status (8th edition)		
1	117	52.7
2	105	47.3
Tumor diameter (cm)		
Median (range)	1.5 (0.2–4)	
Depth of invasion (mm)		
Median (range)	4.48 (0.05–9.97)	
Subsite		
Tongue	128	57.6
Floor of mouth	65	29.3
Buccal mucosa	12	5.4
Retromolar trigone	7	3.2
Gingiva mandible*	7	3.2
Gingiva maxilla*	2	0.9
Lip	1	0.4
Hard palate	0	0.0
Differentiation grade		
Well	59	26.6
Moderate	149	67.1
Poor	14	6.3
Perineural invasion		
Yes	36	19.7
No	147	80.3
Unknown	39	
Lymphovascular invasion		
Yes	56	31.1
No	124	68.9
Unknown	42	
Neck treatment		
Ipsilateral END	146	65.8
Bilateral END	20	9.0
WW	56	25.2

In this small group all patients had SCC arising from the gingiva. However, in five cases the tumor was extending to the adjacent floor of mouth, reaching the maximum DOI at that location.

RESULTS

Study Population

A total of 318 patients were seen in our hospital with pT1/pT2 OCSCC during the study period. Patients were excluded due to the following reasons: a history of head and neck tumor (n = 91), unreliable assessment of the depth of invasion (n = 3), loss to follow-up (n = 2). After exclusion, 222 patients were included for the final analysis, **Table 1**. Of the 222 patients included, the cN0 status was determined by both, clinical examination and imaging in 124 patients (55.9%), by clinical examination only in 51 patients (23%), and by imaging only in 42 patients (18.9%). For the remaining five patients (2.2%) no data was available.

Depth of Invasion

Median DOI for all cases was 4.48 mm; mean was 4.8 mm with a standard deviation of 2.5 mm. In 97 cases the DOI was ≤4 mm and in 125 cases the DOI was >4 mm. Of all adverse histopathologic characteristics, only PNI was associated with DOI >4 mm ($p = 0.001$). The other adverse tumor characteristics such as differentiation grade and LVI were similar in both groups, **Table 2**.

TABLE 2 | Comparison of patient and tumor characteristics for the two depth of invasion groups.

	DOI ≤ 4 mm	%	DOI > 4 mm	%	*p*-value*
pT status (8th edition)					<0.001
1	89	91.8	28	22.4	
2	8	8.2	97	77.6	
Tumor diameter**	1.23 ± 0.69		1.94 ± 0.83		<0.001
DOI**	2.47 ± 0.95		6.62 ± 1.75		<0.001
Subsite					0.670
Tongue	59	60.8	69	55.2	
Floor of mouth	28	28.9	37	29.6	
Buccal mucosa	3	3.1	9	7.2	
Retromolar trigone	3	3.1	4	3.2	
Gingiva mandible	3	3.1	4	3.2	
Gingiva maxilla	0	0.0	2	1.6	
Lip	1	1.0	0	0.0	
Hard palate	0	0.0	0	0.0	
Differentiation grade					0.259
Well	31	32.0	28	22.4	
Moderate	61	62.8	88	70.4	
Poor	5	5.2	9	7.2	
Perineural invasion					0.001
Yes	6	8.2	30	27.3	
No	67	91.8	80	72.7	
Unknown	24		15		
Lymphovascular invasion					0.10
Yes	7	10.4	16	15.1	
No	60	89.6	90	84.9	
Unknown	30		19		

*Chi-square test for categorical data, unpaired T-test for numeric data.
**Expressed as mean ± SD.

TABLE 3 | Association between depth of invasion and occult lymph node metastasis.

DOI (mm)	Total patients (n)	pN0 (n)	pN+** n (%)	Cut-off value (mm)	Sens* (%)	Spec* (%)	PPV* (%)	NPV* (%)
1 (0 < DOI ≤ 1)	2	2	0 (0)	>1	100	2	24	100
2 (1 < DOI ≤ 2)	6	6	0 (0)	>2	100	6	25	100
3 (2 < DOI ≤ 3)	24	20	4 (17)	>3	90	22	26	88
4 (3 < DOI ≤ 4)	21	15	6 (29)	>4	74	34	26	81
5 (4 < DOI ≤ 5)	26	20	6 (23)	>5	59	50	26	80
6 (5 < DOI ≤ 6)	16	14	2 (12)	>6	54	61	30	81
7 (6 < DOI ≤ 7)	24	21	3 (12)	>7	46	77	38	82
8 (7 < DOI ≤ 8)	16	9	7 (44)	>8	28	84	35	79
9 (8 < DOI ≤ 9)	15	9	6 (40)	>9	13	91	31	77
10 (9 < DOI ≤ 10)	16	11	5 (31)	>10	0	100	#N/B	77

Sensitivity, specificity, PPV, and NPV were calculated using the upper limit of the category as a cut-off.
***Percentage is based on the pN+ per categorized DOI (mm).*

TABLE 4 | Association between depth of invasion and occult lymph node metastasis in tongue.

DOI (mm)	Total patients (n)	pN0 (n)	pN+** n (%)	Cut-off value (mm)	Sens* (%)	Spec* (%)	PPV* (%)	NPV* (%)
1 (0 < DOI ≤ 1)	4	4	0 (0)	>1	100	4	31	100
2 (1 < DOI ≤ 2)	12	10	2 (17)	>2	95	16	33	88
3 (2 < DOI ≤ 3)	23	16	7 (30)	>3	77	34	34	77
4 (3 < DOI ≤ 4)	20	12	8 (40)	>4	56	47	32	71
5 (4 < DOI ≤ 5)	19	14	5 (26)	>5	44	63	34	72
6 (5 < DOI ≤ 6)	8	7	1 (12)	>6	41	71	38	73
7 (6 < DOI ≤ 7)	15	12	3 (20)	>7	33	84	48	74
8 (7 < DOI ≤ 8)	7	4	3 (43)	>8	26	89	50	73
9 (8 < DOI ≤ 9)	9	4	5 (56)	>9	13	93	45	71
10 (9 < DOI ≤ 10)	11	6	5 (45)	>10	0	100	#N/A	70

Sensitivity, specificity, PPV, and NPV were calculated using the upper limit of the category as a cut-off.
***Percentage is based on the pN+ per categorized DOI (mm).*

Elective Neck Dissection *Versus* Watchful Waiting

Thirty-nine patients of the 166 patients treated with an END had occult lymph node metastasis. The DOI of all patients was categorized into whole mm (0 mm < DOI ≤ 1 mm, 1 mm < DOI ≤ 2 mm, *etc*), **Table 3**. A separate analysis was performed for 128 patients with SCC of the tongue, **Table 4**.

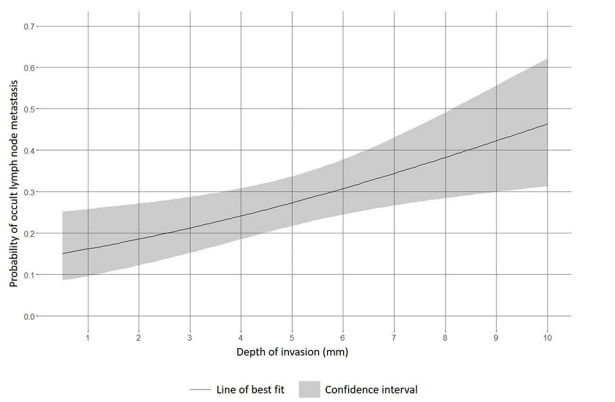

FIGURE 1 | Association between depth of invasion and occult lymph node metastasis.

Figure 1 shows predictions from a logistic regression analysis. This leads to a cut-off value of 4.3 mm, considering the 20% risk (NPV = 80%) (7). In the logistic regression analysis for the tongue population, the risk of 20% (NPV = 80%) is reached between 3 mm and 4 mm.

Predictors for Occult Lymph Node Metastasis

Univariate logistic regression analysis showed depth of invasion (OR = 1.3 per mm DOI; 95% CI: 1.1–1.5, $p = 0.001$) and tumor diameter (OR = 2.0; 95% CI: 1.3–3.1, $p = 0.002$) as predictors for occult lymph node metastasis. Perineural invasion ($p = 0.204$) and differentiation grade ($p = 0.194$) were non-predictors for occult lymph node metastasis.

Follow-Up

The mean follow-up was 67 ± 34 months, ranging from 0.2 to 156 months. No difference was found in the duration of follow-up between the DOI ≤4 mm and >4 mm, $p = 0.969$ (66.7 ± 33.5 months; 66.5 ± 34.9 months, respectively).

No difference was found between the groups DOI ≤ 4 mm and > 4 mm in local recurrence, and distant metastasis. Local recurrence occurred in 19 patients, 8 patients (8.2%) in the group DOI ≤ 4 mm and 11 patients (8.8%) in the group DOI > 4 mm, $p = 1.0$. Distant metastasis occurred in 12 patients, 6 patients (6.2%) in the group DOI ≤ 4 mm and 6 patients (4.8%) in the group DOI > 4 mm, $p = 0.878$.

TABLE 5 | Regional recurrence for the two depth of invasion groups.

	DOI ≤ 4 mm				DOI > 4 mm			
	Number of patients (n = 97)	Regional Recurrence (n)			Number of patients (n = 125)	Regional Recurrence (n)		
		2 yr	5 yr	Total		2 yr	5 yr	Total
WW	44 (45.4%)	8	3	11 (25%)	12 (9.6%)	1	1	2 (16.7%)
END	53 (54.6%)			4 (7.7%)	113 (90.4%)			10 (8.8%)
pN0	43 (81.1%)	2	1		84 (74.3%)	3	3	
pN+	10 (18.9%)	0	1		29 (25.7%)	3	1	

Regional recurrence was also analyzed per DOI group (≤4 mm *versus* >4 *mm*) and per type of treatment (WW *versus* END), **Table 5**. Regional recurrence occurred in 15 patients (15.5%) in the group DOI ≤4 mm and in 12 patients (9.6%) in the group DOI >4 mm, $p = 0.263$.

In the WW group, regional recurrence was seen in 13 patients (23.2%) (11 in the group DOI ≤4 mm and two in the group DOI >4 mm) and 14 patients (8.4%) in the END group (four in the group DOI ≤4 mm and 10 in the group DOI >4 mm), $p = 0.007$.

In this END group, in nine of 14 cases regional recurrence was contralateral (tumor subsite: tongue six, floor of mouth two, and retromolar trigone one). In the remaining five cases the regional recurrence was ipsilateral, four in a level which was not included in the END, one in the level that was included.

Regional recurrence-free survival was similar for a DOI ≤4 mm and a DOI >4 mm (5-year RRFS 86.0 *vs* 90.1%, logrank test p = 0.317).

Disease specific survival was similar for a DOI ≤4 mm and a DOI >4 mm (both 5-year DSS 89.1 *vs* 91.3%, log-rank test p = 0.605).

Overall survival was similar for a DOI ≤4 mm and a DOI >4 mm (5-year OS 73.6 *vs* 70.1%, log-rank test p = 0.527).

The differences in RRFS and DSS were calculated between WW and END only for the group DOI ≤4 mm, because in the group DOI >4 mm the number of patients with WW was not sufficient for statistical analysis.

For the group DOI ≤4 mm, the RRFS for patients with an END compared to those with WW was not different (5-year RRFS 92.2 *vs* 78.4%, log-rank test p = 0.055), **Figure 2**.

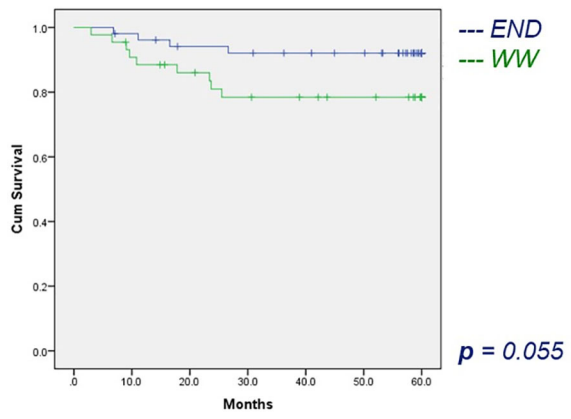

FIGURE 2 | The 5-year regional recurrence-free survival.

For the DOI ≤4 mm, the DSS was similar for the END and WW (5-year DSS 94.3 *vs* 82.6%, log-rank test p = 0.097).

DISCUSSION

Several studies report the DOI as a predictor of occult lymph node metastasis, and it is used as a criterion to decide on END in early OCSCC (19–26).

However, large differences exist between studies in regard to the definition and reliable measurement of the DOI and in the number of cases included from different subsites. This makes comparison of the results between studies unreliable.

The lack of consensus on the DOI cut-off value for the clinical decision on END is caused by the fact that it is used interchangeably with tumor thickness (TT) in different studies (16, 17, 19, 20, 27, 28). The DOI is considered a better prognostic factor than TT because it compensates for exophytic or ulcerative tumors (28). The 8th edition of the AJCC guideline, published in January 2017, provides a clear definition of the DOI (*i.e.*, the distance between the basal membrane of normal adjacent mucosa and the deepest point of tumor invasion) (18). Therefore, many studies are outdated (9, 19, 28–30). Moreover, the studies published after the release of the 8th edition of the AJCC show large variances. A number of studies do not confirm the DOI cut-off value of 4 mm. For instance, Faisal et al. showed 10 mm DOI cut-off value for decision making on END, Tam et al. showed 7.25 mm, and Kozak et al. did not specify another DOI cut-off value (23, 24, 31). On the other hand, van Lanschot et al. confirmed the DOI cut-off value of 4 mm, and Brockhoff et al. calculated DOI cut-off values for most subsites (*i.e.*, tongue = 2mm, floor of mouth = 3mm, and Proc alv/hard palate = 4mm) (20, 22).

The strength of the current study is that the DOI was measured for all cases, according to the current AJCC guideline, on digital H&E slides with high precision. In order to have comparable data, it would be desirable that in future studies the DOI is used and that the conclusions of already published studies based on TT are reassessed based on the DOI.

It is known that the frequency of occult lymph node metastasis differs per OCSCC subsite. It has been reported that occult lymph node metastasis is present in 20–30% of the cases for tongue cancer, 41.7% for the floor of mouth, and 15.4% for the buccal mucosa (20, 32). Therefore, the DOI cut-off value should be determined per subsite. The limited number of cases per subsite included in this study did not allow this analysis.

Aside from the DOI, other tumor characteristics like diameter, differentiation grade, worst pattern of invasion, perineural invasion, and tumor budding can also be associated with occult lymph node metastasis (33–36). In this study, it was not possible to confirm the other tumor characteristics because the multivariate analysis was not performed due to the incomplete pathology reporting between 2006 and 2012. Data on LVI, PNI, and tumor diameter were sometimes missing. Besides, margin status was often not annotated exactly. Instead of numerical values, there was only a description of margins (*e.g.*, radical, free of tumor). The previously published study on this subject by our group involved a relatively recent cohort (2013–2018), in which our protocol for END was based on the DOI (>4 mm = END). On contrary, in the current study an older cohort was involved for which the guideline for END was based on either DOI >5 mm or tumor diameter >1.0 cm. Moreover, for the old cohort the reliable data for LVI, PNI, tumor diameter and margin status were missing and therefore not further analyzed and compared with the newer cohort. Finally, the patient outcome (locoregional recurrence and survival) in the previously published study may be influenced by the fact that our institute started with intra-operative assessment of resection margins in 2013 (22, 37, 38).

However, it was shown that a predictive model for occult lymph node metastasis including all the tumor characteristics is the best approach (39). Objective methods for predicting occult lymph node metastasis are being investigated, like gene-expression profiling or molecular markers (40–43).

In this study, we showed that the DOI is a significant predictor for occult lymph node metastasis ($p = 0.001$) in OCSCC. Therefore, the DOI can be regarded as a parameter for decision making on END. At our institute, the DOI cut-off value >4 mm is used, based on the National Comprehensive Cancer Network (NCCN) guideline (12). Here we confirm with a NPV of 81% the DOI cut-off value >4 mm for decision making on END.

We showed that performing an END in patients with an DOI ≤4 mm had no significant effect on the 5-year DSS compared to WW (94.3 *vs* 82.6%, log-rank test $p = 0.097$). The strength of this study is that this analysis was possible because of the large number of patients treated with an END in the group with a DOI ≤4 mm. In this group, the RRFS reached near significance ($p = 0.055$) for END, when compared to WW. For the group DOI >4 mm, the difference in DSS and RRFS could not be calculated because the number of patients was not sufficient for statistical analysis.

Despite the fact that END was performed, regional recurrence occurred in 8.4% of patients (14 of 166). The recurrences were either ipsilateral and mostly at a neck level that was not included in the END (5), or contralateral (9) to END side. The effectiveness of END is shown by the fact that only one patient had a regional recurrence at a level that was included in the END.

Most authors base their decision on END according to 20% (NPV 80%) risk of occult lymph node metastasis (19, 20, 22–26). The origin of this risk cut-off value is the publication of Weiss et al. in 1994 (7). In this study, the decision for intervention was determined by the side effects of surgery (END) and radiotherapy at that time. It may be assumed that nowadays, 25 years later, the treatment modalities have substantially improved. Therefore, we suggest that a risk lower than 20% should be taken into consideration when deciding on END. This of course, should only be done in agreement with patients, based on the clear information on both, side effects of the END and the risk of occult lymph node metastasis.

DATA AVAILABILITY STATEMENT

The raw data supporting the conclusions of this article will be made available by the authors, without undue reservation.

ETHICS STATEMENT

The studies involving human participants were reviewed and approved by the Medisch Ethische Toetsings Commissie Erasmus MC (MEC-2016-751). The patients/participants provided their written informed consent to participate in this study.

AUTHOR CONTRIBUTIONS

YA designed the study, performed the depth of invasion measurements with SKo, carried out the retrospective database study, and drafted the manuscript. QT designed the study, performed the depth of invasion measurements with SKo, and carried out the retrospective database study. MR was responsible for the statistical analysis of data. MH and BS were responsible for the collection and scanning of histopathologic material and revised the manuscript critically for important intellectual content. CL, EB, MN, IH, HM, RS, AS, DM, SKe, PC, and RB revised the manuscript critically for important intellectual content. TS anticipated the design of the study and revised the manuscript critically for important intellectual content. GP designed the study, supervised the research group, and revised the manuscript critically for important intellectual content and gave the final approval of the version to be published. JH designed, drafted, and supervised this study and gave the final approval of the version to be published. SKo designed, drafted, and supervised this study, was mainly responsible for the depth of the invasion measurements, and gave the final approval of the version to be published. All authors contributed to the article and approved the submitted version.

FUNDING

We thank the Dutch Cancer Society (106467-Optimizing surgical results for oral squamous cell carcinoma by intra-operative assessment of resection margins using Raman spectroscopy) and Eurostars (12076-RA-SURE) for the financial support.

REFERENCES

1. Bray F, Ferlay J, Soerjomataram I, Siegel RL, Torre LA, Jemal A. Global cancer statistics 2018: GLOBOCAN estimates of incidence and mortality worldwide for 36 cancers in 185 countries. *CA Cancer J Clin* (2018) 68(6):394–424. doi: 10.3322/caac.21492
2. Shield KD, Ferlay J, Jemal A, Sankaranarayanan R, Chaturvedi AK, Bray F, et al. The global incidence of lip, oral cavity, and pharyngeal cancers by subsite in 2012. *CA Cancer J Clin* (2017) 67(1):51–64. doi: 10.3322/caac.21384
3. Vigneswaran N, Williams MD. Epidemiologic Trends in Head and Neck Cancer and Aids in Diagnosis. *Oral Maxillofac Surg Clin North Am* (2014) 26 (2):123–41. doi: 10.1016/j.coms.2014.01.001
4. Hashibe M, Brennan P, Chuang S-c, Boccia S, Castellsague X, Chen C, et al. Interaction between Tobacco and Alcohol Use and the Risk of Head and Neck Cancer: Pooled Analysis in the International Head and Neck Cancer Epidemiology Consortium. *Cancer Epidemiol Biomarkers Prev* (2009) 318 (2):541–50. doi: 10.1158/1055-9965.EPI-08-0347
5. Ferlay J, Soerjomataram I, Dikshit R, Eser S, Mathers C, Rebelo M, et al. Cancer incidence and mortality worldwide: sources, methods and major patterns in GLOBOCAN 2012. *Int J Cancer* (2015) 136(5):E359–86. doi: 10.1002/ijc.29210
6. Liu S-A, Wang C-C, Jiang R-S, Lee F-Y, Lin W-J, Lin J-C. Pathological features and their prognostic impacts on oral cavity cancer patients among different subsites – A singe institute's experience in Taiwan. *Sci Rep* (2017) 7 (1):7451. doi: 10.1038/s41598-017-08022-w
7. Weiss MH, Harrison LB, Isaacs RS. Use of Decision Analysis in Planning a Management Strategy for the Stage NO Neck. *Arch Otolaryngol Head Neck Surg* (1994) 120(7):699–702. doi: 10.1001/archotol.1994.01880310005001
8. Xie Y, Shen G. Association of neck dissection with survival for early stage N0 tongue cancer: A SEER population-based study. *Medicine (Baltimore)* (2018) 97(51):e13633. doi: 10.1097/MD.0000000000013633
9. D'Cruz AK, Vaish R, Kapre N, Dandekar M, Gupta S, Hawaldar R, et al. Elective versus Therapeutic Neck Dissection in Node-Negative Oral Cancer. *N Engl J Med* (2015) 373(6):521–9. doi: 10.1056/NEJMoa1506007
10. Gane EM, Michaleff ZA, Cottrell MA, McPhail SM, Hatton AL, Panizza BJ, et al. Prevalence, incidence, and risk factors for shoulder and neck dysfunction after neck dissection: A systematic review. *Eur J Surg Oncol* (2017) 43 (7):1199–218. doi: 10.1016/j.ejso.2016.10.026
11. Bradley PJ, Ferlito A, Silver CE, Takes RP, Woolgar JA, Strojan P, et al. Neck treatment and shoulder morbidity: Still a challenge. *Head Neck* (2011) 33:1060–7 doi: 10.1002/hed.21495
12. National Comprehensive Cancer Network. *NCCN Clinical Practice Guidelines in Oncology (NCCN Guidelines®) Head and Neck. Version 1.* (2016). p. 2016.
13. Civantos FJ, Zitsch RP, Schuller DE, Agrawal A, Smith RB, Nason R, et al. Sentinel lymph node biopsy accurately stages the regional lymph nodes for T1-T2 oral squamous cell carcinomas: Results of a prospective multi-institutional trial. *J Clin Oncol* (2010) 28(8):1395–400. doi: 10.1200/JCO.2008.20.8777
14. Alkureishi LWT, Ross GL, Shoaib T, Soutar DS, Robertson AG, Thompson R, et al. Sentinel node biopsy in head and neck squamous cell cancer: 5-year follow-up of a european multicenter trial. *Ann Surg Oncol* (2010) 17(9):2459–64. doi: 10.1245/s10434-010-1111-3
15. Govers TM, Hannink G, Merkx MAW, Takes RP, Rovers MM. Sentinel node biopsy for squamous cell carcinoma of the oral cavity and oropharynx: A diagnostic meta-analysis. *Oral Oncol* (2013) 49(8):726–32. doi: 10.1016/j.oraloncology.2013.04.006
16. Kuan EC, Clair JM-S, Badran KW, St. John MA. How does depth of invasion influence the decision to do a neck dissection in clinically N0 oral cavity cancer? *Laryngoscope* (2016) 126(3):547–8. doi: 10.1002/lary.25707
17. Shinn JR, Wood CB, Colazo JM, Harrell FE, Rohde SL, Mannion K. Cumulative incidence of neck recurrence with increasing depth of invasion. *Oral Oncol* (2018) 87:36–42. doi: 10.1016/j.oraloncology.2018.10.015
18. Lydiatt WM, Patel SG, O'Sullivan B, Brandwein MS, Ridge JA, Migliacci JC, et al. Head and Neck Cancers—Major Changes in the American Joint Committee on Cancer Eighth Edition Cancer Staging Manual William. *Cancer J Clin* (2018) 68(1):55–63. doi: 10.3322/caac.21389
19. Melchers LJ, Schuuring E, van Dijk BAC, de Bock GH, Witjes MJH, van der Laan BFAM, et al. Tumour infiltration depth ≧4mm is an indication for an elective neck dissection in pT1cN0 oral squamous cell carcinoma. *Oral Oncol* (2012) 48(4):337–42. doi: 10.1016/j.oraloncology.2011.11.007
20. Brockhoff HC, Kim RY, Braun TM, Skouteris C, Helman JI, Ward BB. Correlating the depth of invasion at specific anatomic locations with the risk for regional metastatic disease to lymph nodes in the neck for oral squamous cell carcinoma. *Head Neck* (2017) 39(5):974–9. doi: 10.1002/hed.24724
21. Pentenero M, Gandolfo S, Carrozzo M. Importance of tumor thickness and depth of invasion in nodal involvement and prognosis of oral squamous cell carcinoma: A review of the literature. *Head Neck* (2005) 27(12):1080–91. doi: 10.1002/hed.20275
22. van Lanschot CGF, Klazen YP, de Ridder MAJ, Mast H, ten Hove I, Hardillo JA, et al. Depth of invasion in early stage oral cavity squamous cell carcinoma: The optimal cut-off value for elective neck dissection. *Oral Oncol* (2020) 111:104940. doi: 10.1016/j.oraloncology.2020.104940
23. Faisal M, Abu Bakar M, Sarwar A, Adeel M, Batool F, Malik KI, et al. Depth of invasion (DOI) as a predictor of cervical nodal metastasis and local recurrence in early stage squamous cell carcinoma of oral tongue (ESSCOT). *PLoS One* (2018) 13(8):e0202632. doi: 10.1371/journal.pone.0202632
24. Tam S, Amit M, Zafereo M, Bell D, Weber RS. Depth of invasion as a predictor of nodal disease and survival in patients with oral tongue squamous cell carcinoma. *Head Neck* (2018) 7:hed.25506. doi: 10.1002/hed.25506
25. Liao CT, Wang HM, Ng SH, Yen TC, Lee LY, Hsueh C, et al. Good tumor control and survivals of squamous cell carcinoma of buccal mucosa treated with radical surgery with or without neck dissection in Taiwan. *Oral Oncol* (2006) 42(8):800-9. doi: 10.1016/j.oraloncology.2005.11.020
26. Massey C, Dharmarajan A, Bannuru RR, Rebeiz E. Management of N0 neck in early oral squamous cell carcinoma: A systematic review and meta-analysis. *Laryngoscope* (2019) 129(8):E284–98. doi: 10.1002/lary.27627
27. Fukano H, Matsuura H, Hasegawa Y, Nakamura S. Depth of invasion as a predictive factor for cervical lymph node metastasis in tongue carcinoma. *Head Neck* (1997) 19(3):205–10. doi: 10.1002/(SICI)1097-0347(199705)19:3<205::AID-HED7>3.0.CO;2-6
28. Kane SV, Gupta M, Kakade AC, D'Cruz A. Depth of invasion is the most significant histological predictor of subclinical cervical lymph node metastasis in early squamous carcinomas of the oral cavity. *Eur J Surg Oncol* (2006) 32 (7):795–803. doi: 10.1016/j.ejso.2006.05.004
29. Almagush A, Bello IO, Coletta RD, Makitie AA, Makinen LK, Kauppila JH, et al. For early-stage oral tongue cancer, depth of invasion and worst pattern of invasion are the strongest pathological predictors for locoregional recurrence and mortality. *Virchows Arch* (2015) 467(1):39-46467(1):39–46. doi: 10.1007/s00428-015-1758-z
30. Chen YW, Yu EH, Wu TH, Lo WL, Li WY, Kao SY. Histopathological factors affecting nodal metastasis in tongue cancer: analysis of 94 patients in Taiwan. *Int J Oral Maxillofac Surg* (2008) 37(10):912–6. doi: 10.1016/j.ijom.2008.07.014
31. Kozak MM, Shah J, Chen M, Schaberg K, von Eyben R, Chen JJ, et al. Depth of invasion alone as a prognostic factor in low-risk early-stage oral cavity carcinoma. *Laryngoscope* (2019) 129(9):2082–6. doi: 10.1002/lary.27753
32. Hanai N, Asakage T, Kiyota N, Homma A, Hayashi R. Controversies in relation to neck management in N0 early oral tongue cancer. *Jpn J Clin Oncol* (2019) 49(4):297–305. doi: 10.1093/jjco/hyy196
33. An S, Jung E-J, Lee M, Kwon T-K, Sung M-W, Jeon YK, et al. Factors Related to Regional Recurrence in Early Stage Squamous Cell Carcinoma of the Oral Tongue. *Clin Exp Otorhinolaryngol* (2008) 1(3):166. doi: 10.3342/ceo.2008.1.3.166
34. Lanzer M, Gander T, Kruse A, Luebbers H-T, Reinisch S. Influence of histopathologic factors on pattern of metastasis in squamous cell carcinoma of the head and neck. *Laryngoscope* (2014) 124(5):E160–6. doi: 10.1002/lary.24458
35. Kademani D, Bell RB, Bagheri S, Holmgren E, Dierks E, Potter B, et al. Prognostic Factors in Intraoral Squamous Cell Carcinoma: The Influence of Histologic Grade. *J Oral Maxillofac Surg* (2005) 63(11):1599–605. doi: 10.1016/j.joms.2005.07.011
36. Chatterjee D, Bansal V, Malik V, Bhagat R, Punia RS, Handa U, et al. Tumor Budding and Worse Pattern of Invasion Can Predict Nodal Metastasis in Oral Cancers and Associated With Poor Survival in Early-Stage Tumors. *Ear Nose Throat J* (2019) 98(7):E112–9. doi: 10.1177/0145561319848669

37. Smits RWH, van Lanschot CGF, Aaboubout Y, de Ridder M, Hegt VN, Barroso EM, et al. Intraoperative Assessment of the Resection Specimen Facilitates Achievement of Adequate Margins in Oral Carcinoma. *Front Oncol* (2020) 10:1–9. doi: 10.3389/fonc.2020.614593
38. Aaboubout Y, ten Hove I, Smits RWH, Hardillo JA, Puppels GJ, Koljenovic S. Specimen-driven intraoperative assessment of resection margins should be standard of care for oral cancer patients. *Oral Dis* (2021) 27(1):111–6. doi: 10.1111/odi.13619
39. Wermker K, Belok F, Schipmann S, Klein M, Schulze H-J, Hallermann C. Prediction model for lymph node metastasis and recommendations for elective neck dissection in lip cancer. *J Craniomaxillofac Surg* (2015) 43 (4):545–52. doi: 10.1016/j.jcms.2015.02.002
40. Roepman P, Wessels LFA, Kettelarij N, Kemmeren P, Miles AJ, Lijnzaad P, et al. An expression profile for diagnosis of lymph node metastases from primary head and neck squamous cell carcinomas. *Nat Genet* (2005) 37 (2):182–6. doi: 10.1038/ng1502
41. van Hooff SR, Leusink FKJ, Roepman P, Baatenburg de Jong RJ, Speel E-JM, van den Brekel MWM, et al. Validation of a Gene Expression Signature for Assessment of Lymph Node Metastasis in Oral Squamous Cell Carcinoma. *J Clin Oncol* (2012) 30(33):4104–10. doi: 10.1200/JCO.2011.40.4509
42. Melchers L, Clausen M, Mastik M, Slagter-Menkema L, van der Wal J, Wisman G, et al. Identification of methylation markers for the prediction of nodal metastasis in oral and oropharyngeal squamous cell carcinoma. *Epigenetics* (2015) 10(9):850–60. doi: 10.1080/15592294.2015.1075689
43. Takes RP, Baatenburg de Jong RJ, Alles MJRC, Meeuwis CA, Marres HAM, Knegt PPM, et al. Markers for Nodal Metastasis in Head and Neck Squamous Cell Cancer. *Arch Otolaryngol Neck Surg* (2002) 128(5):512. doi: 10.1001/archotol.128.5.512

Conflict of Interest: The authors declare that the research was conducted in the absence of any commercial or financial relationships that could be construed as a potential conflict of interest.

frontiers in Oncology

ORIGINAL RESEARCH
published: 12 March 2021
doi: 10.3389/fonc.2021.619372

Postoperative Concurrent Chemoradiotherapy *Versus* Radiotherapy Alone for Advanced Oral Cavity Cancer in the Era of Modern Radiation Techniques

*Tae Hyung Kim[1,2], In-Ho Cha[3], Eun Chang Choi[4], Hye Ryun Kim[5], Hyung Jun Kim[3], Se-Heon Kim[4], Ki Chang Keum[1] and Chang Geol Lee[1]**

[1] Department of Radiation Oncology, Yonsei Cancer Center, Yonsei University College of Medicine, Seoul, South Korea, [2] Department of Radiation Oncology, Eulji General Hospital, College of Medicine, Eulji University, Seoul, South Korea, [3] Department of Oral and Maxillofacial Surgery, Yonsei University College of Dentistry, Seoul, South Korea, [4] Department of Otorhinolaryngology, Yonsei University College of Medicine, Seoul, South Korea, [5] Division of Medical Oncology, Department of Internal Medicine, Yonsei Cancer Center, Yonsei University College of Medicine, Seoul, South Korea

OPEN ACCESS

Edited by:
Cesare Piazza, University of Brescia, Italy

Reviewed by:
Nicola Alessandro Iacovelli, Istituto Nazionale dei Tumori (IRCCS), Italy
Gaurisankar Sa, Bose Institute, India

***Correspondence:**
Chang Geol Lee
CGLEE1023@yuhs.ac

Specialty section:
This article was submitted to Head and Neck Cancer, a section of the journal Frontiers in Oncology

Received: *20 October 2020*
Accepted: *20 January 2021*
Published: *12 March 2021*

Citation:
Kim TH, Cha I-H, Choi EC, Kim HR, Kim HJ, Kim S-H, Keum KC and Lee CG (2021) Postoperative Concurrent Chemoradiotherapy Versus Radiotherapy Alone for Advanced Oral Cavity Cancer in the Era of Modern Radiation Techniques. Front. Oncol. 11:619372. doi: 10.3389/fonc.2021.619372

Background/Purpose: Surgery followed by postoperative radiotherapy (RT) has been considered the standard treatment for oral cavity squamous cell carcinoma (OCSCC) of advanced stages or with adverse prognostic factors. In this study, we compared the outcomes in patients with OCSCC who received postoperative concurrent chemoradiotherapy (CCRT) or postoperative RT alone using modern RT techniques.

Methods: A total of 275 patients with OCSCC treated between 2002 and 2018 were retrospectively analyzed. Adverse prognostic factor was defined as extranodal extension (ENE), microscopically involved surgical margin, involvement of ≥2 lymph nodes, perineural disease, and/or lymphovascular invasion (LVI). In total, 148 patients (54%) received CCRT and 127 patients (46%) received RT alone. More patients in the CCRT group had N3 disease and stage IVB disease (46.6% *vs.* 10.2%, $p<0.001$), ENE (56.1% *vs.* 15.7%, $p<0.001$), LVI (28.4% *vs.* 13.4%, $p=0.033$).

Results: With a median follow-up of 40 (range, 5–203) months, there were no significant differences in the 5-year overall survival (OS) and PFS between treatment groups. In the subgroup analysis according to high risk, the concurrent use of chemotherapy showed significantly improved OS in patients with ENE (HR 0.39, $p=0.003$).

Conclusion: Our retrospective study showed that postoperative CCRT group had comparable survival outcomes to those in the RT alone group for advanced OCSCC in the era of modern RT techniques and indicated that concurrent chemotherapy should be administered to patients with ENE. Prospective randomized studies for confirmation are needed.

Keywords: oral cancer, intensity modulated radiotherapy, chemotherapy, treatment outcome, prognosis

INTRODUCTION

Squamous cell carcinoma (SCC) is the most common malignancy of the oral cavity (1). It is estimated that 35,130 people will be diagnosed with oral cavity cancer in 2019 (2). Surgery followed by postoperative radiotherapy (PORT) is considered the standard treatment for oral cavity SCC (OCSCC) of advanced stages or with adverse prognostic factors. In general, patients with OCSCC tend to have worse local and regional control compared to other head and neck subsites (3–5).

Evidence for the concurrent use of chemotherapy was established by the European Organization for Research and Treatment of Cancer (EORTC) 22931 and Radiation Therapy Oncology Group (RTOG) 9501 trials (6, 7). Concurrent chemotherapy with cisplatin was administrated for high risk patients and reported that 5-year overall survival (OS) was approximately 50%.

With advances in radiotherapy (RT) techniques, intensity-modulated RT (IMRT) has been the standard RT for head and neck tumors. In this study, we compared the outcomes in patients with oral cavity SCC (OCSCC) who received postoperative concurrent chemoradiotherapy (CCRT) or PORT alone using modern RT techniques.

MATERIALS AND METHODS

Study Population

A list of consecutive patients who were diagnosed with OCSCC and received RT between 2002 and 2018 was extracted from an institutional cancer registry; a total of 486 patients were identified. The inclusion criteria were as follows: pathologically confirmed SCC of oral cavity, resection of primary tumor with/without neck node dissection, and received postoperative RT using three-dimensional conformal RT (3D-CRT) or IMRT. Exclusion criteria were as follows: PORT followed by salvage resection after recurrence of disease (n = 145); pathologically not a SCC, such as adenoid cystic carcinoma or sarcoma (n = 41); palliative treatment due to distant metastasis (n = 21); and OCSCC with double primary lung cancer (n = 4). After all exclusions, the data of 275 patients were analyzed.

The procedures followed in this study were in accordance with the Helsinki Declaration of 1975, as revised in 2000. This study was approved by our Institutional Review Board (IRB # 4-2019-0401).

Treatment

Pretreatment evaluation included a complete history, physical examination and laboratory studies including a complete blood cell count and serum chemistry profile. Patients underwent imaging studies such as computed tomography (CT), magnetic resonance imaging for primary tumor and neck node involvement evaluation, and positron emission tomography (PET) for systemic evaluation.

The surgical techniques included resection either by open approaches or by trans-oral robotic surgery using da Vinci Robot (Intuitive Surgical Inc., Sunnyvale, CA). Neck dissection was performed on the involved side or both sides of neck in order to examine the regional lymph node involvement.

RT was delivered using megavoltage photons (≥6 MV). Using 3D-CRT, a cone-down technique was used. Using IMRT, the simultaneous integrated boost technique was used in all patients. The high-risk clinical target volume (CTV)1 encompassed the primary tumor bed (based on preoperative imaging, physical examination, and operative findings) and extranodal extension (ENE) or microscopically involved surgical margin lesions (RM+). The intermediate-risk CTV2 encompassed the pathologically positive hemi neck; this frequently required coverage of nodal levels I, IIa-b, III, and IV for most cases. The low-risk CTV3 usually encompassed the prophylactically treated neck with a low risk of harboring microscopic disease (e.g., the uninvolved low or contralateral neck). For the planning target volume (PTV), a 2–5 mm margin was applied to the CTV. The intended total dose for PTV1 was 60–66 Gy in 2.0 Gy per fraction. If ENE or RM+ were present, the region was treated with 64–66 Gy. The intended total doses for PTV2 and PTV3 were 60 Gy and 45-50 Gy, respectively. The target volume was delineated on simulation CT fused with PET and other images. Helical tomotherapy (HT), an image-guided IMRT system using megavoltage CT (MVCT) that provides precise delivery, was used in IMRT. HT was demonstrated to have better target volume dose conformity and homogeneity than other IMRT (8). The daily MVCT images were fused with the original treatment planning based on soft tissue and bony structures at each fraction. The position was corrected manually to align target volume after automatic registration (9).

Concurrent chemotherapy was added to RT in patients with high risk OCSCC. High risk was defined by ENE, RM+, perineural invasion (PNI), lymphovascular invasion (LVI), and/or multiple nodes involvement. ENE was defined as extension of cancer cells through the lymph node capsule. The pathological margins were classified as negative (>5 mm), close (≤5 mm), and positive (presence of cancer cells microscopically [RM+]). Patients received concurrent chemotherapy as follows: cisplatin was administered as a weekly dose of 25–40 mg/m^2 or a triweekly dose of 100 mg/m^2 from the first day of RT.

Each patient was examined by a dental team for pre-radiotherapy dental care, which was completed before the initiation of PORT. In addition to clinical examination, radiographic examination was performed to determine the periodontal status and the presence of periapical inflammation and other dental diseases. Each patient was examined at least once a week to monitor treatment-related toxicities. Treatment-related toxicities were graded according to the Common Toxicity Criteria for Adverse Events version 5.0.

Patterns of first failure were defined as loco-regional failure or distant metastases. The date of failure was the date of tissue confirmation or imaging study showing evidence of failure. Local failure was defined as failure occurring within the same site of the primary tumor, regional failure if occurring within the regional lymph nodes, and distant failure if occurring outside of the local and regional areas.

Statistical Analysis

Statistical analyses were conducted using IBM SPSS version 25.0 (IBM Corp., Armonk, NY). The differences in characteristics and toxicities were compared using chi-square tests, and the Kaplan–Meier method was used to calculate the OS, progression-free survival (PFS), loco-regional failure-free survival and distant metastasis-free survival; differences between the curves were analyzed using the log-rank test. Cox proportional hazards models were used to assess the association of variables with the survival and hazard ratio (HR) and confidence interval (CI). Statistical significance was defined as $p < 0.05$. Factors showing $p < 0.10$ in the univariate analyses were included in the multivariate analyses.

RESULTS

Patient Characteristics

The patient and pathologic characteristics are summarized in **Table 1**. The median age of patients was 58 years (range, 18–86) and the male-to-female ratio was 6:4. The most common primary site was the oral tongue (54%, n = 148), followed by the buccal mucosa (13%, n = 37), retromolar trigone (12%, n = 32), and alveolar ridge (12%, n = 32). The most common pathologic T and N status were T4 (36%, n = 98) and N3 (30%, n = 82). A total of 119 patients (43%) had stage IVA disease according to American Joint Committee On Cancer (AJCC) 8th edition and 82 patients (30%) had stage IVB disease. A total of 103 patients (37%) had ENE and 72 patients (26%) had RM+.

The characteristics that differed by treatment group included pathologic N status, AJCC stage, ENE, resection margin status, RT dose and RT modality. More patients in the CCRT group had N3 disease and AJCC stage IVB disease (46.6% *vs.* 10.2%, $p<0.001$), ENE (56.1% *vs.* 15.7%, $p<0.001$), LVI (28.4% *vs.* 13.4%, $p=0.033$). The mean RT dose was higher in the CCRT group (62.2 Gy *vs.* 60.9 Gy, $p=0.002$) and fewer patients received IMRT (7.4% *vs.* 19.7%, $p=0.004$). The other characteristics were well balanced between treatment groups.

Ipsilateral neck dissection was performed for 268 patients (98%), of whom 129 (47%) received modified radical neck dissection (mRND), 121 (44%) received supra-omohyoid neck dissection (SOND), and 18 (7%) received selective neck dissection (SND). Contralateral neck dissection was performed for 87 patients (32%), of whom 10 (4%) received mRND, 58 (21%) received SOND, and 19 (7%) received SND.

A total of 36 patients (13%) received 3D-CRT and 239 patients (87%) received IMRT. The median RT dose was 63 Gy (range, 50–67.5), median high risk CTV fractional dose was 2.1 Gy (range, 1.8–2.5) and median fraction number was 30 (range, 20-36). The median treatment day of RT was 42 days (range, 32–70) and total treatment time from surgery to finish of RT was 82 days (range, 63–177). A total of 148 patients (54%) received concurrent chemotherapy, three patients received induction chemotherapy consisting of cisplatin and gimeracil, also known as TS-1, before surgery, and one patient received maintenance gimeracil chemotherapy after RT. The median cumulative dose of cisplatin was 200 mg/m^2 (range, 40–300 mg/m^2). Most patients (66%, n = 97) completed chemotherapy without interruption. A total of 17 patients (12%) discontinued concurrent chemotherapy because of grade 3 poor oral intake (n = 7), grade 3 fatigue (n = 5),

TABLE 1 | Patient characteristics.

Variables	Total (n = 275)	CCRT (n = 148)	RT alone (n = 127)	*p* value
Age (median in year)	58 (18-86)	58.5 (18-80)	58.0 (24–86)	
Age (year)				0.904
<60	143 (52.0)	76 (51.4)	67 (52.8)	
≥60	132 (48.0)	72 (48.6)	60 (47.2)	
Sex				0.900
Male	175 (63.6)	95 (64.2)	80 (63.0)	
Female	100 (36.4)	53 (35.8)	47 (37.0)	
Performance status				0.478
ECOG PS 0–1	256 (93.1)	136 (91.9)	120 (94.5)	
ECOG PS 2	19 (6.9)	12 (8.1)	7 (5.5)	
Subsite				0.960
Tongue	148 (53.8)	79 (53.4)	69 (54.3)	
Buccal mucosa	37 (13.5)	20 (13.5)	17 (13.4)	
Retromolar trigone	32 (11.6)	19 (12.8)	13 (10.2)	
Gingiva, alveolar ridge	32 (11.6)	15 (10.1)	17 (13.4)	
Floor of mouth	18 (6.5)	11 (7.4)	7 (5.5)	
Hard palate	8 (2.9)	4 (2.7)	4 (3.2)	
Pathologic T classification				0.157
T1	56 (20.4)	24 (16.2)	32 (25.2)	
T2	82 (29.8)	43 (29.1)	39 (30.7)	
T3	38 (13.8)	20 (13.5)	18 (14.2)	
T4	99 (36.0)	61 (41.2)	38 (29.9)	
Pathologic N classification				<0.001
N0	70 (25.5)	20 (13.5)	50 (39.4)	
N1	46 (16.7)	19 (12.8)	27 (21.3)	
N2	77 (28.0)	40 (27.0)	37 (29.1)	
N3	82 (29.8)	69 (46.6)	13 (10.2)	
AJCC 8th stage				<0.001
I	12 (4.4)	2 (1.4)	10 (7.9)	
II	22 (8.0)	5 (3.4)	17 (13.4)	
III	40 (14.5)	12 (8.1)	28 (22.0)	
IVA	119 (43.3)	60 (40.5)	59 (46.5)	
IVB	82 (29.8)	69 (46.6)	13 (10.2)	
Extranodal extension				<0.001
Yes	103 (37.5)	83 (56.1)	20 (15.7)	
No	172 (62.5)	65 (43.9)	107 (84.3)	
Lymphovascular invasion				0.033
Yes	59 (21.5)	42 (28.4)	17 (13.4)	
No	216 (78.5)	106 (71.6)	110 (86.6)	
Perineural invasion				0.176
Yes	97 (35.3)	63 (42.6)	34 (26.8)	
No	178 (64.7)	85 (57.5)	93 (73.2)	
Resection margin				0.017
Positive	72 (26.2)	47 (31.8)	25 (19.7)	
Close	94 (34.2)	53 (35.8)	41 (32.3)	
Negative	109 (39.6)	48 (32.4)	61 (48.0)	
RT dose, mean (range, Gy)	61.6 (50.0–67.5)	62.2 (53.0–67.5)	60.9 (50.0–66.0)	0.002
RT modality				0.004
3D-CRT	239 (86.9)	137 (92.6)	102 (80.3)	
IMRT	36 (13.1)	11 (7.4)	25 (19.7)	

ECOG, Eastern Cooperative Oncology Group; AJCC, American Joint Committee on Cancer; RT, radiotherapy; 3D-CRT, 3-dimensional conformal radiotherapy; IMRT, intensity modulated radiotherapy.

and grade 3 neutropenia (n = 5). Furthermore, the chemotherapy dose was reduced in 15 (10%) patients because of grade 3 fatigue (n = 8), and grade 3 neutropenia (n = 7).

Survival Analysis, Prognostic Factors

With a median follow-up of 40 months (range, 5–203), the 5-year OS and PFS rates were 65% and 61%, respectively (**Figure 1**). Median OS was not reached, and median PFS was 140 months (95% CI, 67.6–212.4). According to primary site, the 5-year OS were follows: oral tongue (69%), buccal mucosa (64%), retromolar trigone (55%), gingiva and alveolar ridge (56%), floor of mouth (76%), hard palate (42%).

The prognostic factors associated with OS are summarized in **Table 2**. Univariate analysis revealed that pathologic T and N status, AJCC stage, ENE, and PNI were significant prognostic factors associated with OS. In the multivariate analysis, pathologic T status and PNI were associated with poorer OS. The prognostic factors associated with PFS are summarized in **Table 3**. Univariate analysis revealed that pathologic T and N status, AJCC stage, ENE, and PNI were significant prognostic factors associated with PFS. In the multivariate analysis, pathologic T status and PNI were associated with poorer PFS.

Outcomes According to Treatment Group

There were no significant differences in the 5-year OS (64% *vs.* 65%, $p = 0.974$) and PFS (62% *vs.* 60%, p=0.846) between treatment groups (**Figure 2**). No significant difference was observed in the 5-year loco-regional failure-free survival (79% *vs.* 77%, $p = 0.599$) and distant metastasis-free survival (78% *vs.* 81%, $p = 0.475$).

In the subgroup analysis according to high risk (ENE, RM+, PNI, LVI, and multiple node), the concurrent use of chemotherapy showed significantly improved OS in patients with ENE (HR 0.39, 95% CI 0.21–0.43, $p = 0.003$, **Figure 3**), while there was no advantage in OS in patients with RM+, PNI, LVI, and multiple node.

Outcomes According to Indications of Chemotherapy

In total, 103 and 72 patients had ENE and RM+, respectively; 22 patients had both ENE and RM+ and 153 patients had either ENE or RM+. Concurrent chemotherapy significantly improved the 5-year OS in patients with ENE (56% *vs.* 32%, $p = 0.002$); however, it did not improve the 5-year OS in patients with RM+ (64% *vs.* 64%, $p = 0.899$). Moreover, concurrent chemotherapy was not beneficial in patients with either ENE or RM+ ($p = 0.116$), but it was beneficial in terms of survival in patients with both ENE and RM+ ($p < 0.001$). The mean RT dose for patients with ENE was statistically higher than that for patients without ENE (62.7 Gy *vs.* 60.9 Gy, $p < 0.001$). Similarly, the mean RT dose for patients with RM+ was statistically higher than that for patients without RM+ (62.6 Gy *vs.* 61.2 Gy, $p < 0.001$).

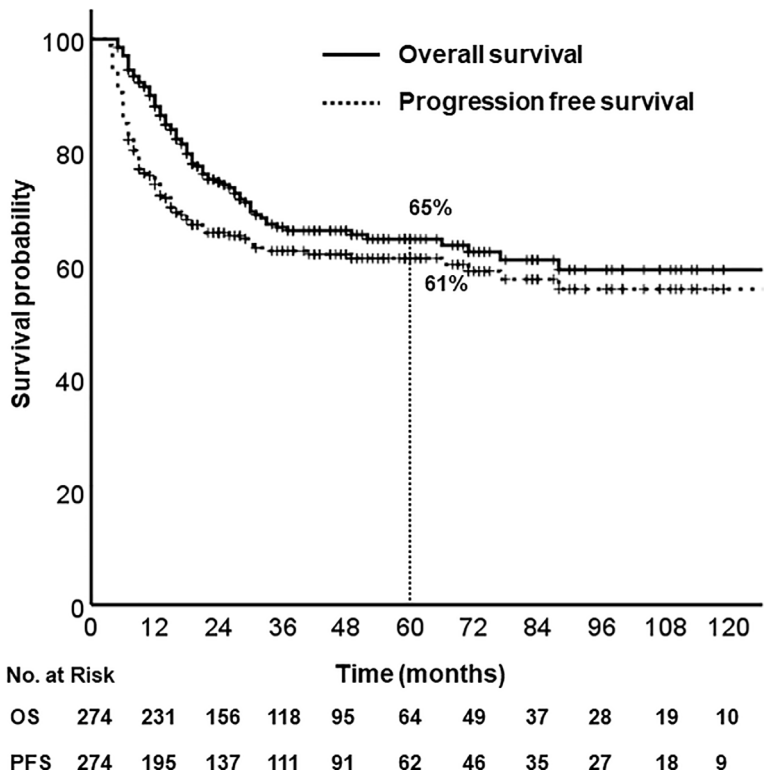

FIGURE 1 | Overall survival and progression free survival.

TABLE 2 | Prognostic factors for overall survival.

Variable	Univariate			Multivariate		
	HR	95% CI	P value	HR	95% CI	P value
Age (<60 *vs.* ≥60)	1.031	0.673–1.579	0.888			
Sex (Female *vs.* Male)	0.974	0.622–1.525	0.908			
Performance (ECOG PS0–1 *vs.* PS2)	0.857	0.347–2.117	0.739			
T classification (T1–2 *vs.* T3–4)	1.800	1.163–2.786	0.008	1.660	1.043–2.642	0.033
N classification (N0–1 *vs.* N2–3)	1.972	1.230–3.163	0.005	1.348	0.694–2.615	0.378
AJCC stage (I–II *vs.* III–IV)	4.372	1.381–13.840	0.012	2.207	0.620–7.852	0.221
ENE (No *vs.* Yes)	2.065	1.348–3.164	0.001	1.525	0.848–2.740	0.159
LVI (No *vs.* Yes)	1.511	0.942–2.425	0.087	1.234	0.757–2.012	0.399
PNI (No *vs.* Yes)	1.868	1.217–2.867	0.004	1.595	1.020–2.495	0.041
RM (Negative *vs.* Close/Positive)	1.481	0.945–2.322	0.087	1.445	0.916–2.277	0.113
Treatment modality (RT alone *vs.* CCRT)	0.993	0.648–1.522	0.974			
RT modality (3D-CRT *vs.* IMRT)	0.869	0.494–1.530	0.627			

The foreparts of the parentheses were set as the reference group.
HR, hazard ratio; CI, confidence interval; ECOG, Eastern Cooperative Oncology Group; AJCC, American Joint Committee on Cancer; ENE, extranodal extension; LVI, lymphovascular invasion; PNI, perineural invasion; RM, resection margin; RT, radiotherapy; CCRT, concurrent chemoradiotherapy; 3D-CRT, three-dimensional conformal radiation therapy; IMRT, intensity-modulated radiation therapy.

TABLE 3 | Prognostic factors for progression free survival.

Variable	Univariate			Multivariate		
	HR	95% CI	P value	HR	95% CI	P value
Age (<60 *vs.* ≥60)	0.930	0.630–1.373	0.715			
Sex (Female *vs.* Male)	0.938	0.621–1.416	0.761			
Performance (ECOG PS0–1 *vs.* PS2)	1.385	0.698–2.747	0.352			
T classification (T1–2 *vs.* T3–4)	1.918	1.287–2.857	0.001	1.881	1.224–2.891	0.004
N classification (N0–1 *vs.* N2–3)	2.056	1.338–3.159	0.001	1.659	0.925–2.975	0.089
AJCC stage (I–II *vs.* III–IV)	3.319	1.347–8.180	0.009	1.387	0.495–3.891	0.534
ENE (No *vs.* Yes)	1.873	1.270–2.762	0.002	1.314	0.791–2.183	0.292
LVI (No *vs.* Yes)	1.375	0.885–2.137	0.156			
PNI (No *vs.* Yes)	1.683	1.138–2.489	0.009	1.572	1.055–2.342	0.026
RM (Negative *vs.* Close/Positive)	1.236	0.827–1.849	0.301			
Treatment modality (RT alone *vs.* CCRT)	0.963	0.652–1.421	0.848			
RT modality (3D-CRT *vs.* IMRT)	0.934	0.544–1.603	0.804			

The foreparts of the parentheses were set as the reference group.
HR, hazard ratio; CI, confidence interval; ECOG, Eastern Cooperative Oncology Group; AJCC, American Joint Committee on Cancer; ENE, extranodal extension; LVI, lymphovascular invasion; PNI, perineural invasion; RM, resection margin; RT, radiotherapy; CCRT, concurrent chemoradiotherapy; 3D-CRT, three-dimensional conformal radiation therapy; IMRT, intensity-modulated radiation therapy.

The most common first pattern of failure in patients with ENE was distant failure (26%), followed by local (16%) and regional failures (15%). In patients with RM+, the rates of local (13%), regional (15%), and distant (13%) failures were similar. The overall rates of distant failure in patients with ENE, RM+, and negative resection margins were 32%, 21%, and 16%, respectively.

Patterns of First Failure

Treatment failure occurred in 48 and 59 patients in the RT alone and CCRT groups, respectively. The patterns of first failure are summarized in **Figure 4**. A total of 37 patients (13%) had local failures, 33 patients (12%) had regional failures, and 37 patients (13%) had distant failures (**Figure 4A**). The most common patterns of failure in CCRT was distant failure (15%) followed by regional (14%) and local (11%) (**Figure 4B**), and the most common patterns of failure in RT alone was local failure (17%), followed by distant (12%) and regional failures (9%) (**Figure 4C**).

Toxicity

A total of 105 patients (38.2%) had grade 3 mucositis, and three patients had grade 3 skin reaction. With respect to late toxicities, 10 patients (3.6%) suffered from osteoradionecrosis (ORN) of the mandible and five patients had orocutaneous fistula. Among the 10 patients with ORN, five patients had a primary tumor near the mandible (one with retromolar trigone and four with gingiva), five had pathologic T4a disease and eight received more than 60 Gy of RT. Among the five patients with orocutaneous fistula, all patients had pathologic T4a disease and received more than 60 Gy, and three had RM+.

DISCUSSION

This study reports outcomes for patients with OCSCC treated with surgery followed by CCRT or RT alone. A total of 239

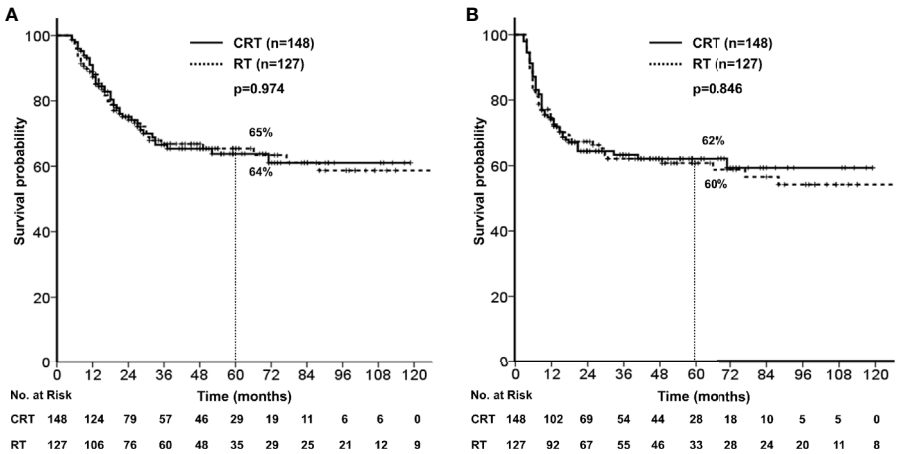

FIGURE 2 | **(A)** Overall survival stratified by concurrent chemotherapy. **(B)** Progression free survival stratified by concurrent chemotherapy.

patients (87%) were treated with IMRT. With a median follow-up of 40 months, there were no significant differences in the OS and PFS between treatment groups. Considering the fact that patients in the CCRT group had more N3 disease, ENE, and LVI, use of concurrent chemotherapy had beneficial effect on survival than RT alone.

In the EORTC 22931 and RTOG 9501 trials (6, 7), ENE and/or RM+ were the most significant prognostic factors, and the concurrent chemotherapy with PORT appeared to improve the survival of patients with OCSCC. The 10-year follow-up results were reported to examine long-term outcomes (6). In the subset analysis limited to patients with ENE and/or RM+, local-regional failure rates were 33.1% *vs.* 21.0% (p=0.02) and the OS was 19.6% *vs.* 27.1% (p=0.07). These results demonstrated improved disease control with concurrent administration of chemotherapy. In our study, there showed improved survival with concurrent administration of chemotherapy for patients with ENE (6). In the subgroup analysis, the mean RT dose for patients with ENE or RM+ was statistically higher than that for patients without ENE or RM+. Radiation dose escalation for RM+ could explain the similar rates of local, regional, and distant failures.

Hsieh C.H. et al. reported that PORT with image guidance results in better OS and LCR than postoperative RT without image guidance (10). Patients who received image-guided IMRT had a better 5-year OS than patients who received non-image-guided IMRT (87% *vs.* 48%). In our institution, all the patients

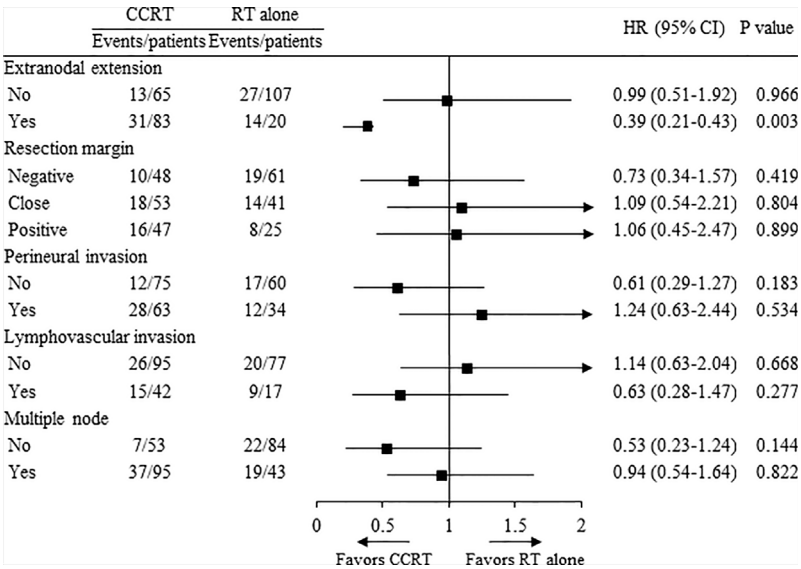

FIGURE 3 | Overall survival in treatment groups.

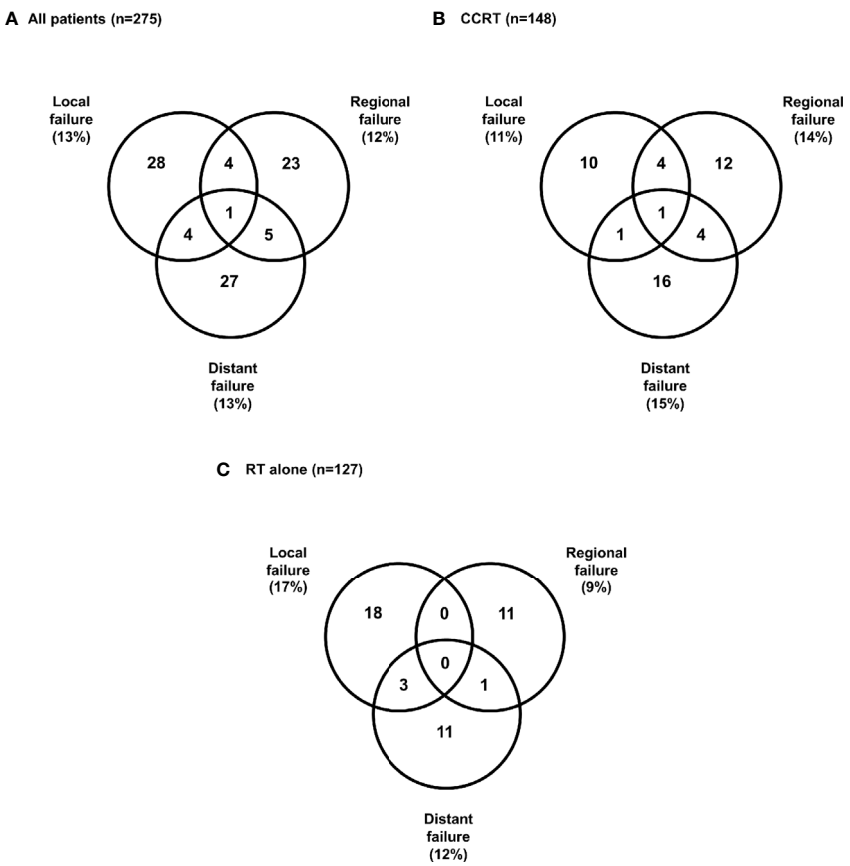

FIGURE 4 | Patterns of first failure **(A)** All patients, **(B)** Concurrent chemoradiotherapy, **(C)** Radiotherapy alone.

with head and neck cancer received image-guided HT, and patients were verified every day with MVCT. In case of weight loss or change in body shape, we made an adaptive plan for these patients.

According to the report by the Memorial Sloan Kettering Cancer center (MSKCC), 44 of 1,023 patients (4.3%) developed ORN. Patients with ORN had poor periodontal status, a history of heavy alcohol use, and received a higher radiation dose (11). Patients with oropharyngeal cancer are prone to develop ORN compared to patients with OCSCC because patients with oropharyngeal cancer receive a higher radiation dose. Similar results were observed in our analysis. Among 10 patients with ORN, most of them received a higher radiation dose and had a primary tumor near the mandible. In a report of oropharyngeal cancer from our institution, approximately 30% of patients had overall grade ≥3 acute toxicities treated with definitive RT (12). In this study, 38% of patients had grade 3 mucositis in the results of OCSCC treated with surgery followed by PORT. With respect to late toxicities, our data showed acceptable results.

Several studies have reported outcomes for specific subsites within the oral cavity. Wang Ling et al. reported the survival outcomes of 210 patients with SCC of the tongue (13). The 5-year OS rate for patients who underwent surgery and surgery with PORT were 58.2% and 45.6%, respectively. PORT was performed for stage III-IV patients, while stage I-II patients received surgery alone. In our data, the 5-year OS for patients with tongue cancer was 65%. Moreover the MSKCC reported the results of SCC of the gingivobuccal complex (14). The 5-year OS rate for patients with tongue (n = 936) and gingivobuccal cancer (n = 486) were 67.8% and 61%, respectively. PORT was performed for 40% of tongue cancer patients and 26% of gingivobuccal cancer patients. Patients with gingivobuccal cancer were more likely to be older and have more advanced disease. In our data, the 5-year OS rate was 64% for patients with buccal mucosa cancer. Nishi H. et al. reported 45 patients with retromolar trigone cancer and reported a 3-year OS rate of 59.8%, as well as pathologic LN involvement as a prognostic factor (15). In our data, the 3-year OS rate for patients with retromolar trigon cancer was 60%. According to a previous retrospective cohort study using the SEER database (Surveillance, Epidemiology, and End Results), the 5-year OS rate for patients with floor of mouth cancer was 40% (16). In our data, the 5-year OS rate for patients with floor of mouth cancer was 76%, although only 18 patients had floor of mouth cancer.

The current study has several limitations. There was heterogeneity of tumor subsites, surgery techniques including neck dissection methods, and radiation dose and field; these

differences may have influenced the local, regional, and distant tumor response. Furthermore, after the first failure, the salvage methods were not uniform. Some patients received re-operation, chemotherapy only, and/or re-irradiation for recurrent tumor; this might have influenced the OS. Because this study was retrospective, the incidence of treatment-related toxicities could be underestimated. However, the current study evaluated a large number of patients with OCSCC who received surgery followed by PORT, and determined the impact of concurrent chemotherapy. Because the EORTC 22931 and RTOG 9501 trials (6, 7) included a heterogeneous group of patients, including those with cancers of the oral cavity, oropharynx, larynx, or hypopharynx, prospective randomized controlled trials are needed for OCSCC. This study could be considered as a preliminary study for such trials. Until such trials have been reported, the recommendation based on the combined analysis of EORTC 22931 and RTOG 9501 still need to be followed (7).

In conclusion, our retrospective study showed that postoperative CCRT group had comparable survival outcomes to those in the RT alone group for advanced OCSCC in the era of modern RT techniques and indicated that concurrent chemotherapy should be administered to patients with ENE. Prospective randomized studies for confirmation are needed.

DATA AVAILABILITY STATEMENT

The raw data supporting the conclusions of this article will be made available by the authors, without undue reservation.

ETHICS STATEMENT

The studies involving human participants were reviewed and approved by IRB #4-2019-0401. The patients/participants provided their written informed consent to participate in this study.

AUTHOR CONTRIBUTIONS

This study was designed and directed by TK and CL. I-HC, EC, HRK, HJK, S-HK, and KK contributed to the data collection and analysis. The manuscript was written by TK and CL, and commented on by all authors. All authors contributed to the article and approved the submitted version.

REFERENCES

1. Kademani D. Oral cancer. *Mayo Clin Proc* (2007) 82(7):878–87. doi: 10.4065/82.7.878
2. Cancer Facts & Figures. (2019). American Cancer Society.
3. Ooishi M, Motegi A, Kawashima M, Arahira S, Zenda S, Nakamura N, et al. Patterns of failure after postoperative intensity-modulated radiotherapy for locally advanced and recurrent head and neck cancer. *Jpn J Clin Oncol* (2016) 46(10):919–27. doi: 10.1093/jjco/hyw095
4. Yao M, Chang K, Funk GF, Lu H, Tan H, Wacha J, et al. The failure patterns of oral cavity squamous cell carcinoma after intensity-modulated radiotherapy-the university of iowa experience. *Int J Radiat Oncol Biol Phys* (2007) 67(5):1332–41. doi: 10.1016/j.ijrobp.2006.11.030
5. Chan AK, Huang SH, Le LW, Yu E, Dawson LA, Kim JJ, et al. Postoperative intensity-modulated radiotherapy following surgery for oral cavity squamous cell carcinoma: patterns of failure. *Oral Oncol* (2013) 49(3):255–60. doi: 10.1016/j.oraloncology.2012.09.006
6. Cooper JS, Zhang Q, Pajak TF, Forastiere AA, Jacobs J, Saxman SB, et al. Long-term follow-up of the RTOG 9501/intergroup phase III trial: postoperative concurrent radiation therapy and chemotherapy in high-risk squamous cell carcinoma of the head and neck. *Int J Radiat Oncol Biol Phys* (2012) 84(5):1198–205. doi: 10.1016/j.ijrobp.2012.05.008
7. Bernier J, Cooper JS, Pajak TF, van Glabbeke M, Bourhis J, Forastiere A, et al. Defining risk levels in locally advanced head and neck cancers: a comparative analysis of concurrent postoperative radiation plus chemotherapy trials of the EORTC (#22931) and RTOG (# 9501). *Head Neck* (2005) 27(10):843–50. doi: 10.1002/hed.20279
8. Murthy V, Mallik S, Master Z, Sharma PK, Mahantshetty U, Shrivastava SK. Does helical tomotherapy improve dose conformity and normal tissue sparing compared to conventional IMRT? A dosimetric comparison in high risk prostate cancer. *Technol Cancer Res Treat* (2011) 10(2):179–85. doi: 10.7785/tcrt.2012.500193
9. Lee TF, Fang FM, Chao PJ, Su TJ, Wang LK, Leung SW. Dosimetric comparisons of helical tomotherapy and step-and-shoot intensity-modulated radiotherapy in nasopharyngeal carcinoma. *Radiother Oncol* (2008) 89(1):89–96. doi: 10.1016/j.radonc.2008.05.010
10. Hsieh CH, Shueng PW, Wang LY, Huang YC, Liao LJ, Lo WC, et al. Impact of postoperative daily image-guided intensity-modulated radiotherapy on overall and local progression-free survival in patients with oral cavity cancer. *BMC Cancer* (2016) 16:139. doi: 10.1186/s12885-016-2165-9
11. Owosho AA, Tsai CJ, Lee RS, Freymiller H, Kadempour A, Varthis S, et al. The prevalence and risk factors associated with osteoradionecrosis of the jaw in oral and oropharyngeal cancer patients treated with intensity-modulated radiation therapy (IMRT): The Memorial Sloan Kettering Cancer Center experience. *Oral Oncol* (2017) 64:44–51. doi: 10.1016/j.oraloncology.2016.11.015
12. Park S, Cho Y, Lee J, Koh YW, Kim SH, Choi EC, et al. Survival and Functional Outcome after Treatment for Primary Base of Tongue Cancer: A Comparison of Definitive Chemoradiotherapy versus Surgery Followed by Adjuvant Radiotherapy. *Cancer Res Treat* (2018) 50(4):1214–25. doi: 10.4143/crt.2017.498
13. Ling W, Mijiti A, Moming A. Survival pattern and prognostic factors of patients with squamous cell carcinoma of the tongue: a retrospective analysis of 210 cases. *J Oral Maxillofac Surg* (2013) 71(4):775–85. doi: 10.1016/j.joms.2012.09.026
14. Gupta P, Migliacci JC, Montero PH, Zanoni DK, Shah JP, Patel SG, et al. Do we need a different staging system for tongue and gingivobuccal complex squamous cell cancers? *Oral Oncol* (2018) 78:64–71. doi: 10.1016/j.oraloncology.2018.01.013
15. Nishi H, Shinozaki T, Tomioka T, Maruo T, Hayashi R. Squamous cell carcinoma of the retromolar trigone: Treatment outcomes. *Auris Nasus Larynx* (2018) 45(2):337–42. doi: 10.1016/j.anl.2017.05.011
16. Saggi S, Badran KW, Han AY, Kuan EC, St John MA. Clinicopathologic Characteristics and Survival Outcomes in Floor of Mouth Squamous Cell Carcinoma: A Population-Based Study. *Otolaryngol Head Neck Surg* (2018) 159(1):51–8. doi: 10.1177/0194599818756815

Conflict of Interest: The authors declare that the research was conducted in the absence of any commercial or financial relationships that could be construed as a potential conflict of interest.

frontiers in Oncology

ORIGINAL RESEARCH
published: 24 March 2021
doi: 10.3389/fonc.2021.626602

Deep Learning for Automatic Segmentation of Oral and Oropharyngeal Cancer Using Narrow Band Imaging: Preliminary Experience in a Clinical Perspective

Alberto Paderno[1], Cesare Piazza[1], Francesca Del Bon[1], Davide Lancini[1], Stefano Tanagli[1], Alberto Deganello[1], Giorgio Peretti[2], Elena De Momi[3], Ilaria Patrini[3], Michela Ruperti[3], Leonardo S. Mattos[4] and Sara Moccia[4,5,6]*

[1] Department of Otorhinolaryngology—Head and Neck Surgery, ASST—Spedali Civili of Brescia, University of Brescia, Brescia, Italy, [2] Department of Otorhinolaryngology—Head and Neck Surgery, IRCCS San Martino Hospital, University of Genoa, Genoa, Italy, [3] Department of Electronics, Information and Bioengineering, Politecnico di Milano, Milan, Italy, [4] Department of Advanced Robotics, Istituto Italiano di Tecnologia, Genoa, Italy, [5] The BioRobotics Institute, Scuola Superiore Sant'Anna, Pisa, Italy, [6] Department of Excellence in Robotics and AI, Scuola Superiore Sant'Anna, Pisa, Italy

OPEN ACCESS

Edited by:
Wojciech Golusiński, Poznan University of Medical Sciences, Poland

Reviewed by:
Remco De Bree, University Medical Center Utrecht, Netherlands
Giuseppe Mercante, Humanitas University, Italy

***Correspondence:**
Alberto Paderno
albpaderno@gmail.com

Specialty section:
This article was submitted to Head and Neck Cancer, a section of the journal Frontiers in Oncology

Received: *06 November 2020*
Accepted: *08 March 2021*
Published: *24 March 2021*

Citation:
Paderno A, Piazza C, Del Bon F, Lancini D, Tanagli S, Deganello A, Peretti G, De Momi E, Patrini I, Ruperti M, Mattos LS and Moccia S (2021) Deep Learning for Automatic Segmentation of Oral and Oropharyngeal Cancer Using Narrow Band Imaging: Preliminary Experience in a Clinical Perspective. Front. Oncol. 11:626602. doi: 10.3389/fonc.2021.626602

Introduction: Fully convoluted neural networks (FCNN) applied to video-analysis are of particular interest in the field of head and neck oncology, given that endoscopic examination is a crucial step in diagnosis, staging, and follow-up of patients affected by upper aero-digestive tract cancers. The aim of this study was to test FCNN-based methods for semantic segmentation of squamous cell carcinoma (SCC) of the oral cavity (OC) and oropharynx (OP).

Materials and Methods: Two datasets were retrieved from the institutional registry of a tertiary academic hospital analyzing 34 and 45 NBI endoscopic videos of OC and OP lesions, respectively. The dataset referring to the OC was composed of 110 frames, while 116 frames composed the OP dataset. Three FCNNs (U-Net, U-Net 3, and ResNet) were investigated to segment the neoplastic images. FCNNs performance was evaluated for each tested network and compared to the gold standard, represented by the manual annotation performed by expert clinicians.

Results: For FCNN-based segmentation of the OC dataset, the best results in terms of Dice Similarity Coefficient (Dsc) were achieved by ResNet with 5(×2) blocks and 16 filters, with a median value of 0.6559. In FCNN-based segmentation for the OP dataset, the best results in terms of Dsc were achieved by ResNet with 4(×2) blocks and 16 filters, with a median value of 0.7603. All tested FCNNs presented very high values of variance, leading to very low values of minima for all metrics evaluated.

Conclusions: FCNNs have promising potential in the analysis and segmentation of OC and OP video-endoscopic images. All tested FCNN architectures demonstrated satisfying outcomes in terms of diagnostic accuracy. The inference time of the processing networks

were particularly short, ranging between 14 and 115 ms, thus showing the possibility for real-time application.

Keywords: oral cancer, oropharyngeal cancer, segmentation, machine learning, neural network, deep learning, narrow band imaging

INTRODUCTION

Surgical data science (SDS) (1) is an emerging field of medicine aimed at extracting knowledge from medical data and providing objective measures to assist in diagnosis, clinical decision making, and prediction of treatment outcomes. In this context, image segmentation, an essential step in computer vision, can be defined as the task of partitioning an image into several non-intersecting coherent parts (2). It is also well known that segmentation is a prerequisite for autonomous diagnosis, as well as for various computer- and robot-aided interventions. Many methodologies have been proposed for image segmentation (3), but the most recent and successful approaches are based on fully convolutional neural networks (FCNNs), applying convolutional filters that learn hierarchical features from data (i.e., input images), and then collecting them in maps. In general, a high number of filters will give better results up to a certain point, when a further increase in their number either does not improve the segmentation performance, or deteriorates it (4).

FCNNs applied to video-analysis are of particular interest in the field of head and neck oncology, since endoscopic examination (and its storage in different ways and media) has always represented a crucial step in diagnosis, staging, and follow-up of patients affected by upper aero-digestive tract cancers. In this view, Narrow Band Imaging (NBI) represents an already consolidated improvement over conventional white light endoscopy, allowing for better and earlier identification of dysplastic/neoplastic mucosal alterations (5–8). However, so far, NBI-based endoscopy remains a highly operator-dependent procedure, and its standardization remains particularly challenging, even when employing simplified pattern classification schemes (9–14). In fact, even though such bioendoscopic tools are aimed at identifying pathognomonic superficial vascular changes in forms of abnormal intrapapillary capillary loops, a relatively long learning curve and intrinsic subjectivity of subtle visual evaluations still hamper their general and widespread adoption in daily clinical practice. Furthermore, subtle differences in NBI patterns according to the head and neck subsite to be analyzed have also been described. This is especially true considering the oral cavity (OC) in comparison with other upper aero-digestive tract sites (9).

The aim of this study was to test FCNN-based methods for semantic segmentation of early squamous cell carcinoma (SCC) in video-endoscopic images belonging to OC and oropharyngeal (OP) subsites to pave the way towards development of intelligent systems for automatic NBI video-endoscopic evaluations.

MATERIALS AND METHODS

This study was performed following the principles of the Declaration of Helsinki and approved by the Institutional Review Board, Ethics Committee of our academic hospital (Spedali Civili of Brescia, University of Brescia, Brescia, Italy). The workflow of the approach used is shown in **Figure 1**. In particular, informative NBI frames were selected from videos of OC and OP SCC through a case by case evaluation ("Original frames", **Figure 1**). Each frame was manually annotated by an expert clinician contouring the lesion margins, thus creating a mask referring to every frame ("Original mask", **Figure 1**). The original frames and masks were then employed to train the FCNNs in order to obtain an automatic tumor segmentation.

Mucosal Cancer Segmentation

Two datasets were retrieved from the institutional registry analyzing 34 and 45 NBI endoscopic videos of OC and OP, respectively. Each video was from a different patient affected by SCC, clinically presenting as a leuko- or erythroplastic lesion. Image acquisition was performed at the Department of Otorhinolaryngology – Head and Neck Surgery, ASST Spedali Civili, University of Brescia, Brescia, Italy between January 2010 and December 2018. Only video-endoscopies of biopsy-proven OC and OP SCC were included in the study. Patients with previous surgical and/or non-surgical treatments for tumors of these anatomical sites and frankly ulcerated neoplasms with significant loss of substance were excluded from the analysis.

All videos were acquired under white light and NBI by a rigid telescope coupled to an Evis Exera II HDTV camera connected to an Evis Exera II CLV-180B light source (Olympus Medical Systems Corporation, Tokyo, Japan). From the total amount of frames constituting the NBI videos, non-informative frames (i.e., blurred, out of focus, dark, or with signs of bleeding) were discarded through a case by case evaluation. After this selection process, the dataset referring to the OC was composed of 110 frames, while a total of 116 frames composed the OP dataset. **Table 1** shows the number of frames tested per patient for each dataset and the relative total amount of frames and patients involved. Each frame in these databases was manually annotated by an expert clinician contouring the lesion margins. The correspondent mean lesion size in percentage of pixels with respect to the entire frame size for each dataset is reported in **Table 2**.

Before segmenting the tumor area with FCNNs, the images underwent a cropping procedure to remove black borders. Given the different dimensions and shapes of extracted NBI video-frames, the cropping was customized for each of them. For memory constraints, frames were down-sampled to dimensions of 256×256 pixels to prevent exceeding the available GPU memory (~14858 MB). Prior to FCNN-based segmentation, images were standardized sample-wise, namely the image mean was removed from each image. Given the small size of the two datasets, data augmentation was performed to avoid

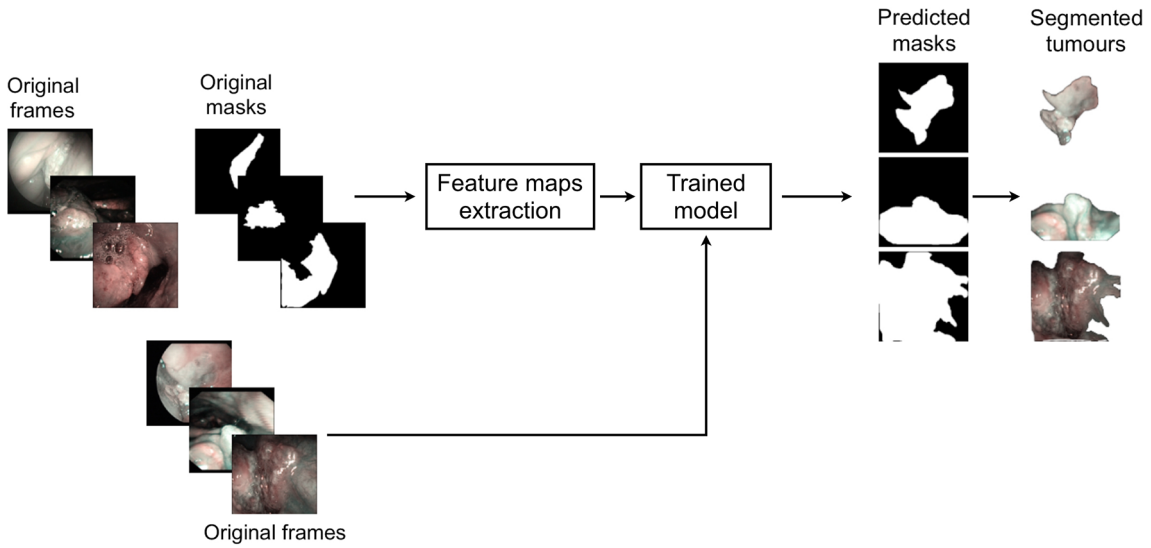

FIGURE 1 | Workflow of the approach used for detection of mucosal SCC in videoendoscopic frames by NBI.

TABLE 1 | Investigated datasets for mucosal SCC segmentation task and corresponding number of NBI videoframes per patient.

Oral cavity			
	No. patients	**No. frames per patient**	**No. frames**
	6	1	6
	26	2	52
	8	4	32
	5	4	20
Total	45		110
Oropharynx			
	No. patients	**No. frames per patient**	**No. frames**
	10	2	20
	8	3	24
	12	4	48
	4	6	24
Total	34		116

TABLE 2 | Investigated datasets for mucosal SCC segmentation task and corresponding amount of mean percentages of lesion pixels per frame and relative standard deviations.

Dataset	**Mean of lesion pixels in %**	**Standard deviation of lesion pixels in %**
Oral cavity	22.84	11.68
Oropharynx	38.04	18.54

overfitting and to increase the ability of the model to better generalize the results. Hence, the training set was augmented by ∼10 times at each cross-validation, imposing the following random transformations to the frames (and corresponding gold-standard masks obtained with manual segmentation): image rotation (random rotation degree in range 0°-90°), shift (random shift in range 0-10% of the frame side length for both width and height), zoom (with zoom values in range 0 and 1), and horizontal and vertical flip.

Three FCNNs were investigated to segment neoplastic images in OC and OP. The architectures tested were:

- U-Net, a fully convolutional U-shaped network architecture for biomedical image segmentation (15);
- U-Net 3, consisting of the previous deep network improved by Liciotti et al. (16) to work with very few training images and yield more precise segmentations;
- ResNet, composed of a sequence of residual units (17).

Technical Definitions

FCNNs are a type of artificial neural networks that have wide application in visual computing. Their deep hierarchical model roughly mimics the nature of mammalian visual cortex, making FCNNs the most promising architectures for image analysis. FCNNs present an input layer, an output layer, and a variable number of hidden layers, that transform the input image through the convolution with small filters, whose weights and biases are learned during a training procedure.

U-Net is a fully convolutional U-shaped neural networks that is especially suitable for biomedical images. The descending path U-Net is made of repeated 3x3 convolutions and max-pooling, for down-sampling the input image. This path acts as an encoder for feature extraction. The ascending path consists of 3x3 convolutions and up-sampling, for restoring the original input image size. This path acts as decoder for feature processing to achieve the segmentation. The encoder and decoder are linked to each other *via* long skip connections. U-Net3 is inspired by U-Net but introduces batch normalization, which makes the training process faster. ResNet is also divided in two parts: the descending and ascending

paths, each consisting of 5 blocks. Each block of the descending path is made of a convolutional sub-block and two identity sub-blocks, whereas in the ascending path there is one up-convolutional sub-block and two identity sub-blocks. The convolutional and identity sub-blocks follow the implementation of (17) and are made of convolution filters. In order to study the complexity of ResNet, in this work we also tested the performance of ResNet considering 1 block, 3 blocks, and 4 blocks per path. In each block, we kept the number of filters for each convolution equal to 16. We also investigated the ResNet with 1 block per path and 8 filters per convolution instead of 16: this represents the simplest model.

Data Analysis

FCNN performance was evaluated for each network tested and compared to the gold standard represented by manual annotation performed by expert clinicians. A contingency table considering true positive (TP), true negative (TN), false negative (FN), and false positive (FP) results was used. The overall accuracy (Acc) was calculated and defined as the ratio of the correctly segmented area by the algorithm over the annotated area by the expert examiner. The positive and negative samples refer to pixels within and outside the segmented region, respectively. Precision (Prec) was defined as the fraction of relevant instances among the retrieved ones (i.e., positive predictive value = true positives over true and false positives). Recall (Rec) was defined as the fraction of the total amount of relevant instances that were actually retrieved (i.e., true positive rate = true positives over true positives and false negatives). The Dice Similarity Coefficient (Dsc) was evaluated as overlapping measure. The Dsc is a statistical validation metric based on the spatial overlap between two sets of segmentations of the same anatomy. The value of Dsc ranges from 0, indicating no spatial overlap between two sets of binary segmentation results, to 1, indicating complete overlap. Tumor detection performance was evaluated by measuring the computational time required by each of the FCNN architectures investigated to perform automatic segmentation per frame.

Analysis of variance (Anova test) with a significance level of 0.05 was performed to check whether the averages of the computed metrics significantly differed from each other. When significant differences were found, a pairwise T-test for multiple comparisons of independent groups was performed.

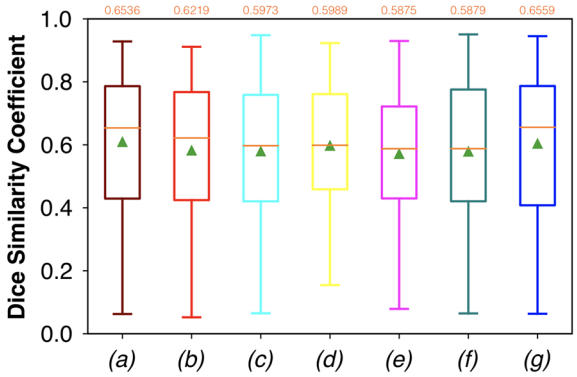

FIGURE 2 | Boxplots of Dsc for the OC dataset, obtained for (a) U-Net architecture, (b) U-Net 3, (c) ResNet with 4(×2) blocks and 16 filters, (d) ResNet with 1(×2) blocks and 8 filters, (e) ResNet with 1(×2) blocks and 16 filters, (f) ResNet with 3(×2) blocks and 16 filters, and (g) ResNet with 5(×2) blocks and 16 filters. Green triangles indicate the mean values, while the orange numbers at the top of each boxplot are the corresponding median values.

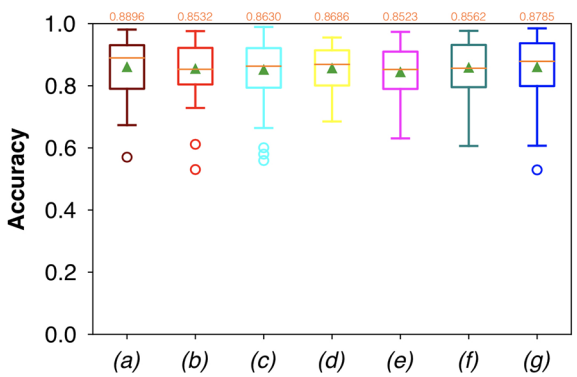

FIGURE 3 | Boxplots of Acc for the OC dataset, obtained for (a) U-Net architecture, (b) U-Net 3, (c) ResNet with 4(×2) blocks and 16 filters, (d) ResNet with 1(×2) blocks and 8 filters, (e) ResNet with 1(×2) blocks and 16 filters, (f) ResNet with 3(×2) blocks and 16 filters, and (g) ResNet with 5(×2) blocks and 16 filters. Green triangles indicate the mean values, while the orange numbers at the top of each boxplot are the corresponding median values.

RESULTS

Oral Cavity Dataset

For FCNN-based segmentation of the OC dataset, the best results in terms of Dsc were achieved by ResNet with 5(×2) blocks (5 for the descending and 5 for the ascending path) and 16 filters, with a median value of 0.6559, as reported in **Figure 2**. The comparison in terms of Acc in **Figure 3** for the tested FCNN architectures showed the best results in terms of median for the U-Net, with a value of 0.8896. Both the abovementioned architectures showed the best results in terms of other metrics. Specifically, ResNet with 5(×2) blocks and 16 filters appeared to be the best in terms of Rec, with a median value of 0.7545, as reported in **Figure 4**. U-Net, in contrast, showed the best result in terms of Prec, with a median value of 0.7079, as reported in **Figure 5**. All FCNNs tested presented very high values of variance, leading to very low values of minima for all metrics evaluated.

No significant difference was found when analyzing variance with the Anova test ($p>0.05$) to the Dsc, Acc, Rec, and Prec vectors constituted by the metrics of each architecture.

The computational times required by the FCNNs for the automated segmentation task for one image are reported in **Table 3**.

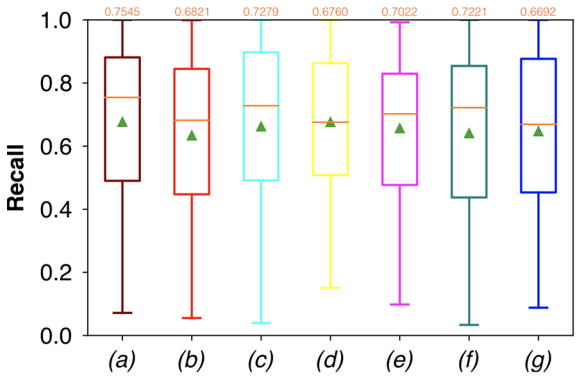

FIGURE 4 | Boxplots of Rec for the OC dataset, obtained for (a) U-Net architecture, (b) U-Net 3, (c) ResNet with 4(×2) blocks and 16 filters, (d) ResNet with 1(×2) blocks and 8 filters, (e) ResNet with 1(×2) blocks and 16 filters, (f) ResNet with 3(×2) blocks and 16 filters, and (g) ResNet with 5(×2) blocks and 16 filters. Green triangles indicate the mean values, while the orange numbers at the top of each boxplot are the corresponding median values.

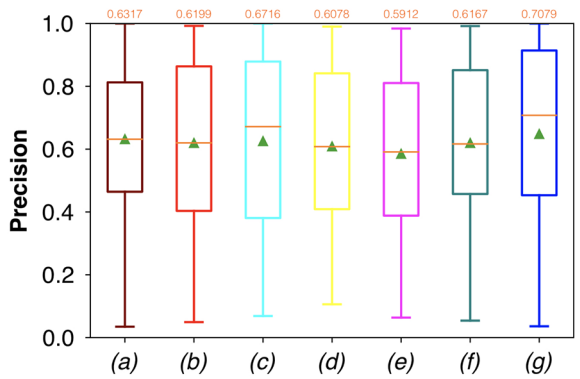

FIGURE 5 | Boxplots of Prec for the OC dataset, obtained for (a) U-Net architecture, (b) U-Net 3, (c) ResNet with 4(×2) blocks and 16 filters, (d) ResNet with 1(×2) blocks and 8 filters, (e) ResNet with 1(×2) blocks and 16 filters, (f) ResNet with 3(×2) blocks and 16 filters, and (g) ResNet with 5(×2) blocks and 16 filters. Green triangles indicate the mean values, while the orange numbers at the top of each boxplot are the corresponding median values.

It is worth noticing that less deep networks, such as ResNet with 1(×2) blocks and 8 filters, and ResNet with 1(×2) blocks and 16 filters, achieved automated segmentation in shorter times than the others. In particular, ResNet with 1(×2) blocks and 8 filters took only 14 ms to predict a single frame.

Oropharyngeal Dataset

Considering FCNN-based segmentation for the OP dataset, the best results in terms of Dsc were achieved by ResNet with 4(×2) blocks and 16 filters, with a median value of 0.7603, as reported in **Figure 6**. The comparison in terms of Acc in **Figure 7** for the FCNN architectures showed the best results in terms of median

TABLE 3 | Tested FCNNs and the corresponding times of inference for each single frame, expressed in milliseconds (ms).

FCNNs	Inference time per frame (ms)
U-Net	~115
U-Net 3	~96
ResNet with 4x2 blocks, 16 filters	~66
ResNet with 1x2 blocks, 8 filters	~14
ResNet with 1x2 blocks, 16 filters	~23
ResNet with 3x2 blocks, 16 filters	~59
ResNet with 5x2 blocks, 16 filters	~59

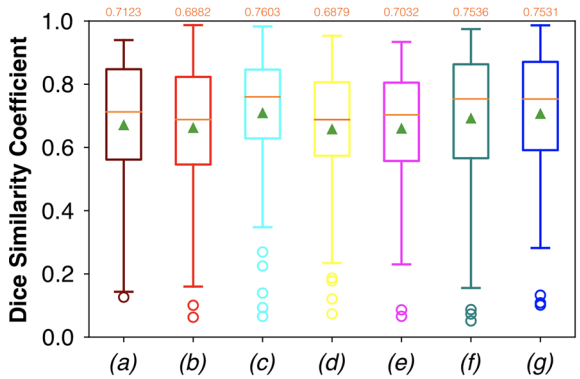

FIGURE 6 | Boxplots of Dsc for the OP dataset, obtained for (a) U-Net architecture, (b) U-Net 3, (c) ResNet with 4(×2) blocks and 16 filters, (d) ResNet with 1(×2) blocks and 8 filters, (e) ResNet with 1(×2) blocks and 16 filters, (f) ResNet with 3(×2) blocks and 16 filters, and (g) ResNet with 5(×2) blocks and 16 filters. Green triangles indicate the mean values, while the orange numbers at the top of each boxplot are the corresponding median values.

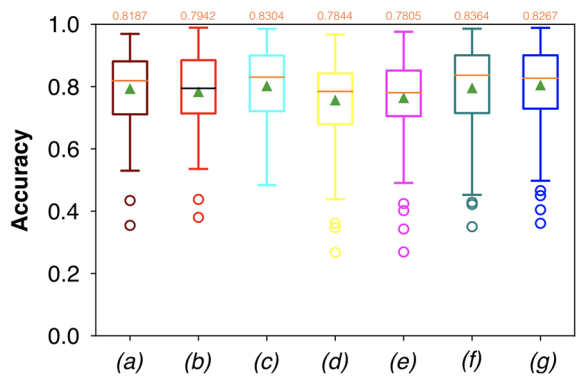

FIGURE 7 | Boxplots of Acc for the OP dataset, obtained for (a) U-Net architecture, (b) U-Net 3, (c) ResNet with 4(×2) blocks and 16 filters, (d) ResNet with 1(×2) blocks and 8 filters, (e) ResNet with 1(×2) blocks and 16 filters, (f) ResNet with 3(×2) blocks and 16 filters, and (g) ResNet with 5(×2) blocks and 16 filters. Green triangles indicate the mean values, while the orange numbers at the top of each boxplot are the corresponding median values.

for the ResNet with 3(×2) blocks and 16 filters, with a median value of 0.8364. Both the abovementioned architectures also showed the best results in terms of Rec, with a median value of 0.8560 for both, as reported in **Figure 8**.

Conversely, considering the comparison in terms of Prec in **Figure 9**, the best result was achieved with a deeper network, the ResNet with 5(×2) blocks and 16 filters. However, no significant difference was found when analyzing variance with the Anova test ($p>0.05$) to the Dsc vectors constituted by the Dsc of each architecture.

A significant difference among the available FCNNs was found applying the same test to the Rec vectors (**Figure 8**). A further investigation was performed using a pairwise T-test for multiple comparisons of independent groups that demonstrated a p value of 0.043 between U-Net 3 and ResNet with 1(×2) blocks and 8 filters, demonstrating that architectures with skip connections (i.e., all the architectures tested except for U-Net and U-Net 3) had greater performances in detecting mucosal sites affected by SCC.

Moreover, a significant difference among the various FCNNs was also found by applying the Anova test to the Prec vectors (**Figure 9**). A further investigation using a pairwise T-test for multiple comparisons of independent groups showed a p value of 0.0454 between ResNet with 5 (×2) blocks and 16 filters, and ResNet with 1(×2) blocks and 8 filters, demonstrating that deeper architectures were more precise in detecting SCC.

Samples of original frames, manual masks, and relative predicted masks for the OC and OP are shown in **Figures 10–12** in order to provide a visual input on the characteristics of correctly and incorrectly segmented tumors, and non-diagnostic cases.

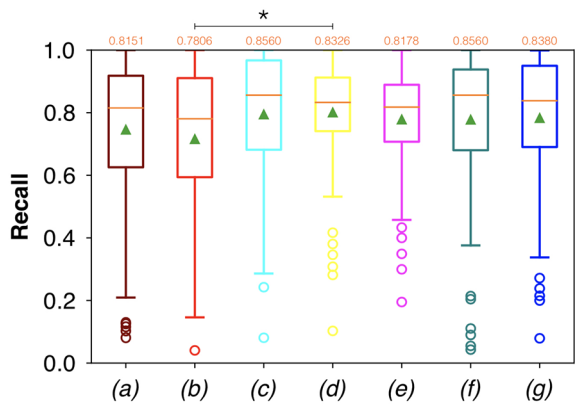

FIGURE 8 | Boxplots of Rec for the OP dataset, obtained for (a) U-Net architecture, (b) U-Net 3, (c) ResNet with 4(×2) blocks and 16 filters, (d) ResNet with 1(×2) blocks and 8 filters, (e) ResNet with 1(×2) blocks and 16 filters, (f) ResNet with 3(×2) blocks and 16 filters, and (g) ResNet with 5(×2) blocks and 16 filters. Green triangles indicate the mean values, while the orange numbers at the top of each boxplot are the corresponding median values. The star indicates a significant difference has been found (Anova test, $p<0.05$).

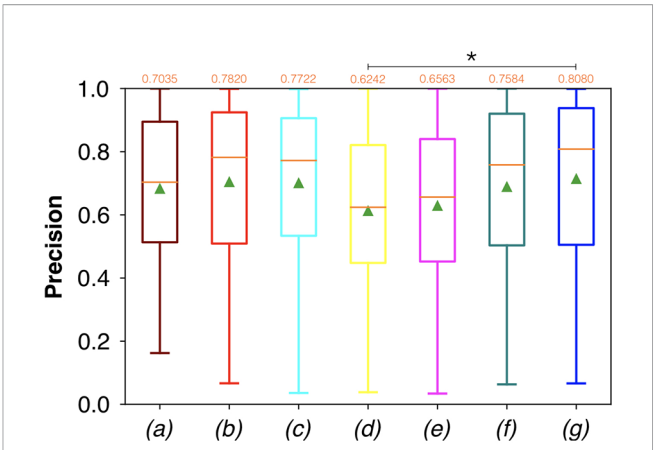

FIGURE 9 | Boxplots of Prec for the OP dataset, obtained for (a) U-Net architecture, (b) U-Net 3, (c) ResNet with 4(×2) blocks and 16 filters, (d) ResNet with 1(×2) blocks and 8 filters, (e) ResNet with 1(×2) blocks and 16 filters, (f) ResNet with 3(×2) blocks and 16 filters, and (g) ResNet with 5(×2) blocks and 16 filters. Green triangles indicate the mean values, while the orange numbers at the top of each boxplot are the corresponding median values. The star indicates a significant difference (Anova test, $p<0.05$).

DISCUSSION

This study presents a computer-aided method for segmentation of SCC through FCNN-based evaluation of NBI video-endoscopic frames afferent to two frequently involved upper aero-digestive tract sites (OC and OP), and evaluates its performance in distinguishing between neoplastic and healthy areas. The overall median Dsc for OC and OP frames of the best performing FCNN [ResNet with 1(×2) blocks and 8 filters] with the shortest time of inference (14 ms) were 0.5989 and 0.6879, respectively.

Of note, this was the first attempt to automatically segment SCC in complex anatomical regions from NBI video-frames. Considering the absence of deep-learning methods in the head and neck literature from which to draw inspiration, this early experience can be considered as a practical approach for segmentation of pathological areas in endoscopic videos, applicable in real time during routine clinical activities, given the short time of inference needed per frame.

Moreover, this approach demonstrates the value of SDS in OC/OP examination and could motivate more structured and regular data storage in the clinic. Indeed, large amounts of data would lead to the possibility of further exploring deep-learning-based algorithms for semantic segmentation, covering a more substantial variability of tissues classification scenarios. In addition, associating such diagnostic videos to subsequently obtained radiologic imaging, pathological specimens, and prognostic characteristics, could pave the way to data mining aimed at understanding adjunctive tumor features (e.g., HPV status, depth of infiltration, risk of regional/distant metastasis) by simple video-endoscopy (18).

In this field, few methodologies have been presented for automatic diagnosis of tumors of the upper aero-digestive tract. As in the present series, most were focused on

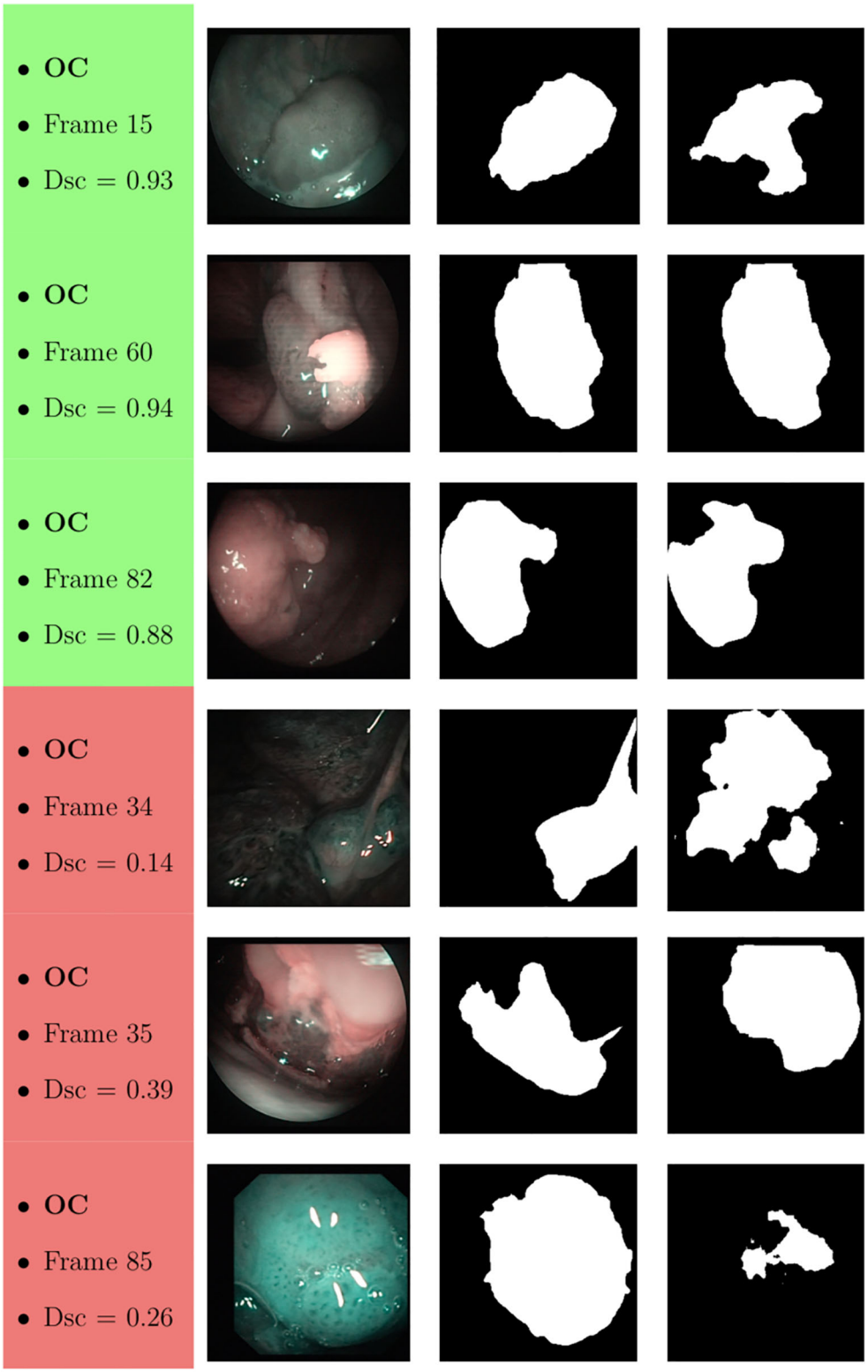

FIGURE 10 | Sample of original OC frames, manual masks, and relative predicted masks for ResNet with 5 (x2) blocks and 16 filters. The red and green boxes correspond to values of Dsc less than 45% (Dsc <0.45) and Dsc greater than 85% (Dsc >0.85), respectively.

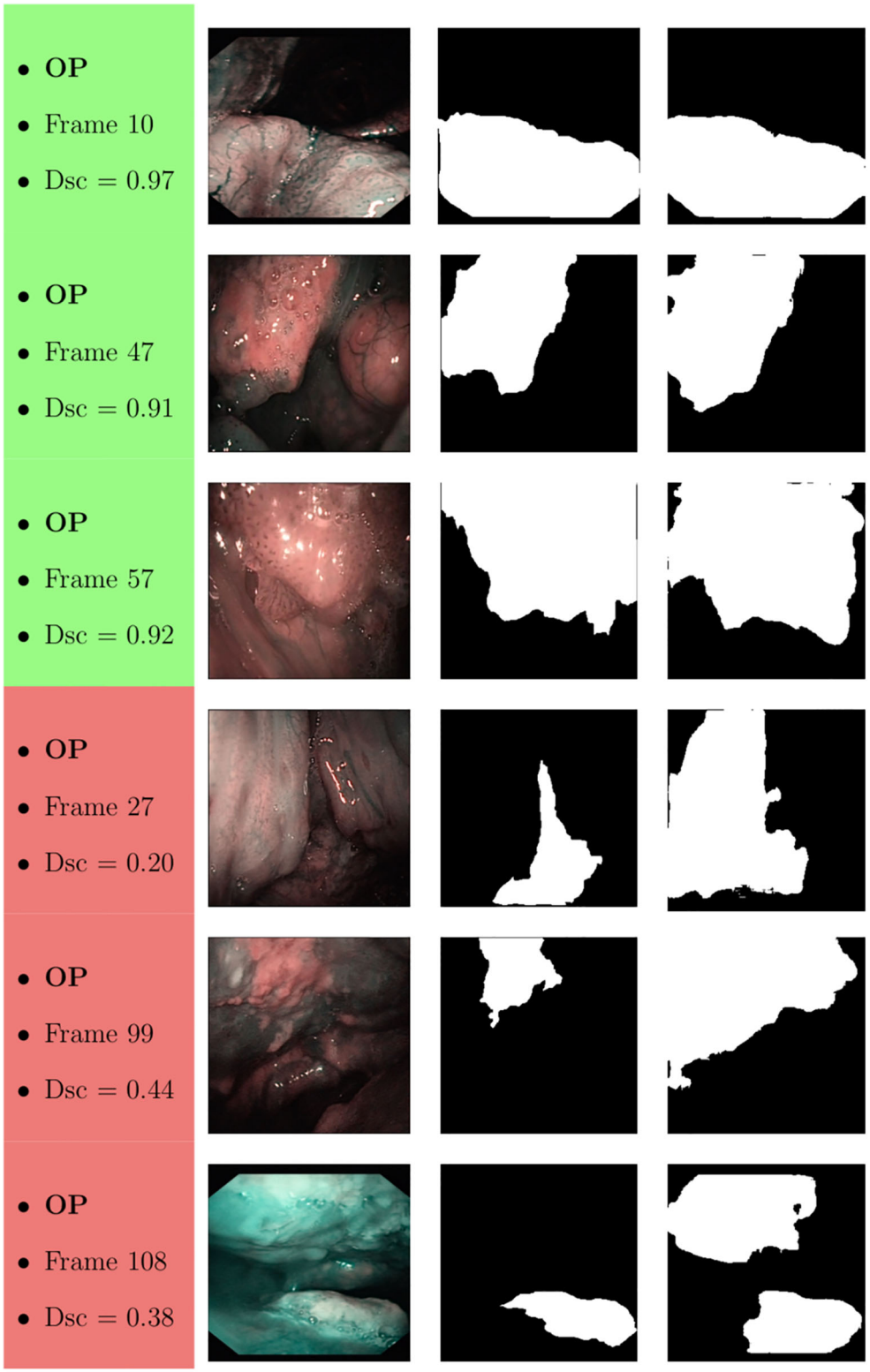

FIGURE 11 | Sample of original OP frames, manual masks, and relative predicted masks for ResNet with 4 (x2) blocks and 16 filters. The red and green boxes correspond to values of Dsc less than 45% (Dsc <0.45) and Dsc greater than 85% (Dsc >0.85), respectively.

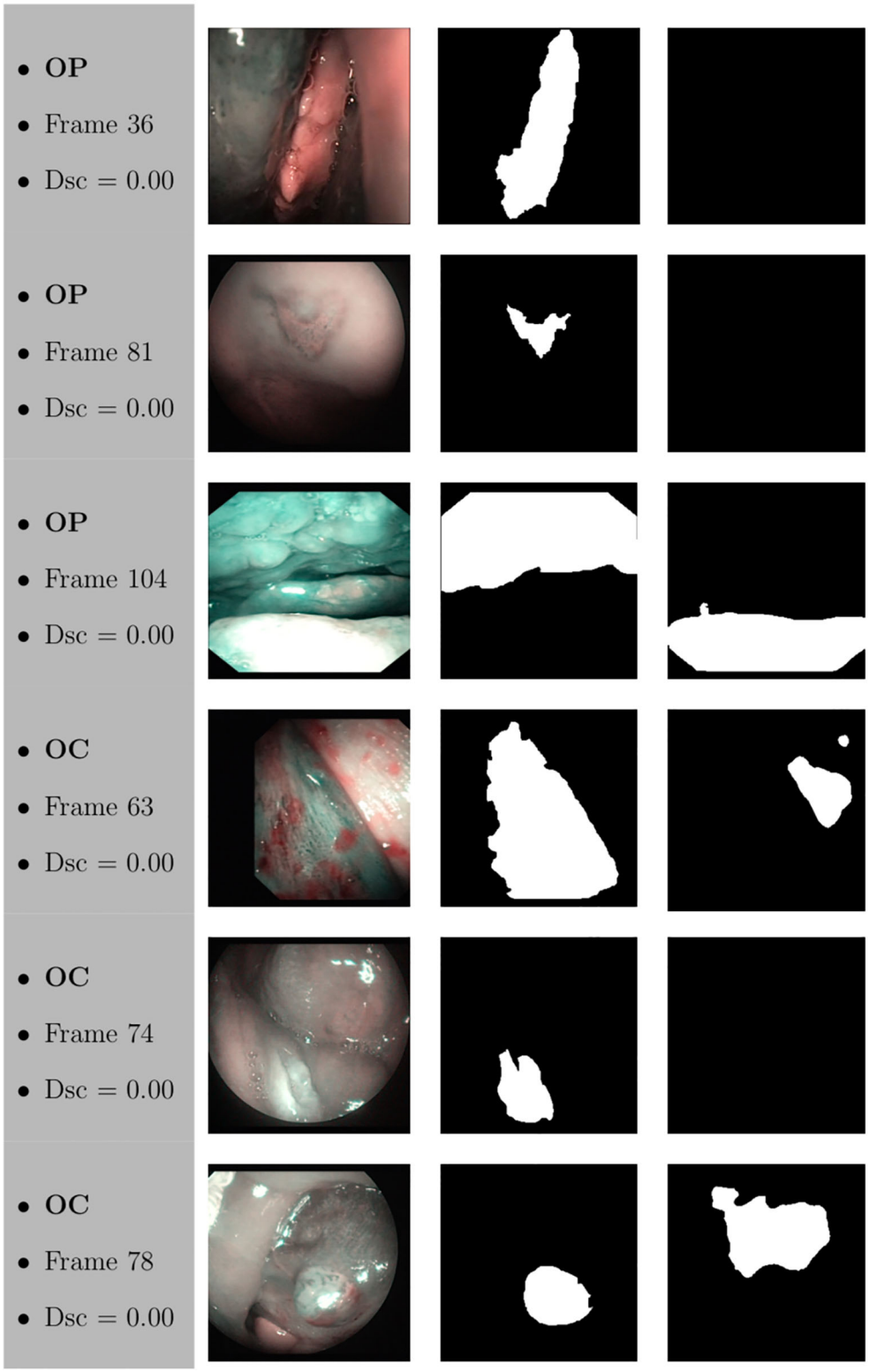

FIGURE 12 | Sample of original frames excluded from the boxplot comparisons due to their Dsc less than 5% (Dsc <0.05) assessed by ResNet with 4 (x2) blocks and 16 filters for OP frames, and ResNet with 5 (x2) blocks and 16 filters for OC frames. The manual masks and relative predicted masks are also reported.

optimizing the analysis by providing adjunctive features (e.g., NBI, autofluorescence) complementing those obtained by conventional white light endoscopy. Taking advantage of the value of autofluorescence in the OC, Song et al. (19) developed an automatic image classification using a smartphone-based system for OC lesions employing CNNs that evaluated dual-modality images (white light and autofluorescence). The final model reached an accuracy of 87%, sensitivity of 85%, and specificity of 89%.

Conversely, different approaches aimed at maximizing extraction of features focusing on tissue vascularization. Specifically, Barbalata et al. (20) proposed a method for automated laryngeal tumor detection based on post-processing of images. Laryngeal tumors were detected and subsequently classified, focusing on their abnormal intrapapillary capillary loops through anisotropic filtering and matched filter. This further reinforces the rationale of using NBI data for our analysis, since this light-filtering system better highlights blood vessels, thus increasing the quality and quantity of data to be analyzed in each image. This concept was also confirmed by Mascharak et al. (21) who took advantage of naïve Bayesian classifiers trained with low-level image features to automatically detect and quantitatively analyze OP SCC using NBI multispectral imaging. The authors showed a significant increase in diagnostic accuracy using NBI compared to conventional white light video-endoscopy.

Recent studies confirmed the potential of FCNNs in the automatic diagnosis of benign and malignant diseases of the upper aero-digestive tract (22–26), demonstrating an outstanding Acc, comparable with that of experienced physicians. However, these studies were only focused on tumor detection and did not include OC and anterior OP tumors since the examination was only based on transnasal/transoral flexible video-endoscopy. Furthermore, no attempt at segmentation of the precise tumor margins was made.

Considering segmentation and margin recognition tasks, a study by Laves et al. (3) put effort into using FCNN to segment a dataset of the human larynx. The dataset, consisting of 536 manually segmented endoscopic images obtained during transoral laser microsurgery, was tested in order to monitor the morphological changes and autonomously detect pathologies. The Intersection-over-Union metric reached 84.7%. To date, no attempt to a precise visual segmentation by FCNN has been described in the pertinent OC/OP cancer literature.

It should be underlined that our investigation is only a preliminary assessment of feasibility and future potential that could encourage collection of additional evidence and support more extensive studies. The datasets, in fact, were relatively small and partially patient-unbalanced, denoting their high variability. In particular, the OC dataset was composed of a relatively low number of frames in relation to its considerable anatomical complexity and variability of epithelia with different histological and NBI-associated features (27). Moreover, the mean percentage of lesion pixels in each frame was only 22.82 ± 11.68% (with respect to the 38.04 ± 18.54% of the OP dataset). Hence, the high values of Acc might be partially due to the small size of the OC lesions with respect to the entire size of each frame presented in the dataset. Finally, it is worth noticing that all FCNNs tested presented very high values of variance, leading to low values of minima. This is probably due to the difficult task related to the small size of datasets and the significant tissue variability in the regions analyzed. Additionally, OC and OP are characterized by very different endoscopic superficial appearances, with the richness in lymphoid tissue of the latter being one of the most prominent diagnostic obstacles when searching for small tumors of this site even by NBI (27). The lower overall accuracy of FCNNs in the OP observed in the present study may be a sign of such a potential confounding factor.

In general, the type of FCNN did not lead to radical differences in the diagnostic performance in both subsites (while some minor differences may be observed in the OP). The same holds true considering inference times, that were always in the range of "real-time detection" (between 14 and 115 ms). However, in the OP it was possible to observe a higher precision in deeper architectures, demonstrating that an added layer of complexity may improve diagnostic results. Still, deeper architectures were also those needing higher inference times, thus requiring more processing power, and potentially impacting on the aim of real-time segmentation. In this view, when dealing with automatic detection and segmentation of mucosal neoplastic lesions, it will be essential to find a balance between depth of the FCNN and time needed to detect lesions and delineate their margins.

At a subjective evaluation, all FCNNs tended to detect malignant areas where illumination was more prominent, usually in the middle of the picture (**Figures 10–12**). This factor hints at the importance of optimal and homogeneous illumination, which should be equally distributed throughout the visual field, and not directed only on its central portion. In fact, the operator usually centers the endoscopic image on the lesion to be identified, leading to a significant bias in automatic segmentation by FCNNs. The key role of illumination has also been emphasized by others (22, 23), even showing different diagnostic performances in relation to the types of endoscopic device employed (23). In this view, novel advances in the field of image analysis should be supported by a parallel technical evolution of endoscopes, especially in terms of homogeneous illumination, high definition, colors, and optimization of image clarity.

An adjunctive limitation of this type of studies is that the "ground truth" (i.e., the image segmentation defining true tumor margins) was defined through a single expert opinion. This issue is related to the current impossibility in creating a histopathologic image to be superimposed to the endoscopic view, defining tumor margins at a microscopic level. However, independent evaluations by multiple experts may lead to a more accurate definition of endoscopic tumor margins.

CONCLUSIONS

SDS has promising potential in the analysis and segmentation of OC and OP video-endoscopic images. All tested FCNN architectures demonstrated satisfying outcomes in terms of

Dsc, Acc, Rec, and Prec. However, further advances are needed to reach a diagnostic performance useful for clinical applicability. On the other hand, the inference time of the processing networks were particularly short, ranging between 14 and 115 ms, thus showing the possibility for real-time application. Future prospective studies, however, should take into account the number and quality of training images, optimizing these variables through accurate planning and data collection.

DATA AVAILABILITY STATEMENT

The raw data supporting the conclusions of this article will be made available by the authors, without undue reservation.

ETHICS STATEMENT

The studies involving human participants were reviewed and approved by Ethics Committee of Spedali Civili di Brescia, University of Brescia, Italy. Written informed consent for participation was not required for this study in accordance with the national legislation and the institutional requirements.

AUTHOR CONTRIBUTIONS

Study design: AP, SM. Manual segmentation: AP, ST. Revision of segmented images: AP, CP, FB, DL, AD, GP. Analysis: SM, EM, IP, MR. All authors contributed to the article and approved the submitted version.

REFERENCES

1. Maier-Hein L, Vedula SS, Speidel S, Navab N, Kikinis R, Park A, et al. Surgical data science for next-generation interventions. *Nat BioMed Eng* (2017) 1:691–6. doi: 10.1038/s41551-017-0132-7
2. Pal NR, Pal SK. A review on image segmentation techniques. *Pattern Recognit* (1993) 26:1277–94. doi: 10.1016/0031-3203(93)90135-J
3. Laves MH, Bicker J, Kahrs LA, Ortmaier T. A dataset of laryngeal endoscopic images with comparative study on convolution neural network-based semantic segmentation. *Int J Comput Assist Radiol Surg* (2019) 14:483–92. doi: 10.1007/s11548-018-01910-0
4. Cernazanu-Glavan C, Holban S. Segmentation of bone structure in X-ray images using convolutional neural network. *Adv Electr Comput Eng* (2013) 13:87–94. doi: 10.4316/AECE.2013.01015
5. Watanabe A, Taniguchi M, Tsujie H, Hosokawa M, Fujita M, Sasaki S. The value of narrow band imaging endoscope for early head and neck cancers. *Otolaryngol Head Neck Surg* (2008) 138:446–51. doi: 10.1016/j.otohns.2007.12.034
6. Piazza C, Dessouky O, Peretti G, Cocco D, De Benedetto L, Nicolai P. Narrow-band imaging: a new tool for evaluation of head and neck squamous cell carcinomas. Review of the literature. *Acta Otorhinolaryngol Ital* (2008) 28:49–54.
7. Piazza C, Bon FD, Peretti G, Nicolai P. 'Biologic endoscopy': optimization of upper aerodigestive tract cancer evaluation. *Curr Opin Otolaryngol Head Neck Surg* (2011) 19:67–76. doi: 10.1097/MOO.0b013e328344b3ed
8. Deganello A, Paderno A, Morello R, Fior M, Berretti G, Del Bon F, et al. Diagnostic Accuracy of Narrow Band Imaging in Patients with Oral Lichen Planus: A Prospective Study. *Laryngoscope* (2021) 131:E1156–61. doi: 10.1002/lary.29035
9. Takano JH, Yakushiji T, Kamiyama I, Nomura T, Katakura A, Takano N, et al. Detecting early oral cancer: narrowband imaging system observation of the oral mucosa microvasculature. *Int J Oral Maxillofac Surg* (2010) 39:208–13. doi: 10.1016/j.ijom.2010.01.007
10. Ni XG, He S, Xu ZG, Gao L, Lu N, Yuan Z, et al. Endoscopic diagnosis of laryngeal cancer and precancerous lesions by narrow band imaging. *J Laryngol Otol* (2011) 125:288–96. doi: 10.1017/S0022215110002033
11. Arens C, Piazza C, Andrea M, Dikkers FG, Tjon Pian Gi RE, Voigt-Zimmermann S, et al. Proposal for a descriptive guideline of vascular changes in lesions of the vocal folds by the committee on endoscopic laryngeal imaging of the European Laryngological Society. *Eur Arch Otorhinolaryngol* (2016) 273:1207–14. doi: 10.1007/s00405-015-3851-y
12. Bertino G, Cacciola S, Fernandes WBJr., Fernandes CM, Occhini A, Tinelli C, et al. Effectiveness of narrow band imaging in the detection of premalignant and malignant lesions of the larynx: validation of a new endoscopic clinical classification. *Head Neck* (2015) 37:215–22. doi: 10.1002/hed.23582
13. Ni XG, Wang GQ, Hu FY, Xu XM, Xu L, Liu XQ, et al. Clinical utility and effectiveness of a training programme in the application of a new classification of narrow-band imaging for vocal cord leukoplakia: A multicentre study. *Clin Otolaryngol* (2019) 44:729–35. doi: 10.1111/coa.13361
14. Ni XG, Zhu JQ, Zhang QQ, Zhang BG, Wang GQ. Diagnosis of vocal cord leukoplakia: The role of a novel narrow band imaging endoscopic classification. *Laryngoscope* (2019) 129:429–34. doi: 10.1002/lary.27346
15. Ronneberger O, Fischer P, Brox T. U-net: Convolutional networks for biomedical image segmentation. In: *International Conference on Medical image computing and computer-assisted intervention*. Berlin: Springer (2015). p. 234–41. doi: 10.1007/978-3-319-24574-4_28
16. Liciotti D, Paolanti M, Pietrini R, Frontoni E, Zingaretti P. Convolutional networks for semantic heads segmentation using top-view depth data in crowded environment. In: *2018 24th international conference on pattern recognition (ICPR)*. IEEE: New York (2018). p. 1384–9. doi: 10.1109/ICPR.2018.8545397
17. He K, Zhang X, Ren S, Sun J. Deep residual learning for image recognition, in: *Proceedings of the IEEE conference on computer vision and pattern recognition*. New York: IEEE (2016) pp. 770–8. doi: 10.1109/CVPR.2016.90
18. Paderno A, Holsinger FC, Piazza C. Videomics: bringing deep learning to diagnostic endoscopy. *Curr Opin Otolaryngol Head Neck Surg* (2021). doi: 10.1097/MOO.0000000000000697
19. Song B, Sunny S, Uthoff RD, Patrick S, Suresh A, Kolur T, et al. Automatic classification of dual-modalilty, smartphone-based oral dysplasia and malignancy images using deep learning. *BioMed Opt Express* (2018) 9:5318–29. doi: 10.1364/BOE.9.005318
20. Barbalata C, Mattos LS. Laryngeal Tumor Detection and Classification in Endoscopic Video. *IEEE J BioMed Health Inform* (2016) 20:322–32. doi: 10.1109/JBHI.2014.2374975
21. Mascharak S, Baird BJ, Holsinger FC. Detecting oropharyngeal carcinoma using multispectral, narrow-band imaging and machine learning. *Laryngoscope* (2018) 128:2514–20. doi: 10.1002/lary.27159
22. Ren J, Jing X, Wang J, Ren X, Xu Y, Yang Q, et al. Automatic Recognition of Laryngoscopic Images Using a Deep-Learning Technique. *Laryngoscope* (2020) 130:E686–93. doi: 10.1002/lary.28539
23. Inaba A, Hori K, Yoda Y, Ikematsu H, Takano H, Matsuzaki H, et al. Artificial intelligence system for detecting superficial laryngopharyngeal cancer with high efficiency of deep learning. *Head Neck* (2020) 42:2581–92. doi: 10.1002/hed.26313
24. Kono M, Ishihara R, Kato Y, Miyake M, Shoji A, Inoue T, et al. Diagnosis of pharyngeal cancer on endoscopic video images by Mask region-based convolutional neural network. *Dig Endosc* (2020). doi: 10.1111/den.13800
25. Abe S, Oda I. Real-time pharyngeal cancer detection utilizing artificial intelligence: Journey from the proof of concept to the clinical use. *Dig Endosc* (2020). doi: 10.1111/den.13833
26. Tamashiro A, Yoshio T, Ishiyama A, Tsuchida T, Hijikata K, Yoshimizu S, et al. Artificial intelligence-based detection of pharyngeal cancer using convolutional neural networks. *Dig Endosc* (2020). doi: 10.1111/den.13653

27. Piazza C, Del Bon F, Paderno A, Grazioli P, Perotti P, Barbieri D, et al. The diagnostic value of narrow band imaging in different oral and oropharyngeal subsites. *Eur Arch Otorhinolaryngol* (2016) 273:3347–53. doi: 10.1007/s00405-016-3925-5

Conflict of Interest: The authors declare that the research was conducted in the absence of any commercial or financial relationships that could be construed as a potential conflict of interest.

frontiers in Oncology

REVIEW
published: 30 March 2021
doi: 10.3389/fonc.2021.628297

Performance of Intraoperative Assessment of Resection Margins in Oral Cancer Surgery: A Review of Literature

Elisa M. Barroso[1,2], Yassine Aaboubout[1,3], Lisette C. van der Sar[1], Hetty Mast[2], Aniel Sewnaik[3], Jose A. Hardillo[3], Ivo ten Hove[4], Maria R. Nunes Soares[1,5], Lars Ottevanger[1,5], Tom C. Bakker Schut[5], Gerwin J. Puppels[5†] and Senada Koljenović[1†]*

[1] Department of Pathology, Erasmus MC, University Medical Center Rotterdam, Rotterdam, Netherlands, [2] Department of Oral and Maxillofacial Surgery, Erasmus MC, University Medical Center Rotterdam, Rotterdam, Netherlands, [3] Department of Otorhinolaryngology and Head and Neck Surgery, Erasmus MC, University Medical Center Rotterdam, Rotterdam, Netherlands, [4] Department of Oral and Maxillofacial Surgery, Leiden UMC, Leiden University Medical Center, Leiden, Netherlands, [5] Department of Dermatology, Erasmus MC, University Medical Center Rotterdam, Rotterdam, Netherlands

OPEN ACCESS

Edited by:
Alberto Paderno, University of Brescia, Italy

Reviewed by:
Rasha Abu Eid, University of Aberdeen, United Kingdom
Pawel Golusinski, University of Zielona Góra, Poland

***Correspondence:**
Senada Koljenović
s.koljenovic@erasmusmc.nl

[†]*These authors share last authorship*

Specialty section:
This article was submitted to Head and Neck Cancer, a section of the journal Frontiers in Oncology

Received: *11 November 2020*
Accepted: *15 March 2021*
Published: *30 March 2021*

Citation:
Barroso EM, Aaboubout Y, van der Sar LC, Mast H, Sewnaik A, Hardillo JA, ten Hove I, Nunes Soares MR, Ottevanger L, Bakker Schut TC, Puppels GJ and Koljenović S (2021) Performance of Intraoperative Assessment of Resection Margins in Oral Cancer Surgery: A Review of Literature. Front. Oncol. 11:628297. doi: 10.3389/fonc.2021.628297

Introduction: Achieving adequate resection margins during oral cancer surgery is important to improve patient prognosis. Surgeons have the delicate task of achieving an adequate resection and safeguarding satisfactory remaining function and acceptable physical appearance, while relying on visual inspection, palpation, and preoperative imaging. Intraoperative assessment of resection margins (IOARM) is a multidisciplinary effort, which can guide towards adequate resections. Different forms of IOARM are currently used, but it is unknown how accurate these methods are in predicting margin status. Therefore, this review aims to investigate: 1) the IOARM methods currently used during oral cancer surgery, 2) their performance, and 3) their clinical relevance.

Methods: A literature search was performed in the following databases: Embase, Medline, Web of Science Core Collection, Cochrane Central Register of Controlled Trials, and Google Scholar (from inception to January 23, 2020). IOARM performance was assessed in terms of accuracy, sensitivity, and specificity in predicting margin status, and the reduction of inadequate margins. Clinical relevance (i.e., overall survival, local recurrence, regional recurrence, local recurrence-free survival, disease-specific survival, adjuvant therapy) was recorded if available.

Results: Eighteen studies were included in the review, of which 10 for soft tissue and 8 for bone. For soft tissue, defect-driven IOARM-studies showed the average accuracy, sensitivity, and specificity of 90.9%, 47.6%, and 84.4%, and specimen-driven IOARM-studies showed, 91.5%, 68.4%, and 96.7%, respectively. For bone, specimen-driven IOARM-studies performed better than defect-driven, with an average accuracy, sensitivity, and specificity of 96.6%, 81.8%, and 98%, respectively. For both, soft tissue and bone, IOARM positively impacts patient outcome.

Conclusion: IOARM improves margin-status, especially the specimen-driven IOARM has higher performance compared to defect-driven IOARM. However, this conclusion is limited by the low number of studies reporting performance results for defect-driven IOARM. The current methods suffer from inherent disadvantages, namely their subjective character and the fact that only a small part of the resection surface can be assessed in a short time span, causing sampling errors. Therefore, a solution should be sought in the field of objective techniques that can rapidly assess the whole resection surface.

Keywords: oral cancer, squamous cell carcinoma, margin status, intraoperative assessment (IOA), specimen-driven, defect-driven, soft tissue, bone tissue

INTRODUCTION

Every year, around 350,000 new patients are diagnosed worldwide with oral cavity cancer. Oral cavity squamous cell carcinoma (OCSCC) is the most prevalent oral cavity cancer type. The worldwide mortality rate is 175,000 per year and the 5-year overall survival is 64.8% (1–4).

Surgery is the primary treatment for OCSCC. The goal of surgery is the complete resection of the tumor with an adequate resection margin (i.e., the shortest distance between the tumor border and the resection surface is > 5 mm) while preserving as much healthy tissue as possible to minimize the loss of function (such as, mastication and swallowing) and facial disfigurement. The resection margin is an important predictor for patient outcome and is the only oncological prognostic factor that pathologists and surgeons can influence (5–7).

For soft tissue, according to the Royal College of Pathologist (RCP), the resection margin is classified as clear when it is more than 5 mm, close when it is 1 to 5 mm, and positive when it is less than 1 mm (8). Clear margins are regarded as adequate, whereas close and positive margins are regarded as inadequate. For bone, the RCP indicates that a resection is adequate when the bone resection surfaces are cancer-negative (5).

It has been proven that inadequate resection margins in soft tissue result in a need for adjuvant therapy (re-excision or post-operative (chemo-) radiotherapy) (8). Adjuvant therapy brings an additional burden for the patient and results in increased morbidity and reduced quality of life (9). Furthermore, inadequate resection margins in soft tissue have a significantly negative effect (almost two fold reduction) on overall survival and disease-free survival (5, 7, 10). Patients with positive bone margins have a twofold reduction of disease-free and overall survival compared to patients with adequate bone margins (11–13).

However, achieving adequate resection margins in the oral cavity is often difficult due to its complex anatomy. During the operation the surgeon relies on pre-operative imaging, visual inspection and palpation.

Recent studies have shown that adequate margins are only achieved in a minority (15% - 26%) of the cases of soft tissue OCSCC (5, 7, 10). Segmental mandible resections have shown considerable improvement over the last years (0% - 14.6% positive bone margins). However, marginal mandible resections and partial maxillectomies still show a high rate of positive bone margins (16% - 35.7% and 44% - 60%, respectively) (11, 13–16).

These results indicate that visual inspection, palpation, and preoperative imaging do not warrant adequate tumor resection. Besides, the final margin status is only known a few days (soft tissue) or weeks (bone) after surgery. If at that point an inadequate margin is encountered, a second surgery is not an option, nor effective, because an accurate relocation of the site of an inadequate margin is almost impossible in most cases (6).

Furthermore, in the case of bone resections, an immediate bone reconstruction is performed (often with a free flap) to limit the loss of continuity and the adverse effects on function and aesthetics, making the second surgery undesirable.

Therefore, for optimal control of resection margins, the surgeon needs additional information during surgery. Intraoperative assessment of resection margins (IOARM) can provide this valuable information, enabling revision of margins (additional tissue resection) during the initial surgery to turn an inadequate resection into an adequate resection (6).

Two methods for soft tissue IOARM can be distinguished: the traditional defect-driven method and the specimen-driven method.

According to a 2005 survey, around 76% of the surgeons perform defect-driven IOARM, while only 14% perform specimen-driven IOARM during OCSCC surgery (17). However, the evidence that specimen-driven IOARM is superior to defect-driven IOARM is growing (5, 18–21). Therefore, the American Joint Committee on Cancer (AJCC) has recommended specimen-driven IOARM as the standard of care since 2017 (22).

In the traditional defect-driven approach, the surgeon samples one or more suspicious pieces of tissue from the wound bed for analysis by frozen section (FS) (i.e., a tissue sample that has been quick-frozen, cut by a microtome, and stained immediately for rapid microscopic diagnosis). The major disadvantage of defect-driven IOARM is that it can only indicate

Abbreviations: IOARM, Intraoperative assessment of resection margins; OCSCC, Oral cavity squamous cell carcinoma; SCC, Squamous cell carcinoma; FS, Frozen sections; RCP, Royal College of Pathologists; AJCC, American Joint Committee on Cancer; M, Male; F, Female; TNM, Tumor, lymph nodes, metastasis (according to the TNM Classification of Malignant Tumors); Acc., Accuracy; Sens.. Sensitivity; Spec., Specificity; PPV, Positive predictive value; NPV, Negative predictive value; OS, Overall Survival; DSS, Disease-specific survival; LR, Local recurrence; RT, Radiotherapy.

the presence of a tumor-positive margin and it cannot provide the exact margin value in millimeters. In the recently recommended specimen-driven method, the margins are assessed on the specimen by visual inspection and palpation followed by perpendicular incisions with or without sampling of tissue for FS examination (6). This approach provides immediate feedback on whether an additional resection is needed.

Here we review the performance of IOARM methods used during OCSCC surgery in predicting margin-status. The impact on patient outcome was assessed with respect to overall survival, disease-specific survival, local recurrence and the need for adjuvant therapy.

MATERIALS AND METHODS

Search Strategy

A search was conducted in the following databases: Embase, Medline, Web of Science Core Collection, Cochrane Central Register of Controlled Trials, and Google Scholar. The following keywords and synonyms were used in the search filter: "oral cavity squamous cell carcinoma", "resection margin" and "intraoperative". Only studies written in English from inception of the database to the 23rd of January 2020 were considered.

The studies were first assessed for eligibility based on the title and abstract. The following inclusion criteria were used: 1) the majority (> 90%) of the patients were surgically treated for OCSCC and 2) the performance of an IOARM method was investigated. The following exclusion criteria used were: 1) the study did not follow the resection margin definition of the RCP, 2) the study comprised a non-human population; 3) the study is a review, a commentary or a letter to the editor. The full text of studies that met the previous criteria was screened to extract and analyze the data.

Data Analysis

Data Extraction

The included studies were divided based on the type of tissue assessed: soft tissue (group 1), and bone tissue (group 2).

The following patient and tumor characteristics were extracted independently by 3 researchers, when available: number of patients, male/female ratio (M/F), mean/median age (years), anatomical subsite, pathological TNM (pTNM) classification, and percentage of patients treated for primary disease. Type of IOARM was extracted from each of the included studies. The following IOARM performance variables were collected: true positives, true negatives, false positives, false negatives, accuracy (Acc.), sensitivity (Sens.), specificity (Spec.), positive predictive value (PPV) and negative predictive value (NPV). IOARM impact on patient outcome (e.g., overall survival (OS), disease-specific survival (DSS), local recurrence (LR) and the need for adjuvant therapy) was also collected.

Analysis of IOARM Performance and Impact on Patient Outcome

Based on the extracted data, IOARM sampling and interpretation errors (a), and the reduction in inadequate resections (b) were calculated.

Sampling and Interpretation Errors

Two types of error can occur during IOARM: sampling error (SE) and interpretation error (IE).

SE is the proportion of inadequate resections that are not identified during IOARM. It occurs due to non-representative sampling of tissue resulting in underestimation of inadequate margins (e.g., tissue is sampled from two suspicious regions but final histopathology indicates that there is a close margin in a region not regarded as suspicious during IOARM).

Interpretation error refers to incorrect diagnosis of the sampled tissue, resulting in under or overestimation of inadequate margins during IOARM.

Reduction of Inadequate Resections

The reduction in the number of inadequate resections (IR) based on IOARM was calculated using

$$Reduction\ IR(\%) = \left(\frac{IR_i - IRL_{Rev}}{IR_i}\right) \times 100$$

where:

IR_i is the number of initially inadequate resections, without revision (additional resection);

IR_{Rev} is the number of inadequate resections after revision.

RESULTS

A total of 1265 records were found in the different databases. After removing duplicates, 699 remained and were screened on title and abstract, see **Figure 1**. This resulted in exclusion of 626 records based on the criteria applied. Of the remaining 43 records, the full text was screened resulting in further exclusion of 25 records based on the criteria of this study, as mentioned above.

Group 1 – IOARM in Soft Tissue

Ten studies investigated the performance of IOARM methods in soft tissue (19, 23–31). The patients and tumor characteristics of the studies are shown in **Table 1**.

The description of the IOARM methods and their performance in the studies included are shown in **Table 2**.

The non-weighted average performance parameters for both methods were calculated over all studies that reported the necessary information (**Table 3**).

For the specimen-driven method the reduction of inadequate resections after revision was 47.1%, based on the report of 5 studies (23, 25, 26, 28, 30). For the defect-driven method, one study has reported that the reduction in inadequate resections amounted 51.3% (27).

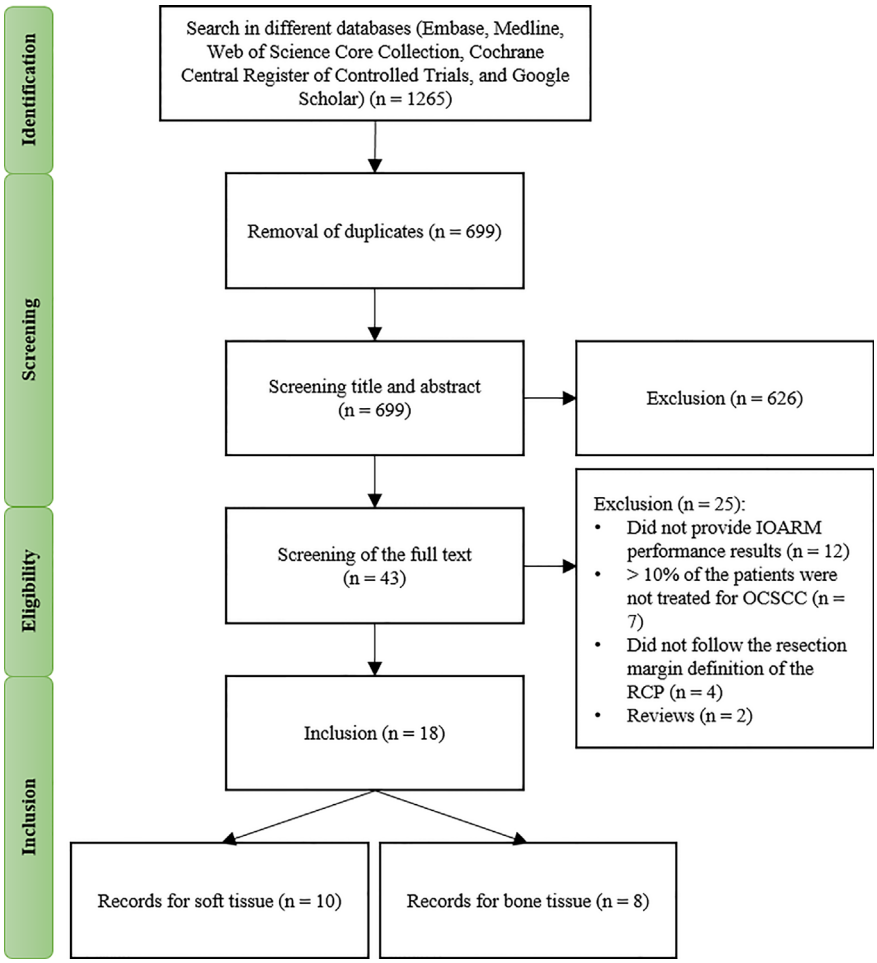

FIGURE 1 | Flow diagram of the study selection process.

IOARM Impact on Patient Outcome

Overall Survival

One study reported that at 5 years follow-up there was no significant difference between defect-driven IOARM and no IOARM (p=0.836) (24). None of the other studies reported on OS.

Disease-Specific Survival

Pathak et al. showed that at 5 years follow-up there was no significant difference between defect-driven IOARM and no IOARM (24). None of the other studies reported on DSS.

Local Recurrence

Three studies reported results on LR (24, 27, 28). Two studies used defect-driven IOARM and one study used specimen-driven IOARM. For defect-driven LR of 14.4% (after 180 months of follow-up) and 23% (after 60 months of follow-up) were shown. For specimen-driven LR of 7.3% (after 14 months of follow-up) was shown (24, 27, 28). From the 3 articles reporting LR, only Pathak et al. compares the defect-driven IOARM group (supported by FS) with a control group without IOARM (22). They showed that the IOARM group had 20.1% of primary failure rate (i.e. LR), while the control group had 25.2% of primary failure rate.

Adjuvant Therapy

Two studies have described the influence of IOARM on the need for adjuvant therapy (19, 30). Datta et al. showed that there was no significant reduction in the need for adjuvant therapy when comparing two groups of patients, patients treated with IOARM vs patients that did not receive IOARM (30). Amit et al. reported that from all patients that underwent defect-driven IOARM 35% required adjuvant therapy. In the specimen-driven IOARM group 8% required adjuvant therapy (19).

Group 2 – IOARM in Bone Tissue

Eight studies investigated the performance of IOARM on bone tissue (11, 12, 32–37). The patients and tumor characteristics are shown in **Table 4**.

The description of the IOARM methods and their performance are shown in **Table 5**.

TABLE 1 | IOARM in soft tissue: patients and tumor characteristics.

Author	Patients (N) (inclusion period)	M/F (%)	Mean age (y)	Tumor characteristics			
				Subsite(s) (%)	pT1/pT2/pT3/pT4 (%) pN0/pN1/pN2/pN3 (%)	Prior therapy (%)	Primary disease (%)
Ord (23)	49.0 (-)	65.0/ 35.0	–	Oral cavity (100.0)	30.6/16.3/14.4/38.7 -/-/-/-	0.0	–
Pathak (24)	416.0 (1973-2003)	58.0/ 42.0	64.0	Floor of the mouth (42.8); Tongue (27.6); Gingiva/Alveolus (12.0); Buccal (8.2); Retromolar trigone (1.9); Hard palate (1.2)	30.8/40.1/10.3/18.8 73.3/15.9/9.9/0.5	0.0	–
Chaturvedi (31)	877.0 (2007-2010)	73.0/ 27.0	48.0	Tongue (100.0)	18.0/45.0/18.0/19.0 65.7/19.8/14.0/0.5	0.0	100.0
Chaturvedi (25)	141.0 (2011-2012)	–	–	Tongue (42.2); Buccal (42.2); Lower and upper alveolus (5.7); Hard palate (2.2); Floor of the mouth (0.7); Lip (0.7); Larynx (2.8); Hypopharynx (3.5)	14.7/26.6/9.1/49.7 -/-/-/-	3.5^{CT} 14.2^{S}	85.8
Ettl (26)	156.0 (2004-2012)	72.0/ 28.0	59.0	Tongue (16.0); Floor of the mouth (45.0); Cheek (7.0); Maxilla and palate (8.0); Larynx/pharynx (8.0); Alveolus (14.0)	35.3/32.0/5.8/26.9 57.0/14.1/28.9/0.0	0.0	100.0
Buchakjian (27)	406.0 (2005-2014)	58.0/ 42.0	61.0	Tongue (45.0); Lower and upper alveolus (20.0); Floor of mouth (18.0); Other (17.0)	45.0/21.0/4.0/30.0 71/10.0/19.0/<1.0	–	100.0
Amit (19)	51.0 (2011-2014)	61.0/ 39.0	59.0	Tongue (49.0); Lip (16.0); Floor of the mouth (9.0); Hard palate (5.0); Buccal (9.0); Mandible (12.0)	29.0/34.0/28.0/9.0 -/-/-/-	0.0	–
	20.0 (2011–2014)	60.0/ 40.0	70.0	Tongue (40.0); Lip (15.0); Floor of the mouth (10.0); Hard palate (5.0); Buccal (15.0); Mandible (15.0)	25.0/35.0/30.0/10.0 -/-/-/-		
Mair (28)	435.0 (2014-2015)	65.0/ 35.0	–	Tongue (28.5); Floor of mouth (1.0); Buccal (48.5); Lower and upper alveolus (18.2); Retromolar trigone (2.1); Lower lip (1.4)	55.9*/44.1** 42.5$^{\#}$/57.5$^{\#\#}$	3.7^{CT} 3.2^{RT} 3.7^{S}	96.3
Abbas (29)	77.0 (2010-2014)	58.0/ 42.0	49.0	Tongue (38.0); Cheek (37.0); Palate (8.0); Other (17.0)	–	0.0	–
Datta (30)	1237.0 (2012-2013)	–	–	Gingivobuccal complex (56.0); Tongue & floor of mouth (36.0); Lip (5.0); Hard palate & upper alveolus (3.0)	–	5.4^{CT} 9.7^{S}	90.3

Percentage of pT1 and pT2.
**Percentage of pT3 and pT4.*
$^{\#}$*Percentage of pN-.*
$^{\#\#}$*Percentage of pN+.*
^{CT}*Percentage of patients treated with neoadjuvant chemotherapy.*
^{RT}*Percentage of patients treated with radiation therapy prior to surgery.*
^{S}*Percentage of patients treated with secondary surgery.*

The non-weighted average performance parameters for both methods were calculated over all studies that reported the necessary information (**Table 6**).

For the specimen-driven method the reduction of inadequate resections after revision was 78.4%, based on the report of 4 studies (11, 32, 35, 36). For the defect-driven method, one study has reported that the reduction in inadequate resections amounted 33% (37).

IOARM Impact on Patient Outcome

Overall Survival

Nieberler et al. demonstrated that at 3 years follow-up OS was higher for patients treated with specimen-driven IOARM compared to the control group (OS: 70% vs 20%, respectively) (11). None of the other studies reported on OS.

Disease-Specific Survival

Nieberler et al. showed that at 3 years follow-up disease-free survival was higher for patients treated with specimen-driven IOARM compared to the control group (DSS: 80% vs 40%, respectively) (11). None of the other studies reported on DSS.

Local Recurrence

None of the studies demonstrated the impact of IOARM on LR.

Adjuvant Therapy

Nieberler et al. have also demonstrated that the group of patients treated with specimen-driven IOARM had a slightly lower rate of adjuvant therapy than the control group (52% RT vs 58% RT, respectively) (11). None of the other studies reported on the impact of IOARM on adjuvant therapy.

DISCUSSION

Surgical treatment of OCSCC patients aims for complete tumor resection with adequate margins, which is the most important prognostic factor. This goal is seldom achieved, underlining that insufficient intraoperative information is available for optimal control of resection margins. IOARM can provide such information.

Here we review the literature reporting on IOARM in OCSCC surgery. The performance of different IOARM methods in predicting margin-status, and their impact on patient outcome were studied.

Despite the pressing need for improving OCSCC surgery, only 18 studies were found that have reported on the performance of IOARM methods; 10 regarding soft tissue resection margins, and 8 regarding bone resection margins.

TABLE 2 | IOARM methods in soft tissue: description and performance.

Author	IOARM		IOARM performance								
	Method	Details of approach	Acc. (%)	Sens. (%)	Spec. (%)	PPV (%)	NPV (%)	IRi (%)	IR Rev. (%)	Reduction IR(%)	SE (%)	IE (%)
Ord (23)	Specimen-driven	Gross examination and FS (taken from mucosal and deep margins)	83.7	30.0	97.0	75.0	84.4	22.4	18.4	17.8	20.0	1.0
Chaturvedi (31)	Specimen-driven	Gross examination and FS (taken from mucosal and deep margins)	99.0	97.0	100.0	100.0	99.4	–	12.2	–	79.0	–
Chaturvedi (25)	Specimen-driven	Gross examination and FS (taken from mucosal and deep margins)	94.0	80.0	100.0	100.0	91.4	31.9	9.9	69.0	20.0	0.0
Ettl (26)	Specimen-driven	FS (taken from mucosal margins)	–	–	–	–	–	51.3	32.0	37.6	–	–
Mair (28)	Specimen-driven	Gross examination alone	83.7	61.9	88.3	53.1	91.2	15.6	7.4	52.6	37.0	12.8
		Gross examination and FS (taken from mucosal and deep margins)	92.9	45.5	98.8	83.3	93.5				48.0	7.7
Datta (30)	Specimen-driven	Gross examination and FS (taken from mucosal and deep margins)	95.4	73.1	100.0	66.0	94.8	18.8	7.8	58.5	44.3	0.0
Pathak (24)	Defect-driven	FS (taken from mucosal and deep margins)	–	–	70.4	–	–	–	–	–	–	–
Buchakjian (27)	Defect-driven	FS (taken from mucosal and deep margins)	–	48.0	72.0	57.0	65.0	37.0	18.0	51.3	64.9	10.1
Abbas (29)	Defect-driven	FS (taken from mucosal and deep margins)	90.9	72.7	95.3	66.6	93.9	–	–	–	27.3	5.2
Amit (19)	Specimen-driven	Gross examination and FS (taken from mucosal and deep margins)	–	91.0	93.0	–	–	–	16.0	–	–	–
	Defect-driven		–	22.0	100.0	–	–	–	45.0	–	–	–

Of the 10 studies that investigated the performance of IOARM for soft tissue, 6 reported on the specimen-driven method, 3 on the defect-driven method and one on both.

In the majority of the specimen-driven studies (4/6), the assessment was performed by gross examination of mucosal and deep margins, followed by FS analysis of locations judged suspicious for inadequate margins (25, 28, 30, 31).

Mair et al. have assessed whether gross examination alone can be as accurate as gross examination combined with FS analysis and found no statistically significant difference in overall incidence of inadequate margins in both groups (28).

In the 3 defect-driven IOARM-studies inspection of the wound bed by the surgeon followed by FS analysis of suspicious mucosal and deep margins was performed (19, 27, 29).

Patient outcome parameters are negatively affected by inadequate resections (5, 7, 10). The studies show that IOARM improves the rate of adequate operations and as a result leads to a decrease in adjuvant therapy. Amit et al. explicitly excluded patients that received adjuvant therapy for other reasons than inadequate resections and showed that of all patients that underwent defect-driven IOARM, 35% required adjuvant therapy while only 8% of all patients that underwent specimen-driven IOARM required adjuvant therapy (19). Only Datta et al. has compared results of adjuvant therapy between patients who received IOARM and those who did not (i.e., control group). The authors demonstrated there was no significant reduction. This result can be explained by the fact that some patients receive adjuvant therapy for other reasons than an inadequate resection (e.g., extra-capsular spread and

TABLE 3 | The non-weighted average IOARM performance parameters for soft tissue: specimen-driven vs defect-driven method.

Performance parameters (average)	Studies using specimen-driven method* (N)	Studies using defect-drivenmethod (N)
Accuracy (%)	91.5 (6.0)	90.9 (1.0)
Sensitivity (%)	68.4 (7.0)	47.6 (3.0)
Specificity (%)	96.7 (7.0)	84.4 (3.0)
[1]PPV (%)	79.6 (6.0)	41.2 (2.0)
[2]NPV (%)	92.5 (6.0)	79.5 (2.0)
[3]SE (%)	41.4 (6.0)	46.1 (2.0)
[4]IE (%)	4.3 (5.0)	7.7 (2.0)

**Four of 6 studies were from the same institute.*

[1]PPV – Positive predictive value.

[2]NPV – Negative predictive value.

[3]SE – Sampling error.

[4]IE – Interpretation error.

N represents the number of studies included in the calculation.

TABLE 4 | IOARM in bone tissue: patients and tumor characteristics.

Author	Patients (N) (inclusion period)	M/F (%)	Mean age (y)	Type of surgery (%)	Tumor characteristics			
					Subsite(s) (%)	pT1/pT2/pT3/pT4 (%) pN0/pN1/ pN2/pN3 (%)	Prior therapy (%)	Primary disease (%)
Forrest (32)	16.0 (–)	–	57.0	Mandible resection: segmental (55.0); marginal (45.0)	–	–	25.0[RT]	–
Wysluch (33)	20.0 (2006–2007)	65.0/ 35.0	67.0	Segmental marginal mandibulectomy (100.0)	Floor of mouth (30.0); Retromular (50.0); Buccal (15.0); Gingiva (5.0)	–	0.0	–
Bilodeau (34)	27.0 (2005–2010)	63.0/ 37.0	59.0	Segmental mandibulectomy (100.0)	Floor of mouth (66.0); Lower and upper alveolus (19.0); Lip (4.0); Retromolar trigone (11.0)	-/-/-/100.0 37.0/19.0/44.0/-	–	85.2
Nieberler (35)	45.0 (2010–2013)	68.0/ 32.0	56.0	Segmental/ marginal mandibulectomy (88.0); partial maxillectomy (12.0)	–	–	–	–
Namin (36)	51.0 (2003–2013)	–	–	Mandible resection: segmental (80.0); marginal (20.0)	Oral cavity (94.0); Oropharynx (6.0)	–	18.0[RT] 4.0[CT]	90.0
Nieberler (11)	102.0 (2009–2014)	69.0/ 31.0	62.0	Segmental/ marginal/ lingual rim mandibulectomy (86.0), partial maxillectomy (13.0); other (1.0)	Floor of mouth (41.0); Mandible (33.0); Maxilla (14.0); Cheek (7.0); Tongue (2.0); Orb. (3.0)	12.0/22.0/18.0/47.0 54.9/10.8/26.5/-	–	89.2
Nieberler (12)	35.0 (2012–2014)	77.0/ 23.0	62.0	Segmental/ partial/ lingual rim mandibulectomy (94.0); partial maxillectomy (3.0); other (3.0)	Floor of mouth (40.0); Mandible (28.6); Maxilla (5.7); Cheek (11.4); Tongue (5.7); Other (8.6)	5.7/25.7/20.0/42.9 51.4/11.4/28.6/-	–	82.9
Cariati (37)	17.0 (2016–2018)	71.0/ 29.0	69.0	Segmental mandibulectomy (100.0)	Tongue (53.0); Floor of mouth (23.5); Retromolar trigone (23.5)	-/-/-/100.0 47.0/29.0/18.0/6.0	0.0	100.0

[CT]*Percentage of patients treated with neoadjuvant chemotherapy.*
[RT]*Percentage of patients treated with radiation therapy prior to surgery.*

perineural involvement) (30). Future studies should be designed to study the impact of IOARM by also including the need for adjuvant therapy, next to other prognostic parameters (e.g., LR, RR, OS, DSS).

Of the 8 studies that investigated the performance of IOARM for bone tissue, 6 reported on the specimen-driven method and 2 on the defect-driven method. Cytological methods were developed for this.

Nieberler et al. demonstrated that the 3 years disease-free survival and overall survival were higher for patients treated with specimen-driven IOARM compared to the control group (DSS: 80% vs 40%; OS: 70% vs 20%). They have also demonstrated that based on specimen-driven IOARM of bone resection margins a number patients did not need to receive adjuvant radiotherapy (11).

When comparing specimen-driven IOARM with defect-driven IOARM we can conclude that for both, soft tissue and bone tissue, the SE and IE are higher for defect-driven IOARM, **Tables 3** and **6**. Consequently, the performance (e.g., average accuracy, sensitivity, specificity, PPV and NPV) of specimen-driven IOARM is better (**Tables 3** and **6**). However, it is important to stress that this conclusion is limited by the low number of available studies reporting performance results for defect-driven IOARM.

TABLE 5 | IOARM methods in bone tissue: description and performance.

Author	IOARM				IOARM performance									
	Method	Sampling tool	Tissue sample	Processing technique (%)	Acc. (%)	Sens. (%)	Spec. (%)	PPV (%)	NPV (%)	IRi (%)	IR Rev (%)	Reduction IR(%)	SE (%)	IE (%)
Forrest (32)	Specimen-driven	Currette	bone marrow	FS (100.0)	93.8	66.7	100.0	100.0	92.9	18.8	6.3	66.5	0.0	6.3
Wysluch (33)	Specimen-driven	Trephine drill technique	cortical bone	FS (100.0)	–	77.0	90.0	–	–	–	–	–	–	–
Nieberler (35)	Specimen-driven	Cytobrush	bone marrow	FS (100.0)	96.0	80.0	98.0	80.0	97.0	11.0	2.2.0	80.0	20.0	2.2
Namin (36)	Specimen-driven	Currette	bone marrow	FS (100.0)	100.0	100.0	100.0	100.0	100.0	19.0	0.0	100.0	0.0	0.0
Nieberler (11)	Specimen-driven	Cytobrush	bone marrow	FS (100.0)	99.0	88.9	100.0	100.0	98.9	8.8	2.9	67.1	11.0	0.0
Nieberler (12)	Specimen-driven	Cytobrush	bone marrow	Fixation with cold methanol (59.0); Papanicolau staining (41.0)	94.0	78.0	100.0	100.0	92.9	–	–	–	22.2	0.0
Bilodeau (34)	Defect-driven	Currette	bone marrow; Inf. alveolar nerve	FS (100.0)	89.0	50.0	100.0	100.0	87.5	–	–	–	50.0	3.7
Cariati (37)	Defect-driven	Currette	bone marrow	FS (100.0)	76.5	33.3	85.7	33.3	85.7	17.6	11.8	33.0	66.7	11.8

TABLE 6 | The non-weighted average IOARM performance parameters for bone tissue: specimen-driven vs defect-driven method.

Performance variables (average)	Studies using specimen-driven method (N)	Studies usingdefect-driven method (N)
Accuracy (%)	96.6 (5.0)	82.8 (2.0)
Sensitivity (%)	81.8 (6.0)	41.7 (2.0)
Specificity (%)	98 (6.0)	92.9 (2.0)
[1]PPV (%)	96 (5.0)	66.7 (2.0)
[2]NPV (%)	96.3 (5.0)	86.6 (2.0)
[3]SE (%)	10.6 (5.0)	58.5 (2.0)
[4]IE (%)	1.7 (5)	7.8 (2)

[1]PPV – Positive predictive value.
[2]NPV – Negative predictive value.
[3]SE – Sampling error.
[4]IE – Interpretation error.
N represents the number of studies included in the calculation.

Another interesting finding was the discrepancy in the reported rate of initially adequate resections for soft tissue specimens. Some recent studies, report adequate resections in only a small minority (15%-26%) of the cases (5, 7, 10). Other studies have shown much higher rates of adequate resections, varying from 48.7% to 81.2% (23, 25–28, 30, 31).

Differences in oral subsite of the tumor might be a reason for this discrepancy. While in Asian countries, a large proportion of the patients have buccal SCC, in Europe and North-America, patients are more often treated for tongue SCC. It has been shown that tongue SCC is significantly more aggressive (more often poorly differentiated) compared to buccal SCC (38). It is harder to achieve a complete resection in poorly differentiated SCC (39). Moreover, differences in surgical approach may play a role; i.e. a difference in balancing the need to remove the tumor, while sparing healthy tissue. However, this information is not available in the papers that were studied.

This literature review shows that there is a low number of studies on the performance of IOARM available. This is the main limitation of this study. However, we firmly believe that with upcoming awareness on the need for IOARM there will be enough evidence in the literature to perform a thorough systematic review/meta-analysis, in the near future. Another limitation of this review is that the studies included performed IOARM according to different protocols. Moreover, the outcome was often evaluated according to different criteria. This makes a comparison of the studies unreliable.

Nevertheless, some conclusions can be drawn: IOARM improves patient outcome and the performance of specimen-driven IOARM is superior to the performance of defect-driven IOARM.

There can be no doubt that IOARM reduces the rate of inadequate margins (average IR Rev. for soft tissue: 47.8%; average IR Rev. for bone tissue: 78.4%), but it still shows low sensitivity

(average Sens. for soft tissue: 62.1%; average Sens. for bone tissue: 71.7%) caused by a high SE (average SE for soft tissue: 42.6%; average SE for bone tissue: 24.3%), **Tables 3** and **6**. The best-performing method; specimen-driven IOARM, is logistically demanding and time-consuming. In addition, grossing fresh tissue is counter-intuitive to most pathologists for fear of interfering with final pathologic assessment. This will continue to stand in the way of IOARM widespread adoption, despite the significant improvement in OCSCC resection results, unless standard protocols and educational programs exist. At our institute we have a comprehensive IOARM protocol including a relocation protocol (6, 40).

The development of objective technology is needed to address these practical hurdles and key to facilitating specimen-driven IOARM in OCSCC. An example of such technology is Raman spectroscopy; an optical technique which has been shown to discriminate between OCSCC and surrounding healthy tissue with high sensitivity and specificity (soft and bone tissue) (41–43). A dedicated instrument employing a fiber optic needle probe for rapid assessment of resection margins on OCSCC specimen is currently under development (44).

AUTHOR CONTRIBUTIONS

EB, YA, and LS designed the study, extracted data, carried out the data analysis and drafted the manuscript. IH, HM, AS, JH, MN, and LO revised the manuscript critically for important intellectual content. TS, GP, and SK designed the study, supervised the research group and revised the manuscript critically for important intellectual content and gave final approval of the version to be published. All authors contributed to the article and approved the submitted version.

FUNDING

We want to thank Dutch Cancer Society (Project 106467 - Optimizing surgical results for oral squamous cell carcinoma by intra-operative assessment of resection margins using Raman spectroscopy) and Eurostars E! (Project 12076 – RA-SURE) for the financial support.

REFERENCES

1. Ferlay J, Colombet M, Soerjomataram I, Mathers C, Parkin DM, Piñeros M, et al. Estimating the global cancer incidence and mortality in 2018: GLOBOCAN sources and methods. *Int J Cancer* (2019) 144(8):1941–53. doi: 10.1002/ijc.31937
2. Sharma SM, Prasad BR, Pushparaj S, Poojary D. Accuracy of intraoperative frozensection in assessing margins in oral cancer resection. *J Maxillofac Oral Surg* (2009) 8(4):357–61. doi: 10.1007/s12663-009-0085-9
3. van der Ploeg T, Datema F, Baatenburg de Jong R, Steyerberg EW. Prediction of Survival with Alternative Modeling Techniques Using Pseudo Values. Pajewski NM, editor. *PloS One* (2014) 9(6):e100234. doi: 10.1371/journal.pone.0100234
4. Chen SW, Zhang Q, Guo ZM, Chen WK, Liu WW, Chen YF, et al. Trends in clinical features and survival of oral cavity cancer: Fifty years of experience with 3,362 consecutive cases from a single institution. *Cancer Manag Res* (2018) 10:4523–35. doi: 10.2147/CMAR.S171251
5. Varvares MA, Poti S, Kenyon B, Christopher K, Walker RJ. Surgical margins and primary site resection in achieving local control in oral cancer resections. *Laryngoscope* (2015) 125(10):2298–307. doi: 10.1002/lary.25397
6. Aaboubout Y, ten Hove I, Smits RWH, Hardillo JA, Puppels GJ, Koljenovic S. Specimen-driven intraoperative assessment of resection margins should be standard of care for oral cancer patients. *Oral Dis* (2020) 27(1):111–6. doi: 10.1111/odi.13619
7. Smits RWH, Koljenović S, Hardillo JA, ten Hove I, Meeuwis CA, Sewnaik A, et al. Resection margins in oral cancer surgery: Room for improvement. Eisele DW, editor. *Head Neck* (2016) 38(S1):E2197–203. doi: 10.1002/hed.24075
8. Baddour HM, Magliocca KR, Chen AY. The importance of margins in head and neck cancer. *J Surg Oncol* (2016) 113(3):248–55. doi: 10.1002/jso.24134
9. Lin A. Radiation Therapy for Oral Cavity and Oropharyngeal Cancers. *Dent Clin North Am* (2018) 62(1):99–109. doi: 10.1016/j.cden.2017.08.007
10. Dik EA, Willems SM, Ipenburg NA, Adriaansens SO, Rosenberg AJWP, Van Es RJJ. Resection of early oral squamous cell carcinoma with positive or close margins: Relevance of adjuvant treatment in relation to local recurrence: Margins of 3 mm as safe as 5 mm. *Oral Oncol* (2014) 50(6):611–5. doi: 10.1016/j.oraloncology.2014.02.014
11. Nieberler M, Häußler P, Kesting MR, Kolk A, Deppe H, Weirich G, et al. Clinical Impact of Intraoperative Cytological Assessment of Bone Resection Margins in Patients with Head and Neck Carcinoma. *Ann Surg Oncol* (2016) 23(11):3579–86. doi: 10.1245/s10434-016-5208-1
12. Nieberler M, Häußler P, Kesting MR, Kolk A, Stimmer H, Nentwig K, et al. Intraoperative cell isolation for a cytological assessment of bone resection margins in patients with head and neck cancer. *Br J Oral Maxillofac Surg* (2017) 55(5):510–6. doi: 10.1016/j.bjoms.2017.02.006
13. Smits RWH, ten Hove I, Dronkers EAC, Bakker Schut TC, Mast H, Baatenburg de Jong RJ, et al. Evaluation of bone resection margins of segmental mandibulectomy for oral squamous cell carcinoma. *Int J Oral Maxillofac Surg* (2018) 47(8):959–64. doi: 10.1016/j.ijom.2018.03.006
14. Murphy J, Isaiah A, Wolf JS, Lubek JE. The influence of intraoperative frozen section analysis in patients with total or extended maxillectomy. *Oral Surg Oral Med Oral Pathol Oral Radiol* (2016) 121(1):17–21. doi: 10.1016/j.oooo.2015.07.014
15. Petrovic I, Montero PH, Migliacci JC, Palmer FL, Ganly I, Patel SG, et al. Influence of bone invasion on outcomes after marginal mandibulectomy in squamous cell carcinoma of the oral cavity. *J Cranio-Maxillofacial Surg* (2017) 45(2):252–7. doi: 10.1016/j.jcms.2016.11.017
16. Kraeima J, Dorgelo B, Gulbitti HA, Steenbakkers RJHM, Schepman KP, Roodenburg JLN, et al. Multi-modality 3D mandibular resection planning in head and neck cancer using CT and MRI data fusion: A clinical series. *Oral Oncol* (2018) 81(April):22–8. doi: 10.1016/j.oraloncology.2018.03.013
17. Meier JD, Oliver DA, Varvares MA. Surgical margin determination in head and neck oncology: Current clinical practice. The results of an International American Head and Neck Society member survey. *Head Neck* (2005) 27(11):952–8. doi: 10.1002/hed.20269
18. Maxwell JH, Thompson LDR, Brandwein-Gensler MS, Weiss BG, Canis M, Purgina B, et al. Early Oral Tongue Squamous Cell Carcinoma. *JAMA Otolaryngol Neck Surg* (2015) 141(12):1104. doi: 10.1001/jamaoto.2015.1351
19. Amit M, Na'ara S, Leider-Trejo L, Akrish S, Cohen JT, Billan S, et al. Improving the rate of negative margins after surgery for oral cavity squamous cell carcinoma: A prospective randomized controlled study. *Head Neck* (2016) 38(S1):E1803–9. doi: 10.1002/hed.24320
20. Tirelli G, Hinni ML, Fernández-Fernández MM, Bussani R, Gatto A, Bonini P, et al. Frozen sections and complete resection in oral cancer surgery. *Oral Dis* (2019) 25(5):1309–17. doi: 10.1111/odi.13101
21. Kain JJ, Birkeland AC, Udayakumar N, Morlandt AB, Stevens TM, Carroll WR, et al. Surgical margins in oral cavity squamous cell carcinoma: Current practices and future directions. *Laryngoscope* (2020) 130(1):128–38. doi: 10.1002/lary.27943
22. Lydiatt WM, Patel SG, O'Sullivan B, Brandwein MS, Ridge JA, Migliacci JC, et al. Head and neck cancers-major changes in the American Joint Committee on cancer eighth edition cancer staging manual. *CA Cancer J Clin* (2017) 67(2):122–37. doi: 10.3322/caac.21389

23. Ord RA, Aisner S. Accuracy of frozen sections in assessing margins in oral cancer resection. *J Oral Maxillofac Surg* (1997) 55(7):663–9. doi: 10.1016/S0278-2391(97)90570-X
24. Pathak KA, Nason RW, Penner C, Viallet NR, Sutherland D, Kerr PD. Impact of use of frozen section assessment of operative margins on survival in oral cancer. *Oral Surgery Oral Med Oral Pathol Oral Radiol Endodontol* (2009) 107 (2):235–9. doi: 10.1016/j.tripleo.2008.09.028
25. Chaturvedi P, Datta S, Nair S, Nair D, Pawar P, Vaishampayan S, et al. Gross examination by the surgeon as an alternative to frozen section for assessment of adequacy of surgical margin in head and neck squamous cell carcinoma. *Head Neck* (2014) 36(4):557–63. doi: 10.1002/hed.23313
26. Ettl T, El-Gindi A, Hautmann M, Gosau M, Weber F, Rohrmeier C, et al. Positive frozen section margins predict local recurrence in R0-resected squamous cell carcinoma of the head and neck. *Oral Oncol* (2016) 55:17–23. doi: 10.1016/j.oraloncology.2016.02.012
27. Buchakjian MR, Tasche KK, Robinson RA, Pagedar NA, Sperry SM. Association of main specimen and tumor bed margin status with local recurrence and survival in oral cancer surgery. *JAMA Otolaryngol - Head Neck Surg* (2016) 142(12):1191–8. doi: 10.1001/jamaoto.2016.2329
28. Mair M, Nair D, Nair S, Dutta S, Garg A, Malik A, et al. Intraoperative gross examination vs frozen section for achievement of adequate margin in oral cancer surgery. *Oral Surg Oral Med Oral Pathol Oral Radiol* (2017) 123 (5):544–9. doi: 10.1016/j.oooo.2016.11.018
29. Abbas SA, Ikram M, Tariq MU, Raheem A, Saeed J. Accuracy of frozen sections in oral cancer resections, an experience of a tertiary care hospital. *J Pak Med Assoc* (2017) 67(5):806–9.
30. Datta S, Mishra A, Chaturvedi P, Bal M, Nair D, More Y, et al. Frozen section is not cost beneficial for the assessment of margins in oral cancer. *Indian J Cancer* (2019) 56(1):19–23. doi: 10.4103/ijc.IJC_41_18
31. Chaturvedi P, Singh B, Nair S, Nair D, Kane SV, D'cruz A, et al. Utility of frozen section in assessment of margins and neck node metastases in patients undergoing surgery for carcinoma of the tongue. *J Cancer Res Ther* (2012) 8 Suppl 1:S100–5. doi: 10.4103/0973-1482.92222
32. Arick Forrest L, Schuller DE, Sullivan MJ, Lucas JG. Rapid analysis of mandibular margins. *Laryngoscope* (1995) 105(5):475–7. doi: 10.1288/00005537-199505000-00004
33. Wysluch A, Stricker I, Hölzle F, Wolff K-D, Maurer P. Intraoperative evaluation of bony margins with frozen-section analysis and trephine drill extraction technique: A preliminary study. *Head Neck* (2010) 32(11):1473–8. doi: 10.1002/hed.21350
34. Bilodeau EA, Chiosea S. Oral Squamous Cell Carcinoma with Mandibular Bone Invasion: Intraoperative Evaluation of Bone Margins by Routine Frozen Section. *Head Neck Pathol* (2011) 5(3):216–20. doi: 10.1007/s12105-011-0264-0
35. Nieberler M, Häusler P, Drecoll E, Stoeckelhuber M, Deppe H, Hölzle F, et al. Evaluation of intraoperative cytological assessment of bone resection margins in patients with oral squamous cell carcinoma. *Cancer Cytopathol* (2014) 122 (9):646–56. doi: 10.1002/cncy.21428
36. Namin AW, Bruggers SD, Panuganti BA, Christopher KM, Walker RJ, Varvares MA. Efficacy of bone marrow cytologic evaluations in detecting occult cancellous invasion. *Laryngoscope* (2015) 125(5):E173–9. doi: 10.1002/lary.25063
37. Cariati P, Cabello Serrano A, Fernandez Solis J, Ferrari S, Torné Poyatos P, Martinez Lara I. Intraoperative cytological examination of bone medullary. A useful technique to predict the extension of bone invasion in segmental mandibulectomy. *Am J Otolaryngol - Head Neck Med Surg* (2019) 40(5):743–6. doi: 10.1016/j.amjoto.2019.07.005
38. Nair S, Singh B, Pawar PV, Datta S, Nair D, Kane S, et al. Squamous cell carcinoma of tongue and buccal mucosa: clinico-pathologically different entities. *Eur Arch Oto-Rhino-Laryngol* (2016) 273(11):3921–8. doi: 10.1007/s00405-016-4051-0
39. Brinkman JN, Hajder E, Van Der Holt B, Den Bakker MA, Hovius SER, Mureau MAM. The effect of differentiation grade of cutaneous squamous cell carcinoma on excision margins, local recurrence, metastasis, and patient survival: A retrospective follow-up study. *Ann Plast Surg* (2015) 75(3):323–6. doi: 10.1097/SAP.0000000000000110
40. van Lanschot CGF, Mast H, Hardillo JA, Monserez D, ten Hove I, Barroso EM, et al. Relocation of inadequate resection margins in the wound bed during oral cavity oncological surgery: A feasibility study. *Head Neck* (2019) 41 (7):2159–66. doi: 10.1002/hed.25690
41. Barroso EM, Smits RWH, Schut TCB, Ten Hove I, Hardillo JA, Wolvius EB, et al. Discrimination between Oral Cancer and Healthy Tissue Based on Water Content Determined by Raman Spectroscopy. *Anal Chem* (2015) 87(4):2419–26. doi: 10.1021/ac504362y
42. Barroso EM, Smits RWH, Van Lanschot CGF, Caspers PJ, Ten Hove I, Mast H, et al. Water concentration analysis by Raman spectroscopy to determine the location of the tumor border in oral cancer surgery. *Cancer Res* (2016) 76 (20):5945–53. doi: 10.1158/0008-5472.CAN-16-1227
43. Barroso EM, ten Hove I, Bakker Schut TC, Mast H, van Lanschot CGF, Smits RWH, et al. Raman spectroscopy for assessment of bone resection margins in mandibulectomy for oral cavity squamous cell carcinoma. *Eur J Cancer* (2018) 92:77–87. doi: 10.1016/j.ejca.2018.01.068
44. Puppels GJ, Barroso EML, Aaboubout Y, Nunes Soares MR, Artyushenko VG, Bocharnikov A, et al. Intra-operative assessment of tumor resection margins by Raman spectroscopy to guide oral cancer surgery (Conference Presentation). In: W Petrich, Z Huang, editors. *Biomedical Vibrational Spectroscopy 2020*. Advances in Research and Industry [Internet] San Francisco, California, United States: SPIE (2020). p. 1. Available at: https://www.spiedigitallibrary.org/conference-proceedings-of-spie/11236/2544394/Intra-operative-assessment-of-tumor-resection-margins-by-Raman-spectroscopy/10.1117/12.2544394.full.

Conflict of Interest: The authors declare that the research was conducted in the absence of any commercial or financial relationships that could be construed as a potential conflict of interest.

frontiers in Oncology

ORIGINAL RESEARCH
published: 12 April 2021
doi: 10.3389/fonc.2021.616653

Survival Outcomes in Oral Tongue Cancer: A Mono-Institutional Experience Focusing on Age

Mohssen Ansarin[1], Rita De Berardinis[1†], Federica Corso[2,3,4], Gioacchino Giugliano[1], Roberto Bruschini[1], Luigi De Benedetto[1], Stefano Zorzi[1], Fausto Maffini[5], Fabio Sovardi[6], Carolina Pigni[7], Donatella Scaglione[8], Daniela Alterio[9], Maria Cossu Rocca [10], Susanna Chiocca[2], Sara Gandini[2†] and Marta Tagliabue[1,11*†‡]*

[1] Division of Otolaryngology and Head and Neck Surgery, IEO, European Institute of Oncology IRCCS, Milan, Italy, [2] Department of Experimental Oncology, IEO, European Institute of Oncology IRCCS, Milan, Italy, [3] Department of Mathematics, DMAT, Politecnico di Milano, Milan, Italy, [4] Center for Analysis Decisions and Society, CADS, Human Technopole, Milan, Italy, [5] Division of Pathology, IEO, European Institute of Oncology IRCCS, Milan, Italy, [6] Department of Otorhinolaryngology, Policlinico San Matteo, IRCCS, Pavia, Italy, [7] Department of Otorhinolaryngology, ASST Ovest Milanese, Legnano, Italy, [8] Division of Data Manager, IEO, European Institute of Oncology IRCCS, Milan, Italy, [9] Division of Radiotherapy, IEO, European Institute of Oncology IRCCS, Milan, Italy, [10] Department of Medical Oncology, Urogenital and Head and Neck Tumors Medical Treatment, IEO, European Institute of Oncology IRCCS, Milan, Italy, [11] Department of Biomedical Sciences, University of Sassari, Sassari, Italy

Objective: The prognostic role of age among patients affected by Oral Tongue Squamous Cell Carcinoma (OTSCC) is a topic of debate. Recent cohort studies have found that patients diagnosed at 40 years of age or younger have a better prognosis. The aim of this cohort study was to clarify whether age is an independent prognostic factor and discuss heterogeneity of outcomes by stage and treatments in different age groups.

Methods: We performed a study on 577 consecutive patients affected by primary tongue cancer and treated with surgery and adjuvant therapy according to stage, at European Institute of Oncology, IRCCS. Patients with age at diagnosis below 40 years totaled 109 (19%). Overall survival (OS), disease-free survival (DFS), tongue specific free survival (TSFS) and cause-specific survival (CSS) were compared by age groups. Multivariate Cox proportional hazards models were used to assess the independent role of age.

Results: The median follow-up time was 5.01 years (range 0–18.68) years with follow-up recorded up to February 2020. After adjustment for all the significant confounding and prognostic factors, age remained independently associated with OS and DSF (respectively, p = 0.002 and p = 0.02). In CSS and TSFS curves, the role of age seems less evident (respectively, p = 0.14 and p = 0.0.37). In the advanced stage sub-group (stages III–IV), age was significantly associated with OS and CSS with almost double increased risk of dying (OS) and dying from tongue cancer (CSS) in elderly compared to younger groups (OS: HR = 2.16 95%, CI: 1.33–3.51, p= 0.001; CSS: HR = 1.76 95%, CI: 1.03–3.01, p = 0.02, respectively). In our study, young patients were more likely to be treated with intensified therapies (glossectomies types III–V and adjuvant radio-chemotherapy). Age was found as a prognostic factor, independently of other

OPEN ACCESS

Edited by:
Alberto Paderno, University of Brescia, Italy

Reviewed by:
Giuseppe Mercante, Humanitas University, Italy
Marco Ferrari, University of Brescia, Italy

***Correspondence:**
Marta Tagliabue
marta.tagliabue@ieo.it
Rita De Berardinis
rita.deberardinis@ieo.it

†ORCID:
Marta Tagliabue
orcid.org/0000-0002-7879-4846
Rita De Berardinis
orcid.org/0000-0003-4959-587X

‡These authors share last authorship

Specialty section:
This article was submitted to Head and Neck Cancer, a section of the journal Frontiers in Oncology

Received: 12 October 2020
Accepted: 11 January 2021
Published: 12 April 2021

Citation:
Ansarin M, De Berardinis R, Corso F, Giugliano G, Bruschini R, De Benedetto L, Zorzi S, Maffini F, Sovardi F, Pigni C, Scaglione D, Alterio D, Cossu Rocca M, Chiocca S, Gandini S and Tagliabue M (2021) Survival Outcomes in Oral Tongue Cancer: A Mono-Institutional Experience Focusing on Age. Front. Oncol. 11:616653. doi: 10.3389/fonc.2021.616653

significant factors and treatment. Also the T–N tract involved by disease and neutrophil-to-lymphocyte ratio ≥3 were independent prognostic factors.

Conclusions: Young age at diagnosis is associated with a better overall survival. Fewer younger people than older people died from tongue cancer in advanced stages.

Keywords: tongue cancer, age, prognosis, head neck cancer, T-N tract, overall survival

INTRODUCTION

One of the hot topics in the field of head and neck tumors concerns the increased incidence of oral tongue squamous cell carcinoma (OTSCC) in young people (1, 2). The reason for these new epidemiological data is still undefined. Above all, etiopathogenesis and prognosis remain unclear when compared to the traditional population affected by oral tongue cancer, which is generally composed of people of over fifty years old with known risk factors such as heavy smoking and alcohol habits (3, 4).

The incidence of mobile tongue cancer in young patients is reported as increasing worldwide, especially in the last three decades (5–8). In particular, the analysis carried out by the National Cancer Institute Surveillance, Epidemiology and End Results Program (SEER) in 2011 on North American data shows that the overall incidence of OTSCC remained stable from 1975 to 2007 but increased in women and more specifically in the sub-population of young white women (9). Many conflicting groups have been published on the etiology, natural history, and prognosis of OTSCC in young adults. As early as 1970, tongue cancer in young people was supposed to be a distinct clinical entity that needed to be treated more aggressively than that in older adults (10). In 2011, Patel et al. also hypothesized a possible hormonal influence as the cause of these tumors (9). In this scenario, also chronic mucosal trauma is considered a possible cause for OTSS in young patients (11).

It is well known that the onset of OTSCC is related to smoking and alcohol abuse and in some countries with the habit of chewing betel leaves (12, 13). In addition, some authors have reported that gender distribution is different depending on the age of onset of oral cancer (12, 14, 15). While in the elderly, males account for over 70% of cases, this percentage drops to 50–65% under 45 years of age. This difference is consolidated if we consider that most of the young, non-smoking and non-drinking patients are reported to be women (12, 14, 15).

Currently, the primary treatment strategy for OTSCC is upfront surgery followed, in advanced stages, by radiotherapy or radio-chemotherapy based on final histopathological findings, according to international guidelines (16, 17).

Locoregional control of OTSCC has improved in recent decades; the reason could be more aggressive surgical resections supported by modern reconstructive methods with free flaps and advances in adjuvant treatment (18–21).

However, despite improved locoregional control, survival rates have remained stable or slightly improved over the past two decades with 5-year overall survival (OS) of approximately 60% for all stages and 33–54% in patients with locally advanced disease (16, 22).

Other treatment strategies such as neoadjuvant chemotherapy followed by surgery or upfront radio-chemotherapy have been employed for OTSCC without any significant improvement in survival (22–24).

In young patients, the prognosis of OTSCC is still controversial. Several early reports on squamous cell carcinoma (SCC) concluded that the disease was more aggressive and the prognosis lower in young adults compared to older patients (10, 25–27). However, recent studies have not found any significant differences in OS between different age groups (2, 28–32). At the same time, several other investigators claim that younger OTSCC patients have better survival compared to elderly patients (6, 8, 29, 33, 34). Conversely, the Memorial Sloan-Kettering Cancer Center reported that younger OTSCC patients had a higher rate of locoregional recurrence, with no significant difference in survival between young and old groups (35).

Many studies reported no difference in biological behavior among young and elderly patients with OTSCC (36–41). In particular, the latest next-generation sequencing techniques indicated that genomic profiles and mutations in the guide genes were very similar among young and elderly OTSCC patients, with similar mechanisms of tumorigenesis (36–41). Moreover, gene-specific mutation and copy number alteration frequencies were the same between young and old OTSCC patients in two independent cohorts (40).

Different results on prognosis and etiology may be attributed both to the small size of the patient cohorts and the different cut-off to define "young" age. Furthermore, there was a considerable heterogeneity both between and also within samples (*i.e.*, matched/unmatched, early/advanced tumor stage). Finally, they did not specify whether or not studies were adjusted for factors such as treatment modality, stage of the disease, presence and absence of metastatic lymph nodes, and percentage of patients between the two age groups. With these premises, the fundamental question about the role of age in cancer outcome of oral tongue cancer remains unanswered.

The aim of the study was to investigate the prognostic role of age and its influence on OTSCC cancer relapse and survival. We collected information on clinical and demographic characteristics of a retrospective cohort of OTSCC patients treated with homogenous modality in our institution, to define which factors could mostly influence survival outcomes.

MATERIAL AND METHODS

Between January 2000 and December 2018, a total of 891 patients with oral cavity cancer underwent surgery at the

Division of Otolaryngology and Head and Neck surgery of the European Institute of Oncology, IRCCS (IEO). The inclusion criteria were: patients with a histologically confirmed primary diagnosis of OTSCC and primary surgical treatment received at IEO. Among these, 173/891 patients were excluded because of previous surgery and/or excisional biopsy which were considered as a complete surgical therapy and not as a mere diagnostic procedure; 105/891 patients were excluded due to histology other than SCC, and 13/891 were excluded because the tumor origin was attributable to the base of the tongue. At the end of the selection, 577 patients with primary diagnosis of OTSCC and primary surgical treatment received at IEO were included in the study cohort.

The current study was approved by the IEO Ethics Committee (cod. IEO 225).

Staging referred to the TNM classification in accordance with the 7th edition American Joint Committee on Cancer system, and all cases were re-classified according to the 8th edition (42, 43). We reported the clinical stages according the 7th TNM editions and the pathological stages in both 7th and 8th TNM editions for completeness of results.

For the study of the paper outcomes, we used the new staging system (8th TNM edition) because it is the prognostic TNM currently used.

Preoperative diagnoses were assessed by a simple biopsy of the lesion, while magnetic resonance imaging or a computed tomography scan was performed for local disease study. Positron emission tomography/computedtomography or total body computed tomography was used for the pre-operative patients' systemic evaluation.

The retrospective information extracted from the electronic medical records included:

- anthropometric and demographic patient characteristics: height, weight, age, gender, pre-operative neutrophil-to-lymphocyte ratio (NLR);
- epidemiologic data: smoking history, family history for tongue cancer and other cancers, alcoholic habits;
- histopathologic features and staging: surgical margins, clinical and pathological TNM 7th and 8th editions, tumor grading, the status of T–N tract (44, 45);
- performed treatment: type of surgery, glossectomies I to V according to the Ansarin et al. classification (from transoral to total glossectomy) (46), adjuvant treatment strategies (radiotherapy and/or chemotherapy)
- follow-up information: type of recurrence (local/locoregional) and/or distant metastases, secondary primary and the patients' status at the last follow-up.

The definition of pack–years of cigarette smoking was used for the evaluation of tobacco consumption (47). Smoking and alcohol status at diagnosis were collected to classify patients as current, former, and never-smoking/drinking.

About the "neck lymph node" status we considered clinical (c)/pathological (p) Nx, N0, N+ as distinct variables. All patients' follow-up were collected and updated to assess their status at the last clinical evaluation and the last contact. Patient deaths and their possible causes were assessed using the Italian national death register.

The NLR cutoff of < or ≥3 was determined based on prior publications (48–51).

All the data were collected in a well-designed database according to good clinical practice guidelines.

In previous studies of OTSCC the most frequent used age cutoff to define young adulthood was 40; moreover, it is reported that the role of risk factors, as smoke and alcohol, start to be significant after the age of 40 (1, 52–54). Thus, the main analysis was carried out considering 40 years of age as the cutoff of interest.

Treatment Modality

All patients received the standard surgical treatment according to the IEO protocol for tongue cancer (46). The clinical early stages (clinical stags I and II) underwent trans-oral glossectomies (type I or II) followed by delayed (within 30 days) neck dissection (I–IV levels) in cases of deep of infiltration (DOI)>3 mm in the tongue. The "wait and see" policy was chosen where DOI was less than 3 mm.

The variable "neck dissection" (**Table 1**) refers to neck dissections performed *en bloc* with the tongue cancer (glossectomies types III to V) or as prophylactic neck dissection after 4 weeks from trans-oral glossectomies (types I or II) for tumor DOI.

Tumor clinically staged as intermediate and advanced (III and IV) were treated with glossectomies types III–to V *en bloc* neck dissection removing the T–N tract in pull-through or with trans-mandibular approaches (compartmental tongue surgery). Adjuvant treatment, such as radiotherapy or radio-chemotherapy, was recommended based on definitive histopathological findings.

Definition of Endpoints

Local recurrence was defined as recurrence in the original tumor bed with the same histopathologic features of the primary tumor in the first three years after treatment. Regional recurrence was described as a metastatic disease in the head and neck region. Distant recurrence was defined as the presence of metastatic disease in all other locations. Any recurrence was reported as any local, regional, or distant metastasis, whichever occurred first. Disease-free survival (DFS) was defined as the time from surgery until any kind of tumor recurrence, including the occurrence of a second primary tumor or death from any cause, or the last contact date if alive with no recurrence. The last contact date was considered the last follow-up visit performed with the patient or the last telephone call ascertaining the patient's state of health.

We considered the second tumor as an event of interest if it appeared after three years of treatment in the oral cavity or in other districts at any time after treatment (55).

Overall survival (OS) was defined as the time from surgery until the date of death from any cause, or the last contact date if alive (56). Patients' deaths were assessed using the Italian national death registers.

TABLE 1 | Patients', tumor and treatments characteristics according to age.

		N (%):	Age ≤ 40 (%)	Age > 40 (%)	P-value
			N = 109	N = 468	
Gender	F	230 (36.57)	43 (39.45)	187 (39.96)	1
	M	347 (60.14)	66 (60.55)	281 (60.04)	
BMI	<24.9	301 (52.17)	57 (52.29)	244 (52.14)	0.13
	25.0–29.9	199 (34.49)	29 (26.61)	170 (36.32)	
	≥30	86 (14.9)	20 (18.35)	66 (14.1)	
	Unknown	11 (1.91)	3 (2.75)	8 (1.71)	
Smoking	Never	208 (36.05)	50 (45.87)	158 (33.76)	0.01
	Current/Former	362 (62.74)	56 (51.38)	306 (65.38)	
	Unknown	7 (1.21)	3 (2.75)	4 (0.85)	
Smoking pack/year	<20	326 (56.5)	89 (81.65)	237 (50.64)	<0.001
	≥20	232 (40.21)	14 (12.84)	218 (46.58)	
Alcohol	Never	288 (49.91)	79 (72.48)	209 (44.66)	<0.001
	Current/Former	280 (48.53)	27 (24.77)	253 (54.06)	
	Unknown	9 (1.56)	3 (2.75)	6 (1.28)	
Family history for tongue squamous cell carcinoma	No	546 (94.63)	101 (92.66)	445 (95.09)	0.69
	Yes	11 (1.91)	1 (0.92)	10 (2.14)	
	Unknown	20 (3.47)	7 (6.42)	13 (2.78)	
Family history for other squamous cell carcinomas	No	311 (53.9)	76 (69.72)	235 (50.21)	<0.001
	Yes	247 (42.81)	27 (24.77)	220 (47.01)	
	Unknown	19 (3.29)	6 (5.5)	13 (2.78)	
Grading	G1	104 (18.02)	19 (17.43)	85 (18.16)	0.62
	G2	267 (46.27)	48 (44.04)	219 (46.79)	
	G3	186 (32.24)	40 (36.7)	146 (31.2)	
	Unknown	20 (3.47)	2 (1.83)	18 (3.85)	
Neutrophil to Lymphocyte Ratio (NLR)	<3	378 (65.51)	86 (78.9)	292 (62.39)	0.006
	≥3	178 (30.85)	21 (19.27)	149 (31.84)	
Clinical Tumor (VII ed)	T1	186 (32.24)	32 (31.19)	152 (32.48)	0.96
	T2	173 (29.98)	33 (30.28)	140 (29.91)	
	T3–T4	218(37.78)	42 (38.53)	176 (37.61)	
Clinical lymph nodes (VII ed)	N0	367 (63.6)	63 (57.8)	304 (64.96)	0.19
	N+	210 (36.4)	46 (42.2)	164 (35.04)	
Pathological Tumor (VII ed.)	T1	186 (32.24)	56 (51.38)	130 (27.78)	0.29
	T2	104 (18.02)	28 (25.69)	76 (16.24)	
	T3–T4	248 (42.98)	58 (53.21)	190 (40.6)	
Pathological Tumor (VIII ed.)	T1	142 (24.61)	24 (22.02)	118 (25.21)	0.63
	T2	136 (23.57)	29 (26.61)	107 (22.86)	
	T3–T4	299 (51.82)	56 (51.38)	243 (51.92)	
Patological lymph nodes N (VII ed.)	N0	158 (27.38)	33 (30.28)	125 (26.71)	0.05
	N+	243 (42.11)	53 (48.62)	190 (40.6)	
	NX	176 (30.5)	23 (21.1)	153 (32.69)	
Patological lymph nodes (VIII ed.)	N0	158 (27.38)	33 (30.28)	125 (26.71)	0.05
	N+	243 (42.11)	53 (48.62)	190 (40.6)	
	NX	176 (30.5)	23 (21.1)	153 (32.69)	
Stage (VII ed.)	I	180 (31.2)	33 (30.28)	147 (31.41)	0.55
	II	70 (12.13)	12 (11.01)	58 (12.39)	
	III	36 (6.24)	10 (9.17)	26 (5.56)	
	IV	291 (50.43)	54 (49.54)	237 (50.64)	
Stage (VIII ed.)	I	130 (22.53)	19 (17.43)	111 (23.72)	0.33
	II	94 (16.29)	21 (19.27)	73 (15.6)	
	III	176 (30.5)	38 (34.86)	138 (29.49)	
	IV	177 (30.68)	31 (28.44)	146 (31.2)	
Lymphovascular invasion	No	548 (94.97)	104 (95.41)	444 (94.87)	1
	Yes	29 (5.03)	5 (4.59)	24 (5.13)	
Perineural infiltration	No	491 (85.1)	90 (82.57)	401 (85.68)	0.50
	Yes	86 (14.9)	19 (17.43)	67 (14.32)	
Tongue Intrinsic muscle infiltration	No	79 (13.69)	12 (11.01)	67 (14.32)	0.45
	Yes	498 (86.31)	97 (88.99)	401 (85.68)	
Tongue Extrinsic muscle infiltration	No	303 (52.51)	56 (51.38)	247 (52.78)	0.86
	Yes	273 (47.31)	53 (48.62)	220 (47.01)	
	Unknown	1 (0.17)	0 (0)	1 (0.21)	
T–N tract status	Free from disease	261 (45.23)	59 (54.13)	202 (43.16)	0.02
	Involved by disease	68 (11.79)	16 (14.68)	52 (11.11)	

(Continued)

TABLE 1 | Continued

		N (%):	Age ≤ 40 (%)	Age > 40 (%)	P-value
	Not removed	248 (42.98)	34 (31.19)	214 (45.73)	
Extracapsular extension	No	461 (79.9)	89 (81.65)	372 (79.49)	0.70
	Yes	116 (20.1)	20 (18.35)	96 (20.51)	
Tumor Side in the tongue	Right	275 (47.66)	52 (47.71)	223 (47.65)	0.60
	Left	284 (49.22)	54 (49.54)	230 (49.15)	
	Bilateral	11 (1.91)	3 (2.75)	8 (1.71)	
	Median	7 (1.21)	0 (0)	7 (1.5)	
Neck dissection	No	176 (30.5)	23 (21.1)	153 (32.69)	0.02
	Yes	401 (69.5)	86 (78.9)	315 (67.31)	
Surgery on Tumor	Glossectomies I-II (transoral)	245 (42.46)	34 (31.19)	211 (45.08)	0.01
	Glossectomies III–V (Compartmental)	332 (57.53)	75 (68.80)	257 (54.91)	
Margins	Free	490 (84.92)	98 (89.91)	392 (83.76)	0.42
	Macroscopic involvement	14 (2.43)	1 (0.92)	13 (2.78)	
	Close	72 (12.48)	10 (9.17)	62 (13.25)	
	Unknown	1 (0.17)	0 (0)	1 (0.21)	
Radiotherapy	No	346 (59.97)	58 (53.21)	288 (61.54)	0.12
	Yes	231 (40.03)	51 (46.79)	180 (38.46)	
Adjuvant radio chemotherapy	No	478 (82.84)	80 (73.39)	398 (85.04)	0.005
	Yes	99 (17.16)	29 (26.61)	70 (14.96)	
Median follow-up (years)		5.01 (0–18.68)	4.22 (0–18.14)	2.63 (0–18.68)	
Overall Survival 5 years		0.65	0.73	0.62	
Disease Free Survival 5 years		0.54	0.60	0.51	
Cause Specific Survival 5 years		0.70	0.75	0.68	
Tongue Specific Free Survival 5 years		0.60	0.70	0.67	

The following tumor-specific clinical outcomes were also evaluated: Cause-specific survival (CSS) defined as the time from surgery until the date of death for tongue cancer. In case of no death for tongue cancer the observation was censored at the last follow-up visit or the date of death for other causes. Tongue specific free survival (TSFS) included the period after a successful treatment during which there were no signs and symptoms of the disease that was treated (tongue cancer) (56–59). The events considered for the TSFS were: local, locoregional recurrence and metastases only for tongue cancer. In case of no events or death for tongue cancer, the observation was censored at the last follow-up visit or the date of death for other causes.

Statistical Analysis

Patient clinical-pathological and tumor characteristics were expressed as relative frequencies and percentages according to age. We choose 40 years old as a cutoff point for age in compliance with previous published studies that evaluated age in head and neck cancer (1, 10, 60–62). We conducted also a sensitivity analysis looking for the best cutoff point in our group for each survival outcome, and we investigated the role of age also as a continuous variable.

Univariate models were performed to evaluate the association of age and other prognostic factors (*e.g.*, smoking pack/year, T–N tract, surgery and stage of 8th TNM edition) with clinical outcomes (DFS, OS, CSS and TSFS). Differences between survival curves were investigated with Log-rank tests and estimated using the Kaplan–Meier method. We assessed the independent prognostic role of age for each outcome with multivariate Cox Proportional Hazard models adjusted for all significant prognostic factors. Hazard ratio (HR) with 95% confidence intervals (CIs) from multivariate Cox proportional hazard models were reported. Sub-group analyses were conducted to investigate whether stage (8th TNM edition) and surgery were associated with any cancer event as local recurrence, secondary primary (DFS) or death of any cause (OS) and recurrence related only to tongue cancer (TSFS) or death of tongue cancer (CSS) depending on age (56–59). We used a Chi-squared test to assess the association of age with frequencies of patients diagnosed recently (between 2010 and 2020), to investigate the influence of time of diagnosis and whether recent diagnoses were associated with sex. Finally, we evaluated whether the proportion of young patients (≤40 years old) was significantly associated with the type of surgery and stage (8th TNM edition). All analyses were carried out with R 4.0 software (http://cran.r-project.org/), and p-values <0.05 were considered statistically significant.

RESULTS

Patients' Characteristics

Clinical-pathological and tumor characteristics of the study population are reported in **Table 1**. Among the young group (n = 109), the median age was 32 (range 27–37), while the median age was 61 (range 50–71) in the elderly group (n = 468).

We did not find any significant difference between the two groups (young and elderly) in terms of sex, BMI, family history for oral tongue tumor, tumor stage (I–IV, 7th and 8th TNM editions), pT (7th and 8th TNM editions), cT and cN according the 7th TNM edition, the status of post-surgery margins, and radiotherapy (RT) as adjuvant treatment.

Among the elderly patients, we found a significantly higher number of current/former smokers (65.38 *vs* 51.38% for older *vs* younger respectively, p = 0.01) as well as patients with family history for other family members with SCC (47.01 *vs* 24.77% for older *vs* younger respectively, p = 0.001). Moreover, comparing the two groups, the youngest population was significantly more treated with type III–V glossectomies (54.9 *vs* 68.8% for older *vs* younger respectively; p =0.01) and with neck dissections (67.31 *vs* 78.9% for older *vs* younger, respectively; p = 0.02).

In the two age groups considered, the preoperative NLR ratio was highly significant for the population over >40 years old with a value equal or greater than 3 (p = 0.006).

Also, for the pathological state of the lymph nodes (pN 7th and 8th editions) and of the T–N tract status (free from disease, involved by disease, not removed), we find a difference between the two populations under examination (p = 0.05 and p = 0.02, respectively). Moreover, adjuvant radio-chemotherapy was administered more in young patients than in elderly (14.96 *vs* 26.61% for older *vs* younger respectively; p = 0.005).

In our sample, the proportion of young diagnoses (≤40 years old) does not seem to be significantly increased over the years: 55% were ≤40 years old between 2000 and 2010, while they were 45% between 2010 and 2020 (p = 0.63).

Furthermore, we also found that the proportion of female cancers was not different from the past: 53% female patients were found between 2000 and 2010, while they totaled 47% between 2010 and 2018 (p = 1).

Events During Follow-Up

The median follow-up time was 5.01 years (range 0–18.68 years) with follow-up recorded up to February 2020.

Overall, we observed 149 (25.8%) locoregional recurrences, 38 (6.5%) distant metastases, and 15 (2.6%) locoregional with synchronous distant metastases as the first site of relapse.

Two hundred and forty-six patients (42.6%) died: 66% died from primary tumor (locoregional-distant recurrence), 10% died

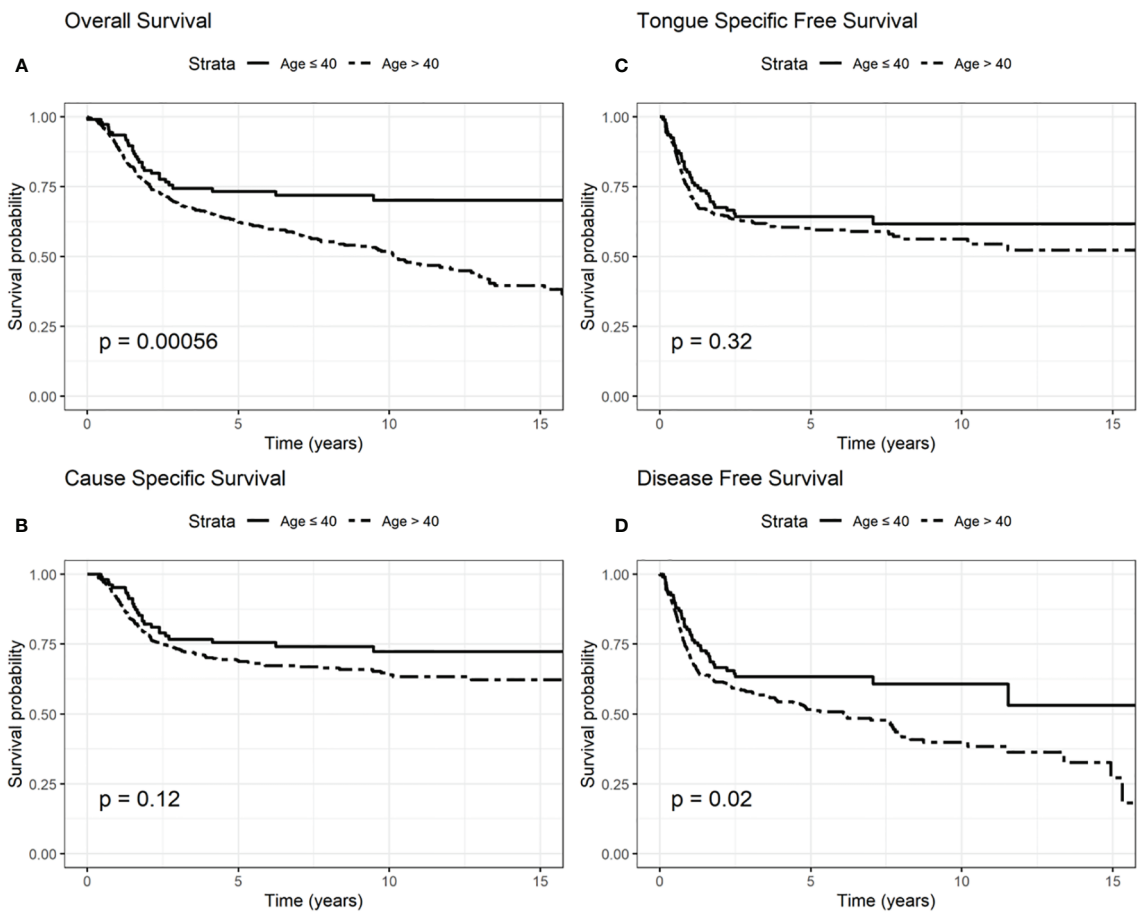

FIGURE 1 | Survival probability: overall survival (OS) **(A)**, cause-specific survival (CSS) **(B)**, tongue specific free survival (TSFS) **(C)**, disease-free survival (DFS) **(D)** according to age.

from a second different tumor, 12% from no cancer related causes, and 12% died from unknown causes.

Forty-six patients had a second primary tumor, of whom two were ≤40 years old.

Regarding OS, elderly 5-year survival was 62% compared to 73% among younger patients, while elderly 10-year survival was 51%, and 70% in younger patients (log rank test p = 0.0006, **Figure 1**).

CSS 5-year survival was 68 and 75% in elderly and younger patients, respectively; CSS 10-year survival was 63 and 72% among elderly and younger patients (log rank test p = 0.12, **Figure 1**).

TSFS at 5-year was 67% for elderly patients and 70% for younger patients; 10-year TSFS was 40% in case of the elderly compared to 50% in younger patients (log-rank test p = 0.32, **Figure 1**).

DFS at 5-year was 51% in elderly than 60% in younger patients; DFS at 10-year was 38 and 53% in elderly and younger patients, respectively (log-rank test p = 0.02, **Figure 1**).

We presented OS, CSS, TSFS, and DFS curves by age, T–N tract involvement and stage 8th edition (**Figures 1**–**3**). Data on OS, CSS, TSFS, and DFS on smoking pack/year (p/y) with 20 p/y as cutoff point, type of intervention (III–V *vs* I, II glossectomies) and stage 8th edition by univariate analysis in association with age (≤/>40) were not significant (data not shown).

In particular, we found that the elderly group was associated with worse overall survival (log-rank test p < 0.001) (**Figure 1**). These results were confirmed by the multivariate analysis, after adjusting for all significant prognostic factors, revealing an almost double risk of death in elderly patients (HR = 1.85 95%, CI: 1.24–2.76; p = 0.002) (**Table 2**). Age was still significantly associated with DFS, as a categorical variable, both in univariate (log-rank test p = 0.02) and multivariate Cox models with a 49% increased risk of relapse in elderly patients (HR = 1.49 95%, CI: 1.05–2.12; p = 0.02) (**Figure 1**, **Table 3**).

Conversely, age was not significantly associated with CSS and TSFS (log-rank test p = 0.14 and p = 0.37 respectively) (**Tables 4**, **5**).

The difference between heavy (<20 p/y) and non-heavy smokers (≥20 p/y) was found to be significantly associated with OS but only in the univariate analysis (log-rank p = 0.05).

The involvement of the T–N tract was found to be significantly associated with all the evaluated clinical outcomes (OS, CSS, DFS, TSFS with p < 0.001) (**Figure 2**, **Tables 2**–**5**). Similarly, patients with advanced stage IV appeared to have a worse prognosis (p < 0.001 for OS, CSS, and DFS) (**Figure 3**).

The multivariable Cox model for OS showed that age remained independently associated with death (p = 0.002), adjusting for T–N tract, stage, vascular invasion together with adjuvant RT and NLR (**Table 2**).

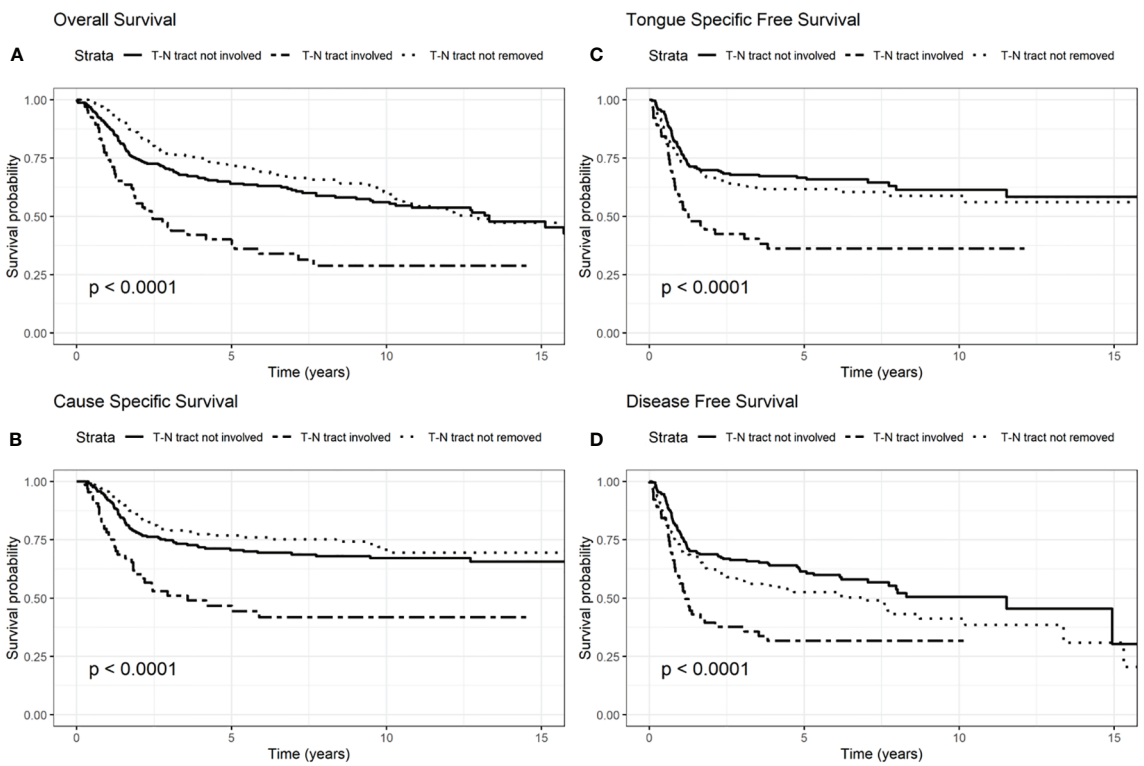

FIGURE 2 | Survival probability: overall survival (OS) **(A)**, cause-specific survival (CSS) **(B)**, tongue specific free survival (TSFS) **(C)**, disease-free survival (DFS) **(D)** according to T–N tract status.

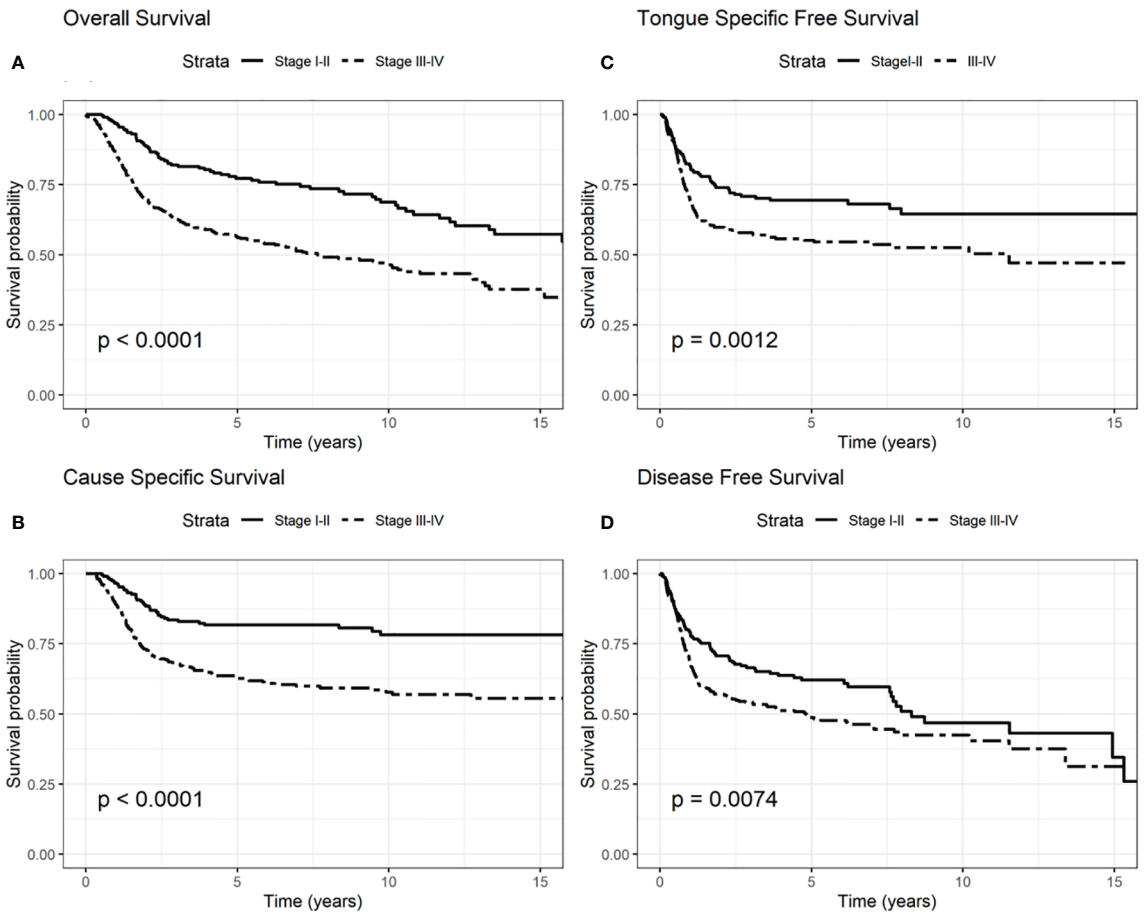

FIGURE 3 | Survival probability: overall survival (OS) **(A)**, cause-specific survival (CSS) **(B)**, tongue specific free survival (TSFS) **(C)**, disease-free survival (DFS) **(D)** according to stages I–II and III–IV according to the 8th edition.

TABLE 2 | Multivariate Cox model for OS.

Variable	Contrast	HR	Low.95	Up.95	P-value
Age	>40 *vs* ≤40	1.85	1.24	2.76	0.002
T–N tract status	Involved *vs* not involved by disease*	1.61	1.11	2.35	0.01
Stage (VIII ed.)	III *vs* I–II	1.73	1.20	2.49	0.003
	IV *vs* I–II	3.70	2.44	5.61	<0.001
Vascular Invasion	yes *vs* no	2.18	1.34	3.56	0.001
Radiotherapy	yes *vs* no	0.53	0.38	0.74	<0.001
NLR^	≥3 *vs* <3	1.47	1.12	1.92	0.004

**not involved by disease (T-N tract not removed for initial stage + removed but free from disease);*
^NLR, Neutrophil to Lymphocyte ratio.

TABLE 3 | Multivariate Cox model for DFS.

Variable	Contrast	HR	Low.95	Up.95	P-value
Age	>40 *vs* ≤40	1.49	1.05	2.12	0.02
T–N tract status	Involved *vs* not involved by disease*	1.48	1.00	2.18	0.04
pN (VIII ed.)	N+ *vs* N0	2.16	1.45	3.22	<0.001
	NX *vs* N0	2.55	1.72	3.78	<0.001
ECE	yes *vs* no	1.48	1.01	2.15	0.04
Vascular Invasion	yes *vs* no	1.58	0.96	2.61	0.07
NLR^	≥3 *vs* <3	1.31	1.00	1.72	0.04

**not involved by disease (T–N tract not removed for initial stage + removed but free from disease);*
^NLR, Neutrophil to Lymphocyte ratio; ECE, extracapsular tumor extension.

Age was independently associated with DFS (p = 0.02), adjusting for other significant prognostic factors such as the T–N tract involvement, pN, extra capsular tumor spread (ECE), vascular invasion, and NLR (**Table 3**).

On the other hand age was not found to be associated with CSS (p = 0.14) adjusting for T–N tract status, pN, pT NLR, and adjuvant radio-chemotherapy. The latter factors were found to be significantly associated with dying of tongue cancer (**Table 4**).

Finally, only T–N tract status, grading, pT and pN were independent prognostic factors associated with TSFS (**Table 5**).

In all the multivariate models in which the variable pN was found to be significant, we see how patients with pN+ and Nx always had a poorer prognosis compared to pN0 patients.

TABLE 4 | Multivariate Cox model for CSS.

Variable	Contrast	HR	Low.95	Up.95	P-value
Age	>40 *vs* ≤40	1.37	0.89	2.12	0.14
T–N tract status	involved *vs* not involved by disease*	1.78	1.16	2.72	0.007
pN (VIII ed.)	N+ *vs* N0	3.27	2.05	5.24	<0.001
	NX *vs* N0	2.86	1.68	4.88	<0.001
pT (VIII ed.)	3–4 *vs* 1–2	1.88	1.25	2.83	0.002
NLR ^	≥3 *vs* <3	1.43	1.04	1.98	0.03
Adjuvant radio-chemotherapy	yes *vs* no	0.63	0.40	0.96	0.03

**not involved by disease (T–N tract not removed for initial stage + removed but free from disease).*
^NLR, Neutrophil to Lymphocyte ratio.

TABLE 5 | Multivariate Cox model for TSFS.

Variable	Contrast	HR	Low.95	Up.95	P-value
Age	>40 *vs* ≤40	1.17	0.82	1.68	0.37
T-N tract status	Involved *vs* not involved by disease*	1.66	1.13	2.45	0.009
Grading	G3–G2 *vs* G1	1.63	1.05	2.54	0.028
pT (VIII ed.)	III–IV *vs* I–II	1.55	1.08	2.24	0.017
pN (VIII ed.)	N+ *vs* N0	3.53	2.23	5.59	<0.001
	NX *vs* N0	3.97	2.75	7.67	<0.001

**not involved by disease (T–N tract not removed for initial stage + removed but free from disease).*

TABLE 6 | Multivariate Cox model for OS, stages III–IV.

Variable	Contrast	HR	Low.95	Up.95	P-value
Age	>40 *vs* ≤40	2.16	1.33	3.51	0.001
T–N tract status	involved *vs* not involved by disease*	1.88	1.30	2.73	<0.001
Vascular Invasion	yes *vs* no	2.24	1.36	3.67	0.001
Radiotherapy	yes *vs* no	0.69	0.50	0.95	0.02
NLR^	≥3 *vs* <3	1.55	1.15	2.11	0.004

**not involved by disease (T–N tract not removed for initial stage + removed but free from disease).*
^NLR, Neutrophil to Lymphocyte ratio.

TABLE 7 | Multivariate Cox model for CSS, stages III–IV.

Variable	Contrast	HR	Low.95	Up.95	P-value
Age	>40 *vs* ≤40	1.76	1.03	3.01	0.02
T–N tract status	Involved *vs* not involved by disease*	1.97	1.29	3.00	0.004
pN (VIII ed.)	N+ *vs* N0	2.85	1.66	4.91	<0.001
	NX *vs* N0	3.31	1.55	7.06	0.001
NLR^	≥3 *vs* <3	1.51	1.04	2.17	0.02
Adjuvant radiochemotherapy	yes *vs* no	0.69	0.44	1.06	0.09

**not involved by disease (T–N tract not removed for initial stage + removed but free from disease); ^NLR, Neutrophil to Lymphocyte ratio.*

We also conducted stratified analyses to evaluate whether the association of age with recurrence (DFS and TSFS) and survival (OS and CSS) was different by stage (8th edition) and treatment.

In the early stages (I–II), age was not found to be significantly associated with death (OS: HR = 1.56 95%, CI: 0.77–3.16, p = 0.21; CSS HR = 0.80 95% CI: 0.38–1.70, p = 0.57).

On the other hand, in multivariate analysis, for the advanced stages (III–IV, 8th edition), age was found to be significantly associated with OS and CSS models, revealing a worse outcome for patients diagnosed at age >40 years (OS: HR = 2.16 95%, CI: 1.33–3.51, p= 0.001; CSS HR = 1.76 95%, CI: 1.03–3.01, p = 0.02) (**Tables 6**, **7**).

Furthermore, we investigated the relationship between age, stage, and performed treatment (glossectomy types I–II *vs* IV–V): we found that for advanced stages (III–IV 8th edition) there were no statistically significant different distributions of types of glossectomies between the two age groups considered (p = 0.07); instead in the initial stages (I–II 8th edition), glossectomies III–V were significantly more frequent at age ≤40 (30%) than at age >40 (14%), (p = 0.02) (**Table S1**).

Then, we analyzed the role of age in multivariate analysis for patients treated with the same surgery stratified by stage.

In the initial stages I–II according to TNM 8th edition for OS and CSS, in glossectomies types I–II we did not find any significant prognostic factor. In contrast, for type III–V glossectomies and early stages low number of events did not allow to estimate independent prognostic factors (data not shown).

For TSFS in type I–II glossectomies and stages I–II, the lymph nodal status (pN+ and pNx) remained significant (p < 0.001) (**Table S2**). Low number of events in early stage treated with type III–V glossectomies did not allow to identify independent prognostic factors associated with TSFS (data not shown).

Focusing on the DFS for early stages, in glossectomies types I–II we found that lymph node status was significantly associated with relapse: worse DFS was found in patients with laterocervical disease (p = 0.001) (**Table S3**). In early stage type III–V glossectomies, the NLR ratio remained significant (p = 0.03) (**Table S4**).

Concerning the advanced stages, for OS we had significance for the NLR ratio (p = 0.006) in type I–II glossectomies (data not shown). In type III–V glossectomies, age remained significant with the T–N tract, vascular invasion, post-operative radiotherapy treatment and NLR ratio (p = 0.001, p = 0.003, p = 0.006, p = 0.007and p = 0.04 respectively) (**Table S5**).

We did not find significant elements in CSS for type I–II glossectomies in advanced stages. In type III–V glossectomies for advanced stages CSS, we confirmed the variables: age, T–N tract, lymph node status and adjuvant radio-chemotherapy as independent risks factors for worse prognosis (p = 0.01, p = 0.01, p < 0.001, and p = 0.06, respectively) (**Table S6**).

In the TSFS model for advanced stages, in type I–II glossectomies, only the presence of pNx remained associated with prognosis (p = 0.05), while in type III–V glossectomies we found that the T–N tract and pN+ status were significantly

associated with worse TSFS (p = 0.005 and < 0.001 respectively) (data not shown).

In DFS of advanced stages, NLR ratio was found to be significantly associated with relapse for type I–II glossectomies (p = 0.05) (data not shown); while for type III–V glossectomies age, T–N tract status, lymph node status, ECE and vascular invasion remained significantly associated with relapse (p = 0.04, p = 0.07, p = 0.001, p = 0.07 and p = 0.04 respectively) (**Table S7**).

Regarding the female sub-group, age appears to be significantly directly associated with prognosis also in multivariate analysis: patients older than 40 years have almost double increased risk of dying (OS) compared to younger groups (OS: HR = 2.02 95%, CI: 1.12–3.84, p = 0.01) (**Table S8**). In the male sub-group results were similar.

We also assessed several sensitivity analyses considering age as continuous variable and considering as cut-off point of age 45 and conclusion did not change (data not shown).

DISCUSSION

Our analyses confirmed better survival outcomes in young patients than in elderly patients.

We choose 40 as the cutoff age to distinguish young from older people in line with the study by Oliver et al. and others (1, 52, 53); moreover it is reported that the role of risk factors, such as smoke and alcohol, seems to be significant after the age of 40 (54).

In the multivariate Cox analysis for OS and CSS, the variable "age" remained highly significant for the OS model: young people were characterized by a better OS regardless of tumor stage, while CSS did not seem to be significantly correlated with age. However, CSS was related to pT, pN, T–N tract status, NLR, and adjuvant radio-chemotherapy.

Analyzing the advanced stage sub-group (stages III–IV), age seemed to be significant in OS and in CSS models with a double risk of dying and dying for tongue cancer in elderly compared to young people.

Focusing on the role of age in multivariate analysis for patients treated with the same surgery stratified by stage, "age" did not seem to play a role for glossectomies types I–II and stages I–II.

In advanced-stage and glossectomies type III–IV patients at age ≥40 showed to have approximately double risk of death compared to younger patients (CSS) and 50% increased risk of relapse.

Many published studies have shown no significant difference in prognosis between young and elderly patients (31, 34, 35, 63–65). However, Goldenberg D et al. affirmed that a better prognosis characterized young patients than older ones (29).

In a matched-pair analysis, Farquhar et al. described a greater recurrence incidence in young people <45 years old, but no differences in overall mortality in the two groups (30).

In 2019 Oliver at al. published a study with a high number of cases (under 40 years old) and revealed that young patients did not have a worse survival than elderly, as previously found in smaller cohorts: controlling for all confounding factors, patients under 40 had a significantly 9% higher 5-year survival (77.1 *vs* 68.2%). In this work, Oliver et al. underline that age alone could not be a factor for treatment intensification beyond the standard of care (1).

Over the years, other authors have demonstrated that young patients have a worse prognosis and suggested that more aggressive approaches could improve locoregional control and OS (8, 10, 66, 67).

Conversely, Oliver et al. reported in a considerable sample that: "the intensification of treatment could be a source of significant increases in morbidity and cost of treatment, without any proven benefits at this time" (1).

Actually, also in our sample, young patients underwent more aggressive treatments as shown by a significant number of glossectomies types II–V (compartmental surgery), neck dissection, and adjuvant therapies.

Studying our data by type of surgery, the difference in surgical treatment seemed to be statistically evident in the initial stages (I–II) where young patients were treated more with aggressive surgery, but these differences did not remain significant in multivariate analysis. In this regard, as reported by Oliver et al., it will be interesting to further investigate whether the intensification of therapy, generally reserved for young patients, really leads to better disease control in young people than in the elderly (1).

Focusing on adjuvant therapy, regardless of age, multivariate analysis showed that radiotherapy remained significantly associated with OS and radio-chemotherapy with CSS; among surgical treatments were not significant, taking into account other factors as stage, pT, pN, and LNR.

Another aspect highlighted in our results was the role of the T–N tract. The T–N tract is the soft tissue between the primary tumor (T) and the neck lymph nodes (N) and it is composed by the sublingual and submandibular glands, mylohyoid muscle, lingual nerve, artery, and vein and all the stromal tissue, and lingual and sublingual lymph nodes of the compartment. This study confirmed that, independently of age, and other factors analyzed in multivariate analysis, the involvement of T–N tract was significant in all studied survival models (OS, DFS, TSFS, and CSS). Consequently, the status of the T–N tract played an important role in prognosis for patients with OTSCC regardless of age. In fact, patients with the T–N tract involved by disease had a 60% increased risk of dying (OS) and a 78% higher risk of dying from tongue cancer (CSS). These data got worse in advanced stages III–IV where OS and CSS worsen almost twice as much as in those who do not have the disease in the T-N tract.

The presence of cervical metastases at diagnosis and the T–N tract status were confirmed as important prognostic factors in all the survival models stratified by stage.

Focusing on lymph nodal status, patients with pN+ and pNx always showed a worse oncological outcome in multivariate analysis. The presence of neck metastases is directly related to the oncological stage and, consequently, to the prognosis.

Special consideration should be made for patients with pNx. In case of pNx, many published works showed that these patients

have a worse OS and a higher frequency of local recurrence, especially compared to pN0 patients. In fact, pNx patients generally did not undergo the neck dissection because of clinical condition or because the "wait and see" protocol was applied. In this way, as reported by the literature, about 30% of these patients remained with undiagnosed neck micro-metastases and then a worse prognosis for local relapses (68–71). Our data confirm this evidence.

Regardless of treatment modality, the role of smoking is still debated among risk factors for the young. The prognosis of young patients with OTSCC is still undefined, and there exists a lack of clear definition of young and old patients in the published literature. Analyzing the OTSCC literature, as already reported, the concept of "young age" has been considered in varying ways: from below 30 going up to 45 years old. However, the majority of studies considered 40 years old as the major age below which patients were defined young (21, 22, 35, 52, 60, 61, 72–76). There is an agreement that in patients below 40 years old, there is too short smoking exposure to develop carcinogenic activity. Thus, chronic mucosal trauma, genetic and/or hormonal features could cause oral tongue cancer, but to date, no certain data have been proven (11, 40, 54, 77).

In our data smoking and alcohol did not influence the prognosis of the two groups in multivariate analysis.

In our sample the proportion of female cancers was not different from the past. On the contrary, in 2011 Patel et al. reported that OTSCC was increasing among young white individuals with age 18 to 44 years, particularly among white women (9). A recent study on Asiatic patients with tongue cancer described an increasing incidence particularly in young females. Younger females with tongue SCC had no significant history of smoking (78, 79). Regarding the prognosis of our study cohort, females older than 40 years have almost double increased risk of dying (OS) compared to younger.

Moreover, our study highlighted the important role of the NLR as independent prognostic factor. As well reported not only in head and neck cancers, a tumor-induced change of the immune system toward a pre-tumoral pattern and worse prognosis are related with high values of the NLR ratio (80). In our sample, an NLR value greater than three was associated with a worse prognosis in the curves for OS, CSS, and DFS, and the pejorative role was confirmed in the OS and CSS for advanced stage in patients treated with both type I–II and III–V glossectomies. These data also showed how the role of the immune system, in addition to the age and stage of the disease, could be a determining factor in cancer aggressiveness. However, further studies are needed to better understand it.

In this study, we presented survival data specifically related to tongue cancer highlighting how young patients died less specifically of tongue cancer (CSS and TSFS).

In the advanced stages, young age and NLR smaller than three were correlated with a better prognosis in terms of OS and CSS.

As reported by the literature, the elderly group shows worse outcomes, and this fact could be related to the associated comorbidities of older people regarding OS (6, 33). Instead, for CSS we may hypothesize a role of the immune system. Some studies attested an increase of LNR in the elderly: these data could favor tumor aggression with a worsening of the specific cancer outcomes (81).

Moreover, the independent and pejorative role of the pNx was well defined in multivariate analysis for CSS, DFS and TSFS. In our sample the pNx was mostly referred to the oldest group which generally had the less invasive surgery and to the application of the "wait and see" protocol with "personalized" surgical approaches also based on their health status.

Nevertheless, this work has several limitations, such as the limited number of young patients, the monocentric and retrospective nature of the data.

Despite this, to the best of our knowledge, this is one of the largest monocentric cohort studies, the first work to describe patients who underwent standard and replicable surgical treatments over a period of years, reporting comprehensive data of known risk factors, with a long and complete period of follow-up and in which the prognostic role of age, T–N tract, and NLR is clearly demonstrated.

CONCLUSION

The peer-reviewed biomedical literature has shown that the role played by age in OTSCC prognosis is a matter of controversy. Our study revealed that young patients had a better prognosis and survived longer than elderly patients. Moreover, young people showed a slightly better recurrence-free survival, and they died less from tongue cancer than older patients, even in advanced tumor stages. In our sample, young patients seem more likely to be treated with intensified mode. Future studies, prospective and multicentric, will be needed to investigate the role of treatment intensification in young patients with OTSCC.

DATA AVAILABILITY STATEMENT

The original contributions presented in the study are included in the article/**Supplementary Material**. Further inquiries can be directed to the corresponding authors.

ETHICS STATEMENT

The studies involving human participants were reviewed and approved by the European Institute of Oncology cometee (cod. IEO 225). Written informed consent to participate in this study was provided by the participants' legal guardian/next of kin.

AUTHOR CONTRIBUTIONS

MA and MT conceptualized and drafted the study. RBe carried out literature review and revised the manuscript. SZ and LB

revised the manuscript. RBr, GG, MC, FM, SC, and DA critically reviewed the manuscript for important intellectual content. DS, FS, and CP collected patients' data. SG and FC realized statistical analysis. All authors contributed to the article and approved the submitted version.

FUNDING

This work was partially supported by the Italian Ministry of Health with Ricerca Corrente and 5x1000 funds.

ACKNOWLEDGMENTS

The authors thank William Russell-Edu for assistance with the English text.

SUPPLEMENTARY MATERIAL

The Supplementary Material for this article can be found online at: https://www.frontiersin.org/articles/10.3389/fonc.2021.616653/full#supplementary-material

REFERENCES

1. Oliver JR, Wu SP, Chang CM, Roden DF, Wang B, Hu KS, et al. Survival of oral tongue squamous cell carcinoma in young adults. *Head Neck* (2019) 41 (9):2960–8. doi: 10.1002/hed.25772
2. Paderno A, Morello R, Piazza C. Tongue carcinoma in young adults: a review of the literature. *Acta Otorhinolaryngol Ital* (2018) 38(3):175–80. doi: 10.14639/0392-100X-1932
3. Choi G, Song JS, Choi SH, Nam SY, Kim SY, Roh JL, et al. Comparison of Squamous Cell Carcinoma of the Tongue between Young and Old Patients. *J Pathol Transl Med* (2019) 53(6):369–77. doi: 10.4132/jptm.2019.09.16
4. Oliveira LL, Bergmann A, Melo AC, Thuler LC. Prognostic factors associated with overall survival in patients with oral cavity squamous cell carcinoma. *Med Oral Patol Oral Cir Bucal* (2020) 25(4):e523–31. doi: 10.4317/medoral.23558
5. Tota JE, Anderson WF, Coffey C, Califano J, Cozen W, Ferris RL, et al. Rising incidence of oral tongue cancer among white men and women in the United States, 1973-2012. *Oral Oncol* (2017) 67:146–52. doi: 10.1016/j.oraloncology.2017.02.019
6. Xu Q, Wang C, Li B, Kim K, Li J, Mao M, et al. The impact of age on oral squamous cell carcinoma: A longitudinal cohort study of 2,782 patients. *Oral Dis* (2019) Apr25(3):730–41. doi: 10.1111/odi.13015
7. Ng JH, Iyer NG, Tan MH, Edgren G. Changing epidemiology of oral squamous cell carcinoma of the tongue: A global study. *Head Neck* (2017) 39(2):297–304. doi: 10.1002/hed.24589
8. Annertz K, Anderson H, Biörklund A, Möller T, Kantola S, Mork J, et al. Incidence and survival of squamous cell carcinoma of the tongue in Scandinavia, with special reference to young adults. *Int J Cancer* (2002) 101 (1):95–9. doi: 10.1002/ijc.10577
9. Patel SC, Carpenter WR, Tyree S, Couch ME, Weissler M, Hackman T, et al. Increasing incidence of oral tongue squamous cell carcinoma in young white women, age 18 to 44 years. *J Clin Oncol* (2011) 29(11):1488–94. doi: 10.1200/JCO.2010.31.7883
10. Sarkaria JN, Harari PM. Oral tongue cancer in young adults less than 40 years of age: rationale for aggressive therapy. *Head Neck* (1994) 16(2):107–11. doi: 10.1002/hed.2880160202
11. Singhvi HR, Malik A, Chaturvedi P. The Role of Chronic Mucosal Trauma in Oral Cancer: A Review of Literature. *Indian J Med Paediatr Oncol* (2017) 38 (1):44–50. doi: 10.4103/0971-5851.203510
12. Sturgis EM, Cinciripini PM. Trends in head and neck cancer incidence in relation to smoking prevalence: an emerging epidemic of human papillomavirus-associated cancers? *Cancer* (2007) 110(7):1429–35. doi: 10.1002/cncr.22963
13. Sankaranarayanan R, Masuyer E, Swaminathan R, Ferlay J, Whelan S. Head and neck cancer: a global perspective on epidemiology and prognosis. *Anticancer Res* (1998) 18(6B):4779–86.
14. Harris SL, Kimple RJ, Hayes DN, Couch ME, Rosenman JG. Never-smokers, never-drinkers: unique clinical subgroup of young patients with head and neck squamous cell cancers. *Head Neck* (2010) 32(4):499–503. doi: 10.1002/hed.21220
15. Hussein AA, Helder MN, de Visscher JG, Leemans CR, Braakhuis BJ, de Vet HCW, et al. Global incidence of oral and oropharynx cancer in patients younger than 45 years versus older patients: A systematic review. *Eur J Cancer* (2017) 82:115–27. doi: 10.1016/j.ejca.2017.05.026
16. Chinn SB, Myers JN. Oral Cavity Carcinoma: Current Management, Controversies, and Future Directions. *J Clin Oncol* (2015) 33(29):3269–76. doi: 10.1200/JCO.2015.61.2929
17. National Comprehensive Cancer Network guidelines. Available at: http://www.nccn.org/professionals/physician_gls/pdf/head-and-neck.pdf (Accessed October, 2020).
18. Calabrese L, Bruschini R, Giugliano G, Ostuni A, Maffini F, Massaro MA, et al. Compartmental tongue surgery: Long term oncologic results in the treatment of tongue cancer. *Oral Oncol* (2011) 47(3):174–9. doi: 10.1016/j.oraloncology.2010.12.006
19. Cooper JS, Pajak TF, Forastiere AA, Jacobs J, Campbell BH, Saxman SB, et al. Postoperative concurrent radiotherapy and chemotherapy for high-risk squamous-cell carcinoma of the head and neck. *N Engl J Med* (2004) 350 (19):1937–44. doi: 10.1056/NEJMoa032646
20. Bernier J, Domenge C, Ozsahin M, Matuszewska K, Lefèbvre JL, Greiner RH, et al. Postoperative irradiation with or without concomitant chemotherapy for locally advanced head and neck cancer. *N Engl J Med* (2004) 350(19):1945–52. doi: 10.1056/NEJMoa032641
21. Piazza C, Grammatica A, Montalto N, Paderno A, Del Bon F, Nicolai P. Compartmental surgery for oral tongue and floor of the mouth cancer: Oncologic outcomes. *Head Neck* (2019) 41(1):110–5. doi: 10.1002/hed.25480
22. Kies MS, Boatright DH, Li G, Blumenschein G, El-Naggar AK, Brandon Gunn G, et al. Phase II trial of induction chemotherapy followed by surgery for squamous cell carcinoma of the oral tongue in young adults. *Head Neck* (2012) 34(9):1255–62. doi: 10.1002/hed.21906
23. Gore SM, Crombie AK, Batstone MD, Clark JR. Concurrent chemoradiotherapy compared with surgery and adjuvant radiotherapy for oral cavity squamous cell carcinoma. *Head Neck* (2015) 37(4):518–23. doi: 10.1002/hed.23626
24. Zhong LP, Zhang CP, Ren GX, Guo W, William WN Jr, Sun J, et al. Randomized phase III trial of induction chemotherapy with docetaxel, cisplatin, and fluorouracil followed by surgery versus up-front surgery in locally advanced resectable oral squamous cell carcinoma. *J Clin Oncol* (2013) 31(6):744–51. doi: 10.1200/JCO.2012.43.8820
25. Byers RM. Squamous cell carcinoma of the oral tongue in patients less than thirty years of age. *Am J Surg* (1975) 130(4):475–8. doi: 10.1016/0002-9610(75)90487-0
26. Brägelmann J, Dagogo-Jack I, El Dinali M, Stricker T, Brown CD, Zuo Z, et al. Oral cavity tumors in younger patients show a poor prognosis and do not contain viral RNA. *Oral Oncol* (2013) 49(6):525–33. doi: 10.1016/j.oraloncology.2013.02.003
27. Son YH, Kapp DS. Oral cavity and oropharyngeal cancer in a younger population. Review of literature and experience at Yale. *Cancer* (1985) 55 (2):441–4. doi: 10.1002/1097-0142(19850115)55:2<441::AID-CNCR2820550225>3.0.CO;2-5
28. Goepfert RP, Kezirian EJ, Wang SJ. Oral tongue squamous cell carcinoma in young women: a matched comparison-do outcomes justify treatment intensity? *ISRN Otolaryngol* (2014) 2014:529395. doi: 10.1155/2014/529395
29. Goldenberg D, Brooksby C, Hollenbeak CS. Age as a determinant of outcomes for patients with oral cancer. *Oral Oncol* (2009) 45(8):e57–61. doi: 10.1016/j.oraloncology.2009.01.011

30. Farquhar DR, Tanner AM, Masood MM, Patel SR, Hackman TG, Olshan AF, et al. Oral tongue carcinoma among young patients: An analysis of risk factors and survival. *Oral Oncol* (2018) 84:7–11. doi: 10.1016/j.oraloncology.2018.06.014
31. Atula S, Grénman R, Laippala P, Syrjänen S. Cancer of the tongue in patients younger than 40 years. A distinct entity? *Arch Otolaryngol Head Neck Surg* (1996) 122(12):1313–9. doi: 10.1001/archotol.1996.01890240021006
32. Myers JN, Elkins T, Roberts D, Byers RM. Squamous cell carcinoma of the tongue in young adults: increasing incidence and factors that predict treatment outcomes. *Otolaryngol Head Neck Surg* (2000) 122(1):44–51. doi: 10.1016/S0194-5998(00)70142-2
33. Mukdad L, Heineman TE, Alonso J, Badran KW, Kuan EC, St John MA. Oral tongue squamous cell carcinoma survival as stratified by age and sex: A surveillance, epidemiology, and end results analysis. *Laryngoscope* (2019) 129 (9):2076–81. doi: 10.1002/lary.27720
34. Verschuur HP, Irish JC, O'Sullivan B, Goh C, Gullane PJ, Pintilie M. A matched control study of treatment outcome in young patients with squamous cell carcinoma of the head and neck. *Laryngoscope* (1999) 109(2 Pt 1):249–58. doi: 10.1097/00005537-199902000-00015
35. Friedlander PL, Schantz SP, Shaha AR, Yu G, Shah JP. Squamous cell carcinoma of the tongue in young patients: a matched-pair analysis. *Head Neck* (1998) 20(5):363–8. doi: 10.1002/(SICI)1097-0347(199808)20:5<363::AID-HED1>3.0.CO;2-W
36. Barnabé L, Batista AC, Mendonça EF, Nonaka CFW, Alves PM. Cell cycle markers and apoptotic proteins in oral tongue squamous cell carcinoma in young and elderly patients. *Braz Oral Res* (2019) 36:1–7. doi: 10.1590/1807-3107bor-2019.vol33.0103
37. Dos Santos Costa SF, Brennan PA, Gomez RS, Fregnani ER, Santos-Silva AR, Martins MD, et al. Molecular basis of oral squamous cell carcinoma in young patients: Is it any different from older patients? *J Oral Pathol Med* (2018) 47 (6):541–6. doi: 10.1111/jop.12642
38. O'Regan EM, Toner ME, Smyth PC, Finn SP, Timon C, Cahill S, et al. Distinct array comparative genomic hybridization profiles in oral squamous cell carcinoma occurring in young patients. *Head Neck* (2006) 28(4):330–8. doi: 10.1002/hed.20354
39. Benevenuto TG, Nonaka CF, Pinto LP, de Souza LB. Immunohistochemical comparative analysis of cell proliferation and angiogenic index in squamous cell carcinomas of the tongue between young and older patients. *Appl Immunohistochem Mol Morphol* (2012) 20(3):291–7. doi: 10.1097/PAI.0b013e31823277f6
40. Pickering CR, Zhang J, Neskey DM, Zhao M, Jasser SA, Wang J, et al. Squamous cell carcinoma of the oral tongue in young non-smokers is genomically similar to tumors in older smokers. *Clin Cancer Res* (2014) 20 (14):3842–8. doi: 10.1158/1078-0432.CCR-14-0565
41. Santos-Silva AR, Ribeiro AC, Soubhia AM, Miyahara GI, Carlos R, Speight PM, et al. High incidences of DNA ploidy abnormalities in tongue squamous cell carcinoma of young patients: an international collaborative study. *Histopathology* (2011) 58(7):1127–35. doi: 10.1111/j.1365-2559.2011.03863.x
42. Amin MB, Edge S, Greene FL, Byrd DR, Brookland RK, Washington MK. *AJCC Cancer Staging Manual*. American Joint Commitee on Cancer (AJCC): Springer International Publishing (2017).
43. Edge SB, Byrd DR, Compton CC, Fritz AG, Greene FL, Trotti A. *AJCC cancer staging manual. 7th ed* Vol. 2010. . New York, NY: Springer (2010).
44. Tagliabue M, Gandini S, Maffini F, Navach V, Bruschini R, Giugliano G, et al. The role of the T-N tract in advanced stage tongue cancer. *Head Neck* (2019) 41(8):2756–67. doi: 10.1002/hed.25761
45. Calabrese L, Giugliano G, Bruschini R, Ansarin M, Navach V, Grosso E, et al. Compartmental surgery in tongue tumours: description of a new surgical technique. *Acta Otorhinolaryngol Ital* (2009) 29(5):259–64.
46. Ansarin M, Bruschini R, Navach V, Giugliano G, Calabrese L, Chiesa F, et al. Classification of GLOSSECTOMIES: Proposal for tongue cancer resections. *Head Neck* (2019) 41(3):821–7. doi: 10.1002/hed.25466
47. Cammarata LM, Zagà V, Pistone G. The pack-year as expression of tobacco use in smokers' lifetime. *Tabaccologia* (2014) 1(2):31–4.
48. Wu CN, Chuang HC, Lin YT, Fang FM, Li SH, Chien CY. Prognosis of neutrophil-to-lymphocyte ratio in clinical early-stage tongue (cT1/T2N0. *cancer Onco Targets Ther* (2017) 10:3917–24. doi: 10.2147/OTT.S140800
49. Zhang B, Du W, Gan K, Fang Q, Zhang X. Significance of the neutrophil-to-lymphocyte ratio in young patients with oral squamous cell carcinoma. *Cancer Manag Res* (2019) 11:7597–603. doi: 10.2147/CMAR.S211847
50. Abbate V, Dell'Aversana Orabona G, Salzano G, Bonavolontà P, Maglitto F, Romano A, et al. Pre-treatment Neutrophil-to-Lymphocyte Ratio as a predictor for occult cervical metastasis in early stage (T1-T2 cN0) squamous cell carcinoma of the oral tongue. *Surg Oncol* (2018) 27(3):503–7. doi: 10.1016/j.suronc.2018.06.002
51. Hasegawa T, Iga T, Takeda D, Amano R, Saito I, Kakei Y, et al. Neutrophil-lymphocyte ratio associated with poor prognosis in oral cancer: a retrospective study. *BMC Cancer* (2020) 20(1):568. doi: 10.1186/s12885-020-07063-1
52. Garavello W, Spreafico R, Gaini RM. Oral tongue cancer in young patients: a matched analysis. *Oral Oncol* (2007) 43(9):894–7. doi: 10.1016/j.oraloncology.2006.10.013
53. de Morais EF, Mafra RP, Gonzaga AKG, de Souza DLB, Pinto LP, da Silveira ÉD. Prognostic Factors of Oral Squamous Cell Carcinoma in Young Patients: A Systematic Review. *J Oral Maxillofac Surg* (2017) 75(7):1555–66. doi: 10.1016/j.joms.2016.12.017
54. Mohideen K, Krithika C, Jeddy N, Bharathi R, Thayumanavan B, Sankari SL. Meta-analysis on risk factors of squamous cell carcinoma of the tongue in young adults. *J Oral Maxillofac Pathol* (2019) 23(3):450–7. doi: 10.4103/jomfp.JOMFP_118_19
55. Priante AV, Castilho EC, Kowalski LP. Second primary tumors in patients with head and neck cancer. *Curr Oncol Rep* (2011) 13(2):132–7. doi: 10.1007/s11912-010-0147-7
56. Birgisson H, Wallin U, Holmberg L, Glimelius B. Survival endpoints in colorectal cancer and the effect of second primary other cancer on disease free survival. *BMC Cancer* (2011) 11:438–2407-11-438. doi: 10.1186/1471-2407-11-438
57. Nahler G. *Disease free interval (DFI)*. Vienna: Springer (2009).
58. Schatzkin A, Freedman LS, Schiffman MH, Dawsey SM. Validation of intermediate end points in cancer research. *J Natl Cancer Inst* (1990) 82 (22):1746–52. doi: 10.1093/jnci/82.22.1746
59. Hudis CA, Barlow WE, Costantino JP, Gray RJ, Pritchard KI, Chapman JA, et al. Proposal for standardized definitions for efficacy end points in adjuvant breast cancer trials: the STEEP system. *J Clin Oncol* (2007) 25(15):2127–32. doi: 10.1200/JCO.2006.10.3523
60. Veness MJ, Morgan GJ, Sathiyaseelan Y, Gebski V. Anterior tongue cancer: age is not a predictor of outcome and should not alter treatment. *ANZ J Surg* (2003) 73(11):899–904. doi: 10.1046/j.1445-2197.2003.02818.x
61. Hyam DM, Conway RC, Sathiyaseelan Y, Gebski V, Morgan GJ, Walker DM, et al. Tongue cancer: do patients younger than 40 do worse? *Aust Dent J* (2003) 48(1):50–4. doi: 10.1111/j.1834-7819.2003.tb00009.x
62. Fang QG, Shi S, Liu FY, Sun CF. Tongue squamous cell carcinoma as a possible distinct entity in patients under 40 years old. *Oncol Lett* (2014) 7 (6):2099–102. doi: 10.3892/ol.2014.2054
63. Randall CJ, Shaw HJ. Malignant tumours of the tongue in young adults. Experience of a secondary referral centre. *J Laryngol Otol* (1986) 100 (11):1295–8. doi: 10.1017/S0022215100101008
64. Lund VJ, Howard DJ. Head and neck cancer in the young: a prognostic conundrum? *J Laryngol Otol* (1990) 104(7):544–8. doi: 10.1017/S002221510011312X
65. Siegelmann-Danieli N, Hanlon A, Ridge JA, Padmore R, Fein DA, Langer CJ. Oral tongue cancer in patients less than 45 years old: institutional experience and comparison with older patients. *J Clin Oncol* (1998) 16(2):745–53. doi: 10.1200/JCO.1998.16.2.745
66. Depue RH. Rising mortality from cancer of the tongue in young white males. *N Engl J Med* (1986) 315(10):647. doi: 10.1056/NEJM198609043151013
67. Jeon JH, Kim MG, Park JY, Lee JH, Kim MJ, Myoung H, et al. Analysis of the outcome of young age tongue squamous cell carcinoma. *Maxillofac Plast Reconstr Surg* (2017) 39(1):41. doi: 10.1186/s40902-017-0139-8
68. Jiang Q, Tang A, Long S, Qi Q, Song C, Xin Y, et al. Development and validation of a nomogram to predict the risk of occult cervical lymph node metastases in cN0 squamous cell carcinoma of the tongue. *Br J Oral Maxillofac Surg* (2019) 57(10):1092–7. doi: 10.1016/j.bjoms.2019.09.024
69. D'Cruz AK, Vaish R, Kapre N, Dandekar M, Gupta S, Hawaldar R, et al. Head and Neck Disease Management Group.Elective versus Therapeutic Neck

Dissection in Node-Negative Oral Cancer. *N Engl J Med* (2015) 373(6):521–9. doi: 10.1056/NEJMoa1506007

70. Abu-Ghanem S, Yehuda M, Carmel NN, Leshno M, Abergel A, Gutfeld O, et al. Elective Neck Dissection vs Observation in Early-Stage Squamous Cell Carcinoma of the Oral Tongue With No Clinically Apparent Lymph Node Metastasis in the Neck: A Systematic Review and Meta-analysis. *JAMA Otolaryngol Head Neck Surg* (2016) 142(9):857–65. doi: 10.1001/jamaoto.2016.1281
71. Tsushima N, Sakashita T, Homma A, Hatakeyama H, Kano S, Mizumachi T, et al. The role of prophylactic neck dissection and tumor thickness evaluation for patients with cN0 tongue squamous cell carcinoma. *Eur Arch Otorhinolaryngol* (2016) 273(11):3987–92. doi: 10.1007/s00405-016-4077-3
72. Pitman KT, Johnson JT, Wagner RL, Myers EN. Cancer of the tongue in patients less than forty. *Head Neck* (2000) 22(3):297–302. doi: 10.1002/(SICI)1097-0347(200005)22:3<297::AID-HED14>3.0.CO;2-3
73. Vargas H, Pitman KT, Johnson JT, Galati LT. More aggressive behavior of squamous cell carcinoma of the anterior tongue in young women. *Laryngoscope* (2000) 110(10 Pt 1):1623–6. doi: 10.1097/00005537-200010000-00009
74. Liao CT, Wang HM, Hsieh LL, Chang JT, Ng SH, Hsueh C, et al. Higher distant failure in young age tongue cancer patients. *Oral Oncol* (2006) 42(7):718–25. doi: 10.1016/j.oraloncology.2005.11.012
75. Kabeya M, Furuta R, Kawabata K, Takahashi S, Ishikawa Y. Prevalence of human papillomavirus in mobile tongue cancer with particular reference to young patients. *Cancer Sci* (2012) 103(2):161–8. doi: 10.1111/j.1349-7006.2011.02149.x
76. Yang AK, Liu TR, Chen FJ, Ma XF, Guo ZM, Song M, et al. Survival analysis of 229 patients with advanced squamous cell carcinoma of the oral tongue. *Ai Zheng* (2008) 27(12):1315–20.
77. Gamez ME, Kraus R, Hinni ML, Moore EJ, Ma DJ, Ko SJ, et al. Treatment outcomes of squamous cell carcinoma of the oral cavity in young adults. *Oral Oncol* (2018) 87:43–8. doi: 10.1016/j.oraloncology.2018.10.014
78. Satgunaseelan L, Allanson BM, Asher R, Reddy R, Low HTH, Veness M, et al. The incidence of squamous cell carcinoma of the oral tongue is rising in young non-smoking women: An international multi-institutional analysis. *Oral Oncol* (2020) 110:104875. doi: 10.1016/j.oraloncology.2020.104875
79. Lin NC, Hsu JT, Tsai KY. Difference between Female and Male Patients with Oral Squamous Cell Carcinoma: A Single-Center Retrospective Study in Taiwan. *Int J Environ Res Public Health* (2020) 17(11):3978. doi: 10.3390/ijerph17113978
80. Mattavelli D, Lombardi D, Missale F, Calza S, Battocchio S, Paderno A, et al. Prognostic Nomograms in Oral Squamous Cell Carcinoma: The Negative Impact of Low Neutrophil to Lymphocyte Ratio. *Front Oncol* (2019) 9:339. doi: 10.3389/fonc.2019.00339
81. Li J, Chen Q, Luo X, Hong J, Pan K, Lin X, et al. Neutrophil-to-Lymphocyte Ratio Positively Correlates to Age in Healthy Population. *J Clin Lab Anal* (2015) 29(6):437–43. doi: 10.1002/jcla.21791

Conflict of Interest: The authors declare that the research was conducted in the absence of any commercial or financial relationships that could be construed as a potential conflict of interest.

frontiers in Oncology

METHODS
published: 23 April 2021
doi: 10.3389/fonc.2021.613945

Step-by-Step Cadaver Dissection and Surgical Technique for Compartmental Tongue and Floor of Mouth Resection

Alberto Grammatica[1], Cesare Piazza[1], Marco Ferrari[1,2], Vincenzo Verzeletti[1], Alberto Paderno[1], Davide Mattavelli[1], Alberto Schreiber[1], Davide Lombardi[1], Enrico Fazio[3], Luca Gazzini[3], Giovanni Giorgetti[3], Barbara Buffoli[4], Luigi Fabrizio Rodella[4], Piero Nicolai[2] and Luca Calabrese[3]*

[1] Department of Otorhinolaryngology – Head and Neck Surgery, University of Brescia, Brescia, Italy, [2] Department of Otorhinolaryngology – Head and Neck Surgery, University of Padua, Padua, Italy, [3] Department of Otorhinolaryngology – Head and Neck Surgery, "San Maurizio" Hospital, Bolzano, Italy, [4] Department of Clinical and Experimental Sciences, Section of Anatomy and Physiopathology, University of Brescia, Brescia, Italy

OPEN ACCESS

Edited by:
Remco De Bree, University Medical Center Utrecht, Netherlands

Reviewed by:
Giuseppe Mercante, Humanitas University, Italy
Raul Pellini, Regina Elena National Cancer Institute (IRCCS), Italy

***Correspondence:**
Alberto Paderno
albpaderno@gmail.com

Specialty section:
This article was submitted to Head and Neck Cancer, a section of the journal Frontiers in Oncology

Received: *04 October 2020*
Accepted: *06 April 2021*
Published: *23 April 2021*

Citation:
Grammatica A, Piazza C, Ferrari M, Verzeletti V, Paderno A, Mattavelli D, Schreiber A, Lombardi D, Fazio E, Gazzini L, Giorgetti G, Buffoli B, Rodella LF, Nicolai P and Calabrese L (2021) Step-by-Step Cadaver Dissection and Surgical Technique for Compartmental Tongue and Floor of Mouth Resection. Front. Oncol. 11:613945. doi: 10.3389/fonc.2021.613945

Background: The aim of oral cancer surgery is tumor removal within clear margins of healthy tissue: the latter definition in the literature, however, may vary between 1 and 2 cm, and should be intended in the three dimensions, which further complicates its precise measurement. Moreover, the biological behavior of tongue and floor of mouth cancer can be unpredictable and often eludes the previously mentioned safe surgical margins concept due to the complexity of tongue anatomy, the intricated arrangements of its intrinsic and extrinsic muscle fibers, and the presence of rich neurovascular and lymphatic networks within it. These structures may act as specific pathways of loco-regional tumor spread, allowing the neoplasm to escape beyond its visible macroscopic boundaries. Based on this concept, in the past two decades, compartmental surgery (CS) for treatment of oral tongue and floor of mouth cancer was proposed as an alternative to more traditional transoral resections.

Methods: The authors performed three anatomical dissections on fresh-frozen cadaver heads that were injected with red and blue-stained silicon. All procedures were documented by photographs taken with a professional reflex digital camera.

Results: One of these step-by-step cadaver dissections is herein reported, detailing the pivotal points of CS with the aim to share this procedure at benefit of the youngest surgeons.

Conclusions: We herein present the CS step-by-step technique to highlight its potential in improving loco-regional control by checking all possible routes of tumor spread. Correct identification of the anatomical space between tumor and nodes (T-N tract), spatial relationships of extrinsic tongue muscles, as well as neurovascular bundles of the floor of mouth, are depicted to improve knowledge of this complex anatomical area.

Keywords: tongue cancer, oral cavity, compartmental tongue surgery, cadaver dissection, surgical technique

INTRODUCTION

Compartmental surgery (CS) has emerged in the last decade as a promising approach for treatment of locally advanced cancers of the tongue and floor of mouth. The term "compartmental" has been borrowed from the field of sarcoma surgery which typically aims to remove an entire anatomical compartment defined as an entire group of muscle fibers, vascular, lymphatic and neural bundles along with the overlaying fascial system that usually drive tumor growth and direction, following the spatial orientation of these structures (1, 2). First conceived and proposed by Calabrese and coworkers in 2009, CS allows better oncological outcomes compared to traditional wide-margin (1-2 cm) resections, in terms of both local and loco-regional control (3, 4). This standardized technique involves the en-bloc resection of one hemitongue and related floor of mouth *via* pull-through or transmandibular approaches, clearing the neck lymph nodes in continuity with the "tumor-nodes" (T-N) tract. This has been demonstrated to achieve optimal loco-regional control, while not substantially impacting functional outcomes and residual quality of life (5–7).

The ideal indications for CS are represented by tongue and/or floor of mouth cancers with a clinical/radiological depth of infiltration (DOI) ≥10 mm (as ascertained by preoperative MR or CT scans with contrast administration). The importance of a DOI threshold ≥10 mm for tongue cancer has been demonstrated to be crucial in various clinical and anatomical studies, clearly showing that the boundary between the vast majority of intrinsic and extrinsic muscle fibers in such a complex anatomy mainly occurs at this depth (8–11). However, such a parameter cannot be considered an absolute cut-off since the thickness of the intrinsic tongue musculature can vary between different patients, and there is still a relatively large confidence interval in DOI quantification by imaging. The abrupt change of the 3D-spatial arrangement between extrinsic and intrinsic muscular fibers at this level is, however, fundamental for the philosophy at the basis of CS, since it is conceivable that the tumor from this location would start spreading following directions of the connective framework, tending to reach the bone insertions of extrinsic tongue muscles (i.e. mandible, hyoid, and styloid process). Moreover, vessels, lymphatics, and nerves travelling within the paramedian and lateral tongue septa are easily involved when the tumor reaches a DOI of 10 mm in the tongue and floor of the mouth, and play a paramount role in clinical and pathological tumor behavior (12).

We herein present the CS technique in a step-by-step fashion, based on a fresh cadaver dissection focusing on the most valuable anatomical details, in order to make it possible for the reader to reproduce the procedure in an oncologically safe way in routine clinical practice.

MATERIALS, EQUIPMENT AND METHODS

Three fresh-frozen cadaver heads (Medcure®, Portland, Oregon, USA) were dissected in the Laboratory of Anatomy at the University of Brescia, Italy. The arterial and venous systems had been previously injected with red and blue-stained silicon, respectively. A complete set of head and neck surgical instrumentation was available for the dissection. All the anatomical procedures were recorded by a VITOM 3D (Karl Storz®, Tuttlingen, Germany) or a 4K endoscope (Olympus®, Tokyo, Japan) for academic purposes. The photographs of all anatomical dissections for each step were taken using a reflex digital camera with a 12.3 megapixel resolution (Nikon D300, Nikon, Japan) coupled with a 60 mm F/2 Macro 1:1 fixed focal length lens, mounted on a tripod.

RESULTS

The best surgical specimen both for quality of tissues and preservation of anatomical details was selected and used for presentation of this step-by-step anatomical/surgical dissection.

Step 1 - Surgical Field Preparation and Level IB Anatomy

Skin incision is performed following a horizontal crease, usually extending it from the mastoid tip to the thyroid notch or thyro-hyoid membrane, crossing the midline in order to allow appropriate bilateral clearance of submental lymph nodes (level IA) (**Figure 1**, continuous line). If mandibulotomy is needed to reach tumors with massive posterior tongue involvement or associated trismus, skin incision can be accordingly modified by extending it to the mandibular symphysis and lower vermilion (**Figure 1**, dotted line).

A subplatismal cervical flap is raised with exposure of the body of the mandible, paying attention to preserve the mandibularis branch of the VII cranial nerve which runs in a plane deep to the superficial cervical fascia. The procedure usually starts by clearing lymph nodes according to clinical needs (selective neck dissection levels I-III, or levels I-IV, or modified radical or radical neck dissections). As a consequence, the internal jugular vein (IJV) and common carotid artery (CCA) with its bifurcation are fully visible when retracting the

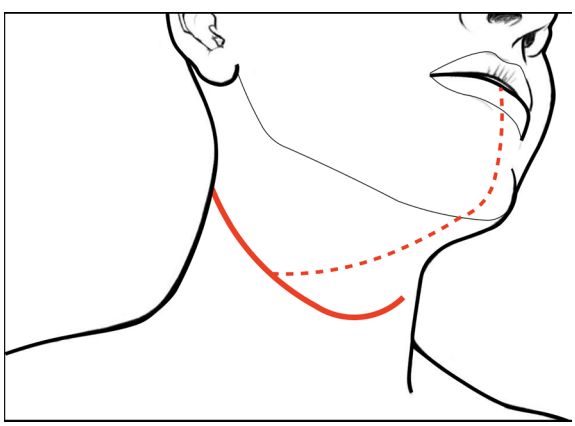

FIGURE 1 | Skin incisions for CS of the tongue and floor of mouth: the continuous line represents that usually followed in case of pull-through approach and unilateral neck dissection (while tracheostomy is performed *via* a separated caudal stab wound); dotted line indicates the incision for the transmandibular approach.

sternocleidomastoid muscle (SCM). The external carotid artery (ECA) with its collateral branches is also in full view. Thyroid and occipital arteries (the latter resected) and their anatomical relationships with the XII cranial nerve can be easily appreciated.

The digastric muscle with its anterior (ABDM) and posterior bellies (PBDM) is skeletonized to correctly delimitate the inferior borders of the submandibular space. The submandibular gland and adjacent fat tissue containing lymph nodes of level IB is then dissected from the surrounding tissues and detached from the mylohyoid muscle (MhM), which represents the deep plane of dissection. Facial artery (FA) and its submental branch (SmA) are found herein and, whenever possible, preserved (**Figure 2A**).

Surgical tips and tricks

- Skin incision in males should be placed caudally to the margin of the beard to make shaving easier in the postoperative period. Usually, putting it in a skin crease minimizes the ensuing aesthetic impact. Great care should be applied to maintain surgical field of the neck separate from the tracheostomy site, thus reducing the risk of contamination and wound infection.
- The facial vessels (artery and vein) are dissected and preserved as long as possible since they represent the first option for subsequent micro-anastomoses during the reconstructive phase.
- The patient is positioned supine with the head extended and turned in order to expose the affected neck side.
- In short necks, it is advisable to put a roll under the patient's shoulders to further improve neck extension.

Step 2 - Submandibular Space Dissection and Lingual Artery Exposure

The FA is ligated to clearly expose the submandibular space. The MhM is completely skeletonized, identifying its bony attachment to the mandible and hyoid bone. The intermediate tendon of the digastric muscle (ITDM) is pulled down along with the stylohyoid muscle (StM) in order to highlight the lingual artery (LA) and the XII cranial nerve. This space, also known as Pirogov's triangle, is bounded by the ITDM, posterior margin of the MhM, and XII cranial nerve cranially. The LA is clearly visible close to its branching point from the ECA while, after 1-2 cm, it lays deep to the hyoglossus muscle (HgM) (**Figure 2B**).

Step 3 - Hypoglossal and Lingual Nerve Identification

Once the inferior aspect of the compartment has been delimited, the next step is to identify the two major neural structures potentially acting as routes for tumor spread: the XII cranial nerve and the lingual nerve (LN). The former is identified from posterior to anterior crossing the ECA, running deeply to the PBDM and StM, and superficially to the HgM (hidden by the silicone background) and LA. Two centimeters cranially and anteriorly, running deeply to the MhM, the LN can be found in close relationship with the sublingual gland and floor of mouth mucosa. The XII cranial nerve must be followed and sectioned, preserving, if feasible, the emergence of its descending loop with the cervical plexus to maintain the strap muscles innervation (**Figure 3**). Dissection continues deeply, in a caudo-cranial way by detaching the HgM from its hyoid insertions, thus exposing and ligating the LA in close proximity to the greater cornu of the hyoid bone.

Surgical tips and tricks

- Frozen sections should be sent from the cranial stump of the hypoglossal nerve, especially in the presence of advanced cancers massively infiltrating the MhM and HgM.
- Identification of the HgM is made easier by gripping the hyoid bone with Ellis forceps and pulling it laterally.
- The LA must be ligated and frozen sections sent for possible vascular invasion evaluation, especially when floor of the

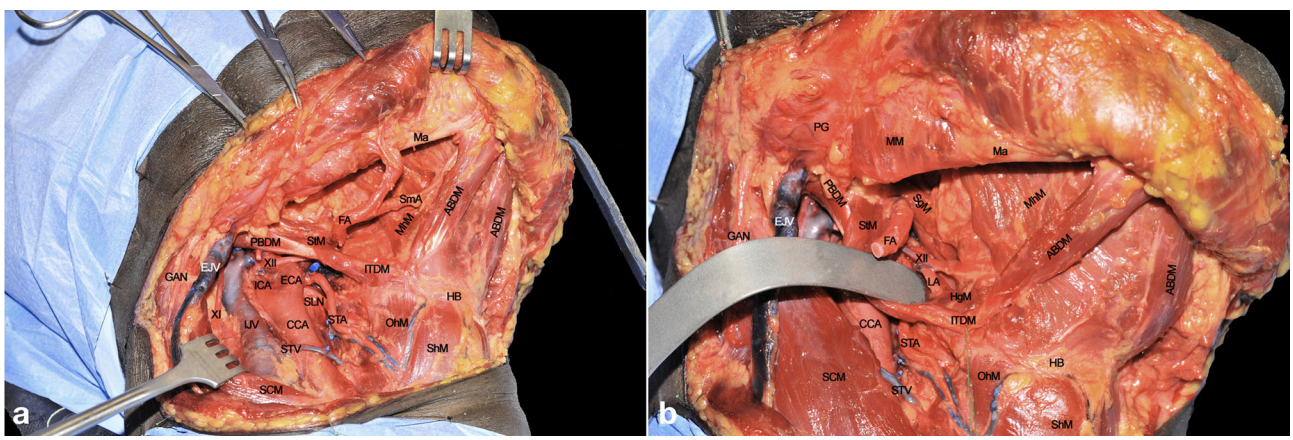

FIGURE 2 | **(A, B)** ABDM, anterior belly of digastric muscle; CCA, common carotid artery; ECA, external carotid artery; EJV, external jugular vein; FA, facial artery; GAN, great auricular nerve; HB, hyoid bone; HgM, hyoglossus muscle; ICA, internal carotid artery; IJV, internal jugular vein; ITDM, intermediate tendon of digastric muscle; LA, lingual artery; Ma, mandible; MhM, mylohyoid muscle; OhM, omohyoid muscle; PBDM, posterior belly of digastric muscle; PG, parotid gland; SCM, sternocleidomastoid muscle; SgM, styloglossus muscle; ShM, sternohyoid muscle; SLN, superior laryngeal nerve; SmA, submental artery; STA, superior thyroid artery; StM, stylohyoid muscle; STV, superior thyroid vein; XI, spinal accessory nerve; XII, hypoglossal nerve.

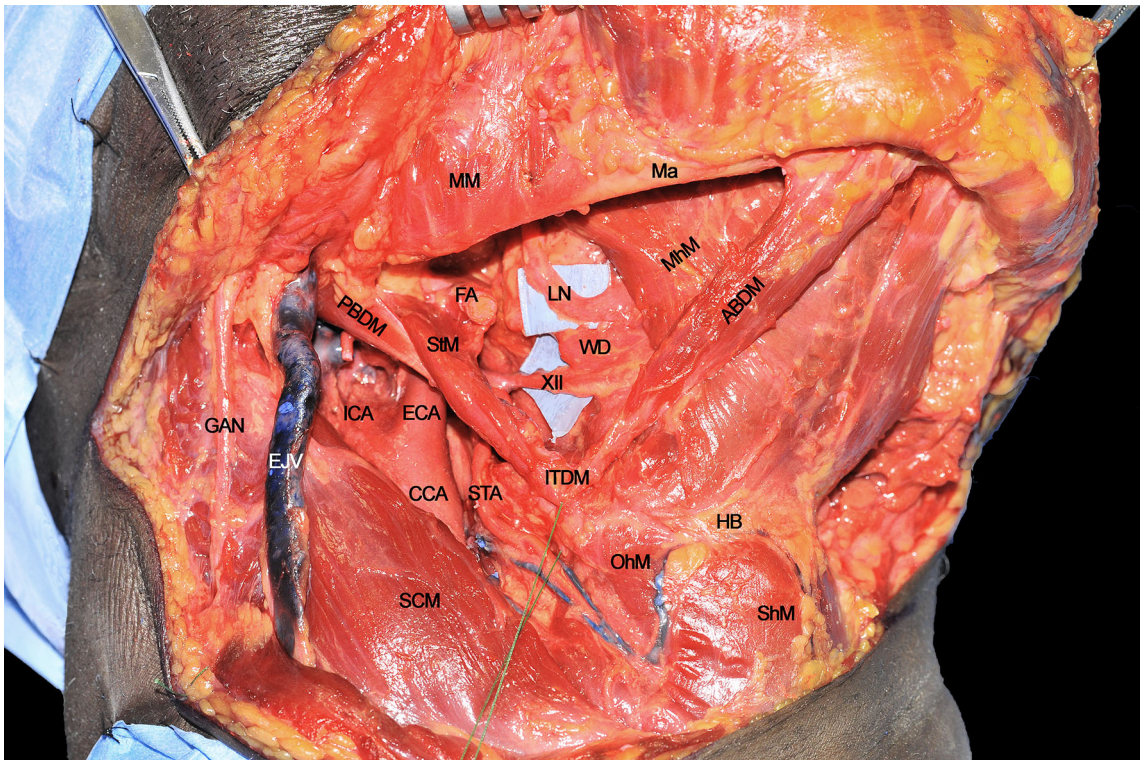

FIGURE 3 | ABDM, anterior belly of digastric muscle; CCA, common carotid artery; ECA, external carotid artery; EJV, external jugular vein; FA, facial artery; GAN, great auricular nerve; HB, hyoid bone; ICA, internal carotid artery; ITDM, intermediate tendon of digastric muscle; LN, lingual nerve; Ma, mandible; MhM, mylohyoid muscle; MM, masseter muscle; OhM, omohyoid muscle; PBDM, posterior belly of digastric muscle; SCM, sternocleidomastoid muscle; ShM, sternohyoid muscle; STA, superior thyroid artery; StM, stylohyoid muscle; WD, Warthon's duct; XII, hypoglossal nerve.

mouth gross involvement is detected. This maneuver will also greatly reduce bleeding during subsequent tongue resection. The LA can be also used as an alternative to the FA as a donor vessel for microvascular anastomoses.

- The anatomical preservation of the descending loop of the XII cranial nerve may improve swallowing in the postoperative period.

Step 4 - Mylohyoid and Hyoglossus Muscles Detachment

Once the above mentioned neurovascular structures have been identified, the dissection proceeds delimitating the T-N tract from caudal to cranial following the bony attachments of the different muscular structures. In this specific case, the digastric muscle has been removed to better expose the extrinsic lingual muscular compartment (even though not necessarily done in all patients treated by CS). The LA, clearly visible at the level of its branching from the ECA, is followed through the HgM (grabbed with forceps), and detached from its hyoid insertions (black dotted line). Cranially, the MhM has been detached from the mylohyoid line (white dotted line) on the internal aspect of the mandibular body, while the LN is exposed and sectioned as cranial as possible. Anteriorly, the ABDM is retracted medially to show the fatty median raphe between the left and right genioglossus muscles (GgM). Anteriorly and superficially the geniohyoid muscle (GhM) and deeply both the GgMs are well visible. Lateral to the right GgM the fat-containing paramedian septum is recognizable (black arrow) (**Figure 4**).

Surgical tips and tricks

- If not oncologically required, it is not advisable to completely skeletonize the hyoid bone, especially in previously irradiated patients, to reduce the risk of postoperative osteonecrosis.
- Conversely, when detaching the MhM from the inner mandibular surface, it is advisable to use monopolar cautery, taking care to cut the fibers directly over the bone in a subperiosteal plane (a blunt dissector can be also used to assist the surgeon in this crucial maneuver). This is of paramount importance, especially when managing tumors involving the antero-lateral floor of the mouth, with close relationship to the mandible, even without radiological signs of erosion, in order to assess a possible limited cortical bone or periosteal neoplastic invasion.

Step 5 - Approach to the Midline in the Submental Area

Once the lateral compartment has been prepared, the head is turned to a neutral position while extended in order to fully

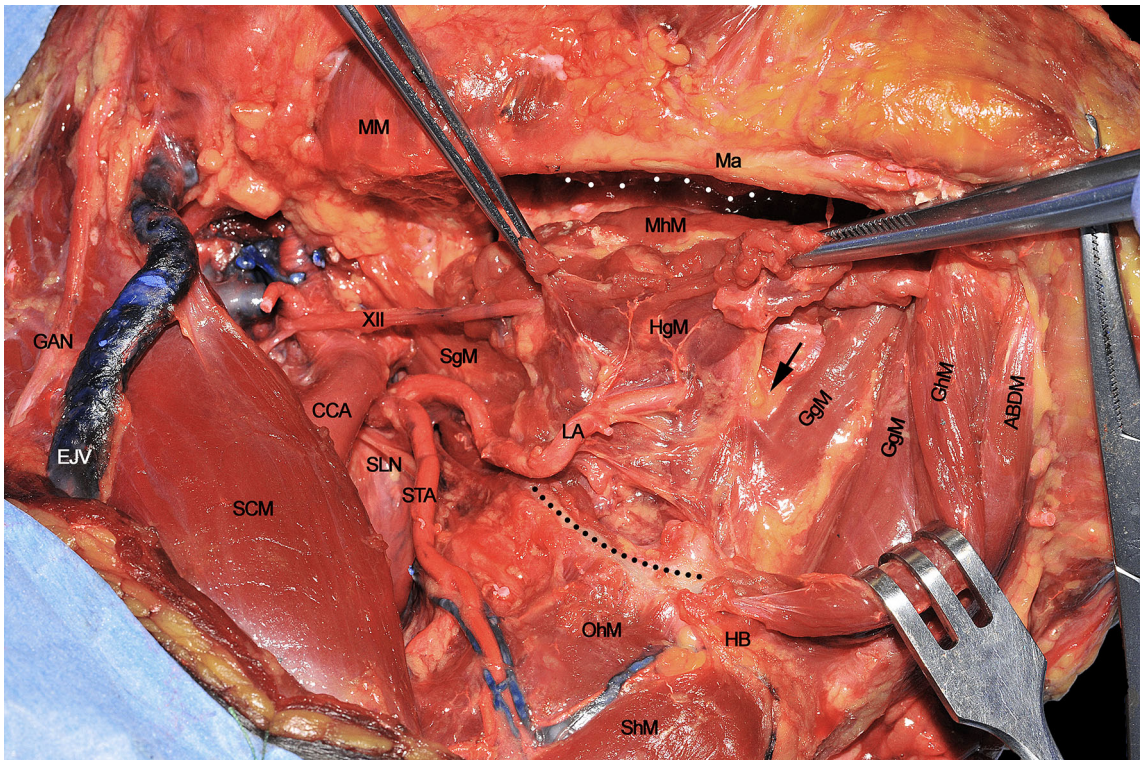

FIGURE 4 | ABDM, anterior belly of digastric muscle; CCA, common carotid artery; EJV, external jugular vein; GAN, great auricular nerve; GgM, genioglossus muscle; GhM, geniohyoid muscle; HB, hyoid bone; HgM, hyoglossus muscle; LA, lingual artery; Ma, mandible; MhM, mylohyoid muscle; MM, masseter muscle; OhM, omohyoid muscle; SCM, sternocleidomastoid muscle; SgM, styloglossus muscle; ShM, sternohyoid muscle; SLN, superior laryngeal nerve; STA, superior thyroid artery; XII, hypoglossal nerve. White dotted line, mylohyoid line of the mandible. Black dotted line, great hyoid cornu. Black arrow, paramedian septum of the tongue.

expose the region from the hyoid bone up to the mandible. The midline is found by sectioning the MhM in between the two ABDMs. The section line (**Figure 5A**) should be traced from the body of the hyoid bone to the genial tubercles of the mandible. In the present cadaver dissection, the right digastric muscle has been removed to better expose the underlying anatomy, while it is easily recognizable on the left side. Particular care should be given to the MhM dissection in order to properly find the midline between the GhMs, just beneath its deeper surface. This step is crucial when treating tumors massively involving the anterior floor of mouth, to exclude possible neoplastic spread through the midline into the opposite compartment. Moreover, adequate intraoperative assessment of the MhM deeper portion is mandatory, due to the possible presence of in-transit nodal metastases and/or tumor satellitosis at this level.

Once the dissection of the MhM has been completed along the midline, this can be retracted laterally to fully expose the underlying GhM. This leads to optimal visualization of the paramedian lingual septum, which contains lymphatic vessels and nodes, neural bundles of the LN, the sublingual gland (SlG), and branches of the sublingual artery (SLA) (**Figure 5B**). This space is of special relevance when performing CS, since it represents one of the most important routes for tumor spread.

The anatomical area in which the T-N tract can be located is defined by the following boundaries: the inferior aspect of the floor of mouth (FoM) mucosa cranially, the GhM anteriorly, and the HB caudally (black dotted line) (**Figure 6**).

Surgical tips and tricks

- When approaching the MhM, it can be difficult to properly identify its midline since the muscle fibers of both sides at this level are usually merged. An easy way for its correct identification is therefore to cut with electrocautery a line running from the genial tubercles to the midline of the HB identified by palpating the thyroid notch.
- Once the MhM is detached from the deeper GhM, particular care should be addressed to obtain accurate hemostasis due to the large number of small perforators between the two muscles. Keeping the surgical field as clean as possible in this phase may be of great help in correctly identifying the median raphe and contralateral muscular compartment.

Step 6 - Deeper Midline Raphe Dissection

Once the GhM has been resected, the midline fibrous raphe between the two hemilingual compartments is clearly

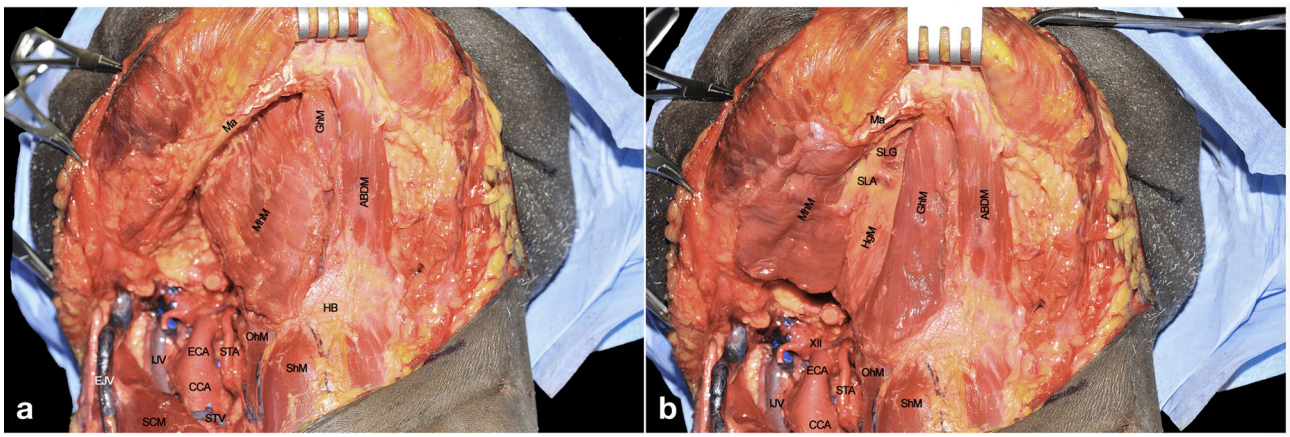

FIGURE 5 | **(A, B)** ABDM, anterior belly of digastric muscle; CCA, common carotid artery; ECA, external carotid artery; EJV, external jugular vein; GhM, geniohyoid muscle; HB, hyoid bone; HgM, hyoglossus muscle; IJV, internal jugular vein; Ma, mandible; MhM, mylohyoid muscle; OhM, omohyoid muscle; SCM, sternocleidomastoid muscle; ShM, sternohyoid muscle; SLA, sublingual artery; SlG, sublingual gland; STA, superior thyroid artery; STV, superior thyroid vein; XII, hypoglossal nerve.

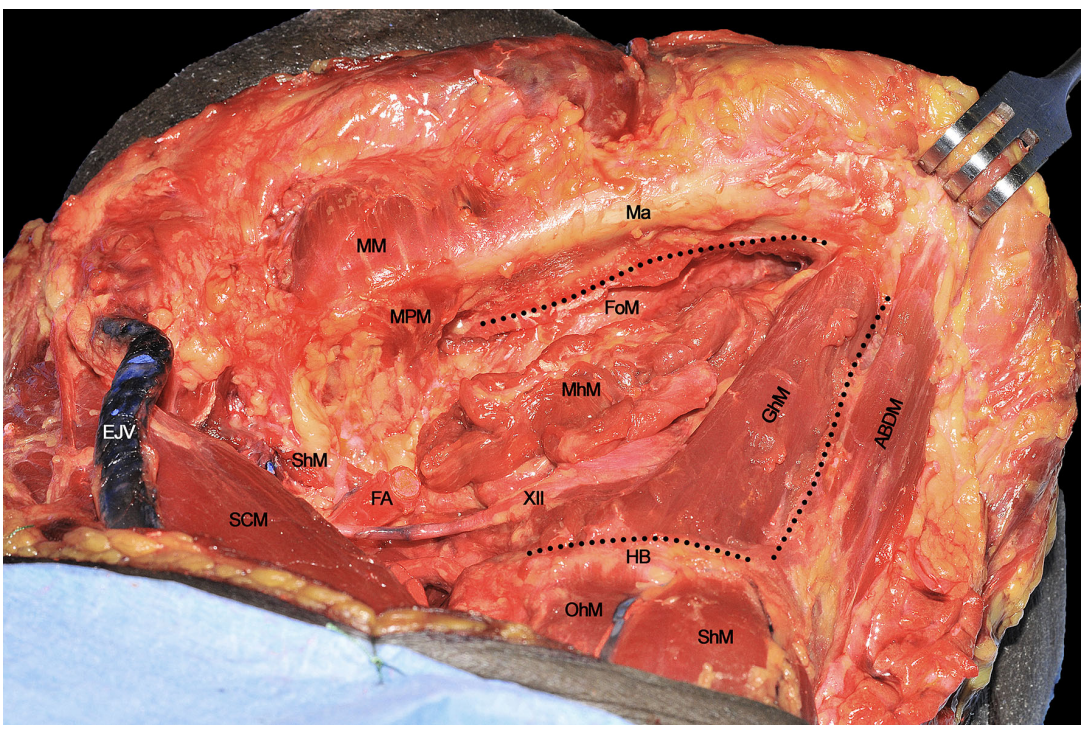

FIGURE 6 | ABDM, anterior belly of digastric muscle; EJV, external jugular vein; FA, facial artery; FoM, floor of mouth; GhM, geniohyoid muscle; HB, hyoid bone; Ma, mandible; MhM, mylohyoid muscle; MM, masseter muscle; MPM, medial pterygoid muscle; OhM, omohyoid muscle; SCM, sternocleidomastoid muscle; ShM, sternohyoid muscle; StM, stylohyoid muscle; XII, hypoglossal nerve. Black dotted line, boundaries of the anatomical area containing the T-N tract.

recognizable. It is imperative to not resect muscular or neurovascular structures of the healthy side in order to minimize any undue functional impairment. Separation of the two compartments at this level is usually easily obtained by blunt dissection, using a cotton swab or dissector. This maneuver is also useful to palpate the lingual body from below in order to assess the tumor characteristics and possible critical issues such as endophytic extension, distance from the midline, or presence of

satellitosis. The insertion of the removed right GhM is visible at the level of the inferior genial tubercle (arrow), while the deeper extrinsic muscular layer (represented by the GgM) is now clearly visible (**Figure 7A**). The latter is the most represented structure of the mobile tongue and is of pivotal importance for tumor spread due to its spatial fan-shaped fibers arrangement, disposed from the upper genial tubercle to the rest of the mobile tongue itself, and its large volume accounting for more than half of the lingual body. The GgM must be separated from the contralateral one using monopolar cautery, starting from its mandibular insertion, to the HB and glosso-epiglottic valleculae (**Figure 7B**).

The resected GgM is laterally and posteriorly displaced, pulling it from its mandibular tendon (**Figure 7C**). Both cranially and caudally, particular care should be paid to not damage the floor of mouth or glosso-epiglottic mucosa. In this way, the median raphe is completely transected up to the intrinsic tongue musculature and mucosa. When the midline dissection is complete, a clear vision of the opposite tongue compartment should be appreciated (**Figure 8**).

Surgical tips and tricks

- A useful trick to correctly identify the midline is to use a cotton swab to manipulate the muscular bundles and avoid annoying bleeding. The GgM and GhM are covered by a thin fascia that give these structures a round and well-defined contour, helping the surgeon to recognize the fascial planes between different muscular layers.
- When the midline is precisely located, the assistant surgeon should apply countertraction from the healthy side to facilitate dissection. Once the muscles are spread apart, the yellowish tissue of the median raphe is exposed. At this point, a gauze can be placed from below in order to keep one compartment separated from the contralateral one and to correctly identify the midline when subsequently performing the transoral resection by incising the mucosa between the two Wharton's ducts.

Step 7 – Assessment of Routes of Tumor Spread

When every extrinsic muscular, neural and vascular structure have been dissected, the entire ipsilateral hemilingual compartment is detached from its anterior/cranial (mandible), caudal (HB), contralateral (opposite lingual compartment), and posterior/cranial insertions (mastoid and styloid processes). The most important advantage of CS is that it allows the most

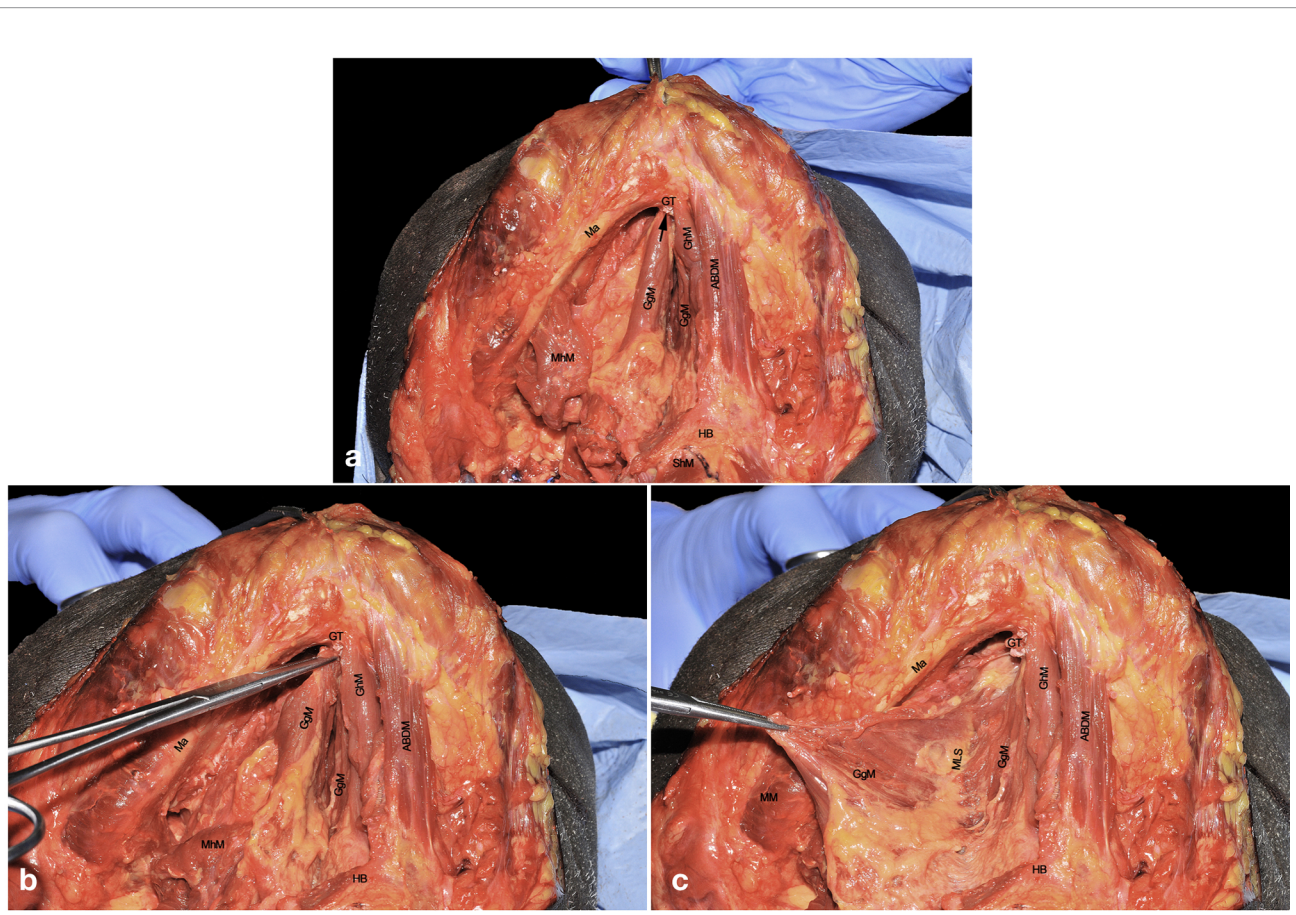

FIGURE 7 | **(A–C)** ABDM, anterior belly of digastric muscle; GgM, genioglossus muscle; GhM, geniohyoid muscle; GT, genial tubercle; HB, hyoid bone; Ma, mandible; MhM, mylohyoid muscle; MM, masseter muscle; MLS, median lingual septum; ShM, sternohyoid muscle. Black arrow, right inferior genial tubercle.

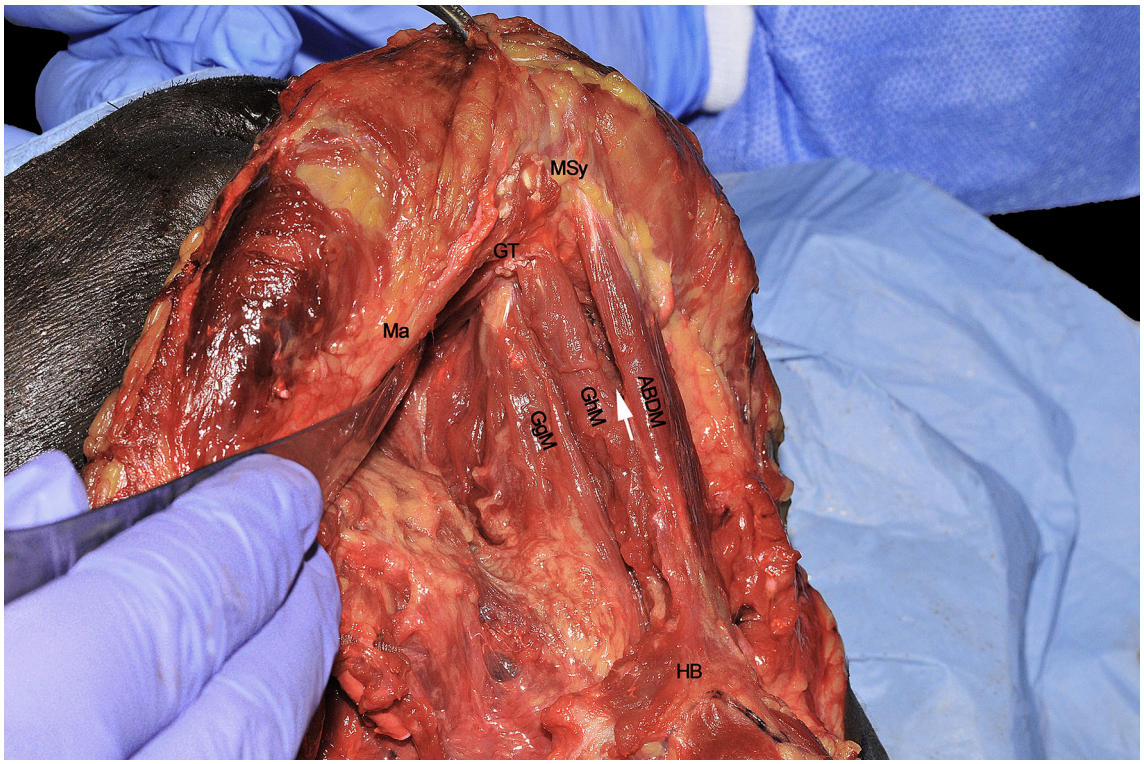

FIGURE 8 | ABDM, anterior belly of digastric muscle; GgM, genioglossus muscle; GhM, geniohyoid muscle; GT, genial tubercle; HB, hyoid bone; Ma, mandible; MSy, mandibular symphysis. White arrow, thin left mylohyoid muscle between the ipsilateral ABDM and GhM.

adequate control of all possible routes for centrifugal tumor spread that, starting from posterior to anterior, in an anti-clockwise direction, are shown herein: 1) SgM (towards the skull base), 2) XII cranial nerve (towards the vascular axis and skull base), 3) LA (towards the vascular axis), 4) HgM (towards the HB), and 5) GgM (towards the mandible) (**Figure 9**). In the middle of this complex surgical space, the MhM and GhM alongside the LN and all the lymphatic and glandular structures are located.

Step 8 - Transoral Resection and Pull-Through Maneuver

When the lingual compartment (right in the present cadaver dissection) has been prepared from the neck, it is possible to access the tumor through the oral cavity. The operating surgeon moves to the patient's head and dissection starts from the anterior FoM, between the two openings of the Wharton's ducts. A communication with the underlying neck space is created at this level and identification of the gauze previously positioned from the neck helps the surgeon to complete the dissection in the correct plane. Next, resection proceeds in a caudo-cranial direction, towards the ventral and dorsal surfaces of the tongue, maintaining the tumor under direct vision/palpation, and strictly following the midline lingual raphe. Dissection can be safely carried *via* the transoral route up to the circumvallate papillae in most patients without trismus (**Figure 10**). According to the posterior extension of the tumor towards the oropharynx, if the surgeon needs to perform a complete tongue base removal, the pull-through maneuver must be performed by cutting the mucosa of the lateral (paramandibular) FoM and pulling the involved hemilingual compartment into the neck. In this way, a complete compartmental resection addressing the posterior aspect of the base of tongue up to the glosso-epiglottic vallecula can be safely accomplished (**Figure 11**). Otherwise, if some mucosa and intrinsic muscles of the base of the tongue can be safely spared since a large (i.e. 2 cm) cuff of healthy tissues is already present at the posterior margin of the tumor, the dissection proceeds in an anterior to posterior direction reaching the hyo-glossal membrane, anterior and deep to the base of tongue, perpendicular to the midline raphe, where surgical resection may change its course from medial to lateral, up to the anterior tonsillar pillar. This surgical step is quite important since the entity of oropharyngeal resection can be modulated under direct view through the neck.

The T-N tract, completely released from all its muscular insertions and neural/vascular supplies, is visible as composed by the sublingual and submandibular glands (previously removed), extrinsic tongue muscles (GhM, GgM, HgM, and SgM) and MhM, LA and vein, XII cranial nerve, LN, and the lymphatic vessels and nodes embedded in the median and

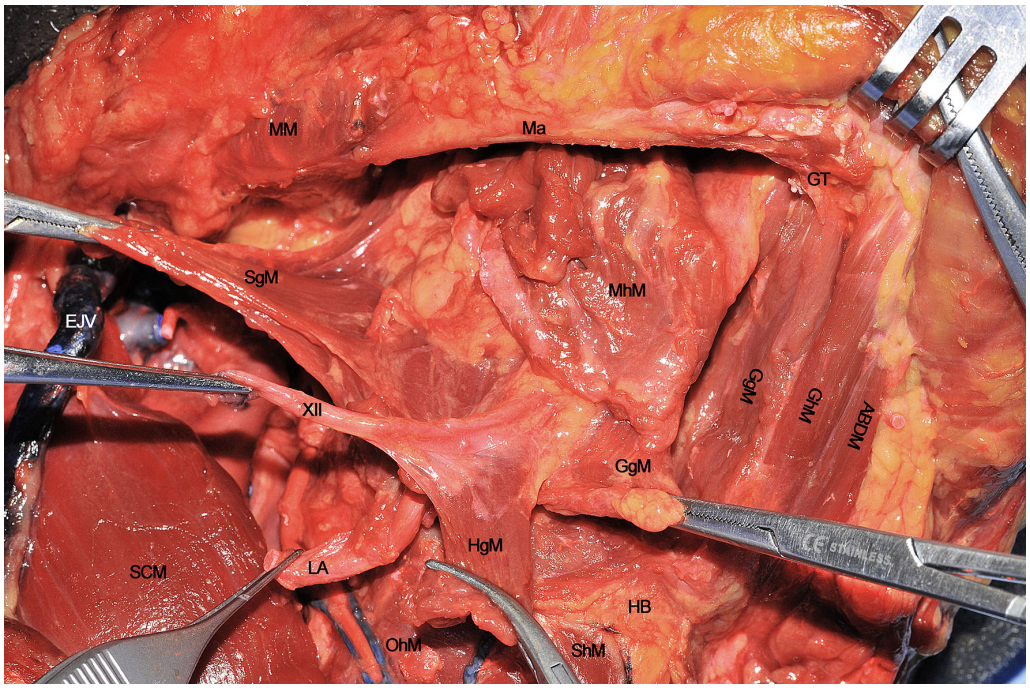

FIGURE 9 | ABDM, anterior belly of digastric muscle; EJV, external jugular vein; GgM, genioglossus muscle; GhM, geniohyoid muscle; GT, genial tubercle; HB, hyoid bone; HgM, hyoglossus muscle; LA, lingual artery; Ma, mandible; MhM, mylohyoid muscle; MM, masseter muscle; OhM, omohyoid muscle; SCM, sternocleidomastoid muscle; SgM, styloglossus muscle; ShM, sternohyoid muscle; XII, hypoglossal nerve.

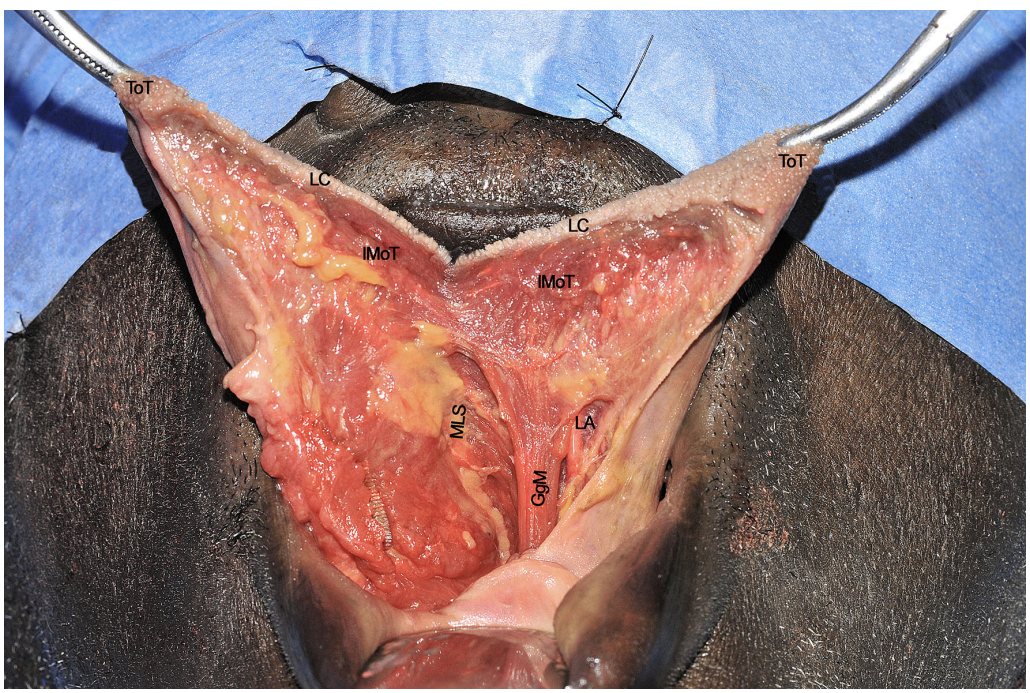

FIGURE 10 | GgM, genioglossus muscle; IMoT, intrinsic musculature of the tongue; LA, lingual artery; LC, lingual cover; MLS, median lingual septum; ToT, tip of tongue. Please note that the nose is covered by the blue drape and the inferior lip pulled down by a retractor.

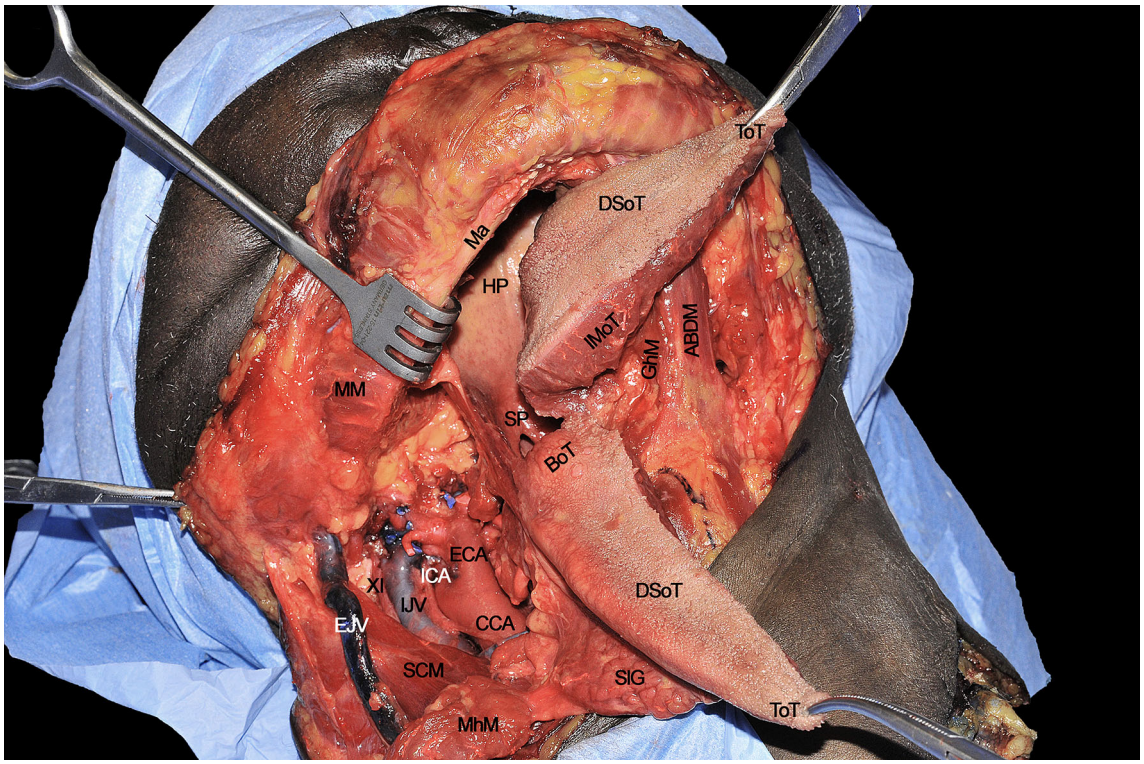

FIGURE 11 | ABDM, anterior belly of digastric muscle; BoT, base of tongue; CCA, common carotid artery; DSoT, dorsal surface of tongue; ECA; external carotid artery; EJV, external jugular vein; IJV, internal jugular vein; GhM, geniohyoid muscle; HP, hard palate; ICA, internal carotid artery; IMoT, intrinsic muscle of tongue; Ma, mandible; MhM, mylohyoid muscle; MM, masseter muscle; SCM, sternocleidomastoid muscle; SlG, sublingual gland; SP, soft palate; ToT, tip of tongue; XI, spinal accessory nerve.

paramedian septa (**Figure 12**). The final step of the CS is represented by the detachment of the specimen from the glosso-epiglottic vallecula, keeping attention to spare healthy mucosa at this level which can be used for an effective flap suture during the reconstructive phase.

Surgical tips and tricks

- The tracheostomy (if not done previously) should be performed to remove the tube from the oral cavity and thus secure the postoperative airways. In some cases, this step can be postponed at the end of surgery if nasotracheal intubation has been performed. Others prefer to perform tracheostomy at the beginning of surgical procedure, to avoid any possible neoplastic seeding at the level of the tracheal wound by "contaminated" instrumentation. In any case, before starting the transoral step, the anesthesiologist should provide an optimal muscle relaxation in order to maximize oral opening.
- A self-retaining mouth and lips retractor and/or bite blocks can be used to optimize the view of the surgical field.
- Electrocautery or ultrasonic scalpels are usually applied to reduce bleeding during this phase, especially at the level of the contralateral (healthy) hemilingual compartment.
- The tip of tongue can be spared when not directly involved by the tumor since it is composed only of intrinsic muscles and not anatomically reached by the GgM fibers. This definitively improves postoperative speech without affecting oncologic outcomes.
- When sampling tissue for frozen sections, especially along the midline of the oral tongue, it is advisable to use a cool blade knife to reduce the shrinkage and cautery/crush artifacts of the specimen to be analyzed.
- When dissection between the two openings of the Wharton's duct in the anterior aspect of the FoM is performed, particular attention should be paid to not accidentally injure the healthy side. The same holds true when suturing, at the end of surgery, the free flap at this level.
- Whenever the midline is reached by the tumor without invasion of the opposite side, a cuff of extrinsic/intrinsic muscles of the healthy hemilingual compartment should be taken as a safe extra-margin.
- When lateral FoM mucosa is incised medial to the mandibular body, at least 5 mm of healthy tissue should be spared at this level, if oncologically feasible, in order to guarantee enough recipient mucosa for the in-set of the free flap. If this is not possible, suturing the flap cutaneous edge to the mucosa of the gum passing the stitches in between teeth can be used as an effective trick to reduce the risk of salivary fistula.

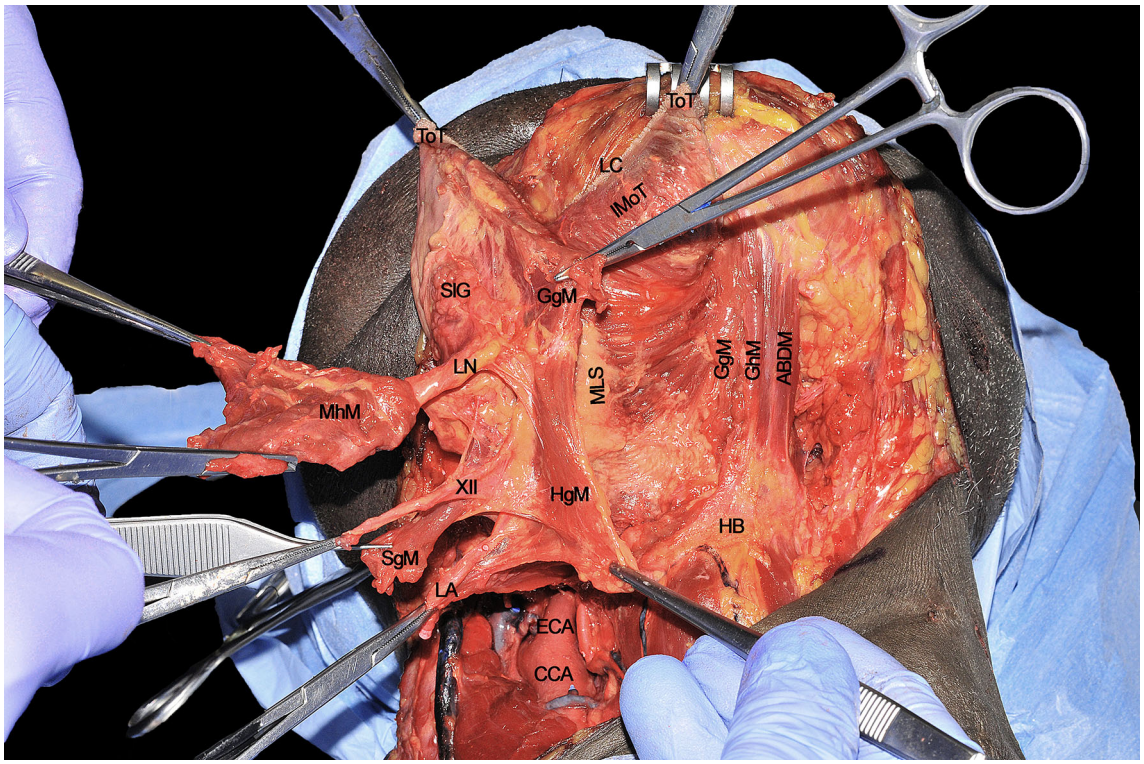

FIGURE 12 | ABDM, anterior belly of digastric muscle; CCA, common carotid artery; ECA; external carotid artery; HB, hyoid bone; HgM, hyglossus muscle; GgM, genioglossus muscle; GhM, geniohyoid muscle; IMoT, intrinsic muscle of tongue; LA, lingual artery; LC, lingual cover; LN, lingual nerve; MhM, mylohyoid muscle; MLS, median lingual septum; SgM, styloglossus muscle; SlG, sublingual gland; ToT, tip of tongue; XII, hypoglossal nerve.

- For tumors massively involving the BoT and/or associated with severe trismus, a median/paramedian mandibulotomy to widen the surgical field and guarantee an optimal visualization and dissection of the tumor may be of great help. All the steps herein described for CS can be equally performed *via* transoral or transmandibular routes.

Step 9 - Surgical Defect and Specimen Evaluation

At the end of procedure, the surgical defect results in a wide communication between oral cavity/oropharynx and neck, delimited by the symphysis and body of the mandible anterolaterally, constrictor muscles and tonsillar region posteriorly, HB and glosso-epiglottic vallecula inferiorly, and healthy contralateral tongue compartment medially (**Figure 13**).

The surgical specimen at the end of CS includes the right hemitongue (from the tip to the circumvallate papillae), ipsilateral FoM with related T-N tract, and the distal fringes of all the extrinsic muscles (**Figure 14**). The latter are herein clearly identifiable: the SgM reaches the tongue from posterior and its inferior muscular fibers intertwine in the posterior-lateral part of the tongue with those coming from the HgM, reaching the organ with an inferior-superior course. The LN runs in a lateral direction ventrally to the MhM adjacent to the SlG, while the XII cranial nerve is in strict relationships with the HgM, and the LA lies deeply to it. The fan-shaped fibers of the GgM are visible below the FoM and form large part of the volume of the tongue just cranially to the GhM.

DISCUSSION

CS of the tongue has been demonstrated to be a sound oncological technique, especially for tumors with a DOI ≥10 mm staged as cT3-T4 according to the 8th Edition of the AJCC-UICC TNM classification (13). The advantages are: 1) complete removal of the primary tumor along with the involved muscle compartment (which can potentially house in-transit perineural and/or lympho-vascular micrometastases and tumor satellitosis), thus improving local and loco-regional control; 2) surgical paradigm shift from a circumferential to an anatomical resection driven by the potential escape routes of the tumor itself; 3) standardization of the surgical ablation with consequent increase of both reproducibility and appropriate reconstructive planning.

This technique, first proposed by Calabrese and coworkers in 2009 (3), is based on the oncological principles of sarcoma surgery of the limbs (1, 2). In this view, the oral tongue is considered as a paired symmetric organ acting as the union of two compartments, identical in terms of spatial arrangement of

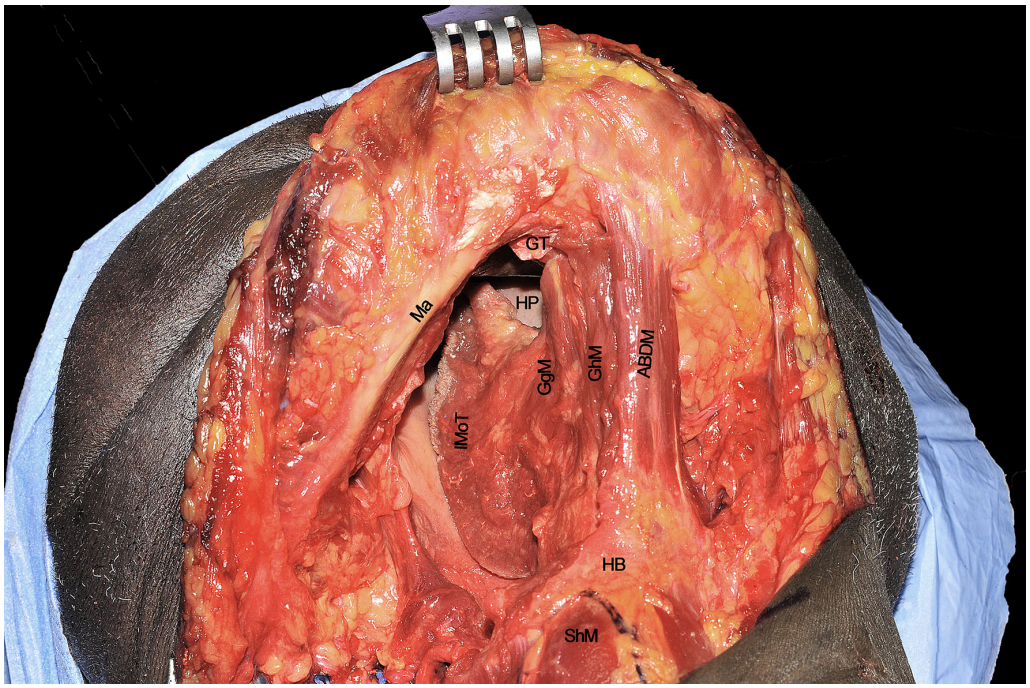

FIGURE 13 | ABDM, anterior belly of digastric muscle; HB, hyoid bone; GgM, genioglossus muscle; GhM, geniohyoid muscle; GT, genial tubercle; HP, hard palate; IMoT, intrinsic muscle of tongue; Ma, mandible; ShM, sternohyoid muscle.

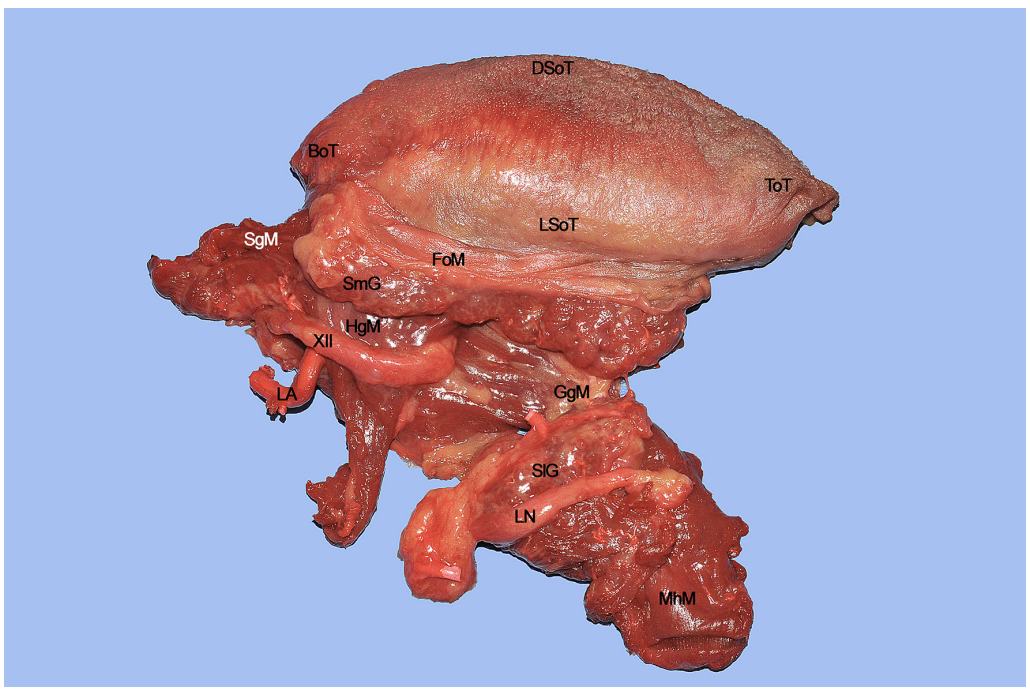

FIGURE 14 | BoT, base of tongue; DSoT, dorsal surface of tongue; FoM, floor of mouth; GgM, genioglossus muscle; HgM, hyoglossus muscle; LA, lingual artery; LN, lingual nerve; LSoT, lateral surface of tongue; MhM, mylohyoid muscle; SgM, styloglossus muscle; SlG, sublingual gland; ToT, tip of tongue; XII, hypoglossal nerve.

extrinsic and intrinsic muscles and presence of intermuscular connective structures (median raphe, paramedian, and lateral septa) (12). The median raphe represents a natural barrier that separates each hemitongue from the opposite one, while laterally and anteriorly the mandibular periosteum represents its peripheral boundary. Inside the lingual body, all the extrinsic muscles, XII cranial nerve and LN, LA, veins and lymphatic vessels act as routes potentially causing persistent/recurrent loco-regional disease if not correctly addressed by surgery. This has been clearly demonstrated in seminal papers assessing the clinical relevance of the longitudinal path of tumor spread along tongue musculature (14, 15), quite similar to what has been described for sarcomas of the musculoskeletal system. Controlling such potential routes of tumor progression by a CS approach may significantly impact local and loco-regional tumor control as well as survival (4, 5, 16–19).

To support this thesis and anatomical considerations, Calabrese et al. in 2011 (4) presented the first case series of 143 patients affected by cT2-T4 cN0-N+ squamous cell carcinoma (SCC) of the oral tongue or floor of the mouth treated by CS compared to 50 patients treated by standard transoral surgery within clear margins (>1 cm). The oncological outcomes showed a 5-year local control (LC) of 88.4% (16.8% improvement compared to the control group), loco-regional control (LRC) of 83.5% (24.4% improvement), and overall survival (OS) of 70.7% (27.3% improvement).

Another study published in 2019 by Piazza et al. (5) focused on a retrospective analysis on 45 patients managed by CS for SCC of the oral tongue/floor of mouth (35 naïve patients and 10 in a salvage setting), showed that 2-year OS, disease free survival (DFS), LC, and LRC were 80%, 91%, 100%, and 94%, respectively, in previously untreated patients. On the other hand, prognosis was poor in those undergoing salvage surgery, showing a 2-year OS, DFS, LC, and LRC of 27%, 26%, 67%, and 36%, respectively. This confirmed that CS has a main role as primary surgical treatment in locally advanced oral tongue cancers, whereas survival remains extremely poor for recurrent disease.

The herein mentioned paradigm shift from a traditional circumferential to a CS approach can draw some criticisms because it can initially appear more aggressive, especially towards anatomical structures that are not macroscopically involved by the tumor. However, from a functional point of view, when a muscle is even partially resected as during standard surgery, its function is completely compromised and scar tissue substitutes it, potentially tethering the tongue residue, and impairing swallowing and speech functions. In fact, Ji et al. (20) demonstrated a significant difference between microsurgical reconstruction after partial *vs*. hemiglossectomies showing more functional impairment in the former. To further analyze functional outcomes in CS followed by microsurgical reconstructions in terms of swallowing and speech, a retrospective study on 48 patients was conducted by Grammatica and coworkers (7). The conclusion of this study was that CS does not significantly affect speech, while sub-clinical liquid food aspiration and vallecular pouch are present in a significant proportion of patients, especially after adjuvant non-surgical treatments. However, this issue is usually not subjectively perceived as a major problem, and no aspiration pneumonia occurred in our surgical series. Of note, when the residual tongue was tested using a device that objectively assesses muscular strength and endurance, it seemed that these were not macroscopically affected when proper reconstruction had been accomplished.

CONCLUSIONS

The landmark concepts of CS herein depicted consist of: 1) anatomically-based approach to the lesion within the tongue and floor of mouth compartment, aiming to control all potential pathways of tumor progression; 2) clear identification of the anatomical space between primary and cervical nodes (the so called T-N tract), potentially acting as a high-risk metastatic basin; 3) good reproducibility and standardization of the surgical technique. A rational resectional approach associated with modern microsurgical reconstructive techniques maximizes oncological outcomes, while not affecting the mobility and function of the contralateral healthy hemitongue.

DATA AVAILABILITY STATEMENT

The original contributions presented in the study are included in the article/supplementary material. Further inquiries can be directed to the corresponding author.

AUTHOR CONTRIBUTIONS

Study design: all authors. Anatomical dissections: AG, CP, MF, VV, LC. Drafting of the manuscript: all authors. Revision of the manuscript: AG, CP, AP, LC. All authors contributed to the article and approved the submitted version.

ACKNOWLEDGMENTS

The authors acknowledge MedCure's provision of anatomical specimens.

REFERENCES

1. Enneking WF, Spanier SS, Goodman MA. A System for the Surgical Staging of Musculoskeletal Sarcoma. *Clin Orthop Relat Res* (1980) 153:106–20. doi: 10.1097/00003086-198011000-00013
2. Azzarelli A. Surgery in Soft Tissue Sarcomas. *Eur J Cancer* (1993) 29A:618–23. doi: 10.1016/s0959-8049(05)80165-0
3. Calabrese L, Giugliano G, Bruschini R, Ansarin M, Navach V, Grosso E, et al. Compartmental Surgery in Tongue Tumors: Description of a New Surgical Technique. *Acta Otorhinolaryngol Ital* (2009) 29:259–64.
4. Calabrese L, Bruschini R, Giugliano G, Ostuni A, Maffini F, Massaro MA, et al. Compartmental Tongue Surgery: Long Term Oncologic Results in the Treatment of Tongue Cancer. *Oral Oncol* (2011) 47:174–9. doi: 10.1016/j.oraloncology.2010.12.006

5. Piazza C, Grammatica A, Montalto N, Paderno A, Del Bon F, Nicolai P. Compartmental Surgery for Oral Tongue and Floor of the Mouth Cancer: Oncologic Outcomes. *Head Neck* (2019) 41:110–5. doi: 10.1002/hed.25480
6. Tagliabue M, Gandini S, Maffini F, Navach V, Bruschini R, Giugliano G, et al. The Role of the T-N Tract in Advanced Stage Tongue Cancer. *Head Neck* (2019) 41:2756–67. doi: 10.1002/hed.25761
7. Grammatica A, Piazza C, Montalto N, Del Bon F, Frittoli B, Mazza M, et al. Compartmental Surgery for Oral Tongue Cancer: Objective and Subjective Functional Evaluation. *Laryngoscope* (2020) 131(1):E176–83. doi: 10.1002/lary.28627. online ahead of print.
8. Fukano H, Matsuura H, Hasegawa Y, Nakamura S. Depth of Invasion as a Predictive Factor for Cervical Lymph Node Metastasis in Tongue Carcinoma. *Head Neck* (1997) 19:205–10. doi: 10.1002/(sici)1097-0347(199705)19:3<205::aid-hed7>3.0.co;2-6
9. Takemoto H. Morphological Analyses of the Human Tongue Musculature for Three-Dimensional Modeling. *J Speech Lang Hear Res* (2001) 44:95–107. doi: 10.1044/1092-4388(2001/009
10. Boland PW, Pataridis K, Eley KA, Golding SJ, Watt-Smith SR. A Detailed Anatomical Assessment of the Lateral Tongue Extrinsic Musculature, and Proximity to the Tongue Mucosal Surface. Does This Confirm the Current TNM T4a Muscular Subclassification? *Surg Radiol Anat* (2013) 35:559–64. doi: 10.1007/s00276-013-1076-6
11. Piazza C, Montalto N, Paderno A, Taglietti V, Nicolai P. Is it Time to Incorporate "Depth of Infiltration" in the T Staging of Oral Tongue and Floor of Mouth Cancer? *Curr Opin Otolaryngol Head Neck Surg* (2014) 22:81–9. doi: 10.1097/MOO.0000000000000038
12. Abd El-Malek S. Observations on the Morphology of the Human Tongue. *J Anat* (1938) 73:201–10.
13. Brierley JD, Gospodarowicz MK, Wittekind C. *Tnm Classification of Malignant Tumors. 8th Edition*. John Wiley & Sons, Oxford UK; Hoboken NJ; Union Int Cancer Control (2017). doi: 10.1002/ejoc.201200111
14. Steinhart H, Kleinsasser O. Growth and Spread of the Squamous Cell Carcinoma of the Floor of the Mouth. *Eur Arch Otorhinolaryngol* (1993) 250:358–61. doi: 10.1007/BF00188386
15. Prince S, Bailey BM. Squamous Carcinoma of the Tongue: Review. *Br J Oral Maxillofac Surg* (1999) 37:164–74. doi: 10.1054/bjom.1999.0031
16. Woolgar JA. T2 Carcinoma of the Tongue: The Histopathologist's Perspective. *Br J Oral Maxillofac Surg* (1999) 37:187–93. doi: 10.1054/bjom.1999.0034
17. De Wever O, Mareel M. Role of Tissue Stroma in Cancer Cell Invasion. *J Pathol* (2003) 200:429–47. doi: 10.1002/path.1398
18. Woolgar JA. Histopathological Prognosticators in Oral and Oropharyngeal Squamous Cell Carcinoma. *Oral Oncol* (2006) 42:229–39. doi: 10.1016/j.oraloncology.2005.05.008
19. Vered M, Dobriyan A, Dayan D, Yahalom R, Talmi YP, Bedrin L, et al. Tumor-Host Histopathologic Variables, Stromal Myofibroblasts and Risk Score, are Significantly Associated With Recurrent Disease in Tongue Cancer. *Cancer Sci* (2010) 101:274–80. doi: 10.1111/j.1349-7006.2009.01357.x
20. Ji YB, Cho YH, Song CM, Kim YH, Kim JT, Ahn HC, et al. Long-Term Functional Outcomes After Resection of Tongue Cancer: Determining the Optimal Reconstruction Method. *Eur Arch Otorhinolaryngol* (2017) 274:3751–6. doi: 10.1007/s00405-017-4683-8

Conflict of Interest: The authors declare that the research was conducted in the absence of any commercial or financial relationships that could be construed as a potential conflict of interest.

frontiers in Oncology

ORIGINAL RESEARCH
published: 23 April 2021
doi: 10.3389/fonc.2021.644306

Contralateral Regional Recurrence in Lateralized or Paramedian Early-Stage Oral Cancer Undergoing Sentinel Lymph Node Biopsy—Comparison to a Historic Elective Neck Dissection Cohort

*Rutger Mahieu[1], Inne J. den Toom[1], Koos Boeve[2,3], Daphne Lobeek[4], Elisabeth Bloemena[5,6,7], Maarten L. Donswijk[8], Bart de Keizer[9], W. Martin C. Klop[10], C. René Leemans[11], Stefan M. Willems[3,12], Robert P. Takes[13], Max J. H. Witjes[2] and Remco de Bree[1]**

[1] Department of Head and Neck Surgical Oncology, University Medical Center Utrecht, Utrecht, Netherlands, [2] Department of Oral and Maxillofacial Surgery, University Medical Center Groningen, University of Groningen, Groningen, Netherlands, [3] Department of Pathology and Medical Biology, University Medical Center Groningen, University of Groningen, Groningen, Netherlands, [4] Department of Radiology, Nuclear Medicine and Anatomy, Radboud University Medical Center, Nijmegen, Netherlands, [5] Department of Oral and Maxillofacial Surgery, Amsterdam University Medical Center, Amsterdam, Netherlands, [6] Oral Pathology, Academic Center for Dentistry (ACTA) Amsterdam, Amsterdam, Netherlands, [7] Department of Pathology, Amsterdam University Medical Center, Amsterdam, Netherlands, [8] Department of Nuclear Medicine, The Netherlands Cancer Institute, Amsterdam, Netherlands, [9] Department of Radiology and Nuclear Medicine, University Medical Center Utrecht, Utrecht, Netherlands, [10] Department of Head and Neck Surgery, The Netherlands Cancer Institute, Amsterdam, Netherlands, [11] Department of Otolaryngology-Head and Neck Surgery, Amsterdam University Medical Center, Amsterdam, Netherlands, [12] Department of Pathology, University Medical Center Utrecht, Utrecht, Netherlands, [13] Department of Otolaryngology-Head and Neck Surgery, Radboud University Medical Center, Nijmegen, Netherlands

OPEN ACCESS

Edited by:
Alberto Paderno, University of Brescia, Italy

Reviewed by:
Jeroen Meulemans, University Hospitals Leuven, Belgium
Samskruthi P. Murthy, Kidwai Memorial Institute of Oncology, India

***Correspondence:**
Remco de Bree
r.debree@umcutrecht.nl

Specialty section:
This article was submitted to Head and Neck Cancer, a section of the journal Frontiers in Oncology

Received: *20 December 2020*
Accepted: *15 February 2021*
Published: *23 April 2021*

Citation:
Mahieu R, den Toom IJ, Boeve K, Lobeek D, Bloemena E, Donswijk ML, de Keizer B, Klop WMC, Leemans CR, Willems SM, Takes RP, Witjes MJH and de Bree R (2021) Contralateral Regional Recurrence in Lateralized or Paramedian Early-Stage Oral Cancer Undergoing Sentinel Lymph Node Biopsy—Comparison to a Historic Elective Neck Dissection Cohort. Front. Oncol. 11:644306. doi: 10.3389/fonc.2021.644306

Introduction: Nowadays, two strategies are available for the management of the clinically negative neck in early-stage (cT1-2N0) oral squamous cell carcinoma (OSCC): elective neck dissection (END) and sentinel lymph node biopsy (SLNB). SLNB stages both the ipsilateral and the contralateral neck in early-stage OSCC patients, whereas the contralateral neck is generally not addressed by END in early-stage OSCC not involving the midline. This study compares both incidence and hazard of contralateral regional recurrences (CRR) in those patients who underwent END or SLNB.

Materials and Methods: A retrospective multicenter cohort study, including 816 lateralized or paramedian early-stage OSCC patients, staged by either unilateral or bilateral END ($n = 365$) or SLNB ($n = 451$).

Results: The overall rate of occult contralateral nodal metastasis was 3.7% (30/816); the incidence of CRR was 2.5% (20/816). Patients who underwent END developed CRR during follow-up more often than those who underwent SLNB (3.8 vs. 1.3%; $p = 0.018$). Moreover, END patients had a higher hazard for developing CRR than SLNB patients (HR = 2.585; $p = 0.030$). In addition, tumor depth of invasion was predictive for developing CRR (HR = 1.922; $p = 0.009$). Five-year disease-specific survival in patients with

CRR was poor (42%) compared to patients in whom occult contralateral nodal metastases were detected by SLNB or bilateral END (88%), although not statistically different ($p = 0.066$).

Conclusion: Our data suggest that SLNB allows for better control of the contralateral clinically negative neck in patients with lateralized or paramedian early-stage OSCC, compared to END as performed in a clinical setting. The prognosis of those in whom occult contralateral nodal metastases are detected at an earlier stage may be favorable compared to those who eventually develop CRR, which highlights the importance of adequate staging of the contralateral clinically negative neck.

Keywords: mouth neoplasms, sentinel lymph node biopsy, neck dissection, lymphatic metastasis, contralateral, recurrence, survival

INTRODUCTION

In patients with early-stage (cT1-2N0) oral squamous cell carcinoma (OSCC), occult metastases are present in 20–30% of patients with a clinically negative neck, despite advanced diagnostic imaging modalities (1–3).

As watchful-waiting in these patients has been associated with a poor prognosis, especially when compared to those in whom the clinically negative neck was electively treated (1), two strategies are available for management of the clinically negative neck in early-stage OSCC: elective neck dissection (END) and sentinel lymph node biopsy (SLNB) (3–6). Although END is considered the best approach by many (5), SLNB has proven to reliably stage the clinically negative neck in early-stage OSCC with a pooled sensitivity and negative predictive value of 87 and 94%, respectively (4, 7–9). While END has the benefit of being a single-stage procedure, without need for specific facilities (e.g., nuclear medicine, advanced histopathology), SLNB is less invasive for the 70–80% of patients without metastatic neck involvement and has overall lower morbidity rates, better quality of life, and lower health care costs compared to END (10–13).

Furthermore, SLNB allows assessment of individual lymphatic drainage patterns and is able to detect aberrant drainage patterns (14, 15). This feature is of particular benefit in OSCC, since even lateralized OSCC occasionally metastasizes to contralateral cervical lymph nodes [2.7% (95% CI 1.2–4.2%)] (8, 9, 14, 16–21). Studies reported contralateral or bilateral lymphatic drainage patterns in 13–23% of lateralized OSCC patients, as detected during the SLNB procedure (8, 9, 14, 22).

Thus, SLNB stages the contralateral clinically negative neck in (lateralized) early-stage OSCC patients as well, whereas the contralateral clinically negative neck is generally not addressed by END in early-stage OSCC not involving the midline (i.e., lateralized or paramedian tumors).

Although the reported incidence of contralateral lymph node metastases in these patients is relatively low, underdiagnosis of the contralateral clinically negative neck is undesirable, especially since the presence of contralateral lymph node metastasis from OSCC has been associated with poor disease-specific survival (DSS) (16, 23, 24).

Therefore, this study aimed to assess whether SLNB allows for better control of the contralateral neck as compared to END, in early-stage OSCC not involving the midline. Accordingly, this study compares both incidence and hazard of contralateral regional recurrences (CRR) in those who underwent either END or SLNB as performed in daily clinical practice. Furthermore, this study compares the prognosis of those in whom occult contralateral nodal metastases were detected at an earlier stage by SLNB or bilateral END (pN2c) and those who eventually developed CRR.

MATERIALS AND METHODS

Ethical Considerations

This study abided the Declaration of Helsinki and was approved by UMC Utrecht's Ethics Committee (no. 17/766) and all participating centers. The Internal Review Board waived requirement for signed informed consent forms for all subjects (4). Samples and data were handled according to General Data Protection Regulation.

Patients

Patients without a history of head and neck cancer requiring treatment of the neck (i.e., neck dissection, neck irradiation) were included from five Dutch Head and Neck Cancer centers. In these centers, SLNB is currently part of standard oncological care in regard to staging the clinically negative neck in early-stage OSCC patients. Data were extracted from two large retrospective cohorts (END cohort and SLNB cohort), which have been extensively described by den Toom et al. (4).

For this study, only patients with early-stage OSCC (cT1-2N0) not involving the midline (i.e., lateralized or paramedian) were included in this study (AJCC UICC TNM-staging 7th Edition). Paramedian tumors were classified as tumors located adjacent to, but not involving, the midline. In all patients, clinical nodal staging was confirmed by palpation, imaging (i.e., ultrasound, CT, and/or MRI), and, in case of suspected lymph nodes, ultrasound-guided fine-needle aspiration cytology.

Patients who underwent unilateral END for tumors from which the specific location was missing were included. In these cases, it was estimated that performing unilateral END, instead

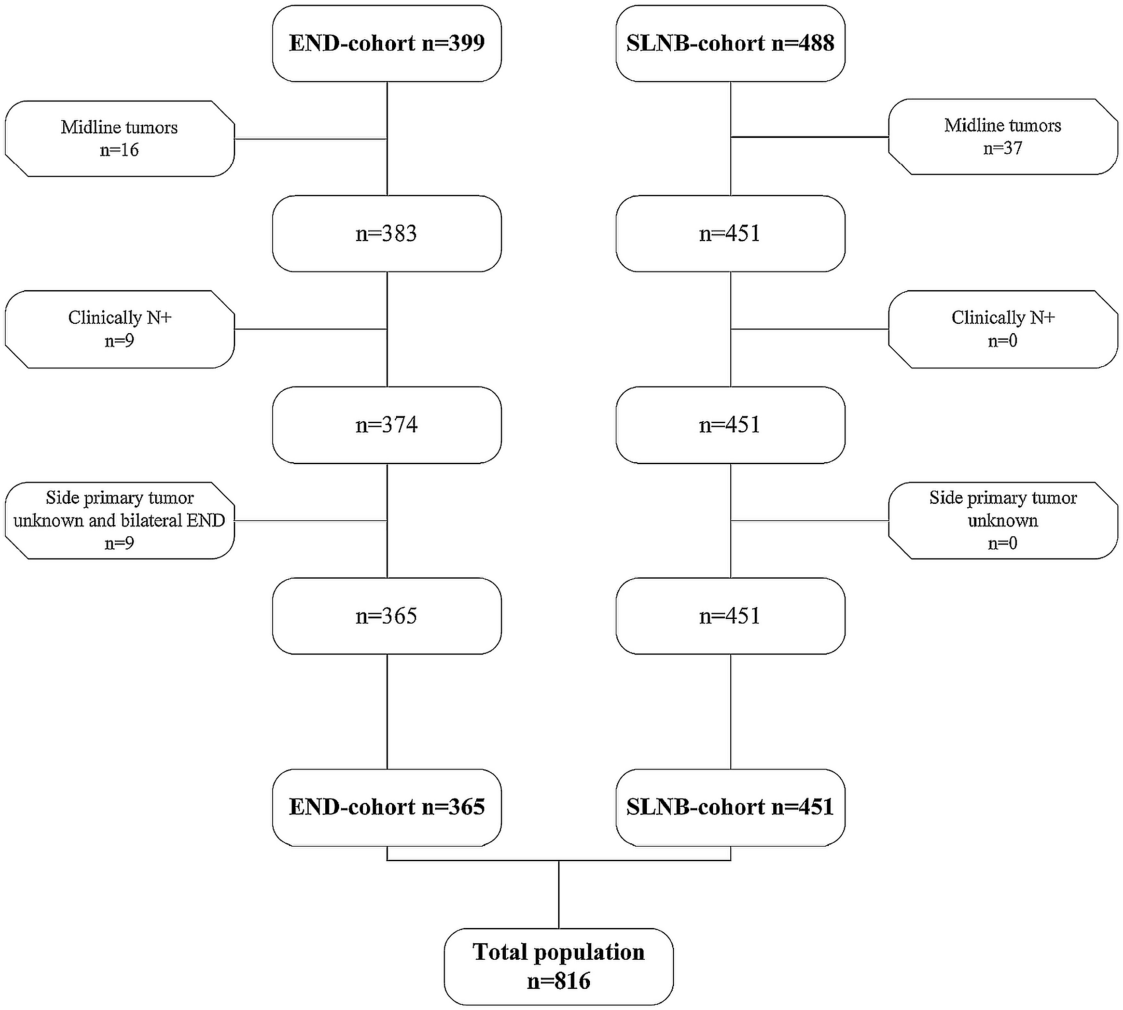

FIGURE 1 | Flowchart for inclusion of patients in both the END cohort ($n = 365$) and the SLNB cohort ($n = 451$).

of bilateral END, was on the basis of non-involvement of the midline. Patients who underwent bilateral END for confirmed lateralized or paramedian early-stage OSCC were included as well.

Patients were excluded if they underwent bilateral END for tumors from which the specific location was missing, as there was insufficient data to reliably assess whether the tumor involved the midline.

Out of 887 patients (END $n = 399$, SLNB $n = 488$), 816 patients met the inclusion criteria (END $n = 365$, SLNB $n = 451$) (**Figure 1**).

Elective Neck Dissection

The END cohort has been previously described by den Toom et al. (4); early-stage OSCC patients who underwent END between 1990 and 2015 were included in the END cohort. END was performed as selective (level I–III/IV; $n = 294$) or modified radical neck dissection (level I–V; $n = 70$). Twenty-eight patients (7.7%) underwent bilateral END for lateralized or paramedian early-stage OSCC. The decision to perform either unilateral or bilateral END was made by the treating physician. The indication for bilateral END was on discretion of the treating physician and multidisciplinary team. END was elected over watchful-waiting when tumor depth of invasion (DOI) was estimated to be >4 mm (25). Neck dissection specimens were histopathologically assessed using conventional hematoxylin–eosin staining on formalin-fixed paraffin-embedded tissue.

Sentinel Lymph Node Biopsy

Early-stage OSCC patients who underwent SLNB between 2007 and 2018 were included in the SLNB cohort. SLNB was performed according to European Association of Nuclear Medicine and Sentinel European Node Trial joint practice guidelines (26–28). SLNB was elected over watchful-waiting irrespective of tumor DOI. In short, the SLNB procedure

consisted of preoperative peritumoral injections with technetium-99m [^{99m}Tc]-labeled nanocolloid (80–240 MBq), followed by planar dynamic and static lymphoscintigraphy including SPECT-CT imaging, in a 1- or 2-day protocol. Intraoperative localization and extirpation of SLNs were performed using a handheld gammaprobe. Harvested SLNs were histopathologically assessed using step-serial sectioning (section thickness 150–500 μm) with hematoxylin–eosin staining and immunohistochemistry (26, 29). In SLNB-negative patients, a wait-and-scan policy was adopted, while SLNB-positive patients underwent complementary neck treatment. The vast majority of SLNB-positive patients underwent neck dissection as complementary neck treatment (85.6%; 89/104). Seven patients (6.7%) underwent complementary neck irradiation and three patients (2.9%) underwent complementary chemoradiation due to irradical resection of the primary tumor ($n = 2$) or presence of extracapsular spread of nodal metastasis ($n = 1$). Radiotherapy was employed only on the affected nodal basin in three patients, whereas in the other seven patients, the side and levels involved in neck irradiation were unknown.

CRR, pN2c and Occult Contralateral Nodal Metastasis

Regional recurrences that occurred in the contralateral neck of the initial primary tumor, within 5 years following treatment, were regarded as event for CRR analyses. In addition, CRR in the presence of ipsilateral regional recurrences were regarded as event for CRR analyses as well. Regional recurrences in the presence of local recurrence or second primary tumors were excluded from final analyses, as differentiation between missed nodal metastasis at initial diagnostic work-up and metastasis developed from reseeding local recurrence is unfeasible.

Nodal metastasis detected in the contralateral neck of the primary tumor at time of initial neck staging, by either SLNB or bilateral END, was classified as pN2c, irrespective of the nodal status of the ipsilateral neck.

Occult contralateral nodal metastasis was defined as lymph node metastasis in the contralateral neck of the initial primary tumor, which was detected by either SLNB or bilateral END (i.e., pN2c) or which became clinically manifest during follow-up (i.e., CRR).

Statistical Analysis

All data were analyzed with IBM SPSS Statistics Version 26.0. Data are expressed as mean ± SD for continuous variables. Number of cases and percentages are presented for categorical variables.

Independent samples *t* test was applied for parametric continuous variables, Mann–Whitney *U* test was applied for non-parametric continuous variables, and χ^2 test was applied for categorical variables. Fisher's exact test was used to compare categorical variables containing small number of cases ($n \leq 5$). *Post-hoc* testing was conducted in case of statistically significant χ^2 test or Fisher's exact test outcomes for categorical variables with ≥3 groups.

For comparing 5-year DSS between patients with occult contralateral nodal metastasis (i.e., pN2c, CRR) and those without, Log-Rank test was conducted and Kaplan–Meier survival curves were computed. Furthermore, 5-year DSS were compared between patients in whom contralateral nodal metastases were detected by SLNB or bilateral END (pN2c) and those who eventually developed CRR during follow-up.

To assess independent predictors of CRR over time, Cox-regression analysis was applied (Method: Backward Likelihood Ratio). Variables that showed univariate association with occult contralateral nodal metastasis (i.e., pN2c and/or CRR), at a level of $p \leq 0.05$, were included in the proportional hazard regression model. Accordingly, covariates were neck management (SLNB/END), initial ipsilateral pN+-status, location of primary tumor (i.e., paramedian or lateralized), vaso-invasive tumor growth, perineural tumor growth, and tumor DOI. Included covariates were analyzed for multicollinearity; variables with correlation of ≥0.5 were not included in Cox-regression analysis (30).

Missing data were handled by pairwise deletion. A *p*-value of <0.05 was regarded statistically significant.

RESULTS

The SLNB cohort contained a higher rate of tongue tumors ($p < 0.001$), whereas the END cohort contained a higher rate of floor-of-mouth tumors ($p = 0.008$) (**Table 1**). The END cohort had a higher rate of cT2-staged tumors ($p < 0.001$) and a higher rate of tumors staged pT2 or higher (52.8 vs. 24.6%; $p < 0.001$). Tumor DOI was higher in the END cohort ($p < 0.001$). Extracapsular spread of nodal metastases was more often present in the END cohort ($p < 0.001$). Median follow-up was longer for the END cohort ($p < 0.001$).

Contralateral Regional Recurrences

The overall rate of CRR was 2.5% (20/816). Tumor DOI was higher in patients who developed CRR ($p < 0.001$) (**Table 2**). Vaso-invasive tumor growth was more frequently present in patients who developed CRR ($p = 0.032$). END patients developed CRR more often (14/365; 3.8%) as compared to SLNB patients (6/451; 1.3%) ($p = 0.021$). None of the patients who underwent bilateral END developed CRR. In one patient, CRR was diagnosed in the presence of distant metastasis. CRR was diagnosed in the presence of ipsilateral regional recurrence in one END patient and in two SLNB patients. The rate of ipsilateral nodal metastases, as detected by END or SLNB, was higher in those who developed CRR ($p = 0.018$). None of the patients in whom occult contralateral nodal metastases were detected by SLNB or bilateral END (i.e., pN2c) developed CRR. Out of those who developed CRR, 15 patients underwent salvage treatment with curative intent; in three patients, no data on salvage treatment was available.

Occult Contralateral Nodal Metastasis (i.e., pN2c and CRR)

The overall rate of occult contralateral nodal metastasis was 3.7% (30/816). Patients with paramedian tumors showed a higher rate of contralateral nodal metastases compared to those with lateralized tumors ($p = 0.018$) (**Table 3**). Tumor DOI was

TABLE 1 | Patient and tumor characteristics comparing END and SLNB cohort.

N = 806	SLNB (*n* = 451)	END (*n* = 365)	*P*-value*
Age; mean (±SD)	62.03 (±11.97)	61.98 (±12.77)	0.960
Gender			0.533
Male (%)	233 (51.8%)	197 (54.0%)	
Site of primary tumor[a]			**<0.001†; 0.003†**
Tongue (%)	300 (66.5%)	195 (53.4%)	
Floor of Mouth (%)	98 (21.7%)	113 (31.0%)	
Buccal Mucosa (%)	34 (7.5%)	35 (9.6%)	
Other (%)	19 (4.3%)	22 (6.0%)	
cT-stage			**<0.001†**
T1 (%)	306 (67.8%)	133 (36.4%)	
T2 (%)	145 (32.2%)	222 (63.6%)	
pT-stage[b]			**<0.001†**
T1 (%)	340 (75.4%)	172 (47.2%)	
T2 (%)	107 (23.7%)	188 (51.5%)	
T3 (%)	4 (0.9%)	3 (0.8%)	
T4 (%)	0 (0%)	2 (0.5%)	
DOI; mean (±SD) in mm	5.32 (±4.28)	6.90 (±4.19)	**<0.001‡**
pN-stage			0.533
pN0 (%)	347 (76.9%)	274 (75.1%)	
pN+ (%)	104 (23.1%)	91 (24.9%)	
pN2c			0.199
Yes (%)	8 (1.8%)	2 (0.5%)	
ECS			**<0.001ⱾX**
Yes (%)	3 (0.7%)	32 (8.8%)	
Follow-up in years; median (IQR)	2.2 (1.0–4.1)	4.6 (2.5–7.3)	**<0.001‡**

SLNB sentinel lymph node biopsy, END elective neck dissection, SD standard deviation, DOI depth of invasion, ECS extracapsular spread, IQR interquartile range.
**Bold script indicates significant value.*
† χ^2 test.
‡ Independent samples t test.
Ⱦ Fisher's exact test.
‡ Mann-Whitney U test.
[a] Significance regarding tumors of the tongue and floor-of-mouth tumors.
[b] Significance regarding tumors staged pT2 or higher.

TABLE 2 | Characteristics associated with contralateral regional recurrence.

N = 816	No CRR (*n* = 796)	CRR (*n* = 20)	*P*-value*
Site of primary tumor			0.655
Tongue (%)	481 (60.4%)	14 (70.0%)	
Floor of Mouth (%)	206 (25.9%)	5 (25.0%)	
Buccal Mucosa (%)	68 (8.5%)	1 (5.0%)	
Other (%)	41 (5.2%)	0 (0%)	
pT-stage[a]			0.097
T1 (%)	503 (63.2%)	9 (45.0%)	
T2 (%)	286 (35.9%)	9 (45.0%)	
T3 (%)	5 (0.6%)	2 (10.0%)	
T4 (%)	2 (0.3%)	0 (0%)	
Location primary tumor			0.154
Lateralized	655 (97.4%)	18 (2.6%)	
Paramedian	23 (92.0%)	2 (8.0%)	
DOI; mean (±SD) in mm	5.90 (±4.21)	9.48 (±6.11)	**<0.001‡**
Non-cohesive growth			0.316
Yes (%)	267 (53.6%)	13 (65.0%)	
Perineural growth			0.071
Yes (%)	110 (18.8%)	7 (35.0%)	
Vasoinvasive growth			**0.032Ⱦ**
Yes (%)	51 (8.9%)	5 (25.0%)	
Procedure neck[b]			**0.021†**
SLNB (%)	445 (98.7%)	6 (1.3%)	
Unilateral END (%)	323 (95.8%)	14 (4.2%)	
Bilateral END (%)	28 (100%)	0 (0%)	
pN-stage			**0.018†**
Ipsilateral pN+ (%)	179 (22.5%)	9 (45.0%)	
pN2c			N.A.
Yes (%)	10 (1.3%)	0 (0%)	
ECS			0.588
Yes (%)	34 (4.3%)	1 (5.0%)	

CRR contralateral regional recurrence, DOI depth of invasion, SD standard deviation, SLNB sentinel lymph node biopsy, END elective neck dissection, ECS extracapsular spread, N.A. not applicable.
**Bold script indicates significant value.*
† χ^2 test.
‡ Independent samples t test.
Ⱦ Fisher's exact test.
[a] p value regarding tumors staged pT1 vs. pT2 or higher.
[b] Significance regarding difference in CRR rate between END and SLNB cohort.

higher in patients with occult contralateral nodal metastasis ($p < 0.002$). Perineural tumor growth and vasoinvasive tumor growth were more often present in those with occult contralateral nodal metastasis ($p = 0.002$, $p = 0.001$). A higher rate of ipsilateral nodal metastases, as detected by SLNB or END, was seen in patients with occult contralateral nodal metastasis ($p = 0.025$). Of those in whom occult contralateral nodal metastasis was detected by either bilateral END or SLNB (i.e., pN2c), ipsilateral nodal metastasis was simultaneously detected in three patients (30%). No significant difference was seen in the rate of occult contralateral nodal metastasis between the END and SLNB cohort.

Survival

Figure 2 shows 5-year DSS for patients with and without occult contralateral nodal metastasis (i.e., pN2c and CRR). Five-year DSS was significantly shorter for patients who developed CRR as compared to patients without occult contralateral nodal metastasis (42 vs. 92%, $p < 0.001$). No difference in 5-year DSS was observed between those in whom occult contralateral nodal metastasis were detected by SLNB or bilateral END (i.e., pN2c) and patients without occult contralateral nodal metastasis (88 vs. 92%; $p = 0.446$). Five-year DSS of patients who developed CRR was worse compared to those in whom occult contralateral metastasis were detected by SLNB or bilateral END (i.e., pN2c), although not statistically significant (42 vs. 88%; $p = 0.066$). Of those who underwent salvage treatment with curative intent for CRR, 67% (10/15) died of disease after an average follow-up of 6.1 months following occurrence of CRR.

TABLE 3 | Characteristics associated with occult contralateral nodal metastasis (i.e., pN2c and CRR).

***N* = 816**	**No contralateral metastases (*n* = 786)**	**Contralateral metastases (*n* = 30)**	***P*-value***
Site of primary tumor			0.394
Tongue (%)	474 (60.3%)	21 (70.0%)	
Floor of mouth (%)	203 (25.8%)	8 (26.7%)	
Buccal mucosa (%)	68 (8.7%)	1 (3.3%)	
Other (%)	41 (5.2%)	0 (0%)	
pT-stage[a]			0.277
T1 (%)	496 (63.1%)	16 (53.3%)	
T2 (%)	283 (36.0%)	12 (40.0%)	
T3 (%)	5 (0.6%)	2 (6.7%)	
T4 (%)	2 (0.3%)	0 (0%)	
Location primary tumor			**0.018**$^{\mathbf{X}}$
Lateralized	657 (96.2%)	26 (3.8%)	
Paramedian	21 (84.0%)	4 (16.0%)	
DOI; mean (±SD) in mm	5.90 (±4.21)	8.46 (±5.75)	**0.002**‡
Non-cohesive growth			0.177
Yes (%)	262 (53.4%)	18 (66.7%)	
Perineural growth			**0.002**†
Yes (%)	106 (18.3%)	11 (42.3%)	
Vasoinvasive growth			**0.001**†
Yes (%)	49 (8.6%)	7 (28.0%)	
Procedure neck			0.334
SLNB (%)	437 (98.7%)	14 (3.1%)	
END (%)	349 (95.6%)	16 (4.4%)	
pN-stage[a]			**0.025**†
Ipsilateral pN+ (%)	176 (22.4%)	12 (40.0%)	
ECS			0.133
Yes (%)	32 (4.1%)	3 (10.0%)	

CRR contralateral regional recurrence, DOI depth of invasion, SD standard deviation, SLNB sentinel lymph node biopsy, END elective neck dissection, ECS extracapsular spread.

**Bold script indicates significant value.*

$^{\mathbf{X}}$*Fisher's exact test.*

‡*Independent samples t test.*

† χ^2 *test.*

[a]*p-value regarding tumors staged pT1 vs. pT2 or higher.*

Mean time of survival in patients who developed CRR was 4.1 years (95% CI 2.29–5.95), whereas mean time of survival of those in whom contralateral nodal metastases were detected by SLNB or bilateral END (i.e., pN2c) was 9.7 years (95% CI 7.37–12.02). The mean time of survival in patients without occult contralateral nodal metastasis was 19.3 years (95% CI 18.81–19.72).

Hazard for Developing CRR

Proportional hazard regression analysis showed that patients who underwent END had a higher hazard for developing CRR as compared to those who underwent SLNB [HR = 2.922 (95% CI 1.11–7.71); $p = 0.030$] (**Figure 3**). In addition, tumor DOI was significantly associated with development of CRR as well [HR = 2.277 (95% CI 1.44–3.60); $p < 0.001$].

DISCUSSION

This is the first study that evaluated incidence and hazard of CRR in early-stage OSCC not involving the midline (i.e., lateralized and paramedian) and compared these outcomes between patients who underwent either END or SLNB.

The overall incidence of occult contralateral nodal metastasis in this study was 3.7% (30/816), which is in concordance with the reported incidence of occult contralateral nodal metastasis in lateralized early-stage OSCC [2.7% (95% CI 1.2–4.2%)] (8, 9, 14, 16–21).

Our results showed higher incidence of CRR in patients who underwent END (3.8%) as compared to those who underwent SLNB (1.3%) ($p = 0.018$). Furthermore, our data showed that patients staged by END had a higher hazard of developing CRR, independent of factors such as tumor DOI, compared to patients staged by SLNB [HR = 2.922 (95% CI 1.11–7.71); $p = 0.030$].

Five-year DSS of patients who developed CRR was poor in our population, in particular when compared to those without occult contralateral nodal metastasis. These findings are in line with previous reports on prognosis of (lateralized) OSCC patients with CRR (16, 23, 24). Moreover, our results suggest that 5-year DSS of patients in whom contralateral nodal metastases were detected at an earlier stage by SLNB or bilateral END (pN2c) may be better than in those who eventually developed CRR. In addition, the successful salvage rate of those who developed CRR was only 33% in our population. This highlights the importance of adequate staging or treatment of the contralateral clinically negative neck.

Nevertheless, elective treatment of the contralateral clinically negative neck in OSCC without midline involvement remains controversial. This controversy is sustained by the varying incidence of occult contralateral nodal metastasis and CRR among institutions and the accompanying morbidity of (bilateral) END (18–20, 23, 24, 31–34). In our population, only two patients who underwent bilateral END had occult contralateral nodal metastasis, indicating that 26/28 patients (93%) underwent unnecessary contralateral END. With this in mind, it is worth noting that SLNB has the benefit of staging the contralateral clinically negative neck simultaneous with the ipsilateral neck. Accordingly, SLNB is able to avoid overtreatment of the contralateral neck by allowing accurate selection of only those that require treatment of the contralateral neck.

Another predictor for development of CRR in our population was tumor DOI [HR = 2.277 (95% CI 1.44–3.60); $p < 0.001$], which is in agreement with previous findings by Ganly et al. (35). In their study, neck failure in the undissected contralateral neck of T1-2N0 oral tongue patients accounted for 39% of all recurrences. Moreover, their results showed that tumor thickness was predicting for CRR. Although tumor thickness and DOI are not equivalent, they have similar prognostic implications for nodal metastases (36). As

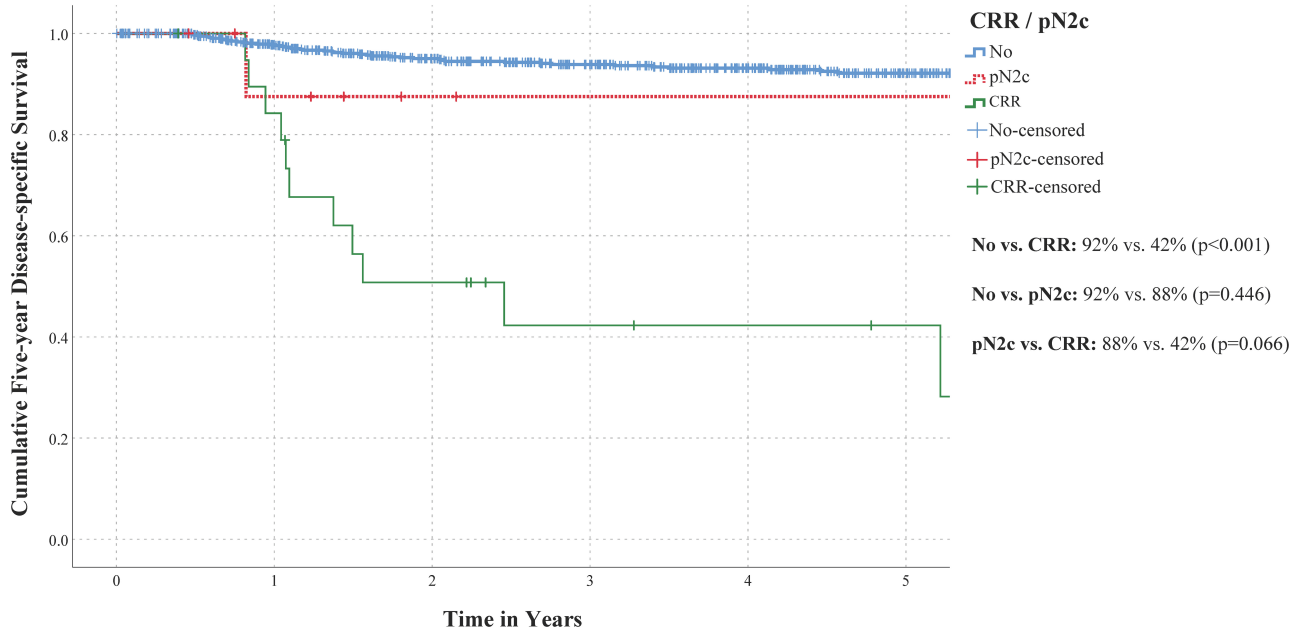

FIGURE 2 | Five-year DSS curves for lateralized or paramedian early-stage OSCC patients without contralateral occult nodal metastasis (*blue bold line*) as compared to those with contralateral occult nodal metastasis: initially staged pN2c by SLNB or bilateral END (*red interrupted line*) or CRR (*green line*).

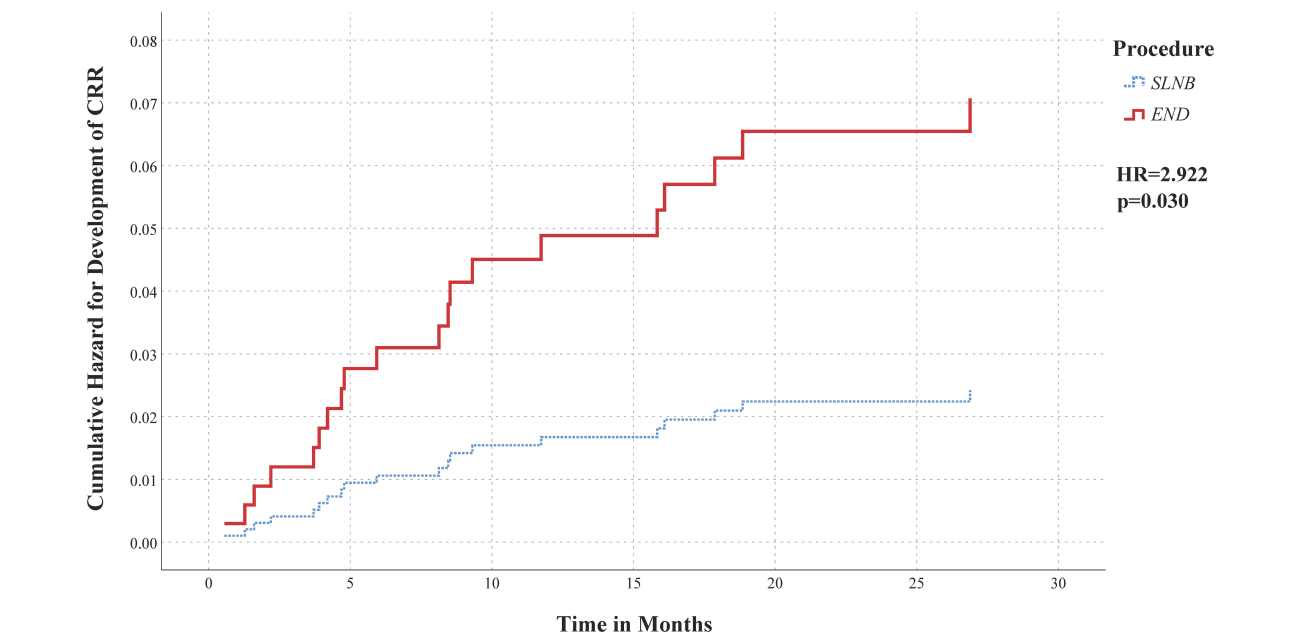

FIGURE 3 | Cumulative hazard curve regarding development of CRR in patients with early-stage OSCC not involving the midline, divided by initial management of the neck: elective neck dissection (*END; red bold line*) or sentinel lymph node biopsy (*SLNB; blue interrupted line*). A significantly higher hazard for developing CRR was observed for patients who underwent END compared to those who underwent SLNB [HR = 2.922 (95% CI 1.11–7.71)].

a consequence, the higher rate of CRR in our END cohort may be explained by greater tumor DOI in these patients. Nevertheless, when correcting for DOI in our proportional hazard regression analysis, a significantly higher hazard for developing CRR was observed in END patients as compared to SLNB patients.

The limitations of our study remain its retrospective design and the heterogeneity in performing SLNB or END among institutions. Secondly, occult contralateral nodal metastases are uncommon in this population, which irrevocably results in a small number of events for analyses. Accordingly, it could be argued that a larger sample, resulting in more CRR and pN2c events for analyses, may result in a significantly better prognosis for those in whom the metastatic involved contralateral neck is correctly staged and treated at an earlier stage, as compared to those who eventually develop CRR. Thirdly, since END patients were included between 1990 and 2015, a substantial proportion may have been elected for END based on potentially dated therapeutic guidelines or aged diagnostic imaging modalities. Moreover, patients were predominantly selected for END based on estimated tumor DOI >4 mm, inevitably resulting in higher tumor DOI in the END cohort. Due to this heterogeneity in therapeutic decision making between both cohorts, they cannot easily be compared, especially since the END cohort had a higher tumor DOI, higher T-stages, a higher rate of extracapsular spread of nodal metastases, and a longer follow-up duration, which might impact the occurrence of occult contralateral nodal metastasis or CRR. Nevertheless, there was no significant difference in the total rate of occult contralateral nodal metastasis (i.e., pN2c and CRR) between both cohorts, which implies that these cohorts can be compared when concerning control of the contralateral clinically negative neck. Furthermore, our proportional hazard regression analysis, which allows adjustment for confounding effects of included variables, showed a higher hazard for developing CRR in the END cohort, independent of confounding factors such as tumor DOI. In addition, both higher T-stages and presence of extracapsular spread of nodal metastases showed no association with contralateral nodal metastases or CRR in our univariate analyses. Besides, although a longer follow-up was available for END patient compared to SLNB patients, local or regional recurrences are uncommon after 2 years post-treatment (37). The follow-up duration of the SLNB cohort was therefore considered long enough for missed occult metastases to become clinically manifest and provides no explanation for the difference in rate of CRR between both cohorts. It could be argued that patients who underwent unilateral END for tumors from which the specific location was missing should be excluded from this study. However, since none of these patients developed CRR, excluding them would result in a relatively higher incidence of CRR in the END cohort, which will presumably induce a distortion of results in favor of SLNB. Fourthly, as there are no clear guidelines in which cases to perform contralateral END in early-stage OSCC, these were likely performed based on preference of the treating physician and on availability of the latest state-of-the-art imaging modalities. This may introduce some bias; however, it reflects daily clinical practice at that time. This strengthens the need for more research to develop evidence-based guidelines on this important topic. Fifthly, in this study, the 7th TNM classification was applied, whereas the 8th edition has already been implemented (38). While tumor diameter reflected pT-stage in the 7th edition, DOI is newly incorporated for T-stage in the 8th edition (36, 39). Due to missing data on DOI in several cases, our results could not be directly translated to the 8th TNM classification. Finally, some clinical and histopathological factors that have been associated with contralateral nodal metastasis in OSCC were not included due to lack of data. These factors include histological grading, surgical margin status, peritumoral inflammation, (adjuvant) radiotherapy to contralateral neck, and time of initial diagnosis (24). In particular, (adjuvant) radiotherapy to contralateral neck could influence the occurrence of CRR in these patients and should therefore be documented and incorporated in further studies. Although non-cohesive growth of the tumor was included as a potential predictor for CRR in our analyses, it was not subdivided by grading of pattern of invasion (i.e., cohesive growth, small islands, thin strands, and individual tumor cells) (24, 40). Nevertheless, the correlation between several of these factors (i.e., histological grading, peritumoral inflammation, and pattern of invasion) and contralateral nodal metastasis is dubious (24).

In conclusion, the incidence of CRR in lateralized or paramedian early-stage OSCC is relatively low (2.5%). As the salvage rate and prognosis of those who develop CRR remain poor, adequate staging of the contralateral clinically negative neck is highly recommended, especially since the prognosis of those in whom occult contralateral nodal metastases are detected at an earlier stage may be favorable compared to those who eventually develop CRR. In our population, a higher incidence of CRR was observed in those who underwent END for lateralized or paramedian early-stage OSCC, as compared to those who underwent SLNB. Furthermore, a higher hazard for developing CRR was observed in patients who underwent END in a clinical setting as compared to patients who underwent SLNB. Accordingly, our data suggest that SLNB allows for better control of the contralateral clinically negative neck in early-stage OSCC not involving the midline.

DATA AVAILABILITY STATEMENT

The raw data supporting the conclusions of this article will be made available by the authors, without undue reservation.

ETHICS STATEMENT

The studies involving human participants were reviewed and approved by UMC Utrecht's Ethics Committee (no. 17/766) and all participating centers. Written informed consent for participation was not required for this study in accordance with the national legislation and the institutional requirements.

AUTHOR CONTRIBUTIONS

RM, IT, KB, RT, MW, and RB: conceptualization. RM, IT, KB, DL, and WK: methodology. RM, IT, and KB: software, formal analysis, and visualization. RM, IT, KB, and DL: validation. RM, IT, KB, DL, WK, MW, and RB: investigation. EB, MD, BK, WK, CL, SW, RT, MW, and RB: resources. IT, KB, DL,

and WK: data curation. RM, IT, KB, MW, and RB: writing—original draft preparation. DL, EB, MD, BK, WK, CL, SW, and RT: writing—review and editing. MW and RB: supervision and project administration. IT and RB: funding acquisition. All authors have read and agreed to the published version of the manuscript.

FUNDING

For setting up these multicenter national databases (END and SLNB cohort), financial support was obtained from SpePharm A.G.—part of the Norgine Group of companies, Amsterdam, The Netherlands.

REFERENCES

1. D'Cruz AK, Vaish R, Kapre N, Dandekar M, Gupta S, Hawaldar R, et al. Head and neck disease management group. elective versus therapeutic neck dissection in node-negative oral cancer. *N Engl J Med.* (2015) 373:521–9. doi: 10.1056/NEJMoa1506007
2. Abu-Ghanem S, Yehuda M, Carmel NN, Leshno M, Abergel A, Gutfeld O, et al. Elective Neck Dissection vs Observation in Early-Stage Squamous Cell Carcinoma of the Oral Tongue With No Clinically Apparent Lymph Node Metastasis in the Neck: A Systematic Review and Meta-analysis. *JAMA Otolaryngol Head Neck Surg.* (2016) 142:857–65. doi: 10.1001/jamaoto.2016.1281
3. de Bree R, Takes RP, Shah JP, Hamoir M, Kowalski LP, Robbins KT, et al. Elective neck dissection in oral squamous cell carcinoma: Past, present and future. *Oral Oncol.* (2019) 90:87–93. doi: 10.1016/j.oraloncology.2019.01.016
4. Den Toom IJ, Boeve K, Lobeek D, Bloemena E, Donswijk ML, de Keizer B, et al. Elective neck dissection or sentinel lymph node biopsy in early stage oral cavity cancer patients: the Dutch experience. *Cancers.* (2020) 12:1783. doi: 10.3390/cancers12071783
5. Schilling C, Shaw R, Schache A, McMahon J, Chegini S, Kerawala C, et al. Sentinel lymph node biopsy for oral squamous cell carcinoma. Where are we now? *Br J Oral Maxillofac Surg.* (2017) 55:757–62. doi: 10.1016/j.bjoms.2017.07.007
6. Cramer JD, Sridharan S, Ferris RL, Duvvuri U, Samant S. Sentinel lymph node biopsy versus elective neck dissection for stage I to II oral cavity cancer. *Laryngoscope.* (2019) 129:162–9. doi: 10.1002/lary.27323
7. Liu M, Wang SJ, Yang X, Peng H. Diagnostic efficacy of sentinel lymph node biopsy in early oral squamous cell carcinoma: a meta-analysis of 66 studies. *PLoS ONE.* (2017) 12:e0170322.
8. Schilling C, Stoeckli SJ, Haerle SK, Broglie MA, Huber GF, Sorensen JA, et al. Sentinel European Node Trial (SENT): 3-year results of sentinel node biopsy in oral cancer. *Eur J Cancer.* (2015) 51:2777–84. doi: 10.1016/j.ejca.2015.08.023
9. Flach GB, Bloemena E, Klop WM, van Es RJ, Schepman KP, Hoekstra OS, et al. Sentinel lymph node biopsy in clinically N0 T1-T2 staged oral cancer: the Dutch multicenter trial. *Oral Oncol.* (2014) 50:1020–4. doi: 10.1016/j.oraloncology.2014.07.020
10. Schiefke F, Akdemir M, Weber A, Akdemir D, Singer S, Frerich B. Function, postoperative morbidity, and quality of life after cervical sentinel node biopsy and after selective neck dissection. *Head Neck.* (2009) 31:503–12. doi: 10.1002/hed.21001
11. Murer K, Huber GF, Haile SR, Stoeckli SJ. Comparison of morbidity between sentinel node biopsy and elective neck dissection for treatment of the n0 neck in patients with oral squamous cell carcinoma. *Head Neck.* (2011) 33:1260–4. doi: 10.1002/hed.21622
12. Govers TM, Schreuder WH, Klop WM, Grutters JP, Rovers MM, Merkx MA, et al. Quality of life after different procedures for regional control in oral cancer patients: cross-sectional survey. *Clin Otolaryngol.* (2016) 41:228–33. doi: 10.1111/coa.12502
13. Govers TM, Takes RP, Baris Karakullukcu M, Hannink G, Merkx MA, Grutters JP, et al. Management of the N0 neck in early stage oral squamous cell cancer: a modeling study of the cost-effectiveness. *Oral Oncol.* (2013) 49:771–7. doi: 10.1016/j.oraloncology.2013.05.001
14. Mølstrøm J, Grønne M, Green A, Bakholdt V, Sørensen JA. Topographical distribution of sentinel nodes and metastases from T1-T2 oral squamous cell carcinomas. *Eur J Cancer.* (2019) 107:86–92. doi: 10.1016/j.ejca.2018.10.021
15. den Toom IJ, Boeve K, van Weert S, Bloemena E, Brouwers AH, Hoekstra OS, et al. High rate of unexpected lymphatic drainage patterns and a high accuracy of the sentinel lymph node biopsy in oral cancer after previous neck treatment. *Oral Oncol.* (2019) 94:68–72. doi: 10.1016/j.oraloncology.2019.05.007
16. Koo BS, Lim YC, Lee JS, Choi EC. Management of contralateral N0 neck in oral cavity squamous cell carcinoma. *Head Neck.* (2006) 28:896–901. doi: 10.1002/hed.20423
17. Kurita H, Koike T, Narikawa JN, Sakai H, Nakatsuka A, Uehara S, et al. Clinical predictors for contralateral neck lymph node metastasis from unilateral squamous cell carcinoma in the oral cavity. *Oral Oncol.* (2004) 40:898–903. doi: 10.1016/j.oraloncology.2004.04.004
18. Lim YC, Lee JS, Koo BS, Kim SH, Kim YH, Choi EC. Treatment of contralateral N0 neck in early squamous cell carcinoma of the oral tongue: Elective neck dissection versus observation. *Laryngoscope.* (2006) 116:461–5. doi: 10.1097/01.mlg.0000195366.91395.9b
19. Zbären P, Nuyens M, Caversaccio M, Stauffer E. Elective neck dissection for carcinomas of the oral cavity: occult metastases, neck recurrences, and adjuvant treatment of pathologically positive necks. *Am J Surg.* (2006) 191:756–60. doi: 10.1016/j.amjsurg.2006.01.052
20. Nobis CP, Otto S, Grigorieva T, Alnaqbi M, Troeltzsch M, Schöpe J, et al. Elective neck dissection in unilateral carcinomas of the tongue: Unilateral versus bilateral approach. *J Craniomaxillofac Surg.* (2017) 45:579–84. doi: 10.1016/j.jcms.2017.01.008
21. Pezier T, Nixon IJ, Gurney B, Schilling C, Hussain K, Lyons AJ, et al. Sentinel lymph node biopsy for T1/T2 oral cavity squamous cell carcinoma–a prospective case series. *Ann Surg Oncol.* (2012) 19:3528–33. doi: 10.1245/s10434-011-2207-0
22. Moya-Plana A, Aupérin A, Guerlain J, Gorphe P, Casiraghi O, Mamelle G, et al. Sentinel node biopsy in early oral squamous cell carcinomas: Long-term follow-up and nodal failure analysis. *Oral Oncol.* (2018) 82:187–94. doi: 10.1016/j.oraloncology.2018.05.021
23. Feng Z, Niu LX, Yuan Y, Peng X, Guo CB. Risk factors and treatment of contralateral neck recurrence for unilateral oral squamous cell carcinoma: a retrospective study of 1482 cases. *Oral Oncol.* (2014) 50:1081–8. doi: 10.1016/j.oraloncology.2014.08.003
24. Fan S, Tang QL, Lin YJ, Chen WL, Li JS, Huang ZQ, et al. A review of clinical and histological parameters associated with contralateral neck metastases in oral squamous cell carcinoma. *Int J Oral Sci.* (2011) 3:180–91. doi: 10.4248/IJOS11068
25. Huang SH, Hwang D, Lockwood G, Goldstein DP, O'Sullivan B. Predictive value of tumour thickness for cervical lymph-node involvement in squamous cell carcinoma of the oral cavity: a meta-analysis of reported studies. *Cancer.* (2009) 115:1489–97. doi: 10.1002/cncr.24161
26. Alkureishi LW, Burak Z, Alvarez JA, Ballinger J, Bilde A, Britten AJ, et al. European Association of Nuclear Medicine Oncology Committee European Sentinel Node Biopsy Trial Committee. Joint practice guidelines for radionuclide lymphoscintigraphy for sentinel node localization in oral/oropharyngeal squamous cell carcinoma. *Ann Surg Oncol.* (2009) 16:3190–210. doi: 10.1245/s10434-009-0726-8
27. Giammarile F, Schilling C, Gnanasegaran G, Bal C, Oyen WJG, Rubello D, et al. The EANM practical guidelines for sentinel lymph node localisation in oral cavity squamous cell carcinoma. *Eur J Nucl Med Mol Imaging.* (2019) 46:623–37. doi: 10.1007/s00259-018-4235-5
28. Schilling C, Stoeckli SJ, Vigili MG, de Bree R, Lai SY, Alvarez J, et al. Surgical consensus guidelines on sentinel node biopsy (SNB) in patients with oral cancer. *Head Neck.* (2019) 41:2655–64. doi: 10.1002/hed.25739
29. Dhawan I, Sandhu SV, Bhandari R, Sood N, Bhullar RK, Sethi N. Detection of cervical lymph node micrometastasis and isolated tumour cells in oral squamous cell carcinoma using immunohistochemistry and serial sectioning. *J Oral Maxillofac Pathol.* (2016) 20:436–44. doi: 10.4103/0973-029X.190946

30. Donath C, Grässel E, Baier D, Pfeiffer C, Bleich S, Hillemacher T. Predictors of binge drinking in adolescents: ultimate and distal factors - a representative study. *BMC Public Health.* (2012) 12:263. doi: 10.1186/1471-2458-12-263
31. Klingelhöffer C, Gründlinger A, Spanier G, Schreml S, Gottsauner M, Mueller S, et al. Patients with unilateral squamous cell carcinoma of the tongue and ipsilateral lymph node metastasis do not profit from bilateral neck dissection. *Oral Maxillofac Surg.* (2018) 22:185–92. doi: 10.1007/s10006-018-0690-1
32. Habib M, Murgasen J, Gao K, Ashford B, Shannon K, Ebrahimi A, et al. Contralateral neck failure in lateralised oral squamous cell carcinoma. *ANZ J Surg.* (2016) 86:188–92. doi: 10.1111/ans.13206
33. Liao CT, Huang SF, Chen IH, Chang JT, Wang HM, Ng SH, et al. Risk stratification of patients with oral cavity squamous cell carcinoma and contralateral neck recurrence following radical surgery. *Ann Surg Oncol.* (2009) 16:159–70. doi: 10.1245/s10434-008-0196-4
34. Shimamoto H, Oikawa Y, Osako T, Hirai H, Mochizuki Y, Tanaka K, et al. Neck failure after elective neck dissection in patients with oral squamous cell carcinoma. *Oral Surg Oral Med Oral Pathol Oral Radiol.* (2017) 124:32–6. S2212-4403(17)30105-0
35. Ganly I, Goldstein D, Carlson DL, Patel SG, O'Sullivan B, Lee N, et al. Long-term regional control and survival in patients with "low-risk," early stage oral tongue cancer managed by partial glossectomy and neck dissection without postoperative radiation: the importance of tumour thickness. *Cancer.* (2013) 119:1168–76. doi: 10.1002/cncr.27872
36. Dirven R, Ebrahimi A, Moeckelmann N, Palme CE, Gupta R, Clark J. Tumour thickness versus depth of invasion - Analysis of the 8th edition American Joint Committee on Cancer Staging for oral cancer. *Oral Oncol.* (2017) 74:30–3. doi: 10.1016/j.oraloncology.2017.09.007
37. Hutchison IL, Ridout F, Cheung SMY, Shah N, Hardee P, Surwald C, et al. Nationwide randomised trial evaluating elective neck dissection for early stage oral cancer (SEND study) with meta-analysis and concurrent real-world cohort. Br J Cancer.2019 121:827–36. doi: 10.1038/s41416-019-0587-2
38. Brierley JD, Gospodarowicz M, Wittekind C. *UICC TNM Classification of Malignant Tumours*. 8th ed. Chichester: Wiley (2017).
39. Lydiatt WM, Patel SG, O'Sullivan B, Brandwein MS, Ridge JA, Migliacci JC, et al. Head and Neck cancers-major changes in the American Joint Committee on cancer eighth edition cancer staging manual. *CA Cancer J Clin.* (2017) 67:122–37. doi: 10.3322/caac.21389
40. De Silva RK, Siriwardena BSMS, Samaranayaka A, Abeyasinghe WAMUL, Tilakaratne WM. A model to predict nodal metastasis in patients with oral squamous cell carcinoma. *PLoS ONE.* (2018) 13:e0201755. doi: 10.1371/journal.pone.0201755

Conflict of Interest: The authors declare that the research was conducted in the absence of any commercial or financial relationships that could be construed as a potential conflict of interest.

frontiers in Oncology

ORIGINAL RESEARCH
published: 28 May 2021
doi: 10.3389/fonc.2021.652553

Derivation and Validation of a Prognostic Scoring Model Based on Clinical and Pathological Features for Risk Stratification in Oral Squamous Cell Carcinoma Patients: A Retrospective Multicenter Study

Jiaying Zhou[1,2†], Huan Li[3†], Bin Cheng[1,2], Ruoyan Cao[1,2], Fengyuan Zou[4], Dong Yang[4], Xiang Liu[4], Ming Song[5*] and Tong Wu[1,2*]*

[1] Hospital of Stomatology, Guanghua School of Stomatology, Sun Yat-sen University, Guangzhou, China, [2] Guangdong Provincial Key Laboratory of Stomatology, Guanghua School of Stomatology, Sun Yat-sen University, Guangzhou, China, [3] Department of ICU, Sun Yat-sen University Cancer Center, State Key Laboratory of Oncology in South China, Collaborative Innovation Center for Cancer Medicine, Guangzhou, China, [4] Department of Data Sciences, AID Cloud Technology Co., Ltd, Guangzhou, China, [5] Department of Head and Neck Surgery, Sun Yat-sen University Cancer Center, State Key Laboratory of Oncology in South China, Collaborative Innovation Center for Cancer Medicine, Guangzhou, China

Objective: To develop and validate a simple-to-use prognostic scoring model based on clinical and pathological features which can predict overall survival (OS) of patients with oral squamous cell carcinoma (OSCC) and facilitate personalized treatment planning.

Materials and Methods: OSCC patients (n = 404) from a public hospital were divided into a training cohort (n = 282) and an internal validation cohort (n = 122). A total of 12 clinical and pathological features were included in Kaplan–Meier analysis to identify the factors associated with OS. Multivariable Cox proportional hazards regression analysis was performed to further identify important variables and establish prognostic models. Nomogram was generated to predict the individual's 1-, 3- and 5-year OS rates. The performance of the prognostic scoring model was compared with that of the pathological one and the AJCC TNM staging system by the receiver operating characteristic curve (ROC), concordance index (C-index), calibration curve, and decision curve analysis (DCA). Patients were classified into high- and low-risk groups according to the risk scores of the nomogram. The nomogram-illustrated model was independently tested in an external validation cohort of 95 patients.

Results: Four significant variables (physical examination-tumor size, imaging examination-tumor size, pathological nodal involvement stage, and histologic grade) were included into the nomogram-illustrated model (clinical–pathological model). The area under the ROC curve (AUC) of the clinical–pathological model was 0.687, 0.719, and 0.722 for 1-, 3- and 5-year survival, respectively, which was superior to that of the pathological model

OPEN ACCESS

Edited by:
Cesare Piazza,
University of Brescia, Italy

Reviewed by:
Chuan Hu,
Qingdao University Medical College, China
Xin-hua Liang,
Sichuan University, China

****Correspondence:***
Xiang Liu
liuxiang@aidcloud.cn
Ming Song
songming@sysucc.org.cn
Tong Wu
wutong23@mail.sysu.edu.cn

†These authors have contributed equally to this work and share first authorship

Specialty section:
This article was submitted to Head and Neck Cancer, a section of the journal Frontiers in Oncology

Received: *12 January 2021*
Accepted: *12 April 2021*
Published: *28 May 2021*

Citation:
Zhou J, Li H, Cheng B, Cao R, Zou F, Yang D, Liu X, Song M and Wu T (2021) Derivation and Validation of a Prognostic Scoring Model Based on Clinical and Pathological Features for Risk Stratification in Oral Squamous Cell Carcinoma Patients: A Retrospective Multicenter Study. Front. Oncol. 11:652553. doi: 10.3389/fonc.2021.652553

(AUC = 0.649, 0.707, 0.717, respectively) and AJCC TNM staging system (AUC = 0.628, 0.668, 0.677, respectively). The clinical–pathological model exhibited improved discriminative power compared with pathological model and AJCC TNM staging system (C-index = 0.755, 0.702, 0.642, respectively) in the external validation cohort. The calibration curves and DCA also displayed excellent predictive performances.

Conclusion: This clinical and pathological feature based prognostic scoring model showed better predictive ability compared with the pathological one, which would be a useful tool of personalized accurate risk stratification and precision therapy planning for OSCC patients.

Keywords: oral squamous cell carcinoma, prediction model, prognosis, risk stratification, nomogram

INTRODUCTION

Prognostic prediction models are widely utilized both in clinic and research to estimate the probability that a certain outcome will occur within a specific time period in an individual (1). A reliable prognostic model is essential in individual risk quantification and stratification, which is fundamental in personalized treatment plan development. Furthermore, it can also help to provide a basis for health economic assessment of cost-effectiveness (2).

Recent global estimates have revealed 377,713 new cases and 177,757 deaths of oral cancer in 2020 (3). Oral squamous cell carcinoma (OSCC) is the most common oral cancer, accounting for more than 90% of all oral cancers (4). Although surgical resection remains the primary treatment at present, more and more therapeutic options such as radiotherapy, chemotherapy and immunotherapy have emerged. Advances in treatments improved the quality of life and life expectancy of patients. However, the 5-year overall survival rate of OSCC patients was still less than 60% (5). Therefore, how to assess the prognostic risk and choose the most suitable treatment for individuals is challenging for clinicians (6).

The most commonly and widely used prognostic model for oral cancer is based on the American Joint Committee on Cancer (AJCC) tumor, lymph node, and metastases (TNM) staging system (7). However, the pathological TNM stage does not allow a comprehensive assessment for the prognosis prediction of patients. Many other risk factors, including age, smoking status, primary site, and clinical examination results, should be considered for individualized prognosis (8). A growing number of tumor molecular biomarker models have been highlighted for their potential predictive abilities (9). But more and more studies demonstrate that due to the methodological heterogeneity, biomarker testing lacks sufficient accuracy, which is difficult to define specific biomarkers for OSCC prognosis prediction (10, 11).

In this study, we aimed to develop a prognostic scoring model using the widely available physical and imaging data, as well as the pathological data to predict 1-, 3- and 5-year OS in OSCC patients after surgery. The model would help the clinician to customize adjuvant treatment program in addition to surgical resection. We combined the most relevant prognosticators into nomogram, which could help clinicians to define the risk profile of individual patient intuitively and effectively. Furthermore, the model was validated in an external patient cohort. This model will not only contribute to provide a more accurate OSCC prognosis, but also help to facilitate personalized treatment planning.

MATERIALS AND METHODS

Patient Selection

In this multicenter retrospective study, we firstly collected 4,089 OSCC patients from the Head and Neck Surgery Department of the Sun Yat-sen University Cancer Center (SYSUCC, Guangdong, China). The inclusion criteria of patients were as follows: (1) received pretreatment clinical assessment including tumor size and nodal involvement of physical and imaging examinations, (2) received curative-intent surgical resection, (3) received postoperative pathological confirmation, (4) follow-up time greater than 6 months. The patients were excluded according to the following criteria: (1) patients experienced distant metastasis at the time of diagnosis, (2) patients with previous history of OSCC, (3) subgroup with small sample size. After applying the criteria, 404 patients from SYSUCC between 2000 and 2016 were enrolled in this study and randomly split into the training cohort (n = 282) and internal validation cohort (n = 122) with 7/3 split ratio.

OSCC patients satisfying the aforementioned inclusion and exclusion criteria were also obtained from the Hospital of Stomatology of the Sun Yat-sen University between 2013 and 2018 (Guangdong, China). In total, 95 patients were designated as the external validation cohort. The screening process are shown in **Figure 1**. All research procedures were approved by the Ethics Committee of the Sun Yat-sen University Cancer Center and Hospital of Stomatology of the Sun Yat-sen University. Informed consents for data collection and analysis were obtained from patients.

Variable Enrollment

A total of 12 key variables were categorized into three data types for each OSCC case. Social demographic data included gender, age, radiotherapy history for head and neck cancer, and smoking

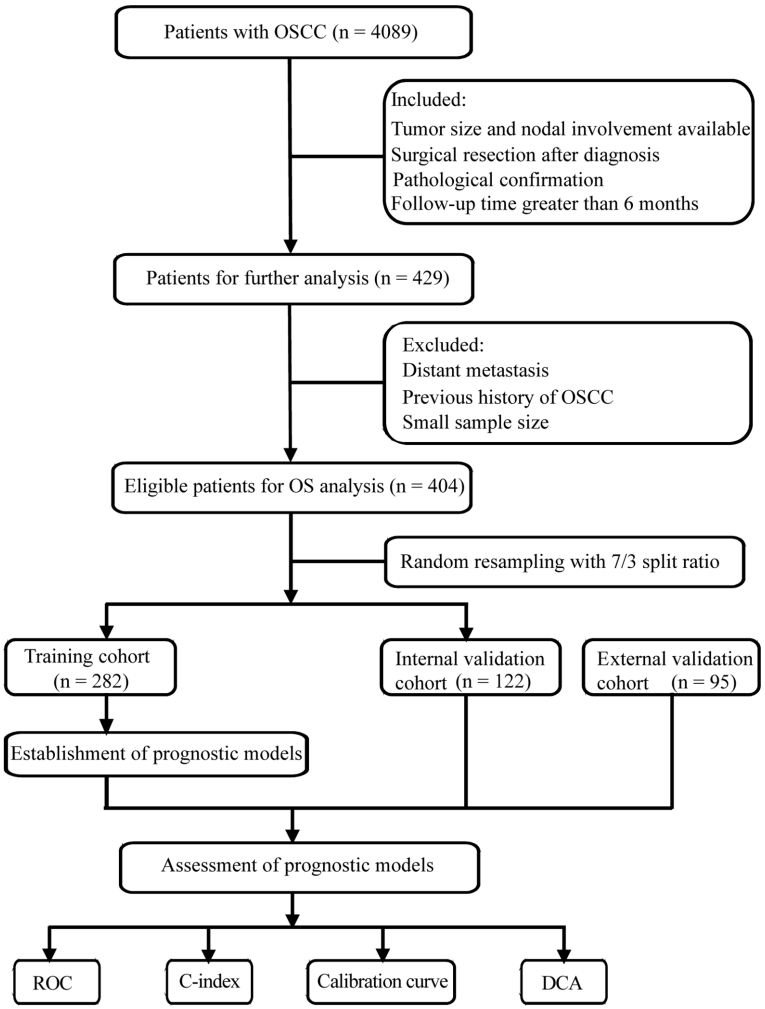

FIGURE 1 | Flow chart of screening process and experimental procedure. OSCC, oral squamous cell carcinoma; ROC, receiver operating characteristic curve; C-index, concordance index; DCA, decision curve analysis.

history. Clinical data included primary site, physical examination-tumor size (PE-T), imaging examination-tumor size (IE-T), physical examination-nodal involvement (PE-N), and imaging examination-nodal involvement (IE-N). Imaging examination only included CT and MRI in our study. Pathological data included pathological tumor stage (P-T), pathological nodal involvement stage (P-N), and histologic grade. All the data were summarized in **Table 1**. The clinical and pathological TN stage were classified according to the 7th edition of the AJCC staging system for oral cancer. The endpoint of this study was overall survival (OS), which referred to the time interval from surgery to death or the last follow-up (12). The survival time of patients who were still alive at the last date of follow-up was given as censored data.

Statistical Analysis

Kaplan–Meier analysis was used to estimate OS and detect intersections between the variables. The independent prognostic factors affecting OS were identified by univariate and multivariate Cox regression analyses. The qualified prognostic factors with significant differences in the univariate analysis were incorporated into the multivariate analysis. Stepwise regression was adopted to remove the non-significant factors, which ensured each variable in the resulting independent variable subset was significant to the dependent variable and the remaining variables were not multicollinear. The results were shown as hazard ratios (HR) with 95% confidence interval (CI). Then, an integrated nomogram was established to predict 1-, 3-, 5-year OS based on multivariate Cox proportional hazards regression model. Finally, the clinical–pathological model was validated internally and externally according to the TRIPOD statement (13).

The performances of the prognostic model were evaluated by various methods, involving the time-dependent receiver operating characteristic (ROC) curve and the value of the area under the ROC curve (AUC), Harrell's concordance index (C-index), calibration curve, and decision curve analysis (DCA). ROC was

TABLE 1 | Characteristics description in the training and validation cohorts.

Characteristics	Subtype	Train cohort (n = 282)	Internal validation cohort (n = 122)	*p*-value	External validation cohort (n = 95)	*p*-value*
Gender	Male	192 (68.09%)	87 (71.31%)	1	64 (67.37%)	1
	Female	90 (31.91%)	35 (28.69%)		31 (32.63%)	
Age	<60	181 (64.18%)	74 (60.66%)	1	64 (67.37%)	1
	≥60	101 (35.82%)	48 (39.34%)		31 (32.63%)	
Radiotherapy history	No/Unknown	271 (96.1%)	118 (96.72%)	1	95 (100%)	NA
	Yes	11 (3.90%)	4 (3.28%)		0 (0%)	
Smoking history	No	150 (53.19%)	71 (58.2%)	0.974	57 (60.0%)	0.870
	Yes	132 (46.81%)	51 (41.8%)		38 (40.0%)	
Primary tumor site	Tongue	142 (50.35%)	71 (58.2%)	0.636	63 (66.31%)	0.047
	Floor of mouth	28 (9.93%)	8 (6.56%)		9 (9.47%)	
	Gingiva	58 (20.57%)	17 (13.93%)		10 (10.53%)	
	Hard palate	33 (11.7%)	18 (14.75%)		2 (2.11%)	
	Others	21 (7.45%)	8 (6.56%)		11 (11.58%)	
PE-T	(0-2] cm	70 (24.82%)	23 (18.85%)	0.459	24 (25.26%)	0.019
	(2-4] cm	138 (48.94%)	78 (63.93%)		63 (66.32%)	
	>4 cm	74 (26.24%)	21 (17.21%)		8 (8.42%)	
IE-T	(0-2] cm	85 (30.14%)	39 (31.97%)	0.867	37 (38.95%)	0.532
	(2-4] cm	147 (52.13%)	69 (56.56%)		50 (52.63%)	
	>4 cm	50 (17.73%)	14 (11.48%)		8 (8.42%)	
PE-N	N0	164 (58.16%)	70 (57.38%)	1	60 (63.16%)	0.199
	N1	71 (25.18%)	27 (22.13%)		31 (32.63%)	
	N2	47 (16.67%)	25 (20.49%)		4 (4.21%)	
IE-N	N0	197 (69.86%)	81 (66.39%)	1	30 (31.58%)	<0.001
	N1	39 (13.83%)	17 (13.93%)		57 (60.0%)	
	N2	46 (16.31%)	24 (19.67%)		8 (8.42%)	
P-T	T1	68 (24.11%)	23 (18.85%)	0.204	18 (18.95%)	0.966
	T2	115 (40.78%)	70 (57.38%)		49 (51.58%)	
	T3	57 (20.21%)	11 (9.02%)		11 (11.58%)	
	T4	42 (14.89%)	18 (14.75%)		17 (17.89%)	
P-N	N0	173 (61.35%)	74 (60.66%)	0.999	68 (71.58%)	0.413
	N1	65 (23.05%)	25 (20.49%)		10 (10.53%)	
	N2	44 (15.6%)	23 (18.85%)		17 (17.89%)	
Histologic grade	Well differentiated	178 (63.12%)	66 (54.1%)	0.459	47 (49.47%)	0.127
	Moderately differentiated	76 (26.95%)	49 (40.16%)		46 (48.42%)	
	Poorly differentiated	28 (9.93%)	7 (5.74%)		2 (2.11%)	
AJCC TNM stage	I	54(19.15%)	17(13.93%)	0.963	16(16.84%)	0.099
	II	72(25.53%)	42(34.43%)		40(42.11%)	
	III	80(28.37%)	28(22.95%)		12(12.63%)	
	IV	76(26.95%)	35(28.69%)		27(28.42%)	
Follow-up months	Median (range)	25.6 (11-71)	29.4 (12-93)	0.222	42 (8-69)	0.184

**Compared with the training cohort. PE-T, physical examination-tumor size; IE-T, imaging examination-tumor size; PE-N, physical examination-nodal involvement; IE-N, imaging examination-nodal involvement; P-T, pathological tumor stage; P-N, pathological nodal involvement stage; NA, not applicable.*

used to assess the sensitivity and specificity of the model. C-index was determined to evaluate the model's discriminative power between the predicted model and actual chance of experiencing the events (14). 1,000 bootstrap resamples were used to obtain the intervals of the C-index. The purpose of the calibration curve is to evaluate the agreement between the predictive values and observation values in the probabilities of 3- and 5-year survival of individuals. DCA was used to determine the net benefit of using the prognostic model at various threshold probabilities, which would be helpful to evaluate the actual needs for clinical decision-making (15). The total risk points of each patient were calculated according to the established nomogram. An optimal cut-off point was determined by the R package "maxstat" in the training cohort to classify patients as high-risk and low-risk groups.

All analyses were conducted using Python version 3.7.1 and R version 4.0.0 (R Foundation for Statistical Computing, Vienna, Austria). All statistical tests were two-sided with statistical significance defined as a $p < 0.05$. The Kolmogorov–Smirnov test was used to compare the distribution in the training and validation cohorts between different subgroups. Kaplan–Meier analysis was performed, and log-rank tests were used to determine the significance of the survival differences. In addition, Hosmer–Lemeshow tests were applied to evaluate the goodness-of-fit of the calibration curve, $p > 0.05$ represented good calibration (16).

RESULTS

Patient Characteristics

The demographic and clinicopathologic characteristics of the training and validation cohorts are summarized in **Table 1**.

Of the 282 individuals in the training cohort, 68.09% of the patients were male, and patients over 60 years accounted for 35.82%. Only minority of patients (3.9%) had a radiotherapy history for head and neck cancer, and about half of patients (46.81%) had a smoking history. The 95 individuals in the external validation cohort were slightly younger with a lower prevalence of smoking. The median period of follow-up of the training cohort was shorter than that of the external validation cohort (25.6 vs. 42 months). The tongue was the most common primary tumor site in both the training and validation cohorts (50.35, 58.2, 66.31%, respectively). There was no statistically significant difference in the distribution of the features between the training and internal validation cohorts ($p > 0.05$), while the distribution of the primary tumor site, PE-T, and IE-N between the training and external validation cohorts was significantly different ($p < 0.05$) (**Table 1**).

Screening Independent Prognostic Factors

Kaplan–Meier analysis showed that smoking history, primary site, PE-T, IE-T, PE-N, IE-N, P-T, P-N, and histologic grade were significantly associated with OS (all $p < 0.05$), while gender, age, and radiotherapy history displayed non-significance ($p > 0.05$) (**Figure 2**). All the available characteristics were included in the univariate analysis. There were statistically significant survival differences in the characteristics of primary tumor site, PE-T, IE-T, PE-N, IE-N, P-T, P-N, histologic grade in the univariate analysis (**Table 2**). These significant variables in the

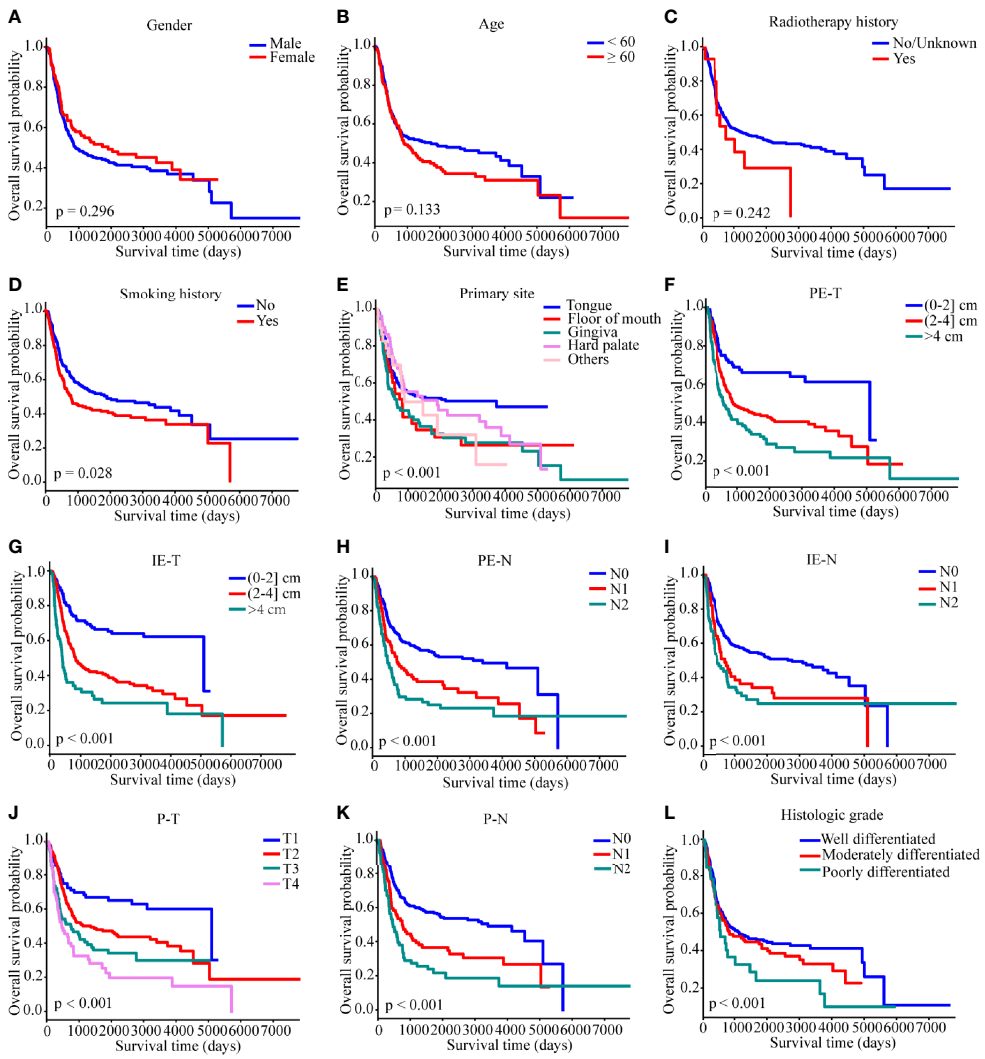

FIGURE 2 | Kaplan–Meier survival curves of overall survival in the SYSUCC cohort. **(A)** gender, **(B)** age, **(C)** radiotherapy history, **(D)** smoking history, **(E)** primary site, **(F)** PE-T, **(G)** IE-T, **(H)** PE-N, **(I)** IE-N, **(J)** P-T, **(K)** P-N, **(L)** histologic grade. Survival curves were compared by the log-rank test, and p <0.05 was considered as statistically significant. PE-T, physical examination-tumor size; IE-T, imaging examination-tumor size; PE-N, physical examination-nodal involvement; IE-N, imaging examination-nodal involvement; P-T, pathological tumor stage; P-N, pathological nodal involvement stage; T, tumor; N, lymph node.

Kaplan–Meier curves and the univariate analysis were included in the multivariate analysis to further screen out significant factors. In the multivariable stepwise regression analysis, PE-T (HR = 3.811; 95% CI, 1.210–12.004; p = 0.022), IE-T (HR = 4.135; 95% CI, 1.343–12.736; p = 0.013), P-N (HR = 1.834; 95% CI, 1.241–2.710; p = 0.002), and histologic grade (HR, 1.649; 95% CI, 1.083–2.511; p = 0.02) were significantly associated with OS in the training cohort (**Table 2**). Meanwhile, P-T, P-N, and histologic grade were significantly related to the outcome in the pathological model (p < 0.05, **Supplementary Table S1**).

Development of the Prognostic Model and Nomogram

Based on the results of the multivariable Cox regression model, four independent variables were incorporated to develop a more accurate nomogram for optimizing personalized prognostic assessment and predicting 1-, 3- and 5-year OS (**Figure 3**). Higher score was associated with a poor prognosis. The nomogram of the pathological model was shown in **Supplementary Figure S1**.

Performance and Validation of the Prognostic Model

The predictive accuracy between the clinical-pathological model and the pathological model has been compared. In the training cohort, the 1-, 3-, and 5-year AUC values of the clinical–pathological model for OS prediction were 0.687, 0.719, 0.722 (**Figure 4A**), which were superior to those of the pathological one (0.649, 0.707, 0.717, respectively) and AJCC TNM staging system (0.628, 0.668, 0.677, respectively), demonstrating

TABLE 2 | Univariate and multivariate Cox analysis for the clinical-pathological model.

Characteristics	Univariate analysis HR (95% CI)	*p*–value	Multivariate analysis HR (95% CI)	*p*–value
Gender	0.862 (0.621–1.195)	0.373		
Age	1.182 (0.869–1.609)	0.286		
Radiotherapy history	1.596 (0.824–3.093)	0.166		
Smoking history	1.287 (0.954–1.736)	0.099		
Site— tongue	Reference			
Site —Floor of mouth	1.758 (1.086–2.846)	0.022		
Site—Gingiva	1.702 (1.171–2.472)	0.005		
Site—Hard palate	1.192 (0.752–1.890)	0.454		
Site—Others	0.916 (0.464–1.807)	0.800		
PE-T	1.285 (1.170–1.411)	<0.001	3.811 (1.210–12.004)	0.022
IE-T	1.301 (1.183–1.432)	<0.001	4.135 (1.343–12.736)	0.013
PE-N	1.490 (1.234–1.800)	<0.001		
IE-N	1.408 (1.171–1.693)	<0.001		
P-T	1.389 (1.196–1.612)	<0.001		
P-N	1.548 (1.282–1.870)	<0.001	1.834 (1.241–2.710)	0.002
Histologic grade	1.290 (1.043–1.596)	0.019	1.649 (1.083–2.511)	0.020

HR, hazard ratio; CI, confidence interval; other abbreviations as in ***Table 1****.*

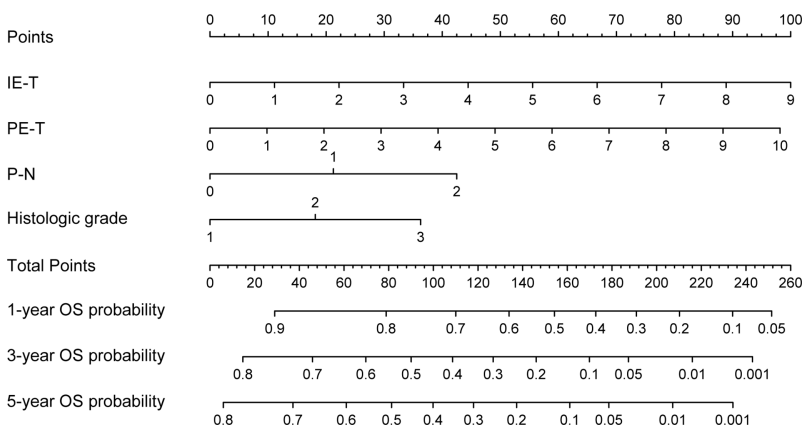

FIGURE 3 | Nomogram based on the clinical-pathological model for the prediction of 1-, 3- and 5-year OS. PE-T, physical examination-tumor size; IE-T, imaging examination-tumor size; P-N, pathological nodal involvement stage; OS, overall survival.

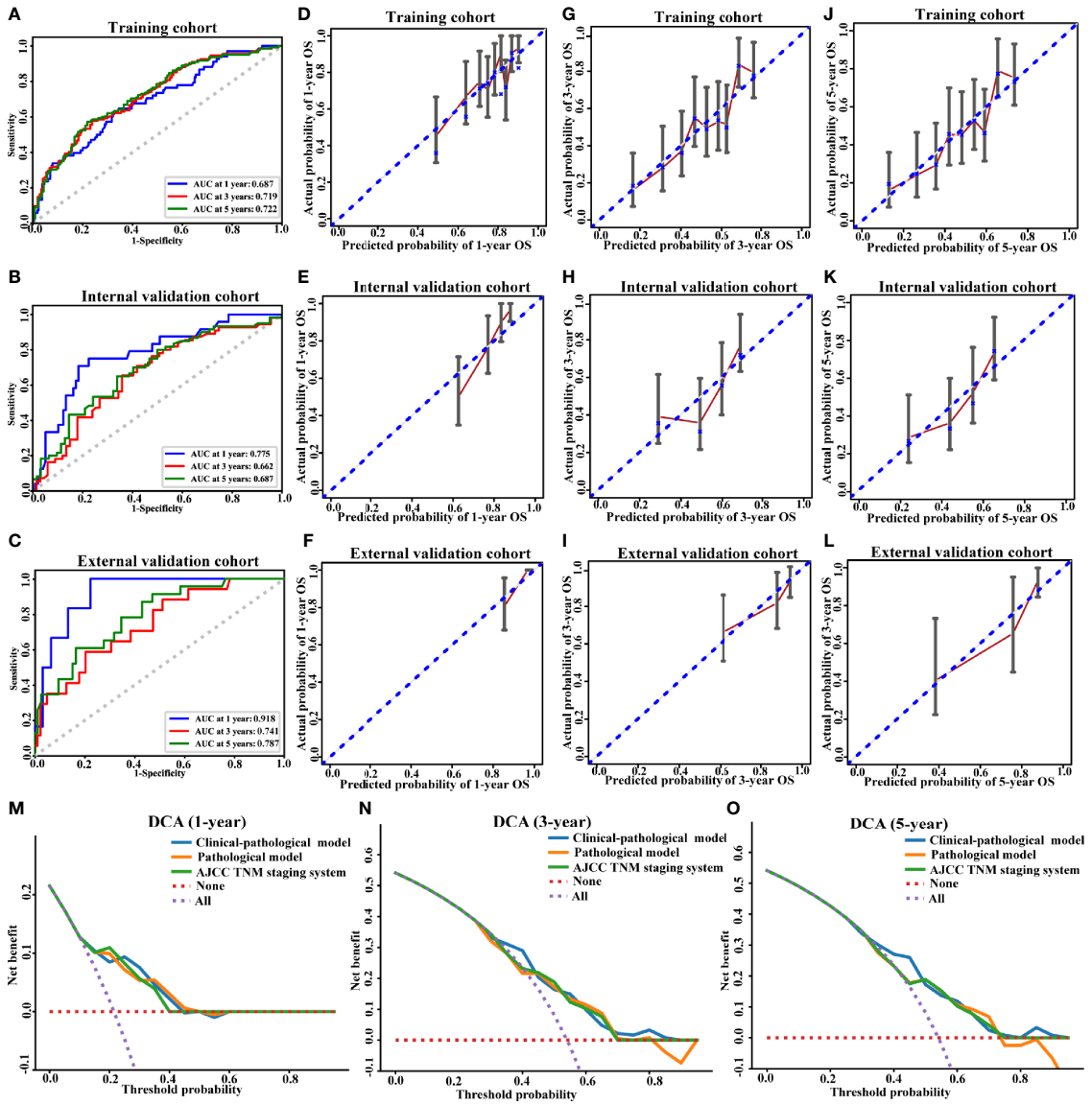

FIGURE 4 | Performance of the clinical-pathological model. ROC curve **(A–C)**, calibration curves for 1-year OS **(D–F)**, calibration curves for 3-year OS **(G–I)**, calibration curves for 5-year OS **(J–L)**, and decision curve analysis **(M–O)** for the training **(A, D, G, J)**, internal validation **(B, E, H, K, M–O)** and external validation cohorts **(C, F, I, L)**. AUC, area under the curve; OS, overall survival.

excellent sensitivity and specificity for the clinical–pathological model (**Supplementary Figures S2A**, **S3A**). Similarly, the 1-, 3-, and 5-year AUCs in the internal validation cohort (0.775, 0.662, 0.687, respectively; **Figure 4B**) and external validation cohort (0.918, 0.741, 0.787, respectively; **Figure 4C**) of the clinical–pathological model also showed better discriminative ability compared with the pathological one and the AJCC TNM staging system (**Supplementary Figures S2B, C**, **S3B, C**).

The C-indices of the clinical–pathological model displayed better predictive performance than that of the pathological model in the training (0.664; 95% CI, 0.615–0.711 vs. 0.638; 95% CI, 0.592–0.683), internal validation (0.679; 95% CI, 0.609–0.75 vs. 0.655; 95% CI, 0.578–0.726) and external validation cohorts (0.755; 95% CI, 0.644–0.853 vs. 0.702; 95% CI, 0.621–0.778) (**Table 3**). The clinical–pathological model exhibited superior discriminative power for OS prediction compared with the pathological model and the AJCC TNM staging system.

The calibration curves of 1-, 3- and 5-year OS and non-significant Hosmer–Lemeshow test demonstrated a good agreement between the prediction and observation values ($p > 0.05$) in the training (**Figures 4D, G, J**) and validation cohorts (**Figures 4E, F, H, I, K, L**), indicating that there was no deviation from the perfect fit. The calibration curves of pathological model were shown in **Supplementary Figures S2D–L**.

TABLE 3 | The C-indices for prediction of overall survival.

Model	Training cohort		Internal validation cohort		External validation cohort	
	C-index	95% CI	C-index	95% CI	C-index	95% CI
Clinical—pathological model	0.664	0.615–0.711	0.679	0.609–0.750	0.755	0.644–0.853
Pathological model	0.638	0.592–0.683	0.655	0.578–0.726	0.702	0.621–0.778
AJCC TNM staging system	0.610	0.564–0.653	0.660	0.594–0.720	0.642	0.567–0.713

C-index, concordance index; CI, confidence interval.

DCA analysis was conducted to evaluate the clinical value of our model. In the validation cohort, for predicted threshold probability between 30 and 70%, both the clinical–pathological and pathological models showed a positive net benefit for 3- and 5-year OS. Furthermore, the clinical–pathological model had a better net benefit for decision-making with the threshold probability within 30 and 50% illustrated by DCA (**Figures 4N, O**). Collectively, the threshold probabilities of the clinical–pathological model had better net benefits for predicting the 1-, 3- and 5-year OS in OSCC patients compared with the pathological one and the AJCC TNM staging system (**Figures 4M–O**).

Risk Stratification Based on the Nomogram

Based on the individualized risk points of the nomogram, patients were divided into low-risk and high-risk groups in the training, internal, and external validation cohorts (**Figures 5A–C**). The optimal cut-off value was 79.08 for the clinical–pathological nomogram, and the Kaplan–Meier curves revealed that the high-risk group (total points > 79.08) was significantly correlated with a poor prognosis. The optimal point effectively distinguished populations of low-risk and high-risk, demonstrating a good prognostic classification for OSCC patients.

DISCUSSION

Reliable prognostic factors are indispensable for properly stratifying the risk of the individual patient and avoid unnecessary overtreatment as well as unjustified toxicity. Clinical prognostic judgement of OSCC mainly focuses on the most classical AJCC TNM staging system (17–19). Besides the

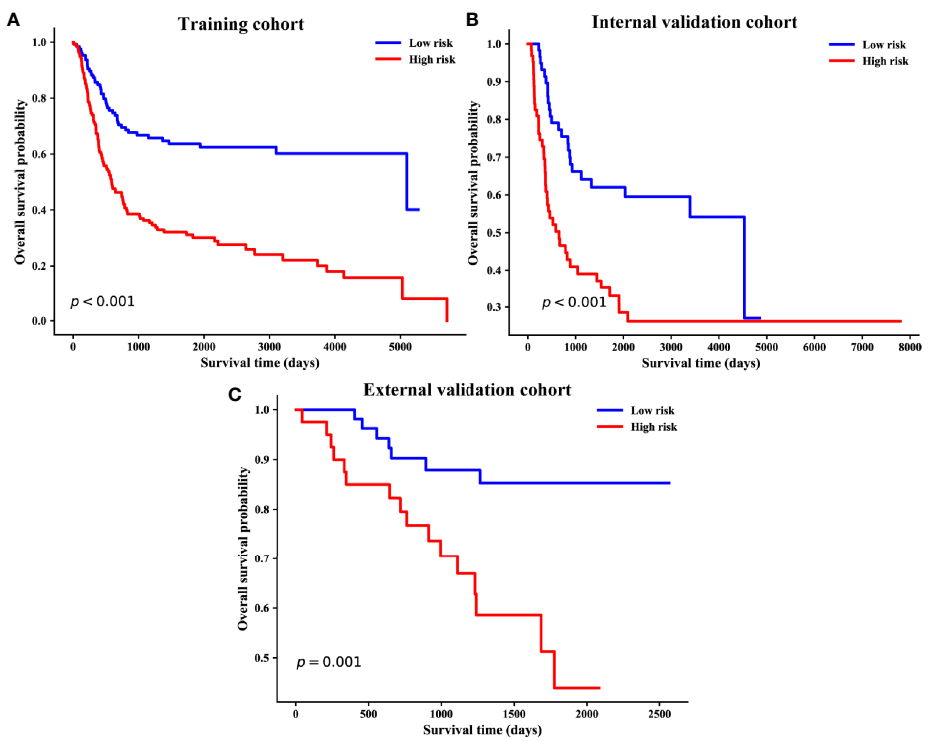

FIGURE 5 | Kaplan–Meier survival curves of overall survival based on risk score of the clinical–pathological nomogram in the training **(A)**, internal validation **(B)** and external validation cohorts **(C)**.

traditional pathological criterion, the multiple biomarkers detection such as protein-coding genes, messenger RNAs, and non-coding RNAs in body fluids (such as saliva and serum) and tumor tissues have gained much attention in prognosis prediction (20–23). However, traditional pathological TNM staging system only considered the anatomical extent of the disease without considering the nonanatomic factors, which can't fully reflect the accurate prognosis (24). A variety of clinicopathological parameters like age, gender, as well as clinical and pathological features of the tumor were also associated with the prognosis of OSCC patients (8, 25, 26). The single characteristic is usually insufficient to predict individual survival, while a combination can provide better prognostic reliability (27). Due to the lack of exact independent predictable biomarker, current biomarker testing was limited in the practical application (28).

Current treatment strategies for OSCC vary from radical surgery and radiotherapy to chemotherapy and molecular targeted therapy (29). Therapeutic effectiveness, health care costs, and personal affordability all will have influence on treatment process (30). From the perspective of patients and clinicians, the prognosis judgement would be of great importance in postoperative risk stratification and personalizing selection of adjuvant treatment for OSCC patients who underwent surgical resection (31). To develop a simple-to-use prediction model, we combined the clinical variables with the pathological TN stage, taking the individual differences in clinical examination into account. The illustrated-nomogram model finally suggested that integrating the preoperative data of physical and imaging examination with pathological data may be a comprehensive, economical and convenient method for clinicians to predict the prognosis of OSCC patients.

Nomograms have been frequently used for cancer prognosis prediction via a simple visualization modality. In our study, a visualized nomogram encompassed clinical and pathological risk factors that were easy to obtain and routinely collected was developed. Through the intuitive nomogram, the interrelation between variables and outcome was demonstrated and the probability of outcome events could be easily calculated by clinicians. Each subtype within these covariates was assigned a point on the point scale. Adding the points together of each variable was able to calculate a total point. The clinician would get the prediction probability of 1-, 3- and 5-year OS by locating the total point on the bottom scales. In our model, individualized score for each patient was calculated according to the nomogram, and the patients were successfully divided into low- and high-risk groups. The two groups showed significantly different prognosis. For high-risk patients, the traditional surgical resection cannot achieve satisfactory outcome, so alternative adjuvant treatment could be considered for the postoperative therapeutic scheme.

In the clinical–pathological model, the four variables including IE-T, PE-T, P-N, and histologic grade were significantly related to the outcome. Data of tumor size in physical examination were acquired by clinicians. Due to the specific location of oral cancer, clinicians could directly observe and measure the extent of the tumor, which ensured the relative accuracy and repeatability of our data (32). As an indispensable tool for clinical decision, physical examination still plays a significant role in the prognostic risk assessment in our study.

Tumor size in imaging examination also played a crucial part in our prognostic model. As a vital part of precision medicine, imaging examination has been proven its utility in identifying the multi-dimensional shape and location characteristics of a tumor (33). In 2017, tumor depth of invasion (DOI) was introduced into the 8th edition AJCC staging system. The AJCC 8th manual suggested that DOI could be reliably defined by the preoperative imaging (34). Weimar et al. successfully used the measurements of tumor thickness as a modifier for T stage in 8th AJCC based on the preoperative imaging examination such as computed tomography (CT) and magnetic resonance imaging (MRI) (35). At present, radiomics have been proven in identifying the shape and location characteristics of the tumor (36). However, radiomics require professional quantitative extraction of high-dimensional mineable data from all types of medical images, which mainly relies on professional radiologist for analysis (37). For most clinical surgeons, it's difficult to complete the complex radiomics analysis and make a prognosis judgement. Therefore, in our research, we only used the simple tumor size and nodal involvement stage obtained by imaging examination. Especially, the tumor size incorporated into the nomogram was analyzed as a continuous variable, which is convenient for clinicians to operate.

Although the background characteristics were different between independent hospitals, our nomogram-illustrated model still showed strong predictive ability in the external validation cohort, indicating our model could be widely applied to predict OS. Remarkably, early postoperative adjuvant therapy may be appropriate for patients considered at high risk for OS, such as those with high nomogram points. However, in the current analysis, the imaging examination data mainly included CT and MRI data. To gain further evidence and confirmation, large-scale prospective study and more up-to-date data from different equipment are needed to validate the generalization.

CONCLUSION

Collectively, a new nomogram-illustrated model was developed and validated for the OSCC patients without distant metastases from retrospective data. The tumor size of physical and imaging examination, pathological nodal involvement stage, and histologic grade were significantly associated with OS. Our clinical–pathological model was accessible and practical, which showed improved discriminatory ability relative to the pathological model. The clinical–pathological model might act as an effective method to improve the individualized prognostic evaluation through patient-specific characteristics, which may help to optimize postoperative therapeutic strategies.

DATA AVAILABILITY STATEMENT

The original contributions presented in the study are included in the article/**Supplementary Material**. Further inquiries can be directed to the corresponding authors.

ETHICS STATEMENT

Written informed consent was obtained from the individual(s) for the publication of any potentially identifiable images or data included in this article.

AUTHOR CONTRIBUTIONS

JZ and TW were involved in the design and conception. HL, RC, FZ, and DY conducted the acquisition of data, statistical analysis, and interpretation of data. JZ, HL, and TW drafted the paper. BC, MS, and XL retrieved the relevant literatures and revised the paper. All authors contributed to the article and approved the submitted version.

FUNDING

This work was supported by the National Natural Science Foundation of China (No. 81600878) and the key project of National Natural Science Foundation of China (No. 81630025).

SUPPLEMENTARY MATERIAL

The Supplementary Material for this article can be found online at: https://www.frontiersin.org/articles/10.3389/fonc.2021.652553/full#supplementary-material

Supplementary Figure 1 | Nomogram based on the pathological model for the prediction of 1-, 3- and 5-year OS. P-T, pathological tumor stage; P-N, pathological nodal involvement stage; OS, overall survival.

Supplementary Figure 2 | Performance of the pathological model. ROC curve **(A–C)**, calibration curves for 1-year OS **(D–F)**, calibration curves for 3-year OS **(G–I)**, and calibration curves for 5-year OS **(J–L)** for the training **(A, D, G, J)**, internal validation **(B, E, H, K)** and external validation cohorts **(C, F, I, L)**.

Supplementary Figure 3 | The ROC curves based on the AJCC TNM staging system for the prediction of 1-, 3- and 5-year OS in the training **(A)**, internal validation **(B)**, and external validation cohorts **(C)**.

REFERENCES

1. Toll DB, Janssen KJ, Vergouwe Y, Moons KG. Validation, Updating and Impact of Clinical Prediction Rules: A Review. *J Clin Epidemiol* (2008) 61:1085–94. doi: 10.1016/j.jclinepi.2008.04.008
2. Moons KG, Royston P, Vergouwe Y, Grobbee DE, Altman DG. Prognosis and Prognostic Research: What, Why, and How? *BMJ* (2009) 338:b375. doi: 10.1136/bmj.b375
3. Sung H, Ferlay J, Siegel RL, Laversanne M, Soerjomataram I, Jemal A, et al. Global Cancer Statistics 2020: GLOBOCAN Estimates of Incidence and Mortality Worldwide for 36 Cancers in 185 Countries. *CA Cancer J Clin* (2021). doi: 10.3322/caac.21660
4. Chi AC, Day TA, Neville BW. Oral Cavity and Oropharyngeal Squamous Cell Carcinoma–an Update. *CA Cancer J Clin* (2015) 65:401–21. doi: 10.3322/caac.21293
5. Bosetti C, Carioli G, Santucci C, Bertuccio P, Gallus S, Garavello W, et al. Global Trends in Oral and Pharyngeal Cancer Incidence and Mortality. *Int J Cancer* (2020) 147:1040–9. doi: 10.1002/ijc.32871
6. Chinn SB, Myers JN. Oral Cavity Carcinoma: Current Management, Controversies, and Future Directions. *J Clin Oncol* (2015) 33:3269–76. doi: 10.1200/JCO.2015.61.2929
7. Amin MB, Greene FL, Edge SB, Compton CC, Gershenwald JE, Brookland RK, et al. The Eighth Edition AJCC Cancer Staging Manual: Continuing to Build a Bridge From a Population-Based to a More "Personalized" Approach to Cancer Staging. *CA Cancer J Clin* (2017) 67:93–9. doi: 10.3322/caac.21388
8. Ferreira AK, Carvalho SH, Granville-Garcia AF, Sarmento DJ, Agripino GG, Abreu MH, et al. Survival and Prognostic Factors in Patients With Oral Squamous Cell Carcinoma. *Med Oral Patol Oral Cir Bucal* (2020) 24242. doi: 10.4317/medoral.24242
9. Sasahira T, Kirita T. Hallmarks of Cancer-Related Newly Prognostic Factors of Oral Squamous Cell Carcinoma. *Int J Mol Sci* (2018) 19:2413. doi: 10.3390/ijms19082413
10. Cervino G, Fiorillo L, Herford AS, Romeo U, Bianchi A, Crimi S, et al. Molecular Biomarkers Related to Oral Carcinoma: Clinical Trial Outcome Evaluation in a Literature Review. *Dis Markers* (2019) 2019:8040361. doi: 10.1155/2019/8040361
11. Ballman KV. Biomarker: Predictive or Prognostic? *J Clin Oncol* (2015) 33:3968–71. doi: 10.1200/JCO.2015.63.3651
12. Touil H, Briki S, Karray F, Bahri I. Malignant Peripheral Nerve Sheath Tumor of the Superficial Cervical Plexus With Parotid Extension. *Eur Ann Otorhinolaryngol Head Neck Dis* (2015) 132:93–5. doi: 10.1016/j.anorl.2013.11.012
13. Moons KG, Altman DG, Reitsma JB, Ioannidis JP, Macaskill P, Steyerberg EW, et al. Transparent Reporting of a Multivariable Prediction Model for Individual Prognosis or Diagnosis (TRIPOD): Explanation and Elaboration. *Ann Intern Med* (2015) 162:W1–73. doi: 10.7326/M14-0698
14. Liang CJ, Heagerty PJ. A Risk-Based Measure of Time-Varying Prognostic Discrimination for Survival Models. *Biometrics* (2017) 73:725–34. doi: 10.1111/biom.12628
15. Vickers AJ, Cronin AM, Elkin EB, Gonen M. Extensions to Decision Curve Analysis, a Novel Method for Evaluating Diagnostic Tests, Prediction Models and Molecular Markers. *BMC Med Inform Decis Mak* (2008) 8:53. doi: 10.1186/1472-6947-8-53
16. Steyerberg EW, Vickers AJ, Cook NR, Gerds T, Gonen M, Obuchowski N, et al. Assessing the Performance of Prediction Models: A Framework for Traditional and Novel Measures. *Epidemiology* (2010) 21:128–38. doi: 10.1097/EDE.0b013e3181c30fb2
17. Moeckelmann N, Ebrahimi A, Tou YK, Gupta R, Low TH, Ashford B, et al. Prognostic Implications of the 8th Edition American Joint Committee on Cancer (AJCC) Staging System in Oral Cavity Squamous Cell Carcinoma. *Oral Oncol* (2018) 85:82–6. doi: 10.1016/j.oraloncology.2018.08.013
18. Lee NCJ, Eskander A, Park HS, Mehra S, Burtness BA, Husain Z. Pathologic Staging Changes in Oral Cavity Squamous Cell Carcinoma: Stage Migration and Implications for Adjuvant Treatment. *Cancer* (2019) 125:2975–83. doi: 10.1002/cncr.32161
19. Almangush A, Pirinen M, Youssef O, Makitie AA, Leivo I. Risk Stratification in Oral Squamous Cell Carcinoma Using Staging of the Eighth American Joint Committee on Cancer: Systematic Review and Meta-Analysis. *Head Neck* (2020) 42:3002–17. doi: 10.1002/hed.26344
20. Chang SW, Abdul-Kareem S, Merican AF, Zain RB. Oral Cancer Prognosis Based on Clinicopathologic and Genomic Markers Using a Hybrid of Feature Selection and Machine Learning Methods. *BMC Bioinf* (2013) 14:170. doi: 10.1186/1471-2105-14-170
21. Zhang L, Meng X, Zhu XW, Yang DC, Chen R, Jiang Y, et al. Long non-Coding RNAs in Oral Squamous Cell Carcinoma: Biologic Function, Mechanisms and Clinical Implications. *Mol Cancer* (2019) 18:102. doi: 10.1186/s12943-019-1021-3

22. Rivera C, Oliveira AK, Costa RAP, De Rossi T, Paes Leme AF. Prognostic Biomarkers in Oral Squamous Cell Carcinoma: A Systematic Review. *Oral Oncol* (2017) 72:38–47. doi: 10.1016/j.oraloncology.2017.07.003
23. Lu Z, Liang J, He Q, Wan Q, Hou J, Lian K, et al. The Serum Biomarker Chemerin Promotes Tumorigenesis and Metastasis in Oral Squamous Cell Carcinoma. *Clin Sci (Lond)* (2019) 133:681–95. doi: 10.1042/CS20181023
24. De Paz D, Kao HK, Huang Y, Chang KP. Prognostic Stratification of Patients With Advanced Oral Cavity Squamous Cell Carcinoma. *Curr Oncol Rep* (2017) 19:65. doi: 10.1007/s11912-017-0624-3
25. Tagliabue M, Belloni P, De Berardinis R, Gandini S, Chu F, Zorzi S, et al. A Systematic Review and Meta-Analysis of the Prognostic Role of Age in Oral Tongue Cancer. *Cancer Med* (2021) 10:2566–78. doi: 10.1002/cam4.3795
26. Oh LJ, Asher R, Veness M, Smee R, Goldstein D, Gopalakrishna Iyer N, et al. Effect of Age and Gender in non-Smokers With Oral Squamous Cell Carcinoma: Multi-institutional Study. *Oral Oncol* (2021) 116:105210. doi: 10.1016/j.oraloncology.2021.105210
27. Kademani D. Oral Cancer. *Mayo Clin Proc* (2007) 82:878–87. doi: 10.4065/82.7.878
28. Kang H, Kiess A, Chung CH. Emerging Biomarkers in Head and Neck Cancer in the Era of Genomics. *Nat Rev Clin Oncol* (2015) 12:11–26. doi: 10.1038/nrclinonc.2014.192
29. Marur S, Forastiere AA. Head and Neck Squamous Cell Carcinoma: Update on Epidemiology, Diagnosis, and Treatment. *Mayo Clin Proc* (2016) 91:386–96. doi: 10.1016/j.mayocp.2015.12.017
30. Siegel R, Ma J, Zou Z, Jemal A. Cancer Statistics, 2014. *CA Cancer J Clin* (2014) 64:9–29. doi: 10.3322/caac.21208
31. Kim KY, Zhang X, Kim SM, Lee BD, Cha IH. A Combined Prognostic Factor for Improved Risk Stratification of Patients With Oral Cancer. *Oral Dis* (2017) 23:91–6. doi: 10.1111/odi.12579
32. Huber MA, Tantiwongkosi B. Oral and Oropharyngeal Cancer. *Med Clin North Am* (2014) 98:1299–321. doi: 10.1016/j.mcna.2014.08.005
33. Kurland BF, Gerstner ER, Mountz JM, Schwartz LH, Ryan CW, Graham MM, et al. Promise and Pitfalls of Quantitative Imaging in Oncology Clinical Trials. *Magn Reson Imaging* (2012) 30:1301–12. doi: 10.1016/j.mri.2012.06.009
34. Dirven R, Ebrahimi A, Moeckelmann N, Palme CE, Gupta R, Clark J. Tumor Thickness Versus Depth of Invasion - Analysis of the 8th Edition American Joint Committee on Cancer Staging for Oral Cancer. *Oral Oncol* (2017) 74:30–3. doi: 10.1016/j.oraloncology.2017.09.007
35. Weimar EAM, Huang SH, Lu L, O'Sullivan B, Perez-Ordonez B, Weinreb I, et al. Radiologic-Pathologic Correlation of Tumor Thickness and Its Prognostic Importance in Squamous Cell Carcinoma of the Oral Cavity: Implications for the Eighth Edition Tumor, Node, Metastasis Classification. *AJNR Am J Neuroradiol* (2018) 39:1896–902. doi: 10.3174/ajnr.A5782
36. Huang YQ, Liang CH, He L, Tian J, Liang CS, Chen X, et al. Development and Validation of a Radiomics Nomogram for Preoperative Prediction of Lymph Node Metastasis in Colorectal Cancer. *J Clin Oncol* (2016) 34:2157–64. doi: 10.1200/JCO.2015.65.9128
37. Parmar C, Grossmann P, Rietveld D, Rietbergen MM, Lambin P, Aerts HJ. Radiomic Machine-Learning Classifiers for Prognostic Biomarkers of Head and Neck Cancer. *Front Oncol* (2015) 5:272. doi: 10.3389/fonc.2015.00272

Conflict of Interest: Authors FZ, DY, and XL were employed by the company AID Cloud Technology Co., Ltd.

The remaining authors declare that the research was conducted in the absence of any commercial or financial relationship that could be construed as a potential conflict of interest.

frontiers in Oncology

ORIGINAL RESEARCH
published: 23 June 2021
doi: 10.3389/fonc.2021.647175

IRAK2, an IL1R/TLR Immune Mediator, Enhances Radiosensitivity *via* Modulating Caspase 8/3-Mediated Apoptosis in Oral Squamous Cell Carcinoma

*Chih-Chia Yu[1,2], Michael W.Y. Chan[3,4,5,6], Hon-Yi Lin[2,7], Wen-Yen Chiou[2,7], Ru-Inn Lin[2], Chien-An Chen[8], Moon-Sing Lee[2,7], Chen-Lin Chi[7,9], Liang-Cheng Chen[2,7], Li-Wen Huang[2,7], Chia-Hui Chew[2,7], Feng-Chun Hsu[2], Hsuan-Ju Yang[2] and Shih-Kai Hung[2,7]**

[1] Department of Medical Research, Dalin Tzu Chi Hospital, Buddhist Tzu Chi Medical Foundation, Chia-Yi, Taiwan, [2] Department of Radiation Oncology, Dalin Tzu Chi Hospital, Buddhist Tzu Chi Medical Foundation, Chia-Yi, Taiwan, [3] Research Center for Environmental Medicine, Kaohsiung Medical University, Kaohsiung, Taiwan, [4] Department of Biomedical Sciences, National Chung Cheng University, Chia-Yi, Taiwan, [5] Epigenomics and Human Disease Research Center, National Chung Cheng University, Chia-Yi, Taiwan, [6] Center for Innovative Research on Aging Society (CIRAS), National Chung Cheng University, Chia-Yi, Taiwan, [7] School of Medicine, Tzu Chi University, Hualian, Taiwan, [8] Department of Radiation Oncology, Zhongxing Branch, Taipei City Hospital, Taipei, Taiwan, [9] Department of Pathology, Chiayi Chang Gung Memorial Hospital, Chia-Yi, Taiwan

OPEN ACCESS

Edited by:
Cesare Piazza, University of Brescia, Italy

Reviewed by:
Gaurisankar Sa, Bose Institute, India
Gunnar Wichmann, University Hospital Leipzig, Germany

***Correspondence:**
Shih-Kai Hung
oncology158@yahoo.com.tw

Specialty section:
This article was submitted to Head and Neck Cancer, a section of the journal Frontiers in Oncology

Received: *29 December 2020*
Accepted: *03 June 2021*
Published: *23 June 2021*

Citation:
Yu C-C, Chan MWY, Lin H-Y, Chiou W-Y, Lin R-I, Chen C-A, Lee M-S, Chi C-L, Chen L-C, Huang L-W, Chew C-H, Hsu F-C, Yang H-J and Hung S-K (2021) IRAK2, an IL1R/TLR Immune Mediator, Enhances Radiosensitivity via Modulating Caspase 8/3-Mediated Apoptosis in Oral Squamous Cell Carcinoma. Front. Oncol. 11:647175. doi: 10.3389/fonc.2021.647175

Predicting and overcoming radioresistance are crucial in radiation oncology, including in managing oral squamous cell carcinoma (OSCC). First, we used RNA-sequence to compare expression profiles of parent OML1 and radioresistant OML1-R OSCC cells in order to select candidate genes responsible for radiation sensitivity. We identified IRAK2, a key immune mediator of the IL-1R/TLR signaling, as a potential target in investigating radiosensitivity. In four OSCC cell lines, we observed that intrinsically low IRAK2 expression demonstrated a radioresistant phenotype (i.e., OML1-R and SCC4), and vice versa (i.e., OML1 and SCC25). Next, we overexpressed IRAK2 in low IRAK2-expression OSCC cells and knocked it down in high IRAK2-expression cells to examine changes of irradiation response. After ionizing radiation (IR) exposure, IRAK2 overexpression enhanced the radiosensitivity of radioresistant cells and synergistically suppressed OSCC cell growth both *in vitro* and *in vivo*, and vice versa. We found that IRAK2 overexpression restored and enhanced radiosensitivity by enhancing IR-induced cell killing *via* caspase-8/3-dependent apoptosis. OSCC patients with high IRAK2 expression had better post-irradiation local control than those with low expression (i.e., 87.4% *vs.* 60.0% at five years, P = 0.055), showing that IRAK2 expression was associated with post-radiation recurrence. Multivariate analysis confirmed high IRAK2 expression as

an independent predictor for local control (HR, 0.11; 95% CI, 0.016 – 0.760; P = 0.025). In conclusion, IRAK2 enhances radiosensitivity, *via* modulating caspase 8/3-medicated apoptosis, potentially playing double roles as a predictive biomarker and a novel therapeutic target in OSCC.

Keywords: IRAK2, radioresistant, apoptosis, radiosensitization, oral squamous cell carcinoma

INTRODUCTION

Radiotherapy (RT) is an essential treatment modality for managing patients with oral squamous cell carcinoma (OSCC) (1). However, cancer radioresistance restricts the clinical efficacy of RT. Although several genes and molecular pathways have been reported (2, 3), the molecular events leading to a radioresistant phenotype of OSCC remain mostly unknown. Therefore, exploring a novel targeted molecular marker that sensitizes tumors to ionizing radiation (IR) is crucial to overcome radioresistance and then decrease post-RT cancer recurrence.

RNA Sequencing (RNA-Seq) technology, widely used in studying whole-genome expression profiles, can help identify possible therapeutic targets (4). To search for genes potentially responsible for OSCC resistance that could predict radiosensitivity, we recently established a stable, radioresistant oral cancer cell subline (i.e., OML1-R) from its parent line (i.e., OML1) *via* step-by-step fractionated irradiations (5). Subsequently, we performed next-generation sequencing (NGS) and bioinformatics techniques to analyze post-IR gene expression between the two cell lines. Finally, we identified that IRAK2 was up-regulated in post-irradiated parental OML1 cells, but not in radioresistant OML1-R cells, implicating that the IRAK2 gene might play a role in the process of radiosensitivity in OSCC.

IRAK2 (Interleukin-1 receptor associated kinase 2) is a component of the interleukin-1 receptor (IL-1R)/Toll-like receptor (TLR) signaling cascade (6). Known to act as an adaptor in the TLR-MyD88-TRAF6 complex, IRAK2 could enable the downstream activation of NF-κB and thereby regulating inflammation (7). Notably, IRAK2 also participates in the regulation of cellular apoptosis *via* inducing the FADD-dependent caspase-8 apoptotic pathway to trigger the Yersinia-induced macrophage cell death (8). Besides, IRAK2 has been recognized as a contributor to ER stress-induced cell death *via* IRE1/CHOP signaling (9). Recently, one family member of IRAK2, i.e., IRAK1, has been reported to play a role in the processes of TLR signaling (10) and intrinsic radioresistance, suggesting a potential chemoradiotherapy target (11). However, the function and biologic effects of IRAK2 in association with intrinsic/acquired radioresistance in the context of solid cancers, including OSCC, remain mostly unknown.

Hence, in the present study, we present new insight into the significance of IRAK2 in radiation response, therefore, tested the role of IRAK2 in OSCC, focusing on exploring its potential function and molecular mechanism in mediating radiosensitization. Our data indicated that IRAK2 is an attractive target, in both predictive and therapeutic aspects, for radioresistant OSCC because the overexpression of IRAK2 may contribute to enhanced/restore IR-induced tumor cell killing.

MATERIALS AND METHODS

Chemicals and Reagents

Antibodies against IRAK2, cleaved caspase-8, cleaved caspase-3, NF-κB-p65, and C/EBP homologous protein (CHOP) were purchased from the Cell Signaling Technology (Beverly, MA). Processes of storage, manipulation, and analysis obeyed the manufacturer's instructions.

Cell Lines and Cell Culture

SCC4 and SCC25 were bought from American Type Culture Collection (ATCC; Manassas, VA) and cultured in DMEM/F12 containing 10% fetal bovine serum (FBS), 1% penicillin-streptomycin and 2 mM L-glutamine. Parental (OML1) and acquired-radioresistant (OML1-R) cell lines were established and maintained in RPMI1640 containing 10% FBS, 1% penicillin-streptomycin, and 2 mM L-glutamine, as previously reported (5, 12). Briefly, we constructed OML-1R from parental OML-1 cells by using fractionated irradiations. A fraction size of 5 Gy was delivered per 5-7 days till every 80% confluent of irradiated cells. By ten fractions, a total of 50 Gy were delivered on parental OML-1 cells to construct OML-1R cells. Then, we applied a 10-Gy single shot to validate the level of acquired radioresistance of OML-1R cells before further experiments [10]. Briefly, a total of 1×10^3 cells were seeded on a 6-cm plate before irradiation. The next day, cells were irradiated with 10 Gy and then cultured for another 2-3 days.

Patient Samples and Radiotherapy Details

From Jan. 2007 to Dec. 2014, we retrospectively identified 41 patients with pathological stage I-II OSCC (i.e., pT1-2N0M0 status) (12, 13). The reason to choose this population was that OSCC patients with microscopic residual disease (R1) or close surgical margins of ≤5 mm (R0) have an increased risk for local failure even if the resected tumor was staged as pT1-2N0M0 and therefore were subjected to postoperative RT according to guidelines (1). All patients received radical surgery and postoperative RT. Indications of RT for these patients were positive or close surgical margin (i.e., ≤5 mm), as mentioned previously (13). All OSCC patient samples (i.e., formalin-fixed paraffin-embedded pathological blocks) were retrospectively re-confirmed, and tumor-burden-enriched regions (i.e., >70% tumor-content area) were re-sliced, re-stained, and retrieved for bench experiments, as previously reported (12).

Postoperative RT was delivered using the intensity-modulated radiotherapy (IMRT) technique (14). Irradiation volumes were designed according to the principle of radiotherapy (15), in terms of high-, moderate-, and low-risk planning target volume (PTV). Notably, total doses of RT to the high-risk PTV (i.e., the oral surgical bed and high-risk lymph-drainage basins) were ranged from 60 Gy to 66 Gy by using a conventional fraction size of 1.8-2.0 Gy (6-MV photons).

Research Database of Clinical Outcomes

For coding post-irradiation clinical outcomes, we used the Dalin Prospective-coding Cancer Registration Database. This database was a regular national-audit cancer database for oncological research. Regular audits were conducted by the multimodality committee of the Health Promotion Administration, Ministry of Health and Welfare, Taiwan (16). At the latest audit in 2018, the overall data-consisting rate was 99.5%. For each involved patient, the following clinicopathological factors were retrospectively retrieved from the database: age, RT dose, pathologic stage, clinical stage, surgical margin, and postoperative adjuvant chemotherapy (17–19). All data were independently validated by a radiation physician and analyzed by a biostatistician according to methods described in the statistical section, as previously reported (12).

Illumina MiSeq System

We used TRIZOL to isolate total RNAs according to the manufacturer's instructions (Invitrogen, Carlsbad, CA). Next, we used the Illumina MiSeq (Illumina, San Diego, CA) to conduct RNA-Seq. The mapped reads (i.e., Reads Per Kilobase Million [RPKM]) were applied to indicate gene expression levels; this value was used to calculate the average expression level for each gene between paired OML1 and OML1-R cell lines treated with or without IR. Gene expression profiles of both cells were obtained from the Gene Expression Omnibus (GEO) database (https://www.ncbi.nlm.nih.gov/geo/query/acc.cgi?acc=GSE165585). First, we selected genes that exhibited a statistically significant difference of higher than 1.5-fold between OML1 and OML1-R cells after IR. Next, we filtered out lowly expressed transcripts by using an absolute value of RPKM < 2. Then, we identified eight genes of IRAK2, KLK6, NSMF, SCO1, TRIP13, LMBR1, SCARB1, and FANCD2. Finally, we investigated IRAK2 because IRAK2 showed the maximum fold change of gene expression.

Colony Formation Assay

OSCC cell lines were treated with indicated irradiation doses of 0, 4, or 10 Gray (Gy) by using 6-MV photons (Varian linear accelerator, US), as previously reported (12). Notably, to provide effective dose delivery, a 0.5-cm bolus was placed over both the upper and downsides of the culture dishes, just like a sandwich design (5). Briefly, cells were cultured in a specific medium for more than 80% fluency. Next, we trypsinized and plated the cells to produce a single-cell suspension in another culture dish. Then, irradiation was delivered per protocol in the irradiating arm; the control arm had no irradiation. At seven days after irradiation, colonies (defined as groups of >50 cells) were fixed and stained with 0.05% crystal violet for further visual quantification. For quantifying cell number, irradiated cells were stained with 0.4% crystal violet (Sigma) and counted at OD580 by using a spectrophotometer (GeneQuant 1300, GE Healthcare, UK) (20).

Western Blotting

We lysed cells with 100μl of PRO-PREP Protein Extraction Solution according to the manufacturer's protocol. Then, protein samples (50 μg/well) were separated by 12% SDS-PAGE electrophoresis and transferred to PVDF membranes (at 260 mA for about 90 minutes), as reported previously (21). Briefly, membranes were blocked with 5% non-fat dried milk in 1X TBS-T buffer (for 1 hour at room temperature) and probed with primary antibodies (diluted with 5% non-fat milk in 1X TBST), followed by HRP-labeled secondary antibodies (also diluted with 5% non-fat milk in 1X TBST). Finally, bands were visualized by using electrochemiluminescence detection reagents (Millipore, Billerica, MA). Quantification was performed by using the image-J software (National Institute of Health, NIH, Bethesda, MD).

RNA Extraction and Quantitative Real-Time-Polymerase Chain Reaction (qRT-PCR)

Total RNA samples were extracted by using the TRIZOL (Invitrogen, Carlsbad, CA) according to the manufacturer's instructions and previously reported (12). Briefly, we used DNase I (amplification grade, Invitrogen) to treat 1μg of total RNA before first-strand cDNA synthesis by using reverse transcriptase (Superscript II RT, Invitrogen). Then, PCR reactions were performed by using the ABI StepOne real-time PCR system (Applied Biosystems, Foster City, CA). For PCR, specific primers were used accordingly. The relative expression of IRAK2 was estimated by using the comparative Ct method. The following primers were used: IRAK2, forward, CCAGCCTGCAGGAGGTGTGTGG and reverse, CATCAAGGCT GGAATTGTCAAC; GAPDH, forward, AGCCACATCGCTCAGA CAC and reverse, GCCCAATACGACCAAATCC.

Flow Cytometry Analysis

Apoptosis was measured by using the FACScan flow cytometer (Becton Dickinson, Franklin Lakes, NJ) with combined-agent Apoptosis Detection Kit (BD Bioscience, Heidelberg, Germany). Annexin V, Fluorescein isothiocyanate (FITC), and 7-aminoactinomycin D (7AAD) were applied and analyzed following the manufacturer's instruction. The cells were treated with or without 4Gy for 48 hours and collected by trypsinization. Cell pellets were resuspended in 400 μl 1X binding buffer and then stained with 5.0 μl annexin V-FITC as well as 2.5 μl 7-AAD for 20 min at room temperature in the dark and then analyzed *via* flow cytometry.

Transient Overexpression

First, cells were plated in a 6-cm culture dish. The plasmid for human IRAK2 (Myc-DDK-tagged) ectopic expression was purchased from Origene (Rockville, MD). We transfected

pCMV6-IRAK2 plasmid into OSCC cells by using Lipofectamine 2000® (Invitrogen, Carlsbad, CA) and Opti-MEM medium, according to the manufacturer's protocols. Cells were finally selected for stable clones by using the medium that contained 400μg/ml Geneticin (G418, Invitrogen).

Transient Knockdown

The human IRAK2 shRNA sequence was purchased from the National RNAi Core Facility at Academia Sinica, Taiwan (clone ID: TRCN0000418431). Lentiviral constructs that expressed IRAK2-shRNA were subcloned into pLKO.1-puro plasmid, a lentiviral vector for cDNA expression (Sigma-Aldrich, St. Louis MO). All lentiviral vectors were transfected into 293T cells by using Lipofectamine 2000 reagent according to the manufacturer's instructions. For lentiviral transduction, cells were treated with 8 μg/ml Polybrene (Sigma-Aldrich). Viral supernatants were added to the cell culture medium for 48 hours. The transduced cells were selected with 3 ug/ml puromycin (Gibco; Thermo Fisher Scientific, Inc., Waltham, MA, USA).

Immunohistochemistry

Paraffin-embedded oral tumor sections were stained with an anti-IRAK2 antibody (monoclonal; Abnova, Taiwan) and then detected by using the Super Sensitive™ Polymer-HRP IHC detection system (Biogenex, San Ramon, CA), according to the manufacturer's instructions. Antigens were retrieved by using EDTA buffer (pH9.0) at 100°C for 25 minutes. Then, the slides were incubated at room temperature with 1:50-diluted IRAK2 antibody for 1 hour, followed by washing with 1XTBS-T. Finally, the sections were incubated with diaminobenzidine (DAB) for 5 minutes to generate signals. The pathologist evaluated stained slides of individual patients. The staining intensity of IRAK2 over the cell membrane or cytoplasmic region was scored by using a scale ranging from 0–3 and percentages (0-100%). The score was a continuous variable, ranging from 0–300. The value was calculated by using the following formula: 1 × (percentage of weakly stained cells, i.e., 1+) + 2 × (percentage of moderately stained cells, i.e., 2+) + 3 × (percentage of strongly stained cells, i.e., 3+). The median IHC score of 110 was applied as a cut-off value to differentiate high or low expression.

In Vivo Tumorigenesis

We used male 6-week-old athymic nude mice (BALB/cAnN.Cg-Foxn1nu/CrlNarl) for the *in vivo* xenograft experiment. Null vector OML1-R cells and stable IRAK2-transfected OML1-R cells (2×10^7 cells) were suspended in 200 ul PBS. Then, these cells were injected subcutaneously into the left and right flanks of each mouse, respectively (n = 3 in each group). Tumor volume was monitored and quantified with a tumor volume growth ratio (final volume/initial volume). For exploring the role of IRAK2 in radiosensitivity *in vivo*, the control and IRAK2-overexpressed groups were designed (n = 3 in each group). IR treatment was started 40 days after cancer cells transplantation. As a similar IR protocol of cell irradiation (5), we delivered IR every four days. A total dose of 50 Gy was given in 10 fractions (Varian linear accelerator, US). All animal protocols were performed according to the instructions of the Institutional Animal Care and Use Committee of National Chung Cheng University (IACUC no.1060703).

Statistical Analysis

All statistical analyses were performed by using the SigmaPlot software, version 10.0 (Systat Software Inc., San Jose, CA, USA) and SPSS (version 12.0; SPSS Inc., Chicago, IL, USA), accordingly. Continuous data were presented as mean ± standard deviation, and their statistically significant levels were calculated by using the Student's t-test. Category data were analyzed by using the chi-square test. Time-to-event endpoints were estimated using the Kaplan-Meier plot, and the log-rank test was applied to assess curve differences between groups. Cox proportional regression analysis was used for univariate and multivariate analysis. All hazard ratios were provided with 95% confidence intervals to demarcate effective size. *P* values of less than 0.05 were defined as statistical significance.

RESULTS

IRAK2 Affected the Sensitivity of OML1 and ML1-R Cells to IR

Clonogenic assay confirmed a higher radiosensitivity of OML1 than that of OML1-R cells. When treated with the same dose of IR, especially 10 Gy, OML1-R cells exhibited a higher survival fraction than that of parental OML1 cells, suggesting that OML1-R is relatively resistant to IR treatment (**Figure 1A**). To identify genes whose expressions were altered after exposure to radiation, we utilized RNA-seq to assess the expression pattern of genes between paired parent (OML1) and radioresistant (OML1-R) cell lines treated with or without IR. By comparing the expression profiles of the two cell lines, we hypothesized that radiation exposure could activate genes responsible for the radiosensitivity process. By using reads per kilobase transcript per million mapped reads (RPKM) to estimate gene expression, we identified 19 genes that exhibited statistically significant differences of higher than 1.5-fold between OML1 and OML1-R cells after IR (**Figure 1B**). We further filtered out lowly expressed transcripts (i.e., an absolute cut-off value of RPKM < 2). As a result, eight genes were identified, including IRAK2, KLK6, NSMF, SCO1, TRIP13, LMBR1, SCARB1, and FANCD2 (**Figure 1B**). Of these, we found that IRAK2 showed the maximum fold change of gene expression (**Figure 1B**). Hence, we chose IRAK2 as our target for further functional analysis because it plays a vital role in regulating innate immunity (22) and may have great potential in predicting radiation response of OSCC cells. The data showed that the RPKM value of IRAK2 expression of the OML1-R was lower than that of OML1 cell lines whether control or IR treatment (**Figure 1C**). Real-time quantitative PCR (qPCR) and Western blotting analysis revealed that both mRNA and protein expressions of IRAK2 were up-regulated in irradiated OML1 cells compared with IR-treated OML1-R cells (**Figures 1D, E**).

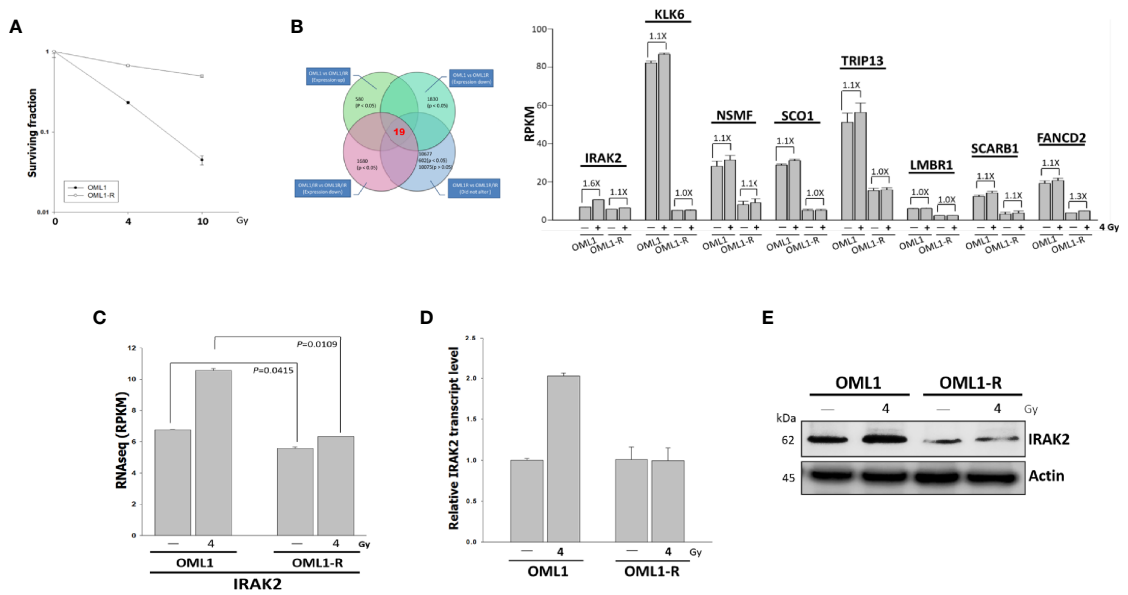

FIGURE 1 | Higher IRAK2 expression was associated with a higher radiosensitivity in the context of parental (i.e., OML1) and radioresistant (i.e., OML1-R) OSCC cells. **(A)** After exposure to 0, 4, and 10 Gy IR, colony-formation assay confirmed that OML1-R cells were relatively radioresistant when compared with parental OML1 cells. **(B)** Venn diagram showed the number of genes with apparent expression change before and after irradiation in OML1 and OML1-R cells (left). Bar graphs displayed 19 genes were up-regulated in OML1 cells, using a filter criterion at least 1.5-fold change with $P < 0.05$. By setting a threshold of RPKM>2, we identified eight reliable transcripts that were largely differentially expressed between the OML1 and OML1-R cells. The graph showed relative fold change in gene expression: control *versus* IR-treated cells (right). **(C)** The RPKM value of IRAK2 expression was plotted for OML1 and OML1-R cells treated with 4 Gy. **(D)** qPCR and **(E)** Western blotting revealed that IRAK2 expression, including mRNA and protein levels, were pronouncedly elevated in parental OML1, but not OML1-R cells. Densitometry-derived values (bottom) were normalized with the control set as 1. β-actin served as the loading control for normalization.

IRAK2 Overexpression Restored Radiosensitivity by Enhancing IR-Induced Cell Killing and Apoptosis in Radioresistant OML1-R Cells

To evaluate whether IRAK2 influences the sensitivity of radioresistant OSCC to IR, we overexpressed IRAK2 in OML1-R cells, which demonstrated an intrinsically low level of IRAK2. As shown in **Figure 2A**, IRAK2-overexpressed OML1-R cells exhibit a higher radiosensitivity than that of control OML1-R cells ($P = 0.0100$), suggesting a role of IRAK2 in the process of restoring radiosensitivity in radioresistant OSCC.

Apoptosis has been well known as a biological indicator for measuring cellular radiosensitivity (23). IRAK2-overexpressed OML1-R cells showed more apoptosis than that of control OML1-R cells, especially after 4Gy IR treatment; quantitative data for apoptosis rate were consistent with this phenomenon (**Figure 2B**).

IRAK2 is critical for apoptosis through FADD-dependent recruitment of caspase-8 activation (8) and the endoplasmic reticulum (ER) stress-induced IRE-1/CHOP signaling pathway (9). After 72 hours of exposure to 4-Gy IR, IRAK2-overexpressed OML1-R cells had higher levels of cleaved caspase-8 and caspase-3, but not NF-κB and CHOP, than that of control OML1-R cells (**Figure 2C**). To further confirm these results, we applied z-IETD-FMK, a caspase-8 inhibitor, to pretreat IRAK2-overexpressed OML1-R cells. Our results revealed that z-IETD-FMK attenuated the overexpression of IRAK2 -induced apoptosis, as shown by significant decreases in cleaved caspase-8 and cleaved caspase-3 (**Figure 2D**). These results simultaneously indicated that IRAK2 overexpression re-sensitizes OML1-R cells to IR treatment *via* enhancing caspase-8- and caspase-3-depended cell apoptosis.

IRAK2 Knockdown Decreased OSCC Radiosensitivity and IR-Induced Apoptosis

To further address whether IRAK2 is sufficient to induce apoptosis and alter cellular radiosensitivity, we quantified the expression of IRAK2 in four OSCC cell lines, finding that OML1 and SCC25 cells exhibited higher expression of IRAK2 (**Figure 3A**). IRAK2-specific shRNA was delivered into OML1 and SCC25 cells to knock down IRAK2 expression. Both IRAK2-knockdown OML-1 and SCC25 cells demonstrated higher survival rates after exposure to IR when compared with their control cells ($P = 0.0009$ and 0.0577, respectively; **Figure 3B**). To exam the apoptotic effects of IRAK2 shRNA combined with radiation in OML1 and SCC25 cell lines. The results revealed that in both cell lines, shRNA-IRAK2 cells were diminished radiation-induced apoptosis compared with their control cells after IR exposure (**Figure 3C**). IRAK2 silencing also decreased the expression of cleaved caspase-8 and -3 in both two types of OSCC cancer cells when compared with their control cells (**Figure 3D**). These data indicated that IRAK2 knockdown in OSCC cells strikingly attenuated radiosensitivity *via* inhibiting caspase-8/3-mediated apoptosis.

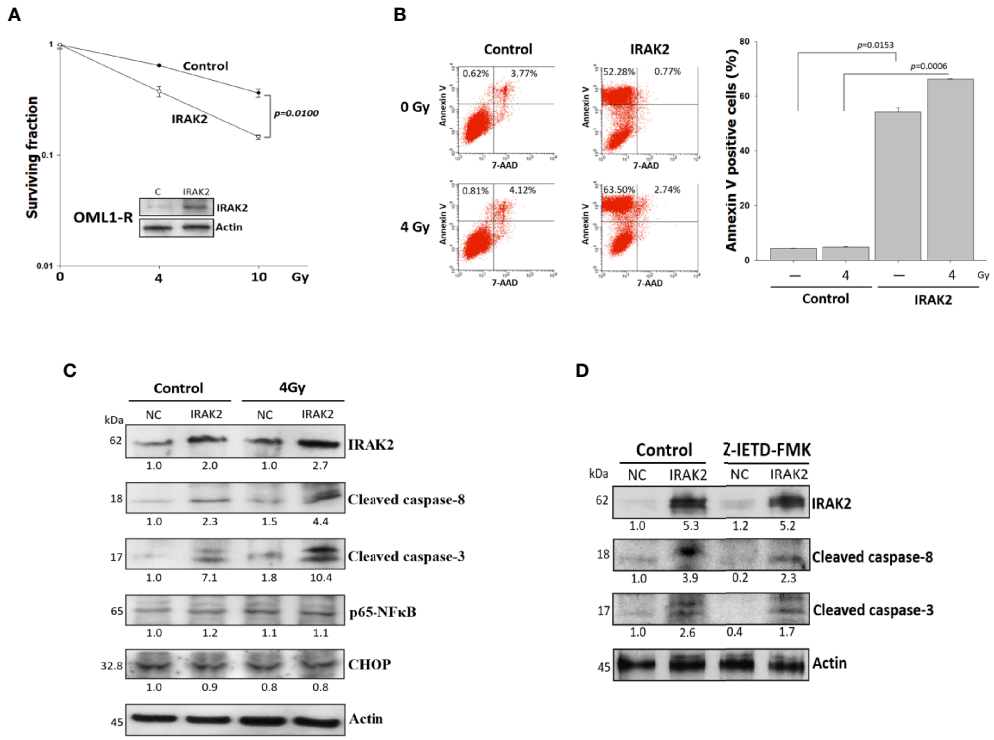

FIGURE 2 | Overexpression of IRAK2 restored radiosensitivity *via* enhancing radiation-induced apoptosis in OML1-R cells. **(A)** Colony formation assay showed that IRAK2-overexpressed OML1-R cells restored their radiosensitivity when compared with that of control OML1-R cells (P = 0.0100). **(B)** Apoptosis-specific flow cytometry represented that overexpression of IRAK2 significantly enhanced apoptosis in OML1-R cells before (52.28% *vs.* 0.62%) and after (63.50% *vs.* 0.81%) 4-Gy IR. The histogram on the right represent Annexin V-positive staining enrichment. **(C)** In OML1-R cells, protein levels of apoptosis-related factors, i.e., cleaved caspase-8, cleaved caspase-3, CHOP, and p65-NF-κB, were elevated by the overexpression of IRAK2, especially after 4-Gy IR (Western blotting, 72 hours after IR). **(D)** Protein levels of IRAK2, cleaved caspase-8 and cleaved caspase-3 were analyzed for OML1-R cells treated with an IRAK2 overexpression followed by the pretreatment with caspase-8 inhibitors (50 mM Z-IETD-FMK) for 1 hour. Densitometry-derived values (bottom) were normalized with the control set as 1. β-actin served as the loading control for normalization.

IRAK2 Overexpression Enhanced IR-Induced Tumor Regression in Radioresistant OSCC Xenografts

To evaluate the radiosensitization potential of IRAK2 *in vivo*, we established a nude mice xenograft model that injected IRAK2-overexpressed OML1-R cells. IRAK2-overexpressed xenografts demonstrated an apparent reduction in tumor volume when compared with the control. IRAK2 overexpression alone inhibited tumor growth, indicating that IRAK2 may function as a tumor suppressor (**Figure 4A**). We then examined the effect of control and IRAK2-overexpressed mice that received a fraction size of 5 Gy every four days to a cumulative dose of 50 Gy, respectively. After exposure to RT, the tumor volume of IRAK2-overexpressed mice was statistically significantly decreased when compared with that of control ones, implicating that IRAK2 enhances the efficacy of IR treatment in radioresistant tumors (**Figure 4B**). The increased expressions of cleaved caspase-8 and cleaved caspase-3 were further confirmed by immunofluorescence staining and western blotting on tumor tissues in IRAK2-overexpressed xenografted mice treated with RT (**Figures 4C, D**).

High IRAK2 Expression Was Associated With Favorable Local Control in Oral Cancer Patients

Finally, we examined the expression of IRAK2 in 41 OSCC patient samples and summarized clinicopathologic factors in **Table 1**. No statistically significant correlation was found between the level of IRAK2 expression and other clinicopathological variables. Immunohistochemical staining showed IRAK2 expression in the cytoplasm and membrane of OSCC tumor samples (**Figure 5A**). Kaplan-Meier survival curves was performed to demonstrate that patients with higher IRAK2 expression (i.e., >110) were associated with better local recurrence-free survival than that of those patients with lower expressions (i.e., ≤110; P = 0.055; **Figure 5B**). Cox proportional hazard regression confirmed this observation (univariate HR, 0.25, being slight in favor of high expression; 95% CI, 0.054 - 1.166; P = 0.055; **Figure 5C**), particularly after multivariable analysis (multivariate HR, 0.11; 95% CI, 0.016 - 0.760; P = 0.025; **Figures 5D, E**). Note that seven factors were used for multivariable analysis of local recurrence: age, gender, pathological stage, radiotherapy dose, chemotherapy, the status of surgical margin, and expression level of IRAK2.

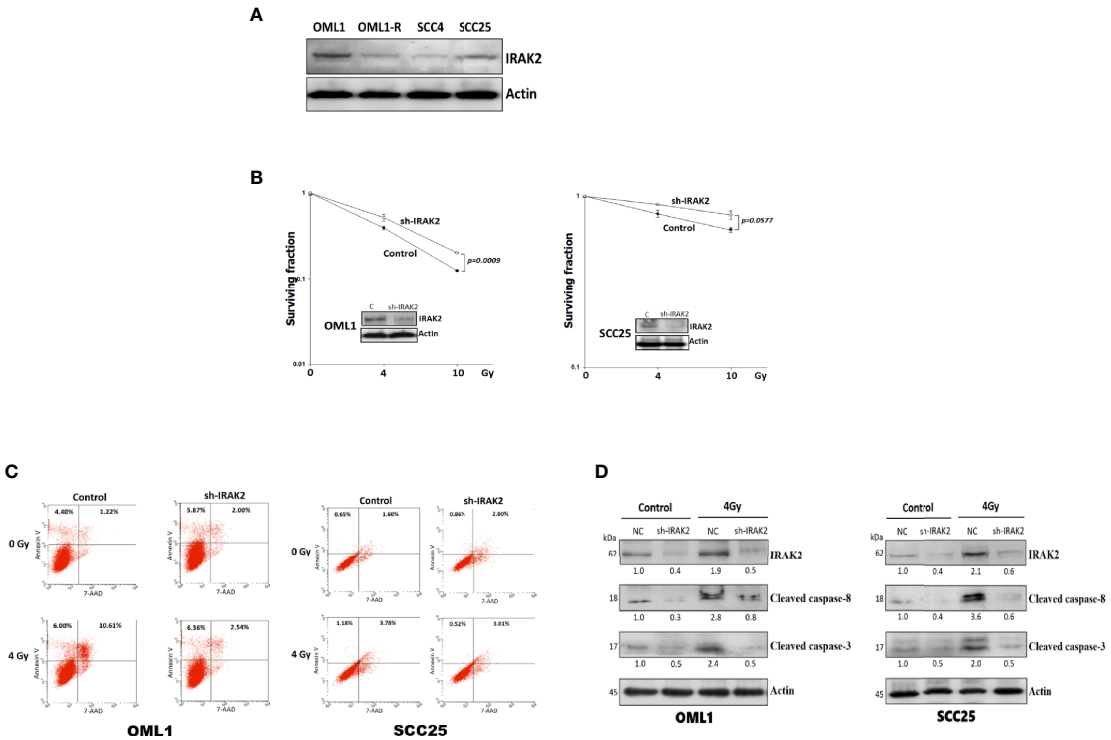

FIGURE 3 | The knockdown of IRAK2 promoted resistance to IR-induced apoptosis in OML1 and SCC25 cells. **(A)** Endogenous IRAK2 expression in different OSCC cell lines, showing higher expressions of IRAK2 in OML1 and SCC25 than that of OML1-R and SCC4 cells. The values under bands represented the relative density that normalized to β-actin. **(B)** When compared with their control cells, post-irradiation colony formation rates were increased in IRAK2-knockdown OML1 ($P = 0.0009$) and SCC25 ($P = 0.0577$) cells. **(C)** Effect of radiation, IRAK2 shRNA or both on cell apoptosis in OML1 and SCC25 cell lines. Flow cytometry analysis using Annexin V and 7-AAD staining was performed to detect apoptotic cells. **(D)** IRAK2-shRNA transfection decreased the expressions of cleaved caspase-8 and caspase-3 in OML1 (left) and SCC25 (right) cancer cells. Densitometry-derived values (bottom) were normalized with the control set as 1. β-actin served as the loading control for normalization.

DISCUSSION

Radioresistance remains a major obstacle for the radiotherapy treatment of OSCC, leading to post-irradiation recurrence and poor clinical outcomes (24, 25). However, so far, few biomarkers are available for identifying potential responders to RT. Based on RNA-seq analysis, we determined that IRAK2 might be an IR-responsive gene whose expression differed significantly between radiosensitive and radioresistant OSCC cells. We found that IRAK2 was downregulated in a radioresistant OML1-R cell line when compared with its parental OML1 cell line. We further examined the expression of IRAK2 in IR-sensitive OML1 and IR-resistant OML1-R cells and showed that the mRNA and protein expression levels of IRAK2 were increased mainly in OML1 cells after IR exposure; however, there was no difference in IRAK2 level between unirradiated and irradiated OML1-R cells, suggesting that the loss of IRAK2 might be an indicator or possibly contribute to mechanisms of radiation resistance. To further clarify the role of IRAK2 in RT, we overexpressed IRAK2 in OML1-R cell lines. Enhanced IRAK2 expression in OML1-R led to decreased colony formation after IR. Conversely, knocking down IRAK2 increased the post-irradiation survival of OSCC cells. Besides, *in vivo*, nude mice exposed to RT had smaller tumors after they were injected with IRAK2-overexpressed OML1-R cells. These sets of data strongly suggested that IRAK2 may serve as a potential therapeutic molecular marker for enhancing radiosensitivity and reversing radioresistance. Therefore, we confirmed that IRAK2 acts as a potential regulator of radiation sensitivity for OSCC.

IRAK2, an immune-responsive protein kinase, is a transducer for the IL1/TLR signaling cascade (6, 26, 27). Recent evidence suggests that TLR-dependent mechanisms contribute to radiation-induced anticancer immunity through the induction of genes associated with programmed cell death (28, 29). Mechanistically, TLR is connected through the interaction of an adaptor molecule (i.e., MyD88), which recruits FADD and caspase-8, leading to the activation of caspase-3 to trigger the apoptotic process subsequently (30). For example, BEAS-2B cells (which were derived from human bronchial epithelium transformed) were treated with a TLR3 agonist [i.e., poly(I:C)]; this manipulation was found to induce apoptosis through the interaction of MyD88 with FADD and caspase-8 (31). Besides, TLR2 was also found to potentiate the MyD88-induced caspase-8 apoptotic pathway in human kidney epithelial 293 cells (32). As

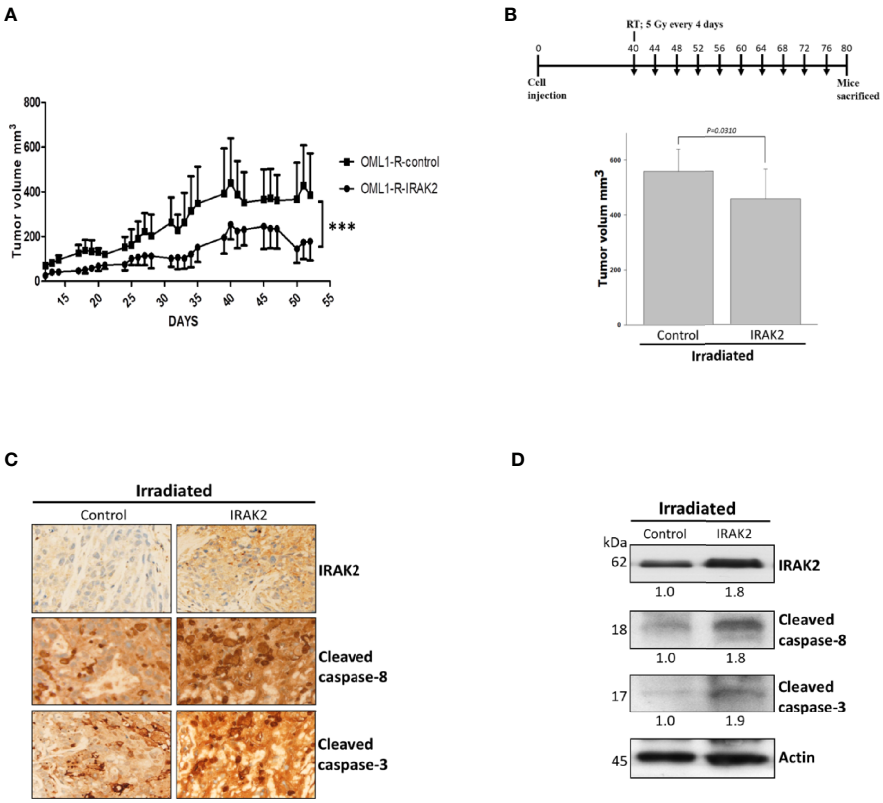

FIGURE 4 | IRAK2 overexpression decreased OML1-R-generated *in vivo* tumor growth and enhanced radiosensitivity in the mice xenograft model. **(A)** In the mice xenograft model, IRAK2-overexpressed OML1-R-generated tumors had a relatively lower tumor growth rate than that of control OML1-R-generated tumors ($P < 0.001$). **(B)** Schema of cell injection and radiation treatments (upper panel). Since the 40th day after cancer cell injection, control and IRAK2-overexpressed mice were treated with RT per 4 days (i.e., a fraction size of 5 Gy by ten fractions to an accumulative dose of 50 Gy). The IRAK2-overexpressed mice had a smaller tumor volume than that of control mice at the time of radiotherapy ($P = 0.0310$; lower panel). **(C)** The expression of IRAK2, cleaved caspase-8, and cleaved caspase-3 in tumor tissues from control and IRAK2-overexpressed mice after radiotherapy were detected by immunohistochemical staining. **(D)** Immunoblotting analysis of the indicated proteins in lung tissues from control and IRAK2-overexpressed mice after irradiation. Densitometry-derived values (bottom) were normalized with the control set as 1. β-actin served as the loading control for normalization. Data were presented as mean ± SD. '***' represented $P < 0.001$. All experiments were performed in triplicate.

a result, IRAK2 demonstrated a mediator of MyD88-dependent signal transduction activation *via* TLRs (6, 33).

IRAK2 also has been reported to be associated with signaling cell death (34). It could induce apoptosis in bacteria-infected macrophages by targeting the FADD/caspase-8 death signaling pathway (35, 36). Moreover, IRAK2 is required for ER stress-induced increases in IRE1 and CHOP expression, which transduces the death signal in ER stress-mediated apoptosis (9). In the present study, we found that overexpression of IRAK2 significantly increased the apoptotic rate in response to IR through cleavage activation of caspase 8 and caspase 3 in irradiated cells, whereas in the presence of z-IETD-FMK (caspase-8 inhibitor) could significantly decrease IRAK2-induced caspase-8 and caspase-3 cleavage. It suggested that IRAK2-induced apoptosis is dependent on the caspase-8 activation.

On the other hand, IRAK2 knockdown diminished the caspase-8 and caspase-3-mediated apoptosis. These findings indicated that IRAK2 might be a superior target for radiosensitization, triggering apoptosis mainly through the activation of caspase-8 and caspase-3 to increase and restore the sensitivity of radioresistant cells to IR-induced cell killing. However, the significant functional role of IRAK2 in mediating apoptosis and anticancer immunity by TLR signaling needs to be further investigated.

Since few reports have discussed the role of IRAK2 in solid tumors (37), we further evaluated the clinical significance of IRAK2 expression in 41 pathological stage I-II OSCC patients who underwent postoperative radiotherapy. Patients with high IRAK2 expression have been demonstrated to be better local control rates than those with low IRAK2 expression. The limitations of the present study are as follows: the nature of retrospective study design and a relatively small case number. Thus, further studies with a large sample size are required to confirm our results. Taken together, we found that IRAK2 was downregulated in radioresistant OSCC cells. We further determined that enhancing IRAK2 activity led to increasing/restoring radiosensitivity in radioresistant OSCC *in vitro* and *in vivo* – and vice versa – operating through a caspase-8/3-

TABLE 1 | Patient characteristics of 41 oral cancer patients according to the expression level of IRAK2.

		IRAK2				
		Low expression (n = 24)		High expression (n = 17)		*P* value
Age (years)	(mean ± SD)	51.3 ± 11.4		52.7 ± 10.1		0.70
RT dose (cGy)	(mean ± SD)	6338.3 ± 1378.4		6559.4 ± 1284.8		0.61
Gender	Male	23	(96%)	16	(94%)	0.80
	Female	1	(4%)	1	(6%)	
Clinical stage	I	8	(33%)	4	(24%)	0.88
	II	11	(46%)	9	(53%)	
	III	2	(8%)	1	(6%)	
	IVA/B	3	(13%)	3	(18%)	
Pathologic stage	I	15	(63%)	7	(41%)	0.18
	II	9	(38%)	10	(59%)	
Surgical margin	<1 mm	6	(25%)	1	(5.9%)	0.21
	≧1~ ≦5 mm	18	(75%)	16	(94.1%)	
Lymphovascular space invasion	No	23	(95.8%)	14	(82.4%)	0.29
	Yes	1	(4.2%)	3	(17.6%)	
Perineural invasion	No	22	(91.7%)	13	(76.5%)	0.18
	Yes	2	(8.3%)	4	(23.5%)	
Chemotherapy	No	17	(71%)	10	(59%)	0.42
	Yes	7	(29%)	7	(41%)	

SD, standard deviation; RT, radiotherapy.

According to the principle of surgical oncology and our treatment policy, re-resection was the first treatment of choice for patients who had close-margin (i.e., ≦5 mm) pathology stage I-II OSCC. However, for those patients who had anatomic difficulty on re-resection and who had refusal of re-operation, salvage therapy of radiotherapy with or without chemotherapy was the alternative treatment choice, as that indicated for the above 41 patients.

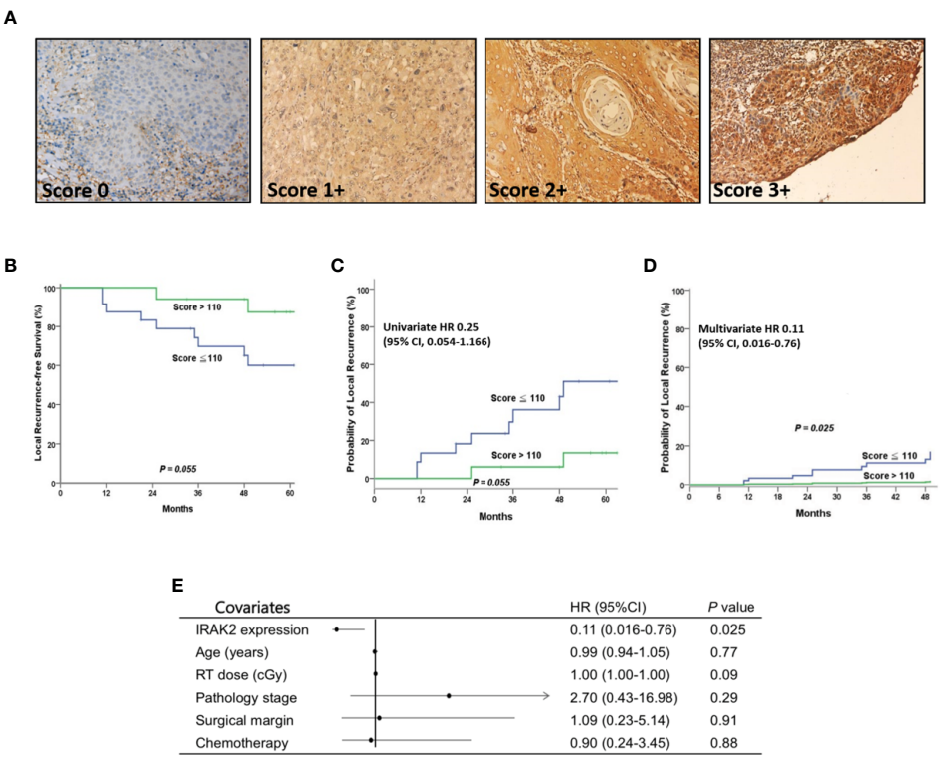

FIGURE 5 | After postoperative radiotherapy, OSCC patients with higher IRAK2 expressions showed better local recurrence-free survival (LRFS) than those with lower IRAK2 expressions. **(A)** Representative micrographs demonstrated the immunohistochemical (IHC) scores of IRAK2 expression in oral squamous cell carcinoma. (magnification, x200). **(B)** Kaplan-Meier survival curves represented that patients with higher IRAK2 expressions (i.e., >110) seemly demonstrated better 5-year LRFS than that of patients with lower expressions (i.e., 87.4% *vs.* 60.0%; P = 0.055, a statistical trend). **(C)** Cox proportional hazard regression confirmed this observation (univariate HR 0.25; 95% CI, 0.054 - 1.166; P = 0.055, a statistical trend). **(D)** Remarkably, after multivariable analysis, the two groups showed a statistically significant difference in terms of post-irradiation LRFS (multivariate HR 0.11; 95% CI, 0.016 - 0.760; P = 0.025). **(E)** Forest plot of multivariate analysis, depending on the Panel **(D)** Note that seven factors were used for multivariate analysis of LRFS (Panel C): age, gender, pathological stage, RT dose, chemotherapy, the status of surgical margin, and the expression level of IRAK2.

dependent apoptosis mechanism. Our data suggested that IRAK2 may affect both the developments of intrinsic and irradiation-acquired radioresistance.

The present study is the first report stating that IRAK2 activation may be associated with modulation of radiosensitivity. IRAK2 may facilitate the process of radiation immunity by inducing cancer cells to undergo apoptosis.

CONCLUSIONS

In the present study, we have established a proof-of-concept platform *in vivo* and *in vitro* that the potential of IRAK2 may serve as both predictive and therapeutic biomarkers for estimating and manipulating radiation sensitivity in OSCC. Overexpressing IRAK2 increases and restores radiosensitivity in intrinsic and treatment-acquired radioresistant OSCC, respectively. Clinically, high IRAK2 expression predicts better local control in irradiated OSCC patients. However, the real-world clinical treatment utilization of IRAK2 in patients with OSCC remains unknown. Accordingly, further research in targeted gene therapy techniques to assess their efficacy and safety in OSCC is required.

DATA AVAILABILITY STATEMENT

The datasets presented in this study can be found in online repositories. The names of the repository/repositories and accession number(s) can be found below: GEO Series, accession number GSE165585.

ETHICS STATEMENT

The studies involving human participants were reviewed and approved by Dalin Tzu Chi Hospital, Buddhist Tzu Chi Medical Foundation, approved number: B10604021. The patients/participants provided their written informed consent to participate in this study. The animal study was reviewed and approved by Animal protocols obeyed the instructions of the Institutional Animal Care and Use Committee of National Chung Cheng University (IACUC no.1060703).

AUTHOR CONTRIBUTIONS

C-CY, R-IL, H-YL, and F-CH performed the experiments. L-CC, L-WH, C-HC, and H-JY collected patient samples. W-YC, C-AC, C-LC, M-SL, and MC performed data analysis. MC, H-YL, and S-KH designed the experiments. C-CY, H-YL and S-KH wrote the manuscript. All authors contributed to the article and approved the submitted version.

FUNDING

This study was supported by grants from the Dalin Tzu Chi Hospital, Buddhist Tzu Chi Medical Foundation (DTCRD105 (2)-E-09, DTCRD106 (2)-E-17, DTCRD107(2)-I-13). This study was also supported by the Ministry of Science and Technology, Taiwan (MOST 108-2314-B-303-001), and Taipei City Hospital Zhongxing Branch (TPCH-107-031).

REFERENCES

1. Pfister DG, Spencer S, Adelstein D, Adkins Y, Anzai Y, Brizel DM, et al. Head and Neck Cancers, Version 2.2020, NCCN Clinical Practice Guidelines in Oncology. *J Natl Compr Canc Netw* (2020) 18(7):873–98. doi: 10.6004/jnccn.2020.0031
2. Ishigami T, Uzawa K, Higo M, Nomura H, Saito K, Kato Y, et al. Genes and Molecular Pathways Related to Radioresistance of Oral Squamous Cell Carcinoma Cells. *Int J Cancer* (2007) 120(10):2262–70. doi: 10.1002/ijc.22561
3. Sankunny M, Parikh RA, Lewis DW, Gooding WE, Saunders WS, Gollin SM. Targeted Inhibition of ATR or CHEK1 Reverses Radioresistance in Oral Squamous Cell Carcinoma Cells With Distal Chromosome Arm 11q Loss. *Genes Chromosomes Cancer* (2014) 53(2):129–43. doi: 10.1002/gcc.22125
4. Ge L, Liu S, Xie L, Sang L, Ma C, Li H. Differential mRNA Expression Profiling of Oral Squamous Cell Carcinoma by High-Throughput RNA Sequencing. *J BioMed Res* (2015) 29(5):397–404. doi: 10.7555/JBR.29.20140088
5. Lin HY, Huang TH, Chan MW. Aberrant Epigenetic Modifications in Radiation-Resistant Head and Neck Cancers. *Methods Mol Biol* (2015) 1238:321–32. doi: 10.1007/978-1-4939-1804-1_17
6. Meylan E, Tschopp J. IRAK2 Takes its Place in TLR Signaling. *Nat Immunol* (2008) 9(6):581–2. doi: 10.1038/ni0608-581
7. Rhyasen GW, Starczynowski DT. IRAK Signalling in Cancer. *Br J Cancer* (2015) 112(2):232–7. doi: 10.1038/bjc.2014.513
8. Ruckdeschel K, Mannel O, Schrottner P. Divergence of Apoptosis-Inducing and Preventing Signals in Bacteria-Faced Macrophages Through Myeloid Differentiation Factor 88 and IL-1 Receptor-Associated Kinase Members. *J Immunol* (2002) 168(9):4601–11. doi: 10.4049/jimmunol.168.9.4601
9. Benosman S, Ravanan P, Correa RG, Hou YC, Yu M, Gulen MF, et al. Interleukin-1 Receptor-Associated Kinase-2 (IRAK2) is a Critical Mediator of Endoplasmic Reticulum (ER) Stress Signaling. *PloS One* (2013) 8(5):e64256. doi: 10.1371/journal.pone.0064256
10. Vollmer S, Strickson S, Zhang T, Gray N, Lee KL, Rao VR, et al. The Mechanism of Activation of IRAK1 and IRAK4 by Interleukin-1 and Toll-like Receptor Agonists. *Biochem J* (2017) 474(12):2027–38. doi: 10.1042/BCJ20170097
11. Liu PH, Shah RB, Li Y, Arora A, Ung PM, Raman R, et al. An IRAK1-PIN1 Signalling Axis Drives Intrinsic Tumour Resistance to Radiation Therapy. *Nat Cell Biol* (2019) 21(2):203–13. doi: 10.1038/s41556-018-0260-7
12. Lin HY, Hung SK, Lee MS, Chiou WY, Huang TT, Tseng CE, et al. DNA Methylome Analysis Identifies Epigenetic Silencing of FHIT as a Determining Factor for Radiosensitivity in Oral Cancer: An Outcome-Predicting and Treatment-Implicating Study. *Oncotarget* (2015) 6(2):915–34. doi: 10.18632/oncotarget.2821
13. Lin HY, Huang TT, Lee MS, Hung SK, Lin RI, Tseng CE, et al. Unexpected Close Surgical Margin in Resected Buccal Cancer: Very Close Margin and DAPK Promoter Hypermethylation Predict Poor Clinical Outcomes. *Oral Oncol* (2013) 49(4):336–44. doi: 10.1016/j.oraloncology.2012.11.005
14. Caudell JJ, Ward MC, Riaz N, Zakem SJ, Awan MJ, Dunlap NE, et al. Volume, Dose, and Fractionation Considerations for IMRT-based Reirradiation in Head and Neck Cancer: A Multi-Institution Analysis. *Int J Radiat Oncol Biol Phys* (2018) 100(3):606–17. doi: 10.1016/j.ijrobp.2017.11.036
15. Halperin EC, Wazer DE, Perez CA, Brady LW. *Perez & Brady's Principles and Practice of Radiation Oncology 7th ed.* Philadelphia: Wolters Kluwer (2018) pp. 859–98.
16. National Health Insurance Research Database. *Taiwan: the Taiwan National Health Research Institutes*. Available at: https://www.nhri.edu.tw/eng/. Accessed January 20, 2019
17. Cannon RB, Kull AJ, Carpenter PS, Francis S, Buchmann LO, Monroe MM, et al. Adjuvant Radiation for Positive Margins in Adult Head and Neck

Sarcomas is Associated With Improved Survival: Analysis of the National Cancer Database. *Head Neck* (2019) 41(6):1873–9. doi: 10.1002/hed.25619
18. Greene FL. *AJCC Cancer Staging Atlas*. New York, NY: Springer (2006).
19. Hsieh MY, Chen G, Chang DC, Chien SY, Chen MK. The Impact of Metronomic Adjuvant Chemotherapy in Patients With Advanced Oral Cancer. *Ann Surg Oncol* (2018) 25(7):2091–7. doi: 10.1245/s10434-018-6497-3
20. Franken NA, Rodermond HM, Stap J, Haveman J, van Bree C. Clonogenic Assay of Cells In Vitro. *Nat Protoc* (2006) 1(5):2315–9. doi: 10.1038/nprot.2006.339
21. Yu CC, Chen CA, Fu SL, Lin HY, Lee MS, Chiou WY, et al. Andrographolide Enhances the Anti-Metastatic Effect of Radiation in Ras-transformed Cells *Via* Suppression of ERK-mediated MMP-2 Activity. *PloS One* (2018) 13(10): e0205666. doi: 10.1371/journal.pone.0205666
22. Boumiza A, Zemni R, Sghiri R, Idriss N, Hassine HB, Chabchoub E, et al. IRAK2 is Associated With Systemic Lupus Erythematosus Risk. *Clin Rheumatol* (2020) 39(2):419–24. doi: 10.1007/s10067-019-04781-1
23. Kunogi H, Sakanishi T, Sueyoshi N, Sasai K. Prediction of Radiosensitivity Using Phosphorylation of Histone H2AX and Apoptosis in Human Tumor Cell Lines. *Int J Radiat Biol* (2014) 90(7):587–93. doi: 10.3109/09553002.2014.907518
24. Smith BD, Haffty BG. Molecular Markers as Prognostic Factors for Local Recurrence and Radioresistance in Head and Neck Squamous Cell Carcinoma. *Radiat Oncol Investig* (1999) 7(3):125–44. doi: 10.1002/(SICI)1520-6823(1999)7:3<125::AID-ROI1>3.0.CO;2-W
25. Liu L, Zhu Y, Liu AM, Feng Y, Chen Y. Long Noncoding RNA LINC00511 Involves in Breast Cancer Recurrence and Radioresistance by Regulating STXBP4 Expression *Via* Mir-185. *Eur Rev Med Pharmacol Sci* (2019) 23 (17):7457–68. doi: 10.26355/eurrev_201909_18855
26. Wang H, Flannery SM, Dickhofer S, Huhn S, George J, Kubarenko AV, et al. A Coding IRAK2 Protein Variant Compromises Toll-like Receptor (TLR) Signaling and is Associated With Colorectal Cancer Survival. *J Biol Chem* (2014) 289(33):23123–31. doi: 10.1074/jbc.M113.492934
27. Lin SC, Lo YC, Wu H. Helical Assembly in the MyD88-IRAK4-IRAK2 Complex in TLR/IL-1R Signalling. *Nature* (2010) 465(7300):885–90. doi: 10.1038/nature09121
28. Trapani S, Manicone M, Sikokis A, D'Abbiero N, Salaroli F, Ceccon G, et al. Effectiveness and Safety of "Real" Concurrent Stereotactic Radiotherapy and Immunotherapy in Metastatic Solid Tumors: A Systematic Review. *Crit Rev Oncol Hematol* (2019) 142:9–15. doi: 10.1016/j.critrevonc.2019.07.006
29. Ratikan JA, Micewicz ED, Xie MW, Schaue D. Radiation Takes its Toll. *Cancer Lett* (2015) 368(2):238–45. doi: 10.1016/j.canlet.2015.03.031
30. Cen X, Liu S, Cheng K. The Role of Toll-Like Receptor in Inflammation and Tumor Immunity. *Front Pharmacol* (2018) 9:878. doi: 10.3389/fphar.2018.00878
31. Koizumi Y, Nagase H, Nakajima T, Kawamura M, Ohta K. Toll-Like Receptor 3 Ligand Specifically Induced Bronchial Epithelial Cell Death in Caspase Dependent Manner and Functionally Upregulated Fas Expression. *Allergol Int* (2016) 65 Suppl:S30–7. doi: 10.1016/j.alit.2016.05.006
32. Aliprantis AO, Yang RB, Weiss DS, Godowski P, Zychlinsky A. The Apoptotic Signaling Pathway Activated by Toll-like Receptor-2. *EMBO J* (2000) 19 (13):3325–36. doi: 10.1093/emboj/19.13.3325
33. Keating SE, Maloney GM, Moran EM, Bowie AG. IRAK-2 Participates in Multiple Toll-Like Receptor Signaling Pathways to NFkappaB *Via* Activation of TRAF6 Ubiquitination. *J Biol Chem* (2007) 282(46):33435–43. doi: 10.1074/jbc.M705266200
34. Huang YS, Misior A, Li LW. Novel Role and Regulation of the Interleukin-1 Receptor Associated Kinase (IRAK) Family Proteins. *Cell Mol Immunol* (2005) 2(1):36–9.
35. Pandey AK, Sodhi A. Recombinant YopJ Induces Apoptotic Cell Death in Macrophages Through TLR2. *Mol Immunol* (2011) 48(4):392–8. doi: 10.1016/j.molimm.2010.07.018
36. Zhou H, Harberts E, Fishelevich R, Gaspari AA. TLR4 Acts as a Death Receptor for Ultraviolet Radiation (UVR) Through IRAK-independent and FADD-dependent Pathway in Macrophages. *Exp Dermatol* (2016) 25 (12):949–55. doi: 10.1111/exd.13222
37. Xu Y, Liu H, Liu S, Wang Y, Xie J, Stinchcombe TE, et al. Genetic Variant of IRAK2 in the Toll-Like Receptor Signaling Pathway and Survival of non-Small Cell Lung Cancer. *Int J Cancer* (2018) 143(10):2400–8. doi: 10.1002/ijc.31660

Conflict of Interest: The authors declare that the research was conducted in the absence of any commercial or financial relationships that could be construed as a potential conflict of interest.

Advantages of publishing in Frontiers

OPEN ACCESS
Articles are free to read for greatest visibility and readership

FAST PUBLICATION
Around 90 days from submission to decision

HIGH QUALITY PEER-REVIEW
Rigorous, collaborative, and constructive peer-review

TRANSPARENT PEER-REVIEW
Editors and reviewers acknowledged by name on published articles

Frontiers
Avenue du Tribunal-Fédéral 34
1005 Lausanne | Switzerland

Visit us: www.frontiersin.org
Contact us: frontiersin.org/about/contact

REPRODUCIBILITY OF RESEARCH
Support open data and methods to enhance research reproducibility

DIGITAL PUBLISHING
Articles designed for optimal readership across devices

FOLLOW US
@frontiersin

IMPACT METRICS
Advanced article metrics track visibility across digital media

EXTENSIVE PROMOTION
Marketing and promotion of impactful research

LOOP RESEARCH NETWORK
Our network increases your article's readership